



University of Verona

Department of Biotechnology

Graduate School of Natural Sciences and Engineering

Doctoral program in Biotechnology

Cycle XXXIII

PhD thesis

**Exploring the participation of VviNAC factors in
the transcriptional regulatory network which
governs grapevine maturation processes**

S.S.D. AGR/07

Coordinator: Prof. Matteo Ballottari

Tutor: Prof. Sara Zenoni

Doctoral Student: Chiara Foresti

ABSTRACT

Grapevine (*Vitis vinifera* L.) is one of the most important fruit crops as it is widely cultivated, and the winemaking industry has a huge worldwide economic relevance.

The global warming has affected viticulture altering the maturation processes; in particular, the anticipation of the onset of the berries ripening (*veraison*) has changed the physiological characteristics of grapes and, consequently, has negatively influenced the wine quality. In this context, uncovering the molecular mechanisms of the ripening could provide the key in maintaining high quality grapes and wine.

For all these reasons, the identification and characterization of master regulators controlling the transition from vegetative-to-mature growth are the challenging but fundamental tasks of this research project. At first, to provide insight into the transcriptional programs controlling the development of grapevine, a global gene expression atlas was generated (Fasoli *et al.*, 2012). Combining this dataset with a berry-specific one (Massonnet *et al.*, 2017), an integrated network analysis was performed (Palumbo *et al.*, 2014) and a new category of genes (*switch genes*), which are significantly up regulated during the developmental shift and inversely correlated with many genes suppressed during the mature growth phase, was identified. Moreover, many transcription factors are present among them, strongly indicating that they could represent master regulators of the developmental phase transition; between them, the plant-specific NAC (NAM/ATAF/CUC) transcription factors represent an interesting family due to their key role in plant development processes and stress responses (Jensen *et al.*, 2014). Fourteen *VviNACs* genes were selected for functional characterization as key candidates of the major transcriptome reprogramming during grapevine development: *VviNAC01*, *VviNAC03* (D'Inca, 2017), *VviNAC08*, *VviNAC11* (D'Inca, 2017), *VviNAC13* (D'Inca, 2017), *VviNAC15*, *VviNAC17*, *VviNAC18*, *VviNAC26*, *VviNAC33* (D'Inca, 2017), *VviNAC38*, *VviNAC39*, *VviNAC60* (D'Inca, 2017) and *VviNAC61*.

Different approaches have been carried out to investigate the function of *VviNACs* gene: the transient over expressions, DAP-seq (DNA Affinity Purification and sequencing, Bartlett *et al.*, 2017) and, only for *VviNAC60*, the ChIP-seq (Chromatin Immunoprecipitation sequencing, Kaufmann *et al.*, 2010). All of them

are powerful techniques used to identify possible targets of the selected transcription factor regulations. VviNAC01 showed its important role in the ethylene pathways; VviNAC03 did not reveal a well-defined identity but seems to be plant growth related; VviNAC08 seems to have a possible role in the gibberellin-related and circadian mechanisms; VviNAC11 seems to be related to the control of the auxin pathways and the chlorophylls degradation; VviNAC13 revealed a probable action in the lignin and phenylpropanoid metabolic processes; VviNAC15, regulating many other TFs, highlighted its role in the regulation mechanisms orchestration; VviNAC17 appeared to be a regulator of the jasmonic acid-induced gene expression; VviNAC18 analyses reported its role in the chlorophyll degradation; VviNAC26 presented the regulation of many genes related to the sugars biosynthesis and the anthocyanin synthesis; VviNAC33 terminates the photosynthetic activity and organ vegetative growth; no data are available for VviNAC38; VviNAC39 resulted to up regulate the transport of sugar and lipids and the ubiquitin-conjugating; VviNAC60 revealed a lot of hormones related up regulated direct target genes and many transcription factors, highlighting again the important and major role of this transcription factor in the grapevine maturation processes; VviNAC61 revealed a predominant role in the regulation of the aromatic compounds biosynthesis. Concerning VviNAC60, ChIP-seq data were also obtained and one interesting gene, the *SRG1- SENESCENCE-RELATED GENE 1 OXIDOREDUCTASE* (VIT_10s0003g02400), was found. In order to define a regulation and co-regulation network between VviNACs, some candidate targets genes taken from the different DAP-seq datasets (*VviNAC01*, *VviNAC05*, *VviNAC08*, *VviNAC34*, *VviNAC37* and *VviNAC61*) were tested by Dual Luciferase Reporter Assays to see by which of the selected TFs were actually regulated. The obtained results showed that VviNAC01 directly repressed *VviNAC05* expression, whereas activated the *VviNAC08* one; moreover, VviNAC01 was validated as repressor of its own transcription. VviNAC03 resulted a repressor of *VviNAC05*. VviNAC11 directly up regulated *VviNAC34*, *VviNAC37* and *VviNAC61*. VviNAC13 resulted to regulate *VviNAC34* and *VviNAC37* expression. VviNAC15 activated *VviNAC34*. VviNAC17 acted as a repressor of *VviNAC05*, *VviNAC08* and *VviNAC61* expression. VviNAC18 resulted a direct activator of *VviNAC05*.

VviNAC26 positively regulated the expression of *VviNAC05* and directly down regulated the *VviNAC08*, *VviNAC34* and *VviNAC61* expression. VviNAC33 was found as a direct activator of *VviNAC05*, *VviNAC08*, *VviNAC34*, *VviNAC37* and *VviNAC61* expression. VviNAC60 showed to induced *VviNAC05*, *VviNAC34* and *VviNAC61* expression.

This PhD thesis lights up the possible roles of some *VviNACs* in the grapevine development and presents a preliminary regulatory network between this family members; further analysis must be conducted to completely elucidate this complex regulation system.

CONTENTS

| | |
|---|-----|
| 1. BACKGROUND KNOWLEDGES..... | 1 |
| 1.1 THE GRAPE RIPENING PROCESS..... | 2 |
| 1.2 THE NAC TRANSCRIPTION FACTORS..... | 9 |
| 1.3 THE REGULATION MECHANISMS OF TRANSCRIPTION..... | 17 |
| 1.4 THE CISTROME LANDSCAPE..... | 29 |
| 2. <i>Vvi</i> NACs SELECTION AND FUNCTIONAL ANALYSES..... | 35 |
| 2.1 INTRODUCTION..... | 36 |
| 2.2 MATERIAL AND METHODS..... | 45 |
| 2.3 RESULTS..... | 50 |
| 3. THE GRAPEVINE CISTROME DISCOVERING..... | 77 |
| 3.1 INTRODUCTION..... | 78 |
| 3.2 MATERIAL AND METHODS..... | 84 |
| 3.3 RESULTS..... | 101 |
| 4. THE <i>Vvi</i> NACs REGULATION NETWORK..... | 191 |
| 4.1 INTRODUCTION..... | 192 |
| 4.2 MATERIAL AND METHODS..... | 193 |
| 4.3 RESULTS..... | 196 |
| 5. DISCUSSION..... | 207 |
| APPENDIX..... | 231 |

OUTLINE OF THE THESIS

The main goal of this PhD project was to investigate the role of the *Vitis vinifera* NAC transcription factors in the grapevine maturation process through genomic, transcriptomic and functional assay techniques.

The attention was focused on 14 *VviNAC* genes: *VviNAC01*, *VviNAC03*, *VviNAC08*, *VviNAC11*, *VviNAC13*, *VviNAC15*, *VviNAC17*, *VviNAC18*, *VviNAC26*, *VviNAC33*, *VviNAC38*, *VviNAC39*, *VviNAC60* and *VviNAC61*.

Chapter 1 reports a general introduction to provide all the current knowledges about the maturation process in grapevine, the NACs transcription factor role in plants, the plant transcription regulatory mechanisms and the last findings concerning the plant cistrome landscape.

Chapter 2 presents the *VviNACs* genes selection criteria and their functional characterization in grapevine. Indeed, after the selection a transient over expression of the selected *VviNACs* was performed to obtain an overview of their primary effects on the grapevine transcriptome and to highlight their hypothetical target genes.

Chapter 3 describes the study of the selected *VviNACs* cistrome through the DAP-seq approach and the first ChIP-seq attempt in grapevine on *VviNAC60*, the master regulator of the berry ripening. A huge bioinformatic work has been done to interpretate the sequencing results and all of them were integrated with the transcriptomic data described in **Chapter 2**.

Chapter 4 reports the validation of the *VviNAC-VviNACs* interactions, aimed at the reconstruction of the grapevine maturation processes regulation. These results were supported by bioinformatic analyses and luciferase assay and permitted to identify a preliminary and partial regulatory network between *VviNACs*.

Chapter 5 discusses all the obtained results and suggests further analyses and technical improvements to fully elucidate the molecular mechanisms underlying the maturation process in grapevine.

1. BACKGROUND KNOWLEDGES

1.1 THE GRAPE RIPENING PROCESS

Grapevine (*Vitis vinifera* L.) is one of the most worldwide cultivated fruit crops as wine industry has a high economic impact on the economy of many developed countries (Martinez-Esteso *et al.*, 2013).

It is a woody temperate perennial plant which presents a period of active growth, from spring to fall, and a dormancy period during winter and until the budburst (Hellman, 2003); to ensure plant survival, all organs undergo an acclimation process for the low temperature toleration during this last phase. It has a biennial reproductive cycle, in fact buds formed in the first year give rise to shoots bearing fruit in the second year.

Berry ripening is a complex and irreversible developmental process affected by many endogenous and exogenous factors (Jackson, 2014; Kuhn *et al.*, 2014). It is tightly coordinated with seed development, originates in the pulp near the stylar end and then moves to the skin and it is genetically and epigenetically programmed (Castellarin *et al.*, 2011).

The berry development exhibits a double sigmoid pattern of growth (Rogiers *et al.*, 2017; **Fig. 1**) which is divided into four distinct stages: a green phase, which lasts from flowering to about 60 days after that, involves rapid growth and cell division; a lag phase, during which the growth slows and the organic acid concentration reaches the highest level; a maturation phase, in which sugars, pigments, volatile secondary metabolites and aromatic molecules are synthesized and organic acids, such as tartrate and malate, accumulate in the vacuole. Moreover, during this last described phase some first growth produced compounds decline, leading to a decrease of acidity and astringency. The third described stage starts with the *veraison* (the onset of ripening), a striking metabolic transition phase characterized by important biochemical and physiological changes, such as softening and coloring of the berries; it is also characterized by an accumulation of specific ROS (Pilati *et al.*, 2014). Berry ripening then proceeds to a fourth phase described as overripening or senescence; during this phase, cell integrity becomes compromised and the berry loses water.

Brassinosteroids, which are well known hormones involved in plant growth and

development, increase at the *veraison*, suggesting they may play a primary role in the regulation of this process (Kuhn *et al.*, 2014). After *veraison*, the levels of ABA increase in berries, playing a role in seed maturation, acquisition of dormancy and resistance to water stress deficit. ABA is also specifically involved in the fruit accumulation of sugar and phenolic compounds (Conde *et al.*, 2007). Despite grape is a non-climacteric fruit, ethylene promotes ripening through complex interactions and may influence berry acidity and the development of flavor and aroma (Fortes *et al.*, 2015; Conde *et al.*, 2007); instead, auxins delay the ripening associated processes (Kuhn *et al.*, 2014).

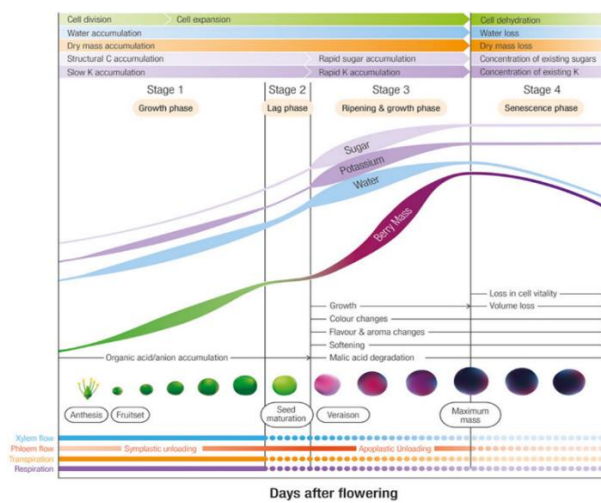


Figure 1: Double sigmoid curve of the four developmental stages of grape berries (Rogiers *et al.*, 2017).

The phenology of grapevine development, which is predominantly influenced by water and inorganic nutrients supply (Jackson, 2014), light exposure (Kuhn *et al.*, 2014) and temperature (Pearce and Coombe 2004; Jones and Davis 2000), is an important aspect that must be considered for the fruit quality and yield (Spayd *et al.*, 2002; Marais *et al.*, 2001; Haselgrove 2000).

The undergoing global warming is changing the timing of grape ripening with consequences on the harvest date and therefore negative impact on wine quality (Webb *et al.*, 2007); low temperatures are necessary to increase total soluble solid and anthocyanin content and to decrease total acidity, while high temperatures cause a reduction in berry weight, total soluble solid, anthocyanins and flavanol contents (Kuhn *et al.*, 2014).

Viticultural, enological and plant culture short-term methods, such as canopy

management (Greer *et al.*, 2010), wine chemistry, the shifting of grapevine growing areas (Hanna *et al.*, 2013; van Leeuwen *et al.*, 2013; Ollat *et al.*, 2011) and the development of new climate adapted cultivars (Ollat *et al.*, 2014; Duchenne *et al.*, 2010), are not sufficient and more powerful solutions are required.

The expansion of genetic resources has provided many useful tools to understand the ripening mechanisms. In fact, a grapevine global gene expression atlas on all *Vitis vinifera* organs was created (Fasoli *et al.*, 2012), showing the transcriptional organization of the whole plant.

The atlas revealed a clear distinction between vegetative/green and mature/woody sample transcriptomes, suggesting a fundamental shift in global gene expression as the plant *switches* from the immature to the mature developmental program (**Fig. 2**). Maturation involves the suppression of diverse metabolic processes, including photosynthesis, energy metabolism, carbohydrate metabolism, cellular component organization, and the cell cycle, which are related to vegetative growth. In contrast, only a few pathways were specifically induced, including secondary metabolic processes and responses to biotic stimuli. This evidence suggests that the transition to mature growth predominantly involves the suppression of vegetative pathways rather than the activation of mature pathways and these results indicate the existence of specific regulatory genes that promote the vegetative-to-mature transcriptomic transition.

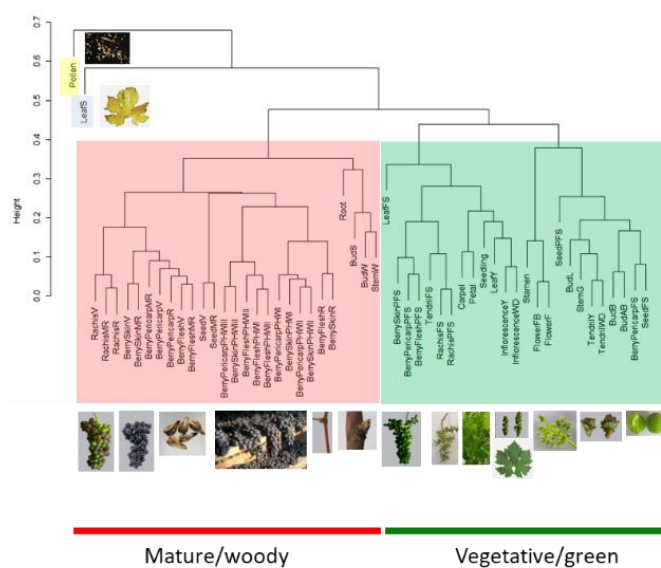


Figure 2: The grapevine global gene expression atlas (Fasoli *et al.*, 2012) showed a clear distinction between samples, which clustered predominantly in relation to temporal dynamics rather than organ identity.

The identification of the key genes involved in deep transcriptome shift that occurs in grapevine was carried out using a gene network analysis (Palumbo *et al.*, 2014) on the gene expression atlas. 1686 differentially expressed genes (DEGs) between vegetative/green and mature/woody samples were identified; among them, 1220 genes were down regulated and 466 were up regulated, suggesting that the transition mainly involves the suppression of vegetative metabolic processes rather than the activation of mature pathways. Moreover, a gene co-expression network with the DEGs was generated and a new subset of 113 genes was identified (**Fig. 3**). These genes were called *switch* genes as they were lowly expressed in the vegetative/green tissues and highly expressed in the mature/woody organs. The most represented functional categories were secondary metabolic process and transcription factors. The same approach was used to analyze the berry-specific transcriptomic dataset (Massonnet *et al.*, 2017) and other *switch* genes involved in the berry development regulation were identified: 190 for the red berry dataset and 212 for the white one. Transcription factors were found as the most significantly over expressed functional category.

By comparing the grapevine atlas and the berry datasets, a list of 131 shared *switch* genes was obtained, representing the key regulators of the global transcriptomic reprogramming necessary for the organ transition.

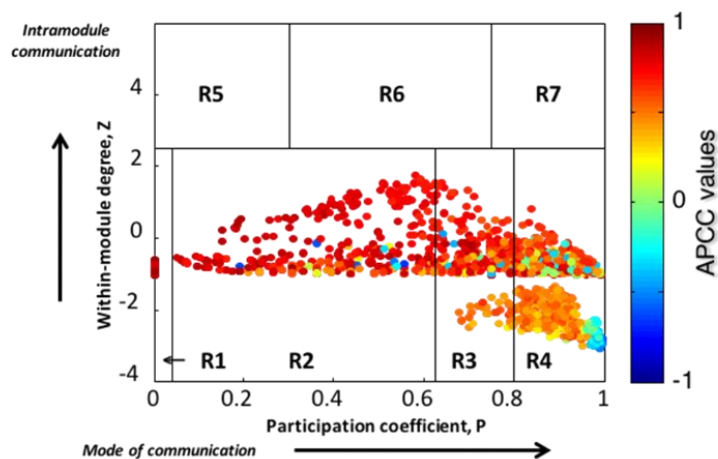


Figure 3: Co-expression network of the differentially expressed genes highlighting a small group of localized *switch* genes that were down regulated during growth phase and up regulated during the mature phase (Palumbo *et al.*, 2014).

To further improve the molecular knowledges related to berry ripening and to identify with more accuracy the key genes involved in the regulation of this process, an RNA-seq transcriptomic analysis has been performed (Fasoli *et al.*, 2018). The results showed that during the progress of berry development and maturation, transcripts are divided into four classes: genes expressed during pre-*veraison* (Class 1), which expression rapidly decreases during berry development; gene expressed during *veraison* (Classes 2 and 3), which expression shows a peak at *veraison* and then subsequently declines; gene expressed during later ripening (Class 4), which are expressed during late-ripening stages with an increasing expression throughout development.

Furthermore, the transcriptomic analysis of berry around *veraison* (early *veraison*, mid-*veraison* and late *veraison*), showed that the onset of berry ripening could be represented by two molecular transitions starting from 14 days before *veraison* (**Fig. 4**). The most represented functional gene categories of both transitions molecular biomarkers were the one related to response to hormone stimulus, cell wall metabolism, secondary metabolic processes and transcription factors; many of these biomarkers were already identified as *switch* genes in the transcriptomic datasets previously analyzed.

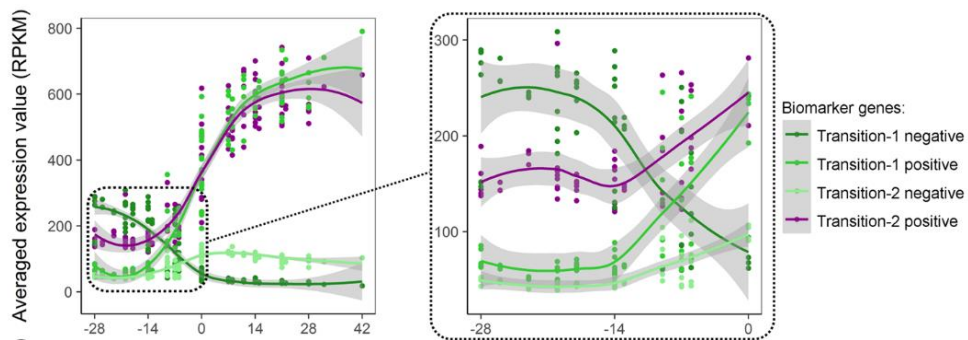


Figure 4: The averaged expression profile of transition-specific putative biomarker genes shown over the whole development (left) and during pre-*veraison* phase (right), (Fasoli *et al.*, 2018).

REFERENCES

Castellarin S., Gambetta G., Wada H., Shackel K., Matthews M. (2011). Fruit ripening in *Vitis vinifera*: spatiotemporal relationships among turgor, sugar accumulation, and anthocyanin biosynthesis. *Journal of Experimental Botany*, Volume 62, Issue 12.

Conde C., Silva P., Fontes N., Dias A. C. P., Tavares R.M., Sousa M. J., Agasse A., Delrot S., Gerós H. (2007). Biochemical Changes throughout Grape Berry Development and Fruit and Wine Quality. *Food*. Vol 1 (1): 1-22.

Coombe BG, Mccarthy MG (2000). Dynamics of grape berry growth and physiology of ripening. *Aust J Grape Wine R.* 6, 131-135.

Duchêne E, Huard F, Dumas V, Schneider C, Merdinoglu D (2010). The challenge of adapting grapevine varieties to climate change. *Clim Res.* 41, 193- 204.

Fasoli M, Dal Santo S, Zenoni S, Tornielli GB, Farina L, Zamboni A, Porceddu A, Venturini L, Bicego M, Murino V, Ferrarini A, Delledonne M, Pezzotti M (2012). The grapevine expression atlas reveals a deep transcriptome shift driving the entire plant into a maturation program. *Plant Cell.* 24(9):3489- 505.

Fasoli M., Richter C. L., Zenoni S., Bertini E., Vitulo N., Dal Santo S., Dokoozlian N., Pezzotti M., Tornielli G.B. (2018). The timing and order of the molecular events that mark the onset of berry ripening in grapevine. *Plant Physiology*. Vol. 178: 1187-1206.

Fortes A. M., Teixeira R. T. and Agudelo-Romero P. (2015). Complex Interplay of Hormonal Signals during Grape Berry Ripening. *Molecules*. Vol. 20: 9326-9343.

Greer DH, Weston C, Weedon M (2010). Shoot architecture, growth and development dynamics of *Vitis vinifera* cv. Semillon vines grown in an irrigated vineyard with and without shade covering. *Funct Plant Biol.* 37, 1061-70.

Hannah L, Roehrdanz PR, Ikegami M, Shepard AV, Shaw MR, Tabor G, et al. (2013). Climate change, wine, and conservation. *Proc Natl Acad Sci USA.* 110, 6907-12.

Haselgrove L. Botting D, Van Heeswijk R, HØJ PB, Dry PR, Ford C, Iland PG (2000). Canopy microclimate and berry composition: The effect of bunch exposure on the phenolic composition of *Vitis vinifera* cv. Shiraz grape berries. *Aust J Grape Wine R.* 6, 141-149.

Hellman EW (2003). Grapevine Structure and Function. *Oregon Viticulture*, 5- 19.

Jackson R. S. (2014). Grapevine Structure and Function. *Wine Science - Principles and Applications*. Chapter 3, 4th edn. Elsevier Inc. 2014.

Jones GV, Davis RE (2000). Climate Influences on Grapevine Phenology, Grape Composition, and Wine Production and Quality for Bordeaux, France. *Am J Enol Vitic.* 51, 249-261.

Kuhn N., Guan L, Wu Dai Z., Wu B. H., Lauvergeat V., Gomès E., Li S. H., Godoy F., Arce-Johnson P. and Serge Delrot S. (2014). Berry ripening: recently heard through the grapevine. *Journal of Experimental Botany*. Vol. 65 (16): 4543–4559.

Marais G, Mouchiroud D, Duret L (2001). Does recombination improve selection on codon usage? Lessons from nematode and fly complete genomes. *Proc Natl Acad Sci USA.* 98, 5688-5692.

Martínez-Esteso MJ, Vilella-Antón MT, Pedreño MA, Valero ML, Bru- Martínez R (2013). iTRAQ-based protein profiling provides insights into the central metabolism changes driving grape berry development and ripening. *BMC Plant Biol.* 13, 167.

Massonnet M, Fasoli M, Tornielli G.B., Altieri M, Sandri M, Zuccolotto P, Paci P, Gardiman M, Zenoni S. and Pezzotti M. (2017). Ripening Transcriptomic Program in Red and White Grapevine Varieties Correlates with Berry Skin Anthocyanin Accumulation. *Plant Physiology*. Vol. 174: 2376–2396.

Ollat N, Bordenave L, Marguerit E, Tandonnet J-P, van Leeuwen K, Destrac A, et al. (2014). Grapevine genetic diversity, a key issue to cope with climate change. Beijing, China: 11th International Conference of Grape Genetics & Breeding, 2014.

Ollat N, Fernandez L, Lecourieux D, Goutouly J-P, van Leeuwen K, Marguerit E, et al. (2011). Multidisciplinary research to select new cultivars adapted to climate changes. Asti-Alba, Italy: 17th International Symposium of GiESCO, 2011.

Palumbo MC, Zenoni S, Fasoli M, Massonnet M, Farina L, Castiglione F, Pezzotti M, Paci P (2014). Integrated network analysis identifies fight-club nodes as a class of hubs encompassing key putative *switch* genes that induce major transcriptome reprogramming during grapevine development. *Plant Cell*. 26(12), 4617-35.

Pearce I, Coombe B (2004). Grapevine phenology. *Viticulture: Volume 1 – Resources*, Eds. P.R. Dry and B.G. Coombe (Winetitles: Adelaide, South Australia) pp. 150-166.

Pilati, S., Bagagli, G., Sonogo, P., Moretto, M., Brazzale, D., Castorina, G., ... Galbiati, M. (2017). Abscisic acid is a major regulator of grape berry ripening onset: new insights into ABA signaling network. *Frontiers in plant science*, 8, 1093.

Rogiers, S. Y., Coetzee, Z. A., Walker, R. R., Deloire, A., & Tyerman, S. D. (2017). Potassium in the grape (*Vitis vinifera* L.) berry: transport and function. *Frontiers in Plant Science*, 8, 1629.

Spayd SE, Tarara JM, Mee DL, Ferguson JC (2002). Separation of sunlight and temperature effects on the composition of *Vitis vinifera* cv. ‘Merlot’ berries. *Amer J Enol and Vitic.* 53, 171-182.

van Leeuwen C, Roby JP, Alonso-Villaverde V, Gindro K (2013). Impact of clonal variability in *Vitis vinifera* Cabernet franc on grape composition, wine quality, leaf blade stilbene content, and downy mildew resistance. *J Agric Food Chem.* 61, 19-24.

Webb L, Whetton P, Barlow EWR (2007). Modelled impact of future climate change on phenology of wine grapes in Australia. *Aust J Grape Wine R.* 13, 165- 175.

1.2 THE NAC TRANSCRIPTION FACTORS

The grapevine global expression atlas (Fasoli *et al.*, 2012) revealed a clear distinction between vegetative/green and mature/woody tissues, reflecting the existence of a deep transcriptome reprogramming occurring during organ phase transition to mature growth. An integrated network analysis (Palumbo *et al.*, 2014) identified the *switch* genes, significantly up regulated in the mature/woody tissues and inversely correlated with many genes down regulated during the developmental transition, which might represent master regulators of transcriptomic rearrangements that drives the entire plant into a maturation program. By combining the atlas dataset with the berries one (Massonnet *et al.*, 2017), *switch* genes, some present in both transcriptomes and other specific for one of them, were identified. All the lists showed several transcription factors (TFs) encoding genes as basic helix-loop-helix (bHLH), MYB, zinc finger (C2H2 and C3HC4 type) family members, some lateral organ boundary (LOB), WRKY DNA-binding and NAC domain-containing proteins (**Fig. 5**).

| <i>GENE_ID</i> | <i>GENE_description</i> | <i>GENE_Name</i> | <i>Atlas</i> |
|--------------------------|---|-------------------------|--------------|
| <i>VIT_17s0000g00430</i> | basic helix-loop-helix (bHLH) family | <i>bHLH075</i> | |
| <i>VIT_15s0046g00150</i> | DOF affecting germination 1 | <i>DAG1</i> | |
| <i>VIT_06s0004g07790</i> | Lateral organ boundaries domain 15 | | * |
| <i>VIT_03s0091g00670</i> | Lateral organ boundaries protein 38 | | |
| <i>VIT_13s0158g00100</i> | putative MADS-box Agamous-like 15a | <i>VvAGL15a</i> | |
| <i>VIT_07s0031g01930</i> | myb TK11 (TSL-KINASE INTERACTING PROTEIN 1) | | |
| <i>VIT_02s0033g00380</i> | R2R3MYB transcription factor | <i>VvMybA2 (C-term)</i> | |
| <i>VIT_02s0033g00390</i> | R2R3MYB transcription factor | <i>VvMybA2</i> | |
| <i>VIT_02s0033g00450</i> | R2R3MYB transcription factor | <i>VvMybA3</i> | |
| <i>VIT_14s0108g01070</i> | NAC domain-containing protein | <i>VvNAC11</i> | |
| <i>VIT_02s0012g01040</i> | NAC domain-containing protein | <i>VvNAC13</i> | |
| <i>VIT_19s0027g00230</i> | NAC domain-containing protein | <i>VvNAC33</i> | * |
| <i>VIT_08s0007g07670</i> | NAC domain-containing protein | <i>VvNAC60</i> | * |
| <i>VIT_07s0005g01710</i> | WRKY Transcription Factor | <i>VvWRKY19</i> | |
| <i>VIT_05s0020g04730</i> | Zinc finger (C3HC4-type ring finger) | | |
| <i>VIT_08s0040g01950</i> | Zinc finger (C3HC4-type ring finger) | | * |
| <i>VIT_18s0001g01060</i> | Zinc finger (C3HC4-type ring finger) | | * |
| <i>VIT_03s0091g00260</i> | Zinc finger protein 4 | | |

Figure 5: Comparison between the Atlas and the berry dataset (Massonnet *et al.*, 2017). The list shows all the transcription factors among the *switch* genes.

Among them the NAC TFs, one of the largest plant-specific family, are particularly interesting as they are functionally involved in the control of late developmental processes (Olsen *et al.*, 2005). Members of this family are involved in flower morphogenesis (Hendelman *et al.*, 2013) and as regulators of the fruit ripening (Zhu *et al.*, 2014). They are implicated in shoot apical meristem development (Nikovics *et al.*, 2006), in lateral root development (He *et al.*, 2005) and in cell division (Kato *et al.*, 2010); they also take part in xylem development (Endo *et al.*, 2015), embryo development (Duval *et al.*, 2002), regulation of secondary cell walls biosynthesis (Mitsuda *et al.*, 2007; Zhong *et al.*, 2006) and cell death (Niu *et al.*, 2014). Moreover, many of these TFs are associated with senescence processes such as the regulation of chlorophyll degradation in leaves (Oda-Yamamizo *et al.*, 2016) and in the regulation of anthocyanin biosynthesis (Zhou *et al.*, 2015).

The NAC TFs are also important for the tolerance to biotic stress response (Jensen *et al.*, 2010; Bu *et al.*, 2008; Fujita *et al.*, 2004; Jensen *et al.*, 2007) and abiotic stress, such as drought and salinity stress response (Mao *et al.* 2012; Nakashima *et al.*, 2012; Christianson *et al.*, 2010; Tran *et al.*, 2004; Puranik *et al.*, 2012). Furthermore, the NAC TFs undergo intensive post-transcriptional regulation that includes microRNA-mediated cleavage of genes (Khraiwesh *et al.*, 2012; Mallory *et al.*, 2004) and are also characterized by a complex post-translational regulation involving ubiquitination, dimerization, phosphorylation or proteolysis (Nakashima *et al.*, 2012; Puranik *et al.*, 2012).

The NAC acronym derives from the first three characterized proteins with the so-called NAC domain (Aida *et al.*, 1997; Souer *et al.*, 1996): NAM (no apical meristem) from petunia, *Arabidopsis* ATAF (*Arabidopsis* transcription activator factor) and CUC (cup-shaped cotyledon). A huge number of putative NAC genes have been identified in many plant species such as *Arabidopsis* (117), rice (151; Nuruzzaman *et al.*, 2010), soybean (152; Le *et al.*, 2011), apple (180; Su *et al.*, 2013), banana (167; Cenci *et al.*, 2014), tomato (104; Su *et al.*, 2015) and so on. In grapevine 74 family members have been identified (Wang *et al.*, 2013), however their specific functions are poorly known.

The wide studies on model plants revealed the presence of a highly conserved N-terminus containing the NAC domain which is approximately 150-160 amino acids

in length and can be divided into five sub-domains (A-E; Ooka *et al.*, 2003; Ernst *et al.*, 2004)): subdomain A may have an important role in the formation of functional NAC dimeric proteins; subdomains C and D are conserved and bind to DNA; the subdomains B and E may confer functional diversity between NAC TFs. If the N-terminus is associated with DNA binding, nuclear localization and the formation of homo- or heterodimers with other NAC proteins (Olsen *et al.*, 2005), the highly divergent C-terminus, which can present a transmembrane motif, has an activation/repression of transcriptional putative regulatory function (Puranik *et al.*, 2011).

The investigation on NAC TFs in grapevine, identified by integrated networking analysis based on the global gene expression atlas and a grapevine berry transcriptomic dataset (Palumbo *et al.*, 2014), started from five members of this gene family (D'Inca, 2017). *VviNAC33* and *VviNAC60* have been selected as *switch* genes of the entire plant development; *VviNAC11* and *VviNAC13* have been selected as *switch* genes of berry development. Thanks to the relevance of tomato as model for fruit development and ripening and the availability of collected tomato-ripening mutants such as *NOR*, *VviNAC03* was also considered as it resulted to be one of the two closest tomato *NOR* homologues.

The high number of TFs related to the selected *NACs* supported the existence of a complex regulatory network during plant development. A correlation between *VviNAC03* and *VviNAC11* was found and was noticed that *VviNAC33* was co-expressed with *VviNAC60*. Moreover, several *switch* genes emerged from the analyses, indicating that the *switch* genes could include putative key regulators of the developmental phase transition but also their direct targets. Furthermore, a correlation between *NACs* and secondary metabolic processes was observed.

To study the role of these TFs, transient ectopic expressions of *VviNAC03*, *VviNAC11*, *VviNAC13*, *VviNAC33* and *VviNAC60* in grapevine plants were carried out and microarray global gene analyses of the transcriptomes were performed.

The attention was focused on those genes linked to metabolic pathways with central roles during grapevine maturation. Secondary metabolic processes were up regulated by all the five *VviNACs*; in particular, many genes implicated in phenylpropanoid pathway, anthocyanin and terpenoid accumulation were

identified. Interestingly, *VviNAC60* up regulated *VviNAC03* and *VviNAC03* down regulated *VviNAC60*. Regarding *VviNAC60*, the up regulation of many germin proteins, involved in development, osmotic regulation, photoperiodic oscillation, defense and apoptosis was noticed; concerning *VviNAC33*, the most down regulated genes were related to photosynthesis.

All these findings provided real evidence that *VviNAC03*, *VviNAC11*, *VviNAC13*, *VviNAC33* and *VviNAC60* participate in the regulation of the transcriptome reprogramming during grapevine development.

VviNAC33 and *VviNAC60* were then stably over expressed in grapevine plants showing that *VviNAC33* affected the chlorophyll metabolism in leaves, causing an anticipated leaf chlorosis and senescence, while *VviNAC60* altered the plant growth and caused a higher accumulation in leaves of anthocyanins, secondary metabolites responsible for the red berry coloring; this confirmed the involvement of both *VviNAC* TFs in the regulation of the organ maturation/senescence associated processes.

To obtain more information about the role of *VviNAC33* and *VviNAC60*, microarray analyses on transgenic stably over expressing leaves were performed.

The number of down regulated genes were higher than the up regulated ones and, moreover, about half of the down regulated genes were shared from both the transcriptomes. Several genes related to the vegetative phase processes, such as photosynthesis, cell cycle and development, were down regulated when plant switched to mature growth, confirming that the transition mainly involved the suppression of vegetative pathways rather than the activation of the maturation ones, as was previously reported (Palumbo *et al.*, 2014).

The results also showed the up regulation of many genes involved in plant development processes associated with ripening and senescence (such as cell wall metabolism, aroma controlling pathways, anthocyanins and stilbenes biosynthesis and ethylene response), suggesting that both *VviNAC33* and *VviNAC60* mainly act as transcriptional activators and confirming, once more, their putative involvement in the regulation of vegetative-to-mature transition in grapevine.

By investigating the result of the microarray analyses performed on both transiently

and stably over expressing plants, the transcription factor activity was present as the most represented functional category. Moreover, a *VviNAC03* up regulation by *VviNAC60* over expression and a *VviNAC60* down regulation by the *VviNAC03* one was seen. Co-expression analyses, which revealed a correlation between *VviNAC03* and *VviNAC11* and between *VviNAC33* and *VviNAC60*, also brought to the hypothesis of a possible regulatory network between *VviNACs*. Moreover, several *switch* genes emerged in the co-expression and microarray analyses, supporting again the existence of a complex regulatory network during plant development.

To complete the functional analysis of both *VviNAC33* and *VviNAC60* and to obtain more information about their role during ripening, they have been converted into transcriptional repressors fusing their coding sequences with the Ethylene-responsive element-binding factor-Associated amphiphilic Repression motif (EAR motif; Kagale and Rozwadowski, 2011) and stably expressing them in grapevine plants (Bertini, 2018- unpublished). Each *VviNAC-EAR* gene was cloned under the control of its endogenous promoter to inhibit the transcription of putative target genes in the same organs and developmental stage when the endogenous *VviNAC* genes are expressed. Their phenotypic and molecular characterization showed a normal vegetative growth and the down regulation of some genes previously induced in the over expressing plants. These results indicated that the addition of the EAR motif was successful in turning these factors into transcriptional repressor and confirmed some of the preliminary data obtained from the over expressing plants.

Overall, *VviNAC33* and *VviNAC60* seem to be master regulator of the immature-to-mature transition phase. In particular, *VviNAC33* could be considered a negative regulator of photosynthesis, due to the phenotypic effects on stably transformed grapevine leaves, and *VviNAC60* seems to play a role in ripening/senescence process, by considering the developmental growth of stably transformed grapevine plants.

REFERENCES

- Aida M, Ishida T, Fukaki H, Fujisawa H, Tasaka M** (1997). Genes involved in organ separation in *Arabidopsis*: an analysis of the cup-shaped cotyledon mutant. *Plant Cell*. 9, 841-857.
- Bertini E.** (2018). Identification and functional characterization of master regulators of the onset of berry ripening in grapevine (*Vitis vinifera* L.). PhD thesis. Verona University.
- Bu Q, Jiang H, Li CB, Zhai Q, Zhang J, Wu X, Sun W, Xie Q, Li C** (2008). Role of the *Arabidopsis thaliana* NAC transcription factors ANAC019 and ANAC055 in regulating jasmonic acid-signaled defense responses. *Cell Res*. 18, 756-767.
- Cenci A, Guignon V, Roux N, Rouard M** (2014). Genomic analysis of NAC transcription factors in banana (*Musa acuminata*) and definition of NAC orthologous groups for monocots and dicots. *Plant Mol Biol*. 85, 63-80.
- Christianson JA, Dennis ES, Llewellyn DJ, Wilson IW** (2010). ATAF NAC transcription factors: regulators of plant stress signaling. *Plant Signal Behav*. 5, 428- 432.
- D'Inca E.** 2017. Master regulators of the vegetative-to-mature organ transition in grapevine: the role of NAC transcription factors. PhD thesis. Verona University.
- Duval M, Hsieh TF, Kim SY, Thomas TL** (2002). Molecular characterization of AtNAM: a member of the Arabidopsis NAC domain superfamily. *Plant Mol. Biol*. 50, 237-248.
- Endo H, Yamaguchi M, Tamura T, Nakano Y, Nishikubo N, Yoneda A, Kato K, Kubo M, Kajita S, Katayama Y, Ohtani M, Demura T** (2015). Multiple classes of transcription factors regulate the expression of VASCULAR-RELATED NAC-DOMAIN7, a master *switch* of xylem vessel differentiation. *Plant Cell Physiol*. 56, 242-254.
- Ernst HA, Olsen AN, Larsen S, Lo Leggio L** (2004). Structure of the conserved domain of ANAC, a member of the NAC family of transcription factors. *EMBO Rep*. 5, 297-303.
- Fasoli M, Dal Santo S, Zenoni S, Tornielli GB, Farina L, Zamboni A, Porceddu A, Venturini L, Bicego M, Murino V, Ferrarini A, Delledonne M, Pezzotti M** (2012). The grapevine expression atlas reveals a deep transcriptome shift driving the entire plant into a maturation program. *Plant Cell*. 24(9):3489-505.
- Fujita M, Fujita Y, Maruyama K, Seki M, Hiratsu K, Ohme-Takagi M, Tran LS, Yamaguchi-Shinozaki K, Shinozaki K** (2004). A dehydration-induced NAC protein, RD26, is involved in a novel ABA-dependent stress-signaling pathway. *Plant J*. 39, 863-76.
- He XJ, Mu RL, Cao WH, Zhang ZG, Zhang JS, Chen SY** (2005). AtNAC2, a transcription factor downstream of ethylene and auxin signaling pathways, is involved in salt stress response and lateral root development. *Plant J*. 44, 903-916.
- Hendelman A, Stav R, Zemach H, Arazi T** (2013). The tomato NAC transcription factor SINAM2 is involved in flower-boundary morphogenesis. *J Exp Bot*. 64, 5497- 5507.
- Jensen MK, Kjaersgaard T, Nielsen MM, Galberg P, Petersen K, O'Shea C, Skriver K** (2010). The *Arabidopsis thaliana* NAC transcription factor family: structure-function relationships and determinants of ANAC019 stress signalling. *Biochem. J*. 426, 183-196.
- Jensen MK, Rung JH, Gregersen PL, Gjetting T, Fuglsang AT, Hansen M, Joehnk N, Lyngkjaer MF, Collinge DB** (2007). The HvNAC6 transcription factor: a positive regulator of penetration resistance in barley and *Arabidopsis*. *Plant Mol Biol*. 65, 137-150.

Kagale S. and Rozwadowski K. (2001). EAR motif-mediated transcriptional repression in plants. An underlying mechanism for epigenetic regulation of gene expression. *Epigenetics*. Vol. 6 (2): 141-146.

Khraiweh B, Zhu JK, Zhu J (2012). Role of miRNAs and siRNAs in biotic and abiotic stress responses of plants. *Biochim Biophys Acta*. 1819(2):137-48.

Le DT, Nishiyama R, Watanabe Y, Mochida K, Yamaguchi-Shinozaki K, Shinozaki K, Trans LS (2011). Genome-Wide Survey and Expression Analysis of the Plant-Specific NAC Transcription Factor Family in Soybean During Development and Dehydration Stress. *DNA Res*. 18, 263-276.

Mallory AC, Dugas DV, Bartel DP, Bartel B (2004). MicroRNA regulation of NAC-domain targets is required for proper formation and separation of adjacent embryonic, vegetative and floral organs. *Curr Biol*. 14:1035-46

Mao X, Zhang H, Qian X, Li A, Zhao G, Jing R (2012). TaNAC2, a NAC-type wheat transcription factor conferring enhanced multiple abiotic stress tolerances in *Arabidopsis*. *J Exp Bot*. 63, 2933-2946.

Massonet M, Fasoli M, Tornielli G.B., Altieri M, Sandri M, Zuccolotto P, Paci P, Gardiman M, Zenoni S. and Pezzotti M. (2017). Ripening Transcriptomic Program in Red and White Grapevine Varieties Correlates with Berry Skin Anthocyanin Accumulation. *Plant Physiology*. Vol. 174: 2376–2396.

Mitsuda N, Seki M, Shinozaki K, Ohme-Takagi M (2005). The NAC transcription factors NST1 and NST2 of *Arabidopsis* regulate secondary wall thickenings and are required for anther dehiscence. *Plant Cell*. 17, 2993-3006.

Nakashima K, Takasaki H, Mizoi J, Shinozaki K, Yamaguchi-Shinozaki K (2012). NAC transcription factors in plant abiotic stress responses. *BiochemBiophys Acta*. 1819, 97-103.

Nikovics K, Bleina T, Peaucellea A, Ishidab T, Morina H, Aidab M, Laufsa P (2006). The balance between the MIR164A and CUC2 genes controls leaf margin serration in *Arabidopsis*. *Plant Cell*, 18, 2929-2945.

Niu F, Wang B, Wu F, Yan J, Li L, Wang C, Wang Y, Yang B, Jiang YQ (2014). Canola (*Brassica napus* L.) NAC103 transcription factor gene is a novel player inducing reactive oxygen species accumulation and cell death in plants. *Biochem Biophys Res Commun*. 454, 30-35.

Nuruzzaman M, Manimekalai R, Sharoni AM, Satoh K, Kondoh H, Ooka H, Kikuchi S (2010). Genome-wide analysis of NAC transcription factor family in rice. *Gene*. 465, 30-44.

Oda-Yamamizo C, Mitsuda N, Sakamoto S, Ogawa D, Ohme-Takagi M, Ohmiya A (2016). The NAC transcription factor ANAC046 is a positive regulator of chlorophyll degradation and senescence in *Arabidopsis* leaves. *Sci Rep*. 6-23609.

Olsen AN, Ernst HA, Lo Leggio L, Skriver K (2005). NAC transcription factors: structurally distinct, functionally diverse. *Trends Plant Sci*. 10, 1360-1385.

Ooka H, Satoh K, Doi K, Nagata T, Otomo Y, Murakami K, Matsubara K, Osato N, Kawai J, Carninci P, Hayashizaki Y, Suzuki K, Kojima K, Takahara Y, Yamamoto K, Kikuchi S (2003). Comprehensive analysis of NAC family genes in *Oryza sativa* and *Arabidopsis thaliana*. *DNA Res*. 10, 239-247.

Palumbo MC, Zenoni S, Fasoli M, Massonet M, Farina L, Castiglione F, Pezzotti M, Paci P (2014). Integrated network analysis identifies fight-club nodes as a class of hubs encompassing key putative *switch* genes that induce major transcriptome reprogramming during grapevine development. *Plant Cell*. 26(12), 4617-35.

Puranik S, Sahu PP, Srivastava PS, Prasad M (2012). NAC proteins: regulation and role in stress tolerance. *Trends Plant Sci.* 17, 369-381.

Puranik S, Bahadur RP, Srivastava PS, Prasad M (2011). Molecular cloning and characterization of a membrane associated NAC family gene, SiNAC from foxtail millet [*Setaria italica* (L.) P. Beauv]. *Mol Biotechnol.* 49, 138-150.

Souer E, van Houwelingen A, Kloos D, Mol J, Koes R (1996). The No Apical Meristem gene of petunia is required for pattern formation in embryos and flowers and is expressed as meristem and primordia boundaries. *Cell* 85, 159-170.

Su H, Zhang S, Yin Y, Zhu D, Han L (2015). Genome-wide analysis of NAM- ATAF1,2-CUC2 transcription factor family in *Solanum lycopersicum* *J Plant Biochem Biotechnol.* 24, 176.

Su H, Zhang S, Yuan X, Chen C, Wang XF, Hao YJ (2013). Genome-wide analysis and identification of stress-responsive genes of the NAM-ATAF1, 2-CUC2 transcription factor family in apple. *Plant Physiol Biochem.* 71, 11-21.

Tran LS, Nakashima K, Sakuma Y, Simpson SD, Fujita Y, Maruyama K, Fujita M, Seki M, Shinozaki K, Yamaguchi-Shinozaki K (2004). Isolation and functional analysis of *Arabidopsis* stress-inducible NAC transcription factors that bind to a drought-responsive cis-element in the early responsive to dehydration stress 1 promoter. *Plant Cell.* 16, 2481-2498.

Wang N, Zheng, Y, Xin H, Fang L, Li S (2013). Comprehensive analysis of NAC domain transcription factor gene family in *Vitis vinifera*. *Plant Cell Rep.* 32,61-75.

Zhu M, Chen G, Zhang J, Zhang Y, Xie Q, Zhao Z, Pan Y, Hu Z (2014). The abiotic stress-responsive NAC-type transcription factor SINAC4 regulates salt and drought tolerance and stress-related genes in tomato (*Solanum lycopersicum*). *Plant Cell Rep.* 33, 1851-1863.

Zhou H, Lin-Wang K, Wang H, Gu C, Dare AP, Espley RV, He H, Allan AC, Han Y (2015). Molecular genetics of blood-fleshed peach reveals activation of anthocyanin biosynthesis by NAC transcription factors. *Plant J.* 82, 105-121.

1.3 THE REGULATION MECHANISMS OF TRANSCRIPTION

Gene expression can be constant or can have a temporal/spatial regulation pattern; in eukaryotic organisms it is multistage, spatially compartmented and controlled by specific factors (Bilas *et al.*, 2016). The primary regulation (**Fig. 6**) occurs with the initiation complex assembling on the available DNA strand (euchromatin) and the RNA polymerase II attachment to the initiation site (IS); both stages require the participation of transcription factors (TFs). After elongation and termination, pre-mRNA is formed; the mRNA maturation step comprises splicing (excising of introns and joining of exons) and attachment of 5' cap and 3' poly-A tail to the transcript ends (Bilas *et al.*, 2016). Mature mRNAs are then moved to the cytoplasm where translation takes place (Klug and Cummings, 2003; Phillips, 2008). The organization of all eukaryotic genomes is similar and most of the regulatory elements are universal. However, substantial differences occur among elements assigned to tissues/organ specific promoters (Twyman, 2003; Venter and Botha, 2010).

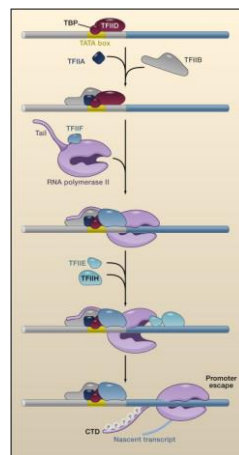


Figure 6: First steps in transcription activation (Levine, 2011).

Generally, the regulators of transcription are classified in terms of their structure as cis regulatory elements (CREs) and trans factors (Bilas *et al.*, 2016). CREs are linear nucleotide fragments of non-coding DNA involved in protein-DNA interaction (Venter and Botha 2010). Plant regulatory sequences are located directly in the transcribed DNA strand (promoters, enhancers, silencers) or may be added during post-transcriptional modifications (5' cap, poly-A tail, signal sequences) (Vaughn *et al.*, 2012). Furthermore, specific regulatory proteins, called trans

elements, interact with cis sequences and other proteins to form active complexes (Bilas *et al.*, 2016).

CREs directly influence gene regulation; depending on the type, they are present in different copy numbers, as well as variable distances (even 10.000-100.000 bp) and orientation in relation to the gene (Venter and Botha, 2010). CREs are also potentially involved in epigenetic pathways (Lu *et al.*, 2018). They are more frequently differentiated based on their activity in each model system and, when they recur in genes ensuring identical functions, are classified as motifs (Bilas *et al.*, 2016).

Gene promoters, located upstream of the gene coding sequence, enable the initiation of transcription by the presence of RNA polymerase II binding sites. This enzyme is attached during the sequential binding of specific proteins, called transcription factors, which results in transcription initiation (Russell 1996; Porto *et al.* 2014). The structure of a promoter, containing cis elements to which trans factors can bind to, can be divided into two regions (Klug and Cummings, 2003; Peremarti *et al.*, 2010; Porto *et al.*, 2014): core promoter and distal region, the last comprising enhancers and silencers. Moreover, the promoters vary in the terms of efficiency, site, and period of action; they may be active throughout all developmental stages in each tissue (constitutive promoters) or in particular tissues or development-stage (tissue-specific promoters). Some promoters may require specific stimuli for activation (inducible promoters) or be operating in the specific developmental stage (Peremarti *et al.*, 2010).

The core promoter (**Fig. 7**) may be composed of TATA box, initiator region (Inr), CAAT box and downstream promoter element (DPE); however, not all these regions are always present at each promoter (Juven-Gershon and Kadonaga, 2010; Kadonaga, 2012). The TATA box, located 25–30 bp upstream of the transcription start site (TSS), is usually flanked with GC-rich regions (Lewin, 2001); it is approximately 8 bp in length and composed of AT base pairs with the consensus sequence TATA(A/T)A(A/T) (Twyman, 2003).

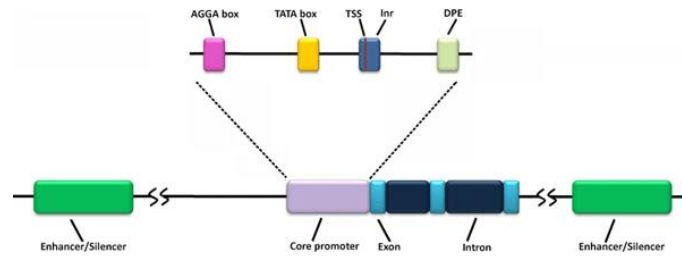


Figure 7: Example of a plant gene organization. Not all the depicted elements are universal; the core promoter may consist of the AGGA box, the TATA box, Inr and DPE. TSS is the transcription start site, Inr is the initiator and DPE is the downstream promoter element. Figure taken from Bilas *et al.*, 2016.

The transcription factors and RNA polymerase II bind to the TATA box in a specific order (Bilas *et al.*, 2016). The transcription factor TFIID is bound first and forms a complex with TFIIA; TFIIB attaches to this complex via TATA-binding protein (TBP), which is a part of TFIID, and because of direct interaction with the DNA strand. RNA polymerase II is bound in the next step and TFIIF attaches to it. TFIIE and TFIIH join the complex and the full transcription apparatus is formed (**Fig. 8**; Kwak and Lis, 2013).

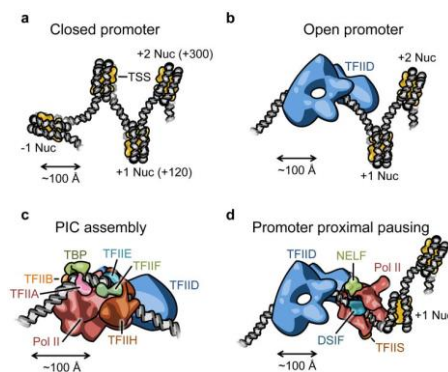


Figure 8: Structure of the promoter and Pol II before and during early elongation (Kwak and Lis, 2013).

A frequently observed conservative promoter element is the CAAT box, located approximately 80 bp upstream of TSS; it is considered as the most important factor as it can act in both directions and is highly susceptible to mutations, significantly influencing the expression efficiency (Bilas *et al.*, 2016). In plants, a similar AGGA box has been identified in place of the CAAT box (Roa-Rodríguez, 2003; Porto *et al.*, 2014).

In the promoters lacking the TATA box, DPE may be responsible for binding TFIID protein; it is usually located 28–32 bp downstream of adenine A+1 of the Inr (Bilas

et al., 2016). Occasionally TATA, Inr and DPE coexist. Even in the case of a single nucleotide alteration between the DPE and Inr, TFIID cannot bind properly to the promoter and the expression efficiency decreases significantly. In plants, several copies of DPE are present upstream the transcription start site and regulate the response to external stimuli (Kutach and Kadonaga, 2000; Sawant *et al.*, 2001).

The 5' untranslated region sequence (5' UTR) is a fragment of mRNA transcript located on its 5' end (Barrett *et al.*, 2012). It is encoded in the DNA strand and submits to transcription but not translation; in fact, it provides a connection between protein translational factors, small 40S ribosomal subunit and the transcript (Bock, 2013). The sequence of 5' UTR comprises the 5' cap (a single 7-methylguanosine nucleotide followed by several methylated riboses), the upstream open reading frame (uORF; Hayden and Jorgensen, 2007), the guanine-rich fragment and the internal ribosome entry site (IRES). Some plant UTRs contain a pyrimidine-rich fragment responsible for high transcription levels (Barrett *et al.* 2012). Presence of 5'UTR stabilizes the transcript (**Fig. 9**) during transport from nucleus to cytoplasm where it protects it from endonuclease activity (Bilas *et al.*, 2016).

The 3' UTR sequence is in the transcript between the stop codon and polyadenylation signal; since the 3' UTR is added after transcription, it is considered an important regulator of translation and act as stabilizers, enhancers and silencers (Bilas *et al.*, 2016). The presence of 3' UTR significantly affect the final gene expression: it influences the transcription termination stage and cooperates with 5' UTR during loop formation, which facilitates the translation initiation and the translation stabilization through the incorporation of specific factors (Papadakis *et al.*, 2004; Vignesh *et al.*, 2013). The 3' UTR also contains sequences complementary to microRNA (miRNA); pairing of complementary sequences between mRNA and miRNA prevents translation, by decreasing the amount of mRNA available in the cytoplasm, and indirectly regulates expression efficiency (Barrett *et al.*, 2012).

The poly-A tail is a polynucleotide sequence composed of around 250 adenines. Both poly-A and 3'UTR are added to the transcript during transcription termination and cooperate in stabilization of mRNA structure (**Fig. 10**), affect the transcript

transport and its fate in the cytoplasm (Li *et al.*, 2012).

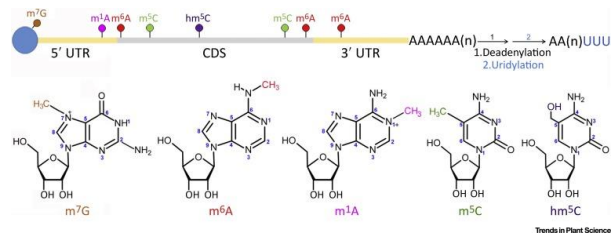


Figure 9: mRNA structure (Shen *et al.*, 2019).

Unlike the previously described elements, enhancers and silencers cis elements could be located further from the TSS, could be included in non-coding intron sequences, could be located near their target core promoter or even within the transcribed region of a gene body, and can act under specific environmental conditions or in definite tissues (Peremarti *et al.*, 2010; Ong and Corces, 2011; Spitz and Furlong, 2012). Furthermore, enhancers generally do not display universal sequence conservation, making them very challenging to locate (Morton *et al.*, 2014; Mejía-Guerra *et al.*, 2015). Mostly they are located at considerable distances, upstream or downstream of the promoter sequence, and enhance gene expression through cooperation with specific transcription factors (Mehrotra *et al.*, 2011). Transcription efficiency improvement is a result of conformational alteration as chromatin state, including dependence on histone modifications, and DNA looping (Alberts *et al.*, 2002). It was recently discovered that many enhancer elements in animal genomes could be identified with relatively high confidence based on a unique combination of flanking histone post translational modifications (PTMs), leading to the annotation of such elements in several animal models and specialized cell types (Heintzman *et al.*, 2009; Bonn *et al.*, 2012). However, the known correlations between plant CREs and histone PTMs appear to be modest (Zhang *et al.*, 2012b; Zhu *et al.*, 2015).

A well-known feature of sequence-specific DNA binding proteins is their ability to displace nucleosomes upon DNA binding, with an increase in nuclease accessibility around the binding region (Gross and Garrard, 1988; Henikoff, 2008). The DNase-seq studies in *Arabidopsis* demonstrate that most open chromatin sites (accessible

chromatin regions, ACRs, with low nucleosome occupancy) exist outside of genes, that differences can be identified between tissues and that a large proportion of intergenic ACRs are in fact regulatory (Zhang *et al.*, 2012a; Pajoro *et al.*, 2014; Zhu *et al.*, 2015). More recent studies on species comparisons confirmed that the majority of ACRs exist outside the transcribed regions; they also tended to cluster within several kilobases upstream of the TSS, despite the large differences in intergenic space between genomes (Maher *et al.*, 2018). When orthologous genes were compared across species, was found that the number and location of ACRs were highly variable, suggesting that regulatory elements are not statically positioned relative to target genes over evolutionary timescales (Maher *et al.*, 2018). However, were found evidence that some sets of gene remain under control of common TFs across species: overall, the suggestion is that the cis regulatory structure of plant genomes is similar, that TF-target gene modules are generally conserved and that the co-regulation of specific gene sets by multiple TFs seems to be frequently maintained across species (Maher *et al.*, 2018).

Consequently, CREs are preferentially located inside ACRs (Thurman *et al.*, 2012; Lu *et al.*, 2018).

Recently published epigenomic datasets revealed that gene distal ACRs are indeed abundant in plant genomes (Lu *et al.*, 2017; Bajic *et al.*, 2018; Zhu *et al.*, 2015; Rodgers-Melnick *et al.*, 2016; Sullivan *et al.*, 2014; Maher *et al.*, 2018; Oka *et al.*, 2017; Mei *et al.*, 2018). ACRs are highly enriched at transcriptional start and end sites, depleted for cytosine DNA methylation (Haring *et al.*, 2010) and exhibit greater GC content compared with nearby intergenic sequences (Wang *et al.*, 2012). The proportion of gene distal ACRs scales with genome size and the amount of intergenic space (Mei *et al.*, 2018) and the number of ACRs also correlates well with the number of annotated genes within the plant species (Lu *et al.*, 2019).

Although genome size varied greatly among the plant species, the total length of sequence occupied by ACRs is consistent and did not scale linearly with genome size (Lu *et al.*, 2019, **Fig. 10**). Interestingly, an increase in distal ACRs (>2kb from a gene) accompanied by a loss of proximal ACRs (within 2 kb of a gene) is clearly correlated with increasing genome sizes (Lu *et al.*, 2019). In *A. thaliana* (135 Mb genome), approximately 80% of ACRs reside within 2000 bp of genes, whereas in

S. lycopersicum (980 Mb genome), only 50% of ACRs reside within 2000 bp of genes (Maher *et al.*, 2018). In *Z. mays* (2.3 Gb genome), a significant proportion of ACRs are found tens to hundreds of kb away from genes (Rodgers-Melnick *et al.*, 2016). A major factor that could have contributed to the strong correlation between genome sizes and the distances between ACRs and genes is the differential activities of transposable elements (TEs); although distal ACRs are generally depleted from TEs, species-specific distal ACRs are strongly enriched within TEs (Lu *et al.*, 2019).

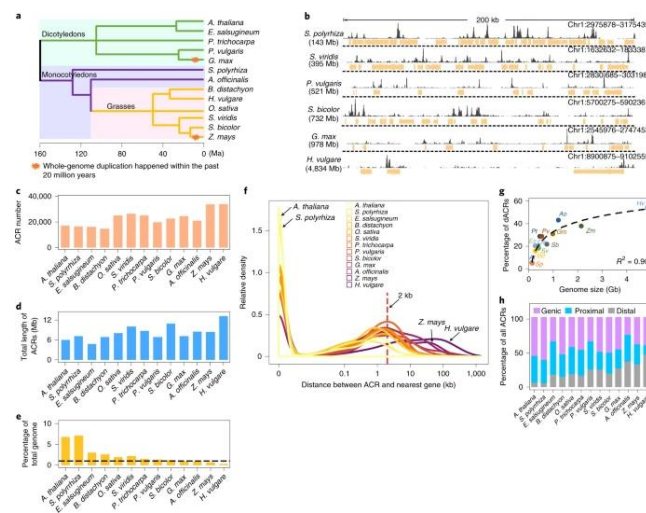


Figure 10: The prevalence of distal accessible regions is a consequence of genome size (Lu *et al.*, 2019).

Distal CREs in plant genomes were identified (Weber *et al.*, 2016; Marand *et al.*, 2017; Dong *et al.*, 2017; Li *et al.*, 2008; Qiu *et al.*, 2016; Zhang *et al.*, 2102; Zhang *et al.*, 2014; Lu *et al.*, 2018) and was seen that sequence variations at several distal CREs cause phenotypic variations that are important for the domestication (Salvi *et al.*, 2007; Xu *et al.*, 2017; Studer *et al.*, 2011; Louwers *et al.*, 2009) and variation in flowering time (Adrian *et al.*, 2010; McGarry *et al.*, 2008; Yang *et al.*, 2005; Liu *et al.*, 2014). Although, the mode of action of distal CREs remain unknown.

Plant species have a considerably lower SNP diversity at distal ACRs compared with flanking intergenic regions; moreover, many distal ACRs are in syntenic regions, making it possible to identify orthologous distal ACRs by sequence similarity and/or chromatin accessibility (Lu *et al.*, 2019). In summary, the vast majority of distal ACR sequences are under strong purifying selection between

species, possibly to retain the sequence specificities for TF binding (Lu *et al.*, 2019). Importantly, histone modifications at orthologous distal ACRs are conserved among species. However, changes in gene expression for distal ACRs exhibiting species specificity are observed (Lu *et al.*, 2019). Genic chromatin modifications are similar between plant species. Expressed genes are enriched in H3K4me3, H3K56ac and H2A.Z at the TSS, and enriched in H3K4me1 and H3K36me3 in gene bodies; by contrast, repressed genes are enriched in H3K27me3 and H2A.Z (Lu *et al.*, 2019).

Chromatin can form long-range loops that bring together distal ACRs with cognate genes during both transcriptional activation and repression; strong loops preferentially contained distal ACRs located upstream of and adjacent to their interacting genes, permitting to assign with reasonable confidence the putative distal CREs to target genes (Lu *et al.*, 2019; Ricci *et al.*, 2019). Studies suggested that long-range regulatory interactions were predictable based on loop strength, orientation and location relative to target genes (Ricci *et al.*, 2019). Moreover, the enhancer activities of distal and proximal ACRs were significantly greater than the activities of control intergenic regions (Ricci *et al.*, 2019).

REFERENCES

- Adrian, J. et al.** (2010). cis-Regulatory elements and chromatin state coordinately control temporal and spatial expression of FLOWERING LOCUS T in Arabidopsis. *Plant Cell* **22**, 1425–1440.
- Alberts B, Johnson A, Lewis J, Raff M, Roberts K, Walter P.** (2002). *Molecular biology of the cell*, 4th edn. Garland Science, New York
- Allen GC.** (2008). The role of nuclear matrix attachment regions in plants. In: Nick P (ed) *Plant cell monographs*. Springer, Berlin, pp 1–29
- Bajic M, Maher KA, Deal RB.** (2018). Identification of open chromatin regions in plant genomes using ATAC-Seq. *Methods Mol Biol*, 1675:183-201.
- Barrett LW, Fletcher S, Wilton SD.** (2012). Regulation of eukaryotic gene expression by the untranslated gene regions and other noncoding elements. *Cell Mol Life Sci* 69:3613–3634
- Bilas, R., Szafran, K., Hnatuszko-Konka, K., & Kononowicz, A. K.** (2016). Cis-regulatory elements used to control gene expression in plants. *Plant Cell, Tissue and Organ Culture (PCTOC)*, 127(2), 269-287.
- Bock R.** (2013). Strategies for metabolic pathway engineering with multiple transgenes. *Plant Mol Biol* 83:21–31
- Bonn, S., Zinzen, R.P., Girardot, C., Gustafson, E.H., Perez-Gonzalez, A., Delhomme, N., Ghavi-Helm, Y., Wilczynski, B., Riddell, A., and Furlong, E.E.** (2012). Tissue-specific analysis of chromatin state identifies temporal signatures of enhancer activity during embryonic development. *Nat. Genet.* 44: 148–156.
- Dong, P. et al.** (2017). 3D chromatin architecture of large plant genomes determined by local A/B compartments. *Mol. Plant* 10, 1497–1509.
- Gross, D.S., and Garrard, W.T.** (1988). Nuclease hypersensitive sites in chromatin. *Annu. Rev. Biochem.* 57: 159–197.
- Haring, M. et al.** (2010). The role of DNA methylation, nucleosome occupancy and histone modifications in paramutation. *Plant J.* 63, 366–378.
- Hayden CA, Jorgensen RA.** (2007). Identification of novel conserved peptide uORF homology groups in Arabidopsis and rice reveals ancient eukaryotic origin of select groups and preferential association with transcription factor-encoding genes. *BMC Biol* 5:32
- Heintzman, N.D., et al.** (2009). Histone modifications at human enhancers reflect global cell-type-specific gene expression. *Nature* 459: 108–112.
- Henikoff, S.** (2008). Nucleosome destabilization in the epigenetic regulation of gene expression. *Nat. Rev. Genet.* 9: 15–26.
- Juven-Gershon T, Kadonaga JT.** (2010). Regulation of gene expression via the core promoter and the basal transcriptional machinery. *Dev Biol* 339:225–229
- Kadonaga JT.** (2012). Perspectives on the RNA polymerase II core promoter. *Wiley Interdiscip Rev Dev Biol* 1(1):40–51
- Klug WS, Cummings MR.** (2003). *Concepts of genetics*. Prentice Hall, Upper Saddle River
- Kutach AK, Kadonaga JT.** (2000). The downstream promoter element DPE appears to be as widely used as the TATA box in *Drosophila* core promoters. *Mol Cell Biol* 20(13):4754–4764

- Kwak H, Lis JT.** (2013). Control of transcriptional elongation. *Annu Rev Renet* 47:483
- Lewin B.** (2001). *Genes VII*. Artmed Editora, Porto Alegre
- Li WJ, Dai LL, Chai ZJ, Yin ZJ, Qu LQ.** (2012). Evaluation of seed storage protein gene 3'-untranslated regions in enhancing gene expression in transgenic rice seed. *Transgenic Res* 21:545–553
- Li, X. et al.** (2008). High-resolution mapping of epigenetic modifications of the rice genome uncovers interplay between DNA methylation, histone methylation, and gene expression. *Plant Cell* 20, 259–276.
- Liu, L. et al.** (2014). Induced and natural variation of promoter length modulates the photoperiodic response of FLOWERING LOCUS T. *Nat. Commun.* 5,4558.
- Louwers, M. et al.** (2009). Tissue- and expression level-specific chromatin looping at maize b1 epialleles. *Plant Cell* 21, 832–842.
- Lu Z, Hofmeister BT, Vollmers C, DuBois RM, Schmitz RJ.** (2017). Combining ATAC-seq with nuclei sorting for discovery of cis-regulatory regions in plant genomes. *Nucleic Acids Res*, 45: e41.
- Lu, P. et al.** (2018). Genome encode analyses reveal the basis of convergent evolution of fleshy fruit ripening. *Nat. Plants* 4, 784–791.
- Lu, Z., Marand, A. P., Ricci, W. A., Ethridge, C. L., Zhang, X., & Schmitz, R. J.** (2019). The prevalence, evolution and chromatin signatures of plant regulatory elements. *Nature Plants*, 5(12), 1250-1259.
- Lu, Z., Ricci, W. A., Schmitz, R. J. & Zhang, X.** (2018). Identification of cis-regulatory elements by chromatin structure. *Curr. Opin. Plant Biol.* 42, 90–94.
- Maher, K. A. et al.** (2017). Profiling of accessible chromatin regions across multiple plant species and cell types reveals common gene regulatory principles and new control modules. *Plant Cell* 30, 15–36.
- Maher, K. A., Bajic, M., Kajala, K., Reynoso, M., Pauluzzi, G., West, D. A., ... & Queitsch, C.** (2018). Profiling of accessible chromatin regions across multiple plant species and cell types reveals common gene regulatory principles and new control modules. *The Plant Cell*, 30(1), 15-36.
- Marand, A. P., Zhang, T., Zhu, B. & Jiang, J. M.** (2017). Towards genome-wide prediction and characterization of enhancers in plants. *Biochim. Biophys. Acta* 1860, 131.
- McGarry, R. C. & Ayre, B. G. A.** (2008). DNA element between At4g28630 and At4g28640 confers companion-cell specific expression following the sink-to-source transition in mature minor vein phloem. *Planta* 228, 839–849.
- Mehrotra R, Gupta G, Sethi R, Bhalothia P, Kumar N, Mehrotra S.** (2011). Designer promoter: an artwork of *cis* engineering. *Plant Mol Biol* 75:527–536
- Mei W, Stetter MG, Gates DJ, Stitzer MC, Ross-Ibarra J.** (2018). Adaptation in plant genomes: bigger is different. *Am J Bot*, 105:16-19.
- Mejía-Guerra, M.K., Li, W., Galeano, N.F., Vidal, M., Gray, J., Doseff, A.I., and Grotewold, E.** (2015). Core promoter plasticity between maize tissues and genotypes contrasts with predominance of sharp transcription initiation sites. *Plant Cell* 27: 3309–3320.
- Morton, T., Petricka, J., Corcoran, D.L., Li, S., Winter, C.M., ...** (2014). Paired-end analysis of transcription start sites in *Arabidopsis* reveals plant specific promoter signatures. *Plant Cell*.

Oka R, Zicola J, Weber B, Anderson SN, Hodgman C, Gent JI, Wesselink JJ, Springer NM, Hoefsloot HCJ, Turck F et al. (2017). Genome-wide mapping of transcriptional enhancer candidates using DNA and chromatin features in maize. *Genome Biol*, 18:137.

Ong, C.T., and Corces, V.G. (2011). Enhancer function: new insights into the regulation of tissue-specific gene expression. *Nat. Rev. Genet.* 12: 283–293.

Pajoro, A., et al. (2014). Dynamics of chromatin accessibility and gene regulation by MADS-domain transcription factors in flower development. *Genome Biol.* 15: R41.

Papadakis ED, Nicklin SA, Baker AH, White SJ. (2004). Promoters and Control elements: designing expression cassettes for gene therapy. *Curr Gene Ther* 4:89–113

Peremarti A, Twyman RM, Gómez-Galera S, Naqvi S, Farré G, Sabalza M, Miralpeix B, Dashevskaya S, Yuan D, Ramessar K, Christou P, Zhu C, Bassie L, Capell T. (2010). Promoter diversity in multigene transformation. *Plant Mol Biol* 73:363–378

Phillips T. (2008). Regulation of transcription and gene expression in eukaryotes. *Nat Educ* 1(1):199

Porto MS, Pinheiro MPN, Batista VGL, Cavalcanti dos Santos R, de Albuquerque Melo Filho P, de Lima LM. (2014). Plant promoters: an approach of structure and function. *Mol Biotechnol* 56:38–49

Qiu, Z. K. et al. (2016). Identification of regulatory DNA elements using genomewide mapping of DNase I hypersensitive sites during tomato fruit development. *Mol. Plant* 9, 1168–1182.

Ricci, W. A., Lu, Z., Ji, L., Marand, A. P., Ethridge, C. L., Murphy, N. G., ... & Johannes, F. (2019). Widespread long-range cis-regulatory elements in the maize genome. *Nature plants*, 5(12), 1237-1249.

Roa-Rodríguez C. (2003). Promoters used to regulate gene expression. CAMBIA Intellectual Property, Canberra

Rodgers-Melnick, E., Vera, D. L., Bass, H. W. & Buckler, E. S. (2016). Open chromatin reveals the functional maize genome. *Proc. Natl Acad. Sci. USA* 113, E3177–E3184.

Russell PJ. (1996). *Genetics*, 4th edn. Harper Collins College, New York

Salvi, S. et al. (2007). Conserved noncoding genomic sequences associated with a flowering-time quantitative trait locus in maize. *Proc. Natl Acad. Sci. USA* 104, 11376–11381.

Sawant SV, Singh PK, Madanala R, Tuli R. (2001). Designing of an artificial expression cassette for high level expression of transgenes in plants. *Theor Appl Genet* 102:635644

Spitz, F., and Furlong, E.E. (2012). Transcription factors: from enhancer binding to developmental control. *Nat. Rev. Genet.* 13: 613–626.

Studer, A., Zhao, Q., Ross-Ibarra, J. & Doebley, J. (2011). Identification of a functional transposon insertion in the maize domestication gene *tb1*. *Nat. Genet.* 43, 1160–1163.

Sullivan AM, Arsovski AA, Lempe J, Bubb KL, Weirauch MT, Sabo PJ, Sandstrom R, Thurman RE, Neph S, Reynolds AP et al. (2014). Mapping and dynamics of regulatory DNA and transcription factor networks in *A. thaliana*. *Cell Rep* 2014, 8:2015-2030.

Thurman RE, Rynes E, Humbert R, Vierstra J, Maurano MT, Haugen E, Sheffield NC, Stergachis AB, Wang H, Vernot B et al. (2012). The accessible chromatin landscape of the human genome. *Nature*, 489:75-82.

Twyman RM. (2003). Growth and development: control of gene expression, regulation of transcription. In: Thomas B, Murphy DJ, Murray B (eds) Encyclopedia of applied plant sciences. Elsevier Science, London, pp 558–567

Vaughn JN, Ellingson SR, Mignone F, von Arnim AG. (2012). Known and novel post-transcriptional regulatory sequences are conserved across plant families. *RNA* 18:368–384

Venter M, Botha FC. (2010). Synthetic promoter engineering. In: Pua EC, Davey MR (eds) Plant developmental biology—biotechnological perspectives. Springer, Berlin/Heidelberg, pp 393–414

Vignesh M, Nepolean T, Hossain F, Singh K, Gupta HS. (2013). Sequence variation in 3'UTR region of crtRB1 gene and its effect on β -carotene accumulation in maize kernel. *J Plant Biochem Biotechnol* 22(4):401–408

Wang, J. et al. (2012). Sequence features and chromatin structure around the genomic regions bound by 119 human transcription factors. *Genome Res.* 22, 1798–1812.

Xu, G. et al. (2017). Complex genetic architecture underlies maize tassel domestication. *New Phytol.* 214, 852–864.

Yang, W. et al. (2005). An egg apparatus-specific enhancer of Arabidopsis identified by enhancer detection. *Plant Physiol.* 139, 1421–1432.

Zhang, W., Wu, Y., Schnable, J.C., Zeng, Z., Freeling, M., Crawford, G.E., and Jiang, J. (2012b). High-resolution mapping of open chromatin in the rice genome. *Genome Res.* 22: 151–162.

Zhang, W., Zhang, T., Wu, Y. & Jiang, J. (2014). Open chromatin in plant genomes. *Cytogenet. Genome Res.* 143, 18–27.

Zhang, W., Zhang, T., Wu, Y., and Jiang, J. (2012a). Genome-wide identification of regulatory DNA elements and protein-binding footprints using signatures of open chromatin in Arabidopsis. *Plant Cell* 24: 2719–2731.

Zhu, B., Zhang, W. L., Zhang, T., Liu, B. & Jiang, J. M. (2015). Genome-wide prediction and validation of intergenic enhancers in Arabidopsis using open chromatin signatures. *Plant Cell* 27, 2415–2426.

1.4 THE CISTROME LANDSCAPE

Recent studies have demonstrated that many important aspects of plant development are regulated by heritable changes in gene expression that do not involve changes in DNA sequence. Rather, these regulatory mechanisms involve modifications of chromatin structure, that affect the accessibility of target genes to regulatory factors that can control their expression, and DNA methylation. Indeed, many TFs are active in different tissues and stages of development, and target genes may differ in a tissue-specific manner depending on chromatin accessibility and the availability of cofactors.

The cistrome is the complete set of TFs binding sites (cis elements, CREs) in an organism (O'Malley *et al.*, 2016). Robust methods to construct comprehensive cistrome maps are critical for elucidating complex transcriptional networks (O'Malley *et al.*, 2016). Comprehensive identification of transcription factor binding sites (TFBS) in a genome is essential for the characterization of regulatory elements and TFs functions (Kheradpour and Kellis, 2014; Stamatoyannopoulos *et al.*, 2012). At present, there are two main approaches for CREs research. One approach is the *in vivo* or *in vitro* DNA–protein interactions study; it led to the development of methods for CREs recognition such as DNase I footprinting (Sullivan *et al.*, 2015), electrophoretic mobility shift assays (EMSA, Hellman *et al.*, 2007), chromatin immunoprecipitation sequencing (ChIP-seq, Kidder *et al.*, 2011; Kaufmann *et al.*, 2010), yeast one-hybrid systems (Reece-Hoyes *et al.*, 2012) and DNA affinity purification sequencing (DAP-seq, Bartlett *et al.*, 2017). The second main approach uses *in silico* algorithms and databases to calculate the probability of predicted regulatory element rightness (Mehrotra *et al.*, 2011), but requires biological confirmation.

The *in vivo* protein-DNA interaction landscape is affected by multiple factors including primary sequence, DNA modifications, and chromatin accessibility, along with stabilizing and destabilizing interactions between proteins associated with the DNA (Lelli *et al.*, 2012; Levo and Segal, 2014).

For this reason, the *in vivo* approach is the most informative considering developmental phase and tissue specificity of plants transcriptomic regulation. Indeed, the ChIP-seq (**Fig. 11**) is a powerful technique used to study interactions

between TFs and DNA *in vivo* (Kaufmann *et al.*, 2010) and, consequently, for TFBS discovery. Unfortunately, genome-wide applications of the ChIP-seq methodology in plants are still relatively scarce. This delay is partly due to technical difficulties in sample preparation related to the properties and complexity of plant tissues. Moreover, ChIP-seq is limited in its throughput by challenging and expensive need to create specific antibodies. As a result, binding site information is available for relatively few TFs and substantial TFBS coverage is only available for humans and several model organisms (O'Malley *et al.*, 2016).

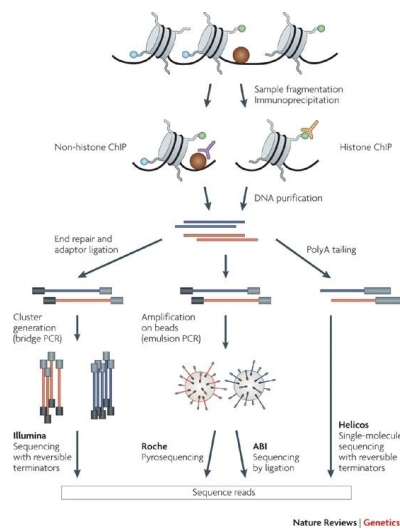


Figure 11: The ChIP-seq assay (Park, 2009).

Methods such as ATAC-seq (Buenrostro *et al.*, 2015a) offer an approach to annotate genome-wide regulatory elements across many organisms and cell types (Buenrostro *et al.*, 2015b; Sullivan *et al.*, 2014; Thurman *et al.*, 2012); however, without comprehensive knowledge of TFs sequence specificity, the targeting TFs of the identified regions cannot be verified.

The *in vitro* mapping of TFBS provides an easier, faster and scalable alternative. In the past the two most used *in vitro* methods were systematic evolution of ligands by exponential enrichment (SELEX, Jolma *et al.*, 2010) and protein binding microarrays (PBM, Berger and Bulyk, 2009). In both methods synthetic DNA oligomers were enriched with an affinity-tagged TF and the preferred binding sequences were used for the identification of binding motifs (Machanick *et al.*, 2011); they permitted to find many TF motifs, but the use of synthetic DNA does

not allow to identify the genomic DNA (gDNA) properties known to impact TF binding *in vivo* (O'Malley *et al.*, 2016).

The gDNA is the native substrate for a TF and therefore ideal for an *in vitro* DNA-TF interaction assay; unlikely synthetic oligomers, gDNA encodes primary sequence and cell-, tissue-, and organism-specific methylation patterns that may impact TFs binding (O'Malley *et al.*, 2016).

Previous TF: DNA binding assays using naked gDNA were effective in identifying motifs and *in vivo* binding sites (Guertin *et al.*, 2012; Liu *et al.*, 2005; Rajeev *et al.*, 2014), but this approach has not been applied for global TFBS characterization or to investigate the impact of *in vivo* important features for the TFs binding.

Instead, the DAP-seq (**Fig. 12**), a fast and high-throughput assay that couples affinity-purified TFs with next-generation sequencing of a genomic DNA library to discover TFBS, allows to capture the impact of the primary sequence but also of the DNA methylation (a parameter that impact binding *in vivo*) on binding affinities at individual TFBS (Bartlett *et al.*, 2017). The ampDAP-seq, which uses a DNA library in which the DNA modifications are removed by PCR, is a valid method to measure the impact of DNA modifications on TFs binding: a comparison between DAP-seq and ampDAP-seq data could bring to a global understanding of the DNA modifications effects on TFs binding.

Moreover, although the DAP-seq technique lacks tissue-specific chromatin accessibility context, a comparison between its results and the ChIP-seq datasets (Zhang *et al.*, 2008) could be useful to find TFBS and to start understanding how the epigenomic variants influence the regulatory dynamics.

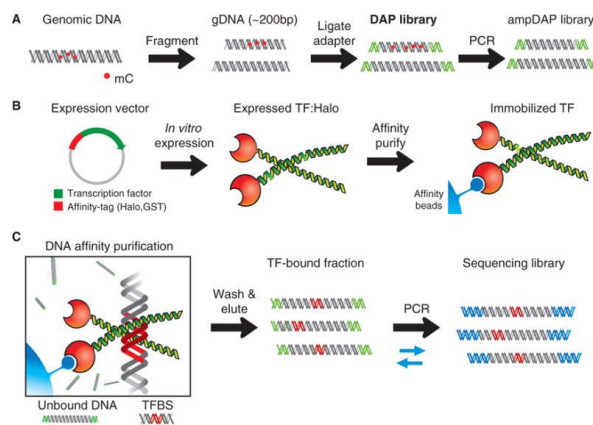


Figure 12: The DAP-seq assay size (O'Malley *et al.*, 2016).

REFERENCES

- Bartlett, A., O'Malley, R. C., Huang, S. S. C., Galli, M., Nery, J. R., Gallavotti, A., & Ecker, J. R.** (2017). Mapping genome-wide transcription-factor binding sites using DAP-seq. *Nature protocols*, 12(8), 1659.
- Berger, M.F., and Bulyk, M.L.** (2009). Universal protein-binding microarrays for the comprehensive characterization of the DNA-binding specificities of transcription factors. *Nat. Protoc.* 4, 393–411.
- Buenrostro, J. D., Wu, B., Chang, H. Y., & Greenleaf, W. J.** (2015a). ATAC-seq: a method for assaying chromatin accessibility genome-wide. *Current protocols in molecular biology*, 109(1), 21–29.
- Buenrostro, J.D., Wu, B., Litzenburger, U.M., Ruff, D., Gonzales, M.L., Snyder, M.P., Chang, H.Y., and Greenleaf, W.J.** (2015b). Single-cell chromatin accessibility reveals principles of regulatory variation. *Nature* 523, 486–490.
- Guertin, M.J., Martins, A.L., Siepel, A., and Lis, J.T.** (2012). Accurate prediction of inducible transcription factor binding intensities in vivo. *PLoS Genet.* 8, e1002610.
- Hellman, L. M., & Fried, M. G.** (2007). Electrophoretic mobility shift assay (EMSA) for detecting protein–nucleic acid interactions. *Nature protocols*, 2(8), 1849.
- Jolma, A., Kivioja, T., Toivonen, J., Cheng, L., Wei, G., Enge, M., Taipale, M., Vaquerizas, J.M., Yan, J., Sillanpää, M.J., et al.** (2010). Multiplexed massively parallel SELEX for characterization of human transcription factor binding specificities. *Genome Res.* 20, 861–873.
- Kaufmann, K., Muino, J. M., Østerås, M., Farinelli, L., Krajewski, P., & Angenent, G. C.** (2010). Chromatin immunoprecipitation (ChIP) of plant transcription factors followed by sequencing (ChIP-SEQ) or hybridization to whole genome arrays (ChIP-CHIP). *Nature protocols*, 5(3), 457–472.
- Kheradpour, P., and Kellis, M.** (2014). Systematic discovery and characterization of regulatory motifs in ENCODE TF binding experiments. *Nucleic Acids Res.* 42, 2976–2987.
- Kidder, B.L., Hu, G., and Zhao, K.** (2011). ChIP-Seq: technical considerations for obtaining high-quality data. *Nat. Immunol.* 12, 918–922.
- Lelli, K.M., Slattery, M., and Mann, R.S.** (2012). Disentangling the many layers of eukaryotic transcriptional regulation. *Annu. Rev. Genet.* 46, 43–68.
- Levo, M., and Segal, E.** (2014). In pursuit of design principles of regulatory sequences. *Nat. Rev. Genet.* 15, 453–468.
- Liu, X., Noll, D.M., Lieb, J.D., and Clarke, N.D.** (2005). DIP-chip: rapid and accurate determination of DNA-binding specificity. *Genome Res.* 15, 421–427.
- Machanick, P., and Bailey, T.L.** (2011). MEME-ChIP: motif analysis of large DNA datasets. *Bioinformatics* 27, 1696–1697.
- Mehrotra R, Gupta G, Sethi R, Bhalothia P, Kumar N, Mehrotra S.** (2011). Designer promoter: an artwork of *cis* engineering. *Plant Mol Biol* 75:527–536
- O'Malley, R. C., Huang, S. S. C., Song, L., Lewsey, M. G., Bartlett, A., Nery, J. R., ... & Ecker, J. R.** (2016). Cistrome and epicistrome features shape the regulatory DNA landscape. *Cell*, 165(5), 1280–1292.

Rajeev, L., Luning, E.G., and Mukhopadhyay, A. (2014). DNA-affinity-purified chip DAP-chip method to determine gene targets for bacterial two component regulatory systems. *J. Vis. Exp.* Jul 21, 89.

Reece-Hoyes, J. S., & Walhout, A. M. (2012). Yeast one-hybrid assays: a historical and technical perspective. *Methods*, 57(4), 441-447.

Stamatoyannopoulos, J.A., Snyder, M., Hardison, R., Ren, B., Gingeras, T., Gilbert, D.M., Groudine, M., Bender, M., Kaul, R., Canfield, T., et al.; Mouse ENCODE Consortium. (2012). An encyclopedia of mouse DNA elements Mouse ENCODE. *Genome Biol.* 13, 418.

Sullivan, A.M., Arsovski, A.A., Lempe, J., Bubb, K.L., Weirauch, M.T., Sabo, P.J., Sandstrom, R., Thurman, R.E., Neph, S., Reynolds, A.P., et al. (2014). Mapping and dynamics of regulatory DNA and transcription factor networks in *A. thaliana*. *Cell Rep.* 8.

Sullivan, A. M., Bubb, K. L., Sandstrom, R., Stamatoyannopoulos, J. A., & Queitsch, C. (2015). DNase I hypersensitivity mapping, genomic footprinting, and transcription factor networks in plants. *Current Plant Biology*, 3, 40-47.

Thurman, R.E., Rynes, E., Humbert, R., Vierstra, J., Maurano, M.T., Haugen, E., Sheffield, N.C., Stergachis, A.B., Wang, H., Vernet, B., et al. (2012). The accessible chromatin landscape of the human genome. *Nature* 489, 75–82.

Zhang, Y., Liu, T., Meyer, C.A., Eeckhoute, J., Johnson, D.S., Bernstein, B.E., Nussbaum, C., Myers, R.M., Brown, M., Li, W., et al. (2008). Model-based analysis of ChIP-seq MACS. *Genome Biol.* 9, R137.1–R137.9.

2. *Vvi*NACs SELECTION AND FUNCTIONAL ANALYSES

2.1 INTRODUCTION

Grapevine is one of the most important fruit crops in the world, reflecting its commercial value in the winemaking, in the vinegar industries and the nutritional benefits of table grapes and raisins.

To provide insight into the transcriptional programs controlling the development of grapevine, at first a global gene expression atlas was generated (Fasoli *et al.*, 2012). Afterwards, a set of *switch* genes were identified by genes co-expression networks analyses (Palumbo *et al.*, 2014) generated from the grapevine global gene expression atlas (Fasoli *et al.*, 2012) and from a large berry transcriptomic dataset (Massonnet *et al.*, 2018). These genes could represent key regulators of transcriptome reprogramming during grapevine development as they are up regulated during the transition from vegetative to mature and inversely correlated with many genes suppressed during the mature growth phase. Among them, VviNAC genes were identified as a good candidate gene family to study and better understand the regulation of the maturation processes (D'Inca, 2017).

NAC (*NAM*, *ATAF1,2*, *CUC2*) are plant specific genes that are often involved in drought and salinity responses. The members of this family are also associated with senescence in different plant organs, including fruits. The NAC genes may represent important signalling components in the control of grapevine maturation processes such as late berry developmental and leaves senescence.

In grapevine 74 family members have been identified (Wang *et al.*, 2013). The relationship among them was investigated through a phylogenetic tree that identified 8 separate clades (**Fig. 13**, Wang *et al.*, 2013). All the family members share the highly conserved NAC domain at N-terminus, divided into five subdomains: subdomain A may have an important role in the formation of functional NAC dimeric proteins, subdomains C and D are conserved and bind to DNA, the highly divergent subdomains B and E may confer functional diversity to NAC TFs (**Fig. 13**).

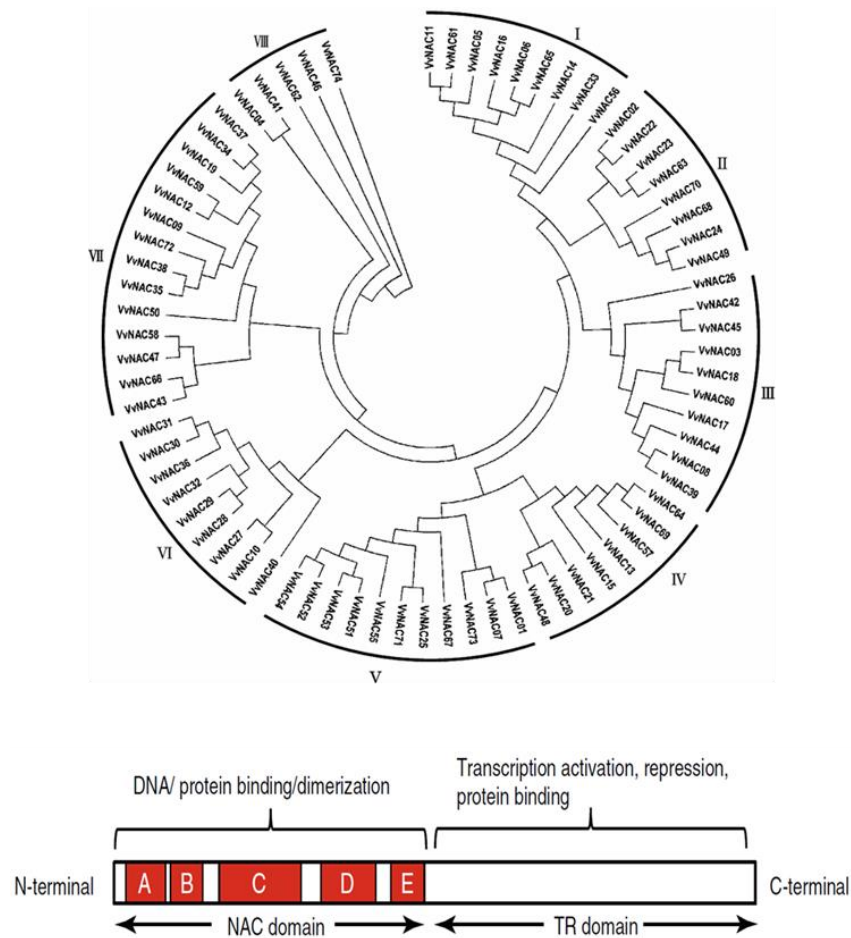


Figure 13: *VviNACs* phylogenetic tree (Wang *et al.*, 2013) and *VviNACs* domain composition.

At first the attention was focused on *VviNAC33* (VIT_19s0027g00230) and *VviNAC60* (VIT_08s0007g07670), selected as they seem to be master regulators of the organ phase transition in the whole plant (D’Inca, 2017). On the base of their expression profiles, which show a very low expression in the vegetative/green tissues and a significantly high expression in the mature/woody organs (**Fig. 14**), they might represent master regulators for the transition from vegetative-to-mature growth, with particular attention to leaves senescence for *VviNAC33* and to berry ripening for *VviNAC60*.

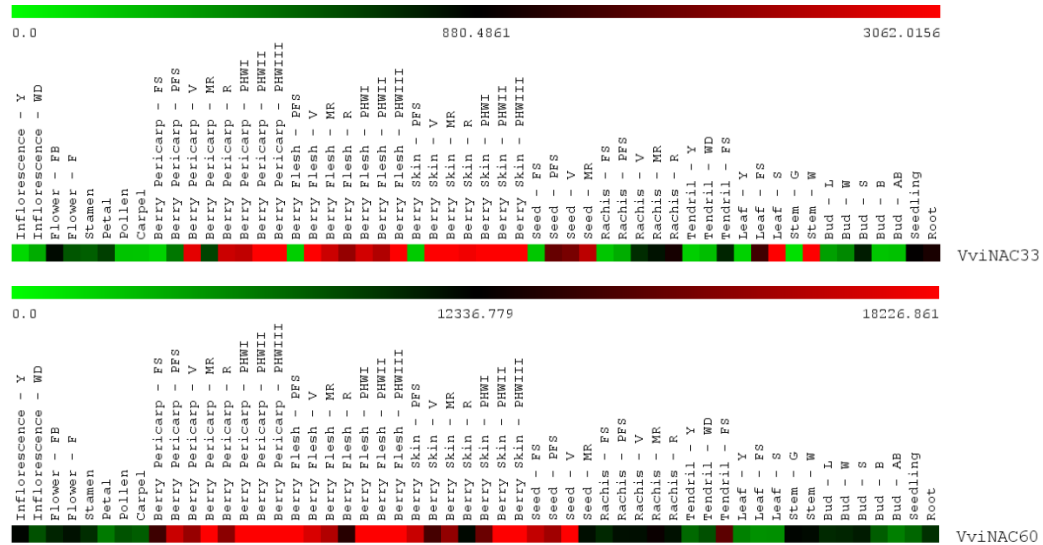


Figure 14: Heatmaps representing the *VviNAC33* and *VviNAC60* expression profiles in all organs and at different developmental stages (data taken from Fasoli *et al.*, 2012).

Description of ATLAS abbreviations (54 developmental stages):

Bud – L = latent bud; – W = winter bud; – S = bud swell; – B = bud burst; – AB = bud after-burst; **Inflorescence** – Y = young inflorescence; – WD = well developed inflorescence; **Flower** – FB = flowering begins; – F = flowering; **Stamen** = pool of stamen from undisclosed flowers; **Pollen** = pollen from disclosed flowers; **Carpel** = pool of carpels from undisclosed flowers; **Petal** = pool of petals from undisclosed flowers; **Tendril** – Y = young tendril; – WD = well developed tendril; – FS = mature tendril; **Leaf** – Y = young leaf; – FS = mature leaf; – S = senescencing leaf; **Berry Pericarp** – FS = fruit set; – PFS = post-fruit set; – V = véraison; – MR = mid-ripening; – R = ripening; – PHWI = post-harvest withering I; – PHWII = post-harvest withering II; – PHWIII = post-harvest withering III; **Berry Skin** – PFS = post-fruit set; – V = véraison; – MR = mid-ripening; – R = ripening; – PHWI = post-harvest withering I; – PHWII = post-harvest withering II; – PHWIII = post-harvest withering III; **Berry Flesh** – PFS = post-fruit set; – V = véraison; – MR = mid-ripening; – R = ripening; – PHWI = post-harvest withering I; – PHWII = post-harvest withering II; – PHWIII = post-harvest withering III; **Seed** – FS = fruit set; – PFS = post-fruit set; – V = véraison; – MR = mid-ripening; **Rachis** – FS = fruit set; – PFS = post-fruit set; – V = véraison; – MR = mid-ripening; – R = ripening; **Stem** – G = green stem; – W = woody stem; **Root** = in-vitro cultivated roots; **Seedling** = pool of 3 developmental stages.

Moreover, embryogenic calli of *Vitis vinifera* cv Shiraz were transformed with *Agrobacterium tumefaciens* harboring a binary vector in which *VviNAC33* and *VviNAC60* were independently over expressed and transgenic grapevines were successfully generated (D’Inca, 2017). *VviNAC33* over expressing plants show normal growth and development; however, a clear bleaching effect on fully expanded leaves was observed (Fig. 15). *VviNAC60* over expressing plants show a slightly reduced growth and earlier stem lignification in comparison to the same-age control plants (Fig. 15). These results confirm the hypothesis that *VviNAC33* and *VviNAC60* may have functions in the transition from vegetative to mature development in grapevine since these changes mirror typical behaviors of plants undergoing ripening and/or senescence.

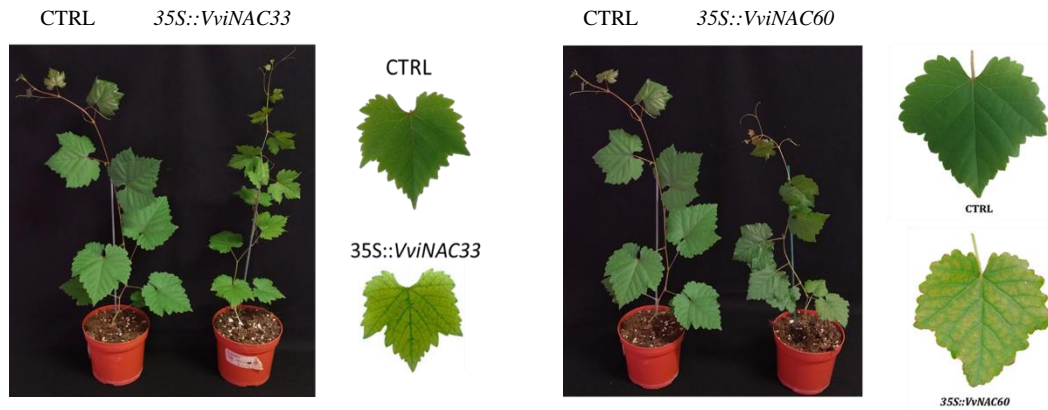


Figure 15: Transgenic plants over expressing *VviNAC33* and *VviNAC60* (D’Inca, 2017).

VviNAC11 (VIT_14s0108g01070) and *VviNAC13* (VIT_02s0012g01040) were also selected as *switch* genes related only to the berry development (D’Inca, 2017); their expression profiles clearly reflect this bioinformatic evidence (**Fig. 16**).

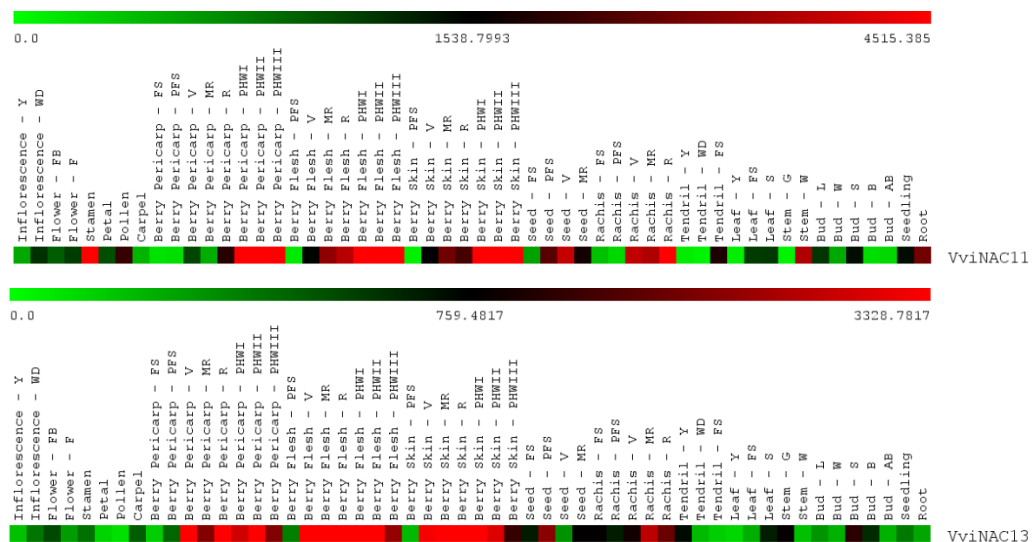


Figure 16: Heatmaps representing the *VviNAC11* and *VviNAC13* expression profiles in all organs and at different developmental stages (data taken from Fasoli *et al.*, 2012).

Description of ATLAS abbreviations (54 developmental stages):

Bud – L = latent bud; – W = winter bud; – S = bud swell; – B = bud burst; – AB = bud after-burst; **Inflorescence** – Y = young inflorescence; – WD = well developed inflorescence; **Flower** – FB = flowering begins; – F = flowering; **Stamen** = pool of stamen from undisclosed flowers; **Pollen** = pollen from disclosed flowers; **Carpel** = pool of carpels from undisclosed flowers; **Petal** = pool of petals from undisclosed flowers; **Tendrill** – Y = young tendrill; – WD = well developed tendrill; – FS = mature tendrill; **Leaf** – Y = young leaf; – FS = mature leaf; – S = senescencing leaf; **Berry Pericarp** – FS = fruit set; – PFS = post-fruit set; – V = véraison; – MR = mid-ripening; – R = ripening; – PHWI = post- harvest withering I; – PHWII = post-harvest withering II; – PHWIII = post-harvest withering III; **Berry Skin** – PFS = post-fruit set; – V = véraison; – MR = mid-ripening; – R = ripening; – PHWI = post-harvest withering I; – PHWII = post-harvest withering II; – PHWIII = post-harvest withering III; **Berry Flesh** – PFS = post-fruit set; – V = véraison; – MR = mid- ripening; – R = ripening; – PHWI = post-harvest withering I; – PHWII = post-harvest withering II; – PHWIII = post-harvest withering III; **Seed** – FS = fruit set; – PFS = post-fruit set; – V = véraison; – MR = mid- ripening; **Rachis** – FS = fruit set; – PFS = post-fruit set; – V = véraison; – MR = mid- ripening; – R = ripening; **Stem** – G = green stem; – W = woody stem; **Root** = in-vitro cultivated roots; **Seedling** = pool of 3 developmental stages.

Since NOR (a NAC-domain transcription factor whose mutation leads to a non-ripening phenotype) has been classified as one of the key regulators of fruit development and ripening in tomato, the two closest grapevine *NOR* orthologues were also selected: *VviNAC03* (VIT_00s0375g00040), already described by D’Inca (2017, **Fig. 17**) and *VviNAC18* (VIT_19s0014g03300).

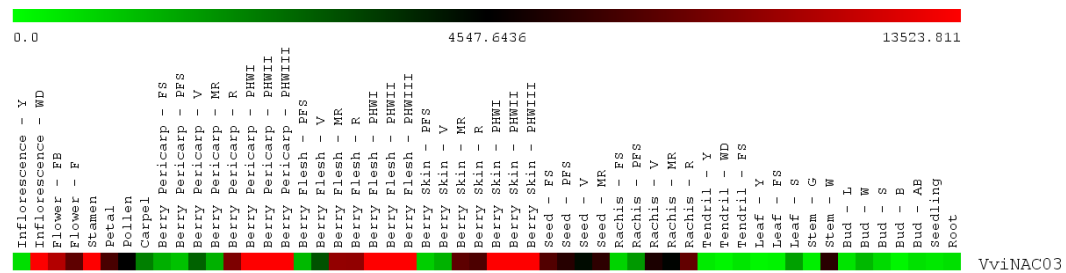


Figure 17: Heatmap representing the *VviNAC03* expression profile in all organs and at different developmental stages (data taken from Fasoli *et al.*, 2012).

Description of ATLAS abbreviations (54 developmental stages):

Bud – L = latent bud; – W = winter bud; – S = bud swell; – B = bud burst; – AB = bud after-burst; **Inflorescence** – Y = young inflorescence; – WD = well developed inflorescence; **Flower** – FB = flowering begins; – F = flowering; **Stamen** = pool of stamen from undisclosed flowers; **Pollen** = pollen from disclosed flowers; **Carpel** = pool of carpels from undisclosed flowers; **Petal** = pool of petals from undisclosed flowers; **Tendril** – Y = young tendril; – WD = well developed tendril; – FS = mature tendril; **Leaf** – Y = young leaf; – FS = mature leaf; – S = senescencing leaf; **Berry Pericarp** – FS = fruit set; – PFS = post-fruit set; – V = véraison; – MR = mid-ripening; – R = ripening; – PHWI = post-harvest withering I; – PHWII = post-harvest withering II; – PHWIII = post-harvest withering III; **Berry Skin** – PFS = post-fruit set; – V = véraison; – MR = mid-ripening; – R = ripening; – PHWI = post-harvest withering I; – PHWII = post-harvest withering II; – PHWIII = post-harvest withering III; **Berry Flesh** – PFS = post-fruit set; – V = véraison; – MR = mid-ripening; – R = ripening; – PHWI = post-harvest withering I; – PHWII = post-harvest withering II; – PHWIII = post-harvest withering III; **Seed** – FS = fruit set; – PFS = post-fruit set; – V = véraison; – MR = mid-ripening; **Rachis** – FS = fruit set; – PFS = post-fruit set; – V = véraison; – MR = mid-ripening; – R = ripening; **Stem** – G = green stem; – W = woody stem; **Root** = in-vitro cultivated roots; **Seedling** = pool of 3 developmental stages.

As the interest is mainly focused on the berry ripening, to choose other candidates all the expression profiles of the *VviNACs* genes were compared. A hierarchical clustering analysis permitted to find those *VviNACs* with a similar profile to the one of *VviNAC60* (**Fig. 18**). Between the genes of this cluster, *VviNAC03*, *VviNAC11*, *VviNAC13* and *VviNAC18* were also found. Some genes presented interesting expression profiles in all berry tissues (*VviNAC01*, *VviNAC05*, *VviNAC15*, *VviNAC20*, *VviNAC37*, *VviNAC38*, *VviNAC48* and *VviNAC61*), where their expression increase during the ripening. Other genes had a very high expression in seeds at the véraison (*VviNAC08*, *VviNAC17*, *VviNAC26* and *VviNAC39*) (**Fig. 18**).

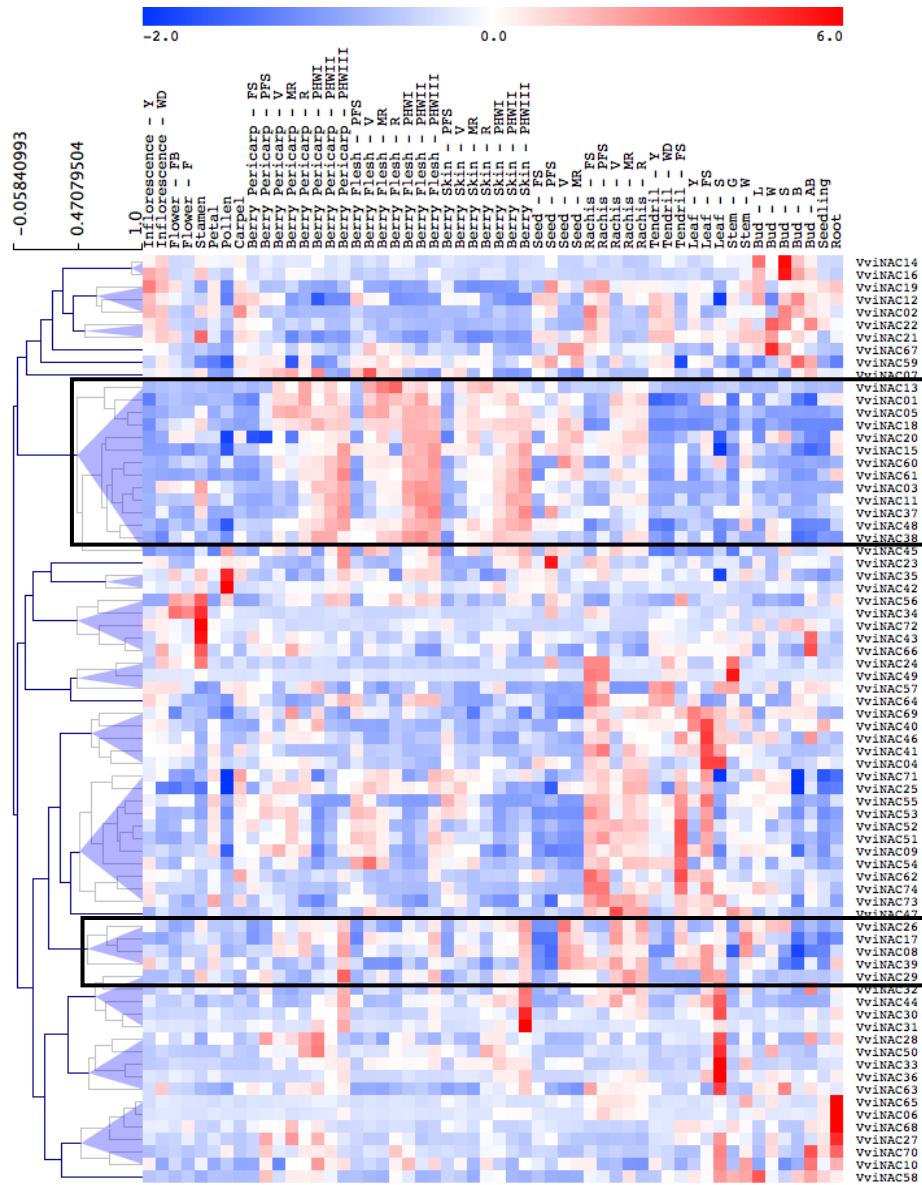


Figure 18: Heatmap representing all the VviNACs expression profiles in all organs and at different developmental stages (data taken from Fasoli *et al.*, 2012). The two clusters of selected NACs are highlighted by black rectangles. Description of ATLAS abbreviations (54 developmental stages):

Bud – L = latent bud; – W = winter bud; – S = bud swell; – B = bud burst; – AB = bud after-burst; **Inflorescence** – Y = young inflorescence; – WD = well developed inflorescence; **Flower** – FB = flowering begins; – F = flowering; **Stamen** = pool of stamen from undisclosed flowers; **Pollen** = pollen from disclosed flowers; **Carpel** = pool of carpels from undisclosed flowers; **Petal** = pool of petals from undisclosed flowers; **Tendril** – Y = young tendril; – WD = well developed tendril; – FS = mature tendril; **Leaf** – Y = young leaf; – FS = mature leaf; – S = senescencing leaf; **Berry Pericarp** – FS = fruit set; – PFS = post-fruit set; – V = véraison; – MR = mid-ripening; – R = ripening; – PHWI = post- harvest withering I; – PHWII = post-harvest withering II; – PHWIII = post-harvest withering III; **Berry Skin** – PFS = post-fruit set; – V = véraison; – MR = mid-ripening; – R = ripening; – PHWI = post-harvest withering I; – PHWII = post-harvest withering II; – PHWIII = post-harvest withering III; **Berry Flesh** – PFS = post-fruit set; – V = véraison; – MR = mid-ripening; – R = ripening; – PHWI = post-harvest withering I; – PHWII = post-harvest withering II; – PHWIII = post-harvest withering III; **Seed** – FS = fruit set; – PFS = post-fruit set; – V = véraison; – MR = mid-ripening; **Rachis** – FS = fruit set; – PFS = post-fruit set; – V = véraison; – MR = mid-ripening; – R = ripening; **Stem** – G = green stem; – W = woody stem; **Root** = in-vitro cultivated roots; **Seedling** = pool of 3 developmental stages.

These clustered genes were selected as they could have an important role, even if marginal compared to the one of the *VviNAC60*, in the vegetative-to-mature phase transition. Afterwards, the previously shown phylogenetic analysis (**Fig. 13**, Wang *et al.*, 2013) was repeated to identify *VviNACs* clustering in the same *VviNAC60* clade (**Fig. 19**). Between the genes of this cluster, *VviNAC03* and *VviNAC18* were also found. The nearest, some of which were also present in the expression profile cluster, were selected (*VviNAC01*, *VviNAC08*, *VviNAC15*, *VviNAC17*, *VviNAC26*, *VviNAC39*, *VviNAC42*, *VviNAC44* and *VviNAC45*).

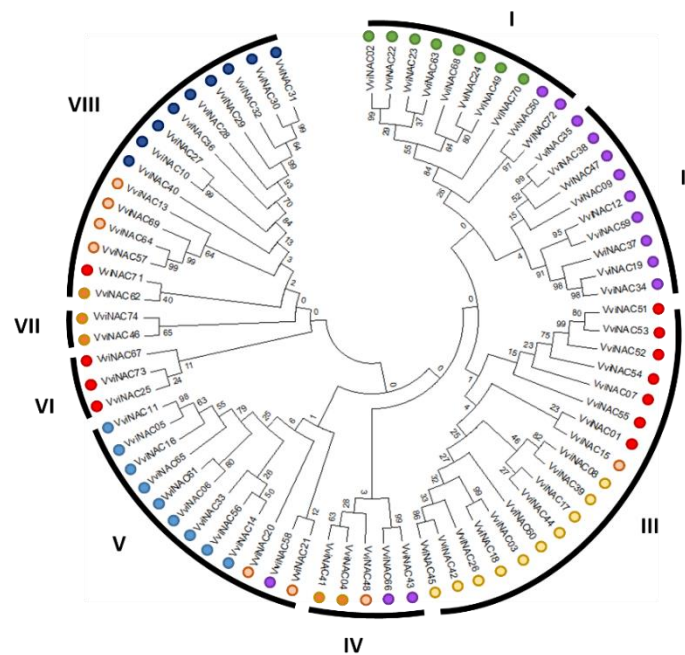


Figure 19: Phylogenetic analysis of the 74 *VviNACs* genes. The previous clade designation (Wang *et al.*, 2013) is shown as a circle of different colours.

Finally, was taken into consideration the new highly detailed transcriptomic map of grape berry development (Fasoli *et al.*, 2018), which is focused on transcriptomic rearrangements close to veraison where two rapid and successive transitions at transcriptional level before veraison were found. Positive and negative markers of each transition were identified, and the expression profile of these genes highlighted the transcriptional rearrangements during the two weeks before veraison. The positive markers of the first transition seem to play a major role as triggers being not expressed until two weeks before veraison and then characterized by a dramatic increase in expression. By looking at the first transition markers list, 3 switch genes

were identified: *VviNAC33*, *VvibHLH075* and *VviWRKY19*. Looking at the genes resulted up regulated by the over expression of *VvibHLH075* and *VviWRKY19*, other *VviNACs* genes were found: *VviNAC05*, *VviNAC17*, *VviNAC26* and *VviNAC61* (**Fig. 20**).

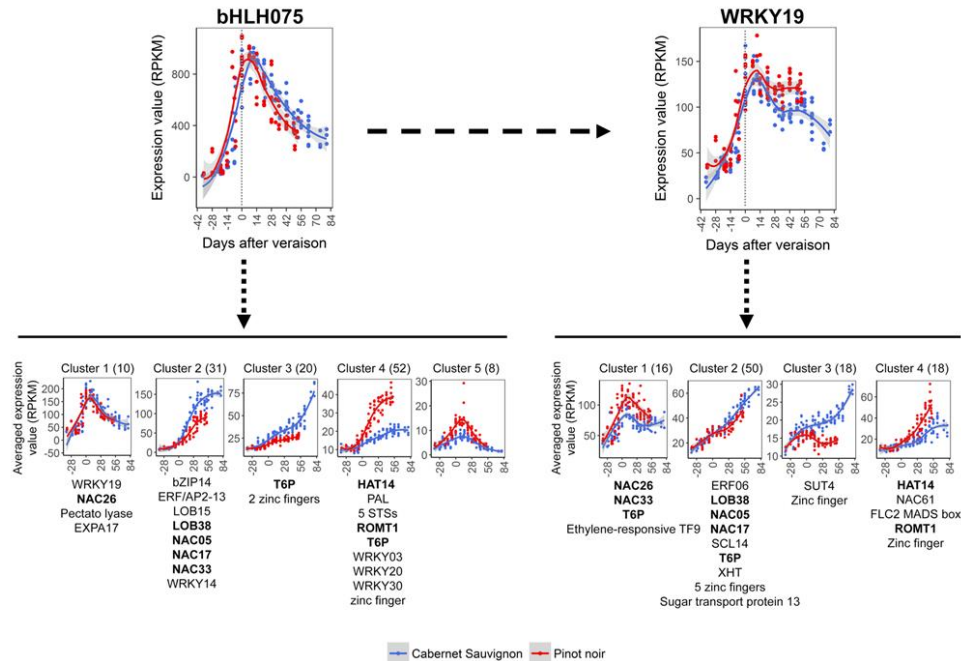


Figure 20: *VvibHLH075* and *VviWRKY19* putative transcriptional activation network (Fasoli *et al.*, 2018).

At the end, comparing the set of genes selected by different criteria, a total of 14 *VviNACs* were selected and isolated for functional studies: *VviNAC01* (VIT_01s0146g00280), *VviNAC03* (VIT_00s0375g00040), *VviNAC08* (VIT_18s0001g02300), *VviNAC11* (VIT_14s0108g01070), *VviNAC13* (VIT_02s0012g01040), *VviNAC15* (VIT_18s0001g01820), *VviNAC17* (VIT_19s0014g03290), *VviNAC18* (VIT_19s0014g03300), *VviNAC26* (VIT_01s0026g02710), *VviNAC33* (VIT_19s0027g00230), *VviNAC38* (VIT_10s0003g00500), *VviNAC39* (VIT_07s0031g02610), *VviNAC60* (VIT_08s0007g07670) and *VviNAC61* (VIT_08s0007g07640).

REFERENCES

D’Inca E. 2017. Master regulators of the vegetative-to-mature organ transition in grapevine: the role of NAC transcription factors. PhD thesis. Verona University.

Fasoli, M., Dal Santo, S., Zenoni, S., Tornielli, G. B., Farina, L., Zamboni, A., ... & Ferrarini, A. (2012). The grapevine expression atlas reveals a deep transcriptome shift driving the entire plant into a maturation program. *The Plant Cell*, 24(9), 3489-3505.

Fasoli, M., Richter, C. L., Zenoni, S., Bertini, E., Vitulo, N., Dal Santo, S., ... & Tornielli, G. B. (2018). Timing and order of the molecular events marking the onset of berry ripening in grapevine. *Plant Physiology*, 178(3), 1187-1206.

Massonnet M, Fasoli M, Tornielli G.B., Altieri M, Sandri M, Zuccolotto P, Paci P, Gardiman M, Zenoni S. and Pezzotti M. (2017). Ripening Transcriptomic Program in Red and White Grapevine Varieties Correlates with Berry Skin Anthocyanin Accumulation. *Plant Physiology*. Vol. 174: 2376–2396.

Palumbo, M. C., Zenoni, S., Fasoli, M., Massonnet, M., Farina, L., Castiglione, F., ... & Paci, P. (2014). Integrated network analysis identifies fight-club nodes as a class of hubs encompassing key putative switch genes that induce major transcriptome reprogramming during grapevine development. *The Plant Cell*, 26(12), 4617-4635.

Wang, N., Zheng, Y., Xin, H., Fang, L., & Li, S. (2013). Comprehensive analysis of NAC domain transcription factor gene family in *Vitis vinifera*. *Plant cell reports*, 32(1), 61-75.

2.2 MATERIAL AND METHODS

Plant material

The ORF of the selected *VviNACs*, except for the already described one (D’Inca, 2017), were isolated from berry pericarp tissue of growth chamber grown *Vitis vinifera* cv Shiraz fruiting cuttings, propagated as described in Mullins *et al.*, 1981. This method permits to have plants for sampling during all the year and is useful to avoid environmental influences. Cuttings were rooted in a heated container (26°C at bases of cuttings) in a cold room (4°C). Buds remained dormant. After four weeks, the rooted cuttings were planted in vermiculite-perlite mixture and transferred in a growth chamber (27°C day and 22°C night, 16 hours photoperiod). At bud burst, leaves basal and adjacent to inflorescences were removed as soon as accessible and the shoot tip was excised. These treatments promote inflorescence growth. A lateral shoot was permitted to grow from an axillary bud of one of the defoliated nodes on the main axis. Development of the bunch to maturity is supported by the foliage of the lateral shoot.

For the transient over expression of the *VviNACs* in grapevine, plantlets of *V. vinifera* cv Sultana were *in vitro* micro-propagated and cultivated in HB medium in a growth chamber at 25°C with a 16 h photoperiod.

Co-expression analysis

Using the global gene expression atlas of *V. vinifera* cv Corvina obtained by microarray approach (Fasoli *et al.*, 2012) a co-expression analysis with the Pearson correlation metric was performed using Cor.To (<http://www.usadellab.org/cms/index.php?page=corto>).

Isolation and Cloning

The total RNA was isolated from 400 mg of ground *Vitis vinifera* cv. Shiraz berry pericarp using Spectrum™ Plant Total RNA kit (Sigma-Aldrich).

RNA samples were quantified with the NanoDrop spectrophotometer (NanoDrop Thermo Scientific Technologies) and 1 µg of RNA was treated with

the TURBO DNA-free™ kit (Ambion). DNase-treated RNA was used for cDNA synthesis using the enzyme Super-Script™ III Reverse Transcriptase (Invitrogen).

The VviNAC ORFs were amplified from cDNA using KAPA HiFi DNA polymerase (KAPA Biosystems, Wilmington, MA, USA) and the primers listed in **Table 1**.

The PCR products were directionally cloned into the Gateway entry vector pENTR/D-TOPO (Invitrogen, Thermo Fisher Scientific, Waltham, MA, USA). Each ORF of interest was then transferred into the binary over expression vector pK7GW2.0 (Laboratory of Plant Systems Biology, PSB; Ghent University, Belgium) by site specific LR Gateway^R recombination.

| Gene ID | TF | Direction | Primer | T _a (°C) | Lenght (bp) |
|-------------------|----------|-----------|------------------------------------|---------------------|-------------|
| VIT_01s0146g00280 | VviNAC01 | For | 5'-CACCATGGAGAAGCTCAATTTTGTGAAG-3' | 55 | 756 |
| | | Rev | 5'-TTATGGTTTTCTCTGAAAGGC-3' | | |
| VIT_18s0001g02300 | VviNAC08 | For | 5'-CACCATGACAGCGGAGTTGCA-3' | 55 | 900 |
| | | Rev | 5'-TCAGAAGGGCTTCTGCA-3' | | |
| VIT_18s0001g01820 | VviNAC15 | For | 5'-CACCATGAAGGTGACAGTGGGT-3' | 55 | 1719 |
| | | Rev | 5'-TCATGAGGGGAGGCATC-3' | | |
| VIT_19s0014g03290 | VviNAC17 | For | 5'-CACCATGGGTGTACCGGAGAC-3' | 55 | 1002 |
| | | Rev | 5'-TTACTGCCTATATCCAAATCCAC-3' | | |
| VIT_19s0014g03300 | VviNAC18 | For | 5'-CACCATGGAGACACCGATTATC-3' | 55 | 1062 |
| | | Rev | 5'-CTAAGCATACCAATTCATGCC-3' | | |
| VIT_01s0026g02710 | VviNAC26 | For | 5'-CACCATGGATGGAAAAGGCAGCT-3' | 55 | 849 |
| | | Rev | 5'-TCACTGAAATTCATACACTGGG-3' | | |
| VIT_10s0003g00500 | VviNAC38 | For | 5'-CACCATGATGGGAAGGGTTCC-3' | 55 | 1458 |
| | | Rev | 5'-TCATGTCAAATAATAGTCACCT-3' | | |
| VIT_07s0031g02610 | VviNAC39 | For | 5'-CACCATGATGAGCGGAGATCAGT-3' | 55 | 885 |
| | | Rev | 5'-TCAAAATGACTTGTTCGAGA-3' | | |
| VIT_08s0007g07640 | VviNAC61 | For | 5'-CACCATGGAAGAGGCTTCATTG-3' | 55 | 1212 |
| | | Rev | 5'-TCAGTAGTCGAGTAAATAATCCA-3' | | |

Table 1: Primers list for the VviNACs isolation from *V. vinifera* cv Shiraz berry pericarp tissue.

***Agrobacterium tumefaciens* C5851 transformation**

A. tumefaciens strain C58C1 was individually transformed by electroporation (Bio-Rad electroporation instrument, 25 μ F, 200 Ω and 2.5 kV) with the pK7WG2.0 transformed vectors containing the 35S:VviNACs (tests) and the empty pK7WG2.0 (control). The transformed colonies were selected by strain antibiotic resistance (tetracycline) and construct antibiotic resistance (streptomycin and spectinomycin).

VviNACs transient over expression

5-week-old *in vitro* plantlets of *Vitis vinifera* cv Sultana were vacuum infiltrated with each of the transformed bacteria strains (tests and control) at 0.5 OD_{600nm}; 6

plants were immersed in the bacterial suspension and vacuum infiltrated two times for 2 min at 90kPa. Immediately after the agroinfiltration, the plants were put in glass jars with sterile perlite and rinsed with sterile water for the *in vitro* recovery. After 7 day from the infiltration, the apical leaves of the 6 plantlets of each over expression were collected and grounded with liquid nitrogen.

The powders were used for the RNA extraction with the Spectrum™ Plant Total RNA kit (Sigma-Aldrich). The extracted RNAs were quantified with the Nanodrop (Thermo Scientific), checked in their quality with a Bioanalyzer Chip RNA 7500 series II (Agilent) for a RIN value over 8 and used in the qPCR Real-Time control.

VviNAC03, *VviNAC11*, *VviNAC13*, *VviNAC33* and *VviNAC60* transient over expression were already performed by D’Inca (2017).

VviNACs stable over expression

VviNAC33 and *VviNAC60* stable over expression were performed by D’Inca (2017).

qPCR Real-Time analyses

Vitis vinifera cv Sultana plantlets were screened for the confirmation of the *VviNACs* transient over expression by qPCR with the primers reported in **Table 2**.

| Gene ID | TF | Direction | Primer | T _a (°C) | Lenght (bp) |
|-------------------|----------|-----------|------------------------------|---------------------|-------------|
| VIT_01s0146g00280 | VviNAC01 | For | 5'- TTGCCAGGTGATTTGGAGCA -3' | 55 | 103 |
| | | Rev | 5'- TCCAGTAACCCGAAACCGTG -3' | | |
| VIT_18s0001g02300 | VviNAC08 | For | 5'- AGCGGAGTTGCAGTTACCTC -3' | 55 | 91 |
| | | Rev | 5'- TTGCGATGCACATTACGGC -3' | | |
| VIT_18s0001g01820 | VviNAC15 | For | 5'- AGGCCGTGCTCCAAGTAAAG -3' | 55 | 91 |
| | | Rev | 5'- CTGCACATTCGGGCATCTCT -3' | | |
| VIT_19s0014g03290 | VviNAC17 | For | 5'- AGAAGTCCAGAGCGGACTCA -3' | 57 | 116 |
| | | Rev | 5'- CGAACGGGTCGAGTGAGTTA -3' | | |
| VIT_19s0014g03300 | VviNAC18 | For | 5'- TTCCACGACAAAGAGGTTCC -3' | 55 | 120 |
| | | Rev | 5'- TGGTGCAATGAAGGAGTCTG -3' | | |
| VIT_01s0026g02710 | VviNAC26 | For | 5'- CGCGTGACCGTAAGTATCCC -3' | 55 | 113 |
| | | Rev | 5'- CCCCACATACTTAGCCCCAC -3' | | |
| VIT_07s0031g02610 | VviNAC39 | For | 5'- CTCTCCAAGGACCGCAAAT -3' | 55 | 118 |
| | | Rev | 5'- AATTCCGACCGTCTTGGGTC -3' | | |
| VIT_08s0007g07640 | VviNAC61 | For | 5'- CGACCAGTACCGTAAGAGCC -3' | 55 | 93 |
| | | Rev | 5'- GCAGAGGCTGACCATAGAC -3' | | |

Table 2: Primers used in the qPCR Real-Time analyses for the confirmation of the *VviNACs* over expression.

All the qPCR analyses were performed as described by Zenoni *et al.* (2010) using SYBR green qPCR Master mix (Promega) and a QuantStudio 3 Real-Time PCR System (Thermo Fisher).

The qPCRs were set up and performed according to the instrument and enzyme manufactures instruction with an appropriate T_a for each set of primers.

Each expression value was determined in triplicate and relatively to the housekeeping gene UBIQUITIN (VIT_16s0098g01190), amplified with the following primers:

For 5'-TCTGAGGCTTCGTGGTGGTA-3'

Rev 5'-AGGCGTGCATAACATTTGCG-3'

Amplification efficiency was calculated from raw data using the LingRegPCR software (Ramakers *et al.*, 2003).

The MNE final expression value were calculated according to Simon (2003).

Microarray analyses

Microarray analyses were performed on the transient over expressing plantlets according to the Agilent Microarray-Based Gene Expression Analysis Guide (V 6.5) protocol. The Agilent custom microarray was designed on the 4pack 44K format (Agilent Sure Print HD 4X44K 60-mer G2514F-048771) and was created by using an Agilent's web-based application (<https://earray.chem.agilent.com/earray/>). 34.651 specific *V. vinifera* 60-mer probes were produced by the software: 29.798 from the *V. vinifera* cv Pinot Noir predicted transcripts V1 version, 4.392 from the new *V. vinifera* cv Pinot Noir loci identified by *V. vinifera* cv Corvina transcriptome reconstruction and analysis and 179 from *V. vinifera* cv Corvina private genes (Venturini *et al.*, 2013). Scanning and Feature Extraction was performed with an Agilent Scanner following the settings and parameters indicated in the instruction manual. For each extraction, the QC report was analyzed to assess the quality of the overall hybridization procedure and a datamatrix was prepared selecting from each single sub-array outcome file the gProcessedSignalvalues, which are the raw fluorescence intensities of each probe. The data were normalized on the 75th percentile and Feature extraction and statistical analysis of the microarray data was conducted as reported in Amato *et al.* (2017). DEGs were identified by TMeV Student's t test ($p < 0.05$), assuming equal variance among samples, and selected by fold change $|1.5|$.

REFERENCES

- Amato, A., Cavallini, E., Zenoni, S., Finezzo, L., Begheldo, M., Ruperti, B., & Tornielli, G. B.** (2017). A grapevine TTG2-like WRKY transcription factor is involved in regulating vacuolar transport and flavonoid biosynthesis. *Frontiers in plant science*, 7, 1979.
- D’Inca E.** 2017. Master regulators of the vegetative-to-mature organ transition in grapevine: the role of NAC transcription factors. PhD thesis. Verona University.
- Fasoli, M., Dal Santo, S., Zenoni, S., Tornielli, G. B., Farina, L., Zamboni, A., ... & Ferrarini, A.** (2012). The grapevine expression atlas reveals a deep transcriptome shift driving the entire plant into a maturation program. *The Plant Cell*, 24(9), 3489-3505.
- Mullins, M. G., & Rajasekaran, K.** (1981). Fruiting cuttings: revised method for producing test plants of grapevine cultivars. *American Journal of Enology and Viticulture*, 32(1), 35-40.
- Ramakers, C., Ruijter, J. M., Deprez, R. H. L., & Moorman, A. F.** (2003). Assumption-free analysis of quantitative real-time polymerase chain reaction (PCR) data. *Neuroscience letters*, 339(1), 62-66.
- Simon, P.** (2003). Q-Gene: processing quantitative real-time RT-PCR data. *Bioinformatics*, 19(11), 1439-1440.
- Venturini, L., Ferrarini, A., Zenoni, S., Tornielli, G. B., Fasoli, M., Dal Santo, S., ... & Zamperin, G.** (2013). De novotranscriptome characterization of *Vitis vinifera* cv. Corvina unveils varietal diversity. *BMC genomics*, 14(1), 41.
- Zenoni, S., Ferrarini, A., Giacomelli, E., Xumerle, L., Fasoli, M., Malerba, G., ... & Delledonne, M.** (2010). Characterization of transcriptional complexity during berry development in *Vitis vinifera* using RNA-Seq. *Plant physiology*, 152(4), 1787-1795.

2.3 RESULTS

Selected VviNACs expression profiles

The genes expression patterns of *VviNAC01*, *VviNAC08*, *VviNAC15*, *VviNAC17*, *VviNAC18*, *VviNAC26*, *VviNAC38*, *VviNAC39* and *VviNAC61* were analyzed by consulting the global gene expression atlas (Fasoli *et al.*, 2012). The expression atlas is a whole-genome expression survey of 54 grapevine tissues and organs collected at various developmental stages, obtained by NimbleGen microarray analysis. As described in the **Introduction** part of this chapter, the above mentioned *VviNACs* were selected as they are in some ways related to *VviNAC60*, the hypothetical master regulator of the berry ripening.

For this reason, the expression profiles of the following genes show high similarity with the *VviNAC60* one (**Fig. 21**).

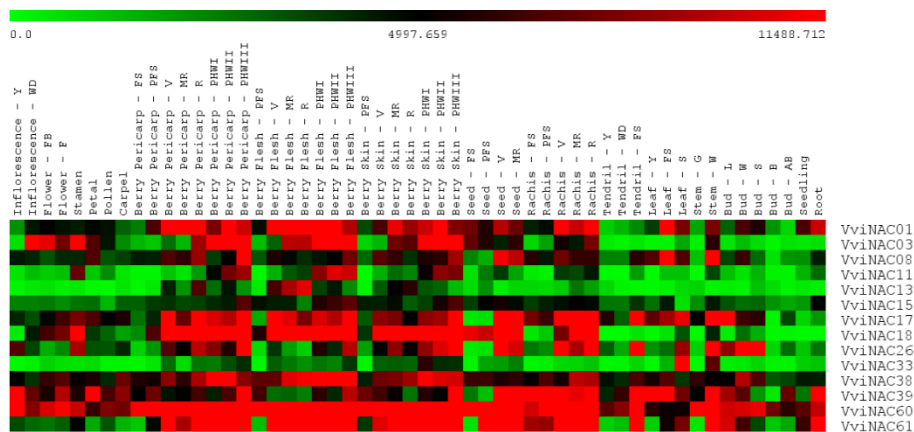


Figure 21: Heatmap representing the selected *VviNACs* expression profiles in all organs and at different developmental stages (data taken from Fasoli *et al.*, 2012).

Description of ATLAS abbreviations (54 developmental stages):

Bud – L = latent bud; – W = winter bud; – S = bud swell; – B = bud burst; – AB = bud after-burst; **Inflorescence** – Y = young inflorescence; – WD = well developed inflorescence; **Flower** – FB = flowering begins; – F = flowering; **Stamen** = pool of stamen from undisclosed flowers; **Pollen** = pollen from disclosed flowers; **Carpel** = pool of carpels from undisclosed flowers; **Petal** = pool of petals from undisclosed flowers; **Tendrils** – Y = young tendril; – WD = well developed tendril; – FS = mature tendril; **Leaf** – Y = young leaf; – FS = mature leaf; – S = senescencing leaf; **Berry Pericarp** – FS = fruit set; – PFS = post-fruit set; – V = véraison; – MR = mid-ripening; – R = ripening; – PHWI = post-harvest withering I; – PHWII = post-harvest withering II; – PHWIII = post-harvest withering III; **Berry Skin** – PFS = post-fruit set; – V = véraison; – MR = mid-ripening; – R = ripening; – PHWI = post-harvest withering I; – PHWII = post-harvest withering II; – PHWIII = post-harvest withering III; **Berry Flesh** – PFS = post-fruit set; – V = véraison; – MR = mid-ripening; – R = ripening; – PHWI = post-harvest withering I; – PHWII = post-harvest withering II; – PHWIII = post-harvest withering III; **Seed** – FS = fruit set; – PFS = post-fruit set; – V = véraison; – MR = mid-ripening; **Rachis** – FS = fruit set; – PFS = post-fruit set; – V = véraison; – MR = mid-ripening; – R = ripening; **Stem** – G = green stem; – W = woody stem; **Root** = in-vitro cultivated roots; **Seedling** = pool of 3 developmental stages.

In details, *VviNAC01* shows an increasing expression during berry developmental phases, in the seeds at veraison, in the rachis from the veraison on, in the mature leaves and in the roots. *VviNAC08* is highly expressed in the berry tissues, in the pericarp and skin from the veraison and in the post-harvesting withering flesh, in the petal, in the seeds from the veraison, in the mature tendril, in the woody stem, in the winter bud and in all the leaf and rachis developmental phases. *VviNAC15* shows an increasing expression during berry development with a peak at post-harvesting withering phase; it is also highly expressed in the seed and rachis all over the growth phases, in the woody stem, in the mature leaf and in the root. *VviNAC17*, has an increased expression in the seed, rachis and berry pericarp and flesh from the veraison on and in the skin at the post-harvesting withering phase III; it is also expressed in the mature tendril, in the woody stem and in the latent bud. *VviNAC18*, is highly expressed in berry tissues after veraison, in the seeds, in the stamen and in the rachis from veraison on ripening. *VviNAC26* shows an increase of expression in the seed, rachis and berry pericarp from veraison on, and in the berry flesh and skin at the post-harvesting withering phases; it also highly expressed in the stamen, in the mature tendril, in the leaves at senescence, in the woody stem and in the bud until burst. *VviNAC38* is expressed in the berry pericarp and skin from the veraison on and in the flesh from the mid-ripening stage on; it also shows high expression in the winter bud and in the mid-ripening stage rachis. *VviNAC39* expression profile shows high expression in the post-harvesting withering phase III of all the berry tissues, in the seed from veraison on, in all the rachis developmental stages, in the mature tendril, in the root, in the young and mature leaves, in the young inflorescences, in the woody stem and in the root. *VviNAC61* increases its expression during the post-harvest withering phases of all the berry tissues but is also highly expressed in the rachis from veraison on, in the mature tendril and in the roots.

Selected *VviNACs* co-expression analyses

To discover genes co-expressed with the selected *VviNACs* and possibly representing their targets or partners, the Atlas transcriptomic dataset was investigated. Thanks to a specific correlation tool named Cor.To, the most

correlated genes with *VviNAC01*, *VviNAC08*, *VviNAC15*, *VviNAC17*, *VviNAC18*, *VviNAC26*, *VviNAC38*, *VviNAC39* and *VviNAC61* were selected. All the ‘no hit’ and ‘unknown’ were eliminated from the list to focus only on the annotated genes with a predicted functional role. At first, a GO enrichment analysis using the on-line tool ShinyGO v0.61 (<http://bioinformatics.sdstate.edu/go/>) was performed on the co-expressed genes for each selected *VviNACs* (**Appendix A**). Then, for each *VviNAC* member the top-20 positive and negative correlated genes were investigated.

VviNAC01 co-expression analysis presented a lot of genes correlated to different catabolic processes, protein modifications and photosynthesis. Among the highest positively correlated genes, *ETHYLENE-RESPONSIVE TRANSCRIPTION FACTOR CORRELATED TO APETALA2 4* (VIT_00s0662g00040), *VviNAC05* (VIT_17s0000g06400) and *VviWRKY19* (VIT_07s0005g01710) were identified, while many *CHLOROPLAST PRECURSORS* (VIT_15s0048g00370, VIT_10s0116g00560, VIT_00s0480g00080 and VIT_09s0018g01870) and a *LHCII* (VIT_19s0014g00160) were found among the negatively correlated genes (**Table 3**).

| Gene ID | Functional annotation | Pearson | Gene ID | Functional annotation | Pearson |
|--------------------|--|---------|-------------------|--|---------|
| VIT_15S0046G02300 | Beta-cyanoalanine synthase | 0.83 | VIT_01S0011G03450 | Alpha-glucosidase | -0.75 |
| VIT_08S0040G01950 | zinc finger (C3HC4-type RING finger) | 0.83 | VIT_11S0016G05840 | protease inhibitor/seed storage/lipid transfer protein (LTP) | -0.74 |
| VIT_00S0404G00040 | ARF GTPase activator, ARF-GAP Domain 5 | 0.81 | VIT_17S0000G06880 | heparanase protein 2 precursor | -0.73 |
| VIT_00S0662G00040 | Ethylene-responsive transcription factor RELATED TO APETALA2 4 | 0.81 | VIT_13S0067G00080 | COP1-interacting protein 7 | -0.73 |
| VIT_17S0000G06400 | NAC domain-containing protein (VvNAC05) | 0.79 | VIT_02S0025G01040 | Receptor protein kinase | -0.73 |
| VIT_14S0060G00410 | EDA32 (embryo sac development arrest 32) | 0.78 | VIT_15S0048G00370 | transketolase, chloroplast precursor | -0.73 |
| VIT_01S0127G00590 | Protein disulfide isomerase | 0.78 | VIT_01S0137G00290 | oxysterol binding protein | -0.73 |
| VIT_08S0007G08840 | Glycosyl transferaseHGA1 | 0.78 | VIT_01S0244G00140 | aspartate kinase | -0.73 |
| VIT_10S0003G02450 | flavonol synthase | 0.77 | VIT_18S0001G00470 | monocopper oxidase SKS5 (SKUS Similar 5) | -0.73 |
| VIT_01S0011G05110 | major latex protein 22 | 0.77 | VIT_10S0116G00560 | polyphenol oxidase II, chloroplast precursor | -0.72 |
| VIT_05S0051G00640 | purple acid phosphatase 23- ATPAP23/PAP23 | 0.77 | VIT_00S0480G00080 | polyphenol oxidase II, chloroplast precursor | -0.72 |
| VIT_06S0004G07560 | ribosomal protein S29 28S | 0.77 | VIT_01S0011G02030 | serine carboxypeptidase S10 | -0.72 |
| VIT_12S0028G000930 | Glutathione S-transferase (VvGST3) | 0.77 | VIT_18S0001G05180 | beta-D-xylosidase | -0.72 |
| VIT_07S0005G01710 | WRKY transcription factor (VvWRKY19) | 0.77 | VIT_03S0063G02490 | glucan endo-1,3-beta-glucosidase 7 precursor | -0.72 |
| VIT_00S0360G00050 | Cyclin-related | 0.77 | VIT_08S0040G00980 | tubulin beta-1 chain | -0.72 |
| VIT_02S0025G04560 | copper amine oxidase | 0.77 | VIT_14S0068G00930 | chalcone synthase 1 | -0.72 |
| VIT_06S0061G00550 | xyloglucan endotransglucosylase/hydrolase 32 | 0.77 | VIT_09S0002G02220 | Protein kinase CDG1 | -0.72 |
| VIT_12S0028G000410 | protein phosphatase 2C | 0.76 | VIT_09S0018G01870 | D-3-phosphoglycerate dehydrogenase | -0.71 |
| VIT_02S0025G04880 | geraniol 10-hydroxylase | 0.76 | VIT_19S0014G00160 | LHCII type I CAB-1 | -0.71 |
| VIT_01S0026G000850 | Zinc finger protein 5 | 0.76 | VIT_14S0108G01660 | biotin carboxyl carrier protein of acetyl-CoA carboxylase | -0.71 |

Table 3: *VviNAC01* positive (left) and negative (right) co-expressed top 20 genes.

VviNAC08 co-expressed genes were highly enriched for the cell cycle and cellular organization and regulation processes categories. Among the highest positively correlated genes, *VviNAC17* (VIT_19s0014g03290), two *ERF/AP2* members (VIT_16s0013g01080 and VIT_18s0001g10150) and *VviWRKY16* (VIT_06s0004g07500) were identified, while *CELL ELONGATION PROTEIN/DWARF1* (VIT_01s0010g01200), *TUBULIN BETA-1 CHAIN*

(VIT_08s0040g00980) and *GIBBERELLIN-REGULATED PROTEIN4/GASA4* (VIT_03s0038g00120) resulted among the negatively correlated gene (**Table 4**).

| Gene ID | Functional annotation | Pearson | Gene ID | Functional annotation | Pearson |
|-------------------|--|---------|-------------------|---|---------|
| VIT_19S0014G03290 | NAC domain-containing protein (VvNAC17) | 0.77 | VIT_18S0072G00330 | Nucleic acid binding | -0.63 |
| VIT_00S0399G00060 | alternative oxidase / immutans protein (IM) | 0.75 | VIT_05S0077G01060 | Aldehyde Dehydrogenase (VvALDH22A1) | -0.62 |
| VIT_11S0016G02580 | MAPK activating protein-like | 0.74 | VIT_06S0004G02480 | Cysteine peptidase | -0.61 |
| VIT_16S0013G01080 | ERF/AP2 Gene Family (VvERF086) | 0.73 | VIT_01S0010G01200 | cell elongation protein / DWARF1 / DIMINUTO (DIM) | -0.60 |
| VIT_12S0028G01410 | heat shock transcription factor A4A | 0.73 | VIT_14S0108G00380 | Protein kinase APK1A | -0.60 |
| VIT_18S0001G12260 | Incomplete root hair elongation | 0.73 | VIT_08S0007G08380 | cellulose synthase CESA3 | -0.60 |
| VIT_06S0004G06750 | armadillo/beta-catenin repeat | 0.73 | VIT_08S0007G08430 | LRR receptor-like kinase 2 | -0.60 |
| VIT_09S0002G03610 | MYB DIVARICATA | 0.71 | VIT_10S0003G04560 | Auxin-Induced in Root cultures 9 AIR9 | -0.60 |
| VIT_06S0004G04950 | scarecrow-like transcription factor 14 SCL14 | 0.71 | VIT_08S0007G01760 | steroid 5 alpha reductase DET2 | -0.59 |
| VIT_13S0019G00830 | armadillo repeat-containing protein | 0.69 | VIT_09S0018G00520 | plastocyanin domain-containing protein | -0.59 |
| VIT_02S0025G03520 | haloacid dehalogenase hydrolase | 0.69 | VIT_08S0040G00980 | tubulin beta-1 chain | -0.59 |
| VIT_01S0026G00190 | armadillo/beta-catenin repeat | 0.69 | VIT_04S0008G05830 | armadillo/beta-catenin repeat | -0.59 |
| VIT_16S0039G01060 | CYP89A2 | 0.69 | VIT_07S0005G05510 | Kinase-like protein TMKL1 | -0.59 |
| VIT_18S0001G10150 | ERF/AP2 Gene Family (VvERF006) | 0.69 | VIT_05S0020G01180 | proteasome 26S AAA-ATPase subunit (RPT5a) | -0.59 |
| VIT_18S0001G01830 | ATP-NAD kinase | 0.68 | VIT_09S0002G08960 | EREBP-4 | -0.58 |
| VIT_18S0122G00320 | PLATZ transcription factor | 0.68 | VIT_00S0218G00090 | exostosin family protein | -0.58 |
| VIT_16S0005G00930 | 4-coumarate-CoA ligase | 0.67 | VIT_03S0038G00120 | gibberellin-regulated protein 4 (GASA4) | -0.58 |
| VIT_14S0006G00430 | plant IF (intermediate filament) | 0.67 | VIT_00S1644G00010 | S-locus protein kinase | -0.58 |
| VIT_01S0010G01840 | GEM-like protein 5 | 0.67 | VIT_17S0000G02010 | atypical receptor kinase MARK | -0.58 |
| VIT_06S0004G07500 | WRKY transcription factor (VvWRKY16) | 0.67 | VIT_03S0088G00380 | Tubulin alpha | -0.58 |

Table 4: VviNAC08 positive (left) and negative (right) co-expressed top 20 genes.

VviNAC15 genes list showed high enrichment in the regulation of the metabolic processes and the protein localization categories. VviNAC15 top highly co-expressed genes list presents four interesting elements: *DENN/AEX-3 DOMAIN-CONTAINING PROTEIN* (VIT_11s0016g01240) and *AUTOPHAGY PROTEIN APG6* (VIT_15s0046g00950), as positively correlated, and *SENESCENCE-INDUCIBLE CHLOROPLAST STAY-GREEN PROTEIN 2* (VIT_18s0001g01250) and *ELIP1-EARLY LIGHT-INDUCIBLE PROTEIN* (VIT_05s0020g04110), as negatively correlated (**Table 5**).

| Gene ID | Functional annotation | Pearson | Gene ID | Functional annotation | Pearson |
|-------------------|--|---------|-------------------|---|---------|
| VIT_01S0011G04520 | programmed cell death 6-interacting protein | 0.89 | VIT_18S0001G06410 | Ribosomal protein 60S | -0.679 |
| VIT_16S0039G01480 | PHD finger transcription factor | 0.87 | VIT_14S0068G00230 | Spiral 1 like 2 | -0.636 |
| VIT_11S0016G01240 | DENN (AEX-3) domain-containing protein | 0.85 | VIT_12S0035G01210 | cytochrome c | -0.615 |
| VIT_19S0015G00930 | hydroxyproline-rich glycoprotein | 0.84 | VIT_00S1491G00020 | lii3 protein | -0.600 |
| VIT_07S0005G02190 | Zinc finger (C2H2 type) family | 0.84 | VIT_07S0104G01270 | kinase interacting family protein | -0.591 |
| VIT_15S0046G00950 | autophagy protein Apg6 | 0.84 | VIT_06S0004G05940 | Uncoupling protein 1 | -0.591 |
| VIT_05S0102G00160 | zinc finger (Ran-binding) | 0.83 | VIT_05S0020G04110 | ELIP1 (early light-inducible protein) | -0.582 |
| VIT_17S0000G03430 | Adaptor-related protein complex 3, delta 1 sub | 0.83 | VIT_15S0046G01130 | myb TRIPYCHON | -0.578 |
| VIT_17S0000G01450 | exocyst subunit EXO70 F1 | 0.83 | VIT_06S0061G00810 | cyclin-dependent kinase regulatory subunit CKS2 | -0.574 |
| VIT_05S0077G00650 | Poly(A) polymerase | 0.83 | VIT_02S0087G00810 | SWIB complex BAF60b domain-containing protein | -0.568 |
| VIT_01S0011G05350 | Cysteine-rich RLK10 | 0.83 | VIT_18S0001G01250 | senescence-inducible chloroplast stay-green protein 2 | -0.567 |
| VIT_07S0104G01600 | MORC family CW-type zinc finger 4 | 0.83 | VIT_19S0027G00200 | photosystem II 10 kDa polypeptide P58R | -0.565 |
| VIT_13S0067G01320 | Alpha-1,2-mannosyltransferase | 0.83 | | | |
| VIT_10S0003G01770 | heat shock transcription factor A4A | 0.83 | | | |
| VIT_08S0007G03880 | Zinc finger (C2H2 type) family | 0.83 | | | |
| VIT_00S0231G00050 | ATP binding protein | 0.82 | | | |
| VIT_06S0004G03180 | zinc finger (FYVE type) | 0.82 | | | |
| VIT_09S0054G01880 | Calreticulin interacted protein | 0.82 | | | |
| VIT_05S0077G01350 | Mov34 STAM-binding protein | 0.82 | | | |
| VIT_06S0009G00250 | Large subunit GTPase 1 | 0.81 | | | |

Table 5: VviNAC15 top 20 positive (left) and all the negative (right) co-expressed genes.

VviNAC17 co-expression analysis revealed that the most represented categories were the one regarding the regulation of metabolic and biosynthetic processes.

VviNAC17 co-expressed genes list presented seven interesting elements: *VviNAC08* (VIT_18s0001g02300), *VviNAC26* (VIT_01s0026g02710), two *ERF/AP2* (VIT_10s0003g00140 and VIT_18s0001g10150), *ETHYLENE-RESPONSIVE DEAD BOX RNA HELICASE/RH30* (VIT_17s0000g09120), *ETHYLENE-RESPONSIVE TRANSCRIPTION FACTOR CORRELATED TO APETALA2 6* (VIT_18s0072g00260) and *VviWRKY16* (VIT_06s0004g07500) as positively correlated (**Table 6**). No interesting genes were found between the negatively correlated.

| Gene ID | Functional annotation | Pearson | Gene ID | Functional annotation | Pearson |
|--------------------|--|---------|-------------------|--|---------|
| VIT_18S0001G02300 | NAC domain-containing protein (VvNAC08) | 0.77 | VIT_05S007G01060 | Aldehyde Dehydrogenase (VvALDH22A1) | -0.64 |
| VIT_01S0026G02710 | NAC domain-containing protein (VvNAC26) | 0.77 | VIT_11S0016G05840 | protease inhibitor/seed storage/lipid transfer protein (LTP) | -0.62 |
| VIT_10S0003G00140 | ERF/AP2 Gene Family (VvERF064) | 0.75 | VIT_14S0108G00380 | Protein kinase APK1A | -0.61 |
| VIT_17S0000G09120 | ethylene-responsive DEAD box RNA helicase (RH30) | 0.71 | VIT_01S0026G02070 | Peptidyl-prolyl cis-trans isomerase cyclophilin-type | -0.61 |
| VIT_16S0050G00390 | 4-coumarate-CoA ligase | 0.71 | VIT_15S0048G00370 | transketolase, chloroplast precursor | -0.61 |
| VIT_06S0004G05660 | glycosyl transferase family 1 protein | 0.70 | VIT_08S0007G01760 | steroid 5 alpha reductase DET2 | -0.60 |
| VIT_08S0056G00180 | Translation initiation factor IF-2B subunit delta | 0.70 | VIT_05S0020G01180 | proteasome 26S AAA-ATPase subunit (RPT5a) | -0.60 |
| VIT_04S0008G02390 | zinc finger (C3HC4-type RING finger) | 0.70 | VIT_06S0004G04610 | fasciclin arabinogalactan-protein (FLA4) | -0.60 |
| VIT_05S0020G01910 | 1,4-alpha-D-glucan maltohydrolase | 0.70 | VIT_04S0008G03610 | Xylan synthase | -0.60 |
| VIT_00S0587G00030 | CBS domain-containing protein | 0.70 | VIT_17S0000G02010 | atypical receptor kinase MARK | -0.60 |
| VIT_18S0001G00180 | protein kinase | 0.70 | VIT_15S0021G00880 | ferredoxin-related | -0.60 |
| VIT_01S0146G00410 | GEM-like protein 5 | 0.70 | VIT_17S0053G00090 | ACCUMULATION AND REPLICATION OF CHLOROPLASTS 6H | -0.59 |
| VIT_11S0016G002580 | MAPK activating protein-like | 0.70 | VIT_12S0028G00310 | Protein kinase family | -0.59 |
| VIT_07S0104G00930 | gibberellin receptor GID1L2 | 0.69 | VIT_07S0151G00140 | NADH dehydrogenase (ubiquinone) Fe-S protein 4 | -0.59 |
| VIT_04S0044G000510 | GT2-like trihelix DNA-binding protein | 0.69 | VIT_12S0059G01320 | glucan endo-1,3-beta-glucosidase 7 precursor | -0.59 |
| VIT_18S0072G00260 | Ethylene-responsive transcription factor RELATED TO APETALA2 6 | 0.69 | VIT_06S0004G08210 | Receptor protein kinase | -0.58 |
| VIT_14S0128G000390 | Mitochondrial FAD carrier | 0.69 | VIT_00S0218G00090 | exostosis family protein | -0.58 |
| VIT_06S0004G07500 | WRKY transcription factor (VvWRKY16) | 0.69 | VIT_07S0141G00240 | NADH dehydrogenase (ubiquinone) flavoprotein 2 | -0.58 |
| VIT_13S0156G000170 | molybdopterin synthase (CNX2) | 0.69 | VIT_06S0004G01540 | Oxidoreductase | -0.58 |
| VIT_18S0001G10150 | ERF/AP2 Gene Family (VvERF006) | 0.69 | VIT_17S0000G08870 | carboxyl-terminal proteinase | -0.58 |

Table 6: *VviNAC17* positive (left) and negative (right) co-expressed top 20 genes.

The most represented enriched categories for *VviNAC18* were the one correlated to different type of catabolic processes, protein modification and localization and photosynthesis. *VviNAC18* co-expressed genes list presented ten interesting elements: *VviNAC05* (VIT_17s0000g06400), an *ERF/EP2* member (VIT_07s0031g00220) and an *UDP-SUGAR PYROPHOSPHARYLASE* (VIT_18s0001g01640) as positively correlated and *LHCB2.1 PHOTOSYSTEM II LIGHT HARVESTING COMPLEX GENE 2.1* (VIT_12s0057g00630), *LHCII TYPE I CAB-1* (VIT_19s0014g00160), *CHLOROPHYLL SYNTHETASE* (VIT_08s0105g00590), *LHCA3* and *LHCA4* (VIT_15s0024g00040 and VIT_17s0000g06350), *PHOTOSYSTEM I REACTION CENTER SUBUNIT III PSFA* (VIT_00s0125g00280) and *PHOTOSYSTEM II 22 KDA PROTEIN PSBS* (VIT_18s0001g02740) as negatively correlated (**Table 7**).

| Gene ID | Functional annotation | Pearson | Gene ID | Functional annotation | Pearson |
|-------------------|--|---------|-------------------|---|---------|
| VIT_19S009G01350 | aspartyl protease | 0.90 | VIT_12S0057G00630 | LHC2.1 (Photosystem II light harvesting complex gene 2.1) | -0.77 |
| VIT_04S0044G01790 | Ribosome assembly protein 1 | 0.88 | VIT_18S0001G13570 | calcium ion binding protein | -0.77 |
| VIT_19S0015G02880 | Glutathione S-transferase 20 GSTU20 | 0.88 | VIT_00S025G600030 | Ankyrin repeat protein | -0.76 |
| VIT_17S0000G05110 | CYP78A4 | 0.88 | VIT_19S0014G00160 | LHCII type I CAB-1 | -0.76 |
| VIT_19S0015G02590 | Glutathione S-transferase 25 GSTU25 | 0.87 | VIT_13S0019G02520 | subtilisin protease C1 | -0.76 |
| VIT_08S0007G00540 | haloacid dehalogenase hydrolase | 0.87 | VIT_12S0142G00420 | Copper-transporting ATPase PAA1 | -0.76 |
| VIT_11S0016G05700 | RabGAP/TBC domain-containing protein | 0.87 | VIT_18S0041G00950 | UDP-glucose: anthocyanidin 5,3-O-glucosyltransferase | -0.75 |
| VIT_05S0020G03860 | homocysteine S-methyltransferase 3 | 0.86 | VIT_00S025G600040 | Ankyrin repeat protein | -0.75 |
| VIT_08S0040G01950 | zinc finger (C3HC4-type RING finger) | 0.86 | VIT_08S0105G00590 | chlorophyll synthetase | -0.75 |
| VIT_17S0000G06400 | NAC domain-containing protein (VvNAC05) | 0.85 | VIT_15S0024G00040 | LHCA3 (Photosystem I light harvesting complex gene 3) | -0.75 |
| VIT_01S0011G04370 | Phosphatidylserine synthase 2 | 0.85 | VIT_00S025G600110 | Ankyrin repeat protein | -0.75 |
| VIT_07S0031G00220 | ERF/AP2 Gene Family (VvAP2-13) | 0.85 | VIT_00S0411G00020 | Ankyrin repeat protein | -0.75 |
| VIT_11S0016G03000 | Phosphoinositide 3-kinase regulatory subunit 4 | 0.85 | VIT_15S0046G03670 | NADP-dependent malic enzyme | -0.75 |
| VIT_05S0051G00640 | purple acid phosphatase 23- ATPAP23/PAP23 | 0.85 | VIT_17S0000G06350 | LHCA4 (Photosystem I light harvesting complex gene 4) | -0.75 |
| VIT_18S0001G01640 | UDP-sugar pyrophosphorylase | 0.85 | VIT_00S0125G00280 | Photosystem I reaction center subunit III (PSAF) | -0.74 |
| VIT_14S0030G01600 | DNA-binding storekeeper protein | 0.85 | VIT_18S0001G02740 | photosystem II 22 kDa protein PSBS | -0.74 |
| VIT_08S0040G00770 | cysteine protease inhibitor | 0.84 | VIT_18S0001G00470 | monocopper oxidase SKS5 (SKU5 similar 5) | -0.74 |
| VIT_01S0127G00680 | SRO2 (SIMILAR TO RCD ONE 2) | 0.84 | VIT_02S0012G00570 | pseudo-response regulator 2 (APRR2) (TOC2) | -0.74 |
| VIT_02S0025G00030 | zinc finger (C3HC4-type RING finger) | 0.84 | VIT_18S0041G01040 | UDP-glycosyltransferase 88A4 | -0.74 |
| VIT_04S0023G03120 | Histone H3 | 0.84 | VIT_18S0001G09040 | LIM domain protein WLIM1 | -0.73 |

Table 7: VviNAC18 positive (left) and negative (right) co-expressed top 20 genes.

VviNAC26 analysis showed a GO enrichment for the regulation of biosynthetic and metabolic processes categories, but also for photosynthesis. VviNAC26 co-expressed genes list presented five interesting elements: VviNAC17 (VIT_19s0014g03290), *ERF/AP2* (VIT_18s0001g10150), VviMYB15 (VIT_05s0049g01020) and *ETHYLENE-RESPONSIVE DEAD BOX RNA HELICASE RH30* (VIT_17s0000g09120) as positively correlated and *LEAF SENESCENCE PROTEIN* (VIT_14s0083g00400) and *PURINE PERMEASE 1 PUP1* (VIT_18s0001g06950) as negatively correlated (**Table 8**).

| Gene ID | Functional annotation | Pearson | Gene ID | Functional annotation | Pearson |
|-------------------|--|---------|-------------------|--|---------|
| VIT_04S0023G02480 | Dehydrin 1b | 0.77 | VIT_01S0026G02070 | Peptidyl-prolyl cis-trans isomerase cyclophilin-type | -0.65 |
| VIT_19S0014G03290 | NAC domain-containing protein (VvNAC17) | 0.77 | VIT_09S0002G01550 | lecithine cholesterol acyltransferase | -0.60 |
| VIT_18S0001G10150 | ERF/AP2 Gene Family (VvERF006) | 0.70 | VIT_15S0046G03520 | phosphomannomutase | -0.60 |
| VIT_00S0076G00010 | S-locus lectin protein kinase family | 0.70 | VIT_05S0077G01060 | Aldehyde Dehydrogenase (VvALDH22A1) | -0.59 |
| VIT_18S0001G11130 | calmodulin-binding protein AR781 | 0.69 | VIT_11S0078G00430 | L-fucokinase | -0.59 |
| VIT_05S0049G01020 | VvMYB15 | 0.68 | VIT_06S0004G05940 | Uncoupling protein 1 | -0.58 |
| VIT_16S0039G01060 | CYP89A2 | 0.67 | VIT_14S0060G00460 | Receptor-like protein kinase | -0.58 |
| VIT_05S0051G00140 | RRS1 (resistant to ralstonia solanacearum 1) | 0.67 | VIT_05S0020G02890 | GPI-anchored protein-like protein II | -0.57 |
| VIT_00S0347G00060 | S-locus lectin protein kinase | 0.67 | VIT_02S0025G01330 | Polygalacturonase GH28 | -0.57 |
| VIT_06S0004G05660 | glycosyl transferase family 1 protein | 0.66 | VIT_05S0049G01860 | receptor-like protein kinase | -0.57 |
| VIT_18S0001G06950 | purine permease 1 (PUP1) | 0.66 | VIT_11S0037G00930 | GDP-L-fucose synthase | -0.57 |
| VIT_00S0743G00020 | S-locus lectin protein kinase | 0.66 | VIT_06S0080G00250 | sialyltransferase | -0.56 |
| VIT_19S0027G01630 | disease resistance protein (NBS-LRR class) | 0.66 | VIT_06S0004G04610 | fasciclin arabinogalactan-protein (FLA4) | -0.56 |
| VIT_04S0008G02980 | Lupeol synthase | 0.66 | VIT_03S0038G02520 | aquaporin PIP3 | -0.56 |
| VIT_04S0023G03630 | WD repeat domain 60 | 0.66 | VIT_12S0057G01020 | fasciclin-like arabinogalactan protein FLA2 | -0.56 |
| VIT_17S0000G09120 | ethylene-responsive DEAD box RNA helicase (RH30) | 0.66 | VIT_14S0030G02180 | GDP-mannose 3,5-epimerase 1 | -0.55 |
| VIT_05S0051G00230 | R protein L6 | 0.65 | VIT_06S0004G01540 | Oxidoreductase | -0.55 |
| VIT_08S0007G07730 | CYP93A1 2-hydroxyisoflavanone synthase | 0.65 | VIT_14S0083G00400 | Leaf senescence protein | -0.55 |
| VIT_02S0025G03510 | bromo-adjacently (BAH) domain-containing protein | 0.65 | VIT_19S0090G00020 | TOR1 (TORTIFOLIA 1) | -0.55 |
| VIT_02S0025G03290 | hydroxyproline-rich glycoprotein | 0.64 | VIT_09S0002G01710 | Zeta-cop, subunit of COP-1 complex | -0.54 |

Table 8: VviNAC26 positive (left) and negative (right) co-expressed top 20 genes.

VviNAC38 co-expressed genes revealed a GO enrichment for the catabolic processes, protein, macromolecule and organic compounds transport and protein modification categories. Among the positively correlated genes with VviNAC38 a *ABC TRANSPORTER F MEMBER 6* (VIT_18s0076g00380) was identified, while the *COPPER-TRANSPORTING ATPase PAA1* (VIT_12s0142g00420) a *BZIP*

TRANSCRIPTION FACTOR (VIT_13s0067g02900), the *LHCB2.1* (VIT_12s0057g00630), the *LHCA4* (VIT_17s0000g06350) and the *PHOTOSYSTEM I REACTION CENTER (PSAF)* resulted negatively correlated with *VviNAC38* (Table 9).

| Gene ID | Functional annotation | Pearson | Gene ID | Functional annotation | Pearson |
|-------------------|--|---------|-------------------|---|---------|
| VIT_08S0217G00030 | Ran-binding protein 1 RanBP1 | 0.84 | VIT_08S0007G06450 | omega-6 fatty acid desaturase, endoplasmic reticulum (FAD2) | -0.70 |
| VIT_02S0025G02760 | Ubiquitin thiolesterase 4 | 0.84 | VIT_01S0244G00140 | aspartate kinase | -0.67 |
| VIT_13S0064G01090 | Zinc finger (CCH-type) family protein | 0.83 | VIT_12S0035G00970 | evolutionarily conserved C-terminal region 11 ECT11 | -0.67 |
| VIT_04S0008G05770 | CBL-interacting protein kinase 25 (CIPK25) | 0.83 | VIT_05S0020G00870 | Ubi/COQ5 methyltransferase | -0.66 |
| VIT_16S0098G00890 | harpin-induced protein | 0.83 | VIT_15S0019G05290 | acyl-CoA binding | -0.64 |
| VIT_08S0040G00770 | cysteine protease inhibitor | 0.82 | VIT_19S0014G01470 | Thioredoxin TTL1 (Tetraatricopeptide-repeat thioredoxin-like 1) | -0.64 |
| VIT_14S0030G01600 | DNA-binding storekeeper protein | 0.82 | VIT_12S0142G00420 | Copper-transporting ATPase PAA1 | -0.64 |
| VIT_06S0004G03440 | Ulp1 protease | 0.82 | VIT_18S0001G08250 | tubulin alpha-3 chain | -0.64 |
| VIT_18S0076G00380 | ABC transporter F member 6 | 0.82 | VIT_03S0038G02790 | Ribosomal protein L2, Chloroplast | -0.63 |
| VIT_18S0001G13790 | Cytochrome P450, family 83, subfamily B, polypeptide 1 | 0.82 | VIT_04S0008G03610 | Xylan synthase | -0.63 |
| VIT_06S0080G00800 | Vesicle-associated membrane protein 714 | 0.81 | VIT_13S0067G02900 | bZIP transcription factor | -0.63 |
| VIT_11S0016G05600 | Zinc finger (ubiquitin-hydrolase) domain-containing | 0.81 | VIT_04S0044G01670 | ankyrin | -0.63 |
| VIT_01S0026G00850 | Zinc finger protein 5 | 0.81 | VIT_13S0019G03210 | Lectin-like protein | -0.62 |
| VIT_07S0255G00100 | Extra-large G-protein (XLG1) | 0.81 | VIT_12S0057G00630 | LHCB2.1 (Photosystem II light harvesting complex gene 2.1) | -0.62 |
| VIT_10S0092G00120 | gamma-soluble NSF attachment protein (GSNAP) | 0.81 | VIT_17S0000G06350 | LHCA4 (Photosystem I light harvesting complex gene 4) | -0.62 |
| VIT_14S0068G00840 | RBR1 (retinoblastoma-related 1) | 0.81 | VIT_07S0104G01150 | RNA-binding protein | -0.61 |
| VIT_09S0002G02070 | Protein kinase PKN/PRK1 | 0.81 | VIT_11S0078G00310 | isoamylase-type starch-debranching enzyme 1 | -0.61 |
| VIT_05S0011G04370 | Phosphatidylserine synthase 2 | 0.80 | VIT_00S0125G00280 | Photosystem I reaction center subunit III (PSAF) | -0.61 |
| VIT_14S0083G00470 | Amino acid permease | 0.80 | VIT_06S0004G00040 | Pur alpha-1 (purin-rich alpha 1) | -0.61 |
| VIT_12S0035G01090 | Regulator of nonsense transcripts 3 UPF3 | 0.80 | VIT_10S0003G02590 | SH3 domain-containing protein 3 (SH3P3) | -0.61 |

Table 9: *VviNAC38* positive (left) and negative (right) co-expressed top 20 genes.

VviNAC39 genes list showed high enrichment in the regulation of the biosynthetic and metabolic processes. *VviNAC39* co-expressed genes list presented eight interesting elements: four *VviWRKYs* (VIT_10s0116g01200, VIT_08s0058g00690, VIT_10s0003g01600 and VIT_06s0004g07500), two *ETHYLENE RESPONSIVE ELEMENTS* (VIT_02s0234g00130 and VIT_18s0072g00260) and *UDP-GLUCOSE: FLAVONOID 7-O-GLUCOSYLTRANSFERASE* (VIT_05s0062g00270) as positively correlated and *AUXIN-INDEPENDENT GROWTH PROMOTER* (VIT_14s0083g00940) as inverse correlated (Table 10).

| Gene ID | Functional annotation | Pearson | Gene ID | Functional annotation | Pearson |
|--------------------|--|---------|-------------------|---|---------|
| VIT_10S0116G01200 | WRKY transcription factor (VvWRKY29) | 0.77 | VIT_06S0004G06610 | peptidyl-prolyl cis-trans isomerase ROC7 (ROTAMASE CYP 7) | -0.54 |
| VIT_02S0234G00130 | Ethylene responsive element binding factor 1 | 0.74 | VIT_08S0007G03490 | Mitochondrial Acyl carrier protein 2 | -0.54 |
| VIT_19S0015G00130 | serine acetyltransferase 3 | 0.74 | VIT_04S0023G00840 | Mitochondrial Acyl carrier protein 2 | -0.54 |
| VIT_06S0004G04960 | scarecrow-like transcription factor 14 SCL14 | 0.72 | VIT_14S0083G00490 | Phosphoglycerate mutase | -0.53 |
| VIT_17S0000G03340 | Wall-associated kinase 4 | 0.72 | VIT_01S0010G03690 | Splicing factor YTS21-B | -0.53 |
| VIT_09S0002G03540 | MYB DIVARICATA | 0.71 | VIT_14S0083G00940 | auxin-independent growth promoter | -0.53 |
| VIT_00S0370G00010 | LRR receptor-like serine/threonine-protein kinase | 0.69 | VIT_17S0000G08540 | lipase GDSL | -0.53 |
| VIT_08S0058G00690 | WRKY transcription factor (VvWRKY24) | 0.69 | VIT_00S0357G00070 | beta-hydroxyacyl-ACP dehydratase | -0.52 |
| VIT_06S0004G06710 | Cys-3-His zinc finger protein | 0.68 | VIT_18S0001G06830 | Methyltransferase type 11 | -0.52 |
| VIT_00S2376G00010 | NADH dehydrogenase, putative | 0.68 | VIT_13S0067G03650 | histone H4 | -0.51 |
| VIT_09S0002G03610 | MYB DIVARICATA | 0.67 | VIT_07S0151G00140 | NADH dehydrogenase (ubiquinone) Fe-S protein 4 | -0.51 |
| VIT_10S0003G01600 | WRKY transcription factor (VvWRKY30) | 0.67 | VIT_06S0004G05470 | sterol 4-alpha-methyl-oxidase 2 (SMO2) | -0.51 |
| VIT_16S00039G01060 | CYP89A2 | 0.67 | VIT_04S0023G00760 | biotin carboxyl carrier protein 2 (BCCP2) | -0.50 |
| VIT_10S0003G05450 | reticuline oxidase precursor | 0.66 | VIT_08S0007G03940 | histone deacetylase HD2A | -0.50 |
| VIT_05S0062G00270 | UDP-glucose:flavonoid 7-O-glucosyltransferase | 0.66 | VIT_04S0023G02390 | Thioredoxin domain-containing protein 9 | -0.50 |
| VIT_06S0004G07500 | WRKY transcription factor (VvWRKY16) | 0.66 | VIT_08S0040G00970 | plectin (myosin-like) | -0.50 |
| VIT_19S0014G04940 | Chitin-inducible gibberellin-responsive protein 1 | 0.65 | VIT_15S0021G00570 | acyl carrier protein, mitochondrial | -0.50 |
| VIT_05S0231G00040 | RPM1-interacting protein 4 | 0.65 | VIT_17S0000G08840 | trans-2-enoyl-CoA reductase | -0.49 |
| VIT_18S0072G00260 | Ethylene-responsive transcription factor RELATED TO APETALA2 6 | 0.65 | VIT_00S0357G00020 | beta-hydroxyacyl-ACP dehydratase | -0.49 |
| VIT_00S2648G00010 | FAD-dependent pyridine nucleotide-disulphide oxidoreductase | 0.65 | VIT_06S0004G00250 | PUMILIO 12 (APUM12) | -0.49 |

Table 10: *VviNAC39* positive (left) and negative (right) co-expressed top 20 genes.

VviNAC61 co-expressed genes were highly enriched for autophagy, inorganic and organic molecules transport, protein modification and transport, catabolic processes and photosynthesis categories. *VviNAC61* co-expressed genes list presented ten interesting elements: *LATERAL ORGAN BOUNDARIES DOMAIN 15* (VIT_06s0004g07790) and *MYB DOMAIN PROTEIN 3R2* (VIT_15s0048g02120), as positively correlated, and *LHCB2.1 PHOTOSYSTEM II LIGHT HARVESTING COMPLEX GENE 2.1* (VIT_12s0057g00630), *LHCA4 PHOTOSYSTEM I LIGHT HARVESTING COMPLEX GENE 4* (VIT_17s0000g06350), *PHOTOSYSTEM I REACTION CENTER SUBUNIT III PSFA* (VIT_00s0125g00280), *2-CYS PEROXIREDOXIN BAS1*, *CHLOROPLAST PRECURSOR* (VIT_08s0007g02490), *PECTINACETYLESTERASE* (VIT_05s0020g01110), *FRUCTOSAMINE KINASE* (VIT_15s0048g01810) and *FRUCTOKINASE-2* (VIT_14s0006g01410) and *MAGNESIUM-PROTOPORPHYRIN IX MONOMETHYL ESTER [OXIDATIVE] CYCLASE* (VIT_08s0040g00390), as inverse correlated (**Table 11**).

| Gene ID | Functional annotation | Pearson | Gene ID | Functional annotation | Pearson |
|-------------------|--|---------|-------------------|--|---------|
| VIT_06s0004g07790 | lateral organ boundaries DOMAIN 15 | 0.89 | VIT_12s0057g00630 | LHCB2.1 (Photosystem II light harvesting complex gene 2.1) | -0.73 |
| VIT_14s0108g00890 | beta-1,3-galactosyltransferase | 0.88 | VIT_11s0016g04850 | carboxylic ester hydrolase | -0.73 |
| VIT_04s0023g01080 | Lys Motif-Type Receptor-Like Kinase LYK4 | 0.88 | VIT_07s0141g00240 | NADH dehydrogenase (ubiquinone) flavoprotein 2 | -0.72 |
| VIT_14s0128g00180 | zinc finger (C3HC4-type RING finger) | 0.88 | VIT_06s0004g05940 | Uncoupling protein 1 | -0.72 |
| VIT_12s0028g03580 | lectin-receptor like protein kinase 3 | 0.87 | VIT_15s0048g01810 | fructosamine kinase | -0.71 |
| VIT_08s0007g05250 | cig3 | 0.87 | VIT_01s0244g00140 | aspartate kinase | -0.71 |
| VIT_11s0016g03780 | CONTINUOUS VASCULAR RING (COV1) | 0.86 | VIT_17s0000g00290 | alpha-mannosidase precursor lysosomal | -0.71 |
| VIT_13s0019g02440 | Mitochondrial substrate carrier family protein | 0.86 | VIT_05s0020g01110 | pectinacetylsterase | -0.71 |
| VIT_12s0059g01100 | PRU-interacting factor K | 0.86 | VIT_17s0000g06350 | LHCA4 (Photosystem I light harvesting complex gene 4) | -0.70 |
| VIT_08s0007g01150 | Unc51-like kinase | 0.86 | VIT_14s0108g01420 | DEFENSE NO death 1 | -0.70 |
| VIT_14s0083g00930 | BIM2 (BES1-interacting Myc-like protein 2) | 0.85 | VIT_14s0006g01410 | fructokinase-2 | -0.70 |
| VIT_14s0068g01360 | GEM-like protein 5 | 0.85 | VIT_08s0040g00390 | Magnesium-protoporphyrin IX monomethyl ester [oxidative] cyclase | -0.70 |
| VIT_13s0019g02440 | Peptide chain release factor eRF subunit 1 | 0.85 | VIT_18s0001g08250 | tubulin alpha-3 chain | -0.70 |
| VIT_14s0068g02240 | 2-hydroxyacyl-CoA lyase 1 | 0.84 | VIT_12s0035g00910 | bile acid sodium symporter | -0.70 |
| VIT_14s0068g02150 | kelch repeat-containing F-box family protein | 0.84 | VIT_11s0016g05840 | protease inhibitor/seed storage/lipid transfer protein (LTP) | -0.70 |
| VIT_15s0048g01160 | phospholipase D beta 1 | 0.84 | VIT_18s0001g00810 | 24-methylenesterol C-methyltransferase 2 | -0.70 |
| VIT_05s0026g01190 | pirin | 0.84 | VIT_12s0035g00270 | ferredoxin, chloroplast (PETF) | -0.70 |
| VIT_01s0127g00680 | SRO2 (SIMILAR TO RCD ONE 2) | 0.84 | VIT_00s0125g00280 | Photosystem I reaction center subunit III (PSFA) | -0.70 |
| VIT_11s0118g00360 | leucoanthocyanidin dioxygenase | 0.84 | VIT_08s0007g02490 | 2-cys peroxidoreoxin BAS1, chloroplast precursor | -0.69 |
| VIT_15s0048g02120 | myb domain protein 3R2 | 0.84 | VIT_06s0004g05280 | troponin reductase | -0.69 |

Table 11: *VviNAC61* positive (left) and negative (right) co-expressed top 20 genes.

Selected *VviNACs* isolation

Starting from *V. vinifera* cv Shiraz fruiting cuttings, all the selected *VviNACs* coding sequences were isolated from cDNA obtained from berry pericarp tissue RNA. Afterwards, the isolated sequences were directionally cloned into the Gateway entry vector pENTR/D-TOPO (Invitrogen) and sequenced.

VviNAC01, *VviNAC08*, *VviNAC15*, *VviNAC17*, *VviNAC18*, *VviNAC26*, *VviNAC38*, *VviNAC39* and *VviNAC61* contain a 756, 900, 1719, 1002, 1062, 849, 1458, 885

and 1212 bp open reading frame encoding a protein of 251, 299, 572, 333, 353, 282, 517, 294 and 403 amino acidic residues with a predicted mass of 28.66, 34.09, 63.40, 37.19, 38.92, 32.46, 57.10, 33.47 and 45.44 kDa and a calculated pI = 9.20, 6.66, 4.73, 8.66, 8.55, 7.70, 5.76, 7.06 and 6.52, respectively.

The sequenced genes taken from cv Shiraz were blasted against the cv Pinot Noir reference genome and the analyses revealed that the predicted *VviNACs* gene sequences were practically identical to the one of the reference genome (**Appendix B**). The nucleotide sequences were translated into aminoacids sequences to see if the SNPs found in the different cultivar genes could bring to deleterious mutations. *VviNAC01* reports only one change, from a G (glycine, non-polar) to a D (aspartic acid, negative polar) at the residue 207 (**Fig. 22A**).

VviNAC15 reports two changes, one from a G (glycine, non-polar) to a D (aspartic acid, negatively polar) at the residue 364 and the other from a I (isoleucine, non-polar) to a M (methionine, non-polar) at the residue 369 (**Fig. 22C**).

VviNAC38 reports a frameshift nucleotides insertion/duplication of 96 bp that does not affect the protein translation but just adds 32 aminoacids to the final protein (**Fig. 22G**).

VviNAC39 reports five changes: from a K (lysine, positively polar) to a E (glutamic acid, negatively polar), from a P (proline, non-polar) to a L (leucine, non-polar), from a Q (glutamine, uncharged polar) to a H (histidine, positively polar), from a N (asparagine, uncharged polar) to a D (aspartic acid, negatively polar) and from a V (valine, non-polar) to a A (alanine, non-polar) at the residues 74, 76, 171, 192 and 194 respectively (**Fig. 22H**).

| | | | |
|----------|--------------------|--|-----|
| A | VviNAC01_Shiraz | MEKLNFKVNGVLRLLPPGFRFHPTDEELVVQYLKRRKAYSCPLPASIIPEVDVCKADPWLDP | 60 |
| | VviNAC01_Reference | MEKLNFKVNGVLRLLPPGFRFHPTDEELVVQYLKRRKAYSCPLPASIIPEVDVCKADPWLDP | 60 |
| | | ***** | |
| | VviNAC01_Shiraz | GDLEQERYFFSTREAKYPNGNRSNRATVSGYWKATGIDKQIVASKGNQVVMKKTILVFYR | 120 |
| | VviNAC01_Reference | GDLEQERYFFSTREAKYPNGNRSNRATVSGYWKATGIDKQIVASKGNQVVMKKTILVFYR | 120 |
| | | ***** | |
| | VviNAC01_Shiraz | GKPPHGSRTDWIMHEYRLVGAETTPQRKSSTTQSSMAQAENWVLCRIFLKKRGTKNDEEM | 180 |
| | VviNAC01_Reference | GKPPHGSRTDWIMHEYRLVGAETTPQRKSSTTQSSMAQAENWVLCRIFLKKRGTKNDEEM | 180 |
| | | ***** | |
| | VviNAC01_Shiraz | MQTNNENRVVQKLRSSRPVFDLFLTRRDDTNLASSNSSGSSGITEVSNTESEEHHEESS | 240 |
| | VviNAC01_Reference | MQTNNENRVVQKLRSSRPVFDLFLTRRDDTNLASSNSSGSSGITEVSNTESEEHHEESS | 240 |
| | | ***** | |
| | VviNAC01_Shiraz | CNSFSPFRKPK | 251 |
| | VviNAC01_Reference | CNSFSPFRKPK | 251 |
| | | ***** | |

B

| | | |
|--------------------|--|-----|
| VviNAC08_Shiraz | MTAELQLPPGFRFHPTDEELVMHYLCRKCASQSIAPVPIAEIDLYKFDPWQLPEMALYGE | 60 |
| VviNAC08_Reference | MTAELQLPPGFRFHPTDEELVMHYLCRKCASQSIAPVPIAEIDLYKFDPWQLPEMALYGE | 60 |
| ***** | | |
| VviNAC08_Shiraz | KEWYFFSPDRKYPNGSRPNRAAGTYWKATGADKPIGHPKPVGIKKALVYFAGKAPRGE | 120 |
| VviNAC08_Reference | KEWYFFSPDRKYPNGSRPNRAAGTYWKATGADKPIGHPKPVGIKKALVYFAGKAPRGE | 120 |
| ***** | | |
| VviNAC08_Shiraz | KTNWIMHEYRLADVDRSARKKNSLRLLDDWVLCRIYNKKGIVEKQHTAARKSDCSDVEDQ | 180 |
| VviNAC08_Reference | KTNWIMHEYRLADVDRSARKKNSLRLLDDWVLCRIYNKKGIVEKQHTAARKSDCSDVEDQ | 180 |
| ***** | | |
| VviNAC08_Shiraz | KPGPLALSRKVGAMPPPPSSSTAPTATAALDDLVIYFSSSDSVPRLHTDSSCEHVVSP | 240 |
| VviNAC08_Reference | KPGPLALSRKVGAMPPPPSSSTAPTATAALDDLVIYFSSSDSVPRLHTDSSCEHVVSP | 240 |
| ***** | | |
| VviNAC08_Shiraz | EFTCEREVQSEPKWKEWENPMDFSYNYMDATVDNAFLSQFPNNQMSPLQDMFMYLQKPF | 299 |
| VviNAC08_Reference | EFTCEREVQSEPKWKEWENPMDFSYNYMDATVDNAFLSQFPNNQMSPLQDMFMYLQKPF | 299 |
| ***** | | |

C

| | | |
|--------------------|---|-----|
| VviNAC15_Shiraz | MKVTVGDSPPCFDGEKSAWPPGFRFHPTDEELVLYLKKKICRRRLKLDIAEVDVYKW | 60 |
| VviNAC15_Reference | MKVTVGDSPPCFDGEKSAWPPGFRFHPTDEELVLYLKKKICRRRLKLDIAEVDVYKW | 60 |
| ***** | | |
| VviNAC15_Shiraz | DPEDLPGLSKLKTGDRQWFFSPDRKYPNGARSNRATRHGYWKATGKDRITISCNIRSVG | 120 |
| VviNAC15_Reference | DPEDLPGLSKLKTGDRQWFFSPDRKYPNGARSNRATRHGYWKATGKDRITISCNIRSVG | 120 |
| ***** | | |
| VviNAC15_Shiraz | VKKTLVFYKGRAPSKERTDWMHEYTMDEEELKRCFNVQDYALYKVFKKSGPGKNGEQ | 180 |
| VviNAC15_Reference | VKKTLVFYKGRAPSKERTDWMHEYTMDEEELKRCFNVQDYALYKVFKKSGPGKNGEQ | 180 |
| ***** | | |
| VviNAC15_Shiraz | YGAPFKEEWADEDLDVSNYSVEETPPEQLNGVISVNNKPNQDCCQADAWDDIWKGLA | 240 |
| VviNAC15_Reference | YGAPFKEEWADEDLDVSNYSVEETPPEQLNGVISVNNKPNQDCCQADAWDDIWKGLA | 240 |
| ***** | | |
| VviNAC15_Shiraz | EAPPVPLRVDDYVNLQAQVIGEEEAQPLVDSSLNGAFVADPISTVLTPTSQQYAVPEN | 300 |
| VviNAC15_Reference | EAPPVPLRVDDYVNLQAQVIGEEEAQPLVDSSLNGAFVADPISTVLTPTSQQYAVPEN | 300 |
| ***** | | |
| VviNAC15_Shiraz | VEFTQSASSQLLHEAPEVTSAPNISEQERGLSEEDFLEMDDLGPPEIPQNYEKTEENL | 360 |
| VviNAC15_Reference | VEFTQSASSQLLHEAPEVTSAPNISEQERGLSEEDFLEMDDLGPPEIPQNYEKTEENL | 360 |
| ***** | | |
| VviNAC15_Shiraz | QFE D GLS R LDLYHDAAMFLRDI G IDQGTVPHPYLNTIENEMVNQLNYQLQPHSVGADQ | 420 |
| VviNAC15_Reference | QFE D GLS R LDLYHDAAMFLRDI G IDQGTVPHPYLNTIENEMVNQLNYQLQPHSVGADQ | 420 |
| ***_***_*:***** | | |
| VviNAC15_Shiraz | ISGQLWTLQDQSVCTSAESIQQIGIIGQPTSGVVYASSSTNVPTTEGNQNMNGEGGNGAGNRF | 480 |
| VviNAC15_Reference | ISGQLWTLQDQSVCTSAESIQQIGIIGQPTSGVVYASSSTNVPTTEGNQNMNGEGGNGAGNRF | 480 |
| ***** | | |
| VviNAC15_Shiraz | SALWSFVESIPTTPASASENALVNRALVRMSSFSRMRMNAINTNAGNGGAATWKGGINNG | 540 |
| VviNAC15_Reference | SALWSFVESIPTTPASASENALVNRALVRMSSFSRMRMNAINTNAGNGGAATWKGGINNG | 540 |
| ***** | | |
| VviNAC15_Shiraz | GFIIILSVIGALIAIFWVLMGFPVKMLGRCLPS | 572 |
| VviNAC15_Reference | GFIIILSVIGALIAIFWVLMGFPVKMLGRCLPS | 572 |
| ***** | | |

D

| | | |
|--------------------|--|-----|
| VviNAC17_Shiraz | MGVPETDPLSQLSLPPGFRFYPTDEELLVQYLCKRVAGQGFSLIIEIDLYKFDPWVLP | 60 |
| VviNAC17_Reference | MGVPETDPLSQLSLPPGFRFYPTDEELLVQYLCKRVAGQGFSLIIEIDLYKFDPWVLP | 60 |
| ***** | | |
| VviNAC17_Shiraz | SKAIFGEKEWYFFSPDRKYPNGSRPNRVAGSGYWKATGTDKVIITTEGRKVGIKKALVYF | 120 |
| VviNAC17_Reference | SKAIFGEKEWYFFSPDRKYPNGSRPNRVAGSGYWKATGTDKVIITTEGRKVGIKKALVYF | 120 |
| ***** | | |
| VviNAC17_Shiraz | VGKAPKGTKTNWIMHEYRLLENSRKNKSSKLDWVLCRIYKKNNSNKKPIAAVLPKSAHS | 180 |
| VviNAC17_Reference | VGKAPKGTKTNWIMHEYRLLENSRKNKSSKLDWVLCRIYKKNNSNKKPIAAVLPKSAHS | 180 |
| ***** | | |
| VviNAC17_Shiraz | NGSSSSSSHLDDVLESLEIDDRFFSPNRMNSLRVSPDEKVNFNHNLGSGNFDWATLAG | 240 |
| VviNAC17_Reference | NGSSSSSSHLDDVLESLEIDDRFFSPNRMNSLRVSPDEKVNFNHNLGSGNFDWATLAG | 240 |
| ***** | | |
| VviNAC17_Shiraz | VSSLQELVSGVQSHAQPPAAVNNSEMYVPSLPLIQAEIEEVQSGRLTRQVDPVMNQGF | 300 |
| VviNAC17_Reference | VSSLQELVSGVQSHAQPPAAVNNSEMYVPSLPLIQAEIEEVQSGRLTRQVDPVMNQGF | 300 |
| ***** | | |
| VviNAC17_Shiraz | PQNSNAFSQSFNSLDPFGFRYPTQPSGFGYRQ | 333 |
| VviNAC17_Reference | PQNSNAFSQSFNSLDPFGFRYPTQPSGFGYRQ | 333 |
| ***** | | |

| | | | |
|----------|--------------------|--|-----|
| E | VviNAC18_Shiraz | MESTDSSSGSPQPQLPPGFRFHPTDEELVVHYLKKKASSAPLPVAIIAEVDLYKFDWPWL | 60 |
| | VviNAC18_Reference | MESTDSSSGSPQPQLPPGFRFHPTDEELVVHYLKKKASSAPLPVAIIAEVDLYKFDWPWL | 60 |
| | VviNAC18_Shiraz | PAKASFGEQEWYFFSPRDRKYPNGARPNRAATSGYWKATGTDKPVLTSGGTQKVGKVKAL | 120 |
| | VviNAC18_Reference | PAKASFGEQEWYFFSPRDRKYPNGARPNRAATSGYWKATGTDKPVLTSGGTQKVGKVKAL | 120 |
| | VviNAC18_Shiraz | VFYGGKPPKGIKTNWIMHEYRLADNKVNTKPPGCDMGKNKNSLRLLDDWVLCRIYKKNNTH | 180 |
| | VviNAC18_Reference | VFYGGKPPKGIKTNWIMHEYRLADNKVNTKPPGCDMGKNKNSLRLLDDWVLCRIYKKNNTH | 180 |
| | VviNAC18_Shiraz | RTLDPDKDDSMDDMLGPVPSISMGQQSLKQFPKVPNYSALLENEQSLFEGMINSGIN | 240 |
| | VviNAC18_Reference | RTLDPDKDDSMDDMLGPVPSISMGQQSLKQFPKVPNYSALLENEQSLFEGMINSGIN | 240 |
| | VviNAC18_Shiraz | SSGTISQLACSSSKPDHLSVAATTSSILPLKRTLPSLYWDDDTAGPSTTKRFQAENTD | 300 |
| | VviNAC18_Reference | SSGTISQLACSSSKPDHLSVAATTSSILPLKRTLPSLYWDDDTAGPSTTKRFQAENTD | 300 |
| | VviNAC18_Shiraz | GNIGRTTDGNNSIATLLSQLPQTPSLHQQSMGLGSLGEGVFRQPFQPLFGMNWYA 353 | |
| | VviNAC18_Reference | GNIGRTTDGNNSIATLLSQLPQTPSLHQQSMGLGSLGEGVFRQPFQPLFGMNWYA 353 | |
| F | VviNAC26_Shiraz | MDGKGSQQLPPGFRFHPTDEELIMYYLKNQATSKPCPVSI IPEVDIYKFEPEWELPEKAEF | 60 |
| | VviNAC26_Reference | MDGKGSQQLPPGFRFHPTDEELIMYYLKNQATSKPCPVSI IPEVDIYKFEPEWELPEKAEF | 60 |
| | VviNAC26_Shiraz | GENEWYFFSPRDRKYPNGARPNRATVSGYWKATGTDKAIYSGAKYGVKVKALVFYKGRPP | 120 |
| | VviNAC26_Reference | GENEWYFFSPRDRKYPNGARPNRATVSGYWKATGTDKAIYSGAKYGVKVKALVFYKGRPP | 120 |
| | VviNAC26_Shiraz | KGIKTDWIMHEYRLSDSRPRPKKHNGSMRLDDWVLCRIYKHKHVGRILEEKEENLGPQIP | 180 |
| | VviNAC26_Reference | KGIKTDWIMHEYRLSDSRPRPKKHNGSMRLDDWVLCRIYKHKHVGRILEEKEENLGPQIP | 180 |
| | VviNAC26_Shiraz | VTNSDDGGEQHVKFPRFTSLAHLDDMEYLGPIISQLLDGNSYHSAPDFQGTISNIAGTDP | 240 |
| | VviNAC26_Reference | VTNSDDGGEQHVKFPRFTSLAHLDDMEYLGPIISQLLDGNSYHSAPDFQGTISNIAGTDP | 240 |
| | VviNAC26_Shiraz | PGVDKFELFQLPCQYNDSTKQVQVNHIPNQPLFVNPVYEFQ | 282 |
| | VviNAC26_Reference | PGVDKFELFQLPCQYNDSTKQVQVNHIPNQPLFVNPVYEFQ | 282 |
| G | VviNAC38_Shiraz | MMGKGSKNCSASHKMFKDKAKNRVDDLQGMFTDLQSARKESSRVDVAVLEEQLHQMLR | 60 |
| | VviNAC38_Reference | MMGKGSKNCSASHKMFKDKAKNRVDDLQGMFTDLQSARKESSRVDVAVLEEQLHQMLR | 60 |
| | VviNAC38_Shiraz | EWKAELENEPSPASSLQGGSLGFSFSDICRLLQLCEEEDDATSALADGAVPKPEPDAQGHQ | 120 |
| | VviNAC38_Reference | EWKAELENEPSPASSLQGGSLGFSFSDICRLLQLCEEEDDATSALADGAVPKPEPDAQGHQ | 120 |
| | VviNAC38_Shiraz | IGASVLFQERYNKGPQEHGFQLVDQCKISPSGAHNMGVHNLEGATQLDYRQFDLQDFEQ | 180 |
| | VviNAC38_Reference | IGASVLFQERYNKGPQEHGFQLVDQCKISPSGAHNMGVHNLEGATQLDYRQFDLQDFEQ | 180 |
| | VviNAC38_Shiraz | NFFAGYDGTGLCGEDAMPHISSFLPSICLPPSAFLGPKCALWDCPRPAQGMDCQNYCSS | 240 |
| | VviNAC38_Reference | NFFAGYDGTGLCGEDAMPHISSFLPSICLPPSAFLGPKCALWDCPRPAQGMDCQNYCSS | 240 |
| | VviNAC38_Shiraz | FHATLALSEGPPGMTPVLRPGGIGLKDGLLFAALSAKVQGDVGIPECEGAATAKSPWNA | 300 |
| | VviNAC38_Reference | FHATLALSEGPPGMTPVLRPGGIGLKDGLLFAALSAKVQGDVGIPECEGAATAKSPWNA | 300 |
| | VviNAC38_Shiraz | PELFDLSVLEGETIREWLFFDKPRRAFESGNRQQRSLPDYSGRGWHESRKQVMNEYGGGLK | 360 |
| | VviNAC38_Reference | PELFDLSVLEGETIREWLFFDKPRRAFESGNRQQRSLPDYSGRGWHESRKQVMNEYGGGLK | 360 |
| | VviNAC38_Shiraz | RSYYMDPQPLNHFWEHLYEYEISKCDACALYRLELKLVDGKKS KAKATTSV | 420 |
| | VviNAC38_Reference | RSYYMDPQPLNHFWEHLYEYEISKCDACALYRLELKLVDGKKS KAKATTSV | 413 |
| | VviNAC38_Shiraz | GRLTAEFPFTMMGKGSKAKATTSV | 480 |
| | VviNAC38_Reference | ADLQKQMGRLTAEFPPLDNKRSVKGRTRKINMKDGVG | 448 |
| | VviNAC38_Shiraz | DVYSTPNRVGPPNQGDYGVGGPYDYLVENLGDYYLT | 517 |
| | VviNAC38_Reference | DVYSTPNRVGPPNQGDYGVGGPYDYLVENLGDYYLT | 485 |

| | | | |
|--------------------|---|--|---|
| H | VviNAC39_Shiraz | MMSGDQLQLPAGFRFHPTDEELVVHYLVRKCASQSI SVPI IAEVDLYKYDPWQLPGMALY | 60 |
| | VviNAC39_Reference | MMSGDQLQLPAGFRFHPTDEELVVHYLVRKCASQSI SVPI IAEVDLYKYDPWQLPGMALY | 60 |
| | VviNAC39_Shiraz | GEKEWYFFSPRDRYINGSRPNRAAGSGYWKATGADKPIGRPKTVGIKKALVYAGKAPR | 120 |
| | VviNAC39_Reference | GEKEWYFFSPRDRYINGSRPNRAAGSGYWKATGADKPIGRPKTVGIKKALVYAGKAPR | 120 |
| | VviNAC39_Shiraz | GVKTNWIMHEYRLANVDRSAGKKNLRLDDDWLVCRIYNKKGSAEKQHTFDKSMKYPELE | 180 |
| | VviNAC39_Reference | GVKTNWIMHEYRLANVDRSAGKKNLRLDDDWLVCRIYNKKGSAEKQHTFDKSMKYPELE | 180 |
| | VviNAC39_Shiraz | DQKPKIISTVQKIVPSSLPGLPMPAPPTNDYLYFETS DSV PRLHTHTDSSGSEQVMS | 240 |
| | VviNAC39_Reference | DQKPKIISTVQKIVPSSLPGLPMPAPPTNDYLYFETS DSV PRLHTHTDSSGSEQVMS | 240 |
| | VviNAC39_Shiraz | PEKEVQSEPKWNDFDFSLYMDGFANDPFASQAQFSGDLLTSSWQDMLMFSNKSF | 294 |
| | VviNAC39_Reference | PEKEVQSEPKWNDFDFSLYMDGFANDPFASQAQFSGDLLTSSWQDMLMFSNKSF | 294 |
| | VviNAC39_Reference | *****:***** | |
| | I | VviNAC61_Shiraz | MEEASLADQGDLDLPPGFRFHPTDEEIIISYLTERRVMNSSFSARAIGEVDLNKCEPWD |
| VviNAC61_Reference | | MEEASLADQGDLDLPPGFRFHPTDEEIIISYLTERRVMNSSFSARAIGEVDLNKCEPWD | 60 |
| VviNAC61_Shiraz | | LPKKAKMGEKEWYFFCQRDRKYPTGMRTNRATESGYWKATGKDKEIYKGGKGLVGMKCTL | 120 |
| VviNAC61_Reference | | LPKKAKMGEKEWYFFCQRDRKYPTGMRTNRATESGYWKATGKDKEIYKGGKGLVGMKCTL | 120 |
| VviNAC61_Shiraz | | VFYRGRAPKGEKSNWVMHEYRLGKFSYYNLPKAAKDEWVVCVRFHKSAGIKRSLIPAPI | 180 |
| VviNAC61_Reference | | VFYRGRAPKGEKSNWVMHEYRLGKFSYYNLPKAAKDEWVVCVRFHKSAGIKRSLIPAPI | 180 |
| VviNAC61_Shiraz | | RMNSFGDDLDCSSLPPLIDPPYSNPKNKNDSCFTNGEDEFKGSSTRFSDGNHHYPYFSP | 240 |
| VviNAC61_Reference | | RMNSFGDDLDCSSLPPLIDPPYSNPKNKNDSCFTNGEDEFKGSSTRFSDGNHHYPYFSP | 240 |
| VviNAC61_Shiraz | | INGHQLQKQDQKSFLLSPNNVHTTSNYQATLSNPTPNSIFYPQVSPSNPLFPFQASPTP | 300 |
| VviNAC61_Reference | | INGHQLQKQDQKSFLLSPNNVHTTSNYQATLSNPTPNSIFYPQVSPSNPLFPFQASPTP | 300 |
| VviNAC61_Shiraz | | SYSHWQMGSSFPSPFGSGFKGSDPTSTVRAQTSQVQRQCKVEQFSSNQSMVSLSDQTGLS | 360 |
| VviNAC61_Reference | | SYSHWQMGSSFPSPFGSGFKGSDPTSTVRAQTSQVQRQCKVEQFSSNQSMVSLSDQTGLS | 360 |
| VviNAC61_Shiraz | TDMNTEISSVLSKHQDTGNRRSYEDLQGPSVGQIGDLDYLLDY 403 | | |
| VviNAC61_Reference | TDMNTEISSVLSKHQDTGNRRSYEDLQGPSVGQIGDLDYLLDY 403 | | |
| VviNAC61_Reference | *****:***** | | |

Figure 22: Alignments of (A) *VviNAC01*, (B) *VviNAC08*, (C) *VviNAC15*, (D) *VviNAC17*, (E) *VviNAC18*, (F) *VviNAC26*, (G) *VviNAC38*, (H) *VviNAC39* and (I) *VviNAC61* aminoacids sequences from Shiraz and Pinot Noir cultivars.

Transient over expression of the selected *VviNACs* in grapevine

To elucidate the functions of *VviNAC01*, *VviNAC08*, *VviNAC15*, *VviNAC17*, *VviNAC18*, *VviNAC26*, *VviNAC38*, *VviNAC39* and *VviNAC61*, a transient over expression of the nine selected *VviNACs* was performed directly in the native species (*V. vinifera* cv. Sultana), avoiding possible problems that may occur with gene expression in heterologous systems. In this way an overview on the putative primary effects of these TFs on grapevine leaf transcriptome was obtain. For each *VviNAC* factor, by vacuum *Agrobacterium*-mediated infection six young *in vitro* grown grapevine plantlets were transfected. Other six plantlets were transformed with the same vector containing a non-coding sequence (control). Agroinfiltrated plants were screened for their over expression through qPCR Real Time analyses

and the three plantlets with the highest transcript amount of transgene, in comparison with their respective *VviNAC* expression level in the three control lines, were selected (**Fig.23**).

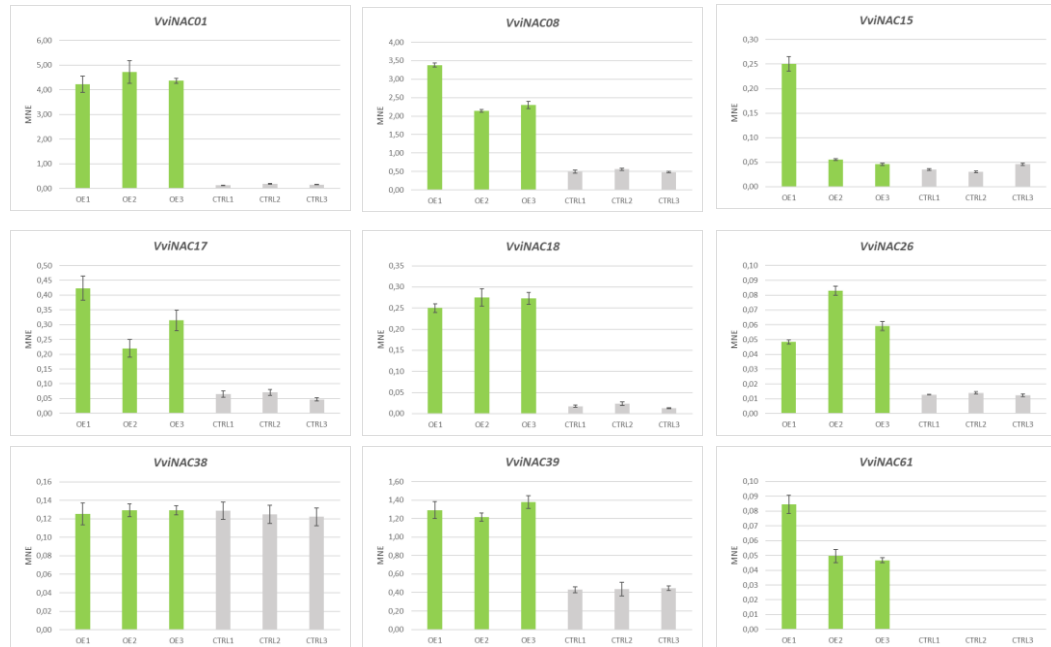


Figure 23: qPCR analysis of *VviNACs* expression level in transiently over expressing leaves and control. Each expression value corresponds to the mean \pm standard deviation (SD) of three technical replicates relative to the *VviUBIQUITIN1* (VIT_16s0098g01190) control.

Unfortunately, *VviNAC15* over expression produced only one over expressing plantlet and concerning the *VviNAC38* one no plantlet at all was transfected. The two over expressions will be performed again in the future but, meanwhile, the only *VviNAC15* over expressing plantlet was used for the further analysis. All the *VviNACs* transiently over expressed grapevine plantlets were collected and used for microarray transcriptomic analyses.

Microarray transcriptomic analyses of the selected *VviNACs*

To gain information about the impact of the ectopic expression of the selected *VviNACs* on the leaf transcriptome and to identify the possible targets of these TFs, microarray analyses were performed on the leaf RNA of the selected lines. T-test analyses were carried out with a p correlation value of 0.05 (TMeV 4.3), comparing the over expressing *VviNACs* samples with the control lines. Considering a |fold

change| > 1.5 and eliminating all the ‘no hit’ and ‘unknow’ annotated genes, up and down regulated genes were identified; these filtered DEGs were annotated using V1 version of the 12X draft annotation of the grapevine genome. Comparing the DEGs lists with the co-expressed genes one, only 2, 9, 39, 5, 48, 86, 6 and 68 genes were found in common for *VviNAC01*, *VviNAC08*, *VviNAC15*, *VviNAC17*, *VviNAC18*, *VviNAC26*, *VviNAC39* and *VviNAC61*, respectively (**Fig. 24**).

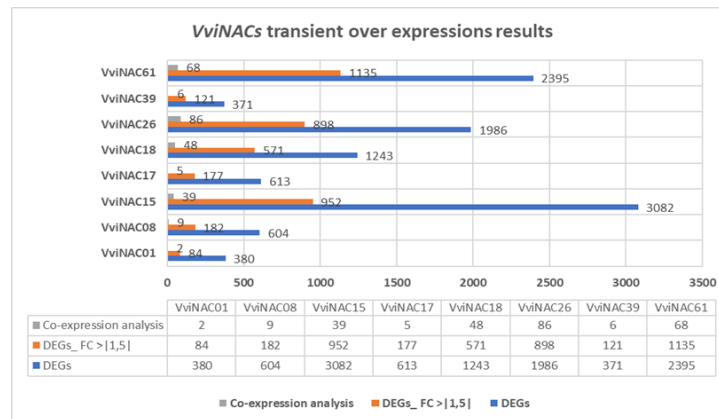


Figure 24: Summary of the general results of the *VviNACs* transient over expression, integrated with the co-expression datasets.

In detail, in the FC>|1.5| DEGs lists were identified 62, 30, 642, 37, 224, 538, 35 and 338 up regulated genes and 22, 152, 310, 140, 347, 360, 86 and 797 down regulated genes regarding *VviNAC01*, *VviNAC08*, *VviNAC15*, *VviNAC17*, *VviNAC18*, *VviNAC26*, *VviNAC39* and *VviNAC61*, respectively (**Fig. 25**). The long DEGs lists represent a good starting point to investigate the hypothetical *VviNACs* targets and to elucidate the role of the transcription factors in a specific regulatory network.

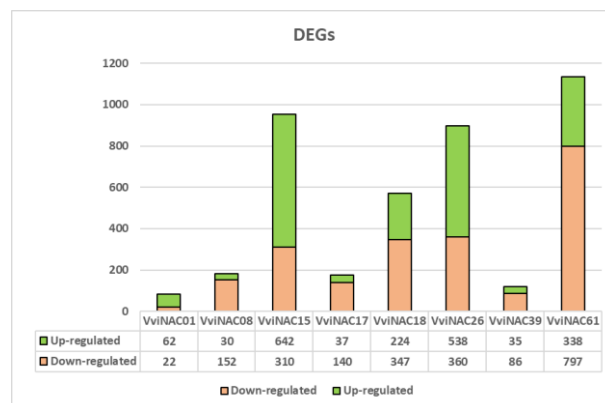


Figure 25: Summary of the number of DEGs, divided into up- and down-regulated, of the *VviNACs* transient over expression.

GO enrichment analyses, divided into two gene sub-groups (up and down regulated) were performed on the DEGs obtained by the over expression of each of the eight *VviNACs* (**Appendix C**).

VviNAC01 over expression up regulated genes were mainly enriched in regulation of biosynthetic and metabolic processes categories but were also found genes concerning the aromatic and organic compound biosynthesis and the calcium transport; among the down regulated DEGs, many genes regarding the response regulation to different type of stress and stimuli resulted enriched.

The most relevant information obtained from the *VviNAC01* over expression was related to the up regulated genes (**Table 12**). At the first place *LIPASE CLASS 3* (VIT_10s0003g04210) was found, which is part of the triacylglycerol lipase family involved in lipid degradation, esterification, and transesterification processes in plants (Nurniwalis *et al.*, 2015). It is indeed well known that the cuticular wax of the grape berries, which is chemically a mixture of long-chain alcohols, esters of such alcohols and fatty acids, free fatty acids, long-chain aldehydes, and hydrocarbons (Grncarevic *et al.*, 1971), is the main barrier to the evaporation of water. Analyses on the grape berry lipid profiles revealed that there is a very high number of double bonds in a fatty acid molecule in skins and juices, which suddenly affect the production of volatile compounds (Arita *et al.*, 2017). For example, linoleic acid is the major components in *V. vinifera* berry and C6 and C9 aldehydes, important volatiles responsible for the 'green aroma' in berry and wine, are generated from it by oxidative cleavage (Arita *et al.*, 2017).

ETHYLENE-RESPONSIVE TRANSCRIPTION FACTOR 9 (VIT_12s0028g03270) was also found between the top 20 up regulated genes.

Another important family found between the up regulated genes is the one of *ERF/AP2*, which was represented by 9 different genes (VIT_16s0013g01050, VIT_16s0013g01060, VIT_16s0013g01030, VIT_16s0013g01000, VIT_16s0013g01070, VIT_16s0013g00990, VIT_16s0013g00980, VIT_16s0013g00900 and VIT_16s0013g00950). The *APETALA 2/ETHYLENE-RESPONSIVE ELEMENT BINDING FACTOR (AP2/ERF)* family is a large group of plant-specific transcription factors involved in plant abiotic stress such as drought, salinity and high temperatures (Mizoi *et al.*, 2012). Traditionally, the

expression of ERF genes has been associated with the molecular response to ethylene and therefore have been suggested as being involved in the ripening process in climacteric fruits; grape is a non-climacteric fruit, but ethylene still plays an important role during development and ripening processes such as anthocyanin accumulation and alcohol dehydrogenase expression (Licausi *et al.*, 2010). Moreover, 149 *ERF/AP2* genes were identified in the grape genome and characterized by their expression patterns in aerial vegetative, inflorescence and berry skin and flesh at two different ripening stages, *veraison* and full ripening (Licausi *et al.*, 2010).

| Gene ID | Functional annotation | FC | Gene ID | Functional annotation | FC |
|-------------------|--|-------|-------------------|---|-------|
| VIT_10s0003g04210 | Lipase class 3 | 21.62 | VIT_11s0052g01570 | MATE efflux family protein | -2.15 |
| VIT_16s0013g01050 | ERF/AP2 Gene Family (VvERF107) | 10.38 | VIT_07s0005g02030 | Lipase GD5L | -2.14 |
| VIT_16s0013g01060 | ERF/AP2 Gene Family (VvERF108) | 10.07 | VIT_08s0007g00570 | WRKY Transcription Factor (VvWRKY27) | -1.96 |
| VIT_12s0134g00240 | Avr9/Cf-9 rapidly elicited protein 20 | 9.97 | VIT_15s0046g01700 | Chitinase, class III | -1.86 |
| VIT_06s0080g00170 | Aluminium-tolerance ALMT1 | 8.09 | VIT_14s0081g00400 | Ankyrin repeat | -1.83 |
| VIT_16s0013g01030 | ERF/AP2 Gene Family (VvERF106) | 7.68 | VIT_13s0156g00450 | R protein disease resistance protein | -1.77 |
| VIT_03s0063g00370 | Nitrite reductase | 7.62 | VIT_19s0014g03770 | Retrotransposon | -1.75 |
| VIT_16s0013g01000 | ERF/AP2 Gene Family (VvERF084) | 6.41 | VIT_18s0001g15410 | Alcohol dehydrogenase 1 | -1.73 |
| VIT_16s0013g01070 | ERF/AP2 Gene Family (VvERF085) | 6.27 | VIT_18s0117g00360 | R protein L6 | -1.65 |
| VIT_16s0013g00990 | ERF/AP2 Gene Family (VvERF105) | 6.25 | VIT_08s0007g00130 | Heat shock protein 70 | -1.64 |
| VIT_03s0063g01790 | Transducin protein | 5.81 | VIT_10s0092g00380 | Multidrug resistance-associated protein 3 | -1.63 |
| VIT_16s0013g00980 | ERF/AP2 Gene Family (VvERF082) | 5.64 | VIT_09s0002g06730 | Longin | -1.60 |
| VIT_12s0028g03270 | Ethylene-responsive transcription factor 9 | 5.48 | VIT_14s0108g01270 | Cyclin-dependent kinase CDC2C | -1.58 |
| VIT_16s0013g00900 | ERF/AP2 Gene Family (VvERF079) | 5.27 | VIT_18s0001g10850 | Patatin | -1.56 |
| VIT_16s0013g00950 | ERF/AP2 Gene Family (VvERF080) | 5.00 | VIT_18s0001g10910 | Patatin | -1.56 |
| VIT_12s0028g03010 | Glutaredoxin | 4.05 | VIT_13s0067g01880 | Other LOB domain-containing protein ASL5 | -1.56 |
| VIT_09s0002g03220 | Acid phosphatase | 3.79 | VIT_02s0033g00700 | Nitrilase | -1.55 |
| VIT_12s0034g00270 | R protein L6 | 3.52 | VIT_18s0001g03710 | R protein L6 | -1.54 |
| VIT_15s0024g00400 | R protein MLA10 | 3.25 | VIT_14s0108g00270 | Aldose 1-epimerase | -1.53 |
| VIT_10s0116g01390 | F-box family protein | 3.00 | VIT_17s0000g07450 | Glycerophosphoryl diester phosphodiesterase | -1.52 |

Table 12: *VviNAC01* (A) top 20 up-regulated and (B) top 20 down-regulated DEGs.

VviNAC08 GO enrichment analysis showed phosphorus metabolic processes and transport as significantly enriched gene categories for the up regulated genes and presented a high number of down regulated gene involved in the regulation of the response to salicylic acid, organic compounds and hydrogen peroxide; moreover, a very represented gene category was the cyanide metabolic/catabolic processes one, which is related to the ethylene production. Looking at the up and down regulated genes found in the *VviNAC08* over expressing plants transcriptome, an *ACID PHOSPHATASE* (VIT_09s0018g01800) and *TRANSCRIPTION FACTOR JUMONJI (JMJC) DOMAIN-CONTAINING PROTEIN* (VIT_00s0179g00180) were found in the first places, respectively (**Table 13**).

Acid phosphatases catalyze the hydrolysis of phosphate, an essential but limiting macronutrient important for plant metabolism and development; it is a key structural constituent of important biomolecules such as ATP, NADPH, nucleic

acids, phospholipids, and sugar-phosphates (Tran *et al.*, 2010).

Gibberellins are well known for their growth control function in fruit and seed development and exogenous gibberellic acid (GA) application plays an important role in viticulture. In a recent study was demonstrated that application of GA to grapevine inflorescences at pre-bloom promoted flower opening, and induced fruit coloring and seed abortion; GA treatment brought to the up regulation of genes encoding acid phosphatase (Cheng *et al.*, 2015).

Instead, a subgroup of JmjC domain-containing proteins were identified in *Arabidopsis thaliana* as a novel clock component involved in controlling the circadian period, in particular affecting the flowering phenotypes (Lu *et al.*, 2011).

| Gene ID | Functional annotation | FC | Gene ID | Functional annotation | FC |
|-------------------|--|------|-------------------|---|-------|
| VIT_09s0018g01800 | Acid phosphatase | 5.34 | VIT_00s0179g00180 | Transcription factor jumoni (jmc) domain-containing protein | -7.54 |
| VIT_14s0066g01210 | Carbonic anhydrase, chloroplast precursor | 2.86 | VIT_05s0094g00330 | Chitinase, class IV [Vitis vinifera] | -3.61 |
| VIT_14s0066g00850 | Nitrate transporter2.5 | 2.77 | VIT_09s0070g00350 | R protein disease resistance protein | -3.44 |
| VIT_07s0031g00920 | Inositol-3-phosphate synthase | 2.33 | VIT_04s0008g01860 | CYP72A58 | -3.43 |
| VIT_11s0016g02350 | Ubiquinone/menaquinone biosynthesis methyltransferase UbiE | 2.18 | VIT_00s0125g00150 | SHR5-receptor-like kinase | -3.34 |
| VIT_15s0046g02390 | ANR2 (anion transporter 2) | 2.03 | VIT_03s0017g01360 | UDP-glycosyltransferase 85A8 | -3.20 |
| VIT_05s0020g04110 | EUIP1 (early light-inducible protein) | 2.02 | VIT_14s0030g02060 | Aldo/keto reductase AKR | -3.19 |
| VIT_17s0000g04030 | Endonuclease | 1.88 | VIT_04s0023g02790 | Dehydration-responsive protein | -3.15 |
| VIT_03s0038g04210 | Phototropin-2 | 1.81 | VIT_16s0022g02230 | Leucine-rich repeat receptor protein kinase EXS | -3.05 |
| VIT_08s0040g03240 | Pentatricopeptide (PPR) repeat | 1.79 | VIT_16s0039g01370 | (9,10) (9',10') cleavage dioxygenase (CCD4) (VvCCD4c) | -3.00 |
| VIT_16s0050g00990 | ferric reduction oxidase 4 | 1.76 | VIT_12s0028g01830 | Peroxidase precursor | -2.86 |
| VIT_18s0001g12510 | 5' nucleotidase | 1.74 | VIT_14s0030g01990 | Perakine reductase aldo/keto reductase | -2.81 |
| VIT_09s0002g02430 | ABC Transporter (VvMRP8 - VvABCC8) | 1.70 | VIT_15s0024g01650 | Glutathione S-transferase 8 GSTU8 | -2.79 |
| VIT_13s0019g02110 | fringe-related protein | 1.69 | VIT_14s0081g00350 | Ankyrin repeat | -2.78 |
| VIT_07s0005g02470 | Cellulose synthase CESA3 | 1.66 | VIT_10s0003g04250 | Glutathione S-transferase GSTU22 | -2.76 |
| VIT_01s0026g01710 | Zinc knuckle | 1.66 | VIT_19s0015g02470 | Zinc finger (C3HC4-type ring finger) | -2.74 |
| VIT_02s0012g01240 | PHD finger transcription factor | 1.62 | VIT_11s0118g00040 | Receptor Like Protein 9 | -2.73 |
| VIT_07s0031g02160 | Protein phosphatase 2C DBP | 1.61 | VIT_08s0040g02600 | F-box protein | -2.63 |
| VIT_17s0000g06610 | Zinc finger (C3HC4-type ring finger) | 1.61 | VIT_02s0025g04890 | CYP76B1 | -2.63 |

Table 13: VviNAC08 (A) top 20 up-regulated and (B) top 20 down-regulated DEGs.

VviNAC15 over expression up regulated genes were mainly enriched in metabolic, catabolic processes and transport categories; among the down regulated were found may genes related to the response to hormones and to protein catabolic processes.

In the up regulated genes list of the VviNAC15 over expression transcriptome, at the first place the *SEVEN IN ABSENTIA SINA5* (VIT_19s0014g00880) was found (Table 14). A recent study on a parthenocarpic somatic variant of a seeded cultivar found that a polymorphism on the *SEVEN-IN-ABSENTIA SINA5* (VIT_02s0025g01660) gene was the one potentially responsible for its parthenocarpic phenotype (Rojo *et al.*, 2016).

Many up regulated *GERMININ-LIKE PROTEIN 3* genes (VIT_14s0128g00540, VIT_14s0128g00660, VIT_14s0128g00610 and VIT_14s0128g00630) were also found. Germin and germin-like proteins (GLPs) constitute a ubiquitous family of plant proteins. They were first discovered in wheat seeds as specific markers of

germination but *GLPs* genes are expressed in all types of organs including leaves, cotyledons, stems, roots, embryos, flowers and seeds, and are involved in the developmental processes (Lu *et al.*, 2010). Moreover, recent studies revealed a close connection between *GLPs* genes and disease resistance phenotypes and the mechanism by which *GLPs* influence plant defense is likely related to ROS (reactive oxygen species) production (Li *et al.*, 2016).

As for *VviNAC08* over expression, a *TRANSCRIPTION FACTOR JUMONJI (JMJC) DOMAIN-CONTAINING PROTEIN* (VIT_00s0179g00180) was found down regulated also in *VviNAC15* DEGs list.

Fruit ripening involves the regulation of numerous biochemical pathways associated with pigmentation, cell wall metabolism, and the production of aromatic and nutritionally important compounds but, additionally, ripening is also characterized by a major increase in susceptibility to necrotrophic pathogens (Wang *et al.*, 2017).

Knowing that the regulatory networks that contribute to fruit ripening are almost always associated with disease resistance, finding *R protein MLA10* (VIT_09s0002g08020) gene as the most down regulated was not strange. Indeed, *MLA10* activity in disease resistance and cell death signalling was already demonstrated in barley and *Nicotiana benthamiana* (Bai *et al.*, 2012).

| Gene ID | Functional annotation | FC | Gene ID | Functional annotation | FC |
|-------------------|--|--------|-------------------|---|--------|
| VIT_19s0014g00880 | Seven in absentia SINA5 | 122.25 | VIT_09s0002g08020 | R protein MLA10 | -10.40 |
| VIT_03s0088g00560 | Citrate synthase | 25.81 | VIT_13s0047g00230 | Pectinesterase family | -9.33 |
| VIT_14s0128g00570 | Germin | 24.41 | VIT_10s0092g00240 | Alpha-glucosidase 1 (AGLU1) | -8.73 |
| VIT_08s0007g05100 | Glycosyl hydrolase family 31 protein | 19.95 | VIT_19s0014g02900 | Ring finger protein 185 | -7.38 |
| VIT_14s0128g00540 | Germin-like protein 3 [Vitis vinifera] | 18.98 | VIT_04s0069g00510 | WD-40 repeat family protein / beige-related | -6.31 |
| VIT_03s0063g01290 | Gibberellin 20 oxidase 2 | 16.92 | VIT_02s0025g02610 | basic helix-loop-helix (bHLH) family | -5.81 |
| VIT_14s0128g00680 | Germin | 16.50 | VIT_16s0022g00860 | Invertase/pectin methyltransferase inhibitor | -5.41 |
| VIT_13s0064g00750 | Polygalacturonase GH28 | 16.08 | VIT_09s0070g00350 | R protein disease resistance protein | -5.23 |
| VIT_11s0016g04160 | Sulfate transporter 3.5 | 15.55 | VIT_12s0035g00610 | CYP82M1v3 | -4.33 |
| VIT_03s0063g01130 | Nodulin 1A, senescence-associated | 15.14 | VIT_19s0085g00010 | Auxin-regulated protein | -4.19 |
| VIT_03s0063g01280 | Gibberellin 20 oxidase 2 | 14.73 | VIT_14s0081g00370 | Ankyrin repeat | -4.15 |
| VIT_14s0128g00600 | Germin-like protein 3 [Vitis vinifera] | 12.98 | VIT_08s0007g01140 | Esterase/lipase/thioesterase family protein | -4.10 |
| VIT_07s0005g05770 | Tetratricopeptide repeat domain male sterility M55 | 12.82 | VIT_19s0014g01360 | Curculin (mannose-binding) lectin | -4.02 |
| VIT_14s0128g00660 | Germin-like protein 3 [Vitis vinifera] | 12.44 | VIT_19s0014g00440 | PMR5 (powdery mildew resistant 5) | -3.66 |
| VIT_14s0128g00610 | Germin-like protein 3 [Vitis vinifera] | 11.99 | VIT_11s0052g01510 | MATE efflux family protein | -3.61 |
| VIT_14s0128g00630 | Germin-like protein 3 [Vitis vinifera] | 11.80 | VIT_00s0179g00180 | Transcription factor jumonji (JMJC) domain-containing protein | -3.55 |
| VIT_05s0020g03860 | Homocysteine S-methyltransferase 3 | 10.99 | VIT_11s0052g01560 | MATE efflux family protein | -3.51 |
| VIT_14s0066g01290 | Exonuclease | 10.76 | VIT_11s0052g01540 | MATE efflux family protein | -3.50 |
| VIT_11s0052g01650 | Pathogenesis-related protein 1 precursor (PRP 1) | 10.60 | VIT_10s0116g00560 | Polyphenol oxidase II, chloroplast precursor | -3.49 |
| VIT_09s0002g05280 | 2-oxoglutarate-dependent dioxygenase | 10.38 | VIT_06s0004g00070 | Expansin (VvEXPAS) | -3.42 |

Table 14: *VviNAC15* (A) top 20 up-regulated and (B) top 20 down-regulated DEGs.

VviNAC17 over expression brought to a high number of up regulated genes related to the regulation of biosynthetic and primary metabolic processes and to the transmembrane transport, while the down regulated clustered into only two categories: generation of precursor metabolites and energy and oxidation-reduction

processes. *VviNAC17* over expression led to an up regulation of many *VviWRKY* genes (VIT_12s0028g01700, VIT_12s0055g00340 and VIT_12s0028g01690), which are involved in the regulation of various physiological processes, such as development and senescence, and in plant response to many biotic and abiotic stresses (Wang et al., 2014); moreover, they resulted important in regulating vacuolar transport and flavonoid biosynthesis (Amato *et al.*, 2017) (**Table 15**).

Among the *VviNAC17* over expression down regulated genes was found again an *ACID PHOSPHATASE* (VIT_09s0018g01800) but, at the first place, a *STEROID 5ALPHA-REDUCTASE* (VIT_19s0014g00080) was present. *STEROID 5ALPHA-REDUCTASE* inhibition has been already studied in relation to the increase of condensed tannins (Liu *et al.*, 2008). Tannins are a type of bitter and astringent polyphenols that occur abundantly in nature; as natural products in plants, they act as a barrier against insects, pathogens and animals because of their ability to react with proteins and their antioxidant properties. In grapes, condensed tannins are mainly found in the stem, skin, flesh and seeds of the berries (WatreLOT *et al.*, 2020).

| ID | Functional annotation | FC | ID | Functional annotation | FC |
|-------------------|---|------|-------------------|--|-------|
| VIT_14s0108g00630 | Amino acid permease | 2.84 | VIT_19s0014g00080 | Steroid 5alpha-reductase | -3.89 |
| VIT_14s0108g00690 | Amino acid permease | 2.76 | VIT_05s0020g04110 | ELIP1 (early light-inducible protein) | -3.28 |
| VIT_18s0001g11630 | Allene oxide synthase (jasmonates from fatty acids) | 2.63 | VIT_09s0018g01800 | Acid phosphatase | -3.06 |
| VIT_05s0049g00100 | DNA-binding protein | 2.24 | VIT_04s0008g02670 | Cryptochrome DASH | -2.90 |
| VIT_16s0098g00900 | Pseudo-response regulator 5 (APRR5) | 2.19 | VIT_12s0035g02150 | ferric reduction oxidase 7 FRO7 | -2.50 |
| VIT_12s0028g01700 | WRKY DNA-binding protein 65 | 2.14 | VIT_18s0041g01150 | Lectin protein kinase | -2.48 |
| VIT_15s0048g01540 | CYP76B1 | 2.12 | VIT_12s0059g02280 | Spg1p (septum-promoting GTPase) | -2.46 |
| VIT_16s0022g00860 | Invertase/pectin methyltransferase inhibitor | 2.03 | VIT_16s0022g00470 | Peroxisomal biogenesis factor 11 (PEX11) | -2.36 |
| VIT_12s0055g00340 | WRKY Transcription Factor (VvWRKY39) | 1.87 | VIT_13s0156g00090 | Protease inhibitor/seed storage/lipid transfer protein (LTP) | -2.35 |
| VIT_19s0014g01120 | Curculin (mannose-binding) lectin | 1.82 | VIT_19s0015g01720 | fructose-bisphosphate aldolase, cytoplasmic isozyme 1 | -2.30 |
| VIT_01s0011g04790 | 1-phosphatidylinositol-3-phosphate 5-kinase | 1.82 | VIT_08s0007g03240 | Carbonic anhydrase precursor | -2.28 |
| VIT_00s0400g00020 | HcrVf1 protein | 1.81 | VIT_04s0044g01530 | UDP-glucuronic acid:anthocyanin glucuronosyltransferase | -2.28 |
| VIT_12s0028g01690 | WRKY DNA-binding protein 65 | 1.80 | VIT_06s0004g06170 | Thylakoid soluble phosphoprotein | -2.26 |
| VIT_05s0062g01120 | PIN1 | 1.80 | VIT_06s0291g00060 | Inorganic phosphate transporter 2-1, chloroplast precursor | -2.24 |
| VIT_13s0064g01510 | Auxin-independent growth promoter | 1.79 | VIT_00s0475g00020 | Zinc finger (C3HC4-type ring finger) | -2.22 |
| VIT_08s0058g00700 | F-box protein (FBL3) | 1.77 | VIT_07s0151g00860 | Hydrolase, alpha/beta fold | -2.16 |
| VIT_09s0002g02700 | basic helix-loop-helix (bHLH) family | 1.76 | VIT_10s0003g03310 | EMB2756 (embryo defective 2756) | -2.16 |
| VIT_13s0067g03260 | Phosphatidase | 1.76 | VIT_06s0061g00080 | Saccharopine dehydrogenase | -2.16 |
| VIT_00s0179g00170 | Indeterminate(ID)-domain 12 | 1.73 | VIT_11s0016g03830 | Protein kinase | -2.15 |
| VIT_10s0003g00130 | ERF Domain protein 12 | 1.71 | VIT_10s0116g00600 | RIC10 (ROP-Interactive crib motif-containing) | -2.15 |

Table 15: *VviNAC17* (A) top 20 up-regulated and (B) top 20 down-regulated DEGs.

The genes related to the phosphate-containing compounds metabolic processes and activity are highly represented in the *VviNAC18* up regulated genes sub dataset. Many genes were also related to the defense response, an important aspect know to be up regulated during the ripening process. As for *VviNAC08*, a very represented gene category was the cyanide metabolic/catabolic processes one. In the *VviNAC18* DEGs list, another ethylene-related gene, *ERF/AP2 GENE FAMILY VVERF022*, *DEHYDRATION RESPONSIVE ELEMENT-BINDING TRANSCRIPTION*

FACTOR VVDREB23 (VIT_16s0100g00380), was found as the most up regulated (**Table 16**).

Among the down regulated genes, the *STEROID 5ALPHA-REDUCTASE* (VIT_19s0014g00080) and the *ACID PHOSPHATASE* (VIT_09s0018g01800) were found again, but the most down regulated one was *MINI ZINC FINGER 2 MIF2* (VIT_08s0056g01130). A recent study has demonstrated that *Arabidopsis thaliana* *MINI ZINC FINGER2* (*AtMIF2*) and its homolog in tomato, *INHIBITOR OF MERISTEM ACTIVITY* (*SIIMA*), participate in the floral meristem termination process; the number of carpels arising from the floral meristem, and consequently the number of fruit locules, is determined during floral meristem termination (Bollier *et al.*, 2018).

| ID | Functional annotation | FC | ID | Functional annotation | FC |
|-------------------|--|-------|-------------------|--|-------|
| VIT_16s0100g00380 | ERF/AP2 Gene Family (VvERF022) | 18.02 | VIT_08s0056g01130 | Mini zinc finger 2 MIF2 | -5.65 |
| VIT_12s0028g03260 | Rooty/superroot1 | 8.48 | VIT_08s0007g05130 | UDP-glucuronosyl/UDP-glucosyl transferase | -5.24 |
| VIT_05s0094g00360 | Chitinase class IV | 5.85 | VIT_19s0014g00080 | Steroid 5alpha-reductase | -4.88 |
| VIT_15s0048g00510 | Pectinesterase family | 5.44 | VIT_09s0018g01800 | Acid phosphatase | -4.51 |
| VIT_16s0100g01070 | Stilbene synthase (VvSTS35) | 4.45 | VIT_01s0026g00570 | Bet v 1 allergen | -4.42 |
| VIT_07s0104g00850 | Pto kinase interactor | 4.41 | VIT_05s0077g01670 | s3_Pathogenesis protein 10 [Vitis vinifera] | -4.17 |
| VIT_05s0077g01600 | s8_Pathogenesis protein 10 [Vitis vinifera] | 4.20 | VIT_13s0156g00090 | Protease inhibitor/seed storage/lipid transfer protein (LTP) | -4.11 |
| VIT_13s0019g01380 | Integral membrane protein | 4.16 | VIT_09s0002g06750 | ERF/AP2 Gene Family (VvERF042) | -4.08 |
| VIT_04s0044g00270 | Monoxygenase (MO3) | 4.12 | VIT_19s0015g00510 | Pectate lyase 2 | -3.79 |
| VIT_09s0002g05410 | ABC Transporter (VvPDR11 - VvABCG41) | 4.04 | VIT_05s0020g04110 | ELIP1 (early light-inducible protein) | -3.38 |
| VIT_16s0100g01200 | Stilbene synthase (VvSTS48) | 3.90 | VIT_11s0052g01620 | Pathogenesis-related protein 1 precursor (PRP 1) | -3.30 |
| VIT_04s0008g00110 | TIFY gene family (VvJAZ3) | 3.77 | VIT_03s0063g01880 | Acyl-CoA synthetase long-chain member 2 | -3.28 |
| VIT_02s0025g04420 | MATE efflux family protein | 3.73 | VIT_00s0230g00080 | Copper-binding family protein | -3.20 |
| VIT_19s0014g04650 | Avr9/Cf-9 rapidly elicited protein 20 | 3.70 | VIT_09s0002g03140 | Lipase GD5L | -3.17 |
| VIT_01s0026g02390 | Glutathione S-transferase 10 GSTU10 | 3.69 | VIT_03s0038g03770 | Auxin-induced SAUR | -3.12 |
| VIT_10s0003g03790 | Jasmonate ZIM domain-containing protein (VvJAZ5) | 3.69 | VIT_04s0069g00750 | AHK5 (Cytokinin independent 2) | -3.08 |
| VIT_16s0100g00910 | Stilbene synthase (VvSTS21) | 3.62 | VIT_17s0000g08680 | IMP dehydrogenase/GMP reductase | -3.07 |
| VIT_01s0026g02400 | Glutathione S-transferase 10 GSTU10 | 3.57 | VIT_17s0000g10060 | Lipase GD5L | -3.05 |
| VIT_18s0041g02010 | 12-oxophytodiene reductase 1 | 3.44 | VIT_16s0050g00100 | Myosin-related | -2.99 |
| VIT_01s0026g02370 | Glutathione S-transferase 10 GSTU10 | 3.40 | VIT_15s0045g00040 | Copper-binding family protein | -2.95 |

Table 16: *VviNAC18* (A) top 20 up-regulated and (B) top 20 down-regulated DEGs.

VviNAC26 over expression up regulated genes were mainly enriched in response to different stimuli, transmembrane transport and biosynthetic processes categories; among the down regulated dataset were found the lipid catabolism category and, again, many genes related to cyanide metabolic/catabolic processes. Between the up regulated genes related to the *VviNAC26* over expression, some already described genes were present: *SEVEN IN ABSENTIA SINA5* (VIT_19s0014g00880) and *ACID PHOSPHATASE* (VIT_09s0018g01800) (**Table 17**).

Moreover, *CITRATE SYNTHASE* (VIT_03s0088g00560) was found; it plays an important role in the Krebs cycle, in β -oxidation of fatty acids and in photo-respiratory glycolate pathways, can affect fruit ripening (Liu *et al.*, 2013).

Among the down regulated *ALPHA-GLUCOSIDASE 1 AGLU1* (VIT_10s0092g00240) and, again, a *R PROTEIN MLA10* (VIT_09s0002g08020) were found. *ALPHA-GLUCOSIDASE 1 AGLU1* occur widely in plants but their function is unknown.

| Gene ID | Functional annotation | FC | Gene ID | Functional annotation | FC |
|-------------------|--|-------|-------------------|---|--------|
| VIT_19s0014g00880 | Seven in absentia SINA5 | 88.46 | VIT_10s0092g00240 | Alpha-glucosidase 1 (AGLU1) | -13.49 |
| VIT_09s0018g01800 | Acid phosphatase | 46.57 | VIT_13s0047g00230 | Pectinesterase family | -8.10 |
| VIT_03s0088g00560 | Citrate synthase | 20.48 | VIT_09s0002g08020 | R protein MLA10 | -8.10 |
| VIT_11s0052g01650 | Pathogenesis-related protein 1 precursor (PRP 1) | 19.08 | VIT_16s0022g00860 | Invertase/pectin methylesterase inhibitor | -7.32 |
| VIT_03s0063g02680 | Radialis-like protein 5 | 10.16 | VIT_19s0014g02900 | Ring finger protein 185 | -7.03 |
| VIT_04s0023g00610 | Protein kinase CRK1 CRK1 protein(Cdc2-related kinase 1) | 6.58 | VIT_00s0179g00180 | Transcription factor jumoni (jmc) domain-containing protein | -6.02 |
| VIT_03s0063g00370 | Nitrite reductase | 6.15 | VIT_16s0039g01370 | (9,10) (9',10') cleavage dioxygenase (CCD4) (VvCCD4c) | -5.38 |
| VIT_01s0127g00400 | Polygalacturonase GH28 | 5.93 | VIT_02s0025g04890 | CYP76B1 | -5.19 |
| VIT_19s0090g00080 | Ubiquitin-conjugating enzyme E2 variant | 5.86 | VIT_00s0371g00100 | Mannitol dehydrogenase | -4.78 |
| VIT_19s0090g00120 | Ubiquitin-conjugating enzyme E2 variant | 5.80 | VIT_06s0061g00120 | Beta-1,3-glucanase [Vitis riparia] | -4.49 |
| VIT_12s0035g01050 | Octicosapeptide/Phox/Bem1p (PB1) domain-containing protein | 5.60 | VIT_09s0070g00350 | R protein disease resistance protein | -4.34 |
| VIT_12s0035g02150 | ferric reduction oxidase 7 FRO7 | 5.56 | VIT_14s0081g00400 | Ankyrin repeat | -4.25 |
| VIT_03s0063g02620 | Myb RAD (Transcription factor RAD) | 5.50 | VIT_03s0038g00360 | Isochorismatase hydrolase | -4.20 |
| VIT_11s0016g02350 | Ubiquinone/menaquinone biosynthesis methyltransferase UbiE | 5.48 | VIT_11s0052g01560 | MATE efflux family protein | -4.07 |
| VIT_17s0000g03890 | Peptidyl-prolyl isomerase C | 5.33 | VIT_19s0014g00250 | Bile acid:sodium symporter | -3.96 |
| VIT_00s0572g00020 | Linalool synthase (VvTP562) | 5.08 | VIT_11s0052g01510 | MATE efflux family protein | -3.93 |
| VIT_11s0016g02860 | Nudix hydrolase 8 | 4.75 | VIT_02s0025g02610 | basic helix-loop-helix (bHLH) family | -3.85 |
| VIT_19s0090g01350 | Aspartyl protease | 4.56 | VIT_08s0007g08910 | Cis-zeatin O-beta-D-glucosyltransferase | -3.83 |
| VIT_14s0030g00420 | Inosine-uridine preferring nucleoside hydrolase family protein | 4.50 | VIT_10s0042g00480 | ABC transporter g family pleiotropic drug resistance 12 PDR12 | -3.79 |
| VIT_09s0002g06970 | Palmitoyl-monogalactosyldiacylglycerol delta-7 desaturase | 4.49 | VIT_13s0067g02130 | Dehydration-induced protein (ERD15) | -3.61 |

Table 17: VviNAC26 (A) top 20 up-regulated and (B) top 20 down-regulated DEGs.

The genes related to the regulation of transcription and pathogenesis were highly represented in the VviNAC39 up regulated genes sub dataset. Many genes were also related to the regulation of biosynthetic and metabolic and to the light response. Concerning the down regulated genes, the most represented categories were the response to different type of stress. VviNAC39 over expression brought to the up regulation of two *SERINE CARBOXYPEPTIDASE II* (VIT_08s0040g01130 and VIT_08s0040g01040) (**Table 18**). Although the biological role remains to be determined, some studies suggest that they are likely to function in a broad range of biochemical pathways including those involved in secondary metabolite biosynthesis (Fraser *et al.*, 2005).

Also, four pathogenesis related genes were up-regulated: three *PORE-FORMING TOXIN-LIKE PROTEIN HFR-2s* (VIT_07s0005g06090, VIT_07s0005g06000 and VIT_07s0005g06060) and a *DISEASE RESISTANCE PROTEIN NBS-LRR CLASS* (VIT_14s0030g00520). Moreover, a *PECTATE LYASE 2* (VIT_19s0015g00510), related to fruit softening (Zenoni *et al.*, 2016) and a *MINI ZINC FINGER 2 MIF2* (VIT_08s0056g01130) were found down regulated. Interestingly a VviNAC and a VviMYB family member, VviNAC74 (VIT_06s0080g00780) and MYB RAD (VIT_03s0063g02620), resulted down regulated too.

| Gene ID | Functional annotation | FC | Gene ID | Functional annotation | FC |
|-------------------|---|------|-------------------|--|-------|
| VIT_08s0040g01130 | Serine carboxypeptidase II | 5.93 | VIT_19s0015g00510 | Pectate lyase 2 | -7.23 |
| VIT_07s0005g06090 | Pore-forming toxin-like protein Hfr-2 | 5.34 | VIT_08s0056g01130 | Mini zinc finger 2 MIF2 | -6.24 |
| VIT_07s0005g06000 | Pore-forming toxin-like protein Hfr-2 | 4.96 | VIT_01s0026g00490 | Nodulin | -4.29 |
| VIT_08s0040g01040 | Serine carboxypeptidase II | 4.74 | VIT_16s0010g00390 | ERF/AP2 Gene Family (VVERF022) | -3.80 |
| VIT_07s0005g06060 | Pore-forming toxin-like protein Hfr-2 | 3.62 | VIT_13s0013g00460 | Annexin ANN4 | -3.49 |
| VIT_06s0009g03670 | F-box family protein | 3.12 | VIT_00s0013g00180 | Annexin ANN4 | -3.48 |
| VIT_09s0002g05590 | ABC Transporter (VVPDR16 - VvABC46) | 2.97 | VIT_07s0151g00250 | Chlorophyllase | -3.43 |
| VIT_14s0030g00520 | Disease resistance protein (NBS-LRR class) | 2.41 | VIT_13s0013g00420 | Annexin ANN4 | -3.27 |
| VIT_10s0071g00430 | GRAM domain-containing protein / ABA-responsive | 2.30 | VIT_09s0002g03520 | Ara bidopsis histidine phosphotransfer AHP4 | -3.25 |
| VIT_09s0054g00530 | Zinc finger (B-box type) | 2.24 | VIT_07s0031g00270 | Tonoplast monosaccharide transporter2 | -3.02 |
| VIT_13s0106g00610 | Tetracycline transporter | 2.19 | VIT_08s0007g02450 | Aspartic Protease (VvA P22) | -3.00 |
| VIT_01s0010g02730 | Chaperone BCS1 mitochondrial | 2.11 | VIT_03s0038g01830 | Proline-rich protein 4 | -2.92 |
| VIT_10s0071g00390 | GRAM domain-containing protein / ABA-responsive | 2.02 | VIT_06s0008g00780 | NA C domain-containing protein (VvNAC74) | -2.78 |
| VIT_01s0026g02620 | Expansin (VvEXPA1) | 2.02 | VIT_13s0019g02160 | Laccase | -2.74 |
| VIT_16s0022g00510 | Heat shock 22 kDa protein | 2.00 | VIT_11s0052g01620 | Pathogenesis-related protein 1 precursor (PRP 1) | -2.69 |
| VIT_04s0008g01110 | Heat shock transcription factor A6B | 1.99 | VIT_08s0007g01680 | Ceramidase | -2.69 |
| VIT_10s0071g00500 | GRAM domain-containing protein / ABA-responsive | 1.89 | VIT_14s0030g02090 | Calcium-transporting ATPase 12 ACA12 | -2.68 |
| VIT_09s0018g00620 | Co-chaperone-curved DNA binding protein A | 1.87 | VIT_03s0063g02620 | Myb RAD (Transcription factor RAD) | -2.63 |
| VIT_16s0050g00020 | Cullin-4 | 1.83 | VIT_13s0019g02760 | Heat shock protein 17.6 kDa class I | -2.53 |
| VIT_00s0179g00150 | Heat shock transcription factor A6B | 1.83 | VIT_07s0005g01860 | Patatin | -2.38 |

Table 18: VviNAC39 (A) top 20 up-regulated and (B) top 20 down-regulated DEGs.

VviNAC61 over expression brought to a high number of up regulated genes related to chitin, amino sugars, lignin, aromatic compounds and cyanide (ethylene related) metabolic processes, while the down regulated mainly clustered into photosynthesis and response to hormones categories.

The findings concerning the *VviNAC61* over expression were perfectly in line with what has already been reported by Zenoni *et al.* (2016) concerning the withering processes, where this *VviNAC* TF (together with *VviNAC60*) seems to play a major role (**Table 19**).

Among the up-regulated DEGs list were found an ethylene-related gene *ERF/AP2 GENE FAMILY VVERF072* (VIT_15s0021g01630), many *LACCASE* genes (VIT_18s0117g00590, VIT_18s0075g00780, VIT_18s0117g00550, VIT_18s0001g00680 and VIT_18s0117g00480), the pathogenesis related gene *R PROTEIN MLA10* (VIT_09s0002g08020), and the *UDP-GLUCORONOSYL AND UDP-GLUCOSYL TRANSFERASE* (VIT_06s0004g07250), which is essential and one of the last steps in anthocyanin pigment biosynthesis.

Among the down regulated, two genes related to the photosynthetic process were found, *CHLOROPHYLLASE* (VIT_07s0151g00250) and *CHLOROPHYLLASE 1* (VIT_07s0151g00190); two *MYB* genes, *MYB RAD* (VIT_03s0063g02620) and *MYB FAMILY* (VIT_04s0023g01910); a *PECTATE LYASE 2* (VIT_19s0015g00510) was also found.

| Gene ID | Functional annotation | FC | Gene ID | Functional annotation | FC |
|-------------------|--|-------|-------------------|---|-------|
| VIT_05s0020g05020 | Inhibitor of trypsin and hageman factor (CMTI-V) | 62.11 | VIT_07s0151g00250 | Chlorophyllase | -7.89 |
| VIT_18s0117g00590 | Laccase | 55.76 | VIT_01s0026g00490 | Nudulin | -7.46 |
| VIT_18s0075g00780 | Laccase | 51.12 | VIT_03s0063g02620 | Myb RAD (Transcription factor RAD) | -7.40 |
| VIT_18s0117g00550 | Laccase | 51.09 | VIT_05s0062g01160 | Pectinesterase family | -6.02 |
| VIT_10s0003g04910 | Sinapyl alcohol dehydrogenase | 43.85 | VIT_16s0022g02090 | Embryo-specific 3 | -5.73 |
| VIT_18s0001g00680 | Laccase | 32.56 | VIT_03s0091g00880 | Endoxylanase | -5.57 |
| VIT_05s0020g05040 | Proteinase inhibitor 1 PPI3B2 | 29.05 | VIT_19s0015g00510 | Pectate lyase 2 | -5.34 |
| VIT_14s0060g02170 | GLUTATHIONE S-TRANSFERASE TAU 8 | 22.81 | VIT_02s0025g00250 | SP1L5 (SPIRAL1-like5) | -5.27 |
| VIT_07s0129g00800 | CYP81E1 Isoflavone 2'-hydroxylase | 21.24 | VIT_09s0002g06750 | ERF/AP2 Gene Family (VVERF042) | -4.98 |
| VIT_09s0002g08020 | R protein MLA10 | 16.52 | VIT_14s0030g02090 | Calcium-transporting ATPase 12 ACA12 | -4.92 |
| VIT_06s0004g07250 | UDP-glucuronosyl and UDP-glucosyl transferase | 15.57 | VIT_07s0151g00190 | Chlorophyllase 1 | -4.76 |
| VIT_08s0007g06160 | Basic Leucine Zipper Transcription Factor (VvbZIP28) | 14.78 | VIT_09s0002g03520 | Arabidopsis histidine phosphotransfer AHP4 | -4.48 |
| VIT_15s0021g01630 | ERF/AP2 Gene Family (VVERF072) | 13.79 | VIT_11s0016g02860 | Nudix hydrolase 8 | -4.47 |
| VIT_13s0019g02180 | Tropinone reductase | 12.89 | VIT_05s0020g00950 | Aspartic Protease (VvAP10) | -4.45 |
| VIT_00s0301g00150 | Late embryogenesis abundant protein | 11.80 | VIT_08s0056g01130 | Mini zinc finger 2 MIF2 | -4.40 |
| VIT_18s0117g00480 | Laccase | 11.31 | VIT_14s0128g00210 | Xyloglucanase inhibitor | -4.40 |
| VIT_05s0094g00360 | Chitinase class IV | 10.86 | VIT_04s0023g01910 | Myb family | -4.29 |
| VIT_08s0040g01130 | Serine carboxypeptidase II | 9.38 | VIT_04s0023g03040 | Lactoylglutathione lyase | -4.28 |
| VIT_00s0301g00120 | Late embryogenesis abundant protein | 8.76 | VIT_11s0103g00050 | High-affinity K ⁺ transporter 1 (HKT1) | -4.26 |
| VIT_01s0010g03040 | Calcium-binding protein CML | 7.97 | VIT_08s0007g02450 | Aspartic Protease (VvAP22) | -4.17 |

Table 19: *VviNAC61* (A) top 20 up-regulated and (B) top 20 down-regulated DEGs.

Then, the attention was focused on the DEGs lists to see if any *VviNACs* would be present as up or down regulated genes under a specific *VviNAC* TF over expression. Interestingly, it was found that the *VviNAC15* and *VviNAC18* over expressions seem to have a role in the up regulation of other *VviNACs*, while the over expression of *VviNAC26*, *VviNAC39* and *VviNAC61* seem to bring to a down regulation of the same family TFs (**Table 20**). For *VviNAC01*, *VviNAC08* and *VviNAC17* no interesting *VviNAC* regulation was found.

VviNAC15 over expression seems to up regulate *VviNAC03* (VIT_00s0375g00040), *VviNAC13* (VIT_02s0012g01040), *VviNAC17* (VIT_19s0014g03290), *VviNAC56* (VIT_07s0005g03610) and *VviNAC61* (VIT_08s0007g07640, this one also present a positive Pearson correlation from the co-expression analysis).

VviNAC18 over expression seems to up regulate *VviNAC46* (VIT_18s0041g00700), which results down regulated by the over expression of *VviNAC39* and *VviNAC61*. *VviNAC39* over expression seems to down regulate *VviNAC64* (VIT_04s0079g00280) and *VviNAC74* (VIT_06s0080g00780), but the *VviNAC74* down regulation does not match with the positive Pearson correlation found in the coexpression analysis.

VviNAC61 over expression seems to down regulate *VviNAC19* (VIT_11s0016g02880).

Moreover, an important evidence is that *VviNAC26* over expression seems to up regulate *VviNAC33* (VIT_19s0027g00230).

Looking at the D'Inca (2017) microarray results, was found that *VviNAC13* over

expression seems to up regulate *VviNAC53* (VIT_15s0048g02300) and the *VviNAC33* one seems to up regulate *VviNAC11* (VIT_14s0108g01070); whereas, the over expression of *VviNAC60* seems to down regulate *VviNAC65* (VIT_04s0008g02710).

No *VviNACs* regulation matches were found for *VviNAC03* and *VviNAC11*.

| Over expressed <i>VviNAC</i> | Regulated <i>VviNAC</i> | | | |
|------------------------------|-------------------------|---|-------|---------|
| | Gene ID | Functional annotation | FC | Pearson |
| <i>VviNAC01</i> | | | | |
| <i>VviNAC03</i> | | | | |
| <i>VviNAC08</i> | | | | |
| <i>VviNAC11</i> | | | | |
| <i>VviNAC13</i> | VIT_15s0048g02300 | NAC domain-containing protein (VvNAC53) | 1,50 | |
| | VIT_00s0375g00040 | NAC domain-containing protein (VvNAC03) | 1,82 | |
| | VIT_02s0012g01040 | NAC domain-containing protein (VvNAC13) | 2,77 | |
| <i>VviNAC15</i> | VIT_19s0014g03290 | NAC domain-containing protein (VvNAC17) | 1,51 | |
| | VIT_07s0005g03610 | NAC domain-containing protein (VvNAC56) | 4,05 | |
| | VIT_08s0007g07640 | NAC domain-containing protein (VvNAC61) | 1,56 | 0,747 |
| <i>VviNAC17</i> | | | | |
| <i>VviNAC18</i> | VIT_18s0041g00700 | NAC domain-containing protein (VvNAC46) | 2,09 | |
| <i>VviNAC26</i> | VIT_19s0027g00230 | NAC domain-containing protein (VvNAC33) | -2,25 | |
| <i>VviNAC33</i> | VIT_14s0108g01070 | NAC domain-containing protein (VvNAC11) | 2,65 | |
| <i>VviNAC39</i> | VIT_18s0041g00700 | NAC domain-containing protein (VvNAC46) | -1,52 | |
| | VIT_04s0079g00280 | NAC domain-containing protein (VvNAC64) | -1,81 | |
| | VIT_06s0080g00780 | NAC domain-containing protein (VvNAC74) | -2,78 | 0,400 |
| <i>VviNAC60</i> | VIT_04s0008g02710 | NAC domain-containing protein (VvNAC65) | -2,00 | |
| <i>VviNAC61</i> | VIT_11s0016g02880 | NAC domain-containing protein (VvNAC19) | -1,52 | |
| | VIT_18s0041g00700 | NAC domain-containing protein (VvNAC46) | -1,60 | |

Table 20: *VviNACs* found in the over expression analyses. The *VviNAC03*, *VviNAC11*, *VviNAC13*, *VviNAC33* and *VviNAC60* data were taken from D'Inca (2017).

Taking together all these results showed that each *VviNAC* seems to have a different role in the ripening processes that needs to be better investigated to be fully understood.

The transcriptome analyses were just a first step to elucidate the specific role of all the *VviNAC* family members but will be useful, integrated with other methods, to select some hypothetical candidates as direct targets of the studied TFs.

Moreover, the final evidence suggested how important could the interaction between *VviNACs* TF be in the complicated grapevine maturation regulatory network.

REFERENCES

- Amato, A., Cavallini, E., Zenoni, S., Finezzo, L., Begheldo, M., Ruperti, B., & Tornielli, G. B.** (2017). A grapevine TTG2-like WRKY transcription factor is involved in regulating vacuolar transport and flavonoid biosynthesis. *Frontiers in plant science*, 7, 1979.
- Arita, K., Honma, T., & Suzuki, S.** (2017). Comprehensive and comparative lipidome analysis of *Vitis vinifera* L. cv. Pinot Noir and Japanese indigenous *V. vinifera* L. cv. Koshu grape berries. *PLoS one*, 12(10), e0186952.
- Bai, S., Liu, J., Chang, C., Zhang, L., Maekawa, T., Wang, Q., ... & Shen, Q. H.** (2012). Structure-function analysis of barley NLR immune receptor MLA10 reveals its cell compartment specific activity in cell death and disease resistance. *PLoS Pathog*, 8(6), e1002752.
- Bollier, N., Sicard, A., Leblond, J., Latrasse, D., Gonzalez, N., Gévaudant, F., ... & Delmas, F.** (2018). At-MINI ZINC FINGER2 and SI-INHIBITOR OF MERISTEM ACTIVITY, a conserved missing link in the regulation of floral meristem termination in Arabidopsis and tomato. *The Plant Cell*, 30(1), 83-100.
- Cheng, C., Jiao, C., Singer, S. D., Gao, M., Xu, X., Zhou, Y., ... & Wang, X.** (2015). Gibberellin-induced changes in the transcriptome of grapevine (*Vitis labrusca* × *V. vinifera*) cv. Kyoho flowers. *BMC genomics*, 16(1), 1-16.
- D'Incà E.** 2017. Master regulators of the vegetative-to-mature organ transition in grapevine: the role of NAC transcription factors. PhD thesis. Verona University.
- Fasoli M, Dal Santo S, Zenoni S, Tornielli GB, Farina L, Zamboni A, Porceddu A, Venturini L, Bicego M, Murino V, Ferrarini A, Delledonne M, Pezzotti M** (2012). The grapevine expression atlas reveals a deep transcriptome shift driving the entire plant into a maturation program. *Plant Cell*. 24(9):3489- 505.
- Fraser, C. M., Rider, L. W., & Chapple, C.** (2005). An expression and bioinformatics analysis of the Arabidopsis serine carboxypeptidase-like gene family. *Plant physiology*, 138(2), 1136-1148.
- Grncarevic, M., & Radler, F.** (1971). A review of the surface lipids of grapes and their importance in the drying process. *American Journal of Enology and Viticulture*, 22(2), 80-86.
- Ju, Y. L., Yue, X. F., Min, Z., Wang, X. H., Fang, Y. L., & Zhang, J. X.** (2020). VvNAC17, a novel stress-responsive grapevine (*Vitis vinifera* L.) NAC transcription factor, increases sensitivity to abscisic acid and enhances salinity, freezing, and drought tolerance in transgenic Arabidopsis. *Plant Physiology and Biochemistry*, 146, 98-111.
- Li, L., Xu, X., Chen, C., & Shen, Z.** (2016). Genome-wide characterization and expression analysis of the germin-like protein family in rice and Arabidopsis. *International journal of molecular sciences*, 17(10), 1622.
- Licausi, F., Giorgi, F. M., Zenoni, S., Osti, F., Pezzotti, M., & Perata, P.** (2010). Genomic and transcriptomic analysis of the AP2/ERF superfamily in *Vitis vinifera*. *BMC genomics*, 11(1), 719.

Liu, J. H., Chi, G. H., Jia, C. H., Zhang, J. B., Xu, B. Y., & Jin, Z. Q. (2013). Function of a citrate synthase gene (MaGCS) during postharvest banana fruit ripening. *Postharvest biology and technology*, *84*, 43-50.

Liu, J., Ando, R., Shimizu, K., Hashida, K., Makino, R., Ohara, S., & Kondo, R. (2008). Steroid 5 α -reductase inhibitory activity of condensed tannins from woody plants. *Journal of wood science*, *54*(1), 68-75.

Lu, M., Han, Y. P., Gao, J. G., Wang, X. J., & Li, W. B. (2010). Identification and analysis of the germin-like gene family in soybean. *Bmc Genomics*, *11*(1), 620.

Lu, S. X., Knowles, S. M., Webb, C. J., Celaya, R. B., Cha, C., Siu, J. P., & Tobin, E. M. (2011). The Jumonji C domain-containing protein JMJ30 regulates period length in the Arabidopsis circadian clock. *Plant physiology*, *155*(2), 906-915.

Massonnet M, Fasoli M, Tornielli G.B., Altieri M, Sandri M, Zuccolotto P, Paci P, Gardiman M, Zenoni S. and Pezzotti M. (2017). Ripening Transcriptomic Program in Red and White Grapevine Varieties Correlates with Berry Skin Anthocyanin Accumulation. *Plant Physiology*. Vol. 174: 2376–2396.

Mizoi, J., Shinozaki, K., & Yamaguchi-Shinozaki, K. (2012). AP2/ERF family transcription factors in plant abiotic stress responses. *Biochimica et Biophysica Acta (BBA)-Gene Regulatory Mechanisms*, *1819*(2), 86-96.

Nurniwalis, A. W., Zubaidah, R., Akmar, A. S. N., Zulkifli, H., Arif, M. M., Massawe, F. J., ... & Parveez, G. K. A. (2015). Genomic structure and characterization of a lipase class 3 gene and promoter from oil palm. *Biologia plantarum*, *59*(2), 227-236.

Royo, C., Carbonell-Bejerano, P., Torres-Pérez, R., Nebish, A., Martínez, Ó., Rey, M., ... & Martínez-Zapater, J. M. (2016). Developmental, transcriptome, and genetic alterations associated with parthenocarpy in the grapevine seedless somatic variant Corinto blanco. *Journal of experimental botany*, *67*(1), 259-273.

Tran, H. T., Hurley, B. A., & Plaxton, W. C. (2010). Feeding hungry plants: the role of purple acid phosphatases in phosphate nutrition. *Plant Science*, *179*(1-2), 14-27.

Wang, W., Cai, J., Wang, P., Tian, S., & Qin, G. (2017). Post-transcriptional regulation of fruit ripening and disease resistance in tomato by the vacuolar protease SIVPE3. *Genome biology*, *18*(1), 1-23.

Wang, M., Vannozzi, A., Wang, G., Liang, Y. H., Tornielli, G. B., Zenoni, S., ... & Cheng, Z. M. M. (2014). Genome and transcriptome analysis of the grapevine (*Vitis vinifera* L.) WRKY gene family. *Horticulture research*, *1*(1), 1-16.

WatreLOT, A. A., & Norton, E. L. (2020). Chemistry and Reactivity of Tannins in *Vitis* spp.: A Review. *Molecules*, *25*(9), 2110.

Zenoni, S., Fasoli, M., Guzzo, F., Dal Santo, S., Amato, A., Anesi, A., ... & Tornielli, G. B. (2016). Disclosing the molecular basis of the postharvest life of berry in different grapevine genotypes. *Plant physiology*, *172*(3), 1821-1843.

3. THE GRAPEVINE CISTROME DISCOVERING

3.1 INTRODUCTION

The DNA of a eukaryotic cell must be compacted to fit into the nucleus. Cells can pack their genetic information still maintain it accessible to regulatory proteins that can activate or repress specific genes, repair damage, mediate recombination and replicate the DNA during the cell cycle.

The term chromatin is used to describe fold DNA. The basic unit of chromatin is the nucleosome, which contains approximately 146 bp of DNA wrapped almost twice around a core histone octamer, composed of two molecules each of the histones H2A, H2B, H3 and H4, organized into an H3–H4 tetramer and two H2A–H2B dimers (Luger *et al.*, 1997). Each nucleosome has a diameter of around 10 nm, although the least compacted chromatin appears in the electron microscope as a 30 nm diameter fiber, which appears to correspond to euchromatin, the component of a eukaryotic genome that is actively transcribed (Goodrich and Tweedie, 2002).

Instead, heterochromatin is typically transcriptionally silent and is characterized by higher order packaging of the nucleosomes; it can be reversibly relaxed into euchromatin, to allow activation of gene expression, or may be permanently inactive, as found in gene-poor regions of the genome (peri-centromeric regions).

The regulation of chromatin structure has a key role in the epigenetic control of gene expression. The core histones can be modified by acetylation, methylation, phosphorylation, ubiquitination or ADP-ribosylation; actively transcribed genes are predominantly associated with highly acetylated histones whereas inactive genes are often characterized by the presence of hypoacetylated histones in the nucleosomes that are associated with them (Fischle *et al.*, 2003; Jenuwein and Allis, 2001; Strahl and Allis, 2000).

In addition, the DNA itself can be modified, most commonly by cytosine methylation, which often characterizes inactive genes (Martienssen and Colot, 2001; Ng and Adrian, 1999). Furthermore, RNA has also been found associated with the heterochromatin structure (Maison *et al.*, 2002).

Gene expression is controlled by not only DNA sequence but also by the interaction of DNA-binding proteins with higher order chromatin structure; indeed, transcription factors play an important part in the initiation of gene expression by

interacting with gene promoters.

ChIP-seq represents a powerful way to study TF-DNA interactions *in vivo*; this methodology has produced numerous applications in studying the composition and dynamics of chromatin landscapes and TF binding, as well as assessing the interplay between different factors in gene regulation under different conditions and developmental phases. ChIP-seq approach can be used to study DNA methylation, chromatin structure/histone modifications, and the cooperative binding of TFs.

The first ChIP protocol was developed by Gilmour and Lis (1984) to monitor RNA polymerase II/ DNA association in *Escherichia coli* and *Drosophila*.

Genome-wide applications of the ChIP-seq methodology in the plant field are still relatively scarce. This delay is partly due to technical difficulties in ChIP sample preparation related to the complexity of plant tissues for the presence of rigid cell walls, high levels of cellulose and lignin and large vacuoles. The establishment of an efficient ChIP-seq protocols for plant systems is hard and many optimizations are required if different types of tissues are sampled or for ChIP performed in different plant species.

A general ChIP assay (**Fig. 26**) consists in the TF-DNA crosslinking by formaldehyde vacuum infiltration of the fresh living tissue, the isolation of chromatin from a nuclear extract, the fragmentation of chromatin (average fragment size varying from 200 to 1000 bp), the precipitation of any insoluble material (pre-clearing step), the immunoprecipitation of the TF-DNA complexes with a specific antibody, the reverse crosslinking for the recovery of DNA and the identification of associated DNA sequences through the sequencing, which provides a powerful method to map protein–DNA interactions genome-wide.

Sequencing libraries are prepared from the immunoprecipitated (IP) DNA as well as from the INPUT (not immunoprecipitated sheared chromatin, control). Sequenced data of the IP and INPUT are then analyzed and compared using bioinformatics.

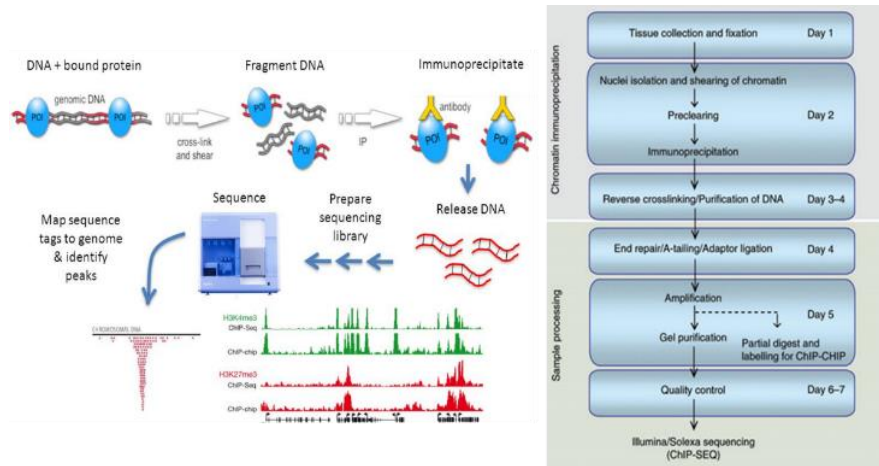


Figure 26: ChIP-seq workflow (Kaufmann *et al.*, 2010).

As *Vitis vinifera* is one of the most important fruit crops in the world, playing a central role in the economy of many developed countries, the regulation of berry ripening has been studied intensely to identify the physiological, biochemical and molecular features that influence fruit quality. Transcriptomic data obtained during berry development and integrated network analyses allowed the identification of several members of the *VviNAC* gene family, functionally involved in a large variety of plant growth and development related programs, as candidate genes for the regulation of the onset of berry ripening. Between these genes, *VviNAC60* was identified as *switch* gene that might represent a master regulator for the transition from vegetative-to-mature growth, since its expression is low in vegetative/green tissues but significantly higher in mature/woody organs and shows a high negatively correlation with genes that are down regulated during ripening.

With the aim to characterize the function of *VviNAC60*, we undertook a ChIP-seq approach on *Vitis vinifera* cv Shiraz plants to identify putative targets of this transcription factor, making a first step in the disclosure of its regulation mechanism. The analysis was performed on berries before veraison, characterized by a very low expression of *VviNAC60*, and berries after veraison, characterized by a high expression of the NAC candidate; given the absence of *VviNAC60* expression in young leaves, these were used as negative control.

The characterization of a specific TF binding profile in the reference genome is essential to identify its regulatory mechanisms of action, especially considering that

the coordination between different TFs via local and/or proximal binding sites influences gene expression. ChIP-seq is the leading method in the *in vivo* determination of TFBS. However, the method is limited in its throughput by the need to create specific antibodies, which can be technically challenging and expensive. Moreover, characterizing TFBS for all TFs within a specific family is crucial to expand the knowledges of complex gene expression networks but is quite difficult and expensive through the ChIP-seq technique.

To obtain cistrome maps of the selected *Vvi*NAC TFs, the DAP-seq (Fig. 27) was performed as it is a fast, high-throughput, inexpensive, and more easily scaled *in vitro* method than ChIP-seq. The binding site data generated by DAP-seq shares similarities to the ChIP-seq one; indeed, DAP-seq data are analysed by standard peak-calling and motif-characterization software, typically allowing uniquely mapped reads to be used in subsequent analyses, effectively masking repeat regions that may give false peaks (Bartlett *et al.*, 2017).

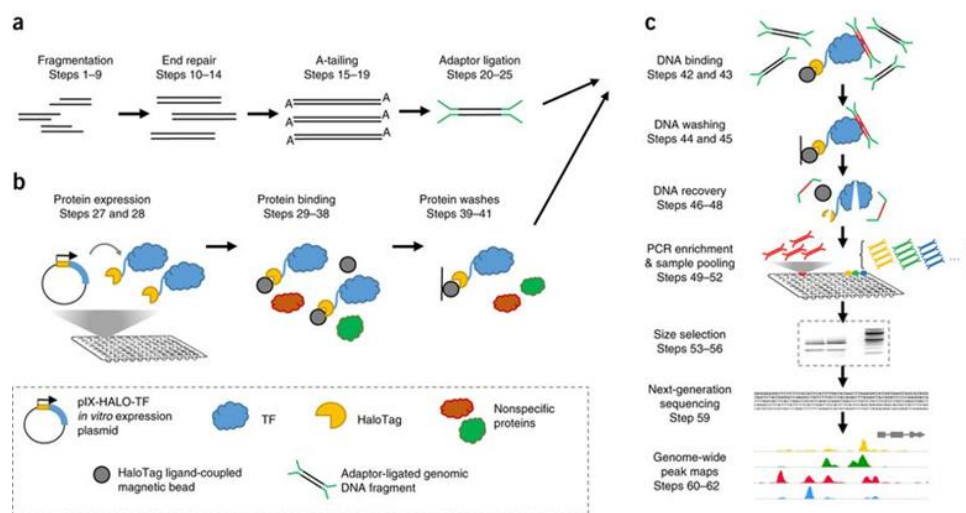


Figure 27: DAP-Seq workflow. (Bartlett *et al.*, 2017). (a) An adaptor-ligated DNA library is prepared by shearing native genomic DNA into ~200-bp fragments and ligating Illumina-based sequencing adaptors to the repaired ends. (b) Transcription factor (TF) ORF clones fused to the Halo affinity tag are expressed *in vitro* and bound to ligand-coupled beads, whereas nonspecific proteins are washed away. (c) Halo Tag-TF fusion proteins are incubated with an adaptor-ligated genomic DNA library, and unbound DNA fragments are washed away. (d) Samples are heated to release TF-bound DNA, and the recovered DNA is PCR-amplified to attach indexed sequencing primers. (e) Indexed DNA samples are subsequently combined and size-selected to remove residual adaptor dimers. (f) Purified DNA libraries are sequenced using next-generation sequencing, and the resulting genome-wide binding events are analysed.

DAP-seq DNA libraries were constructed using gDNA from young leaves of *Vitis vinifera* cv Shiraz, preserving the cytosine methylations that are known to impact

TFs binding. The resulting gDNA libraries were incubated with single HALO-tagged *in vitro* expressed *Vvi*NAC TFs, and TF-DNA complexes were purified using magnetic separation of the affinity tag. The bound gDNA was eluted and sequenced. Sequence reads were mapped to the *Vitis vinifera* cv Pinot Noir reference genome, identifying genome-wide binding locations for each *Vvi*NAC TF. For the expression of the affinity-tagged TFs, individual TF ORFs were transferred into the Gateway-compatible pIX-HALO expression vector, which contains an N-terminal HALO affinity tag sequence. The pIX-HALO-TF constructs were then expressed using rabbit reticulocyte based *in vitro* transcription/translation coupled. The use of a negative control sample (pIX-HALO-GST vector) as background substantially reduced false peak signals. A good *in vitro* expression of the tagged protein is crucial for a successful experiment; for this reason, a Western blot analysis can be performed to verify the expression.

Although DAP-seq retains many of the tissue/cell line-specific secondary modifications and features present in gDNA, the effects of chromatin accessibility and histone modifications are not reflected in DAP-seq datasets. For this reason, a comparison between DAP-seq and ChIP-seq data could be useful to fully uncover the possible CREs of a specific TF, defining its role and mechanism of action.

REFERENCES

- Bartlett, A., O'Malley, R. C., Huang, S. S. C., Galli, M., Nery, J. R., Gallavotti, A., & Ecker, J. R.** (2017). Mapping genome-wide transcription-factor binding sites using DAP-seq. *Nature protocols*, 12(8), 1659.
- Bowler, C., Benvenuto, G., Laflamme, P., Molino, D., Probst, A. V., Tariq, M., & Paszkowski, J.** (2004). Chromatin techniques for plant cells. *The Plant Journal*, 39(5), 776-789.
- Fischle, W., Wang, Y., & Allis, C. D.** (2003). Histone and chromatin cross-talk. *Current opinion in cell biology*, 15(2), 172-183.
- Gilmour, D.S., and Lis, J.T.** (1986). RNA polymerase II interacts with the promoter region of the noninduced hsp70 gene in *Drosophila melanogaster* cells. *Mol. Cell Biol.* **6**: 3984–3989.
- Goodrich, J., & Tweedie, S.** (2002). Remembrance of things past: chromatin remodeling in plant development. *Annual review of cell and developmental biology*, 18(1), 707-746.
- Jenuwein, T., & Allis, C. D.** (2001). Translating the histone code. *Science*, 293(5532), 1074-1080.
- Luger, K., Mäder, A. W., Richmond, R. K., Sargent, D. F., & Richmond, T. J.** (1997). Crystal structure of the nucleosome core particle at 2.8 Å resolution. *Nature*, 389(6648), 251-260.
- Maison, C., Bailly, D., Peters, A. H., Quivy, J. P., Roche, D., Taddei, A., ... & Almouzni, G.** (2002). Higher-order structure in pericentric heterochromatin involves a distinct pattern of histone modification and an RNA component. *Nature genetics*, 30(3), 329-334.
- Martienssen, R. A., & Colot, V.** (2001). DNA methylation and epigenetic inheritance in plants and filamentous fungi. *Science*, 293(5532), 1070-1074.
- Ng, H. H., & Adrian, B.** (1999). DNA methylation and chromatin modification. *Current opinion in genetics & development*, 9(2), 158-163.
- Strahl, B. D., & Allis, C. D.** (2000). The language of covalent histone modifications. *Nature*, 403(6765), 41-45.

3.2 MATERIAL AND METHODS

Plant material

The isolated promoting sequences used for the Dual Luciferase Reporter Assay, the ChIP-seq and the DAP-seq data were obtained by chamber-grown *Vitis vinifera* cv. Shiraz fruiting cuttings, propagated as described in Mullins *et al.*, 1981.

Nicotiana benthamiana, plants were grown from seeds in a greenhouse with temperature between 21 °C and 30°C, relative humidity of approximately 32-50% and a 15h/9h light/dark cycle.

Anti-VviNAC60 polyclonal antibody

The anti-VviNAC60 polyclonal antibodies design has been performed thanks to an initial sequence alignment of the *VviNAC60* against all the other *VviNAC* genes to find the most specific sub-sequences of our gene of interest.

Then, a preliminary structure prediction of the VviNAC60 TF, to evaluate if the selected peptides would have been potentially exposed and could be able to interact with the antibody, has been created thanks to the Robetta server (<https://rosetta.bakerlab.org/>); it uses a fully automated structure prediction procedure that produces a model for an entire protein sequence in the presence or absence of sequence homology to protein(s) of known structure. The protein was visualized by UCSF Chimera (<https://www.cgl.ucsf.edu/chimera/>).

The anti-VviNAC60 polyclonal antibodies was finally produced by Biotem Company (<https://www.biotem-antibody.com/>) and was used for the immunoprecipitation step in the ChIP-Seq protocol.

ChIP-seq protocol

1) Tissue collection and fixation

- Collect the plant material (leaves/ berries) and keep it on ice.
- Wash 2 times for 1 minute with 40 ml sterile MilliQ in a 50 ml falcon tube.
- Sliced the tissue (berries must be without seeds) and put it on ice in a 50 ml falcon tube.

LEAVES: 1g

BERRIES: 3g

- Immediately add to the 50 ml falcon tube 36 ml of MC Buffer and 1 ml of 37% formaldehyde ($C_f = 1\%$ formaldehyde).

NB Better prepare the MC Buffer the evening before the fixation (under laminar flow hood) and keep it at 4°C.

| MC Buffer | | |
|--|--------|--|
| C_i | V_i | C_f |
| Na ₃ PO ₄ 1M pH7 | 10 ml | Na ₃ PO ₄ 10mM pH7 |
| NaCl 5M | 10 ml | NaCl 50mM |
| Sucrose 2M | 50 ml | Sucrose 0,1M |
| H ₂ O | 930 ml | H ₂ O |
| | 1L | |

NB Na₃PO₄ 1M pH7 is prepared adding to the Na₂HPO₄ 1M solution the NaH₂PO₄ 1M solution until a pH of 7 is reached (57,7 ml Na₂HPO₄ 1M + 42,3 ml NaH₂PO₄ 1M).

- Vacuum infiltrate keeping the sample on ice and submerged in the buffer (use a tinfoil ball).

LEAVES: 15 minutes+ 15 minutes (with a pause in the middle to mix the sample)

BERRIES: 4 x 10 minutes (with a pause in the middle to mix the sample)

- Add 3,7 ml of Glycine 1.25M and mix.
- Vacuum infiltrate for 5 minutes keeping the sample on ice and submerged in the buffer (use a tinfoil ball).
- Wash 3 times for 1 minute with 30 ml MC Buffer.
- Wash 1 time for 1 minute with 40 ml sterile MilliQ.

- Dry the plant tissue on tissue paper.
- Grind the sample in a mortar with liquid nitrogen.
- Make a pull and put the sample in a 50 ml falcon tube.
- Store at -80°C.

2) Nuclei isolation and chromatin shearing

- Do not let the sample defrost and add 25 ml of cold M1 Buffer to a 50 ml falcon tube containing 1 g of leaves/berries powder. Mix by inverting the tube until the sample is totally defrost. Keep it on ice for 10 minutes.

NB Better prepare the M1 Buffer the evening before (under laminar flow hood) and keep it at 4°C. Add the β -ME e the protease inhibitors just before use.

| M1 Buffer | | |
|--|----------------|--|
| C _i | V _i | C _f |
| Na ₃ PO ₄ 1M pH7 | 250 μ l | Na ₃ PO ₄ 10mM pH7 |
| NaCl 5M | 500 μ l | NaCl 0,1M |
| 2-methyl 2,4 pentanediol | 3,2 ml | |
| β -ME | 17,5 μ l | |
| Protease inhibitor | 1/2 tablet | |
| | 25 ml | (to volume with sterile MilliQ) |

- Use a 55 μ m sterile filter (the one that is used in the lab for protoplasts) and a sterile Petri dish to collect the nuclei and discard the tissue residues.
- Collect the filtrate in a new 50 ml falcon tube and keep it on ice.
- Centrifuge at 1.000 g for 20 minutes at 4°C.
- Wash the pellet with 5 ml of cold M2 Buffer.

NB Better prepare the M2 Buffer the evening before (under laminar flow hood) and keep it at 4°C. Add the β -ME e the protease inhibitors just before use.

| M2 Buffer | | |
|--|----------------|--|
| C _i | V _i | C _f |
| Na ₃ PO ₄ 1M pH7 | 250 μ l | Na ₃ PO ₄ 10mM pH7 |
| NaCl 5M | 500 μ l | NaCl 0,1M |
| 2-methyl 2,4 pentanediol | 3,2 ml | |
| β -ME | 17,5 μ l | |
| Protease inhibitor | 1/2 tablet | |
| MgCl ₂ 6H ₂ O 1M | 250 μ l | MgCl ₂ 6H ₂ O 10mM |
| Triton X-100 20% | 625 μ l | Triton X-100 0,5% |
| | 25 ml | (to volume with sterile MilliQ) |

- Centrifuge at 1.000 g for 10 minutes at 4°C.
- Discard the supernatant and repeat the wash with the cold M2 Buffer 4 more times.
- Discard the supernatant and wash the pellet with 5 ml of cold M3 Buffer.

NB Better prepare the M3 Buffer the evening before (under laminar flow hood) and keep it at 4°C. Add the β -ME e the protease inhibitors just before use.

| M3 Buffer | | |
|--|----------------|--|
| C _i | V _i | C _f |
| Na ₃ PO ₄ 1M pH7 | 250 μ l | Na ₃ PO ₄ 10mM pH7 |
| NaCl 5M | 500 μ l | NaCl 0,1M |
| β -ME | 17,5 μ l | |
| Protease inhibitor | 1/2 tablet | |
| | 25 ml | (to volume with sterile MilliQ) |

- Centrifuge at 1.000 g for 10 minutes at 4°C.
- Discard the supernatant and resuspend the pellet in 1 ml of cold Sonic Buffer.

NB Prepare, filter and aliquote the Sonic Buffer in 2 ml eppy tubes and store at -20°C. Keep it on ice before use.

| Sonic Buffer | | |
|--|----------------|--|
| C _i | V _i | C _f |
| Na ₃ PO ₄ 1M pH7 | 500 μ l | Na ₃ PO ₄ 10mM pH7 |
| NaCl 5M | 1ml | NaCl 0,1M |
| Sarkosyl 5% | 250mg | |
| EDTA 0,5M pH8 | 1ml | EDTA 10mM pH8 |
| Protease inhibitor | 1/2 tablet | |
| | 50 ml | (to volume with sterile MilliQ) |

- Transfer the solution in a 2 ml eppy tube and keep it on ice.
- Aliquote 130 μ l of the solution in Covaris microTUBEs and sonicate for the maximum time (20 minutes) as describe below.

NB Check the sonication on an agarose gel. The DNA smear should be concentrated between 200 and 1000 bp.

Appendix A: AFA Focused Ultrasonicator Operating Conditions

| Low Tissue Mass Chromatin Shearing Protocol | | | | | | |
|---|---------|---------|------------|----------------|------------|------------|
| Instrument | M220 | ME220 | S220 | E220 Evolution | E220 | LE220 |
| Target Size (bp) | 200-700 | 200-700 | 200-700 | 200-700 | 200-700 | 200-700 |
| PIP | 75 | 75 | 105 | 105 | 105 | 300 |
| Duty Factor (%) | 5 | 5 | 2 | 2 | 2 | 15 |
| CPB | 200 | 1000 | 200 | 200 | 200 | 200 |
| Treatment Time (minutes) | 2-20 | 2-20 | 2-12 | 2-12 | 2-12 | 2-12 |
| Setpoint Temperature (C) ¹ | 7 | 9 | 6 | 6 | 6 | 6 |
| Min/Max Temperature (C) | 4/10 | 6/12 | 3/9 | 3/9 | 3/9 | 3/9 |
| Degassing Mode | NA | NA | Continuous | Continuous | Continuous | Continuous |
| Max Cell Number (Million) | 3M | 3M | 3M | 3M | 3M | 3M |
| AFA Intensifier Required ² | NA | NA | Integrated | Yes | Yes | NA |
| Water Level (run) ³ | Full | 9 | 12 | 6 | 6 | 6 |
| Sample Volume (µl) ⁴ | 130 | 130 | 130 | 130 | 130 | 130 |

Important Notes

1. If using the S220, E220 Evolution, E220, or LE220, set the temperature on the external chiller 3C below the setpoint temperature for the run. The min/max is set in SonoLab
2. If intensifier is required, please ensure PN 500141 is used
3. Water level should always be 1mm below the neck of the microTUBE-130 cap ⁴. Always fill the microTUBE-130 with 130 µl of sample

- Transfer the sonicated solution in a new 2 ml eppy tube.
- Centrifuge at top speed for 20 minutes at 4°C.
- Transfer the supernatant in a new 2 ml eppy tube measuring the correct volume.
- Add an equal volume of cold IP Buffer.

NB Prepare, filter and aliquote the IP Buffer in 2 ml eppy tubes and store at -20°C. Keep it on ice before use.

| IP Buffer | | |
|--|----------------|---|
| C _i | V _i | C _f |
| HEPES 0,5M pH7.5 | 5ml | HEPES 50mM pH7.5 |
| NaCl 5M | 1,5ml | NaCl 150mM |
| MgCl ₂ 6H ₂ O 1M | 250µl | MgCl ₂ 6H ₂ O 5mM |
| ZnSO ₄ 100mM | 5µl | ZnSO ₄ 10µM |
| Triton X-100 20% | 2,5ml | Triton X-100 1% |
| SDS 10% | 250µl | SDS 0,05% |
| | 50 ml | (to volume with sterile MilliQ) |

- Put aside in a 2 ml eppy tube 120 µl of sheared chromatin as control (“input DNA”) and store at -20°C.
- Aliquote 800µl of the remaining sheared chromatin in 1,5 ml low adhesion eppy tube.

3) Chromatin immunoprecipitation

- Prepare the Protein-A Agarose Beads (Protein-A agarose beads (Santa Cruz, cat. no. sc-2001) in a 1,5 ml low-adhesion eppy tube.

NB 160 μ l beads per sample are needed, plus 100 μ l of extra beads in total.

Es. 3 samples = 160 μ l * 3 \rightarrow 480 μ l \rightarrow +100 μ l \rightarrow 580 μ l beads in total

- Wash the beads with 1ml IP Buffer (independently from the volume of the beads) inverting the eppy tube several times.
- Centrifuge at 3.800 g for 3 minutes at 4°C.
- Discard 1ml of supernatant.
- Repeat the wash of the beads with the IP Buffer.
- Add 80 μ l of Protein-A Agarose Beads to the sample using a sterile cut tip.

NB This step is important to remove all the DNA linked to protein containing an IgG before adding the antibody (that is produced in rabbit and contains an IgG) and to avoid false positive. Use a 1,5 ml eppy tube to better visualize the beads pellet.

- Incubate on a rotating wheel for 2h at 4°C.
- Centrifuge at 3.800 g for 5 minutes at 4°C.
- Carefully transfer the supernatant in a new 1,5 ml low adhesion eppy tube (avoid all the beads).
- Add 3 μ g of antibody to the sample (anti-VvNAC60: 1,4mg/ml \rightarrow 2,2 μ l).
- Incubate on a rotating wheel for 2h at room temperature.
- Add 80 μ l of Protein-A Agarose Beads to the sample using a sterile cut tip.
- Incubate on a rotating wheel for 2h at 4°C.
- Centrifuge at 3.800 g for 5 minutes at 4°C.
- Discard the supernatant without touching the beads.
- Wash the beads 3 times with 1ml IP Buffer leaving the eppy tube in rotation at room temperature for 8 minutes; centrifuge every time at 3.800 g for 3 minutes at room temperature and discard 1 ml of supernatant.

- Add 100 μ l of cold Elution Buffer to the beads.

NB Prepare, filter and aliquote the Elution Buffer in 2 ml eppy tubes and store at -20°C . Keep it on ice before use.

| Elution Buffer (pH 2.8 with HCl) | | |
|----------------------------------|------------|---------------------------------|
| C_i | V_i | C_f |
| Glycine 1,25M | 4ml | Glycine 0,1M |
| NaCl 5M | 5ml | NaCl 0,5M |
| Tween 20 | 25 μ l | |
| | 50 ml | (to volume with sterile MilliQ) |

- Incubate with vigorous shaking at 37°C for 1 minute.
- Centrifuge at maximum speed for 1 minute at room temperature.
- Transfer the supernatant in a new 1,5 ml eppy tube and add 50 μ l of Tris-HCl 1M pH9.
- Add 100 μ l of cold Elution Buffer to the beads.
- Incubate with vigorous shaking at 37°C for 1 minute.
- Centrifuge at maximum speed for 1 minute at room temperature.
- Transfer the supernatant in the 1,5 ml eppy tube and add 50 μ l of Tris-HCl 1M pH9.
- Add 100 μ l of cold Elution Buffer to the beads.
- Incubate with vigorous shaking at 37°C for 4 minutes.
- Centrifuge at maximum speed for 1 minute at room temperature.
- Transfer the supernatant in the 1,5 ml eppy tube and add 50 μ l of Tris-HCl 1M pH9.

NB The final volume in the 1,5 ml eppy tube should be of 450 μ l.

- Centrifuge at maximum speed for 2 minutes at room temperature.
- Transfer the supernatant in a new 2 ml eppy tube.
- Recover the 120 μ l of “input DNA” and add 330 μ l of TE Buffer to them.

| TE Buffer | | |
|-----------------|-------------|---------------------------------|
| C_i | V_i | C_f |
| EDTA 0,5M pH8 | 100 μ l | EDTA 1mM pH8 |
| Tris-HCl 1M pH8 | 500 μ l | Tris-HCl 10mM pH8 |
| | 50 ml | (to volume with sterile MilliQ) |

- Add 11,25 μ l of Proteinase K ($C_i = 20\text{mg/ml} \rightarrow C_f = 0,5\text{mg/ml}$) to the sample and to the “input DNA”.
- Incubate at 37°C o/n.
- Add a second aliquote of Proteinase K (11,25 μ l).
- Incubate at 65°C for 6 h.
- Add 2.5 volumes of 100% EtOH, 1/10 volume of 3M NaAc pH 5.4 and 1 μ l of Glycogen.
- Let the DNA precipitate at -20°C o/n.
- Centrifuge at maximum speed for 30 minutes at 4°C.
- Resuspend the pellet with 100 μ l of sterile MilliQ.
- Purify the DNA using the Qiagen PCR Purification Kit and elute in 30 μ l of EB in a new 1,5 ml low adhesion eppy tube.

4) Libraries preparation

The ChIP-seq libraries were prepared using the KAPA Hyper Prep Kit (Roche), starting from 500pg of IP and from 2,5ng of INPUT, using for the purification clean-up the AMPure XP beads (Beckman Coulter) and amplifying the IP and the INPUT libraries for 13 and 10 cycles, respectively.

Finally, the libraries were quantified through qPCR Real Time analysis.

pIX-HALO cloning

The previously isolated *VviNACs* ORF and the one isolated by D’Inca (2017), *VviNAC03*, *VviNAC11*, *VviNAC13*, *VviNAC33* and *VviNAC60*, were transferred from the pENTR/D-TOPO to the Gateway-compatible pIX-HALO destination vector (Bartlett *et al.*, 2017) following the site specific LR recombination manual of the Gateway^R Technology system. A pIX-HALO vector containing the GST sequence, instead of the TF CDS, was used as negative control.

Genomic DNA extraction (from Thomas *et al.*, 1993)

1. Put 1 g of grinded tissue in a 50 ml falcon tube.
2. Add 12,5 ml of CNB buffer (with β -ME added) and vortex.

| CNB Crude Nuclei Buffer pH7.6 | | |
|---|----------------------|--|
| C_i | C_f | Volumes (V_f = 100ml) |
| 5 M NaCl | 0.25 M | 5 ml |
| 1 M Tris-HCl pH 7.6 | 0.2 M | 20 ml |
| PVP 40.000 | 2,5% | 2,5 g |
| 0.5 M Na ₂ EDTA pH 8 | 0.05 M | 10 ml |
| β -ME | 0.1 % | 100 μ l |
| H ₂ O | | to a final volume of 100 ml |
| β -ME must be added just before use | | |
| Store at 4°C | | |

3. Centrifuge at 4.000 rpm for 10 minutes at 4°C and discard the supernatant.
4. Add 5 ml of EtOH/Sark and resuspend the pellet by vortexing.

| DNA Extraction Buffer EtOH/Sark | | |
|--|----------------------|--|
| C_i | C_f | Volumes (V_f = 100ml) |
| 5 M NaCl | 0.5 M | 10 ml |
| 1 M Tris-HCl pH 8 | 0.2 M | 20 ml |
| PVP 40.000 | 2,5% | 2,5 g |
| 0.5 M Na ₂ EDTA pH 8 | 0.05 M | 10 ml |
| N-Lauroyl-Sarcosine | 3% | 3 g |
| EtOH | 20% | 20 ml |
| β -ME | 1% | 1 ml |
| H ₂ O | | to a final volume of 100 ml |
| β -ME and EtOH must be added just before use | | |
| Store at 4°C | | |

5. Put the falcon tube at 55°C for 30 minutes with frequent shaking.
6. Add 5 ml of chloroform and vortex.
7. Transfer the solution to a 15 ml falcon tube to better visualize the phase separation.
8. Centrifuge at 5.000 rpm for 15 minutes at 20°C.
9. Add 2,5 ml of isopropanol into a new 50 ml falcon tube.

10. Transfer the upper phase of the 15 ml falcon tube into the 50 ml falcon tube with isopropanol.
11. Mix very well by inverting the 50 ml falcon tube until a white precipitate is seen.
12. Leave at room temperature for 15 minutes.
13. Centrifuge at 5.000 rpm for 15 minutes at 20°C and discard the supernatant.
14. Put the 50 ml falcon tube upside down on some paper layers to better discard the supernatant drops.
15. Wash the pellet with 5 ml of 70% EtOH.
16. Centrifuge at 5.000 rpm for 10 minutes at 20°C and discard the supernatant.
17. Put the 50 ml falcon tube upside down on some paper layers to better discard the supernatant drops.
18. Let the pellet air dry.
19. Resuspend the pellet with 600 µl of TE buffer added with RNase (3µl of 20mg/ml stock).
20. Place the 50 ml falcon tube at 4°C O/N.
21. Transfer the gDNA solution in a 1,5 ml eppy tube.
22. Add 300 µl of 7.5 M NH₄OAc.
23. Centrifuge at 13.000 rpm for 10 minutes at room temperature.
24. Transfer the supernatant to a new 1,5 ml eppy tube.
25. Add 500 µl of isopropanol.
26. Mix by inverting until a precipitate is seen.
27. Centrifuge at 13.000 rpm for 10 minutes at room temperature and discard the supernatant.
28. Wash the pellet with 1 ml of 70% EtOH.
29. Centrifuge at 13.000 rpm for 10 minutes at room temperature and discard the supernatant.
30. Let the pellet air dry.
31. Resuspend the pellet with 300 µl of TE buffer.
32. Leave the eppy tube at 4°C O/N for a better resuspension.

DAP-seq protocol

- **gDNA library preparation (from Galli *et al.*, 2018)**

1) Fragmentation:

- Measure gDNA concentration using Invitrogen Qubit (Quant-iT™ Assays with Qubit™ dsDNA BR Assay Kit, 2-1000ng, using only thin-wall clear 0,5ml PCR tubes).
- Set up Covaris S2: chill and degas the water (~1h).
- Dilute 7,5µg of gDNA with EB (Elution Buffer, Qiagen) in a finale volume of 130µL and load it into a snap-cap Covaris tube (Covaris cat. 520045, microTUBEs AFA Fiber Pre-Slit Snap-Cap 6X16mm).
- Run 200bp fragment program.

200bp Covaris settings:

Mode: Frequency Sweeping
 Duty Cycle: 10%
 Intensity: 5
 Cycles/Burst: 200
 Time: 60sec
 Number of cycles: 3
 Water level: 12 (between 10-15 on the Covaris)
 T: <10°C (better around 4°C)

- Transfer 125µl of sheared sample to a 1,5ml low- bind eppy tube.
- AMPure XP Beads clean (1X → i.e.: 125µL DNA + 125µL beads).
 - Add beads and vortex 10 seconds; quick spin. Incubate at RT for 10 minutes.
 - Place on magnetic rack (Invitrogen, Dynal, Beads separation) for 5min.
 - Remove most of supernatant with pipet.
 - Immediately add 500µl 80% EtOH (freshly made), remove and rotate tube 180 degrees on the magnet for 6 times to wash beads. Wait 1 minute.
 - Pipet off EtOH and repeat wash as in iv.
 - Pipet off all remaining EtOH.
 - Dry tubes with caps open at 37°C on the magnet until cracks form in beads (~10 minutes).

- viii. Resuspend beads in 35µl EB and mix well by pipetting. Incubate at RT for 10 minutes.
 - ix. Place on magnet for 3 minutes and then aspirate supernatant into new tube being careful not to transfer beads.
- g. Check concentration on Qubit to ensure good yield before continuing (optional).

2) End Repair:

- a. 50µL reaction (End-It kit; Lucigen cat. ER0720 or ER81050):

| | |
|---------------|------|
| DNA sample | 34µL |
| 10x Buffer | 5µL |
| dNTP Mix | 5µL |
| ATP | 5µL |
| End-it Enzyme | 1µL |

- b. Incubate at RT for 45min.
- c. Qiaquick PCR purify (QIAquick PCR Purification Kit; Cat No./ID: 28104).

3) A-tail:

- a. 50µL reaction:

| | |
|-------------------------|------|
| DNA sample | 32µL |
| NEBuffer2 | 5µL |
| 1mM dATP | 10µL |
| Klenow (3'-5'exo-; NEB) | 3µL |

-Klenow (3'-5' exo-) M0212L 5,000U/ml NEB
 -dATP Solution N0440S 100mM NEB

- b. Incubate at 37°C for 30min.
- c. Qiaquick PCR purify and elute off column in 32µl EB.

4) Adapter Ligation:

- a. 50µL reaction:

| | |
|---------------------|------|
| DNA sample | 30µL |
| 10x ligase Buffer | 5µL |
| 30µM Y-Adapter | 10µL |
| T4 DNA Ligase (NEB) | 5µL |

-T4 DNA Ligase M0202L 400,000U/ml NEB
 -Y-Adapter:

5'-/5Phos/GATCGGAAGAGCACACGTCTGAACTCCAGTCAC-3'
 5'-ACACTCTTTCCCTACACGACGCTCTTCCGATCT-3'

- b. Incubate at 16°C for overnight.
- c. Heat inactivate at 70°C for 10min.
- d. Bead clean using commercial AMPure XP beads as described above (1X → i.e.: 50µL DNA + 50µL beads).
- e. Elute in 32µl EB.
- f. Check concentration with Qubit (Quant-iT™ Assays with Qubit™ dsDNA BR Assay Kit using only thin-wall clear 0,5ml PCR tubes).
- g. Store at -20°C.

- **TF in vitro expression (from Bartlett et al., 2017)**

5) In vitro protein expression

- a) Use 1µg of pIX-HALO-ORF plasmid in a 50µl TNT Coupled Reticulocyte Lysate System reaction (*Promega, Catalog number L4601*).

| TNT® Coupled Reticulocyte Lysate Systems | (X1) µl |
|--|------------|
| TNT Rabbit Reticulocyte Lysate | 25 |
| TNT Reaction Buffer | 2 |
| Minus Met 1mM | 1 |
| Minus Leu 1mM | 1 |
| RNasin Ribonuclease Inhibitor | 1 |
| TNT RNA Polymerase (SP6) | 1 |
| pIX-HALO-TF + EB (1µg) | 10 |
| H ₂ O | 9 |
| | 50 |

RNasin Ribonuclease Inhibitor (*Promega, Catalog number N251B*) is not in the kit and must be ordered separately.

- b) Aliquot 40µl of master mix to each PCR.
- c) Add 10µl of EB diluted pIX-HALO-TF and pipet slowly up and down to mix.
- d) Quick spin.
- e) Incubate at 30°C for 2 hours and then let the samples stay at RT.

- **DAP-seq (from Galli et al., 2018)**

6) DAP

- a) Wash 10 μ l of Magne Halo-Tag beads (*Promega, Catalog number G7282*) per DAP sample in 1ml PBSNP wash buffer (1xPBS +0.005%NP40; add 7.5 μ l of 20% NP40 to 30ml 1xPBS).
- b) Flick tube to mix.
- c) Place on magnet (*Invitrogen Dynal Beads Separation*) and remove supernatant. Repeat three times.
- d) Resuspend beads in volume that allows each sample to contain 45 μ l of beads.
- e) Save 5 μ l of each TNT Coupled Reticulocyte Lysate System reaction to check the correct TFs expression on a Western blot. Store at -20°C.
- f) Add 45 μ l of washed Magne Halo-Tag beads to each of the remaining 45 μ l of TNT Coupled Reticulocyte Lysate System reactions.
- g) Rotate at RT for 1 hour.
- h) Place tube on a PCR tubes magnet.
- i) Remove supernatant and wash with 90 μ l PBSNP wash buffer flicking gently the tube to mix. Let the beads settle. Put on the magnet. Repeat for 4 times.
- j) Final resuspend in 40 μ l of PBST.
- k) Dilute 500ng of adapter ligated gDNA library in EB to a final volume of 40 μ l.
- l) Add the 40 μ l of EB diluted gDNA library to the 40 μ l of PBSNP resuspended beads (total final volume of 80 μ l sample).
- m) Rotate at RT for 1 hour.
- n) Place PCR tubes on magnet, remove supernatant.
- o) Wash beads with 90 μ l of PBST as above for 6 times.
- p) Resuspend beads in 25 μ l EB, transfer to new PCR tubes.
- q) Heat tubes at 98°C in PCR machine for 10 min to release DNA and denature protein.

- r) Place on ice 5 min.
- s) Place on magnet, transfer supernatant to new PCR tubes.

The DAP step was performed using 500 ng of libraries for VviNAC01, VviNAC03, VviNAC11, VviNAC13, VviNAC15, VviNAC18, VviNAC38, VviNAC39 and VviNAC61, whereas for VviNAC08, VviNAC17, VviNAC26, VviNAC33 and VviNAC60 1000 ng were used.

7) PCR Enrichment

- a) 50µL reaction (*Phusion High-Fidelity DNA Polymerase, NEB, M0530S or M0530L*).

| Enrichment PCR | |
|--------------------|------|
| | (X1) |
| DAP sample | 25,0 |
| 5x HF Buffer | 10,0 |
| 10mM dNTPs | 2,5 |
| Primer i5* (25µM) | 1,0 |
| Primer i7* (25µM) | 1,0 |
| Phusion polymerase | 1,0 |
| H ₂ O | 9,5 |
| | 50,0 |

95°C X 2 min

98°C X 30 sec

98°C X 15 sec

60°C X 30 sec

72°C X 1 min

X20

72°C X 10 min

4°C X ∞

- b) Transfer the PCR reactions in 1,5ml eppy tubes.
- c) Perform 1x AMPure beads clean-up (i.e. 50µl of beads + 50µl PCR reaction).
- d) Elute in 22µl EB.
- e) Measure the final library concentration using Qubit dsDNA HS kit (*Invitrogen, Catalog number Q32854*).
- f) Check library quality using bioanalyzer or KAPA Library Quantification Kit (Illumina platforms) to confirm absence of adapter dimers prior to sequencing.

g) Store at -20°C.

Sequencing

The DAP-seq and ChIP-seq datasets were obtained through a NextSeq500 sequencing system which gave a total of 60 (ChIP-seq) and 3,5 (DAP-seq) million 75 bp single reads for each sample; VviNAC08, VviNAC17 and VviNAC26 DAP-seq datasets were obtained from a 150 bp paired-end sequencing.

Read mapping, filtering, peak calling and motif analysis

Fastq files were trimmed using trimmomatic (Bolger *et al.*, 2014) with the following parameters: ILLUMINACLIP = TruSeq3-, SE = 2:30:10. LEADING = 3, TRAILING = 3, SLIDINGWINDOW = 4:20, MINLEN = 50. Trimmed reads were mapped to the grape reference genome version 12X.2 (nuclear chromosomes only) at URGI (<https://urgi.versailles.inra.fr/Species/Vitis/Annotations>) using bowtie2 v2.3.4.3 (Langmead and Salzberg, 2012). Reads mapping to multiple locations were filtered, removing all reads with the XS:i field present in the BAM file. Uniquely mapped reads were used for all subsequent steps. Peaks were called using GEM v3.4 (Guo *et al.*, 2012) applying the following parameters: --d Read_Distribution_default.txt --k_min 6 --k_max 20 --outNP; for the DAP-seq samples, a GST-HALO negative control was used for background subtraction. To reduce the number of false positives, in the DAP-seq datasets all peaks with a sample/control ratio < 5 fold were removed. The remaining peaks were associated with nearest genes using the ChipSeeker R package (Yu *et al.*, 2015). For gene annotation, we used the V1 on the 12X.0 assembly transposed to the 12X.2 assembly. The gff3 files were downloaded from URGI. For visualization in the Integrative Genome Browser (IGV), bam files were converted to bigwig files using deepTools v3.4.3, bamCoverage with a 10-bp bin size, and FPKM normalization. Motifs were detected and assigned using RSAT Plants NGS ChIP-Seq peak-motifs analysis and RSAT Plants Motif Discovery dyad-analysis (<http://rsat.eead.csic.es/plants/index.php>). The analyses were performed in collaboration with Prof. Nicola Vitulo (Università degli Studi di Verona).

REFERENCES

- Bartlett, A., O'Malley, R. C., Huang, S. S. C., Galli, M., Nery, J. R., Gallavotti, A., & Ecker, J. R.** (2017). Mapping genome-wide transcription-factor binding sites using DAP-seq. *Nature protocols*, 12(8), 1659.
- Bolger, A. M., Lohse, M., & Usadel, B.** (2014). Trimmomatic: a flexible trimmer for Illumina sequence data. *Bioinformatics*, 30(15), 2114-2120.
- Galli, M., Khakhar, A., Lu, Z., Chen, Z., Sen, S., Joshi, T., ... & Gallavotti, A.** (2018). The DNA binding landscape of the maize AUXIN RESPONSE FACTOR family. *Nature communications*, 9(1), 1-14.
- Guo, Y., Mahony, S., & Gifford, D. K.** (2012). High resolution genome wide binding event finding and motif discovery reveals transcription factor spatial binding constraints. *PLoS Comput Biol*, 8(8), e1002638.
- Kaufmann, K., Muino, J.M., Osteras, M., Farinelli, L., Krajewski, P., and Angenent, G.C.** (2010). Chromatin immunoprecipitation (ChIP) of plant transcription factors followed by sequencing (ChIP-SEQ) or hybridization to whole genome arrays (ChIP-CHIP). *Nat. Protoc.* **5**: 457-472.
- Kim, David E., Dylan Chivian, and David Baker.** (2004). Protein structure prediction and analysis using the Robetta server. *Nucleic acids research* 32. Suppl 2, W526-W531.
- Langmead, B., & Salzberg, S. L.** (2012). Fast gapped-read alignment with Bowtie 2. *Nature methods*, 9(4), 357.
- Mullins, M. G., & Rajasekaran, K.** (1981). Fruiting cuttings: revised method for producing test plants of grapevine cultivars. *American Journal of Enology and Viticulture*, 32(1), 35-40.
- Pettersen, Eric F., et al.** (2004). UCSF Chimera—a visualization system for exploratory research and analysis. *Journal of computational chemistry* 25.13, 1605-1612.
- Thomas, M. R., & Scott, N. S.** (1993). Microsatellite repeats in grapevine reveal DNA polymorphisms when analysed as sequence-tagged sites (STSs). *Theoretical and Applied Genetics*, 86(8), 985-990.
- Yu, G., Wang, L. G., & He, Q. Y.** (2015). ChIPseeker: an R/Bioconductor package for ChIP peak annotation, comparison and visualization. *Bioinformatics*, 31(14), 2382-2383.

3.3 RESULTS

The selected *VviNACs* sequences were transferred into the pIX-Halo vector and *in vitro* translated; afterwards, they were used in a DAP-seq assay to study the specific cistrome for each of them.

Considering the enormous datasets derived from the DAP-seq assays, the decision was to keep analyzing only the FC>5 (compared to GST-Halo expressed protein, the negative control) filtered peaks obtained from each *VviNAC*, which correspond to more than the 90% average of the starting dataset.

Unexpectedly, most of the binding sites were not found in the ‘standard’ studied promoting regions; indeed, many features were found in the ‘distal intergenic’ and in the ‘intron’ regions. Considering the recent discoveries concerning the mechanisms of transcription regulation, it is extremely risky not to give relevance to all these genic regions as a lot of information could be obtained from newly studied long-distance features; despite this consideration, these type of regulation mechanisms are still unknown or not well defined and it will be difficult to presume a hypothetical regulatory network based on them.

For this reason, the attention for further considerations about the *VviNACs* targets was focused only on the ‘promoter’ (up to 2Kb from the transcription start site) and ‘5’UTR’ genic regions. These ‘standard’ and well-known transcription promoting regions are the most intuitive and obligatory starting point in the difficult but fascinating world of the fine *VviNACs* regulatory network.

Between the target of each TF, a lot of *switch* genes (Palumbo *et al.*, 2014) and transition markers (Fasoli *et al.*, 2018) were found, indicating that the selected *VviNACs* represent the regulators of many maturation-related genes.

Interestingly but also in line with the well know cooperative family role of the *VviNAC* TFs, many genes were found to be targets of more than one of the selected *VviNACs*.

All the filtered DAP-seq datasets were also crossed with the transient and stable over expression results to highlight some particularly interesting genes.

The results clearly show how the over expression could reveal the general and final principal effects of a TF on the plant biological processes, without necessarily

highlighting the effective direct targets of the TF transcriptional regulation, which are correctly recognized and reported in the DAP-seq assay.

VviNAC01

The DAP-seq assay reported 20730 binding sites (peaks), which were reduced to 20153 after the FC>5 filtering; even considering the very stringent filter used, the loss was very low, only the 3% (**Fig. 28**). The distribution of peaks revealed that 24% were located within the promoter regions (up to 2 kb upstream from a transcription start site), 1% were in 5' untranslated regions (UTRs), 12% were located in exons, 18% were located within introns, 3% were located in 3' UTRs, 7% were located in the 3 kb downstream region, and 32% were intergenic.

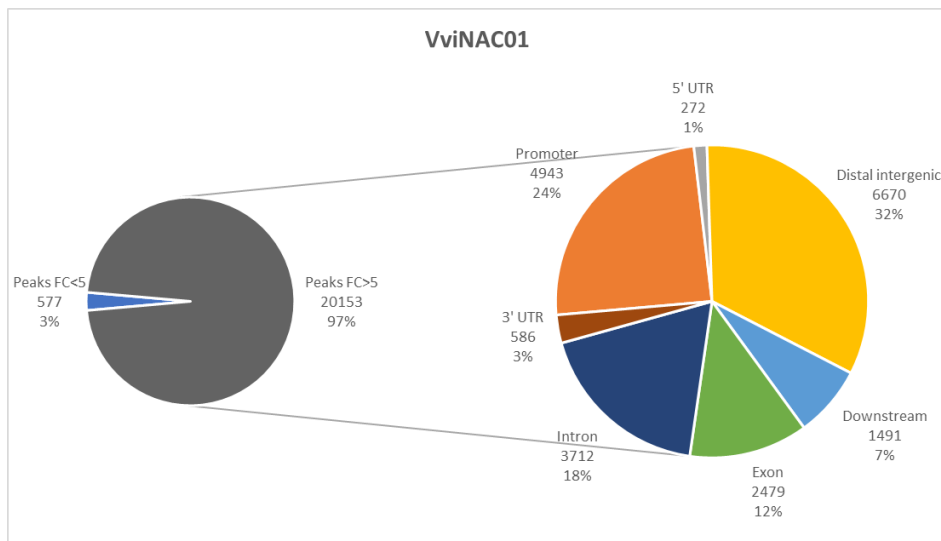


Figure 28: Double pie chart of the VviNAC01 DAP-seq results. The pie on the left represents the total binding sites (peaks) obtained, divided between the FC>5 and FC<5 (compared to the GST-Halo negative control peaks). The pie on the right represents the subdivision into the different genic region of the selected filtered peaks.

Three major binding motifs (TT[G/A][C/A][G/T]TG[T/A]) were identified with strong significance (**Fig. 29**) and the phylogenetic footprints correlate with ANAC092, considered the key positive regulator of leaf senescence, involved in a delicately balanced feed-forward loop that promotes ethylene-mediated chlorophyll degradation (Kim *et al.*, 2009).

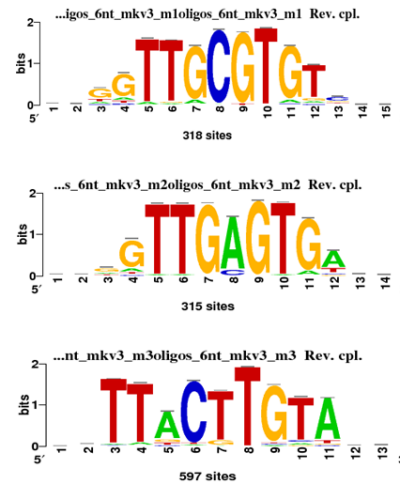


Figure 29: RSAT Plants NGS ChIP-Seq peak motifs analysis on the *VviNAC01* DAP-seq results. Three top-ranking binding motifs identified in the DAP-seq FC>5 filtered dataset, based on the detection of overrepresented oligonucleotides (oligo analysis). The overall height of each letter stack indicates the sequence conservation at that position, and the height of symbols within the stack reflects the relative frequency of the corresponding nucleic acid at that position.

The attention was focused only on the 25% of the final analyzed binding sites, which belongs to the ‘promoter’ and ‘5’UTR’ genic regions, for a total of 5215 sites; this percentage, at first considered low compared to the number of sites, was perfectly in line with other DAP-seq published papers.

After the elimination of all the ‘no hit’ and ‘unknown’ elements, 4215 binding sites were obtained for a total of 3545 unique genes regulated by *VviNAC01*.

A GO enrichment analysis was performed on this sub-dataset, revealing a predominance of genes related to general categories such as biological regulation, in particular to the regulation of different biological and metabolic processes and transcription (**Fig. 30**).

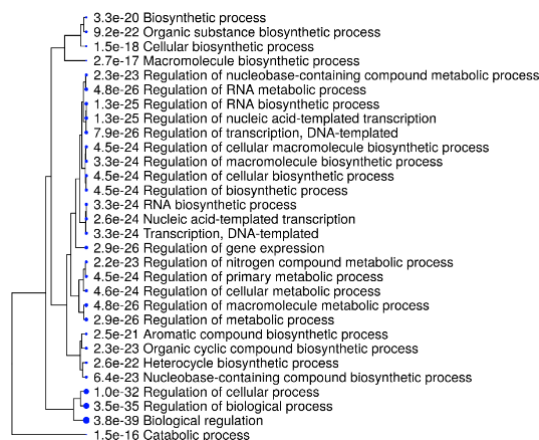


Figure 30: GO enrichment analysis of the *VviNAC01* targets found to be regulated in the promoter and 5’UTR regions. The analysis was performed on ShinyGO.

Between the top 20 (q-value based) promoter and 5'UTR located binding sites some interesting genes were found (**Table 21**).

| q-value | Genic region | Gene ID | Distance to TSS | Functional annotation |
|---------------|------------------|-------------------|-----------------|--|
| 114.67 | Promoter (1-2kb) | VIT_16s0098g01150 | -1172 | Auxin-responsive SAUR29 * |
| 83.07 | Promoter (1-2kb) | VIT_07s0191g00050 | -1919 | Peroxidase 17 * |
| 78.94 | Promoter (<=1kb) | VIT_07s0255g00110 | -145 | WD40 |
| 77.17 | Promoter (<=1kb) | VIT_01s0026g01030 | -974 | Zinc finger (C3HC4-type ring finger) |
| 76.64 | Promoter (1-2kb) | VIT_13s0067g00600 | -1194 | Arginine-tRNA-protein transferase 1 |
| 73.98 | Promoter (<=1kb) | VIT_17s0000g06970 | -424 | Diacylglycerol kinase 1 |
| 69.67 | Promoter (<=1kb) | VIT_18s0001g14950 | -543 | EMB2170 (embryo defective 2170) |
| 68.94 | Promoter (<=1kb) | VIT_04s0044g00710 | -159 | UTP--glucose-1-phosphate uridylyltransferase * |
| 67.78 | Promoter (<=1kb) | VIT_06s0061g01190 | -132 | SWI/SNF matrix-associated regulator of chromatin sbfamily A mber 3 2 |
| 65.87 | Promoter (1-2kb) | VIT_08s0056g01480 | -1033 | Cation exchanger, CAX7 |
| 65.13 | Promoter (1-2kb) | VIT_12s0059g00870 | -1271 | MAPKKK15 |
| 64.48 | Promoter (1-2kb) | VIT_18s0001g09420 | -1850 | Progesterone 5-beta-reductase |
| 62.39 | Promoter (<=1kb) | VIT_18s0001g08300 | 0 | Tubulin alpha-6 chain |
| 62.17 | Promoter (<=1kb) | VIT_10s0003g00140 | -733 | ERF/AP2 Gene Family (VvERF064) |
| 61.59 | Promoter (<=1kb) | VIT_19s0177g00070 | -505 | Polyubiquitin (UBQ14) |
| 60.66 | Promoter (1-2kb) | VIT_18s0001g14980 | -1611 | 3-methyl-2-oxobutanoate dehydrogenase |
| 60.66 | Promoter (1-2kb) | VIT_11s0118g00220 | -1417 | Chloride channel protein CLC |
| 60.1 | Promoter (<=1kb) | VIT_06s0004g04180 | -452 | Zinc finger (C2H2 type) protein (ZAT11) * |
| 59.8 | Promoter (<=1kb) | VIT_17s0000g06410 | -525 | MYB transcription factor MIXTA-like 2 |
| 59.52 | Promoter (<=1kb) | VIT_06s0080g00970 | -157 | NAC domain-containing protein (VvNAC67) |

Table 21: Top 20 (q-value based) represented direct target genes of VviNAC01. In bold are reported the *switch* genes and the asterisk (*) refers to the transition markers.

The most sequenced represented gene was an auxin-related gene, the *AUXIN-RESPONSIVE SAUR29* (VIT_16s0098g01150). Moreover, in agreement with what found in **Chapter 2**, the ethylene-related gene *ERF/AP2 GENE FAMILY VvERF064* (VIT_10s0003g00140) was found. Two transcription factors, *MYB TRANSCRIPTION FACTOR MIXTA-LIKE 2* (VIT_17s0000g06410) and *VviNAC67* (VIT_06s0080g00970), were also present in the list.

Afterwards, the list of the VviNAC01 targets was used to find all the possible VviNACs targets of the TF. 23 VviNACs target genes were found (**Table 22**), some of which harboring multiple VviNAC01 binding sites, *VviNAC29* (VIT_19s0027g00880), *VviNAC34* (VIT_12s0028g03050) and *VviNAC37* (VIT_10s0003g00350), for a total of 28 VviNAC01-VviNACs defined interactions. Intriguingly, between them *VviNAC01* itself was found, indicating an autoregulation of the TF. Moreover, *VviNAC08*, *VviNAC17*, *VviNAC39* and *VviNAC61* were also found.

| q-value | Genic region | Gene ID | Distance to TSS | Functional annotation |
|---------|------------------|-------------------|-----------------|--|
| 59,52 | Promoter (<=1kb) | VIT_06s0080g00970 | -157 | NAC domain-containing protein (VvNAC67) |
| 27,26 | Promoter (<=1kb) | VIT_08s0007g07640 | 0 | NAC domain-containing protein (VvNAC61) |
| 25,66 | Promoter (<=1kb) | VIT_11s0016g02880 | 0 | NAC domain-containing protein (VvNAC19) |
| 23,31 | Promoter (1-2kb) | VIT_13s0019g05240 | -1179 | NAC domain-containing protein (VvNAC20) |
| 21,71 | Promoter (<=1kb) | VIT_12s0028g03050 | -353 | NAC domain-containing protein (VvNAC34) |
| 16,86 | Promoter (1-2kb) | VIT_07s0031g02610 | -1560 | NAC domain-containing protein (VvNAC39) |
| 15,38 | Promoter (<=1kb) | VIT_10s0003g00350 | 0 | NAC domain-containing protein (VvNAC37) |
| 15,31 | Promoter (<=1kb) | VIT_18s0001g10250 | -5 | NAC domain containing protein 19 |
| 14,8 | Promoter (1-2kb) | VIT_14s0068g01490 | -1124 | NAC domain-containing protein (VvNAC73) |
| 13,63 | Promoter (<=1kb) | VIT_10s0003g00350 | -905 | NAC domain-containing protein (VvNAC37) |
| 12,84 | Promoter (<=1kb) | VIT_17s0000g06400 | 0 | NAC domain-containing protein (VvNAC05) |
| 9,34 | Promoter (<=1kb) | VIT_12s0028g03050 | -229 | NAC domain-containing protein (VvNAC34) |
| 8,79 | Promoter (<=1kb) | VIT_01s0146g00280 | -6 | NAC domain-containing protein (VvNAC01) |
| 8,12 | Promoter (<=1kb) | VIT_18s0089g01120 | -84 | NAC domain-containing protein (VvNAC70) |
| 7,79 | Promoter (<=1kb) | VIT_13s0019g05230 | -5 | NAC domain-containing protein (VvNAC21) |
| 7,34 | Promoter (<=1kb) | VIT_08s0007g07660 | 0 | NAC domain-containing protein (VvNAC60bis) |
| 7 | Promoter (<=1kb) | VIT_07s0005g03610 | -885 | NAC domain-containing protein (VvNAC56) |
| 5,22 | Promoter (1-2kb) | VIT_04s0044g01500 | -1416 | NAC domain-containing protein (VvNAC47) |
| 3,69 | Promoter (1-2kb) | VIT_04s0079g00280 | -1293 | NAC domain-containing protein (VvNAC64) |
| 3,21 | Promoter (<=1kb) | VIT_19s0014g03290 | -502 | NAC domain-containing protein (VvNAC17) |
| 2,97 | Promoter (1-2kb) | VIT_18s0072g01060 | -1329 | NAC domain-containing protein (VvNAC63) |
| 2,63 | Promoter (<=1kb) | VIT_10s0003g00350 | -272 | NAC domain-containing protein (VvNAC37) |
| 2,59 | Promoter (1-2kb) | VIT_02s0025g03020 | -1632 | NAC domain-containing protein (VvNAC25) |
| 2,4 | Promoter (<=1kb) | VIT_18s0001g02300 | -327 | NAC domain-containing protein (VvNAC08) |
| 2,4 | Promoter (<=1kb) | VIT_08s0007g02940 | -106 | NAC domain-containing protein (VvNAC62) |
| 2,25 | Promoter (<=1kb) | VIT_15s0048g02300 | -246 | NAC domain-containing protein (VvNAC53) |
| 2,2 | Promoter (<=1kb) | VIT_19s0027g00880 | -819 | NAC domain-containing protein (VvNAC29) |
| 2,02 | Promoter (<=1kb) | VIT_19s0027g00880 | 0 | NAC domain-containing protein (VvNAC29) |

Table 22: VviNAC01 DAP-seq *VviNACs* targets genes.

Then, the previously reported *VviNAC01* transient over expression results ($FC > |1.5|$) were crossed with the DAP-seq promoter and 5'UTR sub-dataset, revealing 20 correlated binding sites (15 unique genes), all of them resulted up regulated (**Table 23**); none of them were present between the top 20 reported genes.

| q-value | Genic region | Gene ID | Distance to TSS | Functional annotation | Transient OE FC |
|---------|------------------|-------------------|-----------------|--|-----------------|
| 45,37 | Promoter (<=1kb) | VIT_03s0038g02680 | -40 | Zeta-carotene desaturase | 1,88 |
| 27,53 | Promoter (<=1kb) | VIT_12s0028g03270 | -102 | Ethylene-responsive transcription factor 9 | 5,48 |
| 15,32 | Promoter (1-2kb) | VIT_18s0001g05250 | -1274 | Dehydration Responsive Element-Binding Transcription Factor (VvDREB27) | 1,80 |
| 10,77 | Promoter (1-2kb) | VIT_08s0058g00790 | -1700 | Secoisolaricresinol dehydrogenase | 1,58 |
| 9,05 | Promoter (<=1kb) | VIT_01s0026g00550 | -883 | Nodulin MTN21 family | 2,07 |
| 7,79 | Promoter (1-2kb) | VIT_13s0019g02280 | -1890 | Regulator of chromosome condensation (RCC1) | 1,87 |
| 7,3 | Promoter (<=1kb) | VIT_17s0000g04030 | -74 | Endonuclease | 2,10 |
| 7,26 | Promoter (<=1kb) | VIT_00s0620g00010 | -685 | Triacylglycerol lipase | 2,82 |
| 6,5 | Promoter (1-2kb) | VIT_13s0019g02280 | -1444 | Regulator of chromosome condensation (RCC1) | 1,87 |
| 6,25 | Promoter (<=1kb) | VIT_04s0023g00580 | -172 | Auxin-responsive SAUR32 | 2,19 |
| 5,52 | Promoter (<=1kb) | VIT_03s0063g01790 | 0 | Transducin protein | 5,81 |
| 5,52 | Promoter (<=1kb) | VIT_01s0026g01460 | -238 | Thioredoxin H-type 2 (Trx-H-2) | 1,56 |
| 5,28 | Promoter (<=1kb) | VIT_08s0058g00790 | -911 | Secoisolaricresinol dehydrogenase | 1,58 |
| 4,03 | Promoter (<=1kb) | VIT_01s0026g01460 | -507 | Thioredoxin H-type 2 (Trx-H-2) | 1,56 |
| 3,76 | Promoter (1-2kb) | VIT_08s0007g03530 | -1095 | Zf A20 and AN1 domain-containing stress-associated protein 4 | 2,00 |
| 3,67 | Promoter (<=1kb) | VIT_18s0001g00560 | -183 | Alpha-amylase / 1,4-alpha-D-glucan glucanohydrolase | 1,53 |
| 2,48 | Promoter (1-2kb) | VIT_03s0063g01790 | -1685 | Transducin protein | 5,81 |
| 2,25 | Promoter (1-2kb) | VIT_11s0052g01210 | -1084 | Xyloglucan endotransglycosylase 6 | 1,84 |
| 2,2 | Promoter (<=1kb) | VIT_17s0000g01010 | -119 | Lysophospholipase homolog | 1,72 |
| 2,19 | Promoter (<=1kb) | VIT_00s0620g00010 | -145 | Triacylglycerol lipase | 2,82 |

Table 23: VviNAC01 DAP-seq targets genes which have a match in the *VviNAC01* transient over expression dataset.

At the first place *ZETA-CAROTENE DESATURASE* (VIT_03s0038g02680), which catalyzes the conversion of zeta-carotene to lycopene, was found and resulted up regulated by the *VviNAC01* transient over expression. An *ETHYLENE-RESPONSIVE TRANSCRIPTION FACTOR 9* (VIT_12s0028g03270), with a very high fold change of up-regulation, was also found in the list, reflecting the already reported *VviNAC01* role described in **Chapter 2**.

Moreover, with the highest fold change value, two binding sites on the *TRANSDUCIN PROTEIN* (VIT_03s0063g01790) were determined. Transducin proteins mediate diverse protein-protein interactions; they serve as multi-interacting platforms in cellular networks for the assembly of protein complexes or mediators of transient interplay among other proteins (Gachomo *et al.*, 2014). Transducin repeated domains have been reported to play central roles in biological processes such as cell division, apoptosis, light signalling and vision, flowering, floral development, meristem organization, protein trafficking, chromatin modification and transcriptional mechanism (Gachomo *et al.*, 2014).

VviNAC03

The DAP-seq assay reported 3461 binding sites (peaks), which were reduced to 3276 after the FC>5 filtering; even considering the very stringent filter used, the loss was very low, only the 5% (**Fig. 31**). The distribution of peaks revealed that 30% were located within the promoter regions (up to 2 kb upstream from a transcription start site), 2% were in 5' untranslated regions (UTRs), 20% were located in exons, 9% were located within introns, 3% were located in 3' UTRs, 7% were located in the 3 kb downstream region, and 24% were intergenic.

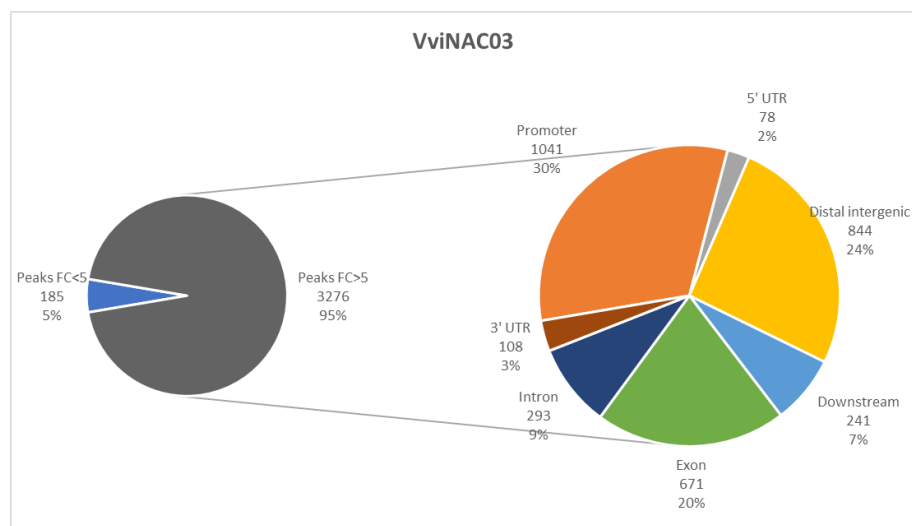


Figure 31: Double pie chart of the VviNAC03 DAP-seq results. The pie on the left represents the total binding sites (peaks) obtained, divided between the FC>5 and FC<5 (compared to the GST-Halo negative control peaks). The pie on the right represents the subdivision into the different genic region of the selected filtered peaks.

Three major binding motifs (GT[T/G][G/A]CGT[G/A][T/A]C) were identified with strong significance (**Fig. 32**) and the phylogenetic footprints correlate with ANAC047, which is involved in embryo development ending in seed dormancy, positive regulation of ethylene biosynthetic process and regulation of transcription (<https://www.arabidopsis.org/servlets/TairObject?type=locus&name=At3g04070>). Moreover, a recent work reported that ANAC047 plays a decisive role in regulating root waterlogging-induced leaf movement by directly or indirectly stimulating localized cell expansion at the abaxial petiole side through ethylene formation (Rauf *et al.*, 2013).

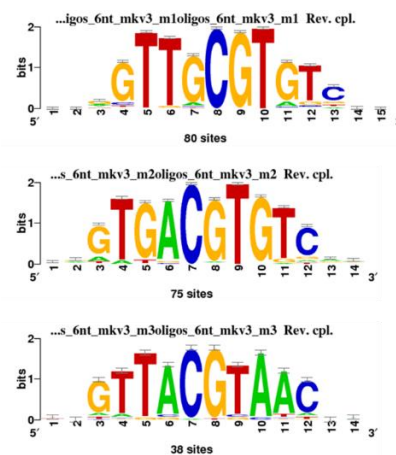


Figure 32: RSAT Plants NGS ChIP-Seq peak motifs analysis on the VviNAC03 DAP-seq results. Three top-ranking binding motifs identified in the DAP-seq FC>5 filtered dataset, based on the detection of overrepresented oligonucleotides (oligo analysis). The overall height of each letter stack indicates the sequence conservation at that position, and the height of symbols within the stack reflects the relative frequency of the corresponding nucleic acid at that position.

The attention was focused only on the 32% of the final analysed binding sites, which belongs to the ‘promoter’ and ‘5’UTR’ genic regions, for a total of 1119 sites; this percentage was even higher than the one found in other DAP-seq published papers.

After the elimination of all the ‘no hit’ and ‘unknown’ elements, 909 binding sites were obtained for a total of 870 unique genes regulated by VviNAC03.

A GO enrichment analysis was performed on this sub-dataset, revealing a predominance of genes related to the general categories of regulation of cellular and biological processes, but also genes important for the cellular differentiation, the homeostatic processes, localization, transport and the response to stimulus (**Fig. 33**).

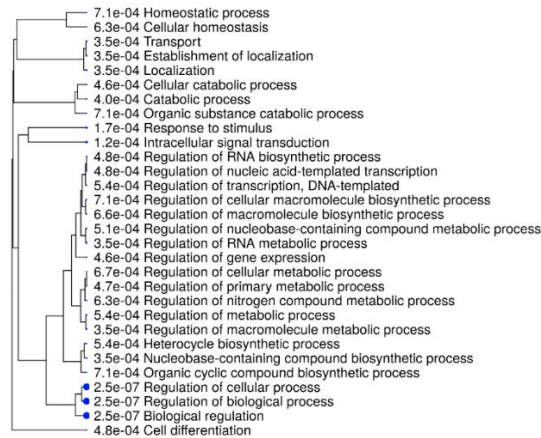


Figure 33: GO enrichment analysis of the VviNAC03 targets found to be regulated in the promoter and 5'UTR regions. The analysis was performed on ShinyGO.

Between the top 20 (q-value based) promoter and 5'UTR located binding sites some interesting genes were found (**Table 24**).

| q-value | Genic region | Gene ID | Distance to TSS | Functional annotation |
|---------|------------------|-------------------|-----------------|---|
| 22,62 | Promoter (<=1kb) | VIT_15s0048g01740 | -376 | Growth-regulating factor 9 |
| 22,42 | Promoter (1-2kb) | VIT_18s0001g14980 | -1600 | 3-methyl-2-oxobutanoate dehydrogenase |
| 20,39 | Promoter (1-2kb) | VIT_05s0062g01120 | -1261 | PIN1 |
| 18,55 | Promoter (1-2kb) | VIT_18s0001g09420 | -1844 | Progesterone 5-beta-reductase |
| 18,16 | 5' UTR | VIT_17s0000g05610 | 502 | Isopiperitenol dehydrogenase |
| 18,04 | Promoter (<=1kb) | VIT_05s0020g02310 | 0 | Pyruvate,orthophosphate dikinase |
| 16,94 | Promoter (<=1kb) | VIT_17s0000g06410 | -525 | MYB transcription factor MIXTA-like 2 |
| 16,01 | Promoter (1-2kb) | VIT_02s0025g04130 | -1354 | Rhomboid ATRBL2 |
| 16 | Promoter (<=1kb) | VIT_05s0020g05060 | -953 | Cellulose synthase CSLG2 |
| 15,23 | Promoter (<=1kb) | VIT_13s0019g00550 | -32 | Cofilin |
| 14,08 | Promoter (<=1kb) | VIT_07s0255g00110 | -148 | WD40 |
| 14,07 | Promoter (<=1kb) | VIT_15s0048g02260 | -118 | Calcium-binding EF hand |
| 14,01 | Promoter (<=1kb) | VIT_01s0011g04760 | -74 | myb domain protein 4 (VvMybC2-L1) |
| 13,31 | Promoter (<=1kb) | VIT_10s0003g04650 | -226 | Nuclear transcription factor Y subunit A-7 |
| 12,99 | Promoter (<=1kb) | VIT_16s0098g01830 | 0 | Transcription factor jumjC (jnjC) domain-containing protein |
| 12,16 | Promoter (<=1kb) | VIT_17s0000g06970 | -421 | Diacylglycerol kinase 1 |
| 12,15 | Promoter (<=1kb) | VIT_16s0050g00120 | -973 | B57 |
| 11,93 | Promoter (<=1kb) | VIT_18s0001g14950 | -544 | EMB2170 (embryo defective 2170) |
| 11,66 | Promoter (<=1kb) | VIT_08s0058g00450 | -775 | Substrate carrier, Mitochondrial |
| 11,51 | Promoter (<=1kb) | VIT_05s0020g02160 | 0 | Squamosa promoter-binding protein (VvSBP6) |

Table 24: Top 20 (q-value based) represented direct target genes of VviNAC03.

The most sequenced represented gene was the *GROWTH-REGULATING FACTOR 9* (VIT_15s0048g01740), which is demonstrated to exerts a negative effect on leaf growth controlling the final leaf dimensions by restricting cell number in the leaf primordium, while the size of the leaf cells remains unaltered (Omidbakhshfard et al., 2018). Moreover, two *MYB* genes were found, *MYB TRANSCRIPTION FACTOR MIXTA-LIKE 2* (VIT_17s0000g06410) and *MYB DOMAIN PROTEIN 4 VvMybC2-L1* (VIT_01s0011g04760), together with other two transcription factors, *NUCEAR TRANSCRIPTION FACTOR Y SUBUNIT A-7* (VIT_10s0003g04650) and *jmjC* (VIT_16s0098g01830).

Another interesting gene was the *PINI* (VIT_05s0062g01120), an auxin efflux facilitator which controls auxin transport and signalling, regulating plant growth and development (Kong *et al.*, 2019).

Afterwards, the list of the *VviNAC03* targets was used to find all the possible *VviNACs* targets of the TF. 2 *VviNACs* target genes were found (**Table 25**), *VviNAC05* (VIT_17s0000g06400) and *VviNAC73* (VIT_14s0068g01490).

| q-value | Genic region | Gene ID | Distance to TSS | Functional annotation |
|---------|------------------|-------------------|-----------------|---|
| 6,66 | Promoter (1-2kb) | VIT_17s0000g06400 | -1859 | NAC domain-containing protein (VvNAC05) |
| 2,82 | Promoter (1-2kb) | VIT_14s0068g01490 | -1111 | NAC domain-containing protein (VvNAC73) |

Table 25: *VviNAC03* DAP-seq *VviNACs* targets genes.

Then, the *VviNAC03* transient over expression results (D’Incà, 2017) were crossed with the DAP-seq promoter and 5’UTR sub-dataset, revealing 7 correlated binding sites (7 unique genes), 3 up regulated and 4 down regulated (**Table 26**); none of them were present between the top 20 reported genes.

| q-value | Genic region | Gene ID | Distance to TSS | Functional annotation | Transient OE |
|---------|------------------|-------------------|-----------------|---|--------------|
| 11,09 | Promoter (1-2kb) | VIT_13s0019g02080 | -1041 | DNA-binding protein | -1,59 |
| 6,11 | Promoter (<=1kb) | VIT_05s0062g00710 | -879 | UDP-glucose:flavonoid 7-O-glucosyltransferase | 4,67 |
| 4,26 | Promoter (<=1kb) | VIT_16s0022g01210 | -797 | myb domain protein 85 | -3,24 |
| 3,71 | Promoter (1-2kb) | VIT_16s0098g01350 | -1315 | Oligopeptide transporter 6 | -1,75 |
| 3,7 | Promoter (<=1kb) | VIT_13s0019g04060 | -261 | MLO1 | 1,82 |
| 3,18 | Promoter (1-2kb) | VIT_00s0125g00180 | -1318 | Zinc finger (C3HC4-type ring finger) | -2,07 |
| 2,9 | Promoter (1-2kb) | VIT_14s0006g02530 | -1122 | Non-specific lipid-transfer protein 2 (LTP 2) | 2,54 |

Table 26: *VviNAC03* DAP-seq targets genes which have a match in the *VviNAC03* transient over expression dataset.

With a high positive fold change and at second place in the list (q-value based), the *UDP-GLUCOSE:FLAVONOID 7-O-GLUCOSYLTRANSFERASE* (VIT_05s0062g00710) was found; glycosylation of flavonoids, which have roles in UV protection, pathogen defense and coloration, is usually mediated by the glycosyltransferases, which use UDP-sugars as the glycosyl donor (Kim *et al.*, 2006). Also, a *MYB* gene was found down regulated, *MYB DOMAIN PROTEIN 85* (VIT_16s0022g01210), and *MLO1* (VIT_13s0019g04060), another plant immunity related gene (Acevedo-Garcia *et al.*, 2014), resulted up regulated.

VviNAC08

The DAP-seq assay reported 150 binding sites (peaks), which were reduced to 116 after the FC>5 filtering; the loss was a little bit higher than the standard of the other assays, about the 23% (**Fig. 34**). The distribution of peaks revealed that 7% were located within the promoter regions (up to 2 kb upstream from a transcription start site), 2% were in 5' untranslated regions (UTRs), 5% were in exons, 4% were located within introns, no gene was located in 3' UTRs, 1% were located in the 3 kb downstream region, and 58% were intergenic.

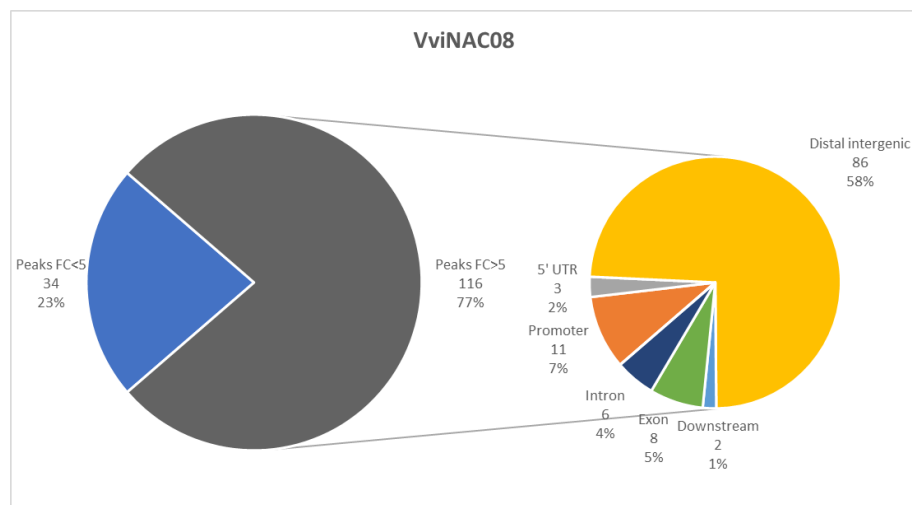


Figure 34: Double pie chart of the VviNAC08 DAP-seq results. The pie on the left represents the total binding sites (peaks) obtained, divided between the FC>5 and FC<5 (compared to the GST-Halo negative control peaks). The pie on the right represents the subdivision into the different genic region of the selected filtered peaks.

Due to the low number of sequenced reads, only one binding motif (CGGTACTC) was identified and not with a strong significance (**Fig. 35**); moreover, no phylogenetic footprint was found.

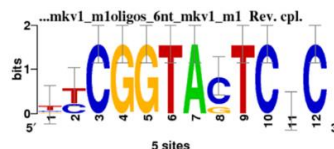


Figure 35: RSAT Plants NGS ChIP-Seq peak motifs analysis on the VviNAC08 DAP-seq results. Top-ranking binding motif identified in the DAP-seq FC>5 filtered dataset, based on the detection of overrepresented oligonucleotides (oligo analysis). The overall height of each letter stack indicates the sequence conservation at that position, and the height of symbols within the stack reflects the relative frequency of the corresponding nucleic acid at that position.

Focusing the attention only on the 9% of the final analyzed binding sites, which

belongs to the ‘promoter’ and ‘5’UTR’ genic regions and presents a total of 14 sites, would not have been possible to perform further analyses. Indeed, this percentage is very low considering the what was normally found in the other DAP-seq assays. However, the DAP-seq was performed two times on this specific TF, and nothing changed; this means that the low number of binding sites reported is not due to a technical issue but could be related to a VviNAC08- specific folding difficulty during the *in vitro* translation or to the biological role of this TF. Trying to better investigate the cistrome landscape of VviNAC08, the GO enrichment analysis was performed on the whole FC>5 DAP-seq dataset (**Fig. 36**). The most represented categories were the one of regulation of biosynthetic processes; the aromatic compound biosynthetic processes, protein catabolic processes and ubiquitination, and electron transport chain categories were also found. Moreover, eliminating all the ‘no hit’ and ‘unknown’ elements, only 8 binding sites were obtained for a total of 8 unique genes regulated by VviNAC08 (**Table 27**). No matches were found between the DAP-seq and the transient over expression results and no *VviNAC* gene was found to be regulated by this TF. However, in the small final targets list an interesting gene was found: the *UDP-GLUCURONOSYL/UDP-GLUCOSYLTRANSFERASE* (VIT_06s0004g07280). Glycosyltransferases catalyze the transfer of a sugar portion from an activated sugar donor to acceptor molecules and this sugar conjugation results in increased stability and water solubility (Bonisch *et al.*, 2014). In grapevine, several classes of phenylpropanoids, including flavonols, anthocyanidins, flavanones, flavones, isoflavones, a stilbene, simple phenols, and monoterpenols, were among the substrates glucosylated, indicating that glycosylation in grape has a big impact on the berries composition, which results in the wine flavor (Bonisch *et al.*, 2014).

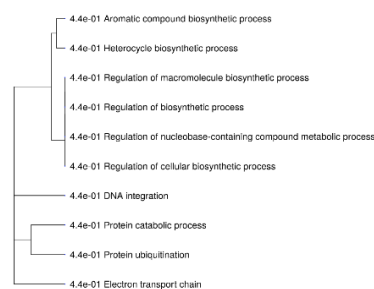


Figure 36: GO enrichment analysis of all the VviNAC08 targets. The analysis was performed on ShinyGO.

| q-value | Genic region | Gene ID | Distance to TSS | Functional annotation |
|---------|------------------|-------------------|-----------------|--|
| 662 | Promoter (1-2kb) | VIT_18s0001g14980 | -1668 | 3-methyl-2-oxobutanoate dehydrogenase |
| 571 | Promoter (<=1kb) | VIT_06s0004g07280 | -103 | UDP-glucuronosyl/UDP-glucosyltransferase |
| 344 | 5' UTR | VIT_09s0054g00520 | 196 | Membrane protein ycf1 (RF1) |
| 238 | Promoter (1-2kb) | VIT_09s0002g00280 | -1021 | Ubiquitin-conjugating enzyme E2 J2 |
| 237 | Promoter (<=1kb) | VIT_00s2634g00010 | -833 | Receptor kinase RK20-1 |
| 221 | 5' UTR | VIT_13s0064g01680 | 112 | RNA polymerase beta" |
| 216 | Promoter (<=1kb) | VIT_17s0000g09270 | -803 | MATE efflux family protein |
| 214 | Promoter (1-2kb) | VIT_03s0063g01470 | -1137 | Steroid nuclear receptor, ligand-binding |

Table 27: Direct target genes of VviNAC08.

VviNAC11

The DAP-seq assay reported 2678 binding sites (peaks), which were reduced to 2459 after the FC>5 filtering; even considering the very stringent filter used, the loss was low, only the 8 (**Fig. 37**). The distribution of peaks revealed that 28% were located within the promoter regions (up to 2 kb upstream from a transcription start site), 2% were in 5' untranslated regions (UTRs), 12% were located in exons, 13% were located within introns, 3% were located in 3' UTRs, 7% were located in the 3 kb downstream region, and 27% were intergenic.

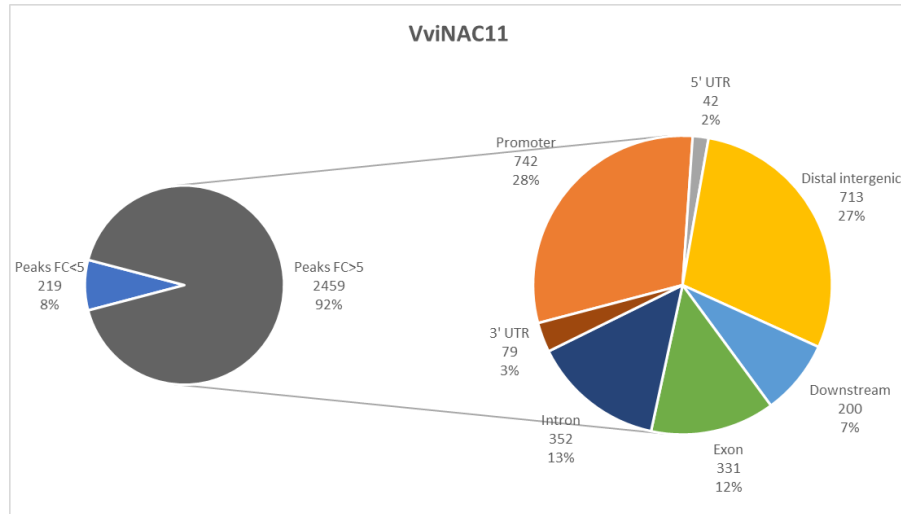


Figure 37: Double pie chart of the VviNAC11 DAP-seq results. The pie on the left represents the total binding sites (peaks) obtained, divided between the FC>5 and FC<5 (compared to the GST-Halo negative control peaks). The pie on the right represents the subdivision into the different genic region of the selected filtered peaks.

Two major binding motifs (GGTTGCGTGT and ACACGCAACCA) were identified with strong significance (**Fig. 38**) and the phylogenetic footprints correlate with ANAC092 and ANCA046, respectively. As said before, ANAC092

is considered the key positive regulator of leaf senescence (Kim *et al.*, 2009); ANAC046 too is a positive regulator of chlorophyll degradation and senescence in *Arabidopsis* leaves (Oda-Yamamizo *et al.*, 2016).

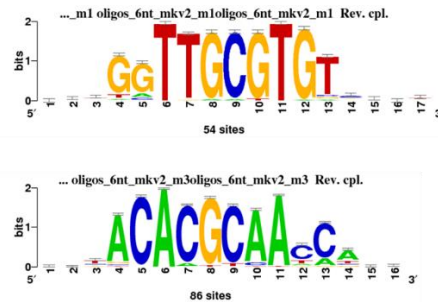


Figure 38: RSAT Plants NGS ChIP-Seq peak motifs analysis on the VviNAC11 DAP-seq results. Two top-ranking binding motifs identified in the DAP-seq FC>5 filtered dataset, based on the detection of overrepresented oligonucleotides (oligo analysis). The overall height of each letter stack indicates the sequence conservation at that position, and the height of symbols within the stack reflects the relative frequency of the corresponding nucleic acid at that position.

The attention was focused only on the 30% of the final analysed binding sites, which belongs to the ‘promoter’ and ‘5’UTR’ genic regions, for a total of 784 sites. This percentage was perfectly in line with other DAP-seq published papers, even higher.

After the elimination of all the ‘no hit’ and ‘unknown’ elements, 640 binding sites were obtained for a total of 610 unique genes regulated by VviNAC11.

A GO enrichment analysis was performed on this sub-dataset, revealing a predominance of genes related to the general categories of biological regulation and regulation of metabolic and biosynthetic processes; moreover, developmental and homeostatic processes genes were also highly represented (**Fig. 39**).

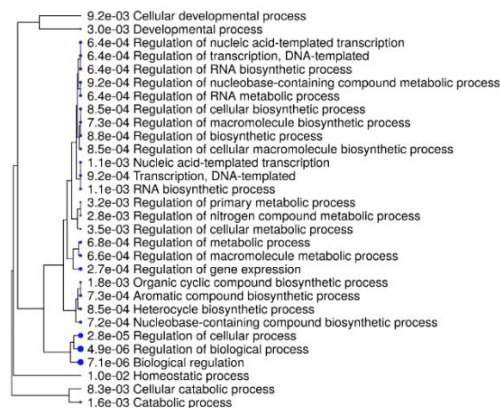


Figure 39: GO enrichment analysis of the VviNAC11 targets found to be regulated in the promoter and 5’UTR regions. The analysis was performed on ShinyGO.

Between the top 20 (q-value based) promoter and 5'UTR located binding sites some interesting genes were found (**Table 28**).

At the first place (q-value based) the *ARGININE_TRNA-PROTEIN TRANSFERASE 1 ATE1* (VIT_13s0067g00600) was found. It is involved in the post-translational conjugation of arginine to the N-terminal aspartate or glutamate of a protein. This arginylation is required for degradation of the protein via the ubiquitin pathway. Moreover, was also seen that the delayed-senescence phenotypes are associated with undetectable levels of *AtATE1* transcripts (Yoshida *et al.*, 2002).

The *SENESCENCE-INDUCIBLE CHLOROPLAST STAY-GREEN PROTEIN 1* (VIT_02s0025g04660) is involved in chlorophyll and photosystem degradation.

VviWRKY52 (VIT_17s0000g01280) is associated with the transcriptional regulation of three genes putatively involved in the jasmonic acid signalling pathway and in the reduced susceptibility to downy mildew infection (Vannozzi *et al.*, 2018); moreover, it is a red berry *switch* gene (Massonnet *et al.*, 2017).

UDP-GLUCOSE:ISOFLAVONE 7-O-GLUCOSYLYTRANSFERASE (VIT_16s0050g01670), as said before, has a role in the coloration (Kim *et al.*, 2006).

| q-value | Genic region | Gene ID | Distance to TSS | Functional annotation |
|---------|------------------|-------------------|-----------------|--|
| 28,52 | Promoter (1-2kb) | VIT_13s0067g00600 | -1194 | Arginine-tRNA-protein transferase 1 |
| 26,82 | Promoter (1-2kb) | VIT_16s0098g01150 | -1172 | Auxin-responsive SAUR29 * |
| 26,73 | Promoter (1-2kb) | VIT_17s0000g09210 | -1926 | No pollen (Osnop) |
| 26,73 | Promoter (<=1kb) | VIT_02s0025g04660 | -164 | Senescence-inducible chloroplast stay-green protein 1 |
| 26,21 | Promoter (1-2kb) | VIT_18s0001g14980 | -1615 | 3-methyl-2-oxobutanoate dehydrogenase |
| 22,74 | Promoter (<=1kb) | VIT_03s0038g00750 | 0 | Ubiquitin fusion degradation protein UFD1 |
| 22,7 | Promoter (<=1kb) | VIT_06s0061g01190 | -122 | SWI/SNF matrix-associated regulator of chromatin sbfamily A mber 3 2 |
| 21,81 | Promoter (<=1kb) | VIT_13s0019g02180 | 0 | Tropinone reductase |
| 21,6 | Promoter (<=1kb) | VIT_04s0044g00710 | -159 | UTP--glucose-1-phosphate uridylyltransferase * |
| 21,31 | Promoter (<=1kb) | VIT_05s0020g02310 | -134 | Pyruvate,orthophosphate dikinase |
| 20,15 | Promoter (<=1kb) | VIT_17s0000g01280 | -76 | WRKY Transcription Factor (VvWRKY52) |
| 18,9 | Promoter (<=1kb) | VIT_11s0052g00180 | -746 | Las1 |
| 17,03 | Promoter (<=1kb) | VIT_12s0057g01420 | -9 | Exostosin |
| 17,03 | Promoter (<=1kb) | VIT_05s0020g02160 | 0 | Squamosa promoter-binding protein (VvSBP6) |
| 16,43 | Promoter (1-2kb) | VIT_11s0118g00220 | -1415 | Chloride channel protein CLC |
| 16,42 | Promoter (<=1kb) | VIT_00s0207g00200 | 0 | Integral membrane protein, putative |
| 15,9 | Promoter (1-2kb) | VIT_08s0058g00960 | -1899 | basic helix-loop-helix (bHLH) family |
| 15,46 | Promoter (1-2kb) | VIT_16s0050g01670 | -1436 | UDP-glucose:isoflavone 7-O-glucosyltransferase |
| 14,56 | Promoter (<=1kb) | VIT_18s0001g11990 | -88 | Methyltransferase-like protein 2, meth 7 |
| 13,71 | Promoter (1-2kb) | VIT_09s0002g02490 | -1105 | Dof zinc finger protein 1 |

Table 28: Top 20 (q-value based) represented direct target genes of VviNAC11. In bold are reported the *switch* genes and the asterisk (*) refers to the transition markers.

Afterwards, the list of the VviNAC11 targets was used to find all the possible VviNACs targets of the TF. 6 VviNACs target genes were found (**Table 29**): *VviNAC19* (VIT_11s0016g02880), *VviNAC34* (VIT_12s0028g03050), *VviNAC37* (VIT_10s0003g00350), *VviNAC45* (VIT_08s0040g02110), *VviNAC47* (VIT_04s0044g01500) and, interestingly, *VviNAC61* (VIT_08s0007g07640).

| q-value | Genic region | Gene ID | Distance to TSS | Functional annotation |
|---------|------------------|-------------------|-----------------|---|
| 4,13 | Promoter (<=1kb) | VIT_11s0016g02880 | 0 | NAC domain-containing protein (VvNAC19) |
| 3,26 | Promoter (<=1kb) | VIT_12s0028g03050 | -353 | NAC domain-containing protein (VvNAC34) |
| 3,25 | Promoter (1-2kb) | VIT_04s0044g01500 | -1416 | NAC domain-containing protein (VvNAC47) |
| 2,75 | Promoter (<=1kb) | VIT_10s0003g00350 | 0 | NAC domain-containing protein (VvNAC37) |
| 2,55 | Promoter (<=1kb) | VIT_08s0007g07640 | 0 | NAC domain-containing protein (VvNAC61) |
| 2,05 | Promoter (1-2kb) | VIT_08s0040g02110 | -1157 | NAC domain-containing protein (VvNAC45) |

Table 29: VviNAC11 DAP-seq *VviNACs* targets genes.

Then, the previously reported *VviNAC11* transient over expression (D'Inca, 2017) results ($FC > |1.5|$) were crossed with the DAP-seq promoter and 5'UTR sub-dataset, revealing 5 correlated binding sites (5 unique genes), all of them resulted up regulated with exception for *GROWTH-REGULATING FACTOR RELATED* (VIT_08s0007g06690) which was down regulated (**Table 30**); none of them were present between the top 20 reported genes.

| q-value | Genic region | Gene ID | Distance to TSS | Functional annotation | Transient OE |
|---------|------------------|-------------------|-----------------|----------------------------------|--------------|
| 3,65 | Promoter (<=1kb) | VIT_17s0000g03740 | -443 | Constans-like 16 | 1,86 |
| 3,42 | Promoter (<=1kb) | VIT_07s0031g02780 | -315 | Cyclase/dehydrase | 1,58 |
| 2,59 | Promoter (<=1kb) | VIT_08s0007g06690 | -975 | Growth-regulating factor related | -1,65 |
| 2,54 | Promoter (<=1kb) | VIT_05s0020g04040 | -565 | Chlorophyllase (CLH2) | 2,14 |
| 2,22 | Promoter (<=1kb) | VIT_06s0004g04000 | -140 | Beta-ketoacyl-CoA synthase | 1,64 |

Table 30: VviNAC11 DAP-seq targets genes which have a match in the *VviNAC11* transient over expression dataset.

Concerning the up regulated genes, very informative features were found.

CONSTANS-LIKE 16 (VIT_17s0000g03740), which was already reported to enhance chlorophyll accumulation in petals and leaves (Ohmiya *et al.*, 2019) was found at the first place (q-value based) of the list.

CHLOROPHYLLASE CLH2 (VIT_05s0020g04040), which catalyzes the hydrolysis of chlorophyll to chlorophyllide and phytol and possesses a predicted signal-peptide for chloroplast localization, was for a very long time considered as the first enzyme of chlorophylls breakdown during leaf senescence and fruit ripening (Schenk *et al.*, 2007). However, a very recent study demonstrated that CLH2 is not involved in chlorophylls breakdown during senescence in *Arabidopsis* (Hu *et al.*, 2020).

BETA-KETOACYL-COA SYNTHASE (VIT_06s0004g04000) represents the key enzyme in very-long-chain fatty acids biosynthesis (Wang *et al.*, 2017). Knowing that cuticular waxes are complex mixtures of very-long-chain fatty acids and their derivatives, forming a natural barrier on aerial surfaces of terrestrial plants against biotic and abiotic stresses, this gene could be an interesting element in the berry

maturation mechanisms.

The only down regulated gene found, the *GROWTH-REGULATING FACTOR RELATED GRF* (VIT_08s0007g06690), is a plant-specific transcription factor, conserved in all land plants, which has growth-promoting activities in lateral organs; indeed, loss-of-function mutations of *GRFs* resulted in small narrow leaves and petals (Lee *et al.*, 2018).

VviNAC13

The DAP-seq assay reported 1670 binding sites (peaks), which were reduced to 1619 after the FC>5 filtering; even considering the very stringent filter used, the loss was very low, only the 3% (**Fig. 40**). The distribution of peaks revealed that 20% were located within the promoter regions (up to 2 kb upstream from a transcription start site), 2% were in 5' untranslated regions (UTRs), 11% were located in exons, 23% were located within introns, 2% were located in 3' UTRs, 7% were located in the 3 kb downstream region, and 32% were intergenic.

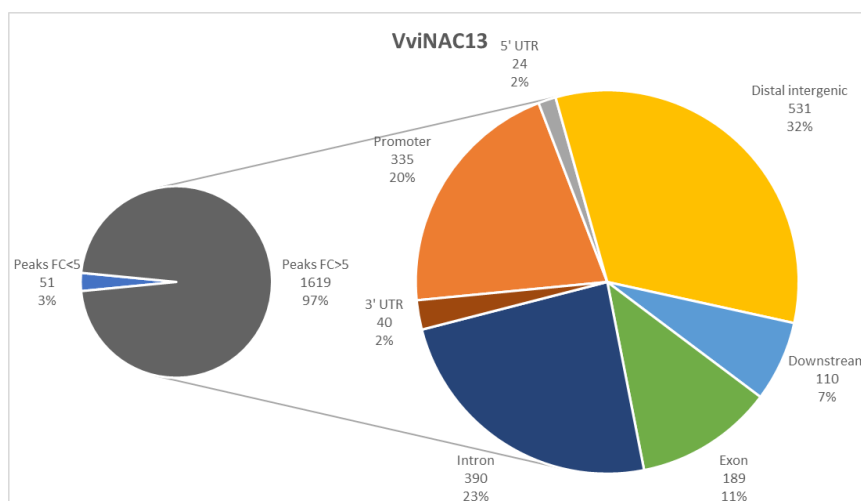


Figure 40: Double pie chart of the VviNAC13 DAP-seq results. The pie on the left represents the total binding sites (peaks) obtained, divided between the FC>5 and FC<5 (compared to the GST-Halo negative control peaks). The pie on the right represents the subdivision into the different genic region of the selected filtered peaks.

Three major binding motifs (TT[A/G/T]CTT[G/C]) were identified with strong significance (**Fig. 41**) and the phylogenetic footprints correlate with ANAC055, which may function as transcription activator to regulate jasmonic acid-induced

expression of defense genes (Bu *et al.*, 2008).

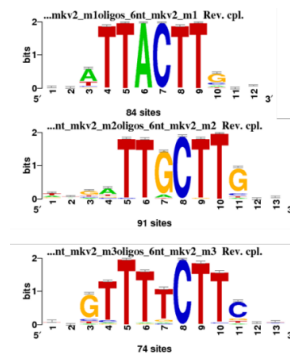


Figure 41: RSAT Plants NGS ChIP-Seq peak motifs analysis on the VviNAC13 DAP-seq results. Three top-ranking binding motifs identified in the DAP-seq FC>5 filtered dataset, based on the detection of overrepresented oligonucleotides (oligo analysis). The overall height of each letter stack indicates the sequence conservation at that position, and the height of symbols within the stack reflects the relative frequency of the corresponding nucleic acid at that position.

The attention was focused only on the 22% of the final analysed binding sites, which belongs to the ‘promoter’ and ‘5’UTR’ genic regions, for a total of 359 sites. This percentage is a little bit lower compared to the number of sites normally found in other DAP-seq published papers. After the elimination of all the ‘no hit’ and ‘unknown’ elements, 283 binding sites were obtained for a total of 275 unique genes regulated by VviNAC13. A GO enrichment analysis was performed on this sub-dataset, revealing a predominance of genes related to regulation of biological and metabolic processes and to catabolic processes; moreover, the response to stimulus and to chitin, the lignin metabolic processes, the phenylpropanoid metabolic processes and the defense response to Gram negative bacterium categories were present (**Fig. 42**).

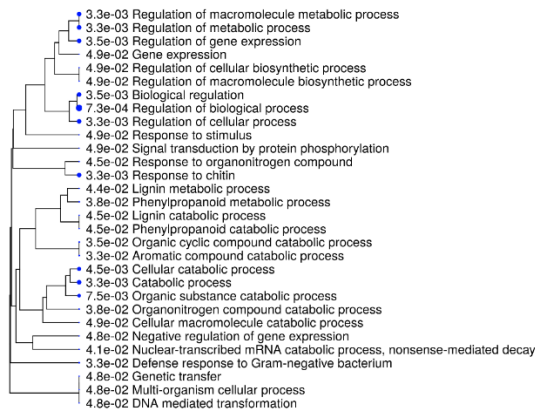


Figure 42: GO enrichment analysis of the VviNAC13 targets found to be regulated in the promoter and 5’UTR regions. The analysis was performed on ShinyGO.

Between the top 20 (q-value based) promoter and 5'UTR located binding sites some interesting genes were found (**Table 31**).

| q-value | Genic region | Gene ID | Distance to TSS | Functional annotation |
|---------|------------------|-------------------|-----------------|--|
| 35,28 | Promoter (<=1kb) | VIT_12s0057g01420 | 0 | Exostosin |
| 31,33 | Promoter (1-2kb) | VIT_13s0067g00600 | -1191 | Arginine-tRNA-protein transferase 1 |
| 27,99 | Promoter (<=1kb) | VIT_18s0001g08290 | -172 | Poly(ADP-ribose) polymerase * |
| 25,06 | Promoter (1-2kb) | VIT_01s0011g01300 | -1061 | Polygalacturonase QRT3 |
| 21,24 | Promoter (1-2kb) | VIT_14s0066g00620 | -1362 | Chitinase, class III |
| 21,23 | Promoter (<=1kb) | VIT_07s0005g00310 | -149 | Zinc finger (CCCH type) helicase family protein |
| 21,21 | Promoter (<=1kb) | VIT_06s0061g01210 | -619 | Lysine histidine transporter 1 |
| 18,54 | Promoter (1-2kb) | VIT_08s0007g04510 | -1907 | RPG related protein 1 RR1 |
| 18,19 | Promoter (1-2kb) | VIT_09s0002g02490 | -1114 | Dof zinc finger protein 1 |
| 16,89 | Promoter (<=1kb) | VIT_17s0000g06970 | -438 | Diacylglycerol kinase 1 |
| 16,8 | Promoter (<=1kb) | VIT_06s0061g01190 | -132 | SWI/SNF matrix-associated regulator of chromatin sbfamily A mber 3 2 |
| 14,32 | Promoter (1-2kb) | VIT_18s0001g14980 | -1605 | 3-methyl-2-oxobutanoate dehydrogenase |
| 13,97 | Promoter (<=1kb) | VIT_08s0058g01360 | -96 | Vacuolar sorting receptor 1 |
| 13,82 | Promoter (<=1kb) | VIT_01s0011g05210 | -965 | Phosphoglucomutase |
| 13,78 | Promoter (<=1kb) | VIT_18s0122g00500 | 0 | Basic Leucine Zipper Transcription Factor (VvbZIP41) |
| 13,55 | Promoter (1-2kb) | VIT_13s0019g05240 | -1179 | NAC domain-containing protein (VvNAC20) |
| 13,52 | Promoter (<=1kb) | VIT_12s0142g00130 | -530 | Mitogen-activated Protein Kinase (VvMPK8) |
| 12,95 | Promoter (<=1kb) | VIT_14s0068g01710 | 0 | Metal-nicotianamine transporter YSL6 |
| 12,2 | Promoter (<=1kb) | VIT_18s0001g09230 | -761 | Salt tolerance zinc finger |
| 11,6 | Promoter (1-2kb) | VIT_06s0009g02500 | -1409 | Plastocyanin domain-containing protein |

Table 31: Top 20 (q-value based) represented direct target genes of VviNAC13. The asterisk (*) refers to the transition markers.

The most sequenced represented gene was the *EXOSTOSIN* (VIT_12s0057g01420), which is an animal glycosyltransferase that catalyze the synthesis a glycosaminoglycan with many roles in cell differentiation and development; this also suggests that the plant cell wall, as the animal extracellular matrix, is synthesized by evolutionarily related enzymes even though the structures of the polysaccharides are different from each other (Madson *et al.*, 2003).

ARGININE-TRNA-PROTEIN TRANSFERASE 1 (VIT_13s0067g00600), described before as senescence phenotypes associated (Yoshida *et al.*, 2002), was again found.

Chitinases constitute a group of defense molecules for which a direct activity against pathogens has been demonstrated. In the DAP-seq list a *CHITINASE, CLASS III* (VIT_14s0066g00620) was found; class III chitinases possess a similar domain to the prokaryotic chitinases one and display lysozyme activity (Robert *et al.*, 2002).

A *BASIC LEUCINE ZIPPER TRANSCRIPTION FACTOR VvbZIP41* (VIT_18s0122g00500) was found. bZIP transcription factors are candidates for the regulation of ABA-mediated fruit ripening. Indeed, in a recent study was seen that the bZIP *VvABF2* was ubiquitously expressed in different grape organs and its transcript accumulated just before the onset of grape berry ripening, when ABA concentrations increase (Nicolas *et al.*, 2014).

Moreover, was very interesting to see that in the top 20 list *VviNAC20* (VIT_13s0019g05240) was present.

Afterwards, the list of the *VviNAC13* targets was used to find all the possible *VviNACs* targets of the TF.

6 *VviNACs* target genes were found (**Table 32**): *VviNAC19* (VIT_11s0016g02880), *VviNAC20* (VIT_13s0019g05240) and *VviNAC21* (VIT_13s0019g05230), *VviNAC34* (VIT_12s0028g03050) and *VviNAC37* (VIT_10s0003g00350). *VviNAC37* harbors multiple *VviNAC13* binding sites.

| q-value | Genic region | Gene ID | Distance to TSS | Functional annotation |
|---------|------------------|-------------------|-----------------|---|
| 13,55 | Promoter (1-2kb) | VIT_13s0019g05240 | -1179 | NAC domain-containing protein (VvNAC20) |
| 9,64 | Promoter (<=1kb) | VIT_10s0003g00350 | 0 | NAC domain-containing protein (VvNAC37) |
| 9,17 | Promoter (<=1kb) | VIT_13s0019g05230 | -3 | NAC domain-containing protein (VvNAC21) |
| 8,71 | Promoter (<=1kb) | VIT_11s0016g02880 | 0 | NAC domain-containing protein (VvNAC19) |
| 6,76 | Promoter (<=1kb) | VIT_12s0028g03050 | -200 | NAC domain-containing protein (VvNAC34) |
| 2,3 | Promoter (<=1kb) | VIT_10s0003g00350 | -926 | NAC domain-containing protein (VvNAC37) |

Table 32: *VviNAC13* DAP-seq *VviNACs* targets genes.

Then, the D'Inca (2017) reported *VviNAC13* transient over expression results ($FC > |1.5|$) were crossed with the DAP-seq promoter and 5'UTR sub-dataset, revealing 4 correlated binding sites (4 unique genes, **Table 33**); none of them were present between the top 20 reported genes.

The two up regulated genes were *ZINC METALLOPROTEASE PITRILYSIN SUB A* (VIT_03s0063g00680) and *FERREDOXIN* (VIT_04s0008g04240), whereas the down regulated one were *HEAT SHOCK PROTEIN 70* (VIT_13s0019g01430) and *RETROTRANSPOSON PROTEIN, UNCLASSIFIED* (VIT_18s0075g00520).

| q-value | Genic region | Gene ID | Distance to TSS | Functional annotation | Transient OE |
|---------|------------------|-------------------|-----------------|---------------------------------------|--------------|
| 3,2 | Promoter (<=1kb) | VIT_13s0019g01430 | -178 | Heat shock protein 70 | -1,62 |
| 2,63 | Promoter (<=1kb) | VIT_03s0063g00680 | 0 | Zinc metalloprotease pitrilysin sub A | 1,54 |
| 2,43 | Promoter (<=1kb) | VIT_04s0008g04240 | -935 | ferredoxin | 1,95 |
| 2,32 | Promoter (<=1kb) | VIT_18s0075g00520 | 0 | Retrotransposon protein, Unclassified | -2,21 |

Table 33: *VviNAC13* DAP-seq targets genes which have a match in the *VviNAC13* transient over expression dataset.

VviNAC15

The DAP-seq assay reported 3461 binding sites (peaks), which were reduced to 3321 after the FC>5 filtering; even considering the very stringent filter used, the loss was very low, only the 4% (**Fig. 43**). The distribution of peaks revealed that 20% were located within the promoter regions (up to 2 kb upstream from a transcription start site), 2% were in 5' untranslated regions (UTRs), 17% were located in exons, 20% were located within introns, 2% were located in 3' UTRs, 6% were located in the 3 kb downstream region, and 29% were intergenic.

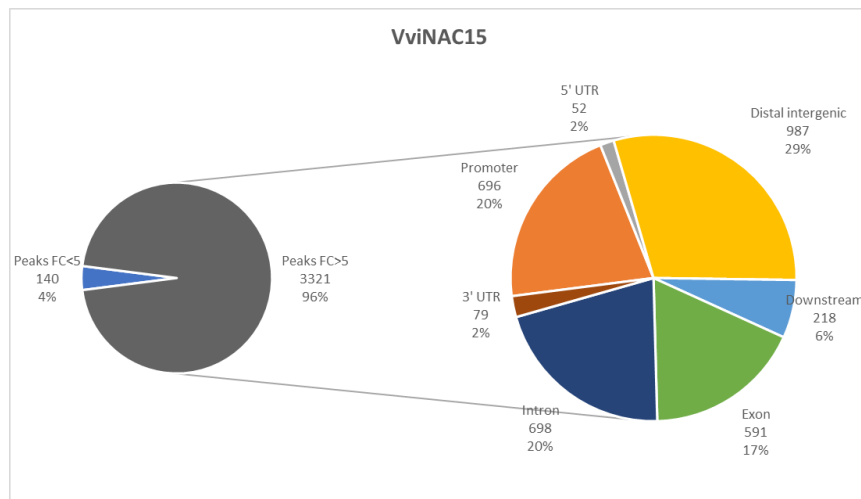


Figure 43: Double pie chart of the VviNAC15 DAP-seq results. The pie on the left represents the total binding sites (peaks) obtained, divided between the FC>5 and FC<5 (compared to the GST-Halo negative control peaks). The pie on the right represents the subdivision into the different genic region of the selected filtered peaks.

Three major binding motifs (TT[A/T]CTTG) were identified with strong significance (**Fig. 44**) and the phylogenetic footprints correlate with ANAC076, which is also known as VND2 and belongs to a group of NAC domain transcription factors that function as master regulators of xylem vessel element differentiation in cotyledons (Tan *et al.*, 2018).

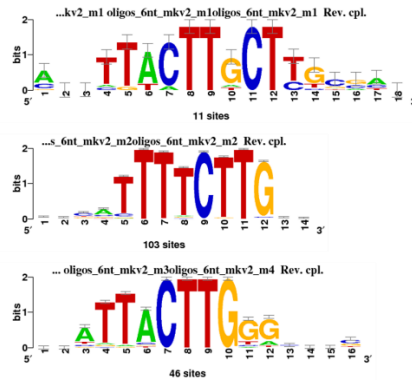


Figure 44: RSAT Plants NGS ChIP-Seq peak motifs analysis on the VviNAC15 DAP-seq results. Three top-ranking binding motifs identified in the DAP-seq FC>5 filtered dataset, based on the detection of overrepresented oligonucleotides (oligo analysis). The overall height of each letter stack indicates the sequence conservation at that position, and the height of symbols within the stack reflects the relative frequency of the corresponding nucleic acid at that position.

The attention was focused only on the 22% of the final analysed binding sites, which belongs to the ‘promoter’ and ‘5’UTR’ genic regions, for a total of 748 sites. This percentage is a little bit lower compared to the number of sites normally found in other DAP-seq published papers.

After the elimination of all the ‘no hit’ and ‘unknown’ elements, 590 binding sites were obtained for a total of 573 unique genes regulated by VviNAC15.

A GO enrichment analysis was performed on this sub-dataset, revealing a predominance of genes related to regulation of gene expression, metabolic (also aromatic compound) and cellular processes (**Fig. 45**).

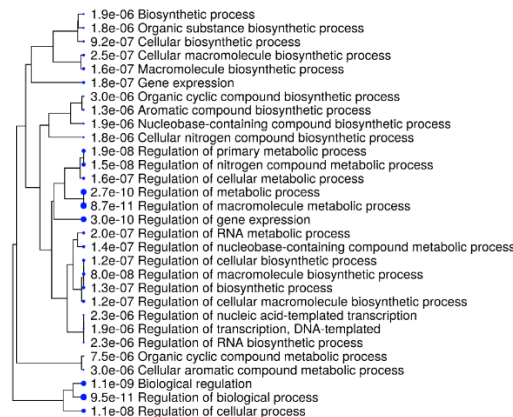


Figure 45: GO enrichment analysis of the VviNAC15 targets found to be regulated in the promoter and 5’UTR regions. The analysis was performed on ShinyGO.

Between the top 20 (q-value based) promoter and 5’UTR located binding sites some interesting genes were found (**Table 34**).

| q-value | Genic region | Gene ID | Distance to TSS | Functional annotation |
|---------|------------------|-------------------|-----------------|---|
| 78,08 | Promoter (1-2kb) | VIT_18s0001g14980 | -1618 | 3-methyl-2-oxobutanoate dehydrogenase |
| 46,74 | Promoter (<=1kb) | VIT_06s0004g04180 | -455 | Zinc finger (C2H2 type) protein (ZAT11) |
| 37,53 | Promoter (<=1kb) | VIT_17s0000g01280 | -68 | WRKY Transcription Factor (VvWRKY52) |
| 37,15 | Promoter (<=1kb) | VIT_12s0035g00650 | -293 | Zinc Finger Homeodomain Transcription Factor (VvZHD5) |
| 36,55 | Promoter (1-2kb) | VIT_17s0000g09890 | -1345 | Tetrapeptide repeat (TPR)-containing |
| 31,77 | Promoter (<=1kb) | VIT_12s0028g02510 | -2 | DNA-binding bromodomain-containing protein |
| 31,76 | Promoter (<=1kb) | VIT_13s0019g00840 | 0 | UDP-glucuronate decarboxylase. |
| 31,03 | Promoter (<=1kb) | VIT_16s0050g00700 | -198 | Zinc finger (C2H2 type) family |
| 29,21 | Promoter (1-2kb) | VIT_06s0004g07030 | -1246 | MRH1 (morphogenesis of root hair 1) |
| 26 | Promoter (1-2kb) | VIT_06s0004g08190 | -1315 | ERF/AP2 Gene Family (VvERF055) |
| 25,45 | Promoter (<=1kb) | VIT_08s0007g07640 | 0 | NAC domain-containing protein (VvNAC61) |
| 24,42 | Promoter (<=1kb) | VIT_18s0001g14960 | -324 | Pentapeptide repeat (PPR) repeat-containing |
| 24,22 | Promoter (1-2kb) | VIT_10s0003g00390 | -1237 | Glutaredoxin |
| 19,83 | Promoter (<=1kb) | VIT_09s0070g00210 | 0 | Metal transporter Nramp1 |
| 19,83 | Promoter (<=1kb) | VIT_03s0038g00750 | 0 | Ubiquitin fusion degradation protein UFD1 |
| 19,66 | Promoter (<=1kb) | VIT_04s0008g07010 | 0 | Dynammin-like protein 2b |
| 19,05 | Promoter (<=1kb) | VIT_10s0042g01180 | -30 | ARGONAUTE 2 (AGO2) |
| 18,79 | Promoter (1-2kb) | VIT_11s0016g00350 | -1111 | Sec34/COG3 |
| 18,23 | Promoter (<=1kb) | VIT_17s0000g01920 | -595 | Nuclear transcription factor, X-box binding 1 |
| 17,94 | Promoter (1-2kb) | VIT_13s0067g01740 | -1194 | Receptor protein kinase |

Table 34: Top 20 (q-value based) represented direct target genes of VviNAC15. In bold are reported the *switch* genes.

An ethylene-related gene, *ERF/AP2 GENE FAMILY VvERF055* (VIT_06s0004g08190), was found. Moreover, many transcription factors were present in the list as two *ZINC FINGER* (VIT_06s0004g04180, VIT_12s0035g00650 and VIT_16s0050g00700) and a *NUCLEAR TRANSCRIPTION FACTOR, X-BOX BINDING 1* (VIT_17s0000g01920); however, the main interest is upon *VviWRKY52* (VIT_17s0000g01280), an already mentioned red berry *switch* (Massonnet *et al.*, 2017), known to be involved in the jasmonic acid signalling pathway (Vannozzi *et al.*, 2018), and one of the selected *VviNAC* family member, *VviNAC61* (VIT_08s0007g07640).

Afterwards, the list of the VviNAC15 targets was used to find all the possible *VviNACs* targets of the TF. 12 *VviNACs* target genes were found (**Table 35**) and, interestingly, two of the selected *VviNACs* were in this group, *VviNAC39* (VIT_07s0031g02610) and, as said before, *VviNAC61* (VIT_08s0007g07640).

| q-value | Genic region | Gene ID | Distance to TSS | Functional annotation |
|---------|------------------|-------------------|-----------------|---|
| 25,45 | Promoter (<=1kb) | VIT_08s0007g07640 | 0 | NAC domain-containing protein (VvNAC61) |
| 17,55 | Promoter (<=1kb) | VIT_12s0028g03050 | -203 | NAC domain-containing protein (VvNAC34) |
| 14,99 | Promoter (1-2kb) | VIT_13s0019g05240 | -1176 | NAC domain-containing protein (VvNAC20) |
| 12,25 | Promoter (<=1kb) | VIT_11s0016g02880 | 0 | NAC domain-containing protein (VvNAC19) |
| 7,52 | Promoter (<=1kb) | VIT_10s0003g00350 | -3 | NAC domain-containing protein (VvNAC37) |
| 5,53 | Promoter (<=1kb) | VIT_15s0048g02300 | -177 | NAC domain-containing protein (VvNAC53) |
| 5,02 | Promoter (<=1kb) | VIT_15s0048g02320 | -280 | NAC domain-containing protein (VvNAC51) |
| 4,63 | Promoter (1-2kb) | VIT_07s0031g02610 | -1604 | NAC domain-containing protein (VvNAC39) |
| 3,37 | Promoter (<=1kb) | VIT_16s0098g00760 | 0 | NAC domain-containing protein (VvNAC71) |
| 3,08 | Promoter (<=1kb) | VIT_15s0048g02290 | -308 | NAC domain-containing protein (VvNAC54) |
| 2,31 | Promoter (<=1kb) | VIT_18s0001g10250 | -14 | NAC domain containing protein 19 |
| 2,1 | Promoter (<=1kb) | VIT_06s0080g00970 | -191 | NAC domain-containing protein (VvNAC67) |

Table 35: VviNAC15 DAP-seq *VviNACs* targets genes.

Then, the already reported *VviNAC15* transient over expression results ($FC > |1.5|$) were crossed with the DAP-seq promoter and 5'UTR sub-dataset, revealing 27 correlated binding sites (27 unique genes, **Table 36**).

3 of these genes, all up regulated, were also present between the top 20 reported genes: *VviWRKY52* (VIT_17s0000g01280), *VviNAC61* (VIT_08s0007g07640) and *METAL TRANSPORTER NRAMP1* (VIT_09s0007g00210).

For the last one, unfortunately, not much information is present in literature; one single study has correlated its role in plants growth under low manganese conditions (Cailliatte et al., 2010).

| q-value | Genic region | Gene ID | Distance to TSS | Functional annotation | Transient OE |
|---------|------------------|-------------------|-----------------|--|--------------|
| 37,53 | Promoter (<=1kb) | VIT_17s0000g01280 | -68 | WRKY Transcription Factor (VvWRKY52) | 1,94 |
| 25,45 | Promoter (<=1kb) | VIT_08s0007g07640 | 0 | NAC domain-containing protein (VvNAC61) | 1,56 |
| 19,83 | Promoter (<=1kb) | VIT_09s0007g00210 | 0 | Metal transporter Nramp1 | 2,26 |
| 16,4 | Promoter (<=1kb) | VIT_17s0000g07670 | -240 | Betaine-aldehyde dehydrogenase | -1,59 |
| 14,15 | Promoter (<=1kb) | VIT_07s0104g00150 | 0 | Outer envelope membrane protein | -1,64 |
| 10,37 | Promoter (<=1kb) | VIT_13s0019g05200 | -667 | MATE efflux family protein | 2,36 |
| 9,5 | Promoter (<=1kb) | VIT_05s0020g04130 | -270 | Perakine reductase aldo/keto reductase * | 2,06 |
| 8,79 | Promoter (1-2kb) | VIT_04s0023g00700 | -1553 | Serine carboxypeptidase S10 | 2,10 |
| 8,24 | Promoter (<=1kb) | VIT_16s0098g00890 | -737 | Harpin-induced protein | 1,55 |
| 7,24 | Promoter (<=1kb) | VIT_13s0019g02180 | 0 | Tropinone reductase | 3,24 |
| 5,74 | Promoter (<=1kb) | VIT_07s0005g01760 | -183 | Glycerol-3-phosphate acyltransferase 3 (AtGPAT3) | -1,95 |
| 5,49 | Promoter (1-2kb) | VIT_01s0026g01050 | -1888 | Myb family * | 1,91 |
| 5,29 | Promoter (<=1kb) | VIT_12s0059g02510 | -96 | Zinc finger (B-box type) | 2,29 |
| 5,17 | Promoter (<=1kb) | VIT_14s0219g00120 | -502 | PQ-loop repeat / transmembrane | 1,79 |
| 5,16 | Promoter (<=1kb) | VIT_13s0019g02160 | -275 | Laccase | -1,72 |
| 5,07 | Promoter (<=1kb) | VIT_06s0004g05710 | 0 | Glutathione S-transferase GSTU7 | -1,74 |
| 4,02 | Promoter (<=1kb) | VIT_11s0016g02800 | -138 | Myo-inositol oxygenase | 1,83 |
| 3,92 | Promoter (<=1kb) | VIT_13s0019g01430 | -181 | Heat shock protein 70 | 1,66 |
| 3,92 | Promoter (1-2kb) | VIT_13s0019g01940 | -1220 | Laccase | -2,13 |
| 3,11 | Promoter (<=1kb) | VIT_07s0005g03470 | -84 | Structural maintenance of chromosomes (SMC1) | 1,65 |
| 2,85 | Promoter (<=1kb) | VIT_18s0001g11740 | -299 | Ring zinc finger ariadne protein AR12 | -1,76 |
| 2,37 | Promoter (1-2kb) | VIT_10s0003g03490 | -1640 | GA 2-oxidase | 5,13 |
| 2,3 | Promoter (1-2kb) | VIT_15s0046g00740 | -1068 | Tetratricopeptide repeat (TPR)-containing | 1,81 |
| 2,27 | Promoter (1-2kb) | VIT_08s0007g02860 | -1373 | RNA-binding protein | 1,54 |
| 2,17 | Promoter (<=1kb) | VIT_18s0157g00020 | 0 | GIGANTEA protein | 1,65 |
| 2,1 | Promoter (1-2kb) | VIT_01s0011g06650 | -1820 | Beta-Ig-H3/fasciclin | 2,42 |
| 2,1 | Promoter (<=1kb) | VIT_07s0197g00080 | -598 | SNF1 protein kinase 2-3 AKIP OST1 | -2,14 |

Table 36: *VviNAC15* DAP-seq targets genes which have a match in the *VviNAC15* transient over expression dataset. In bold are reported the *switch* genes and the asterisk (*) refers to the transition markers.

Moreover, in the list an up regulated *MYB* gene, *MYB FAMILY* (VIT_01s0026g01050) was present and two down regulated *LACCASE* (VIT_13s0019g02160 and VIT_13s0019g01940), which have a role in the flavonoid biosynthesis in grapes (Braidot et al., 2008).

VviNAC17

The DAP-seq assay reported 8599 binding sites (peaks), which were reduced to 8307 after the $FC > 5$ filtering; even considering the very stringent filter used, the loss was very low, only the 3% (**Fig. 46**). The distribution of peaks revealed that

29% were located within the promoter regions (up to 2 kb upstream from a transcription start site), 2% were in 5' untranslated regions (UTRs), 14% were located in exons, 12% were located within introns, 3% were located in 3' UTRs, 8% were located in the 3 kb downstream region, and 29% were intergenic.

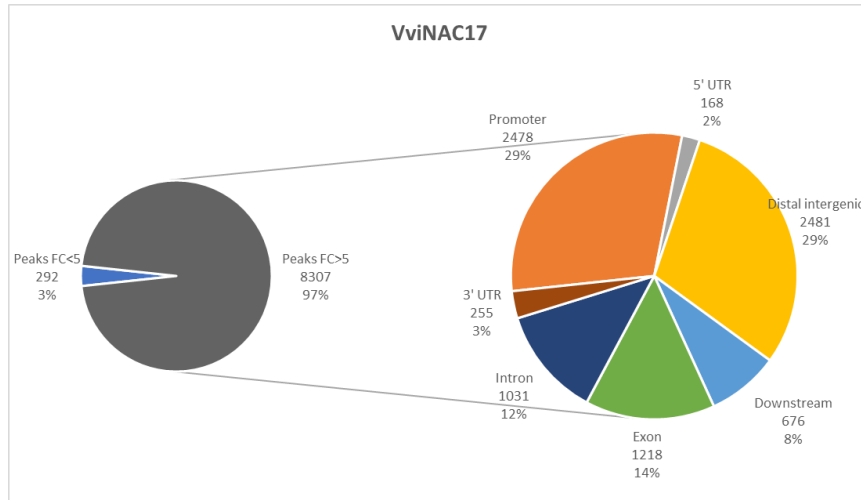


Figure 46: Double pie chart of the VviNAC17 DAP-seq results. The pie on the left represents the total binding sites (peaks) obtained, divided between the FC>5 and FC<5 (compared to the GST-Halo negative control peaks). The pie on the right represents the subdivision into the different genic region of the selected filtered peaks.

Three major binding motifs ([T/A][T/G][A/C]CGT[G/A]) were identified with strong significance (**Fig. 47**) and the phylogenetic footprints correlate with ANAC055, which may function as transcription activator to regulate jasmonic acid-induced expression of defense genes (Bu *et al.*, 2008).

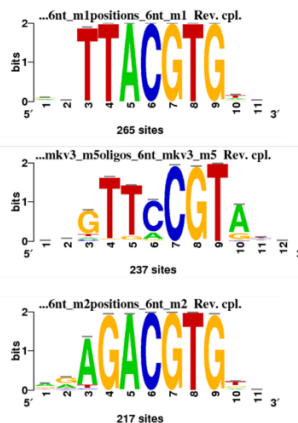


Figure 47: RSAT Plants NGS ChIP-Seq peak motifs analysis on the VviNAC17 DAP-seq results. Three top-ranking binding motifs identified in the DAP-seq FC>5 filtered dataset, based on the detection of overrepresented oligonucleotides (oligo analysis). The overall height of each letter stack indicates the sequence conservation at that position, and the height of symbols within the stack reflects the relative frequency of the corresponding nucleic acid at that position.

The attention was focused only on the 31% of the final analysed binding sites, which belongs to the ‘promoter’ and ‘5’UTR’ genic regions, for a total of 2646 sites. This was a very high percentage, compared to the number of sites normally found in other DAP-seq published papers.

After the elimination of all the ‘no hit’ and ‘unknown’ elements, 2149 binding sites were obtained for a total of 1913 unique genes regulated by VviNAC17.

A GO enrichment analysis was performed on this sub-dataset, revealing a predominance of genes related to regulation of biological and metabolic processes, aromatic compound biosynthesis, response to stimuli and transmembrane transport (Fig. 48).

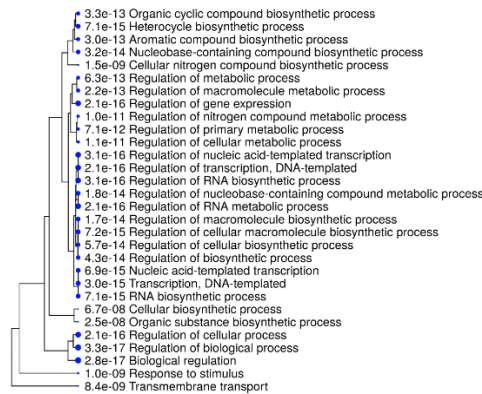


Figure 48: GO enrichment analysis of the VviNAC17 targets found to be regulated in the promoter and 5’UTR regions. The analysis was performed on ShinyGO.

Between the top 20 (q-value based) promoter and 5’UTR located binding sites some interesting genes were found (Table 37).

| q-value | Genic region | Gene ID | Distance to TSS | Functional annotation |
|---------|------------------|-------------------|-----------------|--|
| 14868 | Promoter (<=1kb) | VIT_15s0048g01740 | -347 | Growth-regulating factor 9 |
| 10149 | Promoter (<=1kb) | VIT_19s0177g00070 | -529 | Polyubiquitin (UBQ14) |
| 7108 | Promoter (1-2kb) | VIT_18s0041g02010 | -1916 | 12-oxophytodienoate reductase 1 |
| 5621 | Promoter (<=1kb) | VIT_05s0020g02310 | 0 | Pyruvate,orthophosphate dikinase |
| 5442 | Promoter (<=1kb) | VIT_17s0000g06970 | -412 | Diacylglycerol kinase 1 |
| 5223 | Promoter (1-2kb) | VIT_18s0001g14980 | -1611 | 3-methyl-2-oxobutanoate dehydrogenase |
| 5028 | Promoter (<=1kb) | VIT_11s0016g03000 | -20 | Phosphoinositide 3-kinase regulatory subunit 4 |
| 4861 | 5' UTR | VIT_03s0038g04390 | 24 | Dehydrin 1 |
| 4601 | Promoter (<=1kb) | VIT_19s0015g02950 | 0 | Secologanin synthase CYP72A1 |
| 4515 | 5' UTR | VIT_17s0000g05610 | 473 | Isopiperitenol dehydrogenase |
| 4402 | Promoter (<=1kb) | VIT_17s0000g01280 | -77 | WRKY Transcription Factor (VvWRKY52) |
| 4384 | Promoter (<=1kb) | VIT_05s0062g00710 | -892 | UDP-glucose:flavonoid 7-O-glucosyltransferase |
| 4304 | Promoter (<=1kb) | VIT_05s0077g00220 | 0 | Expansin A4 |
| 4256 | Promoter (<=1kb) | VIT_07s0031g00100 | 0 | flavonol synthase |
| 4202 | Promoter (<=1kb) | VIT_00s0207g00200 | 0 | Integral membrane protein, putative |
| 4158 | Promoter (<=1kb) | VIT_01s0011g04760 | -66 | myb domain protein 4 (VvMybC2-L1) |
| 4122 | 5' UTR | VIT_09s0002g04290 | 40 | Hydroxyphenylpyruvate reductase (HPPR) |
| 4064 | Promoter (<=1kb) | VIT_07s0255g00110 | -146 | WD40 |
| 3742 | Promoter (<=1kb) | VIT_14s0006g02620 | -273 | Cg167 serine protease * |
| 3648 | Promoter (<=1kb) | VIT_07s0005g01240 | -594 | Triacylglycerol lipase |

Table 37: Top 20 (q-value based) represented direct target genes of VviNAC17. In bold are reported the switch genes and the asterisk (*) refers to the transition markers.

As the most represented gene the *GROWTH-REGULATING FACTOR 9* (VIT_15s0048g01740) was found; it controls the final leaf dimensions by restricting cell number in the leaf primordium (Omidbakhshfard et al., 2018).

In the list two red berry *switches* were found (Massonnet *et al.*, 2017), the *DEHYDRIN 1* (VIT_03s0038g04390), which is related to the acquisition of desiccation tolerance in plants and is generally accumulated during the late stages of seed development (Liu et al., 2017) and the many times presented *VviWRKY52* (VIT_17s0000g01280).

Moreover, a MYB gene, *MYB DOMAIN PROTEIN 4 VvMybC2-L1* (VIT_01s0011g04760) and *UDP-GLUCOSE:FLAVONOID 7-O-GLUCOSYLTRANSFERASE* (VIT_05s0062g00710), which have roles in UV protection, pathogen defense and coloration (Kim *et al.*, 2006), were also important features.

Afterwards, the list of the *VviNAC17* targets was used to find all the possible *VviNACs* targets of the TF.

10 *VviNACs* target genes were found (**Table 38**). Interestingly, between them also *VviNAC08* (VIT_18s0001g02300) and *VviNAC61* (VIT_08s0007g07640) were found.

| q-value | Genic region | Gene ID | Distance to TSS | Functional annotation |
|---------|------------------|-------------------|-----------------|---|
| 3045 | Promoter (1-2kb) | VIT_14s0068g01490 | -1125 | NAC domain-containing protein (VvNAC73) |
| 1869 | Promoter (<=1kb) | VIT_08s0007g07640 | 0 | NAC domain-containing protein (VvNAC61) |
| 853 | Promoter (1-2kb) | VIT_17s0000g06400 | -1911 | NAC domain-containing protein (VvNAC05) |
| 663 | Promoter (<=1kb) | VIT_06s0080g00970 | -155 | NAC domain-containing protein (VvNAC67) |
| 652 | Promoter (1-2kb) | VIT_13s0019g05240 | -1180 | NAC domain-containing protein (VvNAC20) |
| 423 | Promoter (1-2kb) | VIT_04s0044g01500 | -1417 | NAC domain-containing protein (VvNAC47) |
| 253 | Promoter (<=1kb) | VIT_12s0055g00510 | -271 | NAC domain-containing protein (VvNAC58) |
| 208 | Promoter (<=1kb) | VIT_15s0048g02300 | -245 | NAC domain-containing protein (VvNAC53) |
| 204 | Promoter (<=1kb) | VIT_18s0001g10250 | -81 | NAC domain containing protein 19 |
| 204 | Promoter (<=1kb) | VIT_18s0001g02300 | -29 | NAC domain-containing protein (VvNAC08) |

Table 38: *VviNAC17* DAP-seq *VviNACs* targets genes.

Afterwards, the already reported *VviNAC17* transient over expression results (FC>|1.5|) were crossed with the DAP-seq promoter and 5'UTR sub-dataset, revealing 19 correlated binding sites (17 unique genes, **Table 39**).

PINI (VIT_05s0062g01120), present with two *VviNAC17* binding sites on its promoting region, is related to the auxin transport and signalling (Kong *et al.*, 2019).

Also, a *VviWRKY* gene was present in the list, *VviWRKY45* (VIT_14s0108g01280); unfortunately, no information is available concerning this TF. However, *WRKY* gene family is well known to be involved in the regulation of development and senescence (Wang et al., 2014).

Moreover, the presence of *ALLENE OXIDE SYNTHASE - JASMONATES FROM FATTY ACIDS* (VIT_18s0001g11630), which also resulted up regulated, confirm the correlation with ANAC055, found with the motif analysis.

| q-value | Genic region | Gene ID | Distance to TSS | Functional annotation | Transient OE |
|---------|------------------|-------------------|-----------------|--|--------------|
| 2027 | Promoter (1-2kb) | VIT_13s0019g02080 | -1368 | DNA-binding protein | 1,52 |
| 1775 | Promoter (1-2kb) | VIT_13s0019g02080 | -1042 | DNA-binding protein | 1,52 |
| 1732 | Promoter (<=1kb) | VIT_16s0100g00010 | -878 | Carboxylesterase 20 CXE20 | 1,68 |
| 1473 | Promoter (<=1kb) | VIT_01s0011g06280 | -356 | Oxidoreductase | 1,50 |
| 1398 | Promoter (1-2kb) | VIT_05s0062g01120 | -1260 | PIN1 | 1,80 |
| 983 | Promoter (<=1kb) | VIT_09s0002g06970 | -148 | Palmitoyl-monogalactosyldiacylglycerol delta-7 desaturase, chloroplast | -1,94 |
| 839 | Promoter (<=1kb) | VIT_05s0020g01670 | -430 | GTP1/OBG | -1,53 |
| 599 | Promoter (<=1kb) | VIT_18s0001g11630 | -304 | Allene oxide synthase (jasmonates from fatty acids) | 2,63 |
| 424 | 5' UTR | VIT_08s0007g04550 | 119 | NCS1 nucleoside transporter family protein | -1,77 |
| 357 | Promoter (<=1kb) | VIT_10s0116g01730 | -138 | Soluble starch synthase 3, chloroplast precursor | -1,68 |
| 331 | 5' UTR | VIT_08s0007g00920 | 12 | Tropinone reductase | -2,00 |
| 276 | Promoter (<=1kb) | VIT_05s0062g01120 | -708 | PIN1 | 1,80 |
| 253 | Promoter (1-2kb) | VIT_14s0108g01280 | -1509 | WRKY DNA-binding protein 4 (WRKY-18), WRKY Transcription Factor (VvWRKY45) * | 1,51 |
| 253 | 5' UTR | VIT_04s0008g07310 | 14 | AarF domain-containing kinase ABC1 | -1,64 |
| 244 | Promoter (<=1kb) | VIT_16s0050g02520 | 0 | RNA polymerase sigma subunit SigE (sigE) | -1,65 |
| 242 | Promoter (<=1kb) | VIT_09s0018g01800 | -55 | Acid phosphatase | -3,06 |
| 241 | Promoter (1-2kb) | VIT_11s0016g02350 | -1639 | Ubiquinone/menaquinone biosynthesis methyltransferase UbiE | -1,75 |
| 204 | Promoter (<=1kb) | VIT_14s0066g00160 | -655 | Ubiquinone/menaquinone biosynthesis methyltransferase UbiE * | -1,90 |
| 203 | Promoter (<=1kb) | VIT_07s0129g01000 | -616 | F-box family protein | 1,66 |

Table 39: VviNAC17 DAP-seq targets genes which have a match in the *VviNAC17* transient over expression dataset. In bold are reported the *switch* genes and the asterisk (*) refers to the transition markers.

VviNAC18

The DAP-seq assay reported 1409 binding sites (peaks), which were reduced to 1233 after the FC>5 filtering; this time the loss was higher, about the 12% (**Fig. 49**). The distribution of peaks revealed that 29% were located within the promoter regions (up to 2 kb upstream from a transcription start site), 3% were in 5' untranslated regions (UTRs), 15% were located in exons, 8% were located within introns, 3% were located in 3' UTRs, 6% were located in the 3 kb downstream region, and 24% were intergenic.

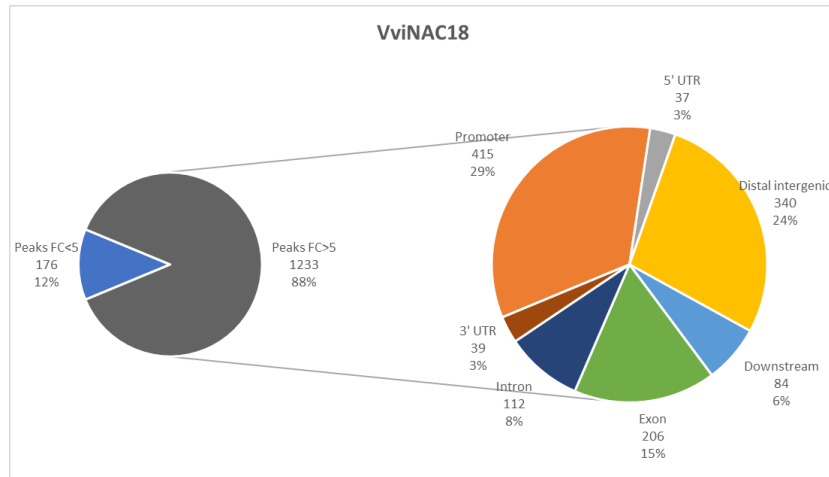


Figure 49: Double pie chart of the VviNAC18 DAP-seq results. The pie on the left represents the total binding sites (peaks) obtained, divided between the FC>5 and FC<5 (compared to the GST-Halo negative control peaks). The pie on the right represents the subdivision into the different genic region of the selected filtered peaks.

Three major binding motifs (GT[T/G][G/A/C]CGTG) were identified with strong significance (**Fig. 50**) and the phylogenetic footprints correlate with ANAC058 (no information available).

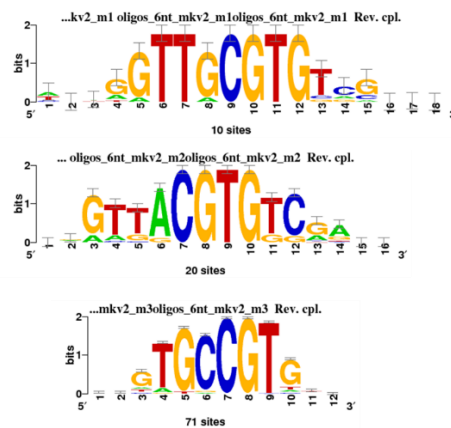


Figure 50: RSAT Plants NGS ChIP-Seq peak motifs analysis on the VviNAC18 DAP-seq results. Three top-ranking binding motifs identified in the DAP-seq FC>5 filtered dataset, based on the detection of overrepresented oligonucleotides (oligo analysis). The overall height of each letter stack indicates the sequence conservation at that position, and the height of symbols within the stack reflects the relative frequency of the corresponding nucleic acid at that position.

The attention was focused only on the 32% of the final analyzed binding sites, which belongs to the 'promoter' and '5'UTR' genic regions, for a total of 452 sites; the percentage of sites belonging to these regulatory regions is, in this case, very high.

After the elimination of all the ‘no hit’ and ‘unknown’ elements, 359 binding sites were obtained for a total of 351 unique genes regulated by VviNAC18.

A GO enrichment analysis was performed on this sub-dataset, revealing a predominance of genes related to regulation of cellular and biological processes, transport, localization, vesicle docking and cold acclimation; moreover, many categories of genes concerning to different types of responses were found (**Fig. 51**).

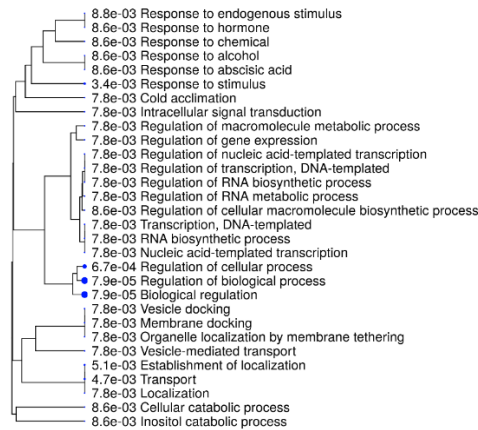


Figure 51: GO enrichment analysis of the VviNAC18 targets found to be regulated in the promoter and 5’UTR regions. The analysis was performed on ShinyGO.

Between the top 20 (q-value based) promoter and 5’UTR located binding sites some interesting genes were found (**Table 40**).

| q-value | Genic region | Gene ID | Distance to TSS | Functional annotation |
|---------|------------------|-------------------|-----------------|---|
| 13,92 | Promoter (<=1kb) | VIT_16s0050g00120 | -973 | B57 |
| 13,7 | 5' UTR | VIT_17s0000g05610 | 502 | Isopiperitenol dehydrogenase |
| 13,18 | Promoter (<=1kb) | VIT_15s0048g01740 | -376 | Growth-regulating factor 9 |
| 12,95 | Promoter (<=1kb) | VIT_19s0015g00930 | -208 | Hydroxyproline-rich glycoprotein |
| 10,62 | 5' UTR | VIT_06s0004g01140 | 764 | GRIK1 (geminivirus rep interacting kinase 1) |
| 9,89 | Promoter (1-2kb) | VIT_17s0000g08950 | -1069 | D111/G-patch |
| 9,55 | Promoter (<=1kb) | VIT_05s0020g02160 | 0 | Squamosa promoter-binding protein (VvSBP6) |
| 9,15 | 5' UTR | VIT_10s0003g01300 | 128 | Transcription factor |
| 7,91 | Promoter (1-2kb) | VIT_05s0062g01120 | -1261 | PIN1 |
| 7,6 | Promoter (1-2kb) | VIT_00s0179g00140 | -1186 | Protein phosphatase 2C / PP2C |
| 7,04 | Promoter (<=1kb) | VIT_10s0003g04650 | -226 | Nuclear transcription factor Y subunit A-7 |
| 6,87 | Promoter (<=1kb) | VIT_18s0001g00360 | -370 | Dehydrin (VvDHN2) |
| 6,61 | Promoter (<=1kb) | VIT_17s0000g06410 | -525 | MYB transcription factor MIXTA-like 2 |
| 6,37 | Promoter (<=1kb) | VIT_18s0001g08300 | 0 | Tubulin alpha-6 chain |
| 6,36 | Promoter (1-2kb) | VIT_16s0098g01150 | -1172 | Auxin-responsive SAUR29 * |
| 6,32 | Promoter (1-2kb) | VIT_18s0001g09420 | -1844 | Progesterone 5-beta-reductase |
| 6,26 | Promoter (<=1kb) | VIT_06s0004g03870 | 0 | CCT motif constans-like |
| 6,17 | Promoter (<=1kb) | VIT_05s0020g05060 | -953 | Cellulose synthase CSLG2 |
| 6,17 | Promoter (<=1kb) | VIT_00s0181g00230 | -75 | LSD ONE like 2 |
| 6,15 | Promoter (<=1kb) | VIT_13s0019g00550 | -32 | Cofilin |

Table 40: Top 20 (q-value based) represented direct target genes of VviNAC18. In bold are reported the *switch* genes and the asterisk (*) refers to the transition markers.

GRIK1 (VIT_06s0004g01140), a white berry *switch*, is a kinase that can activate SnRK1, which plays a central role in coordinating energy balance and nutrient metabolism in plants (Shen et al., 2009).

PIN1 (VIT_05s0062g01120), *GROWTH-REGULATING FACTOR 9* (VIT_15s0048g01740) and *MYB TRANSCRIPTION FACTOR MIXTA-LIKE 2* (VIT_17s0000g06410) were also found again between the targets even of this TF.

Only one *VviNAC* target genes was found concerning the *VviNAC18-VviNACs* defined interactions: *VviNAC05* (VIT_17s0000g06400).

Then, the previously reported *VviNAC18* transient over expression results (FC>|1.5|) were crossed with the DAP-seq promoter and 5'UTR sub-dataset, revealing 9 correlated binding sites (9 unique genes; **Table 41**); none of them were present between the top 20 reported genes.

Between the five up regulated genes, the already described *SENESCENCE-INDUCIBLE CHLOROPLAST STAY-GREEN PROTEIN 1 SGR1* (VIT_02s0025g04660) returned. Interestingly and in line with literature, the *SENESCENCE-INDUCIBLE CHLOROPLAST STAY-GREEN PROTEIN 2 SGR2* (VIT_18s0001g01210) was also found and, on the opposite of its companion gene *SGR1* (VIT_02s0025g04660), it resulted down regulated. *SGRs* are nuclear gene encoding a chloroplast protein and are senescence-associated genes; they are constitutively expressed at low levels and low amounts of protein are always detected during leaf development (Park *et al.*, 2007). *SGR1* interacts with chlorophyll catabolic enzymes and light-harvesting complex II at the thylakoid membrane and acts as a key regulator of leaf yellowing (Sakuraba *et al.*, 2014).

Under senescence-inducing conditions, *SGR2* expression is highly up regulated, similarly to *SGR1* expression; *SGR1* and *SGR2* formed homo- or heterodimers, strongly suggesting a role for *SGR2* in negatively regulating chlorophylls degradation by possibly interfering with the proposed chlorophyll catabolic enzymes recruiting function of *SGR1* (Sakuraba *et al.*, 2014).

Moreover, *STEROID SULFOTRANSFERASE* (VIT_13s0084g00240), a white berry *switch* and a negative second transition marker, was also found down regulated.

| q-value | Genic region | Gene ID | Distance to TSS | Functional annotation | Transient OE |
|-------------|------------------|-------------------|-----------------|---|--------------|
| 3,74 | Promoter (<=1kb) | VIT_12s0142g00610 | -8 | Citrate synthase, glyoxysomal precursor | 1,55 |
| 3,29 | Promoter (<=1kb) | VIT_02s0025g04660 | -196 | Senescence-inducible chloroplast stay-green protein 1 | 2,58 |
| 2,95 | Promoter (<=1kb) | VIT_11s0016g03180 | 0 | ABI1 (ABA insensitive 1) | -1,51 |
| 2,5 | Promoter (1-2kb) | VIT_13s0067g00260 | -1302 | Nematode-resistance protein | 2,41 |
| 2,47 | Promoter (<=1kb) | VIT_05s0077g00850 | -84 | Ubiquitin-conjugating enzyme E2 O | 1,73 |
| 2,45 | Promoter (<=1kb) | VIT_18s0001g01210 | -44 | Senescence-inducible chloroplast stay-green protein 2 | -2,20 |
| 2,44 | Promoter (1-2kb) | VIT_17s0000g08080 | -1008 | Armadillo/beta-catenin repeat protein / U-box domain-containing protein | 2,31 |
| 2,31 | Promoter (<=1kb) | VIT_16s0098g01790 | -477 | Calmodulin-binding region IQD21 | -1,53 |
| 2,01 | Promoter (<=1kb) | VIT_13s0084g00240 | -8 | Steroid sulfotransferase * | -1,51 |

Table 41: VviNAC18 DAP-seq targets genes which have a match in the *VviNAC18* transient over expression dataset. In bold are reported the *switch* genes and the asterisk (*) refers to the transition markers.

VviNAC26

The DAP-seq assay reported 12245 binding sites (peaks), which were reduced to 11795 after the $FC > 5$ filtering; even considering the very stringent filter used, the loss was very low, only the 4% (**Fig. 52**). The distribution of peaks revealed that 30% were located within the promoter regions (up to 2 kb upstream from a transcription start site), 2% were in 5' untranslated regions (UTRs), 15% were located in exons, 11% were located within introns, 3% were located in 3' UTRs, 8% were located in the 3 kb downstream region, and 27% were intergenic.

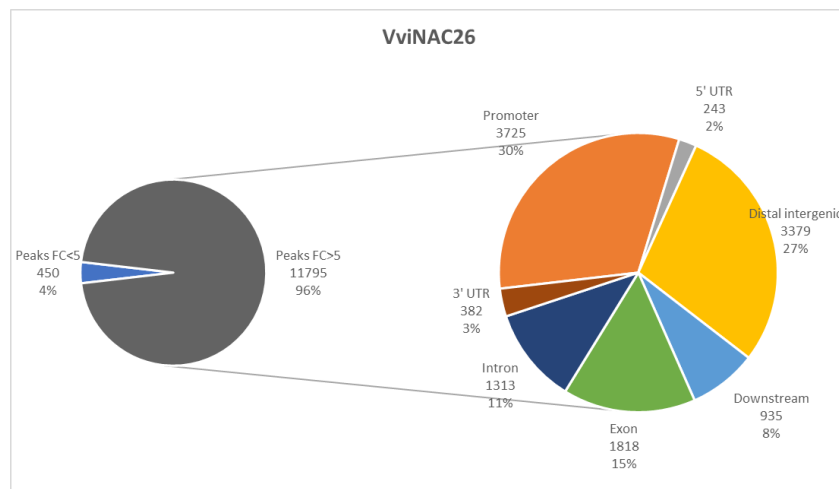


Figure 52: Double pie chart of the VviNAC26 DAP-seq results. The pie on the left represents the total binding sites (peaks) obtained, divided between the $FC > 5$ and $FC < 5$ (compared to the GST-Halo negative control peaks). The pie on the right represents the subdivision into the different genic region of the selected filtered peaks.

Two major binding motifs ([G/T]ACGT[G/A]) were identified with strong significance (**Fig. 53**) and the phylogenetic footprints correlate with ANAC055, which may function as transcription activator to regulate jasmonic acid-induced expression of defense genes (Bu *et al.*, 2008).

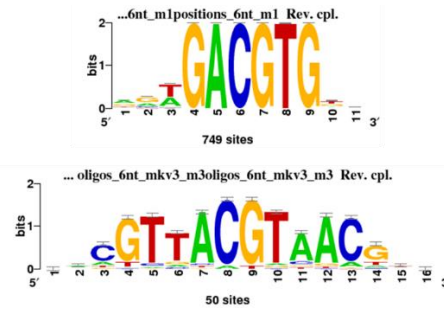


Figure 53: RSAT Plants NGS ChIP-Seq peak motifs analysis on the VviNAC26 DAP-seq results. Two top-ranking binding motifs identified in the DAP-seq FC>5 filtered dataset, based on the detection of overrepresented oligonucleotides (oligo analysis). The overall height of each letter stack indicates the sequence conservation at that position, and the height of symbols within the stack reflects the relative frequency of the corresponding nucleic acid at that position.

The attention was focused only on the 32% of the final analysed binding sites, which belongs to the ‘promoter’ and ‘5’UTR’ genic regions, for a total of 3968 sites. The percentage of sites belonging to these regulatory regions is, in this case, very high.

After the elimination of all the ‘no hit’ and ‘unknown’ elements, 3236 binding sites were obtained for a total of 2765 unique genes regulated by VviNAC26.

A GO enrichment analysis was performed on this sub-dataset, revealing a predominance of genes related to regulation of biological processes category; many regulations of metabolic processes genes, also concerning the aromatic compounds, were present (**Fig. 54**).

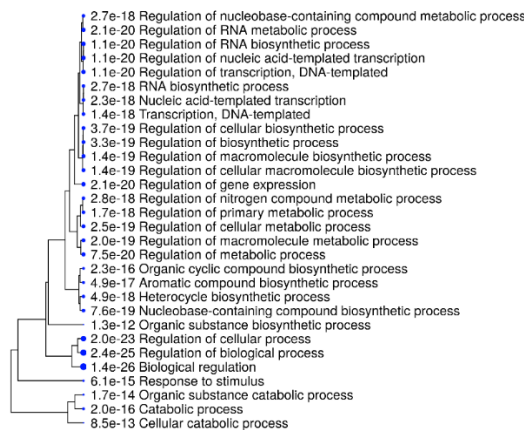


Figure 54: GO enrichment analysis of the VviNAC26 targets found to be regulated in the promoter and 5’UTR regions. The analysis was performed on ShinyGO.

Between the top 20 (q-value based) promoter and 5’UTR located binding sites some interesting genes were found (**Table 42**).

| q-value | Genic region | Gene ID | Distance to TSS | Functional annotation |
|---------|------------------|-------------------|-----------------|---|
| 18661 | Promoter (<=1kb) | VIT_15s0048g01740 | -377 | Growth-regulating factor 9 |
| 18556 | Promoter (1-2kb) | VIT_18s0001g14980 | -1611 | 3-methyl-2-oxobutanoate dehydrogenase |
| 16898 | Promoter (<=1kb) | VIT_19s0177g00070 | -496 | Polyubiquitin (UBQ14) |
| 16516 | Promoter (<=1kb) | VIT_07s0255g00110 | -145 | WD40 |
| 14631 | Promoter (<=1kb) | VIT_05s0020g02310 | 0 | Pyruvate,orthophosphate dikinase |
| 14485 | Promoter (1-2kb) | VIT_18s0001g09420 | -1843 | Progesterone 5-beta-reductase |
| 13904 | Promoter (<=1kb) | VIT_01s0011g04760 | -73 | myb domain protein 4 (VvMybC2-L1) |
| 13529 | Promoter (1-2kb) | VIT_13s0019g02080 | -1042 | DNA-binding protein |
| 12778 | Promoter (<=1kb) | VIT_17s0000g01280 | -65 | WRKY Transcription Factor (VvWRKY52) |
| 12245 | Promoter (1-2kb) | VIT_05s0062g01120 | -1260 | PIN1 |
| 11953 | Promoter (<=1kb) | VIT_12s0142g00610 | 0 | Citrate synthase, glyoxysomal precursor |
| 11061 | 5' UTR | VIT_03s0038g04390 | 24 | Dehydrin 1 |
| 10904 | Promoter (<=1kb) | VIT_05s0062g00710 | -875 | UDP-glucose:flavonoid 7-O-glucosyltransferase |
| 10775 | Promoter (<=1kb) | VIT_16s0039g02750 | -834 | NADH glutamate dehydrogenase |
| 10659 | Promoter (1-2kb) | VIT_18s0041g02010 | -1897 | 12-oxophytodienoate reductase 1 |
| 10566 | Promoter (<=1kb) | VIT_15s0048g02260 | -126 | Calcium-binding EF hand |
| 10384 | Promoter (<=1kb) | VIT_18s0001g08300 | 0 | Tubulin alpha-6 chain |
| 10134 | Promoter (1-2kb) | VIT_13s0067g00570 | -1194 | En/Spm transposon protein |
| 10071 | Promoter (<=1kb) | VIT_14s0006g02620 | -273 | Cgi67 serine protease * |
| 9248 | 5' UTR | VIT_17s0000g05610 | 464 | Isopiperitenol dehydrogenase |

Table 42: Top 20 (q-value based) represented direct target genes of VviNAC26. In bold are reported the *switch* genes and the asterisk (*) refers to the transition markers.

The most sequenced represented gene was the already mentioned *GROWTH-REGULATING FACTOR 9* (VIT_15s0048g01740).

Other genes continually return in the targets lists and were present also in the VviNAC26 dataset: *MYB DOMAIN PROTEIN 4* VvMYBC2-L1 (VIT_01s0011g04760), *PIN1* (VIT_05s0062g01120) and *UDP-GLUCOSE:FLAVONOID 7-O-GLUCOSYLTRANSFERASE* (VIT_05s0062g00710).

Moreover, two red berry *switches* were present in this small list; *VviWRKY52* (VIT_17s0000g01280) returned also in this VviNAC TF targets, together with the *DEHYDRIN 1* (VIT_03s0038g04390).

Afterwards, the list of the VviNAC26 targets was used to find all the possible VviNACs targets of the TF. 13 VviNACs target genes were found (**Table 43**), three of which harboring multiple VviNAC26 binding sites: *VviNAC05* (VIT_17s0000g06400), *VviNAC40* (VIT_12s0035g02020) and *VviNAC61* (VIT_08s0007g07640), for a total of 17 VviNAC26-VviNACs defined gene interactions. Moreover, *VviNAC08*, one of the studied TFs, was also found.

| q-value | Genic region | Gene ID | Distance to TSS | Functional annotation |
|---------|------------------|-------------------|-----------------|---|
| 4704 | Promoter (<=1kb) | VIT_08s0007g07640 | 0 | NAC domain-containing protein (VvNAC61) |
| 1976 | Promoter (1-2kb) | VIT_17s0000g06400 | -1867 | NAC domain-containing protein (VvNAC05) |
| 1855 | Promoter (<=1kb) | VIT_08s0007g07640 | 0 | NAC domain-containing protein (VvNAC61) |
| 1812 | Promoter (1-2kb) | VIT_07s0031g02610 | -1550 | NAC domain-containing protein (VvNAC39) |
| 1353 | Promoter (1-2kb) | VIT_12s0035g02020 | -1029 | NAC domain-containing protein (VvNAC40) |
| 1295 | Promoter (<=1kb) | VIT_17s0000g06400 | 0 | NAC domain-containing protein (VvNAC05) |
| 1113 | Promoter (<=1kb) | VIT_04s0008g06550 | 0 | NAC domain-containing protein (VvNAC66) |
| 729 | Promoter (<=1kb) | VIT_06s0080g00970 | -179 | NAC domain-containing protein (VvNAC67) |
| 636 | Promoter (<=1kb) | VIT_18s0001g02300 | -341 | NAC domain-containing protein (VvNAC08) |
| 471 | Promoter (<=1kb) | VIT_12s0055g00510 | -303 | NAC domain-containing protein (VvNAC58) |
| 404 | Promoter (1-2kb) | VIT_12s0035g02020 | -1485 | NAC domain-containing protein (VvNAC40) |
| 352 | Promoter (<=1kb) | VIT_18s0001g02300 | -29 | NAC domain-containing protein (VvNAC08) |
| 348 | Promoter (<=1kb) | VIT_12s0028g03050 | -390 | NAC domain-containing protein (VvNAC34) |
| 306 | Promoter (<=1kb) | VIT_18s0001g10250 | 0 | NAC domain containing protein 19 |
| 279 | Promoter (1-2kb) | VIT_14s0068g01490 | -1139 | NAC domain-containing protein (VvNAC73) |
| 4 | Promoter (1-2kb) | VIT_04s0023g03110 | -1736 | NAC domain-containing protein (VvNAC23) |
| 2 | Promoter (1-2kb) | VIT_06s0004g02350 | -1933 | NAC domain-containing protein 25 |

Table 43: VviNAC26 DAP-seq *VviNACs* targets genes.

Then, the previously reported *VviNAC26* transient over expression results ($FC > |1.5|$) were crossed with the DAP-seq promoter and 5'UTR sub-dataset, revealing 155 correlated binding sites (132 unique genes), 82 of them up regulated (**Table 44**) and 50 down regulated (**Table 45**); one of them was also present between the top 20 reported genes, *DNA-BINDING PROTEIN* (VIT_13s0019g02080).

Many *switch* genes and transition markers were found between the up and down regulated genes; moreover, other maturation related genes were present.

For example, between the up regulated, the *SUCROSE-PHOSPHATE SYNTHASE* (VIT_05s0029g01140) and a *FRUCTOSE-1,6-BISPHOSPHATASE, CYTOSOLIC* (VIT_18s0072g00770) are related to the sucrose biosynthetic pathways and are important in the leaves and berries maturation processes (Wu *et al.*, 2011 and Daie, 1993). Even more interesting is the presence in the list of *VvMYBA6* (VIT_14s0006g01290), which has a role in the control of anthocyanin synthesis (Matus *et al.*, 2017), and a *bHLH* gene (VIT_11s0052g00100), which are important TFs mainly implicated in the jasmonic acid signalling and in the response to stresses (Heim *et al.*, 2003, Goossnes *et al.*, 2017 and Sun *et al.*, 2018).

Looking at the down regulated genes, a NAC domain containing protein (VIT_18s0001g10250) and other two *bHLH* (VIT_07s0031g00450 and VIT_02s0025g02610) are also direct target of *VviNAC26*.

| q-value | Genic region | Gene ID | Distance to TSS | Functional annotation | Transient OE |
|---------|------------------|-------------------|-----------------|---|--------------|
| 5982 | Promoter (<=1kb) | VIT_16s0098g01790 | -478 | Calmodulin-binding region IQD21 | 1,74 |
| 4646 | Promoter (<=1kb) | VIT_00s0207g00200 | 0 | Integral membrane protein, putative | 1,69 |
| 4247 | Promoter (<=1kb) | VIT_01s0026g01030 | -962 | Zinc finger (C3HC4-type ring finger) | 1,76 |
| 3167 | Promoter (<=1kb) | VIT_17s0000g09540 | 0 | CYP71A26 | 3,17 |
| 2248 | Promoter (<=1kb) | VIT_19s0090g01350 | -201 | Aspartyl protease | 4,56 |
| 2058 | Promoter (1-2kb) | VIT_01s0011g05600 | -1997 | Receptor-like protein kinase | 2,77 |
| 1871 | Promoter (1-2kb) | VIT_07s0005g00210 | -1400 | Thiamin pyrophosphokinase | 1,61 |
| 1785 | Promoter (1-2kb) | VIT_14s0066g01240 | -1951 | L-aspartate oxidase | 1,78 |
| 1743 | Promoter (1-2kb) | VIT_01s0011g04630 | -1409 | Ribose 5-phosphate isomerase | 2,23 |
| 1723 | Promoter (<=1kb) | VIT_19s0090g01350 | 0 | Aspartyl protease | 4,56 |
| 1691 | Promoter (<=1kb) | VIT_02s0012g00530 | -20 | Ribose-phosphate pyrophosphokinase 1 | 1,96 |
| 1664 | Promoter (<=1kb) | VIT_13s0019g02200 | -523 | Protein phosphatase 2CA AHG3 PP2CA (VvPP2C-3) | 2,17 |
| 1637 | Promoter (<=1kb) | VIT_00s0227g00140 | 0 | MLO1 | 2,57 |
| 1379 | 5' UTR | VIT_08s0007g04550 | 122 | NCS1 nucleoside transporter family protein | 2,57 |
| 1362 | Promoter (<=1kb) | VIT_19s0090g00120 | -198 | Ubiquitin-conjugating enzyme E2 variant | 5,80 |
| 1267 | Promoter (<=1kb) | VIT_11s0016g03180 | -7 | AB11 (ABA insensitive 1) | 3,37 |
| 1254 | Promoter (<=1kb) | VIT_12s0028g03010 | -56 | Glutaredoxin | 1,62 |
| 1227 | Promoter (<=1kb) | VIT_00s0216g00060 | 0 | Nuclear transport factor 2 (NTF2) | 2,16 |
| 1213 | Promoter (<=1kb) | VIT_08s0007g08290 | -664 | GTP-binding protein TypA/BipA | 2,32 |
| 1104 | Promoter (<=1kb) | VIT_05s0029g01140 | -26 | Sucrose-phosphate synthase | 4,37 |
| 1094 | Promoter (1-2kb) | VIT_15s0046g01440 | -1776 | Basic Leucine Zipper Transcription Factor (VvbZIP40) | 2,00 |
| 1042 | Promoter (<=1kb) | VIT_05s0077g02150 | 0 | Chalcone reductase * | 2,93 |
| 1042 | Promoter (1-2kb) | VIT_05s0020g01150 | -1504 | Cation/hydrogen exchanger (CHX19) | 2,69 |
| 1022 | Promoter (<=1kb) | VIT_17s0000g09570 | -321 | CYP71A26 | 3,05 |
| 1012 | Promoter (<=1kb) | VIT_17s0000g06610 | 0 | Zinc finger (C3HC4-type ring finger) | 3,40 |
| 995 | Promoter (<=1kb) | VIT_05s0077g00280 | -252 | Beta-amylase | 2,25 |
| 914 | Promoter (1-2kb) | VIT_01s0011g04630 | -1788 | Ribose 5-phosphate isomerase | 2,23 |
| 884 | Promoter (<=1kb) | VIT_13s0084g00310 | -301 | AC112 | 1,57 |
| 834 | Promoter (<=1kb) | VIT_02s0012g01240 | -233 | PHD finger transcription factor | 2,21 |
| 781 | Promoter (<=1kb) | VIT_16s0050g00990 | 0 | ferric reduction oxidase 4 | 2,91 |
| 767 | Promoter (<=1kb) | VIT_07s0031g01530 | 0 | Stress enhanced protein 2 (SEP2) | 2,22 |
| 738 | 5' UTR | VIT_08s0007g04980 | 22 | Phosphoadenosine phosphosulfate (PAPS) reductase | 1,56 |
| 729 | Promoter (1-2kb) | VIT_01s0026g00300 | -1441 | Zinc finger (C3HC4-type ring finger) | 1,88 |
| 626 | Promoter (<=1kb) | VIT_14s0066g01200 | -25 | Protein kinase beta-1 subunit 5'-AMP-activated | 1,58 |
| 625 | Promoter (1-2kb) | VIT_04s0008g06050 | -1396 | Phytosulfokine receptor precursor | 1,69 |
| 612 | Promoter (<=1kb) | VIT_07s0005g00180 | -407 | TOC159 (translocon outer membrane complex 159) | 1,68 |
| 578 | 5' UTR | VIT_02s0012g01240 | 255 | PHD finger transcription factor | 2,21 |
| 578 | Promoter (<=1kb) | VIT_12s0034g02390 | 0 | T-complex protein 11 | 1,60 |
| 576 | Promoter (<=1kb) | VIT_01s0137g00560 | 0 | CYP71B34 | 1,79 |
| 573 | Promoter (<=1kb) | VIT_03s0132g00150 | -135 | GTP cyclohydrolase I | 1,89 |
| 573 | Promoter (<=1kb) | VIT_05s0020g04210 | -663 | Sulfate adenylyltransferase 3 | 1,73 |
| 554 | Promoter (<=1kb) | VIT_11s0016g03180 | -379 | AB11 (ABA insensitive 1) | 3,37 |
| 523 | Promoter (<=1kb) | VIT_05s0020g03970 | -697 | Sulfate transporter 3.1 (AST12) (AtST1) | 3,83 |
| 471 | Promoter (<=1kb) | VIT_07s0005g03680 | -56 | CCR4-NOT complex subunit CAF16 | 2,43 |
| 471 | Promoter (<=1kb) | VIT_01s0127g00220 | -7 | PMR5 (powdery mildew resistant 5) | 1,97 |
| 471 | Promoter (<=1kb) | VIT_19s0090g01440 | -53 | Fimbrin 2 | 1,94 |
| 471 | Promoter (<=1kb) | VIT_00s0477g00030 | -371 | MATE efflux family protein ripening responsive | 1,78 |
| 458 | 5' UTR | VIT_16s0050g00390 | 260 | 4-coumarate-CoA ligase * | 2,40 |
| 448 | Promoter (<=1kb) | VIT_08s0007g08290 | 0 | GTP-binding protein TypA/BipA | 2,32 |
| 448 | Promoter (<=1kb) | VIT_05s0077g00280 | -16 | Beta-amylase | 2,25 |
| 426 | Promoter (1-2kb) | VIT_01s0011g00250 | -1298 | 6-phosphogluconolactonase | 1,93 |
| 426 | Promoter (<=1kb) | VIT_17s0000g01680 | 0 | Adenylate kinase family | 1,83 |
| 424 | Promoter (<=1kb) | VIT_09s0002g06480 | -668 | CYP81B2v1 | 4,05 |
| 424 | Promoter (1-2kb) | VIT_06s0004g02140 | -1083 | MATE efflux family protein | 2,94 |
| 421 | Promoter (<=1kb) | VIT_09s0002g06970 | -148 | Palmitoyl-monogalactosyldiacylglycerol delta-7 desaturase, chloroplast * | 4,49 |
| 421 | Promoter (<=1kb) | VIT_13s0019g02200 | -839 | Protein phosphatase 2CA AHG3 PP2CA (VvPP2C-3) | 2,17 |
| 395 | Promoter (<=1kb) | VIT_02s0012g00530 | -269 | Ribose-phosphate pyrophosphokinase 1 | 1,96 |
| 394 | Promoter (<=1kb) | VIT_18s0072g00770 | -580 | fructose-1,6-bisphosphatase, cytosolic | 2,45 |
| 389 | Promoter (<=1kb) | VIT_08s0056g01230 | -683 | Cycling DOF factor 2 | 2,07 |
| 382 | Promoter (1-2kb) | VIT_06s0004g00260 | -1318 | Shoot1 protein | 2,66 |
| 376 | Promoter (<=1kb) | VIT_18s0089g01410 | -295 | Purine permease 4 PUP4 | 2,44 |
| 352 | Promoter (<=1kb) | VIT_03s0063g00370 | -682 | Nitrite reductase | 6,15 |
| 344 | Promoter (1-2kb) | VIT_19s0015g00130 | -1259 | Serine acetyltransferase 3 | 2,63 |
| 344 | Promoter (<=1kb) | VIT_00s0216g00060 | -197 | Nuclear transport factor 2 (NTF2) | 2,16 |
| 344 | Promoter (<=1kb) | VIT_08s0040g01470 | -39 | Cis-zeatin O-beta-D-glucosyltransferase | 1,89 |
| 322 | Promoter (1-2kb) | VIT_13s0084g00310 | -1095 | AC112 | 1,57 |
| 321 | Promoter (<=1kb) | VIT_13s0019g02200 | -156 | Protein phosphatase 2CA AHG3 PP2CA (VvPP2C-3) | 2,17 |
| 319 | Promoter (<=1kb) | VIT_06s0004g06540 | -7 | Undecaprenyl pyrophosphate synthetase | 2,33 |
| 306 | Promoter (<=1kb) | VIT_05s0077g00810 | -622 | Sodium-inducible calcium-binding protein (ACP1) | 2,34 |
| 295 | Promoter (<=1kb) | VIT_11s0052g01480 | -347 | Salt-inducible protein kinase | 1,89 |
| 295 | Promoter (<=1kb) | VIT_14s0030g02230 | 0 | Unfertilized embryo sac 12 UNE12 | 1,59 |
| 283 | Promoter (<=1kb) | VIT_14s0066g01240 | -286 | L-aspartate oxidase | 1,78 |
| 278 | Promoter (<=1kb) | VIT_05s0020g04430 | 0 | MPBQ/MSBQ methyltransferase 1 | 1,65 |
| 269 | Promoter (<=1kb) | VIT_00s0187g00380 | -998 | Phosphatidate cytidyltransferase | 1,53 |
| 247 | Promoter (<=1kb) | VIT_19s0015g00130 | -952 | Serine acetyltransferase 3 | 2,63 |
| 247 | Promoter (1-2kb) | VIT_11s0037g01210 | -1702 | Eceriferum 1 (CER1 protein) Sterol desaturase | 2,52 |
| 247 | Promoter (<=1kb) | VIT_00s0207g00010 | 0 | Anthrnilate N-benzoyltransferase protein 1 | 2,19 |
| 247 | Promoter (<=1kb) | VIT_14s0030g01340 | -777 | Beta-ketoacyl-CoA synthase | 1,79 |
| 239 | Promoter (<=1kb) | VIT_16s0050g00140 | -847 | Heavy-metal-associated domain-containing protein | 2,83 |
| 239 | Promoter (1-2kb) | VIT_11s0016g05740 | -1675 | Calmodulin-5 (CAM5) | 1,61 |
| 239 | Promoter (<=1kb) | VIT_08s0032g00790 | -763 | ABC Transporter (VvWBC18 - VvABCg18) | 1,58 |
| 239 | Promoter (<=1kb) | VIT_08s0007g04980 | 0 | Phosphoadenosine phosphosulfate (PAPS) reductase | 1,56 |
| 239 | Promoter (1-2kb) | VIT_01s0011g04830 | -1352 | Extensin | 1,51 |
| 218 | Promoter (<=1kb) | VIT_11s0052g00100 | 0 | basic helix-loop-helix (bHLH) family | 3,03 |
| 201 | Promoter (<=1kb) | VIT_14s0006g01290 | -12 | myb domain protein 113 (VvMYB46) | 3,56 |
| 201 | Promoter (1-2kb) | VIT_00s0218g00100 | -1901 | Metal transporter Nramp6 | 3,37 |
| 201 | Promoter (1-2kb) | VIT_08s0007g04890 | -1790 | ACT domain-containing protein | 2,32 |
| 201 | Promoter (<=1kb) | VIT_18s0001g14310 | -403 | flavanone-3-hydroxylase 2 (F3H2) [Vitis vinifera] | 1,66 |
| 198 | Promoter (<=1kb) | VIT_13s0019g02200 | -379 | Protein phosphatase 2CA AHG3 PP2CA (VvPP2C-3) | 2,17 |
| 121 | Promoter (<=1kb) | VIT_18s0001g01030 | -547 | Protein disulfide isomerase * | 2,05 |
| 82 | Promoter (1-2kb) | VIT_00s0304g00080 | -1774 | Trehalose-6-phosphate phosphatase | 2,07 |
| 71 | 5' UTR | VIT_10s0523g00030 | 23 | Photoregulatory zinc-finger protein COP1 | 1,72 |
| 63 | Promoter (<=1kb) | VIT_02s0012g01240 | -295 | PHD finger transcription factor | 2,21 |
| 57 | Promoter (<=1kb) | VIT_11s0016g04580 | -528 | ABC Transporter (VvPDR2 - VvABCg32) | 1,88 |
| 43 | Promoter (<=1kb) | VIT_14s0066g00770 | -704 | Glycosyl transferase family 8 protein | 3,67 |
| 43 | Promoter (1-2kb) | VIT_06s0009g02640 | -1772 | Hydroxymethylglutaryl-CoA lyase | 2,05 |
| 42 | Promoter (1-2kb) | VIT_11s0016g02350 | -1642 | Ubiquinone/menaquinone biosynthesis methyltransferase UbiE | 5,48 |
| 36 | Promoter (<=1kb) | VIT_17s0000g09350 | -394 | Dehydration-induced 19 | 1,85 |
| 3 | Promoter (1-2kb) | VIT_11s0016g02350 | -1545 | Ubiquinone/menaquinone biosynthesis methyltransferase UbiE | 5,48 |
| 3 | Promoter (<=1kb) | VIT_12s0028g03350 | -777 | Squamosa promoter-binding protein (VvSBP11) * | 2,16 |

Table 44: VviNAC26 DAP-seq up regulated targets genes. In bold are reported the *switch* genes and the asterisk (*) refers to the transition markers.

| q-value | Genic region | Gene ID | Distance to TSS | Functional annotation | Transient OE |
|--------------|------------------|-------------------|-----------------|---|--------------|
| 13529 | Promoter (1-2kb) | VIT_13s0019g02080 | -1042 | DNA-binding protein | -1.62 |
| 7261 | Promoter (<=1kb) | VIT_06s0004g07930 | 0 | Nucleotidyltransferase family | -1.65 |
| 2952 | Promoter (<=1kb) | VIT_07s0031g00450 | -796 | Basic helix-loop-helix protein SPATULA | -2.18 |
| 2164 | Promoter (<=1kb) | VIT_06s0004g03870 | 0 | CCT motif constans-like | -1.53 |
| 1751 | Promoter (<=1kb) | VIT_12s0057g00910 | -242 | Sterile apetala | -1.69 |
| 1581 | 5' UTR | VIT_03s0017g00090 | 1287 | Serine/threonine-protein kinase bri1 | -2.13 |
| 1296 | Promoter (<=1kb) | VIT_05s0020g04850 | 0 | H1fk | -1.78 |
| 1287 | Promoter (<=1kb) | VIT_15s0048g01000 | -690 | 2'-hydroxy isoflavone/dihydroflavonol reductase | -1.68 |
| 1147 | Promoter (1-2kb) | VIT_13s0019g02080 | -1368 | DNA-binding protein | -1.62 |
| 1131 | Promoter (1-2kb) | VIT_16s0022g02230 | -1541 | Leucine-rich repeat receptor protein kinase EXS | -2.88 |
| 961 | Promoter (<=1kb) | VIT_19s0015g00710 | -374 | Cellulose synthase CSLE1 | -2.95 |
| 947 | Promoter (<=1kb) | VIT_04s0008g00610 | -508 | Zinc finger (CCH-type) family protein | -2.05 |
| 941 | Promoter (1-2kb) | VIT_06s0004g05710 | -1438 | Glutathione S-transferase GSTU7 | -2.43 |
| 941 | Promoter (<=1kb) | VIT_17s0000g00240 | -649 | Mei2 AML1 | -1.88 |
| 888 | Promoter (1-2kb) | VIT_17s0000g07520 | -1068 | Ribosomal-protein S6 kinase p70 | -1.58 |
| 875 | Promoter (<=1kb) | VIT_04s0023g02970 | 0 | UPF0183 protein | -1.59 |
| 834 | Promoter (1-2kb) | VIT_07s0014g00360 | -1803 | Lipase class 3 | -1.87 |
| 657 | Promoter (<=1kb) | VIT_12s0034g02220 | -839 | RKF3 (receptor-like kinase IN in flowers 3) | -1.91 |
| 653 | Promoter (<=1kb) | VIT_02s0012g00410 | 0 | Naringenin,2-oxoglutarate 3-dioxygenase | -1.58 |
| 629 | Promoter (1-2kb) | VIT_02s0025g02610 | -1990 | basic helix-loop-helix (bHLH) family | -3.85 |
| 603 | Promoter (<=1kb) | VIT_12s0059g01450 | -307 | Zinc finger CCH domain-containing protein ZFN-like 4 | -1.52 |
| 549 | Promoter (1-2kb) | VIT_11s0118g00480 | -1843 | Leucine-rich repeat | -1.52 |
| 548 | Promoter (1-2kb) | VIT_07s0031g01270 | -1220 | Ring-H2 finger A2A | -1.73 |
| 523 | Promoter (<=1kb) | VIT_01s0011g05660 | -831 | Zinc finger (Ran-binding) family | -1.50 |
| 513 | Promoter (1-2kb) | VIT_15s0048g01530 | -1401 | Geraniol 10-hydroxylase | -1.71 |
| 505 | Promoter (<=1kb) | VIT_06s0004g06290 | -62 | Binding | -2.52 |
| 497 | Promoter (<=1kb) | VIT_18s0001g06950 | -367 | Purine permease 1 (PUP1) | -1.74 |
| 497 | Promoter (<=1kb) | VIT_04s0044g01620 | 0 | RGLG1 (ring Domain LIGASE1) | -1.57 |
| 472 | Promoter (<=1kb) | VIT_06s0004g06290 | -307 | Binding | -2.52 |
| 448 | Promoter (1-2kb) | VIT_02s0025g04890 | -1766 | CYP76B1 | -5.19 |
| 445 | Promoter (<=1kb) | VIT_03s0038g00360 | -72 | Isochorismatase hydrolase | -4.20 |
| 403 | Promoter (1-2kb) | VIT_19s0014g02900 | -1756 | Ring finger protein 185 | -7.03 |
| 403 | Promoter (<=1kb) | VIT_18s0001g10910 | -423 | Patatin | -1.84 |
| 366 | 5' UTR | VIT_07s0104g00830 | 36 | Sugar transporter ERD6-like 7 * | -2.29 |
| 344 | Promoter (<=1kb) | VIT_19s0014g02900 | -243 | Ring finger protein 185 | -7.03 |
| 344 | Promoter (1-2kb) | VIT_17s0000g08010 | -1616 | Trehalose 6-phosphate synthase | -1.73 |
| 343 | Promoter (1-2kb) | VIT_07s0104g00830 | -1410 | Sugar transporter ERD6-like 7 * | -2.29 |
| 329 | Promoter (<=1kb) | VIT_05s0020g02710 | -457 | Slingshot | -1.80 |
| 321 | Promoter (<=1kb) | VIT_13s0064g01370 | -369 | Polygalacturonase inhibiting protein 1 PGIP1 | -2.89 |
| 306 | Promoter (<=1kb) | VIT_18s0001g10250 | 0 | NAC domain containing protein 19 | -1.52 |
| 295 | Promoter (<=1kb) | VIT_06s0004g06290 | -598 | Binding | -2.52 |
| 266 | Promoter (1-2kb) | VIT_07s0129g00490 | -1291 | Hydrogenobrynic acid a,c-diamide synthase | -1.70 |
| 247 | Promoter (<=1kb) | VIT_18s0122g00620 | -383 | Cinnamoyl-CoA reductase * | -2.55 |
| 247 | Promoter (<=1kb) | VIT_15s0045g00370 | -575 | Phosphatidylglycerol specific phospholipase C | -2.53 |
| 223 | Promoter (<=1kb) | VIT_03s0063g01780 | -315 | Extra-large G-protein (XLG1) | -3.39 |
| 223 | Promoter (<=1kb) | VIT_03s0017g02110 | -125 | Anthocyanidin 3-O-glucosyltransferase | -2.79 |
| 223 | Promoter (<=1kb) | VIT_01s0127g00910 | -109 | AERO1 (arabidopsis endoplasmic reticulum oxidoreductins 1) | -2.43 |
| 223 | Promoter (1-2kb) | VIT_04s0008g03660 | -1566 | Embryonic flower 1 | -1.61 |
| 219 | Promoter (1-2kb) | VIT_13s0067g03820 | -1605 | chalcone isomerase 1 [Vitis vinifera] (VvCHI1) * | -1.78 |
| 201 | Promoter (<=1kb) | VIT_05s0094g00290 | -797 | Chitinase, class IV [Vitis vinifera] | -2.31 |
| 158 | Promoter (<=1kb) | VIT_06s0004g06930 | -171 | Zinc finger (C3HC4-type ring finger) | -2.13 |
| 43 | Promoter (<=1kb) | VIT_09s0054g00860 | -228 | Lipase GDSL | -1.78 |
| 34 | Promoter (1-2kb) | VIT_18s0001g04500 | -1775 | Enhanced EM level EEL (VvABF-2), Basic Leucine Zipper Transcription Factor (VvblzP43) | -2.00 |
| 4 | Promoter (<=1kb) | VIT_07s0031g02250 | -911 | Zinc finger (C3HC4-type ring finger) | -1.86 |

Table 45: VviNAC26 DAP-seq down regulated targets genes. In bold are reported the *switch* genes and the asterisk (*) refers to the transition markers.

VviNAC33 (New Phytologist, Volume: 231, Issue: 2, Pages: 726-746, First published: 10 February 2021, DOI: (10.1111/nph.17263))

VviNAC33 promotes organ de-greening and represses vegetative growth during the vegetative-to-mature phase transition in grapevine

Erica D'Inca¹, Stefano Cazzaniga¹, Chiara Foresti¹, Nicola Vitulo¹, Edoardo Bertini¹, Mary Galli², Andrea Gallavotti², Mario Pezzotti¹, Giovanni Battista Tornielli¹, Sara Zenoni^{1*}

¹ Department of Biotechnology, University of Verona, 37134 Verona, Italy

² Waksman Institute of Microbiology, Rutgers University, Piscataway, NJ 08854-8020, USA

* Corresponding author: Sara Zenoni, +39 045 802 7941, sara.zenoni@univr.it

Summary

- Plants undergo several developmental transitions during their life cycle. In grapevine, a perennial woody fruit crop, the transition from vegetative/green to mature/woody growth involves transcriptomic reprogramming orchestrated by a small group of genes encoding regulators, but the underlying molecular mechanisms are not fully understood.
- We investigated the function of the transcriptional regulator *VviNAC33* by generating and characterizing transgenic overexpressing grapevine lines and a chimeric repressor, and by exploring its putative targets through DAP-seq approach combined with transcriptomic data.
- We demonstrated that *VviNAC33* induces leaf de-greening, inhibits organ growth and directly activates the expression of *STAY-GREEN PROTEIN 1 (SGR1)*, involved in chlorophyll and photosystem degradation, and *AUTOPHAGY 8f (ATG8f)* involved in the maturation of autophagosomes. Furthermore, we show that *VviNAC33* directly inhibits *AUXIN EFFLUX FACILITATOR PIN1* and *RopGEF1* and *ATP SYNTHASE GAMMA CHAIN 1T (ATPC1)* involved in photosystem II integrity and activity.
- Our results show that *VviNAC33* plays a major role in terminating photosynthetic activity and organ growth as part of a regulatory network governing the vegetative-to-mature phase transition.

Introduction

Plants develop through a succession of distinct growth phases and the correct timing of the transitions is important for plant fitness and agronomic performance (Demura and Ye, 2010). In seed plants, shoots pass through a vegetative growth phase, further divided into juvenile and adult stages, characterized by an increase in photosynthetic capacity and organ size. A reproductive phase follows, during which the vegetative shoot apical meristem assumes an inflorescence meristem identity (Huijser and Schmid, 2011). An essential transition to survive adverse environmental conditions is the shift from an active to a dormant state involving the cessation of growth, the repression of auxin responses, cell wall thickening, and adaptations to survive cold temperatures. For example, seed dormancy prevents germination out of season whereas bud dormancy and shoot lignification in perennial woody plants allows overwinter survival (Schrader *et al.*, 2004).

In fleshy fruit species, the transition from unripe fruit (that must be protected against herbivory) to ripe fruit (that must appeal to the same herbivores to facilitate seed dispersal) is another dramatic shift in survival strategy. Fruit ripening involves a tightly coordinated sequence of chemical and physiological alterations (Giovannoni *et al.*, 2017).

Senescence is the last part of the plant developmental program before cell death (Woo *et al.*, 2013). The transition to senescence involves the ordered disassembly of molecules and cellular components that accumulated during vegetative growth (Lim *et al.*, 2007). The earliest and most significant change in cell structure is the disassembly of the chloroplast, an organelle that contains up to 70% of the total leaf protein content. Like fruit ripening, leaf senescence is a complex genetic and epigenetic program that integrates endogenous developmental signals and environmental cues.

In recent years it has become evident that the genetic networks underlying these phase transitions share certain common factors. For example, the juvenile-to-adult and vegetative-to-reproductive phase transitions involve two evolutionarily conserved microRNAs (miR156 and miR172) and their targets (Huijser and Schmid, 2011; Ma *et al.*, 2020). Recently, certain NAM/ATAF/CUC (NAC) transcription factors were found to be key regulators of both fruit ripening and senescence, such as tomato NOR, a well-characterized master regulator of the onset of fruit ripening and a positive regulator of leaf senescence (Ma *et al.*, 2019).

NAC proteins form a large plant-specific family of transcription factors (TFs) that control the

expression of target genes by forming heterodimers with other NAC proteins as well as other TF families (Kim *et al.*, 2016). The analysis of NAC genes in different crops has shed light on their role in integrating developmental age and environmental signals during plant development (Liang *et al.*, 2014; Podzimska-Sroka *et al.*, 2015). For example, genetic studies have identified ANAC092/ORESARA1 (ORE1), ANAC029/Arabidopsis NAC-LIKE Activated by AP3/PI (AtNAP), ANAC059/ORESARA1 SISTER1 (ORS1), and ANAC016 as positive regulators of leaf senescence (Kim *et al.*, 2009; Guo *et al.*, 2006; Balazadeha *et al.*, 2011; Sakuraba *et al.*, 2015), whereas ANAC042/JUNGBRUNNEN1 (JUB1) and ANAC083/VND-INTERACTING2 (VNI2) are negative regulators (Wu *et al.*, 2012; Yang *et al.*, 2011). ANAC092/ORE1 is considered the key positive regulator of leaf senescence, involved in a delicately balanced feed-forward loop that promotes ethylene-mediated chlorophyll degradation.

Grapevine (*Vitis vinifera* L.) is an important perennial fruit crop and a useful model of developmental phase transition in woody species, featuring all the major developmental and physiological processes and benefiting from a well characterized fruit development process. We previously revealed major transcriptomic reprogramming in all the organs and tissues during the shift from vegetative/green to mature/woody development (Fasoli *et al.*, 2012). Co-expression network analysis uncovered a small group of genes that potentially act as switches for this phase transition (Palumbo *et al.*, 2014; Massonnet *et al.*, 2017), including the NAC family member *VviNAC33* whose sudden expression was among the earliest molecular signals of the onset of berry ripening (Fasoli *et al.*, 2018). Preliminary results indicate that *VviNAC33* is controlled by two transcription factors, *VvibHLH075* and *VviWRKY19*, previously identified as potential regulators of berry phase transition (Fasoli *et al.*, 2018).

Here we characterize the activity of *VviNAC33* by characterizing transient and stable overexpression lines and the creation of a chimeric repressor in planta. We also used the DAP-seq coupled with transcriptomic analysis to identify putative direct targets of *VviNAC33*, revealing that it acts as an activator and repressor of transcription. We propose that *VviNAC33* functions in a regulative network controlling the de-greening and the suppression of organ growth during the transition from the vegetative to the mature phase of development.

Material and Methods

Plant material

N. benthamiana plants, *V. vinifera* cv. Sultana plantlets, cv. Syrah embryogenic calli for the *VviNAC33* genetic transformation, cv. Garganega embryogenic calli for the *VviNAC33-EAR* genetic transformation, *VviNAC33* and *VviNAC33-EAR* transgenic plants were grown as described in Amato *et al.* (2019). For the DAP-seq analysis, cv. Syrah fruiting cuttings were propagated as described in Mullins *et al.* (1981).

Protoplast isolation

Protoplasts were prepared from 0.5 g of leaf tissue as described by Zhao *et al.* (2016). For *VviNAC33* subcellular localization, protoplasts were isolated from a pool of four leaves each from three cv. Corvina plants. For chloroplast distribution analysis, protoplasts were isolated from a pool created by four fully expanded leaves each taken from three plants of every transgenic overexpressing line plus a control.

Bioinformatics

NAC protein sequences from different species were aligned using MUSCLE with default settings. The unrooted phylogenetic tree was constructed in MEGA v7.0 (<http://www.megasoftware.net/>; Kumar *et al.*, 2016) using the neighbour-joining method based on the following parameters: pairwise deletion and bootstrap analysis with 1000 replicates. Conserved motifs were identified using the MEME suite (<http://meme-suite.org/tools/meme>) (Bailey *et al.*, 2009) with standard parameters, maximum 20 motifs and an optimum motif width of 4–60 amino acids. Transcriptomic data for gene expression analysis were retrieved from the Corvina atlas and two berry-specific expression maps (Fasoli *et al.*, 2012; Massonnet *et al.*, 2017; Fasoli *et al.*, 2018). Co-expression analysis based on Pearson's correlation coefficient was carried out using CorTo software and *VviNAC33* (VIT_19s0027g00230) as the bait in the Corvina atlas. ShinyGO v0.61 was used for enrichment analysis (Ge *et al.*, 2020).

Isolation and cloning

The *VviNAC33* coding sequence (with 3' UTR) and *VviNAC33-EAR* were amplified from cv. Corvina mid-ripening and ripening berry skin using KAPA HiFi DNA polymerase (KAPA Biosystems, Wilmington, MA, USA) and the primers used listed in **Table S1**. The PCR products were directionally cloned into the Gateway entry vector pENTR/D-TOPO (Invitrogen, Thermo Fisher Scientific, Waltham, MA, USA). For agroinfiltration in *N. benthamiana* and the transient expression, the *VviNAC33* sequence was transferred into the binary overexpression vector pK7GW2.0 (Laboratory of Plant Systems Biology, Ghent University, Belgium) by site-specific LR recombination. For stable overexpression, the sequence was transferred to the modified binary vector pK7GW2.0 containing an eGFP expression cassette driven by the Arabidopsis ubiquitin 10 promoter. The *VviNAC33-EAR* chimeric repressor was transferred into the modified pK7GW2 vector, harbouring the 1320-bp endogenous *VviNAC33* promoter (isolated from cv. Corvina genomic DNA) instead of the CaMV 35S promoter. For subcellular localization, the GFP sequence was fused to the C-terminus of *VviNAC33*.

Subcellular localization

Protoplasts were transfected with 50 µg of the pK7FWG2:*VviNAC33* vector or the control vector (pK7FWG2:eGFP) as described by Amato *et al.* (2019).

DAP-seq

Genomic DNA was extracted from 1 g of ground young *V. vinifera* cv. Syrah leaves as described by Thomas *et al.* (1993) and the Illumina libraries were prepared as described in Galli *et al.* (2018). The *VviNAC33* sequence was transferred from the pENTR/D-TOPO to the Gateway-compatible destination vector pIX-HALO (Bartlett *et al.*, 2017). The HALO-*VviNAC33* and GST-HALO (used as negative control) fusion proteins were *in vitro* translated using the TNTR SP6 coupled reticulocyte lysate system (Promega). The DAP-seq was performed as described in Galli *et al.* (2018) and a total of 3.5 million of 75 bp single reads were obtained for each sample.

Read mapping, filtering, peak calling and motif analysis

Fastq files were trimmed using trimmomatic (Bolger *et al.*, 2014) with the following parameters: ILLUMINACLIP = TruSeq3-, SE = 2:30:10. LEADING = 3, TRAILING = 3, SLIDINGWINDOW = 4:20, MINLEN = 50. Trimmed reads were mapped to the grape reference genome version 12X.2 (nuclear chromosomes only) at URGI (<https://urgi.versailles.inra.fr/Species/Vitis/Annotations>) using bowtie2 v2.3.4.3 (Langmead and Salzberg, 2012). Reads mapping to multiple locations were filtered, removing all reads with the XS:i field present in the BAM file. Uniquely mapped reads were used for all subsequent steps. Peaks were called using GEM v3.4 (Guo *et al.*, 2012) and the GST-HALO negative control sample for background subtraction, applying the following parameters: --d Read_Distribution_default.txt --k_min 6 --k_max 20 --outNP. To reduce the number of false positives, we removed all peaks with a sample/control ratio < 5-fold. The remaining peaks were associated with nearest genes using the ChipSeeker R package (Yu *et al.*, 2015). For gene annotation, we used the V1 on the 12X.0 assembly transposed to the 12X.2 assembly. The gff3 files were downloaded from URGI. For visualization in the Integrative Genome Browser (IGV), bam files were converted to bigwig files using deepTools v3.4.3, bamCoverage with a 10-bp bin size, and FPKM normalization. Motifs were detected and assigned using RSAT Plants NGS ChIP-Seq peak-motifs analysis (http://rsat.eead.csic.es/plants/peak-motifs_form.cgi) and RSAT Plants Motif Discovery dyad-analysis (http://rsat.eead.csic.es/plants/dyad-analysis_form.cgi).

Transient expression

For *N. benthamiana*, pK7GW2.0 vectors containing 35S:*VviNAC33* or a non-coding sequence (negative control) were transferred to *A. tumefaciens* strain C58C1 by electroporation (Hellens *et al.*, 2000) and three fully expanded leaves each from four plants were syringe infiltrated for both vectors. Phenotypic analysis was carried out 3 days after agroinfiltration. The same vectors were used for transient expression in cv Sultana. 5-week-old *in vitro* plantlets (eight plants for *VviNAC33* overexpression and seven for the control) were vacuum infiltrated as previously described (Amato *et al.*, 2017). Molecular analyses were carried out on leaf samples collected 7 days after the agroinfiltration.

Transgenic plants

The pK7WG2.0 vectors containing 35S:VviNAC33 or VviNAC33-EAR or the eGFP sequence (negative control) were transferred to *A. tumefaciens* strain EHA105 by electroporation. The genetic transformations were performed as described in Amato *et al.* (2019).

Leaf area measurement

Leaf area was estimated as proposed by Smith and Kliewer (1984) by measuring maximum length and width of three laminae of mature leaves (at the 6th/7th node from apex) each from four plants per transgenic line plus control. Mean \pm Standard Deviation (SD) of 12 biological replicates was calculated.

Pigment analysis and photosynthetic parameters

For *N. Benthamiana*, four biological replicates each consisting of a pool of infiltrated leaves from each plant were analyzed. For OXNAC33 and EARNAC33 transgenic plants, four biological replicates each consisting of a pool of three young leaves for each OX1,2,3 lines plus control and four biological replicates each consisting of a pool of three fully expanded leaves for each EAR1, 2, 3 lines plus control were analyzed. Pigments were measured according to Cazzaniga *et al.* (2020). Photosynthetic parameters, and OJIP curves were measured using a DUAL-PAM-100 fluorimeter (Heinz-Walz, Effeltrich, Germany) as previously described (Baker, 2008). Proton motive force was measured by electrochromic shift (ECS) using a MultispeQ V2.0 (PhotosynQ, East Lansing, MI, USA) as previously described (Kuhlgert *et al.*, 2016). For each analysis mean \pm SD of four biological replicates was calculated.

Thylakoid preparation and immunoblotting

For OX2 line plus control four separated pools of leaves, chosen with the same criteria used for pigment analysis, were analyzed. Thylakoid membranes were isolated and fractionated as previously described (Pinnola *et al.*, 2015). Proteins were separated by SDS-PAGE in a Tris-Tricine buffer system (Schägger and von Jagow, 1987). Immunotitration was performed as described in (Cazzaniga *et al.*, 2020) with antibodies (Agriserä Vännäs, Sweden) against the proteins CP47 (AS11 1787), PSAA (AS06 172) LHCII (AS01 004) and AtpC (AS08312). For each analysis mean \pm SD of four biological replicates was calculated.

Chloroplast distribution

Protoplast images were captured using a Leica DM2500 microscope equipped with a DFC7000T camera. The distribution of chloroplasts was analysed with ImageJ software on 70 images for each of the three transgenic lines and the control.

Plant NAA treatment

In vitro cv. Syrah stems of OX2 line and control, consisting of two apical leaves, one fully expanded and the other newly developing, were transferred to MS medium without or with two different 1-Naphthaleneacetic acid (NAA) concentrations (5 and 20 mg/L). For each treatment, four stems of OX2 line and four stems of control were maintained in a growth chamber at 25°C with a 16 h photoperiod. Phenotype was observed 14 days after hormone treatment.

Real time qPCR

For transient expression RNA was extracted from a pool of two apical well-expanded leaves from each plant. For OXNAC33 and EARNAC33 transgenic plants, RNA was extracted from leaves collected and pooled following the same criteria used for pigment analysis. Total RNA was isolated from 50-100 mg of ground material using the Spectrum Plant Total RNA kit. Gene expression analysis by qPCR was performed as previously described (Zenoni *et al.*, 2011) using the primer sequences listed in **Table S1**. Each value corresponds to the mean \pm SD of three technical replicates relative to the VviUBIQUITIN1 (VIT_16s0098g01190) control.

Transcriptomic analysis

The microarray analysis was performed with the RNA isolated for qPCR. For transient expression, the four most highly overexpressing plants (#3, #5, #6 and #7) were selected and used as biological replicates, while for OXNAC33 transgenic lines, the OX1, 2 and 3 lines were used as biological replicates. The cDNA synthesis, labelling, hybridization and washing reactions were performed

according to the Agilent Microarray-Based Gene Expression Analysis Guide (V 6.5). Each sample was hybridized to an Agilent custom microarray four-pack 44K format (Agilent Sure Print HD 4X44K 60-mer; G2514F-048771; Dal Santo *et al.*, 2016) and scanned using an Agilent Scanner (Agilent Technologies; G2565CA). Feature extraction and statistical analysis of the microarray data was conducted as reported in Amato *et al.*, 2017. DEGs were identified by Student's t test ($\alpha = 0.05$), assuming equal variance among samples, and selected by fold change ≥ 1.5).

Dual luciferase assay

The *VviNAC33* (1320 bp), *SGR1* (1558 bp), *ATG8f* (1616 bp), *RopGEF1* (1604 bp), *PIN1* (1637 bp) and *ATPC1* (1573 bp) promoter regions were amplified by PCR from Corvina genomic DNA using KAPA HiFi DNA polymerase. The cloning steps and Dual Luciferase Reporter Assay were carried out as described by Amato *et al.* (2019), using as effector vectors 35S:*VviNAC33* with 35S:*VviWRKY19* (VIT_07s0005g01710) and 35S:*VviBHLH75* (VIT_17s0000g00430), both previously reported by Fasoli *et al.* (2018). Mean \pm SD of four biological replicates was calculated.

Data availability

Microarray data for the transient expression experiments are available at GEO under the series entry GSE155037 (<https://www.ncbi.nlm.nih.gov/geo/query/acc.cgi?acc=GSE155037>). Microarray data for the transgenic plants are available at GEO under the series entry GSE156105 (<https://www.ncbi.nlm.nih.gov/geo/query/acc.cgi?acc=GSE156105>). DAP-seq data are available at GEO under the series entry GSE155445 (<https://www.ncbi.nlm.nih.gov/geo/query/acc.cgi?acc=GSE155445>).

Results

VviNAC33 is upregulated during the vegetative-to-mature transition of several organs and is strongly expressed in leaves undergoing senescence

The analysis of previously released transcriptomic databases (Fasoli *et al.*, 2012) revealed that *VviNAC33* is expressed at high levels during senescence in leaves and in woody stems, but only weakly expressed in the young leaf, green stem, flower organs, pollen, bud and tendrils. *VviNAC33* expression is also induced before veraison in developing seeds and at veraison in berries (**Fig. 1a**), and a similar sharp increase was observed during berry softening in different grapevine genotypes and during the 10 days before veraison (**Figs S1a,b**; Massonnet *et al.*, 2017; Fasoli *et al.*, 2018). Moreover, the *VviNAC33* expression profile during berry development belonged to a stage-specific cluster (Dal Santo *et al.*, 2018), thus unaffected by environmental conditions or G×E interactions (**Figs S1c,d**).

Co-expression analysis using a grapevine expression atlas (Fasoli *et al.*, 2012) revealed 92 genes positively correlated to *VviNAC33*, given a Spearman coefficient > 0.7 (**Dataset S1**). The top-30 strongly co-expressed genes with putative functional annotations formed two clusters based on their expression profiles during organ development. The first was characterized by a sharp increase in expression during berry and seed development, similar to that observed during leaf senescence (**Fig. 1b**; upper cluster). This large cluster included another NAC member, *VviNAC60*, and genes involved in stress responses and cellular processes, such as *AUTOPHAGY 8f* (*ATG8f*). The second was characterized by a stronger induction of expression during senescence (**Fig. 1b**; lower cluster). This smaller cluster included the $\alpha 6$ tubulin chain gene, the *SENESCENCE-INDUCIBLE CHLOROPLAST STAY-GREEN PROTEIN 1* (*SGR1*), and genes encoding the S-locus lectin protein kinase and the UDP-glycosyltransferase 85A8.

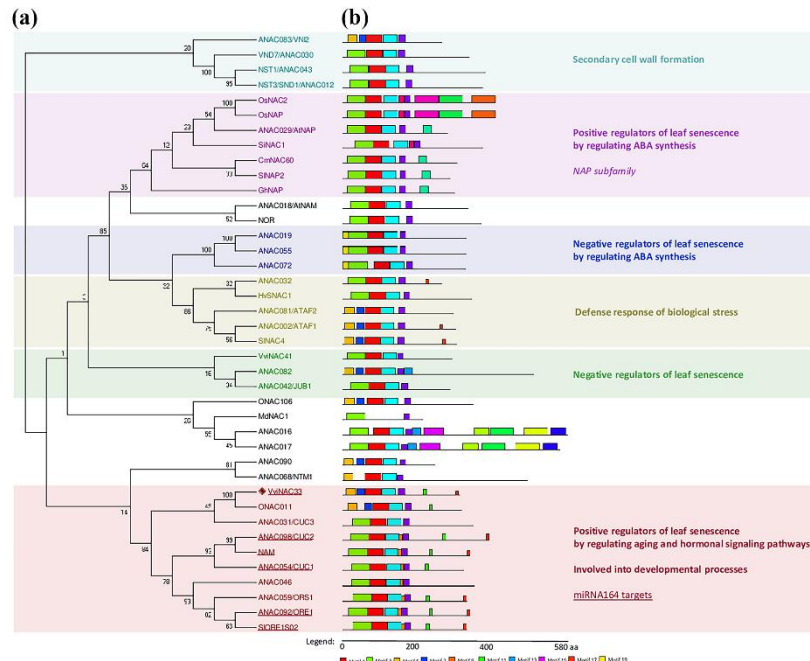


Fig. 2 Phylogenetic relationships and motif compositions of VviNAC33 and 39 additional NAC protein sequences. (a) Phylogenetic tree (neighbour-joining method) of VviNAC33 and 36 additional NAC protein sequences with functional annotations from various species prepared in MEGA v7 (Kumar et al., 2016). The numbers next to the nodes are bootstrap values from 1000 replicates. VviNAC33 is labelled with a red rhombus. The following GenBank accession numbers were used: *Arabidopsis thaliana* ATAF1/ANAC002 (AT1G01720), ATAF2 (AT5G08790), ANAC016 (AT1G34180), ANAC017 (AT1G34190), ANAC019 (AT1G52890), ANAC032 (AT1G77450), ANAC046 (AT3G04060), ANAC055 (AT3G15500), ANAC072 (AT4G27410), ANAC082 (AT5G09330), ANAC090 (AT5G22380), *Azadirachta indica* ANAM (AT1G52880), *Azadirachta indica* ANAP/ANAC029 (AT1G69490), CUC1 (AT3G15170), CUC2 (AT5G53950), CUC3 (AT1G76420), JUB1/ANAC042 (AT2G43000), *Oryza sativa* ORE1/ANAC092 (AT5G39610), ORS1/ANAC059 (AT3G29035), NTM1 (AT4G01540), NST1/ANAC043 (AT2G46770); *Nicotiana glauca* NST3/SND1/ANAC012 (AT1G32770); VND7/ANAC030 (AT1G71930); VNI2/ANAC083 (AT5G13180); *Cucumis melo* CmNAC60 (XM_008448163); *Hordeum vulgare* HvSNAC1 (AEG21060.1); *Gossypium hirsutum* GhNAP (ALG62640.1); *Oryza sativa* ONAC011 (Os06g0675600), ONAC106 (Os08g0433500), OsNAC2 (Os03g0327800), OsNAP (Os03g0327800); *Malus domestica* MdNAC1 (MF401514.1); *Petunia hybrida* NAM (CAA63101); *Setaria italica* SiNAC1 (XP_004967928.1); *Solanum lycopersicum* NOR (Solyc10g006880), SINAC4 (Solyc11g017470), SINAP2 (Solyc04g005610.2.1), STIRE1S02 (Solyc02g088180). (b) Schematic representation of motifs in the same set of NAC proteins identified by MEME analysis. Each color represents a specific motif. See also sequence LOGO in Figure S5.

VviNAC33 localizes in the nucleus and binds to a conserved NAC motif

The subcellular localization of VviNAC33 was assessed through protoplasts transformation with the construct 35S:VviNAC33-GFP or the control vector 35S:GFP. In protoplasts transformed with the control vector, GFP fluorescence was detected in both the nucleus and cytosol, but in protoplasts transformed with 35S:VviNAC33-GFP the GFP fluorescence was concentrated in the nuclei and co-localized with the nuclear stain Hoechst 33342 (**Fig. 3a**).

Next, we carried out DNA affinity purification sequencing (DAP-seq) assays to identify the putative direct targets of VviNAC33. We initially observed 4427 enriched peaks (**Dataset S2**), which was reduced to 3910 by removing those with a sample/control ratio < 5 (**Dataset S3**). The distribution of peaks revealed that 25% were located within promoter regions (up to 2 kb upstream from a transcription start site), 2% were located in 5' untranslated regions (UTRs), 14% were located in exons, 17% were located within introns, 3% were located in 3' UTRs, 7% were located in the 3-kb downstream region, and 32% were intergenic (**Fig. 3b**), leading to 3457 candidate target genes.

We identified three major binding motifs (GTTG[C/A][T/G]TGT) with strong significance (**Fig. 3c**) and phylogenetic footprints correlating with ANAC092/ORE1 (**Fig. S6a**). Distribution analysis revealed that 1024 peaks (27% of the total) were in the upstream region (promoter or 5' UTR) of 971 genes, highlighting potential VviNAC33 direct targets. We focused our analysis on this specific set and found three slightly different top-ranking binding motifs, but the correlation with ANAC092/ORE1 was maintained (**Fig. S6b**). We found three top VviNAC33 dimeric binding motifs, confirming that the well-known characteristic of NAC TFs to bind DNA as stable homodimers or heterodimers is preserved in grapevine (**Fig. S6b**). GO enrichment analysis of the 971 putative direct target genes revealed a significant overrepresentation (FDR < 0.01) of genes in categories including 'Regulation of biosynthetic process', 'Regulation of transcription', 'Regulation of gene expression', 'Auxin-activated signaling pathway' and 'Cellular response to auxin stimulus' (**Fig. 3d**).

By ranking the putative targets by p value, we found that the top position was occupied by the

photosystem II gene *PsbA*, followed by the regulator of chlorophyll degradation *SGRI* (**Dataset S3**). Interestingly, the 971 putative VviNAC33 targets included 14 switch genes from the 113 identified in the atlas dataset (Fasoli *et al.*, 2012), 17 of the 225 berry-specific switch genes reported by Massonnet *et al.* (2017) and several markers of the transcriptional transition characterizing the onset of berry ripening (**Dataset S3**).

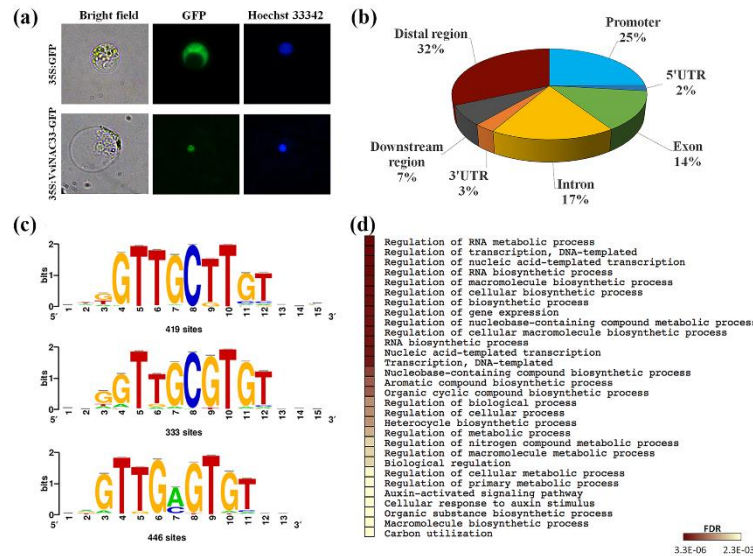


Fig. 3 VviNAC33 subcellular localization and DAP-seq results. (a) Subcellular localization of VviNAC33. Grapevine protoplasts isolated from Corvina leaves were transformed with the 35S:GFP and 35S:VviNAC33-GFP constructs. (b) Distribution of VviNAC33 binding sites. (c) VviNAC33 binding to three core motifs identified by RSAT Plants. (d) GO enrichment analysis on 971 putative VviNAC33 targets. Hierarchical clustering tree summarizes correlations among the 20 most significant pathways (p-value cut-off, FDR ≤ 0.01). Enrichment analysis was based on hypergeometric distribution followed by FDR correction. Pathways with many shared genes are clustered together. Bigger dots indicate more significant p-values.

Transient overexpression of VviNAC33 identifies positively and negatively regulated targets

To investigate the ability of VviNAC33 to activate or inhibit gene expression, we infiltrated grapevine plantlets (cv. Sultana) with *Agrobacterium tumefaciens* (Amato *et al.*, 2017) carrying the 35S:VviNAC33 overexpression construct. The infiltrated plants did not show any overt phenotype, so we used qRT-PCR to quantify transgene expression and selected four lines strongly overexpressing VviNAC33 for transcriptomic analysis (**Fig. S7**). We identified 1027 differentially expressed genes (DEGs) based on a t-test with a significance threshold of $p < 0.05$ (**Dataset S4**), 379 of which satisfied the fold-change criterion ($|FC| > 1.5$). This comprised 122 upregulated and 257 downregulated genes. GO distribution and enrichment analysis showed that the upregulated genes mainly represented the functional categories ‘DNA/RNA metabolic process’, ‘Transport’ and ‘Cellular response to ions’ (**Fig. 4a**), whereas the downregulated genes mainly represented the functional categories ‘Response to hormone stimulus’, ‘Auxin transport and signaling’ and ‘Photosynthesis’ (**Fig. 4b**). Interestingly, some of the most strongly upregulated DEGs were co-expressed with VviNAC33, including *SGRI*, *IAGLU* (indole-3-acetate β -glucosyltransferase), *VviCCD4b*, encoding a (9,10) (9',10') cleavage dioxygenase, and the $\alpha 6$ tubulin chain gene (**Dataset S4**).

By aligning the 1027 DEGs with the 971 putative VviNAC33 targets determined by DAP-seq analysis, we identified 40 genes common to both lists, 24 of which were upregulated and 16 downregulated, suggesting VviNAC33 acts directly as both an activator and repressor (**Fig. 4c**). *SGRI* was the most strongly upregulated direct target candidate with the highest DAP-seq signal, with *IAGLU* and the $\alpha 6$ tubulin chain gene also ranking highly. Downregulated putative targets included several genes encoding signaling components such as *RopGEF1*, an activator of plant Rho GTPases (ROPs) involved in the polar distribution of auxin influx carrier AUX1 and the accumulation of PIN efflux carriers (Liu *et al.*, 2017).

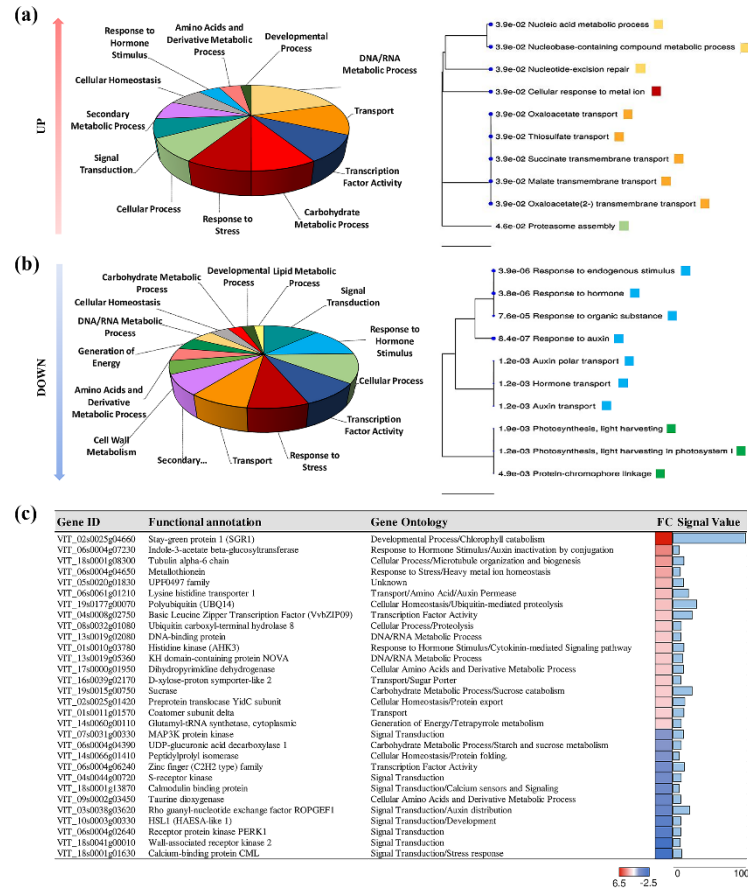


Fig. 4 Transcriptomic analysis of grapevine leaves in transient expression experiments. (a) GO distribution (left) and GO enrichment (right) analysis of the 122 upregulated genes in leaves transiently overexpressing VviNAC33 (threshold $|FC| > 1.5$). (b) GO distribution (left) and GO enrichment (right) analysis of 257 downregulated genes in leaves transiently overexpressing VviNAC33 ($|FC| > 1.5$). The hierarchical clustering trees summarize correlations among the 10 most significant pathways ($FDR \leq 0.05$). Pathways with many shared genes are clustered together. Bigger dots indicate more significant p-values. (c) Common genes in the list of DEGs identified by transient expression and the list of putative VviNAC33 targets based on DAP-seq analysis. Only the 33 functionally annotated genes are reported.

The stable overexpression of VviNAC33 induces leaf de-greening by modulating photosynthetic complexes and leaf expansion

The preliminary functional analysis of VviNAC33 in *Nicotiana benthamiana* leaves by transient expression revealed the acceleration of leaf de-greening compared to vector controls, confirmed by a significant reduction in chlorophyll amount, chlorophyll/carotenoid ratio and maximum quantum efficiency (Fv/Fm) of PSII (Figs S8a-d).

We therefore generated transgenic grapevine plants expressing VviNAC33 under the control of the cauliflower mosaic virus (CaMV) 35S promoter (OXNAC33 lines). We recovered 40 PCR-positive OXNAC33 plantlets and 10 vector controls (data not shown). Ten of the OXNAC33 transgenic lines expressed VviNAC33 at significantly higher levels than the control lines and we observed a positive correlation between phenotypic alterations and level of transgene expression (Figs S9a,b). Three independent lines with the highest VviNAC33 expression (#4, #5 and #8) were selected for further analysis and renamed OX1, OX2, OX3 for simplicity. Southern blot analysis revealed that all three lines as well as the vector control contained a single-copy transgene (Fig. S9c).

The growth rate, height and general habitus of the OXNAC33 transgenic lines were similar to the controls (Fig. 5a). However, as described above for *N. benthamiana*, mature leaves exhibited a clearly visible de-greening effect leading to a green/pale green variegated phenotype that became more apparent with age. Pigment analysis revealed a sharp reduction (~40%) in the levels of chlorophyll and carotenoids (Fig. 5b). The leaf area of the transgenic plants was ~35% lower than the controls (Fig. S9d). We isolated protoplasts from transgenic and control leaves and found a significant (~20%) reduction in the cell area occupied by chloroplasts in the transgenic lines, which only partially explained the loss of pigments (Fig. 5c). We therefore measured the chlorophyll a/b and chlorophyll/carotenoid ratios, both of which were lower in the OXNAC33 transgenic lines.

More detailed analysis of the carotenoid content revealed that the lower chlorophyll/carotenoid ratio in the transgenic plants was almost entirely due to the higher levels of lutein. The analysis of the fluorescence yield in dark-adapted leaves revealed a significant decrease in Fv/Fm in the three transgenic lines. Whereas Fm (normalized to the chlorophyll content) remained stable, F0 was significantly higher in the transgenic leaves (Figs 5d-g).

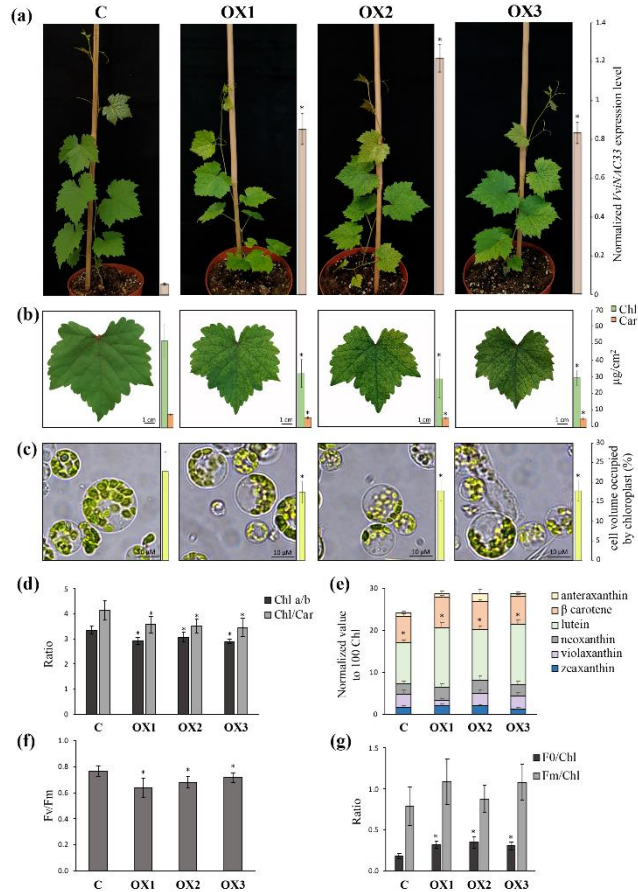


Fig. 5 Phenotypic changes in transgenic grapevine plants overexpressing VviNAC33. (a) Whole-plant phenotype caused by the stable expression of VviNAC33 in selected OXNAC33 lines compared to vector controls. The expression levels detected by qPCR are indicated by the bars next to the pictures. Each value corresponds to the mean \pm standard deviation (SD) of three technical replicates relative to the VviUBIQUITINI (VIT_16s0098g01190) control. (b) Fully expanded leaves showing the phenotype caused by the stable overexpression of VviNAC33 in the three OXNAC33 lines compared to the vector control. Total chlorophyll (chl) and carotenoid (car) levels are indicated by the bars next to the pictures. (c) Distribution of chloroplasts in protoplasts isolated from the three OXNAC33 lines compared to the vector control. The proportion of cell volume occupied by chloroplasts, as determined by light microscopy, is indicated by the bars next to the pictures. (d) Chlorophyll a and b (Chl a/b) and chlorophyll carotenoid (Chl/Car) ratio. (e) Carotenoid content, with individual carotenoid values were normalized to 100 chlorophyll equivalents. (f) F0 and Fm normalized to Chl. (g) PSII maximum quantum efficiency (Fv/Fm). All pigment and photosynthetic performance data are expressed as mean \pm SD (n = 4). Asterisks (*) indicate significant differences (t-test; p < 0.05) in the OXNAC33 lines compared to the vector control.

We selected line OX2, which expressed VviNAC33 at the highest level, for the analysis of photosynthetic parameters in more detail at different light intensities. The PSII operating efficiency (Φ PSII), electron transport rate (ETR) and electrochemical proton gradient (determined by ECS) were significantly lower in OX2 compared to the control at all light intensities, whereas the 1-qL parameter representing the redox state of the plastoquinone pool was higher in OX2, suggesting the plastoquinone pool was more reduced by electrons (Figs 6a-d). Non-photochemical quenching (NPQ) was enhanced in the OX2 leaves at higher light intensities (Fig. S10a). Finally, dark-adapted leaves were exposed to saturating actinic light and the OJIP curve was registered in order to monitor the polyphasic rise from F0 to Fm (Stirbet *et al.*, 2018). The steeper O–J part of the curve (Fig. S10b) indicates lower electron-trapping efficiency in the OX2 leaf and thus an increase in the dissipation of absorbed light energy by fluorescence (Stirbet and Govindjee, 2011).

We then measured the relative amounts of photosynthetic components by immunoblotting on isolated thylakoid membranes. We found that CP47 (PSII core), PSAA (PSI core) and ATPC1 were significantly depleted in OX2 leaves compared to controls whereas LHCII was present at similar levels. We also fractionated the native chlorophyll binding complexes on a sucrose gradient following thylakoid solubilization. The analysis of free pigments, monomeric LHCB, trimeric

LHCII, PSII core and PSI-LHCI confirmed a relative increase in the content of antenna subunits, particularly LHCII, and a relative decrease in the PSII and PSI fractions in OX2 compared to the control (**Figs 6e-g**).

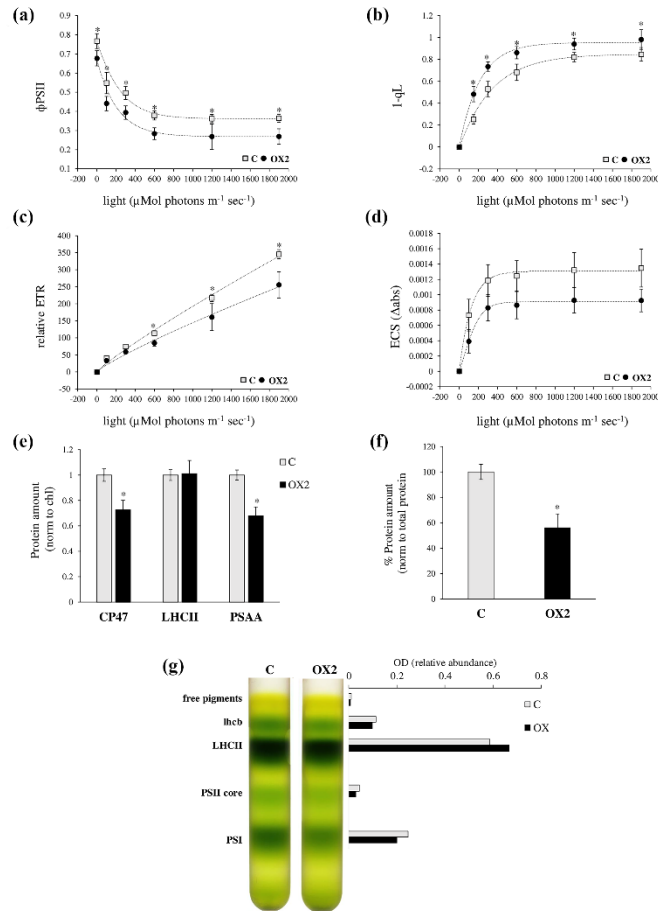


Fig. 6 Photosynthetic parameters and organization of thylakoid membranes. (a) Dependence of PSII operating efficiency (Φ_{PSII}), (b) 1-qL (estimates the fraction of PSII centers with reduced QA), (c) electron transport rate (ETR) and (d) total proton motive force (ECS) on actinic light intensity for the OX2 line compared to the vector control. (e) Immunotitration of thylakoid proteins using specific antibodies against PSAA, LHCII and PSAA corrected for chlorophyll content, and (f) ATPCI corrected for total protein content. (g) Sucrose density gradient fractionation. The composition of the green bands is shown on the left, and the relative abundance of the band (normalized to total green content on the gradient) is shown on the right. All data are expressed as mean \pm standard deviation (SD, $n = 4$). Asterisks (*) indicate significant differences (t-test; $p < 0.05$) between the OX2 line and vector control.

Transcriptomic analysis of transgenic leaves reveals additional putative direct targets of VviNAC33

We analyzed leaves of OXNAC33 transgenic lines and controls for genes that are differentially expressed before the phenotype appears. In total, we identified 2650 DEGs (t-test, $p < 0.05$), 617 of which were upregulated and 1388 downregulated with a $|\text{FC}| > 1.5$ (**Dataset S5**). GO enrichment analysis showed that ‘Glutamate signaling pathway’, ‘Transport’ and ‘Carbohydrate metabolic process’ were the most significant overrepresented functional categories for the upregulated genes whereas ‘Response to auxin’, ‘Developmental growth’, ‘Cell morphogenesis’ and ‘Signaling pathway’ were the most significant overrepresented functional categories for the downregulated genes (**Fig. 7a**), in agreement with our transient expression experiments (**Figs 4a,b**).

We identified 127 common DEGs among the 2650 identified in transgenic plants and the 1027 identified by transient expression (**Fig. 7b**, **Table S3**, **Fig. 7c**).

By combining the DEGs identified in the transgenic plants and transient expression experiments with the DAP-seq data, we resolved to a list of 139 genes that are most likely to be direct targets of VviNAC33 (**Fig. 7b**, **Table S4**). All 139 genes were screened against the three leaf development stages included in the transcriptomic atlas, revealing four major expression trends: upregulation at senescence, downregulation at senescence, peak of expression in the mature leaf, and trough of expression in the mature leaf. There was consistency between the behaviour of these genes in the expression atlas and transgenic plants, with those induced by VviNAC33 tending to be upregulated at senescence or in the mature leaf and those suppressed by VviNAC33 tending to be downregulated

at senescence or in the mature leaf (**Fig. 7d**; **Table S4**). Interestingly, most of the DEGs identified by transient expression corresponded to those modulated at senescence, indicating that transient expression highlights the impact of *VviNAC33* at its highest expression level. Genes strongly expressed at senescence included *SGRI*, *IAGLU* and the $\alpha 6$ tubulin chain gene (**Table S4**).

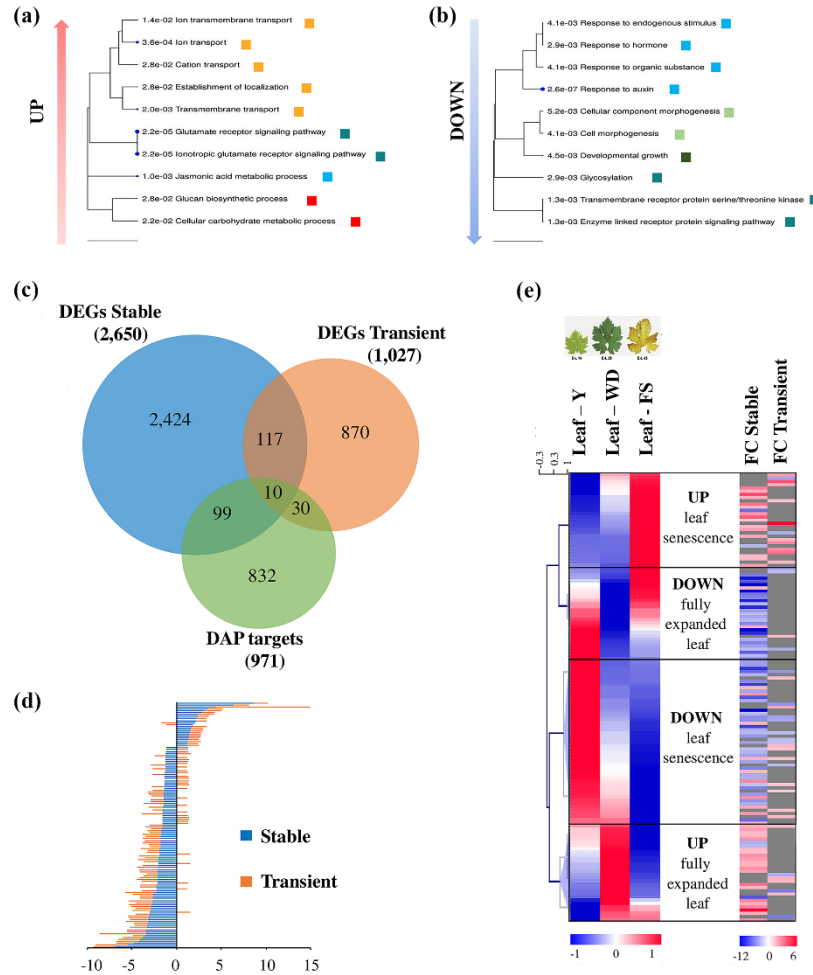


Fig. 7 Transcriptomic analysis of transgenic grapevine plants overexpressing *VviNAC33*. (a) GO enrichment analysis of the upregulated (left) and downregulated (right) genes in transgenic leaves with $|FC| > 1.5$. (b) Venn diagram showing genes common to the lists of differentially expressed genes (DEGs) in the transgenic plants and transient expression experiments, and to the targets identified by DAP-seq analysis. (c) Histogram showing the fold changes (FC) in expression of the genes classed as DEGs by both transient expression experiments and transgenic plants. (d) Heat map of the 139 putative direct targets of *VviNAC33* in three leaf developmental stages (Fasoli et al., 2012). Clusters were generated by hierarchical clustering in TMeV, considering the expression value of each gene in the different stages (left) and the FC of the 139 putative targets. Boxes indicated four expression trends: the upregulated and downregulated genes at senescence and in the fully expanded leaves.

Putative target genes upregulated by stable *VviNAC33* overexpression included several involved in nutrient transport, metabolism and recycling, such as genes encoding a substrate carrier, D xylose proton symporter-like 2, sucrose, and *ATG8f* (**Table S4**). On the other hand, putative targets downregulated by stable *VviNAC33* overexpression included several genes involved in auxin signaling, such as *RopGEF1* and *PINI*, as well as *ATPCI*, encoding the ATP synthase γ chain 1t involved in photosystem II integrity and activity.

In addition to putative direct targets, in *OXNAC33* transgenic lines we found several downregulated genes involved in the synthesis of chlorophyll and carotenoids, in the spatial regulation of chloroplast division and in auxin signaling (**Dataset S5**).

Considering several clues about the possible role of *VviNAC33* in controlling auxin signaling and metabolism emerged from DAP-seq and transcriptomic analyses (**Table S5**), we tested if exogenous auxin treatment was able to rescue the de-greening phenotype in stable *VviNAC33* overexpressing plants. We treated *in vitro* shoots of the *OX2* and control line with two NAA concentrations (**Fig. S11**). After two weeks, we found that both NAA concentrations were able to restore the green phenotype in newly formed leaves, that appeared similar to the controls, while the fully expanded leaves maintained the de-greening effect (**Fig. S11**).

A VviNAC33-EAR chimeric repressor boosts the chlorophyll content and growth of transgenic grapevine leaves

To create a dominant suppressor which overcomes the activity of endogenous VviNAC33, we fused the C-terminal domain of VviNAC33 to the plant-specific EAR repression domain (Ohta *et al.*, 2001; Hiratsu *et al.*, 2002) and placed the chimeric repressor under the control of the endogenous VviNAC33 promoter. The chimeric repressor construct was used to stably transform embryogenic grapevine callus and produce transgenic vines. We recovered four PCR-positive plantlets containing VviNAC33-EAR and two containing the vector control (data not shown). Transgene expression was confirmed by qRT-PCR in fully expanded leaves, when the expression of endogenous VviNAC33 begins to increase. Three independent EARNAC33 lines (#1, #2 and #4) were selected based on their strong transgene expression and were renamed EAR1, EAR2, EAR3 for simplicity (Figs S12a,b).

The three EARNAC33 lines showed normal vegetative growth, but the fully expanded leaves were significantly larger than controls (Figs 8a,b, S12c). Pigment content analysis revealed a significant increase in the chlorophyll and carotenoid content of the transgenic lines (Fig. 8b). However, the chlorophyll a/b and chlorophyll/carotenoid ratios, Fv/Fm, F0/chlorophyll and Fm/chlorophyll were similar in transgenic plants and vector controls (Figs S13a-c), possibly reflecting the partial but not complete dominance of the chimeric repressor.

The chimeric repressor system was also used to evaluate the expression of six putative VviNAC33 direct target genes by qPCR analysis, comparing transgenic lines OX2 and EAR2 and their controls. We assessed the upregulated candidate genes *SGR1*, the sucrose gene, and *ATG8f* and the downregulated candidate genes *PIN1*, *RopGEF1* and *ATPC1*. We found that *SGR1*, *ATG8f* and the sucrose gene were strongly upregulated by VviNAC33 but inhibited by VviNAC33-EAR, conversely, *PIN1*, *RopGEF1* and *ATPC1* were strongly downregulated by VviNAC33 but not inhibited by VviNAC33-EAR (Fig. 8c). This indicates that the addition of the EAR motif could have impaired the VviNAC33 repressor activity possibly by destabilizing putative interactions with binding partners involved in repression or by inhibiting the expression of a repressor that is itself transcriptionally activated by VviNAC33.

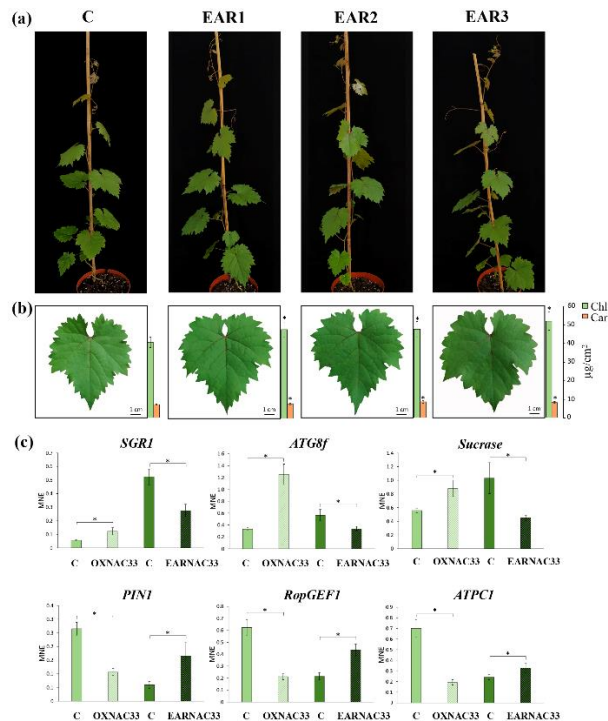


Fig. 8 Phenotypic changes in transgenic grapevine plants expressing the repressor NAC33- EAR and the expression level of VviNAC33 targets. (a) Whole-plant phenotype caused by the stable expression of VviNAC33-EAR in the three EARNAC33 lines compared to the vector control. (b) Fully expanded leaf phenotype caused by the stable expression of VviNAC33-EAR in the three EARNAC33 lines compared to the vector control. Total chlorophyll (Chl) and carotenoid (Car) levels are indicated by the bars next to the pictures. Data are mean \pm standard deviations (SD, n = 4). Asterisks (*) indicate significant differences (t-test; $p < 0.05$) between the EARNAC33 lines and vector control. (c) Expression levels of *SGR1*, *ATG8f*, sucrose, *PIN1*, *RopGEF1* and *ATPC1* in the leaves of transgenic plants overexpressing VviNAC33 (OXNAC33) or expressing VviNAC33-EAR (EARNAC33) determined by qPCR. Each value corresponds to the mean \pm SD of three technical replicates relative to the VviUBIQUITIN1 (VIT_16s0098g01190) control. Asterisks (*) indicate significant differences (t-test; $p < 0.05$) between the OXNAC33 or EARNAC33 lines and the vector control. MNE, mean expression level.

We then tested the ability of VviNAC33 to directly induce or repress the expression of the putative target genes validated by qPCR by a dual-luciferase assay in *N. benthamiana* leaves. The upstream regions of these genes containing a NAC33 DAP-seq peaks (**Fig. 9a**) were cloned upstream of a 35S promoter-Luciferase cassette. Sequence analysis of these putative promoter regions showed several putative VviNAC33 binding sites, including a conserved motif near the summit of each DAP-seq peak (**Fig. S14**). The dual-luciferase assay showed that VviNAC33 significantly activates the *SGRI* and *ATG8f* promoters and represses the *PIN1*, *RopGEF1* and *ATPC1* promoters (**Fig. 9b**). Finally, we investigate the ability of VvibHLH75 and VviWRKY19, two TFs previously suggested to regulate *VviNAC33* in grape berry (Fasoli *et al.*, 2018), to activate the *VviNAC33* expression. The analysis showed that *VviNAC33* is positively regulated by both VvibHLH75 and VviWRKY19 (**Fig. S15**).

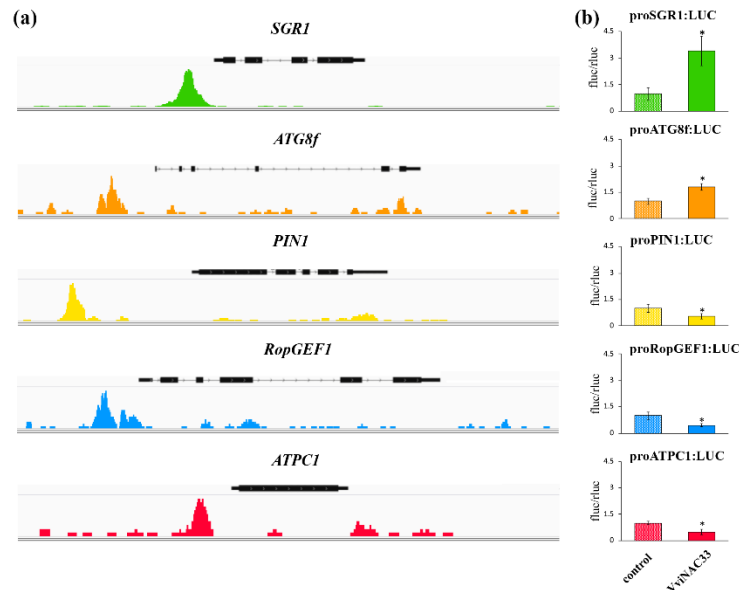


Fig. 9 VviNAC33 binding sites and regulation of *SGRI*, *ATG8f*, *PIN1*, *RopGEF1* and *ATPC1*. (a) IGV images of the VviNAC33 DAP-seq reads mapping to the promoters of the grapevine *SGRI*, *ATG8f*, *PIN1*, *RopGEF1* and *ATPC1* genes and (b) promoter activation tested by dual-luciferase reporter assays in infiltrated *Nicotiana benthamiana* leaves. The activity of these promoters was tested in the presence and absence of the 35S:VviNAC33 effector vector. LUC values are reported relative to the REN value and normalized against the control (empty effector vector). LUC values represent the mean of four biological replicates \pm standard deviation (SD). Asterisks (*) indicate significant differences in promoter activation compared with the control (t-test; $p < 0.01$).

Discussion

In this work we characterized the function of VviNAC33 in regulating vegetative/green to mature/woody growth shift (Fasoli *et al.*, 2012; Palumbo *et al.*, 2014). By transgenic approaches we found that VviNAC33 induces organ de-greening and suppresses vegetative growth. DAP-seq and transcriptomic analyses evidenced that 139 genes, bound by VviNAC33 in the upstream region, were differentially expressed in plants stably or transiently expressing VviNAC33, thus likely representing direct targets of regulation.

SGRI was one of the putative direct targets of VviNAC33 and was strongly co-expressed with VviNAC33 throughout grapevine organ development. We demonstrated that VviNAC33 directly activates *SGRI* expression, as previously shown for the Arabidopsis close homolog ANAC092/ORE1 (Qiu *et al.*, 2015). *SGRI* removes magnesium from chlorophyll a as the first step to initiate its degradation in multiple species (Park *et al.*, 2007; Sato *et al.*, 2007; Hortensteiner, 2009; Zhou *et al.*, 2011). The phenotypes of OXNAC33 and EARNAC33 transgenic leaves showed that VviNAC33 induces leaf de-greening by reducing the total chlorophyll content. There was also a significant depletion of the PSI and PSII core relative to antenna subunits in OXNAC33 leaves. Given that chlorophyll b is bound only by antenna proteins whereas chlorophyll a is bound both by core and antenna subunits, this result agrees with the lower chlorophyll a/b ratio in the OXNAC33 lines. In Arabidopsis, ectopic expression of *SGRI* in fully greened leaves reduces the abundance of chlorophyll-binding proteins in PSI/II and LCH, indicating that *SGRI* directly attacks the pigment-protein complexes and the chlorophyll-depleted apoproteins may then be immediately degraded in

the thylakoid membranes (Shimoda *et al.* 2016). The loss of pigment-binding proteins in our OXNAC33 leaves supports this hypothesis.

We found that leaf de-greening in our transgenic plants was, at least in part, associated with a smaller area occupied by chloroplasts. A similar phenotype was observed in Arabidopsis *glk1 glk2* double mutants, which featured pale green leaves with mesophyll cells containing small chloroplasts with sparse thylakoid membranes that failed to form grana (Waters *et al.*, 2009). GOLDEN2-LIKE1 (GLK1) and GLK2 activate genes responsible for key steps in chlorophyll biosynthesis, contributing to photosystem assembly and chloroplast development and maintenance (Waters *et al.*, 2009).

The gene encoding the PSII central core reaction protein D1 (*PsbA*) showed the highest p value in our DAP-seq data, and additional genes in this dataset included LOW PSII accumulation 1 (*LPA1*) and photosystem one 3 (*APO3*), which are required for efficient PSII and PSI assembly (**Dataset S3**). Although the control of these putative targets by VviNAC33 requires confirmation, our results strongly indicate that VviNAC33 plays a key role in the assembly and stability of the photosynthetic apparatus. In this context, we also found that VviNAC33 negatively regulates the expression of *ATPC1*, which encodes the ATP synthase γ chain It involved in the production of ATP from ADP in the presence of a proton gradient across the membrane. Interestingly, the inactivation of this gene in Arabidopsis abolishes photophosphorylation and alters PSII activity by increasing NPQ and F0 while reducing Fv/Fm (Dal Bosco *et al.*, 2003). Our data clearly demonstrated that VviNAC33 directly activates *SGR1* expression and suppresses *ATPC1*, which combined with the identification of *PsbA* and other PSII component genes among putative VviNAC33 targets strongly indicates that VviNAC33 is directly involved in shutting down photosynthesis in greened organs that enter the vegetative-to-mature phase transition.

Chlorophyll degradation is an integral aspect of senescence occurring during the final phase of development (Lim *et al.*, 2007). Senescence involves a massive cellular proteolysis carried out by organelles known as autophagosomes, which form under the control of ATG proteins to break down damaged and superfluous proteins (Zhai *et al.*, 2016; Fu *et al.*, 2020). A role of VviNAC33 in the control of autophagy is suggested by the fact that one of the direct targets of VviNAC33 is *ATG8f*, and by the upregulation of the *ATG8d* and *ATG18d* genes (Mizushima and Komatsu, 2011; Su *et al.*, 2020) in OXNAC33 leaves. Autophagy includes steps of ubiquitination (Mizushima *et al.*, 1998; Ichimura *et al.*, 2000) and delivery of autophagosomes to the vacuole, via the microtubule cytoskeleton. Interestingly, the polyubiquitin gene *UBQ14* and the α 6-tubulin chain, both strongly induced during senescence, were identified among the VviNAC33 targets (**Table S4**). Our data suggest that VviNAC33 directly orchestrates the elimination of chloroplasts by controlling the expression of genes involved in autophagy and photosynthetic activity.

The leaves of the OXNAC33 plants were significantly smaller than controls whereas those of the EARNAC33 plants were significantly larger, suggesting that VviNAC33 controls organ growth. In Arabidopsis plants overexpressing *ANAC092/ORE1*, the length of the root meristem differed from control plants and the primary roots were shorter, reflecting a slower rate of meristematic cell division based on the suppression of *PIN*, *YUCCA2*, and *ARF* (Xi *et al.*, 2019). Although we did not determine the cause of the OXNAC33 and EARNAC33 leaf phenotypes, we hypothesize that VviNAC33 and *ANAC092/ORE1* play similar roles in the regulation of organ growth. Indeed, several auxin-related genes were found among the 139 direct target candidates that were downregulated (**Table S4**). Furthermore, we demonstrated that VviNAC33 directly binds to the auxin influx carrier *PINI* promoter, inhibiting its expression. Two other *PIN* genes were downregulated in OXNAC33 leaves, and *PIN8* has a VviNAC33-binding site within an exon. We also found that the expression of *ARF3*, *ARF4*, *ARF6* and *ARF8* was modulated by VviNAC33 in the OXNAC33 lines, although we did not find VviNAC33 sites in their promoters. These data provide strong evidence that VviNAC33 is a negative regulator of the auxin pathway, thus suppressing cell division during leaf development.

We also demonstrated that *RopGEF1* is directly suppressed by VviNAC33. RopGEF1 maintains polar auxin transport by regulating the properties of auxin influx and efflux carriers such as AUX1 and PIN proteins, thereby influencing auxin-dependent growth and development (Swarup and Péret, 2012; Liu *et al.*, 2017). Interestingly, *AUX1* was downregulated in leaves overexpressing VviNAC33, supporting the role of VviNAC33 as a negative regulator of auxin transport and distribution by inhibiting *PINI* and *RopGEF1*.

The *CRY1* gene encoding cryptochrome 1, a blue light photoreceptor, was also one of the putative VviNAC33 direct targets and was upregulated by the overexpression of VviNAC33. *CRY1* negatively regulates the phytochrome-interacting transcription factors PIF4 and PIF5, which in turn

activate PIN genes (Ma *et al.*, 2016; Pedmale *et al.*, 2016; Boccaccini *et al.*, 2020).

The ability of exogenous auxin treatment to rescue the de-greening phenotype of VviNAC33 overexpressing shoots, further supports that the senescence-like phenotype of transgenic leaves could be due to an impairment of auxin signaling triggered by VviNAC33. Senescence is controlled by multiple hormones; ethylene, jasmonic acid (JA), salicylic acid, abscisic acid and brassinosteroids act as inducers, while cytokinins, gibberellic acid and auxin, as inhibitors (Gan and Amasino, 1997). Given this complexity, the involvement of other hormones besides auxin in the leaf de-greening phenotype and a role of VviNAC33 in their control, could not be ruled out.

We provided several lines of evidence showing that VviNAC33 is a key regulator of the shift toward organ senescence acting through molecular mechanisms similar to those previously described for the Arabidopsis protein ANAC092/ORE1 (Kim *et al.*, 2006; Balazadeh *et al.*, 2010). Both activate genes such as *SGR1* that trigger chlorophyll degradation (Qiu *et al.*, 2015) while repressing the expression of auxin transporter *PIN* genes to control growth (Xi *et al.*, 2019). The VviNAC33 and ANAC092/ORE1 genes are also regulated in a similar manner, both being repressed by *miR164* (Kim *et al.*, 2009; Sun *et al.*, 2012). Interestingly, *miR164* is expressed strongly in young grapevine leaves but only weakly in old leaves and fruits, the inverse of VviNAC33 (Belli Kullan *et al.*, 2015). There is strong evidence that some tomato NAC TFs involved in the control of leaf senescence are also involved in fruit ripening. SIORE1S02, SIORE1S03, and SIORE1S06 induce leaf senescence and source–sink sugar partitioning, affecting the final sugar level (Lira *et al.*, 2017). Recently, NOR, a NAC TF that regulates fruit ripening in tomato, was shown to induce leaf senescence (Ma *et al.*, 2019). While we could not determine the effects of VviNAC33 or VviNAC33-EAR in transgenic berries because neither the transgenic plants nor vector controls flower under our growing conditions, a role for VviNAC33 at the onset of berry ripening is indicated by increased expression level over a few days before veraison.

Consistently, several genes previously identified as markers of the onset of berry ripening together with VviNAC33 (Fasoli *et al.*, 2018) were highlighted in this work among the DAP-seq hits as potential direct targets of VviNAC33. In addition, we confirmed that the two berry ripening markers VvibHLH75 and VviWRKY19 are able to directly activate the expression of VviNAC33.

Our data defined VviNAC33 as a central hub in a regulatory network that controls de-greening and growth of grapevine organs during the vegetative to mature phase transition (**Fig. 10**). It represents a key step towards a comprehensive understanding of the intricate molecular circuits that combine developmental and environmental cues in grapevine.

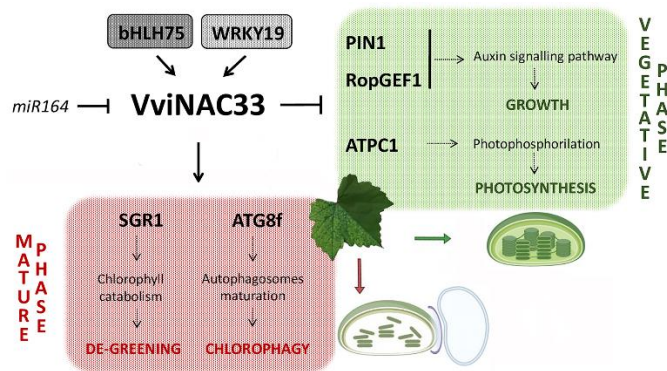


Fig. 10 Proposed regulatory network model of the VviNAC33 mechanisms of action. Induced and repressed VviNAC33 targets identified in this work and the biological processes they are involved in, are indicated together with the transcription factors controlling VviNAC33 expression. The negative regulation of VviNAC33 by *miR164* was demonstrated by Sun *et al.* (2012). The figure also shows the chloroplast images corresponding to vegetative and mature phase (lower right corner). The chloroplast images were created with BioRender.com.

Acknowledgments

The University of Verona, Italy, supported this work with a Grant Ricerca di Base to S.Z. ‘Definition of master regulator genes of fruit ripening in grapevine’. Cost Action 17111 to M.P., S.Z and G.B.T., is acknowledged. M.G and A.G. acknowledge funding from the National Science Foundation (IOS#1916804).

Author Contributions

E.D., S.C., and C.F. performed the research. E.D., S.C, and S.Z. analysed the data. M.G., A.G., and N.V. contributed new analytic and computational tools. S.Z., G.B.T., and M.P. designed the research. S.Z., E.D., and G.B.T. wrote the paper.

REFERENCES

- Amato A, Cavallini E, Zenoni S, Finezzo L, Begheldo M, Ruperti B, Tornielli GB. 2017. A grapevine TTG2-like WRKY transcription factor is involved in regulating vacuolar transport and flavonoid biosynthesis. *Frontiers in Plant Science*. 7:1979. doi: 10.3389/fpls.2016.01979. PMID: 28105033; PMCID: PMC5214514.
- Amato A, Cavallini E, Walker AR, Pezzotti M, Blik M, Quattrocchio F, Koes R, Ruperti B, Bertini E, Zenoni S, Tornielli GB. 2019. The MYB5-driven MBW complex recruits a WRKY factor to enhance the expression of targets involved in vacuolar hyper-acidification and trafficking in grapevine. *The Plant Journal*. 99(6):1220-1241. doi: 10.1111/tpj.14419. PMID: 31125454.
- Bailey TL, Boden M, Buske FA, Frith M, Grant CE, Clementi L, Ren J, Li WW, Noble WS. 2009. MEME SUITE: tools for motif discovery and searching. *Nucleic Acids Research*. 37(Web Server issue): W202-8. doi: 10.1093/nar/gkp335. PMID: 19458158; PMCID: PMC2703892.
- Balazadeh S, Siddiqui H, Allu AD, Matallana-Ramirez LP, Caldana C, Mehrnia M, Zanon MI, Köhler B, Mueller-Roeber B. 2010. A gene regulatory network controlled by the NAC transcription factor ANAC092/AtNAC2/ORE1 during salt-promoted senescence. *The Plant Journal*. 62(2):250-64. doi: 10.1111/j.1365-313X.2010.04151.x. PMID: 20113437.
- Balazadeh S, Kwasniewski M, Caldana C, Mehrnia M, Zanon MI, Xue GP, Mueller-Roeber B. 2011. ORS1, an H₂O₂-responsive NAC transcription factor, controls senescence in *Arabidopsis thaliana*. *Mol Plant*. 4(2):346-60. doi: 10.1093/mp/ssp080. Epub 2011 Feb 8. PMID: 21303842; PMCID: PMC3063519.
- Baker NR. 2008. Chlorophyll fluorescence: a probe of photosynthesis in vivo. 2008. *Annual Review of Plant Biology*. 59:89-113. doi: 10.1146/annurev-arplant.59.032607.092759. PMID: 18444897.
- Bartlett A, O'Malley RC, Huang SC, Galli M, Nery JR, Gallavotti A, Ecker JR. 2017. Mapping genome-wide transcription-factor binding sites using DAP-seq. *Nature Protocols*. 12(8):1659-1672. doi: 10.1038/nprot.2017.055. PMID: 28726847; PMCID: PMC5576341.
- Belli Kullari J, Lopes Paim Pinto D, Bertolini E, Fasoli M, Zenoni S, Tornielli GB, Pezzotti M, Meyers BC, Farina L, Pè ME, Mica E. 2015. miRVine: a microRNA expression atlas of grapevine based on small RNA sequencing. *BMC Genomics*. 16(1):393. doi: 10.1186/s12864-015-1610-5.
- Boccaccini A, Legris M, Krahmer J, Allenbach-Petrolati L, Goyal A, Galvan-Ampudia C, Vernoux T, Karayekov E, Casal JJ, Fankhauser C. 2020. Low blue light enhances phototropism by releasing cryptochrome1-mediated inhibition of PIF4 expression. *Plant Physiology*. 183(4):1780-1793. doi: 10.1104/pp.20.00243. PMID: 32554507.
- Bolger AM, Lohse M, Usadel B. 2014. Trimmomatic: a flexible trimmer for Illumina sequence data. *Bioinformatics*. 30(15):2114-20. doi: 10.1093/bioinformatics/btu170. PMID: 24695404; PMCID: PMC4103590.
- Canaguier A, Grimplet J, Di Gasparo G, Scalabrin S, Duchêne E, Choise N, Mohellibi N, Guichard C, Rombauts S, Le Clairche I, Bérard A, Chauveau A, Bounon R, Rustenholz C, Morgante M, Le Paslier MC, Brunel D, Adam-Blondon AF. 2017. A new version of the grapevine reference genome assembly (12X.v2) and of its annotation (VCost.v3). *Genomics Data*. 14:56-62. doi: 10.1016/j.gdata.2017.09.002. PMID: 28971018; PMCID: PMC5612791.
- Cazzaniga S, Kim M, Bellamoli F, Jeong J, Lee S, Perozeni F, Pompa A, Jin E, Ballottari M. 2020. Photosystem II antenna complexes CP26 and CP29 are essential for nonphotochemical quenching in *Chlamydomonas reinhardtii*. *Plant, Cell & Environment*. 43(2):496-509. doi: 10.1111/pce.13680. PMID: 31724187; PMCID: PMC7004014.
- Dal Bosco C, Lezhneva L, Biehl A, Leister D, Strotmann H, Wanner G, Meurer J. 2003. Inactivation of the chloroplast ATP synthase gamma subunit results in high non-photochemical fluorescence quenching and altered nuclear gene expression in *Arabidopsis thaliana*. *The Journal of Biological Chemistry*. 279(2):1060-9. doi: 10.1074/jbc.M308435200. PMID: 14576160.
- Dal Santo S, Commisso M, D'Inca E, Anesi A, Stocchero M, Zenoni S, Ceoldo S, Tornielli GB, Pezzotti M, Guzzo F. 2016. The terroir concept interpreted through grape berry metabolomics and transcriptomics. *Journal of Visualized Experiments*. (116):54410. doi: 10.3791/54410. PMID: 27768042; PMCID: PMC5092147.
- Dal Santo S, Zenoni S, Sandri M, De Lorenzis G, Magris G, De Paoli E, Di Gasparo G, Del Fabbro C, Morgante M, Brancadoro L, Grossi D, Fasoli M, Zuccolotto P, Tornielli GB, Pezzotti M. 2018. Grapevine field experiments reveal the contribution of genotype, the influence of environment and the effect of their interaction (G×E) on the berry transcriptome. *The Plant journal: for cell and molecular biology*. 93(6), 1143–1159. <https://doi.org/10.1111/tpj.13834>
- Demura T, Ye ZH. 2010. Regulation of plant biomass production. *Current Opinion in Plant Biology*. 13(3):299-304. doi: 10.1016/j.pbi.2010.03.002. PMID: 20381410.
- El Mannai Y, Akabane K, Hiratsu K, Satoh-Nagasawa N, Wabiko H. 2017. The NAC transcription factor gene OsY37 (ONAC011) promotes leaf senescence and accelerates heading time in rice. *International Journal of Molecular Sciences*. 18(10):2165. doi: 10.3390/ijms18102165. PMID: 29039754; PMCID: PMC5666846.
- Fasoli M, Dal Santo S, Zenoni S, Tornielli GB, Farina L, Zamboni A, Porceddu A, Venturini L, Bicego M, Murino V, Ferrarini A, Delledonne M, Pezzotti M. 2012. The grapevine expression atlas reveals a deep transcriptome shift driving the entire plant into a maturation program. *Plant Cell*. 24(9):3489-505. doi: 10.1105/tpc.112.100230. PMID: 22948079; PMCID: PMC3480284.
- Fasoli M, Richter CL, Zenoni S, Bertini E, Vitulo N, Dal Santo S, Dokoozlian N, Pezzotti M, Tornielli GB. 2018. Timing and order of the molecular events marking the onset of berry ripening in grapevine. *Plant Physiology*. 178(3):1187-1206. doi: 10.1104/pp.18.00559. PMID: 30224433; PMCID: PMC6236592.
- Fu C, Zhang X, Lu Y, Wang F, Xu Z, Liu S, Zheng H, Liu X. 2020. Geniposide inhibits NLRP3 inflammasome activation via autophagy in BV-2 microglial cells exposed to oxygen-glucose deprivation/reoxygenation. *International Immunopharmacology*. 84:106547. doi: 10.1016/j.intimp.2020.106547. PMID: 32361652.
- Galli M, Khakhar A, Lu Z, Chen Z, Sen S, Joshi T, Nemhauser JL, Schmitz RJ, Gallavotti A. 2018. The DNA binding landscape of the maize AUXIN RESPONSE FACTOR family. *Nature Communications*. 9(1):4526. doi: 10.1038/s41467-018-06977-6. PMID: 30375394; PMCID: PMC6207667.
- Gan S, and Amasino RM. 1997 Making Sense of Senescence (Molecular Genetic Regulation and Manipulation of Leaf Senescence). *Plant Physiol*. 113(2): 313–319. doi: 10.1104/pp.113.2.313 PMCID: PMC158144 PMID: 12223609
- Ge SX, Jung D, Yao R. 2020. ShinyGO: a graphical gene-set enrichment tool for animals and plants. *Bioinformatics*. 36(8):2628-2629. doi: 10.1093/bioinformatics/btz931. PMID: 31882993; PMCID: PMC7178415.
- Giovannoni J, Nguyen C, Ampofo B, Zhong S, Fei Z. 2017. The epigenome and transcriptional dynamics of fruit ripening. *Annual Review of Plant Biology*. 68:61-84. doi: 10.1146/annurev-arplant-042916-040906. PMID: 28226232.
- Guo Y, Gan S. 2006. AtNAP, a NAC family transcription factor, has an important role in leaf senescence. *Plant J. May*. 46(4):601-12. doi: 10.1111/j.1365-313X.2006.02723.x. PMID: 16640597.
- Guo Y, Mahony S, Gifford DK. 2012. High resolution genome wide binding event finding and motif discovery reveals transcription factor spatial binding constraints. *PLoS Computational Biology*. 8(8): e1002638. doi: 10.1371/journal.pcbi.1002638. PMID: 22912568; PMCID: PMC3415389.
- Hellens R, Mullineaux P, Klee H. 2000. Technical focus: a guide to Agrobacterium binary Ti vectors. *Trends in Plant Science*. 5(10):446-51. doi: 10.1016/s1360-1385(00)01740-4. PMID: 11044722.
- Hiratsu K, Ohta M, Matsui K, Ohme-Takagi M. 2002. The SUPERMAN protein is an active repressor whose carboxy-terminal repression domain is required for the development of normal flowers. *FEBS Lett*. 514: 351–354
- Hörtensteiner S. 2009. Stay-green regulates chlorophyll and chlorophyll-binding protein degradation during senescence. *Trends in Plant Science*. 14(3):155-62. doi: 10.1016/j.tplants.2009.01.002. PMID: 19237309.
- Huijser P, Schmid M. 2011. The control of developmental phase transitions in plants. *Development*. 138(19):4117-29. doi: 10.1242/dev.063511. PMID: 21896627.

- Ichimura Y, Kirisako T, Takao T, Satomi Y, Shimonishi Y, Ishihara N, Mizushima N, Tanida I, Kominami E, Ohsumi M, Noda T, Ohsumi Y. 2000. A ubiquitin-like system mediates protein lipidation. *Nature*. 408(6811):488-92. doi: 10.1038/35044141. PMID: 11100732.
- Liang C, Wang Y, Zhu Y, Tang J, Hu B, Liu L, Ou S, Wu H, Sun X, Chu J, Chu C. 2014. OsNAP connects abscisic acid and leaf senescence by fine-tuning abscisic acid biosynthesis and directly targeting senescence-associated genes in rice. *PNAS*. 111(27):10013-8. doi: 10.1073/pnas.1321568111. PMID: 24951508; PMCID: PMC4103337.
- Kim YS, Kim SG, Park JE, Park HY, Lim MH, Chua NH, Park CM. 2006. A membrane-bound NAC transcription factor regulates cell division in Arabidopsis. *Plant Cell*. 18(11):3132-44. doi: 10.1105/tpc.106.043018. PMID: 17098812; PMCID: PMC1693948.
- Kim JH, Woo HR, Kim J, Lim PO, Lee IC, Choi SH, Hwang D, Nam HG. 2009. Trifurcate feed-forward regulation of age-dependent cell death involving miR164 in Arabidopsis. *Science*. 323(5917):1053-7. doi: 10.1126/science.1166386. PMID: 19229035.
- Kim HJ, Nam HG, Lim PO. 2016. Regulatory network of NAC transcription factors in leaf senescence. *Current Opinion in Plant Biology*. 33:48-56. doi: 10.1016/j.pbi.2016.06.002. PMID: 27314623.
- Kuhlgert S, Austic G, Zegarac R, Osei-Bonsu I, Hoh D, Chilvers MI, Roth MG, Bi K, TerAvest D, Weebadde P, Kramer DM. 2016. MultispeQ Beta: a tool for large-scale plant phenotyping connected to the open PhotosynQ network. *Royal Society Open Science*. 3(10):160592. doi: 10.1098/rsos.160592. PMID: 27853580; PMCID: PMC5099005.
- Kumar S, Stecher G, Tamura K. 2016. MEGA7: molecular evolutionary genetics analysis version 7.0 for bigger datasets. *Molecular Biology and Evolution*. 33(7):1870-4. doi: 10.1093/molbev/msw054. PMID: 27004904.
- Langmead B, Salzberg SL. 2012. Fast gapped-read alignment with Bowtie 2. *Nature Methods*. 9(4):357-9. doi: 10.1038/nmeth.1923. PMID: 22388286; PMCID: PMC3322381.
- Lim PO, Kim HJ, Nam HG. 2007. Leaf senescence. *Annual Review of Plant Biology*. 58:115-36. doi: 10.1146/annurev.arplant.57.032905.105316. PMID: 17177638.
- Lira BS, Gramagna G, Trench BA, Alves FRR, Silva EM, Silva GFF, Thirumalaikumar VP, Lupi ACD, Demarco D, Purgatto E, Nogueira FTS, Balazadeh S, Freschi L, Rossi M. 2017. Manipulation of a senescence-associated gene improves fleshy fruit yield. *Plant Physiology*. 175(1):77-91. doi: 10.1104/pp.17.00452. PMID: 28710129; PMCID: PMC5580748.
- Liu Y, Dong Q, Kita D, Huang JB, Liu G, Wu X, Zhu X, Cheung AY, Wu HM, Tao LZ. 2017. RopGEF1 plays a critical role in polar auxin transport in early development. *Plant Physiology*. 175(1):157-171. doi: 10.1104/pp.17.00697. PMID: 28698357; PMCID: PMC5580763.
- Ma D, Li X, Guo Y, Chu J, Fang S, Yan C, Noel JP, Liu H. 2016. Cryptochrome 1 interacts with PIF4 to regulate high temperature-mediated hypocotyl elongation in response to blue light. *PNAS*. 113(1):224-9. doi: 10.1073/pnas.1511437113. PMID: 26699514; PMCID: PMC4711866.
- Ma X, Balazadeh S, Mueller-Roeber B. 2019. Tomato fruit ripening factor NOR controls leaf senescence. *Journal of Experimental Botany*. 70(10):2727-2740. doi: 10.1093/jxb/erz098. PMID: 31002305; PMCID: PMC6506771.
- Ma J, Zhao P, Liu S, Yang Q, Guo H. 2020. The control of developmental phase transitions by microRNAs and their targets in seed plants. *International Journal of Molecular Sciences*. 21(6):1971. doi: 10.3390/ijms21061971. PMID: 32183075; PMCID: PMC7139601.
- Massonnet M, Fasoli M, Tornielli GB, Altieri M, Sandri M, Zuccolotto P, Paci P, Gardiman M, Zenoni S, Pezzotti M. 2017. Ripening transcriptomic program in red and white grapevine varieties correlates with berry skin anthocyanin accumulation. *Plant Physiology*. 174(4):2376-2396. doi: 10.1104/pp.17.00311. PMID: 28652263; PMCID: PMC5543946.
- Mizushima N, Noda T, Yoshimori T, Tanaka Y, Ishii T, George MD, Klionsky DJ, Ohsumi M, Ohsumi Y. 1998. A protein conjugation system essential for autophagy. *Nature*. 395(6700):395-8. doi: 10.1038/26506. PMID: 9759731.
- Mizushima N and Komatsu M. 2011. Autophagy: renovation of cells and tissues. *Cell*. 147(4), 728–741. <https://doi.org/10.1016/j.cell.2011.10.026>
- Mullins MG & Rajasekaran K. 1981. Fruiting cuttings: revised method for producing test plants of grapevine cultivars. *American Journal of Enology and Viticulture*. 32(1), 35-40.
- Ohta M, Matsui K, Hiratsu K, Shinshi H, Ohme-Takagi M. 2001. Repression domains of class II ERF transcriptional repressors share an essential motif for active repression. *Plant Cell*. 13: 1959–68.
- Palumbo MC, Zenoni S, Fasoli M, Massonnet M, Farina L, Castiglione F, Pezzotti M, Paci P. 2014. Integrated network analysis identifies fight-club nodes as a class of hubs encompassing key putative switch genes that induce major transcriptome reprogramming during grapevine development. *Plant Cell*. 26(12):4617-35. doi: 10.1105/tpc.114.133710. PMID: 25490918; PMCID: PMC4311215.
- Park SY, Yu JW, Park JS, Li J, Yoo SC, Lee NY, Lee SK, Jeong SW, Seo HS, Koh HJ, Jeon JS, Park YI, Paek NC. 2007. The senescence-induced staygreen protein regulates chlorophyll degradation. *Plant Cell*. 19(5):1649-64. doi: 10.1105/tpc.106.044891. PMID: 17513504; PMCID: PMC1913741.
- Pedmale UV, Huang SC, Zander M, Cole BJ, Hetzel J, Ljung K, Reis PAB, Sridevi P, Nito K, Nery JR, Ecker JR, Chory J. 2016. Cryptochromes interact directly with PIFs to control plant growth in limiting blue light. *Cell*. 164(1-2):233-245. doi: 10.1016/j.cell.2015.12.018. PMID: 26724867; PMCID: PMC4721562.
- Pinnola A, Cazzaniga S, Alboresi A, Nevo R, Levin-Zaidman S, Reich Z, Bassi R. 2015. Light-harvesting complex stress-related proteins catalyze excess energy dissipation in both photosystems of *Physcomitrella patens*. *The Plant Cell*. 27(11), 3213–3227. <https://doi.org/10.1105/tpc.15.00443>
- Podzimska-Sroka D, O'Shea C, Gregersen PL, Skriver K. 2015. NAC transcription factors in senescence: from molecular structure to function in crops. *Plants (Basel)*. 4(3):412-48. doi: 10.3390/plants4030412. PMID: 27135336; PMCID: PMC4844398.
- Qiu K, Li Z, Yang Z, Chen J, Wu S, Zhu X, Gao S, Gao J, Ren G, Kuai B, Zhou X. 2015. EIN3 and ORE1 accelerate degreening during ethylene-mediated leaf senescence by directly activating chlorophyll catabolic genes in Arabidopsis. *PLoS Genetics*. 11(7): e1005399. doi: 10.1371/journal.pgen.1005399. PMID: 26218222; PMCID: PMC4517869.
- Raman S, Greb T, Peaucelle A, Blein T, Laufs P, Theres K. 2008. Interplay of miR164, CUP-SHAPED COTYLEDON genes and LATERAL SUPPRESSOR controls axillary meristem formation in Arabidopsis thaliana. *Plant Journal*. 55(1):65-76. doi: 10.1111/j.1365-313X.2008.03483.x. PMID: 18346190.
- Sato Y, Morita R, Nishimura M, Yamaguchi H, Kusaba M. 2007. Mendel's green cotyledon gene encodes a positive regulator of the chlorophyll-degrading pathway. *PNAS*. 104, 14169–14174.
- Schägger H, von Jagow G. 1987. Tricine-sodium dodecyl sulfate-polyacrylamide gel electrophoresis for the separation of proteins in the range from 1 to 100 kDa. *Analytical Biochemistry*. 166(2):368-79. doi: 10.1016/0003-2697(87)90587-2. PMID: 2449095.
- Schrader J, Moyle R, Bhalerao R, Hertzberg M, Lundeberg J, Nilsson P, Bhalerao RP. 2004. Cambial meristem dormancy in trees involves extensive remodelling of the transcriptome. *The Plant Journal*. 40(2):173-87. doi: 10.1111/j.1365-313X.2004.02199.x. PMID: 15447645.
- Shimoda Y, Ito H, Tanaka A. 2016. Arabidopsis STAY-GREEN, Mendel's green cotyledon gene, encodes magnesium-dechelatease. *Plant Cell*. 28(9):2147-2160. doi: 10.1105/tpc.16.00428. PMID: 27604697; PMCID: PMC5059807.
- Souer E, van Houwelingen A, Kloos D, Mol J, Koes R. 1996. The no apical meristem gene of *Petunia* is required for pattern formation in embryos and flowers and is expressed at meristem and primordia boundaries. *Cell*. 85(2):159-70. doi: 10.1016/s0092-8674(00)81093-4. PMID: 8612269.

- Smith RJ & Kliewer WK. 1984. Estimation of Thompson Seedless grapevine leaf area. *American Journal of Enology and Viticulture*. 35:16-22.
- Stirbet A, Govindjee J. 2011. On the relation between the Kautsky effect (chlorophyll a fluorescence induction) and Photosystem II: basics and applications of the OJIP fluorescence transient. *Journal of Photochemistry and Photobiology B*. 104(1-2):236-57. doi: 10.1016/j.jphotobiol.2010.12.010. PMID: 21295993.
- Stirbet A, Lázár D, Kromdijk, Govindjee J. 2018. Chlorophyll a fluorescence induction: Can just a one-second measurement be used to quantify abiotic stress responses? *Photosynthetic*. 56, 86–104. Doi: 10.1007/s11099-018-0770-3.
- Su T, Li X, Yang M, Shao Q, Zhao Y, Ma C, Wang P. 2020. Autophagy: an intracellular degradation pathway regulating plant survival and stress response. *Frontiers in Plant Science*. 11:164. doi: 10.3389/fpls.2020.00164. PMID: 32184795; PMCID: PMC7058704.
- Sun X, Korir NK, Han J, Shangguan LF, Kayesh E, Leng XP, Fang JG. 2012. Characterization of grapevine microR164 and its target genes. *Molecular Biology Reports*. 39(10):9463-72. doi: 10.1007/s11033-012-1811-9. PMID: 22733489.
- Swarup R, Péret B. 2012. AUX/LAX family of auxin influx carriers-an overview. *Frontiers in Plant Science*. 3:225. doi: 10.3389/fpls.2012.00225. PMID: 23087694; PMCID: PMC3475149.
- Thomas MR, Scott NS. 1993. Microsatellite repeats in grapevine reveal DNA polymorphisms when analysed as sequence-tagged sites (STSs). *Theoretical and Applied Genetics*. 86(8):985-90. doi: 10.1007/BF00211051. PMID: 24194007.
- Vroemen CW, Mordhorst AP, Albrecht C, Kwaaitaal MA, de Vries SC. 2003. The CUP-SHAPED COTYLEDON3 gene is required for boundary and shoot meristem formation in *Arabidopsis*. *Plant Cell*. 15(7):1563-77. doi: 10.1105/tpc.012203. PMID: 12837947; PMCID: PMC165401.
- Wang N, Zheng Y, Xin H, Fang L, Li S. 2013. Comprehensive analysis of NAC domain transcription factor gene family in *Vitis vinifera*. *Plant Cell Reports*. 32(1):61-75. doi: 10.1007/s00299-012-1340-y. PMID: 22983198.
- Waters MT, Wang P, Korkaric M, Capper RG, Saunders NJ, Langdale JA. 2009. GLK transcription factors coordinate expression of the photosynthetic apparatus in *Arabidopsis*. *Plant Cell*. 21(4):1109-28. doi: 10.1105/tpc.108.065250. PMID: 19376934; PMCID: PMC2685620.
- Woo HR, Kim HJ, Nam HG, Lim PO. 2013. Plant leaf senescence and death - regulation by multiple layers of control and implications for aging in general. *Journal of Cell Science*. 126(21):4823-33. doi: 10.1242/jcs.109116. PMID: 24144694.
- Wu A, Allu AD, Garapati P, Siddiqui H, Dortay H, Zanon MI, Asensi-Fabado MA, Munné-Bosch S, Antonio C, Tohge T, Fernie AR, Kaufmann K, Xue GP, Mueller-Roeber B, Balazadeh S. 2012. JUNGBRUNNEN1, a reactive oxygen species-responsive NAC transcription factor, regulates longevity in *Arabidopsis*. *Plant Cell*. 24(2):482-506. doi: 10.1105/tpc.111.090894. Epub 2012 Feb 17. PMID: 22345491; PMCID: PMC3315228.
- Xi D, Chen X, Wang Y, Zhong R, He J, Shen J, Ming F. 2019. *Arabidopsis* ANAC092 regulates auxin-mediated root development by binding to the ARF8 and PIN4 promoters. *Journal of Integrative Plant Biology*. 61(9):1015-1031. doi: 10.1111/jipb.12735. PMID: 30415491.
- Yang SD, Seo PJ, Yoon HK, Park CM. 2011. The *Arabidopsis* NAC transcription factor VNI2 integrates abscisic acid signals into leaf senescence via the COR/RD genes. *Plant Cell*. 23(6):2155-68. doi: 10.1105/tpc.111.084913. Epub 2011 Jun 14. PMID: 21673078; PMCID: PMC3160032.
- Yu G, Wang LG, He QY. 2015. ChIPseeker: an R/Bioconductor package for ChIP peak annotation, comparison and visualization. *Bioinformatics*. 31(14):2382-3. doi: 10.1093/bioinformatics/btv145. PMID: 25765347.
- Zenoni S, D'Agostino N, Tornielli GB, Quattrocchio F, Chiusano ML, Koes R, Zethof J, Guzzo F, Delledonne M, Frusciantè L, Gerats T, Pezzotti M. 2011. Revealing impaired pathways in the an11 mutant by high-throughput characterization of *Petunia axillaris* and *Petunia inflata* transcriptomes. *The Plant Journal*. 68(1):11-27. doi: 10.1111/j.1365-3113X.2011.04661.x. PMID: 21623977.
- Zhai Y, Guo M, Wang H, Lu J, Liu J, Zhang C, Gong Z, Lu M. 2016. Autophagy, a conserved mechanism for protein degradation, responds to heat, and other abiotic stresses in *capsicum annum* L. *Frontiers in Plant Science*. 7:131. doi: 10.3389/fpls.2016.00131. PMID: 26904087; PMCID: PMC4746239.
- Zhao FL, Li YJ, Hu Y, Gao YR, Zang XW, Ding Q, Wang YJ, Wen YQ. 2016. A highly efficient grapevine mesophyll protoplast system for transient gene expression and the study of disease resistance proteins. *Plant Cell, Tissue and Organ Culture*. 125(1):43–57. doi.org/10.1007/s11240-015-0928-7.
- Zhou C, Han L, Pislariu C, Nakashima J, Fu C, Jiang Q, Quan L, Blancaflor EB, Tang Y, Bouton JH, Udvardi M, Xia G, Wang ZY. 2011. From model to crop: functional analysis of a STAY-GREEN gene in the model legume *Medicago truncatula* and effective use of the gene for alfalfa improvement. *Plant Physiology*. 157(3):1483-96. doi: 10.1104/pp.111.185140. PMID: 21957014; PMCID: PMC3252161.

VviNAC38

The DAP-seq assay reported only 68 binding sites (peaks), which remain the same after the FC>5 filtering (**Fig. 55**). The distribution of peaks revealed that 56% were located within the promoter regions (up to 2 kb upstream from a transcription start site), no genes were in 5' untranslated regions (UTRs), 10% were located in exons, 7% were located within introns, 3% were located in 3' UTRs, 6% were located in the 3 kb downstream region, and 18% were intergenic.

Even though the number of regulatory sites was very low, it was curious but significant that more than the half of these peaks belonged to the promoter regions; from this observation many questions concerning the success or failure of the experiment came out. Considering that also the transient over expression of the gene did not work and will be repeated, probably the DAP-seq is going to be redo on this specific TF to validate (or not) this first result.

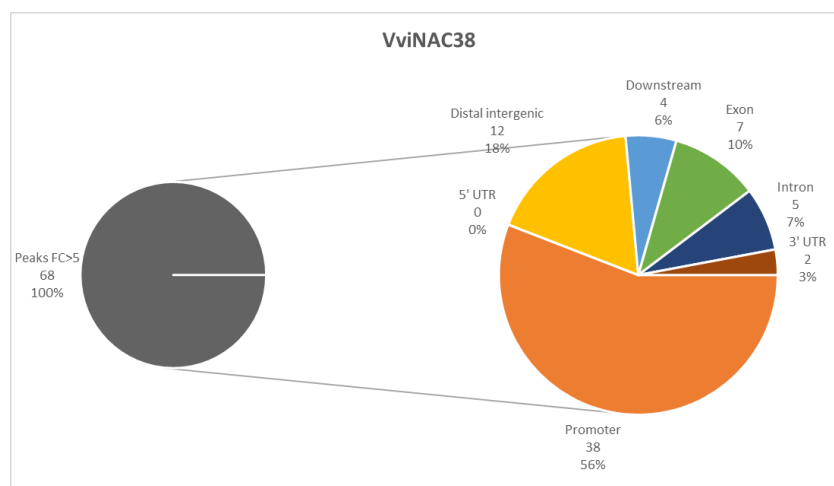


Figure 55: Double pie chart of the VviNAC38 DAP-seq results. The pie on the left represents the total binding sites (peaks) obtained, divided between the FC>5 and FC<5 (compared to the GST-Halo negative control peaks). The pie on the right represents the subdivision into the different genic region of the selected filtered peaks.

Three top binding motifs (GCGTG[G/C]A) were identified but not with a very high significance (**Fig. 56**); the phylogenetic footprints correlate with ANAC046, a positive regulator of chlorophyll degradation and senescence in *Arabidopsis* leaves (Oda-Yamamizo *et al.*, 2016).

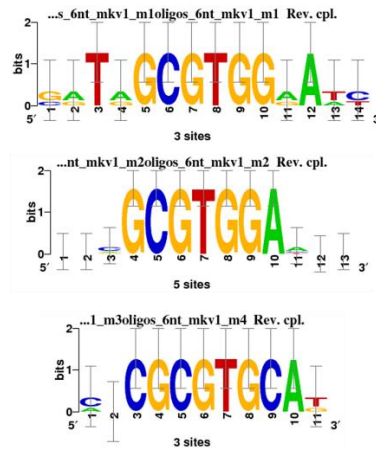


Figure 56: RSAT Plants NGS ChIP-Seq peak motifs analysis on the VviNAC38 DAP-seq results. Three top-ranking binding motifs identified in the DAP-seq FC>5 filtered dataset, based on the detection of overrepresented oligonucleotides (oligo analysis). The overall height of each letter stack indicates the sequence conservation at that position, and the height of symbols within the stack reflects the relative frequency of the corresponding nucleic acid at that position.

The attention was not focused only on the 56% of the final analysed binding sites, which belongs to the ‘promoter’ and ‘5’UTR’ genic regions and were 38 sites in total, but all the DAP-seq resulting dataset was used to obtain a not limited view of the few regulated genes.

However, the ‘no hit’ and ‘unknown’ elements were eliminated, and 55 binding sites were obtained for a total of 48 unique genes regulated by VviNAC38.

A GO enrichment analysis was performed on this sub-dataset, revealing a predominance of genes related to protein modification and cellular response to stress and stimulus (**Fig. 57**).

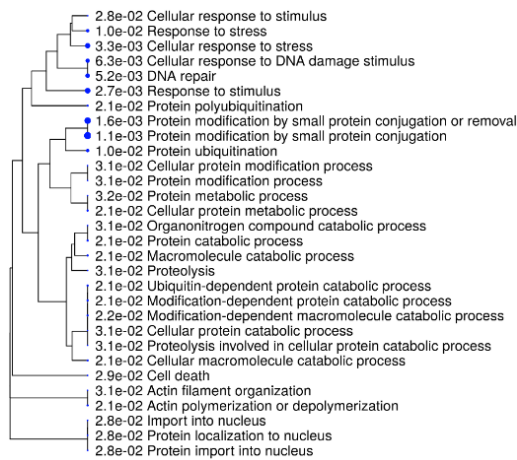


Figure 57: GO enrichment analysis of the VviNAC38 targets found to be regulated in the promoter and 5’UTR regions. The analysis was performed on ShinyGO.

Between the remaining binding sites, many transition markers were present (**Table 46**) but no *VviNACs* target.

Unfortunately, as said before, no transient over expression results ($FC > |1.5|$) were available to be crossed with the DAP-seq promoter and 5'UTR sub-dataset. The cv Sultana transient over expression needs to be repeated to be able to obtain at least three over expressing plantlets and complete the study concerning these *VviNAC* family members.

| q-value | Genic region | Gene ID | Distance to TSS | Functional annotation |
|---------|---|-------------------|-----------------|--|
| 137,37 | Promoter (1-2kb) | VIT_08s0040g03360 | -1144 | Cofilin |
| 127,97 | Intron (mRNA24461/VIT_08s0040g02470, intron 1 of 8) | VIT_08s0040g02470 | 247 | Inorganic pyrophosphatase |
| 96,43 | Promoter (<=1kb) | VIT_04s0044g00710 | -165 | UTP--glucose-1-phosphate uridylyltransferase * |
| 96,26 | Promoter (<=1kb) | VIT_06s0004g02750 | -879 | Auxin response factor 16 |
| 95,45 | Exon (mRNA8524/VIT_03s0038g00790, exon 1 of 3) | VIT_03s0038g00790 | 42 | V-type H+-transporting ATPase 16kDa proteolipid subunit |
| 71,2 | Promoter (<=1kb) | VIT_07s0031g00160 | -132 | Ubiquitin-conjugating enzyme E2 I * |
| 67,26 | Distal Intergenic | VIT_11s0016g02790 | -3336 | Zinc finger (CCCH-type) family protein * |
| 61,32 | Distal Intergenic | VIT_13s0064g01510 | -3624 | Auxin-independent growth promoter |
| 56,51 | Promoter (<=1kb) | VIT_02s0087g00790 | -33 | F-box domain containing protein * |
| 54,59 | Exon (mRNA6780/VIT_06s0004g03710, exon 1 of 2) | VIT_06s0004g03710 | 472 | PRL1-interacting factor G |
| 48,74 | Promoter (<=1kb) | VIT_07s0130g00190 | -742 | Suppressor of gene silencing 3 (SGS3) |
| 25,17 | Promoter (<=1kb) | VIT_04s0008g00490 | 0 | Profilin 5 (PRO5) (PRF5) |
| 24,88 | Promoter (<=1kb) | VIT_07s0130g00190 | -631 | Suppressor of gene silencing 3 (SGS3) |
| 21,37 | Downstream (<1kb) | VIT_14s0060g00200 | 2117 | Pentatricopeptide repeat-containing protein |
| 19,64 | Promoter (<=1kb) | VIT_11s0016g04780 | 0 | Ras GTP-binding protein (RAN2) |
| 18,93 | Promoter (<=1kb) | VIT_04s0008g05020 | 0 | Ras GTP-binding protein (RAN3) |
| 17,37 | Promoter (<=1kb) | VIT_03s0038g00750 | 0 | Ubiquitin fusion degradation protein UFD1 |
| 14,64 | Intron (mRNA3084/VIT_18s0001g08890, intron 1 of 3) | VIT_18s0001g08890 | 87 | Haemolysin-III related |
| 13,8 | Promoter (<=1kb) | VIT_02s0012g00400 | -55 | 1-aminocyclopropane-1-carboxylate oxidase |
| 11,14 | Promoter (<=1kb) | VIT_04s0008g04210 | 0 | GLB3 (2-on-2 hemoglobin like gene 3) |
| 10,6 | Promoter (1-2kb) | VIT_09s0002g02490 | -1135 | Dof zinc finger protein 1 |
| 10,41 | Promoter (<=1kb) | VIT_14s0108g00140 | -330 | Ubiquitin-conjugating enzyme E2 A |
| 10,03 | Promoter (<=1kb) | VIT_13s0019g01980 | 0 | Aspartic Protease (VvAP32) |
| 8,79 | 3' UTR | VIT_02s0025g04170 | 12575 | Heat shock transcription factor B2B |
| 8,71 | Exon (mRNA26154/VIT_08s0040g02950, exon 1 of 1) | VIT_08s0040g02950 | 316 | Zinc finger (C3HC4-type ring finger) |
| 7,91 | Promoter (<=1kb) | VIT_19s0090g00420 | -93 | Translation initiation factor eIF-1 |
| 7,65 | Promoter (1-2kb) | VIT_05s0029g00070 | -1797 | Calcium-binding protein CML |
| 7,41 | Intron (mRNA13633/VIT_01s0010g01480, intron 12 of 16) | VIT_01s0010g01460 | 42749 | Pentatricopeptide (PPR) repeat-containing protein |
| 6,61 | Distal Intergenic | VIT_05s0062g00020 | -82081 | F-box family protein |
| 6,47 | Promoter (1-2kb) | VIT_19s0014g02860 | -1377 | Cellulase |
| 6,45 | Exon (mRNA14093/VIT_15s0048g02390, exon 5 of 13) | VIT_15s0048g02390 | 3914 | Wall-associated receptor kinase-like 14 * |
| 6,36 | Promoter (<=1kb) | VIT_10s0003g02790 | 0 | Double-stranded DNA-binding protein |
| 6 | Promoter (<=1kb) | VIT_07s0005g05670 | -6 | Alba, DNA binding |
| 5,29 | Promoter (1-2kb) | VIT_17s0000g08970 | -1075 | Proline-rich family protein |
| 5,15 | Promoter (1-2kb) | VIT_12s0059g00870 | -1229 | MAPKK15 |
| 5,09 | Promoter (<=1kb) | VIT_04s0044g00710 | -248 | UTP--glucose-1-phosphate uridylyltransferase * |
| 4,47 | Distal Intergenic | VIT_11s0052g01840 | -4551 | Diacylglycerol kinase |
| 4,26 | Distal Intergenic | VIT_03s0091g01010 | -8277 | LIM domain protein WLIM1 |
| 4,21 | Exon (mRNA19274/VIT_08s0007g08420, exon 1 of 2) | VIT_08s0007g08420 | 1173 | R protein MLA10 |
| 4,01 | Distal Intergenic | VIT_02s0154g00400 | 7950 | Scarecrow transcription factor 6 (SCL6) |
| 3,75 | Distal Intergenic | VIT_03s0091g01010 | -8419 | LIM domain protein WLIM1 |
| 3,74 | Promoter (<=1kb) | VIT_05s0020g02820 | 0 | Ubiquitin activating enzyme E1c (ECR1) |
| 3,48 | Promoter (<=1kb) | VIT_02s0087g00790 | 0 | F-box domain containing protein * |
| 3,25 | Promoter (<=1kb) | VIT_01s0011g05060 | -451 | Major latex-like protein 34 |
| 3,25 | Distal Intergenic | VIT_18s0001g05250 | -2048 | Dehydration Responsive Element-Binding Transcription Factor (VvDREB27) |
| 2,95 | Promoter (1-2kb) | VIT_05s0029g00070 | -1685 | Calcium-binding protein CML |
| 2,86 | Downstream (1-2kb) | VIT_08s0007g07930 | 4919 | Clavata1 receptor kinase (CLV1) |
| 2,38 | Distal Intergenic | VIT_17s0053g00990 | -9034 | Expansin (VvEXPA18) * |
| 2,33 | Promoter (1-2kb) | VIT_08s0007g00560 | -1964 | ftsh3 (Ftsh protease 3) |
| 2,21 | Exon (mRNA699/VIT_05s0020g03440, exon 3 of 4) | VIT_05s0020g03440 | 1468 | Photosystem II 11 kDa protein PSB27 |
| 2,17 | Promoter (1-2kb) | VIT_15s0048g02900 | -1359 | CYP78A3p |
| 2,12 | Promoter (<=1kb) | VIT_08s0040g03290 | -84 | Mini-chromosome maintenance protein MCM8 |
| 2,01 | Distal Intergenic | VIT_19s0014g01460 | -2931 | Ubiquitin-conjugating enzyme E2 N |

Table 46: *VviNAC38* direct target genes. The asterisk (*) refers to the transition markers.

VviNAC39

The DAP-seq assay reported 5870 binding sites (peaks), which were reduced to 4682 after the $FC > 5$ filtering; with this stringent filter used, the dataset loss was a

little bit higher, about the 20% (**Fig. 58**). The distribution of peaks revealed that 20% were located within the promoter regions (up to 2 kb upstream from a transcription start site), 1% were in 5' untranslated regions (UTRs), 7% were located in exons, 15% were located within introns, 2% were located in 3' UTRs, 5% were located in the 3 kb downstream region, and 30% were intergenic.

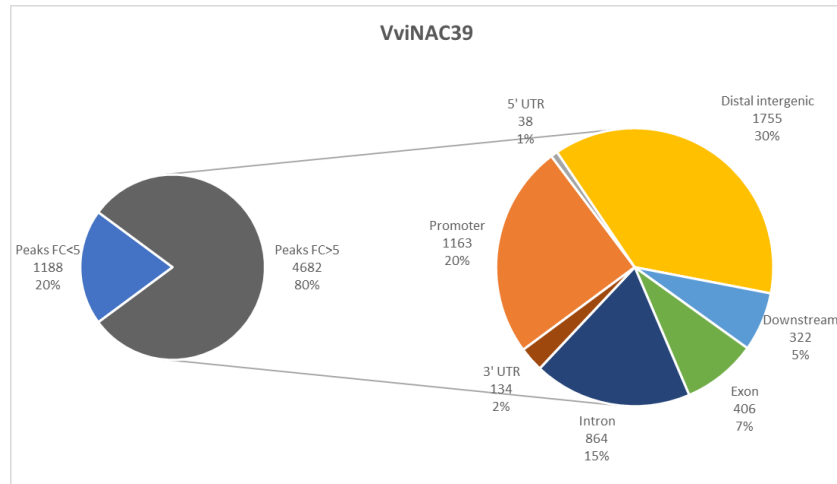


Figure 58: Double pie chart of the VviNAC39 DAP-seq results. The pie on the left represents the total binding sites (peaks) obtained, divided between the FC>5 and FC<5 (compared to the GST-Halo negative control peaks). The pie on the right represents the subdivision into the different genic region of the selected filtered peaks.

Two major binding motifs (CAA[A/T]TTG) were identified with strong significance (**Fig. 59**) but the phylogenetic footprints do not correlate with other known NAC.

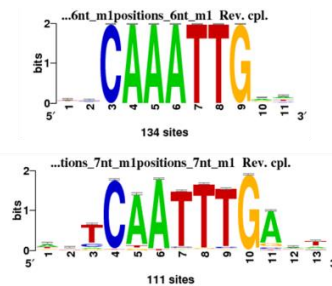


Figure 59: RSAT Plants NGS CHIP-Seq peak motifs analysis on the VviNAC39 DAP-seq results. Two top-ranking binding motifs identified in the DAP-seq FC>5 filtered dataset, based on the detection of overrepresented oligonucleotides (oligo analysis). The overall height of each letter stack indicates the sequence conservation at that position, and the height of symbols within the stack reflects the relative frequency of the corresponding nucleic acid at that position.

The attention was focused only on the 21% of the final analyzed binding sites, which belongs to the ‘promoter’ and ‘5’UTR’ genic regions, for a total of 1201

sites. This percentage is low compared to the average number of DAP-seq sites found in literature.

After the elimination of all the ‘no hit’ and ‘unknown’ elements, 993 binding sites were obtained for a total of 915 unique genes regulated by VviNAC39.

A GO enrichment analysis was performed on this sub-dataset, revealing a predominance of genes related to oxidation-reduction processes, response to jasmonic acid, biological regulation, carboxylic acid metabolic processes, different biosynthetic processes (also fatty acids), carbon utilization, transport and localization (**Fig. 60**).

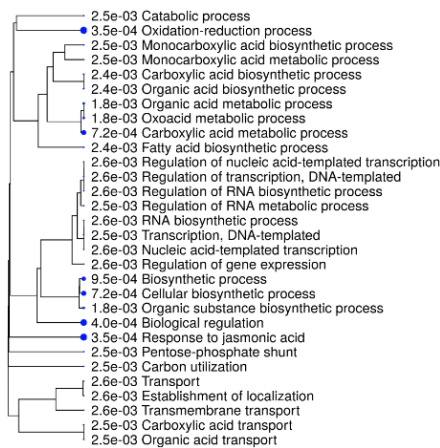


Figure 60: GO enrichment analysis of the VviNAC39 targets found to be regulated in the promoter and 5'UTR regions. The analysis was performed on ShinyGO.

Between the top 20 (q-value based) promoter and 5'UTR located binding sites some interesting genes were found (**Table 47**).

The most represented gene was *3-METHYL-2-OXOBUTANOATE DEHYDROGENASE* (VIT_18s0001g14980), which is present in the DAP-seq dataset of almost all the selected VviNAC TFs but not much information is available concerning its specific role in the plant development.

Moreover, ethylene- and auxin-related genes were found: *ERF/AP2 GENE FAMILY VvERF054* (VIT_16s0050g02400) and *AUXIN-RESPONSIVE SAUR11* (VIT_02s0154g00010). Interestingly, the already mentioned *MYB DOMAIN PROTEIN 4 VvMybC2-L1* (VIT_01s0011g04760) was also present in the list.

| q-value | Genic region | Gene ID | Distance to TSS | Functional annotation |
|---------|------------------|-------------------|-----------------|---|
| 999 | Promoter (1-2kb) | VIT_18s0001g14980 | -1612 | 3-methyl-2-oxobutanoate dehydrogenase |
| 305,44 | Promoter (<=1kb) | VIT_02s0025g02390 | -613 | Oligopeptide transporter OPT7 |
| 284,87 | Promoter (<=1kb) | VIT_11s0016g04270 | -797 | Hydrolase, alpha/beta fold |
| 260,94 | Promoter (<=1kb) | VIT_01s0010g03780 | -887 | Histidine kinase (AHK3) |
| 240,92 | Promoter (<=1kb) | VIT_10s0116g01730 | -170 | Soluble starch synthase 3, chloroplast precursor |
| 238,33 | Promoter (<=1kb) | VIT_17s0000g08450 | -727 | Carbonic anhydrase chloroplast |
| 205,89 | Promoter (1-2kb) | VIT_00s0225g00090 | -1298 | Copper amine oxidase |
| 202,78 | Promoter (1-2kb) | VIT_01s0011g03020 | -1443 | HAK5 (High affinity K ⁺ transporter 5) |
| 182,08 | Promoter (1-2kb) | VIT_16s0050g02400 | -1308 | ERF/AP2 Gene Family (VVERF054) |
| 180,61 | Promoter (<=1kb) | VIT_08s0058g01100 | -227 | Armadillo/beta-catenin repeat / U-box domain-containing protein |
| 178,85 | Promoter (1-2kb) | VIT_00s0394g00020 | -1917 | Pentatricopeptide (PPR) repeat-containing protein |
| 163,9 | Promoter (<=1kb) | VIT_06s0004g07280 | -116 | UDP-glucuronosyl/UDP-glucosyltransferase |
| 155,69 | Promoter (<=1kb) | VIT_01s0011g04760 | -91 | myb domain protein 4 (VvMybC2-L1) |
| 154,96 | Promoter (1-2kb) | VIT_12s0028g00340 | -1210 | Protein kinase |
| 153,69 | Promoter (<=1kb) | VIT_13s0067g03060 | -860 | Methionyl-tRNA synthetase |
| 146,6 | Promoter (1-2kb) | VIT_10s0003g00870 | -1233 | TCP family transcription factor 4 |
| 145,76 | Promoter (1-2kb) | VIT_14s0068g00520 | -1963 | F-box domain containing protein |
| 144,65 | Promoter (<=1kb) | VIT_17s0000g08460 | -540 | Carbonic anhydrase, chloroplast precursor |
| 131,38 | Promoter (<=1kb) | VIT_01s0026g02430 | -900 | Calcineurin B |
| 126,44 | Promoter (1-2kb) | VIT_02s0154g00010 | -1743 | Auxin-responsive SAUR11 |

Table 47: Top 20 (q-value based) represented direct target genes of VviNAC39.

Afterwards, the list of the VviNAC39 targets was used to find all the possible VviNACs targets of the TF. 4 VviNACs target genes were found (**Table 48**): VviNAC12 (VIT_01s0011g02990), VviNAC15 (VIT_18s0001g01820), VviNAC23 (VIT_04s0023g03110) and VviNAC73 (VIT_14s0068g01490).

| q-value | Genic region | Gene ID | Distance to TSS | Functional annotation |
|---------|------------------|-------------------|-----------------|---|
| 8,43 | Promoter (1-2kb) | VIT_14s0068g01490 | -1161 | NAC domain-containing protein (VvNAC73) |
| 8,17 | Promoter (1-2kb) | VIT_04s0023g03110 | -1126 | NAC domain-containing protein (VvNAC23) |
| 3,84 | Promoter (<=1kb) | VIT_18s0001g01820 | -46 | NAC domain-containing protein (VvNAC15) |
| 2,04 | Promoter (<=1kb) | VIT_01s0011g02990 | 0 | NAC domain-containing protein (VvNAC12) |

Table 48: VviNAC39 DAP-seq VviNACs targets genes.

Then, the previously reported VviNAC39 transient over expression results (FC>|1.5|) were crossed with the DAP-seq promoter and 5'UTR sub-dataset, revealing 8 correlated binding sites (7 unique genes; **Table 49**); none of them were present between the top 20 reported genes.

Only two genes were found up regulated: the ABC TRANSPORTER VvPDR16 - VvABCG46 (VIT_09s0002g05590) and the UBIQUITIN-CONJUGATING ENZYME E2 VARIANT (VIT_19s0090g00080).

ABC transporters function as ATP-dependent pumps but also as ion channels and channel regulators; the substrates of these transporters include sugars, lipids, heavy metal chelates, polysaccharides, alkaloids, steroids, inorganic acids and glutathione conjugates (Theodoulou, 2000). Whereas ubiquitin-conjugating (UBC) E2 enzyme plays crucial roles in plant growth and development; indeed, a recent study has demonstrated that most VvUBCs are involved in ripening and post-harvest stage in

grapevine and feature functional roles in grape organs (Gao *et al.*, 2017).

The other five genes resulted down regulated by *VviNAC39*. Between them a *CA2+-TRANSPORTING ATPase TYPE 2 ISOFORM 8* (VIT_14s0030g02110), a *CHUP1* (VIT_08s0007g04330), which is essential for chloroplast anchorage to the plasma membrane and chloroplast movement (Oikawa *et al.*, 2008) and a *GLYCOSYL HYDROLASE FAMILY 17 PROTEIN* (VIT_11s0016g00220) were found. Moreover, two genes were related to pathogenesis mechanisms: *PATHOGENESIS-RELATED PROTEIN 1 PRECURSOR PRP 1* (VIT_11s0052g01620) and *PECTATE LYASE 2* (VIT_19s0015g00510).

A recent study has also demonstrated that another pectate lyase (VIT_17s0000g09810) was found down regulated by grape powdery mildew and methyl salicylate treatments (Toth *et al.*, 2016).

| q-value | Genic region | Gene ID | Distance to TSS | Functional annotation | Transient OE |
|---------|------------------|-------------------|-----------------|--|--------------|
| 67,46 | Promoter (<=1kb) | VIT_08s0007g04330 | -115 | CHUP1 (chloroplast unusual positioning 1) | -1,80 |
| 18,97 | Promoter (1-2kb) | VIT_09s0002g05590 | -1402 | ABC Transporter (VvPDR16 - VvABCG46) | 2,97 |
| 8,69 | Promoter (1-2kb) | VIT_09s0002g05590 | -1918 | ABC Transporter (VvPDR16 - VvABCG46) | 2,97 |
| 8,17 | Promoter (<=1kb) | VIT_19s0015g00510 | -325 | Pectate lyase 2 | -7,23 |
| 8,11 | Promoter (<=1kb) | VIT_19s0090g00080 | -404 | Ubiquitin-conjugating enzyme E2 variant | 1,67 |
| 3,65 | Promoter (<=1kb) | VIT_14s0030g02110 | -815 | Ca2+-transporting ATPase type 2 isoform 8 | -1,79 |
| 2,86 | Promoter (<=1kb) | VIT_11s0016g00220 | -308 | Glycosyl hydrolase family 17 protein | -2,20 |
| 2,64 | Promoter (1-2kb) | VIT_11s0052g01620 | -1082 | Pathogenesis-related protein 1 precursor (PRP 1) | -2,69 |

Table 49: *VviNAC39* DAP-seq targets genes which have a match in the *VviNAC39* transient over expression dataset.

VviNAC60

The DAP-seq assay reported 7489 binding sites (peaks), which were reduced to 6571 after the $FC > 5$ filtering; a 12% of the peaks was lost (**Fig. 61**). The distribution of peaks revealed that 27% were located within the promoter regions (up to 2 kb upstream from a transcription start site), 1% were in 5' untranslated regions (UTRs), 9% were located in exons, 13% were located within introns, 2% were located in 3' UTRs, 8% were located in the 3 kb downstream region, and 28% were intergenic.

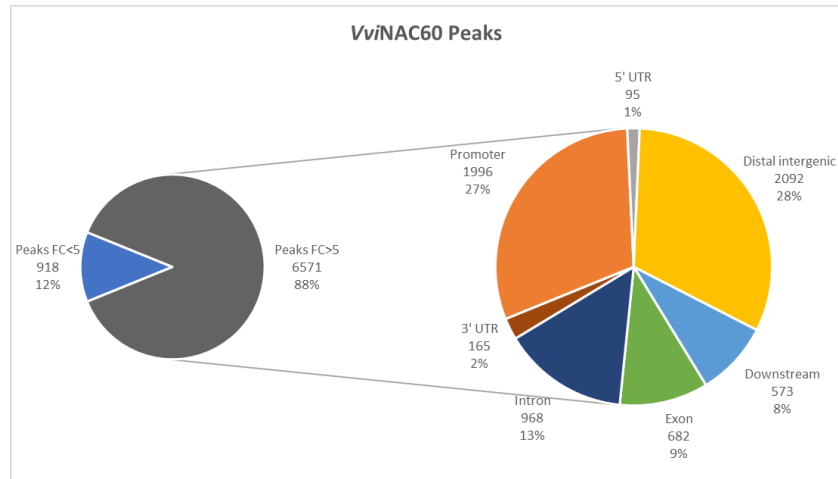


Figure 61: Double pie chart of the VviNAC60 DAP-seq results. The pie on the left represents the total binding sites (peaks) obtained, divided between the FC>5 and FC<5 (compared to the GST-Halo negative control peaks). The pie on the right represents the subdivision into the different genic region of the selected filtered peaks.

Two major binding motifs (AC[G/A][T/C]GT) were identified with strong significance (**Fig. 62**) and the phylogenetic footprints correlate with ANAC055, a transcription activator that regulates jasmonic acid-induced expression of defense genes (Bu *et al.*, 2008).

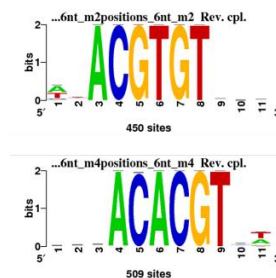


Figure 62: RSAT Plants NGS ChIP-Seq peak motifs analysis on the VviNAC60 DAP-seq results. Three top-ranking binding motifs identified in the DAP-seq FC>5 filtered dataset, based on the detection of overrepresented oligonucleotides (oligo analysis). The overall height of each letter stack indicates the sequence conservation at that position, and the height of symbols within the stack reflects the relative frequency of the corresponding nucleic acid at that position.

The attention was focused only on the 28% of the final analysed binding sites, which belongs to the ‘promoter’ and ‘5’UTR’ genic regions, for a total of 2091 sites.

After the elimination of all the ‘no hit’ and ‘unknown’ elements, 1688 binding sites were obtained for a total of 1511 unique genes regulated by VviNAC60.

A GO enrichment analysis was performed on this sub-dataset, revealing a

predominance of genes related to regulation of cellular, biological and metabolic processes, aromatic compound biosynthetic processes categories, and revealing possible actions concerning transmembrane transport and protein modifications (Fig. 63).

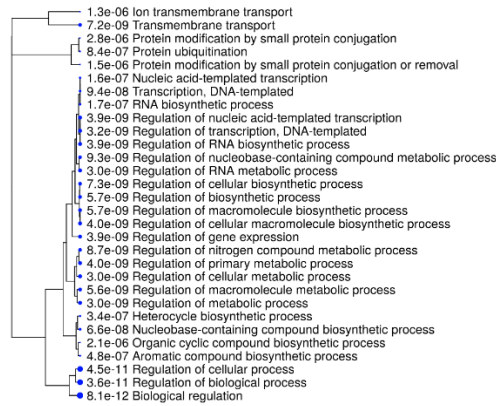


Figure 63: GO enrichment analysis of the VviNAC60 targets found to be regulated in the promoter and 5'UTR regions. The analysis was performed on ShinyGO.

Between the top 20 (q-value based) promoter and 5'UTR located binding sites some interesting genes were found (Table 50).

| q-value | Genic region | Gene ID | Distance to TSS | Functional annotation |
|---------|------------------|-------------------|-----------------|---|
| 999 | Promoter (1-2kb) | VIT_18s0001g14980 | -1609 | 3-methyl-2-oxobutanoate dehydrogenase |
| 242,9 | Promoter (<=1kb) | VIT_01s0011g04760 | -88 | myb domain protein 4 (VvMybC2-L1) |
| 242,78 | Promoter (<=1kb) | VIT_17s0000g01280 | -75 | WRKY Transcription Factor (VvWRKY52) |
| 216,51 | Promoter (<=1kb) | VIT_17s0000g08450 | -733 | Carbonic anhydrase chloroplast |
| 181,24 | Promoter (<=1kb) | VIT_05s0062g00700 | -157 | UDP-glucose:flavonoid 7-O-glucosyltransferase |
| 178,68 | Promoter (1-2kb) | VIT_13s0067g00600 | -1193 | Arginine-tRNA-protein transferase 1 |
| 178,4 | Promoter (<=1kb) | VIT_05s0020g02310 | 0 | Pyruvate,orthophosphate dikinase |
| 165,09 | 5' UTR | VIT_10s0003g01800 | 101 | Zinc finger (FYVE type) |
| 162,67 | Promoter (1-2kb) | VIT_05s0062g01120 | -1262 | PIN1 |
| 155,9 | Promoter (1-2kb) | VIT_18s0041g02010 | -1882 | 12-oxophytodienoate reductase 1 |
| 152,37 | Promoter (<=1kb) | VIT_15s0021g01150 | -568 | Calcium-dependent protein kinase-related |
| 144,42 | Promoter (<=1kb) | VIT_12s0142g00610 | -7 | Citrate synthase, glyoxysomal precursor |
| 143 | Promoter (<=1kb) | VIT_07s0255g00110 | -147 | WD40 |
| 142,63 | Promoter (<=1kb) | VIT_06s0004g07930 | 0 | Nucleotidyltransferase family |
| 137,08 | Promoter (<=1kb) | VIT_19s0177g00070 | -494 | Polyubiquitin (UBQ14) |
| 125,17 | Promoter (<=1kb) | VIT_04s0008g03430 | 0 | Exostosin family |
| 123,51 | Promoter (<=1kb) | VIT_18s0001g08300 | 0 | Tubulin alpha-6 chain |
| 115,1 | Promoter (<=1kb) | VIT_15s0048g01740 | -355 | Growth-regulating factor 9 |
| 114,52 | Promoter (1-2kb) | VIT_07s0005g02250 | -1782 | ABC transporter G member 21 |
| 114,29 | Promoter (<=1kb) | VIT_09s0002g01470 | -771 | 4-phosphopantetheinyl transferase sfp |

Table 50: Top 20 (q-value based) represented direct target genes of VviNAC60. In bold are reported the *switch* genes.

The most represented gene (q-value based) was, once again, the *3-METHYL-2-OXOBUTANOATE DEHYDROGENASE* (VIT_18s0001g14980) but not much information is available concerning its specific role in the plant development; however, this is an interesting gene as it was found in almost all the DAP-seq datasets of the studied VviNACs.

The *VvWRKY52* (VIT_17s0000g01280), a red berry *switch* gene which has been shown to play roles in biotic stress responses (Wang *et al.*, 2017 and Wang *et al.*, 2018), was also present. Moreover, returned the *MYB DOMAIN PROTEIN 4* *VvMYBC2-L1* (VIT_01s0011g04760), the *ARGININE_tRNA-PROTEIN TRANSFERASE 1 ATE1* (VIT_13s0067g00600), the *PINI* (VIT_05s0062g01120) and the *GROWTH-REGULATING FACTOR 9* (VIT_15s0048g01740).

Another *UDP-GLUCOSE:FLAVONOID 7-O-GLUCOSYLTRANSFERASE* (VIT_05s0062g00700) was also found; these class of enzymes has a role in UV protection, pathogen defense and coloration (Kim *et al.*, 2006)

Afterwards, the list of the *VviNAC60* targets was used to find all the possible *VviNACs* targets of the TF. 6 *VviNACs* target genes were found (**Table 51**); interestingly, *VviNAC05* (VIT_17s0000g06400), which was bounded in two different sites by the TF, and *VviNAC61* (VIT_08s0007g07640) were also found in the list.

| q-value | Genic region | Gene ID | Distance to TSS | Functional annotation |
|---------|------------------|-------------------|-----------------|---|
| 59,84 | Promoter (<=1kb) | VIT_08s0007g07640 | 0 | NAC domain-containing protein (VvNAC61) |
| 33,15 | Promoter (1-2kb) | VIT_17s0000g06400 | -1862 | NAC domain-containing protein (VvNAC05) |
| 18,08 | Promoter (<=1kb) | VIT_17s0000g06400 | 0 | NAC domain-containing protein (VvNAC05) |
| 13,32 | Promoter (1-2kb) | VIT_14s0068g01490 | -1137 | NAC domain-containing protein (VvNAC73) |
| 5,76 | Promoter (<=1kb) | VIT_12s0028g03050 | -414 | NAC domain-containing protein (VvNAC34) |
| 5,48 | Promoter (<=1kb) | VIT_04s0008g06550 | 0 | NAC domain-containing protein (VvNAC66) |
| 2,01 | Promoter (1-2kb) | VIT_08s0040g02110 | -1326 | NAC domain-containing protein (VvNAC45) |

Table 51: *VviNAC60* DAP-seq *VviNACs* targets genes.

Then, the previously reported (D'Inca, 2017) *VviNAC60* stable and transient over expression results ($FC > |1.5|$) were crossed with the DAP-seq promoter and 5'UTR sub-dataset, revealing 196 (170 unique genes) and 34 (25 unique genes) correlated binding sites, respectively (**Table 52-53** and **Table 54-55**).

Only two genes were found in common between the two different over expression experiments and, in both cases, resulted up regulated: *ORGANIC CATION/CARNITINE TRANSPORTER4* (VIT_19s0014g04790) and *CELLULOSE SYNTHASE CSLG2* (VIT_05s0020g05060).

Between the up regulated genes found in the stable over expression of *VviNAC60*, three were also present in the top 20 DAP-seq most represented (**Table 52**): 3-

METHYL-2-OXOBUTANOATE DEHYDROGENASE (VIT_18s0001g14980), *CITRATE SYNTHASE, GLYOXYSOMAL PRECURSOR* (VIT_12s0142g00610) and a *NUCLEOTIDYLTRANSFERASE FAMILY* (VIT_06s0004g07930).

Moreover, a *MYB FAMILY* (VIT_09s0054g01620) and the *VvWRKY16* (VIT_06s0004g07500) were up regulated.

Interestingly many genes related to hormones were present: four auxin-related genes, *AUXIN-RESPONSIVE SAUR* (VIT_15s0048g00530 and VIT_01s0146g00180), *ARF* (VIT_00s0404g00040), and *AUXIN RESPONSE FACTOR 10* (VIT_13s0019g04380); three ethylene-related genes, *ERF/AP2 GENE FAMILY VvERF006, DEHYDRATION RESPONSIVE ELEMENT-BINDING TRANSCRIPTION FACTOR VvDREB28* (VIT_18s0001g10150), *ETHYLENE-RESPONSIVE TRANSCRIPTION FACTOR 9* (VIT_12s0028g03270), *ERF/AP2 GENE FAMILY VvERF017, DEHYDRATION RESPONSIVE ELEMENT-BINDING TRANSCRIPTION FACTOR VvDREB30* (VIT_18s0089g01030); and a *GIBBERELLIN RECEPTOR GID1L2* (VIT_07s0104g00930).

A marker of the second transition, and a berry *switch* gene, was also identified with the DAP assay as up regulated: *LATE EMBRYOGENESIS ABUNDANT PROTEIN 5* (VIT_07s0005g00660). The Late Embryogenesis Abundant (LEA) protein gene family is associated with salt and drought stress tolerance in many plant species and is well known that abiotic stresses have the potential to negatively affect both yield and berry quality in grapes (Ibrahime *et al.*, 2019).

Regarding the DAP-seq genes which were also found down regulated in the *VviNAC60* stable over expression (**Table 53**), the *VviNAC34* (VIT_12s0028g03050) and a *BASIC HELIX-LOOP-HELIX bHLH FAMILY* (VIT_08s0058g00960) were present. Moreover, the most down regulated gene was a *PAPAIN CYSTEINE PROTEINASE* (VIT_18s0001g13380); this class of genes is known to play important functions in multiple processes of plant growth including seed germination, leaf senescence, programmed cell death, abiotic stress response and plant immunity (Liu *et al.*, 2018).

| q-value | Genic region | Gene ID | Distance to TSS | Functional annotation | Stable OE |
|---------------|-------------------|-------------------|-----------------|--|--------------|
| 999 | Promoter (-1.2kb) | VIT_18x0001g14980 | -1609 | 3-methyl-2-oxobutanoate dehydrogenase | 3.05 |
| 144.42 | Promoter (-1.1kb) | VIT_12x0142g00610 | -7 | Citrate synthase, glyoxysomal precursor | 1.59 |
| 142.63 | Promoter (-1.1kb) | VIT_06x0004g07930 | 0 | Nucleotidyltransferase family | 2.82 |
| 85.5 | Promoter (-1.2kb) | VIT_18x0001g09420 | -1845 | Progesterone 5-beta-reductase | 1.57 |
| 79.94 | Promoter (-1.2kb) | VIT_05x0020g05060 | -1053 | Cellulose synthase CSLG2 | 2.17 |
| 71.69 | Promoter (-1.1kb) | VIT_11x0149g00280 | -793 | Chitinase A | 3.12 |
| 64.43 | Promoter (-1.1kb) | VIT_18x0001g07400 | -317 | Carbonic anhydrase, chloroplast precursor | 2.11 |
| 58.06 | Promoter (-1.1kb) | VIT_07x0104g00860 | -195 | WD40 | 1.55 |
| 55.11 | Promoter (-1.1kb) | VIT_04x0044g00220 | 0 | Monoxygenase | 1.95 |
| 52.2 | Promoter (-1.1kb) | VIT_01x0011g00780 | -868 | Beta-glucosidase | 7.82 |
| 48.91 | Promoter (-1.1kb) | VIT_01x0144g00180 | 0 | Auxin responsive SAUR protein | 2.41 |
| 47.53 | Promoter (-1.1kb) | VIT_09x0054g01620 | 0 | myb family | 1.59 |
| 46.86 | Promoter (-1.1kb) | VIT_06x0004g04590 | -91 | Epsin N-terminal homology (ENTH) domain-containing | 6.49 |
| 41.26 | Promoter (-1.2kb) | VIT_13x0011g04620 | -1931 | OTU cysteine protease | 1.58 |
| 41.01 | Promoter (-1.1kb) | VIT_00x0304g00030 | -937 | VQ motif-containing protein | 2.69 |
| 35.96 | Promoter (-1.2kb) | VIT_05x0020g05060 | -1084 | Cellulose synthase CSLG2 | 2.17 |
| 33.95 | Promoter (-1.2kb) | VIT_09x0002g03410 | -1582 | Phytochrome-associated protein 1 (PAP1) | 2.12 |
| 32.73 | Promoter (-1.1kb) | VIT_05x0062g00980 | -14 | Aldo/keto reductase AKR | 1.80 |
| 30.18 | Promoter (-1.1kb) | VIT_07x0005g04890 | 0 | Glutathione S-transferase 25 GSTU7 | 3.82 |
| 29.03 | Promoter (-1.1kb) | VIT_18x0001g08430 | -350 | Branched-chain-amino-acid aminotransferase 2, chloroplast (Atbcat-2) * | 11.12 |
| 28.78 | Promoter (-1.2kb) | VIT_07x0104g00930 | -1733 | Gibberellin receptor GID1L2 | 3.07 |
| 24.63 | Promoter (-1.1kb) | VIT_05x0049g01980 | 0 | 3-isopropylmalate dehydratase large subunit 2 | 9.61 |
| 22.26 | Promoter (-1.1kb) | VIT_18x0001g01100 | -433 | BTB/POZ domain-containing protein POB1 | 1.83 |
| 21.75 | Promoter (-1.2kb) | VIT_13x0011g04620 | -1994 | OTU cysteine protease | 1.58 |
| 21.63 | Promoter (-1.1kb) | VIT_06x0004g04010 | -97 | Exocyst subunit EXO70 H7 | 2.45 |
| 17.94 | Promoter (-1.1kb) | VIT_18x0001g15010 | -913 | F-box and leucine-rich repeat protein 1 | 2.19 |
| 16.19 | Promoter (-1.1kb) | VIT_00x0179g00260 | -282 | Calcium-transporting ATPase 12 ACA12 | 1.96 |
| 15.77 | Promoter (-1.1kb) | VIT_07x0005g00660 | -538 | Late embryogenesis abundant protein 5 * | 6.76 |
| 15.55 | Promoter (-1.1kb) | VIT_01x0011g05560 | -822 | TIFY gene family (VvIAZ1) | 1.94 |
| 13.88 | Promoter (-1.2kb) | VIT_18x0044g00730 | -1076 | Peptide chain release factor eRF subunit 1 | 1.82 |
| 13.32 | Promoter (-1.1kb) | VIT_02x0025g00880 | -536 | BTB/POZ domain-containing protein POB1 | 1.83 |
| 13.24 | Promoter (-1.2kb) | VIT_13x0011g04380 | -1343 | Auxin response factor 10 | 1.57 |
| 13.06 | Promoter (-1.1kb) | VIT_09x0002g08670 | -67 | Acetylmethionine aminotransferase | 1.52 |
| 13.05 | 5' UTR | VIT_00x0404g00040 | 113 | ARF GTPase activator, ARF-GAP Domain 5 | 1.68 |
| 12.56 | Promoter (-1.1kb) | VIT_18x0001g01100 | -433 | ERF/AP2 Gene Family (VvERF006), Dehydration Responsive Element-Binding Transcription Factor (VvDREB28) | 1.90 |
| 11.61 | Promoter (-1.2kb) | VIT_05x0020g00890 | -1704 | Zinc finger (C3HC4-type ring finger) | 1.84 |
| 11.55 | Promoter (-1.1kb) | VIT_18x0001g06310 | -56 | snRK2.8 | 2.12 |
| 10.75 | Promoter (-1.1kb) | VIT_14x0083g00440 | -477 | PHD finger transcription factor | 1.59 |
| 10.23 | Promoter (-1.1kb) | VIT_19x0015g00710 | -386 | Cellulose synthase CSL1E1 | 2.34 |
| 10.05 | Promoter (-1.1kb) | VIT_10x0116g00960 | -709 | Transcription factor jumonji (jmiC) domain-containing protein | 1.55 |
| 9.95 | 5' UTR | VIT_00x0404g00040 | 17 | ARF GTPase activator, ARF-GAP Domain 5 | 1.68 |
| 9.76 | Promoter (-1.1kb) | VIT_17x0000g05420 | -793 | AAA-type ATPase family | 3.18 |
| 8.97 | Promoter (-1.1kb) | VIT_00x0203g00100 | -102 | AarF domain-containing kinase ABC1 | 1.57 |
| 8.95 | Promoter (-1.1kb) | VIT_18x0001g06310 | -4 | snRK2.8 | 2.12 |
| 8.48 | Promoter (-1.1kb) | VIT_17x0000g05420 | 0 | AAA-type ATPase family | 3.18 |
| 8.41 | Promoter (-1.1kb) | VIT_00x0181g00280 | -935 | High-level expression of sugar-inducible like 1 | 1.50 |
| 8.36 | Promoter (-1.1kb) | VIT_09x0002g00270 | -717 | R protein disease resistance protein | 1.56 |
| 8.32 | Promoter (-1.2kb) | VIT_13x0047g00010 | -1981 | ZIF2 [Zinc induced facilitator-like 1] | 1.74 |
| 8.23 | Promoter (-1.1kb) | VIT_05x0051g00730 | -43 | Zinc finger (C3HC4-type ring finger) | 1.75 |
| 8.15 | Promoter (-1.1kb) | VIT_09x0002g01590 | -256 | Nuclear transcription factor Y subunit A-8 | 2.15 |
| 8.12 | Promoter (-1.1kb) | VIT_18x0001g13450 | -588 | SLAH1 (SLAC1 homologue 1) | 3.50 |
| 7.75 | Promoter (-1.2kb) | VIT_14x0060g01970 | -1879 | F-box domain containing protein | 1.74 |
| 7.62 | Promoter (-1.2kb) | VIT_12x0028g00930 | -1278 | Glutathione S-transferase (VvGST3) | 1.81 |
| 7.61 | Promoter (-1.2kb) | VIT_09x0002g02680 | -1887 | Early flowering 3 | 2.00 |
| 7.41 | Promoter (-1.1kb) | VIT_01x0127g00590 | 0 | Protein disulfide isomerase | 2.75 |
| 7.41 | 5' UTR | VIT_01x0026g00280 | 290 | Trehalose 6-phosphate synthase | 1.51 |
| 7.16 | Promoter (-1.1kb) | VIT_08x0040g02180 | -126 | Mlo3 | 3.28 |
| 7.02 | Promoter (-1.1kb) | VIT_18x0001g00360 | -154 | Dehydrin (VvDHN2) | 1.86 |
| 6.91 | Promoter (-1.1kb) | VIT_04x0000g06330 | -157 | TPR1 (topless-related 1) | 2.08 |
| 6.85 | Promoter (-1.1kb) | VIT_11x0011g00740 | -95 | TIFY gene family (VvIAZ9) | 2.55 |
| 6.85 | Promoter (-1.1kb) | VIT_19x0014g04600 | -985 | S-kinase protein kinase | 1.79 |
| 6.83 | Promoter (-1.2kb) | VIT_14x0066g01240 | -1949 | L-aspartate oxidase | 2.91 |
| 6.78 | Promoter (-1.1kb) | VIT_04x0008g03770 | 0 | Aspartate aminotransferase P1 | 2.14 |
| 6.77 | Promoter (-1.2kb) | VIT_07x0005g00860 | -1673 | U3 snoRNP-associated helicase Ecm16 | 1.60 |
| 6.67 | Promoter (-1.2kb) | VIT_17x0000g00830 | -1879 | Nodulin MtN3 family | 6.09 |
| 6.61 | Promoter (-1.2kb) | VIT_08x0058g01130 | -1108 | WNKS (Arabidopsis WNK kinase 5) | 3.15 |
| 6.58 | Promoter (-1.1kb) | VIT_18x0001g00360 | -371 | Dehydrin (VvDHN2) | 1.86 |
| 6.07 | 5' UTR | VIT_11x0011g04490 | 444 | IAA16 | 1.66 |
| 6.06 | Promoter (-1.1kb) | VIT_07x0005g00660 | -590 | Late embryogenesis abundant protein 5 * | 6.76 |
| 5.95 | Promoter (-1.1kb) | VIT_10x0003g01500 | -816 | Zinc finger (C3HC4-type ring finger) | 2.63 |
| 5.83 | Promoter (-1.1kb) | VIT_15x0048g00530 | -644 | Auxin-responsive SAUR11 | 2.85 |
| 5.54 | Promoter (-1.1kb) | VIT_09x0002g00700 | -979 | Dormancy/auxin associated protein | 4.73 |
| 5.16 | Promoter (-1.1kb) | VIT_11x0011g00740 | -10 | Aspartic protease (VvAP23) | 2.77 |
| 4.92 | Promoter (-1.1kb) | VIT_08x0040g00040 | -233 | Ubiquitin-conjugating enzyme E2 D/E | 1.50 |
| 4.88 | Promoter (-1.1kb) | VIT_17x0000g07790 | -146 | N-hydroxythioamide 5-beta-glucosyltransferase | 3.22 |
| 4.78 | Promoter (-1.2kb) | VIT_03x0091g00690 | -1874 | Salt tolerance zinc finger | 1.66 |
| 4.64 | Promoter (-1.2kb) | VIT_17x0000g00830 | -1169 | Nodulin MtN3 family | 6.09 |
| 4.55 | Promoter (-1.1kb) | VIT_09x0002g02940 | -5 | Myo-inositol oxygenase 1 | 1.59 |
| 4.52 | Promoter (-1.1kb) | VIT_13x0011g02200 | -525 | Protein phosphatase 2CA AHG3 PP2CA (VvPPP2C-3) | 1.65 |
| 4.41 | Promoter (-1.1kb) | VIT_13x0011g02200 | -377 | Protein phosphatase 2CA AHG3 PP2CA (VvPPP2C-3) | 1.65 |
| 4.3 | Promoter (-1.1kb) | VIT_06x0004g07500 | -580 | WRKY Transcription Factor (VvWRKY16) | 2.27 |
| 4.1 | Promoter (-1.1kb) | VIT_01x0011g06460 | -54 | Deoxymugineic acid synthase | 2.86 |
| 4.01 | Promoter (-1.1kb) | VIT_12x0028g00930 | 0 | Glutathione S-transferase (VvGST3) | 1.81 |
| 3.94 | Promoter (-1.1kb) | VIT_06x0009g01630 | -412 | Cc-nbs-lrr resistance protein | 1.52 |
| 3.75 | Promoter (-1.1kb) | VIT_05x0020g05060 | -954 | Cellulose synthase CSLG2 | 2.17 |
| 3.72 | Promoter (-1.1kb) | VIT_04x0044g00110 | -215 | High-mobility group B 2 | 1.86 |
| 3.71 | Promoter (-1.1kb) | VIT_05x0020g01800 | -687 | Zinc finger (C3HC4-type ring finger) | 1.84 |
| 3.71 | Promoter (-1.1kb) | VIT_09x0002g09280 | 0 | Cysteine peptidase | 1.74 |
| 3.58 | Promoter (-1.1kb) | VIT_18x0001g07980 | -422 | CBL-interacting protein kinase 8 (CIPK8) | 1.59 |
| 3.54 | Promoter (-1.2kb) | VIT_10x0003g01390 | -1512 | Cupin, RmlC-type | 2.21 |
| 3.49 | Promoter (-1.1kb) | VIT_03x0063g00370 | -684 | Nitrite reductase | 3.38 |
| 3.11 | Promoter (-1.1kb) | VIT_16x0098g00290 | -644 | GLT1 (NADH-dependent glutamate synthase 1 gene) | 1.89 |
| 3.05 | Promoter (-1.2kb) | VIT_08x0007g04470 | -1484 | Vacuolar protein sorting 37C | 1.64 |
| 3.01 | Promoter (-1.1kb) | VIT_12x0028g03270 | -79 | Ethylene-responsive transcription factor 9 | 2.02 |
| 3 | Promoter (-1.2kb) | VIT_19x0014g00470 | -1470 | RKF1 (receptor-like kinase in flowers 1) | 1.53 |
| 2.88 | Promoter (-1.2kb) | VIT_19x0090g01870 | -1850 | ABC transporter (VvMRP26 - VvABC26) | 2.08 |
| 2.88 | Promoter (-1.1kb) | VIT_08x0003g02300 | 0 | High mobility group protein B1 | 1.70 |
| 2.83 | Promoter (-1.1kb) | VIT_19x0090g01530 | -794 | Pirin | 2.14 |
| 2.83 | Promoter (-1.1kb) | VIT_00x0424g00020 | -154 | Receptor serine/threonine kinase | 1.96 |
| 2.82 | 5' UTR | VIT_07x0104g00830 | 34 | Sugar transporter ERD6-like 7 * | 1.79 |
| 2.66 | Promoter (-1.1kb) | VIT_18x0001g07630 | -401 | NADPH-cytochrome P450 oxidoreductase isoform 1 | 1.75 |
| 2.63 | Promoter (-1.2kb) | VIT_18x0089g01030 | -1430 | ERF/AP2 Gene Family (VvERF017), Dehydration Responsive Element-Binding Transcription Factor (VvDREB30) | 4.04 |
| 2.63 | Promoter (-1.2kb) | VIT_11x0118g00480 | -1644 | Leucine-rich repeat | 1.75 |
| 2.63 | Promoter (-1.1kb) | VIT_09x0002g02940 | -269 | Myo-inositol oxygenase 1 | 1.59 |
| 2.62 | Promoter (-1.2kb) | VIT_01x0146g00180 | -1983 | Auxin responsive SAUR protein | 2.41 |
| 2.43 | Promoter (-1.1kb) | VIT_04x0044g00110 | -194 | High-mobility group B 2 | 1.86 |
| 2.22 | Promoter (-1.1kb) | VIT_19x0090g01170 | -194 | UPFD041 | 3.29 |
| 2.22 | Promoter (-1.2kb) | VIT_19x0014g04790 | -1503 | Organic cation/carnitine transporter4 | 2.94 |
| 2.22 | Promoter (-1.1kb) | VIT_15x0048g00530 | -749 | Auxin-responsive SAUR11 | 2.85 |
| 2.22 | Promoter (-1.1kb) | VIT_13x0147g00310 | 0 | ferredoxin | 2.00 |
| 2.21 | 5' UTR | VIT_05x0077g01140 | 104 | Basic Leucine Zipper Transcription Factor (VvZBP14) | 2.83 |
| 2.21 | Promoter (-1.1kb) | VIT_02x0012g02650 | -834 | Purple acid phosphatase 2 PAP2 | 2.44 |
| 2.21 | Promoter (-1.2kb) | VIT_00x0179g00260 | -1425 | Calcium-transporting ATPase 12 ACA12 | 1.96 |
| 2.21 | Promoter (-1.1kb) | VIT_04x0044g01620 | 0 | RGLG1 (ring Domain LIGASE1) | 1.88 |
| 2.15 | Promoter (-1.1kb) | VIT_14x0030g00570 | -233 | Copine BON3 (BONZAI 3) | 1.82 |

Table 52: VviNAC60 DAP-seq targets genes which have a match in the VviNAC60 stable over expression dataset and resulted up regulated.

In bold are reported the *switch* genes and the asterisk (*) refers to the transition markers.

| q-value | Genic region | Gene ID | Distance to TSS | Functional annotation | Stable OE |
|---------|------------------|-------------------|-----------------|--|-----------|
| 48.47 | Promoter (<=1kb) | VIT_02s0025g02390 | -587 | Oligopeptide transporter OPT7 | -2,37 |
| 48.47 | Promoter (<=1kb) | VIT_09s0002g06970 | -150 | Palmitoyl-monogalactosyl diacylglycerol delta-7 desaturase, chloroplast | -2,00 |
| 31.22 | Promoter (<=1kb) | VIT_01s0150g00480 | -853 | Protein binding protein | -2,16 |
| 27.56 | Promoter (1-2kb) | VIT_07s0031g01600 | -1342 | Shikimate kinase | -1,64 |
| 25.41 | Promoter (1-2kb) | VIT_10s0003g03690 | -1593 | Beta-1,3-glucanase precursor | -4,43 |
| 22.91 | Promoter (<=1kb) | VIT_15s0021g02280 | -456 | Matrix metalloproteinase | -2,88 |
| 22.51 | Promoter (<=1kb) | VIT_04s0069g00860 | -352 | Sarcosine oxidase * | -5,81 |
| 21.46 | Promoter (<=1kb) | VIT_06s0004g06730 | -422 | Microsomal omega-3 fatty acid desaturase | -16,75 |
| 21.2 | Promoter (<=1kb) | VIT_01s0026g02500 | -167 | Amino acid transport protein | -5,98 |
| 19.77 | Promoter (1-2kb) | VIT_08s0040g02470 | -1035 | Inorganic pyrophosphatase | -1,56 |
| 17.34 | Promoter (<=1kb) | VIT_17s0000g05470 | -3 | Nodulin | -1,69 |
| 17.28 | Promoter (<=1kb) | VIT_05s0020g04210 | -661 | Sulfate adenylyltransferase 3 | -2,64 |
| 16.46 | Promoter (<=1kb) | VIT_00s0227g00140 | 0 | MLO1 | -1,66 |
| 14.96 | Promoter (<=1kb) | VIT_18s0001g12990 | -881 | Anthranilate N-benzoyltransferase protein 1 | -3,27 |
| 13.03 | Promoter (1-2kb) | VIT_02s0025g04720 | -1484 | Leucoanthocyanidin dioxygenase (VvLDOX) [Vitis vinifera] | -4,08 |
| 12.61 | Promoter (<=1kb) | VIT_06s0004g02380 | 0 | Cinnamyl alcohol dehydrogenase | -1,78 |
| 12.49 | Promoter (1-2kb) | VIT_08s0058g00960 | -1898 | basic helix-loop-helix (bHLH) family | -2,62 |
| 10.57 | Promoter (1-2kb) | VIT_17s0000g04810 | -1963 | Auxin-independent growth promoter | -1,75 |
| 10.34 | Promoter (<=1kb) | VIT_06s0004g00720 | -256 | Glucan endo-1,3-beta-glucosidase 4 precursor | -1,98 |
| 9.98 | Promoter (1-2kb) | VIT_01s0011g05600 | -1986 | Receptor-like protein kinase | -3,05 |
| 9.69 | Promoter (1-2kb) | VIT_02s0025g04720 | -1399 | Leucoanthocyanidin dioxygenase (VvLDOX) [Vitis vinifera] | -4,08 |
| 9.69 | Promoter (<=1kb) | VIT_01s0026g01480 | -47 | Adenosine/AMP deaminase active site | -1,70 |
| 8.9 | Promoter (<=1kb) | VIT_10s0003g00330 | -881 | HSL1 (HAESA-like 1) | -2,31 |
| 8.9 | Promoter (<=1kb) | VIT_16s0022g00540 | -190 | Glycerol 3-phosphate permease | -1,90 |
| 8.66 | Promoter (<=1kb) | VIT_18s0117g00130 | 0 | Pi starvation-induced protein * | -1,60 |
| 7.9 | Promoter (<=1kb) | VIT_19s0090g00830 | 0 | Aspartic Protease (VvAP45) * | -3,28 |
| 7.9 | Promoter (1-2kb) | VIT_14s0068g00920 | -1576 | chalcone synthase 2 (CHS2) | -2,82 |
| 7.35 | Promoter (1-2kb) | VIT_07s0104g00540 | -1850 | CYCP1.1; CYCP1.1 * | -1,86 |
| 6.83 | Promoter (<=1kb) | VIT_14s0068g00920 | -749 | chalcone synthase 2 (CHS2) | -2,82 |
| 6.55 | Promoter (<=1kb) | VIT_04s0008g01120 | -709 | Glutaredoxin | -1,82 |
| 6.38 | Promoter (<=1kb) | VIT_06s0004g01890 | -778 | Cu2+-exporting ATPase HMA5 (heavy metal ATPase 5) | -2,12 |
| 5.76 | Promoter (<=1kb) | VIT_12s0028g03050 | -414 | NAC domain-containing protein (VvNAC34) | -2,51 |
| 5.49 | Promoter (1-2kb) | VIT_00s0445g00010 | -1276 | Strubbelig receptor family 1 | -1,64 |
| 5.36 | Promoter (<=1kb) | VIT_01s0011g05600 | 0 | Receptor-like protein kinase | -3,05 |
| 5.36 | Promoter (<=1kb) | VIT_12s0059g01560 | -131 | Protein disulfide-isomerase A6 | -2,19 |
| 5.15 | Promoter (1-2kb) | VIT_05s0049g00880 | -1481 | Activating signal cointegrator | -1,86 |
| 5.12 | Promoter (<=1kb) | VIT_18s0001g10040 | -570 | LRX1 (leucine-rich repeat/extensin 1) | -2,41 |
| 5.04 | Promoter (<=1kb) | VIT_03s0091g00630 | 0 | YGGT family protein | -2,04 |
| 5.04 | Promoter (<=1kb) | VIT_06s0004g06930 | -173 | Zinc finger (C3HC4-type ring finger) | -1,99 |
| 5.01 | Promoter (<=1kb) | VIT_11s0016g04630 | -938 | GAI protein. | -2,77 |
| 4.92 | Promoter (1-2kb) | VIT_06s0004g01050 | -1215 | Calcineurin phosphoesterase | -7,08 |
| 4.86 | Promoter (<=1kb) | VIT_05s0051g00660 | -797 | Octicosapeptide/Phox/Bem1p; Protein kinase | -2,58 |
| 4.71 | Promoter (<=1kb) | VIT_12s0059g01560 | -343 | Protein disulfide-isomerase A6 | -2,19 |
| 4.71 | Promoter (<=1kb) | VIT_17s0000g08080 | -251 | Armadillo/beta-catenin repeat protein / U-box domain-containing protein | -1,96 |
| 4.44 | Promoter (1-2kb) | VIT_06s0004g05850 | -1708 | Zinc finger (C3HC4-type ring finger) | -1,53 |
| 4.17 | Promoter (<=1kb) | VIT_01s0011g03910 | -95 | Protein phosphatase 2C | -1,63 |
| 4.1 | Promoter (<=1kb) | VIT_19s0015g01760 | -201 | Photosystem I reaction center subunit V (PSAV) | -2,13 |
| 4.09 | Promoter (<=1kb) | VIT_06s0004g03810 | -36 | Kinesin motor protein * | -2,12 |
| 4.06 | Promoter (<=1kb) | VIT_07s0005g00010 | -95 | Glutathione S-transferase 8 GSTF8 | -2,24 |
| 4.06 | Promoter (<=1kb) | VIT_18s0001g09460 | -423 | GASAs | -1,64 |
| 4.04 | Promoter (<=1kb) | VIT_14s0068g01540 | -74 | PBS1 (avrPphB susceptible 1) | -1,51 |
| 3.88 | Promoter (1-2kb) | VIT_08s0007g02000 | -1938 | Glycerol-3-phosphate acyltransferase 8 | -3,26 |
| 3.72 | Promoter (1-2kb) | VIT_11s0103g00550 | -1927 | Subtilisin-like serine protease 3 | -1,92 |
| 3.71 | Promoter (<=1kb) | VIT_10s0003g01490 | -476 | NIK3 (NSP-interacting kinase 3) | -1,81 |
| 3.66 | Promoter (<=1kb) | VIT_18s0001g13380 | -431 | Papain cysteine proteinase isoform I | -19,77 |
| 3.49 | Promoter (<=1kb) | VIT_14s0066g02020 | -160 | Proton-dependent oligopeptide transport (POT) family protein | -5,63 |
| 3.45 | Promoter (<=1kb) | VIT_07s0104g00350 | -139 | Circadian clock coupling factor ZGT | -1,80 |
| 3.11 | Promoter (1-2kb) | VIT_08s0007g03060 | -1583 | Beta-fructofuranosidase | -2,09 |
| 3.11 | Promoter (<=1kb) | VIT_10s0003g05420 | -239 | S-2-hydroxy-acid oxidase, peroxisomal | -2,06 |
| 3.05 | Promoter (<=1kb) | VIT_18s0001g10580 | -684 | Glycosyl transferase family 8 protein | -2,49 |
| 3.05 | Promoter (1-2kb) | VIT_17s0000g08290 | -1344 | Dof zinc finger protein DOFS 6 | -2,49 |
| 2.74 | Promoter (1-2kb) | VIT_04s0008g01150 | -1766 | Beta-fructosidase (BFRUCT1) | -3,58 |
| 2.72 | Promoter (<=1kb) | VIT_17s0000g08080 | -400 | Armadillo/beta-catenin repeat protein / U-box domain-containing protein | -1,96 |
| 2.7 | Promoter (<=1kb) | VIT_06s0004g00030 | 0 | S-adenosyl-L-methionine:salicylic acid carboxyl methyltransferase | -1,92 |
| 2.66 | Promoter (1-2kb) | VIT_18s0001g04680 | -1042 | RPG related protein 1 RR1 | -1,75 |
| 2.62 | Promoter (<=1kb) | VIT_15s0021g00050 | -758 | Eceriferum 1 (CER1 protein) Sterol desaturase | -4,69 |
| 2.62 | Promoter (1-2kb) | VIT_04s0069g00780 | -1613 | Cellulose synthase CSLC05 * | -2,80 |
| 2.54 | Promoter (<=1kb) | VIT_05s0020g01980 | -106 | Acyl carrier protein, mitochondrial 3 | -4,54 |
| 2.49 | Promoter (<=1kb) | VIT_05s0020g04100 | -712 | Dymeclin | -1,77 |
| 2.43 | Promoter (<=1kb) | VIT_04s0069g00860 | -431 | Sarcosine oxidase * | -5,81 |
| 2.43 | Promoter (<=1kb) | VIT_00s0179g00150 | -946 | Heat shock transcription factor A6B | -2,95 |
| 2.43 | Promoter (<=1kb) | VIT_04s0023g01800 | -13 | Maf, septum formation protein * | -1,62 |
| 2.42 | Promoter (<=1kb) | VIT_18s0089g01410 | -293 | Purine permease 4 PUP4 | -1,63 |
| 2.22 | Promoter (<=1kb) | VIT_11s0103g00370 | -949 | Cd2+-exporting ATPase HMA2 (Heavy metal ATPase 2) | -2,34 |
| 2.22 | Promoter (<=1kb) | VIT_16s0050g02520 | 0 | RNA polymerase sigma subunit SigE (SigE) | -2,08 |
| 2.22 | Promoter (1-2kb) | VIT_12s0059g00670 | -1917 | NADP-dependent oxidoreductase | -1,80 |
| 2.21 | Promoter (1-2kb) | VIT_05s0051g00050 | -1769 | Myosin-like protein XIB | -2,99 |
| 2.21 | Promoter (1-2kb) | VIT_05s0077g02330 | -1555 | Transducin protein | -2,61 |
| 2.01 | Promoter (1-2kb) | VIT_04s0008g01150 | -1913 | Beta-fructosidase (BFRUCT1) | -3,58 |
| 2.01 | Promoter (<=1kb) | VIT_01s0137g00560 | 0 | CYP71B34 | -2,12 |
| 2.01 | Promoter (<=1kb) | VIT_03s0063g00390 | 0 | Lag one homologue 2 | -2,05 |

Table 53: VviNAC60 DAP-seq targets genes which have a match in the VviNAC60 stable over expression dataset and resulted down regulated. In bold are reported the *switch* genes and the asterisk (*) refers to the transition markers.

Looking at the DAP-seq correlation with the VviNAC60 transient over expression, between the up regulated genes (Table 54) a *CELLULOSE SYNTHASE CSLG2* (VIT_05s0020g05060) was found; this is a gene related to the pectin metabolism

genes and is associated with the inner pollen grain wall or intine (Fasoli *et al.*, 2012). Low auxin levels are required to trigger the onset of ripening but, at the same time, high auxin levels at pre-veraison stages are required for the induction of genes involved in the ripening inception (Zenoni *et al.*, 2017). The regulation of auxin levels is associated with the conjugation of indole acetic acid by the indol-3-acetate beta-glucosyltransferase, which allows an increase in the conjugated form of auxin after veraison. Interestingly, an *INDOLE-3-ACETATE BETA-GLUCOSYLTRANSFERASE* (VIT_06s0004g07230) was found between the *VviNAC60* targets and up regulated by *VviNAC60* transient over expression.

The *SENESCENCE-INDUCIBLE CHLOROPLAST STAY-GREEN PROTEIN 1* (VIT_02s0025g04660), with three *VviNAC60* binding sites in its promoter region, was also found up regulated; it is involved in chlorophyll and photosystem degradation.

Between the DAP-found *VviNAC60* transient over expression down regulated genes (Table 55), no particularly relevant gene was present.

| q-value | Genic region | Gene ID | Distance to TSS | Functional annotation | Transient OE |
|---------|------------------|-------------------|-----------------|---|--------------|
| 79,94 | Promoter (1-2kb) | VIT_05s0020g05060 | -1053 | Cellulose synthase CSLG2 | 2,07 |
| 71,32 | Promoter (<=1kb) | VIT_18s0001g11740 | -375 | Ring zinc finger ariadne protein ARI2 | 1,57 |
| 35,96 | Promoter (1-2kb) | VIT_05s0020g05060 | -1084 | Cellulose synthase CSLG2 | 2,07 |
| 31,94 | Promoter (<=1kb) | VIT_18s0001g09910 | -102 | L-asparaginase | 2,17 |
| 29,09 | Promoter (<=1kb) | VIT_06s0004g07230 | 0 | Indole-3-acetate beta-glucosyltransferase | 3,45 |
| 21,46 | Promoter (1-2kb) | VIT_02s0025g04660 | -1062 | Senescence-inducible chloroplast stay-green protein 1 | 5,74 |
| 17,24 | Promoter (<=1kb) | VIT_18s0001g12040 | -185 | Coniferyl-alcohol glucosyltransferase | 1,73 |
| 16,11 | Promoter (1-2kb) | VIT_18s0075g00550 | -1310 | RuvB DNA helicase protein | 1,98 |
| 15 | Promoter (<=1kb) | VIT_02s0025g04660 | -129 | Senescence-inducible chloroplast stay-green protein 1 | 5,74 |
| 12,02 | Promoter (1-2kb) | VIT_08s0007g02100 | -1896 | Alpha-1,4-glycosyltransferase | 1,85 |
| 11,28 | Promoter (1-2kb) | VIT_10s0003g03190 | -1612 | RNA recognition motif (RRM)-containing | 1,62 |
| 10,92 | Promoter (<=1kb) | VIT_10s0003g05690 | -884 | Ribulose biphosphate carboxylase, large chain | 1,88 |
| 9,17 | 5' UTR | VIT_18s0001g14710 | 237 | Ketol-acid reductoisomerase precursor | 1,61 |
| 6,06 | Promoter (<=1kb) | VIT_16s0050g00950 | -606 | Scarecrow-like transcription factor 8 (SCL8) | 1,82 |
| 5,04 | Promoter (<=1kb) | VIT_10s0003g05690 | 0 | Ribulose biphosphate carboxylase, large chain | 1,88 |
| 4,8 | Promoter (<=1kb) | VIT_02s0025g04660 | -174 | Senescence-inducible chloroplast stay-green protein 1 | 5,74 |
| 4,65 | Promoter (1-2kb) | VIT_15s0046g00490 | -1346 | Wax synthase | 3,12 |
| 4,18 | 5' UTR | VIT_18s0001g14710 | 437 | Ketol-acid reductoisomerase precursor | 1,61 |
| 3,82 | Promoter (<=1kb) | VIT_13s0156g00590 | -34 | S-receptor kinase | 2,23 |
| 3,75 | Promoter (<=1kb) | VIT_05s0020g05060 | -954 | Cellulose synthase CSLG2 | 2,07 |
| 2,74 | 5' UTR | VIT_16s0050g00950 | 137 | Scarecrow-like transcription factor 8 (SCL8) | 1,82 |
| 2,65 | Promoter (<=1kb) | VIT_15s0046g03380 | -932 | Thiol protease | 1,62 |
| 2,43 | Promoter (<=1kb) | VIT_08s0007g02100 | -136 | Alpha-1,4-glycosyltransferase | 1,85 |
| 2,42 | Promoter (<=1kb) | VIT_05s0077g00280 | -32 | Beta-amylase | 1,56 |
| 2,22 | Promoter (1-2kb) | VIT_19s0014g04790 | -1503 | Organic cation/carnitine transporter4 | 1,55 |

Table 54: *VviNAC60* DAP-seq targets genes which have a match in the *VviNAC60* transient over expression dataset and resulted up regulated. In bold are reported the *switch* genes and the asterisk (*) refers to the transition markers.

| q-value | Genic region | Gene ID | Distance to TSS | Functional annotation | Transient OE |
|---------|------------------|-------------------|-----------------|------------------------------|--------------|
| 50,7 | Promoter (<=1kb) | VIT_19s0014g03370 | 0 | Methyltransferase type 11 | -1,68 |
| 9,43 | Promoter (<=1kb) | VIT_14s0068g01570 | -405 | Glutaredoxin-like | -1,99 |
| 7,1 | Promoter (<=1kb) | VIT_10s0003g04270 | -76 | BCL2 binding anthogene | -1,70 |
| 4,32 | Promoter (<=1kb) | VIT_10s0003g04270 | -22 | BCL2 binding anthogene | -1,70 |
| 3,71 | Promoter (<=1kb) | VIT_02s0154g00080 | -114 | Multi-copper oxidase (SKU5) | -2,29 |
| 3,64 | Promoter (1-2kb) | VIT_05s0077g00620 | -1296 | O-acetyltransferase | -1,54 |
| 3,58 | Promoter (1-2kb) | VIT_16s0050g01610 | -1530 | UDP-glycosyltransferase 88A4 | -1,77 |
| 3,27 | 5' UTR | VIT_05s0094g01140 | 1817 | Allyl alcohol dehydrogenase | -2,46 |
| 2,21 | 5' UTR | VIT_01s0010g02910 | 3862 | ATP binding protein | -2,09 |

Table 55: *VviNAC60* DAP-seq targets genes which have a match in the *VviNAC60* transient over expression dataset and resulted down regulated.

VviNAC61

The DAP-seq assay reported only 76 binding sites (peaks), which were reduced to 73 after the $FC > 5$ filtering; the loss was around the 4% (**Fig. 64**).

The distribution of peaks revealed that 30% were located within the promoter regions (up to 2 kb upstream from a transcription start site), 3% were in 5' untranslated regions (UTRs), 13% were located in exons, 5% were located within introns, 3% were located in 3' UTRs, 12% were located in the 3 kb downstream region, and 30% were intergenic.

The number of regulatory sites was very low but the percentage of binding sites in the promoter and 5' UTR regions was in line, even a little bit higher, with literature. Considering the good results obtained in the transient over expression of the gene, the DAP-seq assay on VviNAC61 is going to be repeated as soon as possible to validate the findings of the transient over expression and improve the knowledges on the post-harvest (withering) processes (Zenoni *et al.*, 2016).

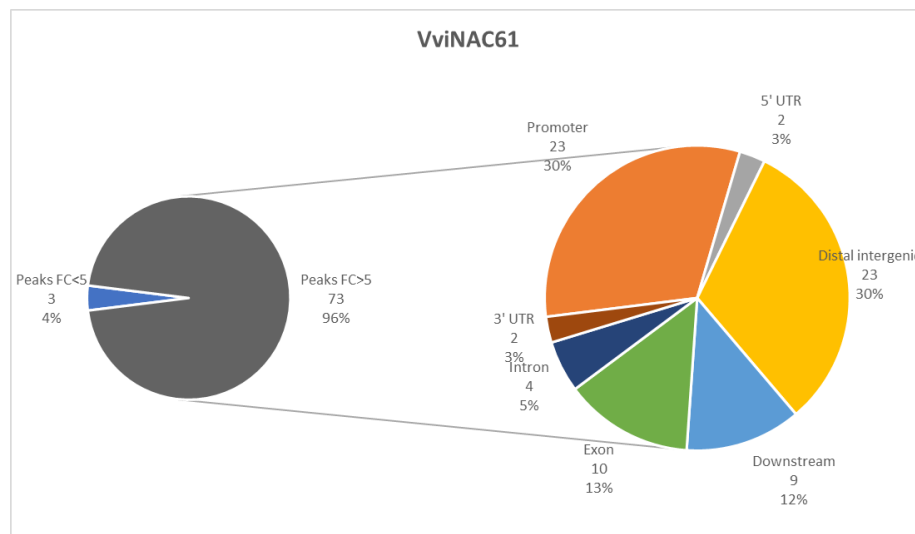


Figure 64: Double pie chart of the VviNAC61 DAP-seq results. The pie on the left represents the total binding sites (peaks) obtained, divided between the $FC > 5$ and $FC < 5$ (compared to the GST-Halo negative control peaks). The pie on the right represents the subdivision into the different genic region of the selected filtered peaks.

A principal binding motif (TTGCGTGT) was identified (**Fig. 65**) and the phylogenetic footprints correlate with ANAC058, for which not much information is available.

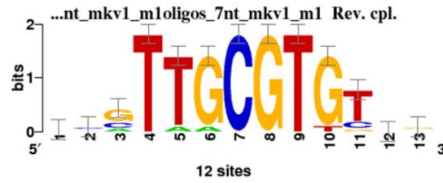


Figure 65: RSAT Plants NGS ChIP-Seq peak motifs analysis on the VviNAC61 DAP-seq results. Top-ranking binding motif identified in the DAP-seq FC>5 filtered dataset, based on the detection of overrepresented oligonucleotides (oligo analysis). The overall height of each letter stack indicates the sequence conservation at that position, and the height of symbols within the stack reflects the relative frequency of the corresponding nucleic acid at that position.

The attention was not focused only on the 33% (25 sites) of the final analyzed binding sites, as was done for almost all the VviNACs TF.

All the DAP-seq dataset was taken in consideration but the ‘no hit’ and ‘unknown’ elements were eliminated as usual.

59 binding sites were obtained for a total of 59 unique genes regulated by VviNAC61.

A GO enrichment analysis was performed, revealing a predominance of genes related to the regulation of metabolic processes, aromatic compounds biosynthetic processes and response to jasmonic acid (**Fig. 66**).

Then, the previously reported *VviNAC61* transient over expression results (FC>|1.5|) were crossed with the DAP-seq dataset, revealing only 3 correlated binding sites (**Table 56**): the up regulated *DISEASE RESISTANCE PROTEIN NBS-LRR CLASS* (VIT_19s0027g01630), which TF binding site is in the ‘promoter’ region, and *EMB2454 EMBRYO DEFECTIVE 2454* (VIT_17s0000g05480), and the down regulated *FRUCTOSE-1,6-BISPHOSPHATASE, CYTOSOLIC* (VIT_18s0072g00770). Always in the ‘promoter’ region, the *VviWRKY14* (VIT_05s0077g00730), which is known to be highly expressed in berries and rachis during or following veraison (Wang *et al.*, 2014), and two ethylene-related genes, *ETHYLENE-RESPONSIVE TRANSCRIPTION FACTOR 9* (VIT_12s0028g03270) and *ERF/AP2 GENE FAMILY VvERF058* (VIT_05s0077g01860), were found.

Interestingly, also a *LACCASE* (VIT_18s0122g00520) was found between the VviNAC61 target genes; unfortunately, the TF binding site was revealed in the ‘distal intergenic’ region at -16831 bp from the TSS and is difficult to validate with other methods the real interaction.

Unfortunately, no VviNACs target genes were found. However, these first findings

are a good result and the new DAP-seq assay will certainly unravel the VviNAC61 regulatory network.

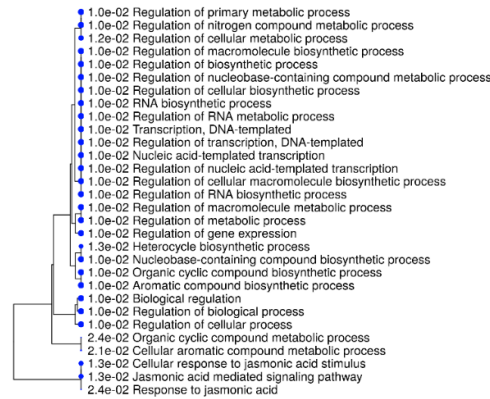


Figure 66: GO enrichment analysis of the VviNAC61 targets found to be regulated in the promoter and 5'UTR regions. The analysis was performed on ShinyGO.

| q-value | Genic region | Gene ID | Distance to TSS | Functional annotation | Transient OE |
|---------|--|-------------------|-----------------|--|--------------|
| 5.57 | Exon (mRNA27258/VIT_04s0008g02380, exon 1 of 2) | VIT_04s0008g02380 | 819 | Kelch repeat-containing F-box protein | |
| 4.29 | Distal Intergenic | VIT_08s0105g00230 | -13948 | BLH1 (embryo sac development arrest 29) | |
| 4.06 | Downstream (1-2kb) | VIT_17s0000g04850 | 1832 | OBF binding protein 4 | |
| 4.05 | Distal Intergenic | VIT_18s0086g00180 | -147831 | MATE efflux family protein | |
| 4.04 | Distal Intergenic | VIT_14s0081g00520 | -12785 | ERF12 | |
| 3.59 | Promoter (1-2kb) | VIT_07s0191g00050 | -1874 | Peroxidase 17 * | |
| 3.52 | Promoter (<=1kb) | VIT_12s0028g03270 | -100 | Ethylene-responsive transcription factor 9 | |
| 3.52 | Distal Intergenic | VIT_06s0009g00580 | -5284 | Receptor protein kinase | |
| 3.51 | Distal Intergenic | VIT_10s0003g02010 | -3315 | RKF1 (receptor-like kinase in flowers 1) | |
| 3.43 | Promoter (1-2kb) | VIT_12s0059g00870 | -1273 | MAPKKK15 | |
| 3.31 | Exon (mRNA11075/VIT_14s0036g00870, exon 1 of 1) | VIT_14s0036g00870 | 653 | Acyl-CoA ligase | |
| 3.08 | Promoter (<=1kb) | VIT_19s0015g00930 | -272 | Hydroxyproline-rich glycoprotein | |
| 3 | Distal Intergenic | VIT_19s0015g01930 | 2462 | LAS (lateral suppressor) | |
| 2.85 | Downstream (2-3kb) | VIT_15s0048g01320 | 4494 | Gibberellin 20-oxidase | |
| 2.65 | Intron (mRNA11877/VIT_18s0041g02430, intron 2 of 9) | VIT_18s0041g02430 | 3416 | abscisic aldehyde oxidase (AAO3) (VVA003) | |
| 2.65 | Exon (mRNA14409/VIT_15s0046g01600, exon 1 of 2) | VIT_15s0046g01600 | 23 | Acidic endochitinase (CHIB1) | |
| 2.64 | Exon (mRNA13719/VIT_17s0000g08720, exon 6 of 7) | VIT_17s0000g08720 | 2549 | RKF2 (receptor-like serine/threonine kinase 2) | |
| 2.63 | Distal Intergenic | VIT_12s0134g00160 | -2133 | Xyloglucan endotransglycosylase/hydrolase 16 | |
| 2.51 | Promoter (1-2kb) | VIT_17s0000g08950 | -1089 | D111/G-patch | |
| 2.51 | Downstream (1-2kb) | VIT_19s0015g00770 | 6363 | Protein kinase G11A | |
| 2.51 | Distal Intergenic | VIT_01s0011g05560 | 10260 | TIFY gene family (VvJAZ1) | |
| 2.49 | Exon (mRNA2054/VIT_11s0037g00580, exon 2 of 2) | VIT_11s0037g00580 | 1010 | Anthranilate N-hydroxycinnamoyl/benzoyltransferase | |
| 2.47 | Distal Intergenic | VIT_01s0026g00740 | -7622 | Nucleobase-ascorbate transporter 6 (NAT6) | |
| 2.36 | Promoter (<=1kb) | VIT_06s0004g03900 | -540 | Calcium-transporting ATPase 1, endoplasmic reticulum-type ECA1 | |
| 2.35 | Distal Intergenic | VIT_13s0158g00370 | 6396 | RNA recognition motif (RRM)-containing CCHC | |
| 2.35 | Distal Intergenic | VIT_04s0044g00870 | -3866 | U-box domain containing protein | |
| 2.31 | Promoter (<=1kb) | VIT_04s0044g00710 | -161 | UTP--glucose-1-phosphate uridylyltransferase * | |
| 2.31 | Downstream (2-3kb) | VIT_07s0130g00460 | 2972 | SWIB complex BAF60b domain-containing protein | |
| 2.31 | Downstream (<1kb) | VIT_08s0007g08320 | 3417 | Pentatricopeptide (PPR) repeat-containing | |
| 2.3 | Promoter (<=1kb) | VIT_10s0042g01150 | -6 | ARGONAUTE 2 (AGO2) | |
| 2.3 | Promoter (<=1kb) | VIT_11s0016g01130 | -360 | MTD1 | |
| 2.3 | Intron (mRNA20379/VIT_08s0007g08270, intron 2 of 2) | VIT_08s0007g08280 | 1991 | Remorin | |
| 2.29 | Promoter (<=1kb) | VIT_17s0000g05480 | -519 | EMB2454 (embryo defective 2454) | 1.57 |
| 2.29 | Promoter (<=1kb) | VIT_04s0008g04370 | -903 | Nucleic acid binding | |
| 2.29 | Exon (mRNA21353/VIT_13s0064g00390, exon 7 of 10) | VIT_13s0064g00390 | 4340 | Polyamine oxidase | |
| 2.29 | Distal Intergenic | VIT_19s0014g03000 | 21567 | Leucine-rich repeat-containing protein 40 | |
| 2.28 | Distal Intergenic | VIT_08s0040g02900 | -4051 | Aluminum sensitive 3 | |
| 2.26 | Exon (mRNA29767/VIT_06s0009g02110, exon 1 of 2) | VIT_06s0009g02110 | 714 | Kelch repeat-containing F-box family protein | |
| 2.21 | Promoter (<=1kb) | VIT_18s0001g13270 | 0 | Papain cysteine peptidase XBCP3 | |
| 2.21 | Promoter (<=1kb) | VIT_06s0061g01190 | -134 | SWI/SNF matrix-associated regulator of chromatin sbfamily A mber 3 2 | |
| 2.15 | Exon (mRNA14074/VIT_05s0020g03310, exon 3 of 4) | VIT_05s0020g03310 | 1399 | Diamine oxidase | |
| 2.15 | Distal Intergenic | VIT_08s0040g02730 | -3066 | Exocyst subunit EXO70 H4 | |
| 2.14 | Promoter (1-2kb) | VIT_10s0003g02820 | -1128 | O-acetyltransferase | |
| 2.14 | Promoter (<=1kb) | VIT_05s0077g01860 | -204 | ERF/AP2 Gene Family (VvERF058) | |
| 2.13 | Downstream (1-2kb) | VIT_18s0072g00770 | 6002 | fructose-1,6-bisphosphatase, cytosolic | |
| 2.13 | Distal Intergenic | VIT_17s0000g08150 | 6259 | basic helix-loop-helix (bHLH) family | -1.62 |
| 2.13 | Distal Intergenic | VIT_05s0051g00580 | -10927 | Inosine triphosphate pyrophosphatase | |
| 2.12 | Promoter (1-2kb) | VIT_04s0023g01230 | -1203 | T-complex protein 1 subunit delta | |
| 2.12 | Promoter (<=1kb) | VIT_05s0062g01000 | -989 | Aldo/keto reductase * | |
| 2.12 | Intron (mRNA26650/VIT_00s0324g00050, intron 1 of 2) | VIT_00s0324g00050 | 4476 | UDP-glucose glucosyltransferase | |
| 2.12 | Intron (mRNA19400/VIT_05s0102g00360, intron 5 of 11) | VIT_05s0102g00360 | 8794 | On-specific serine/threonine protein kinase | |
| 2.12 | Distal Intergenic | VIT_19s0027g01630 | 15308 | Disease resistance protein (NBS-LRR class) | 1.65 |
| 2.11 | Promoter (<=1kb) | VIT_13s0067g01920 | 0 | Exportin 7 | |
| 2.11 | Distal Intergenic | VIT_18s0122g00050 | -16831 | Laccase | |
| 2.07 | Downstream (2-3kb) | VIT_01s0026g02030 | 3322 | basic helix-loop-helix (bHLH) family | |
| 2.06 | Promoter (<=1kb) | VIT_08s0040g02210 | -861 | Lectin protein kinase | |
| 2.06 | Distal Intergenic | VIT_18s0001g00840 | -14933 | Syringolide-induced protein 14-1-1 | |
| 2.06 | 5' UTR | VIT_06s0004g06240 | 328 | Zinc finger (C2H2 type) family | |
| 2.05 | Promoter (1-2kb) | VIT_05s0077g00730 | -1909 | WRKY Transcription Factor (VvWRKY14) | |

Table 56: VviNAC61 DAP-seq targets genes and VviNAC61 transient over expression fold-change values. The asterisk (*) refers to the transition markers.

VviNACs regulation of the *Vitis vinifera* genes

After all the individual analyses on all the 14 above described VviNACs, with the aim to try understanding the general regulative role of the selected VviNAC family members on the grapevine transcriptome, a global analysis of all the possible interactions obtained with the DAP-seq assays was performed.

All the annotated *V. vinifera* genes were listed and, once eliminated all the ‘no hit’ and ‘unknown’, the most represented genes between all the DAP-seq results were identified. In this case all the binding sites in all the possible genic regions were taken into consideration, not only the promoter and 5’UTR one.

Ideally, in this way a general observation concerning the mostly regulated (by these TFs) classes of genes should be possible.

13713 genes resulted as direct targets of at least one of the 14 selected VviNACs.

In **Figure 67** are reported the numbers of genes regulated by a different number of TFs.

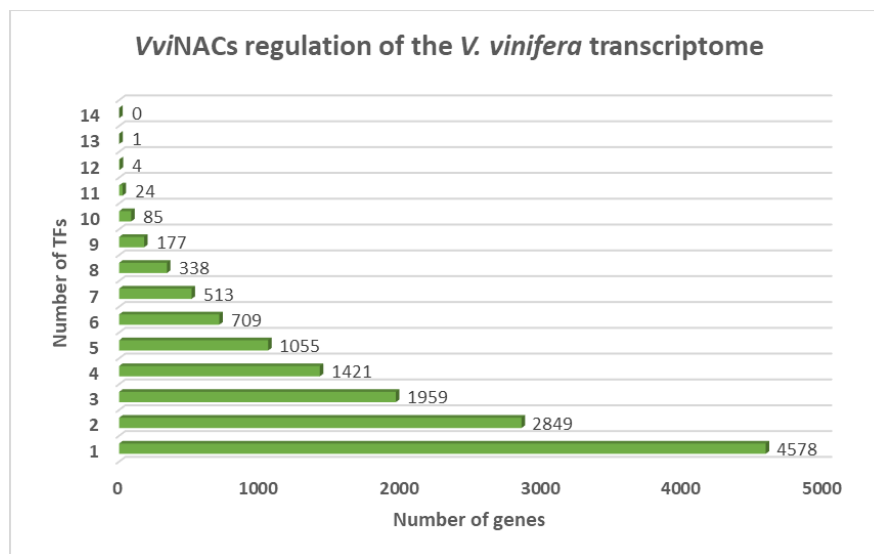


Figure 67: Bar chart reporting the number of annotated *V. vinifera* genes regulated by a different number of the selected VviNACs.

4578 genes were specifically regulated by only one the previously described TFs and only one gene, *UTP--GLUCOSE-1-PHOSPHATE URIDYLYLTRANSFERASE* (VIT_04s0044g00710), was regulated by 13 of the 14 VviNACs; the only TF which did not regulate this gene was VviNAC08.

Not much information is available in literature concerning this gene, excluding the

fact that it encodes for an enzyme obviously related to the carbohydrate metabolism. For this reason, the Atlas (Fasoli *et al.*, 2012) was again investigated to see if this gene could have an interesting expression profile. Considering its role in the sugar metabolism, a specific focus was done on the berry and seed tissues at the different developmental stages (**Fig. 68**).

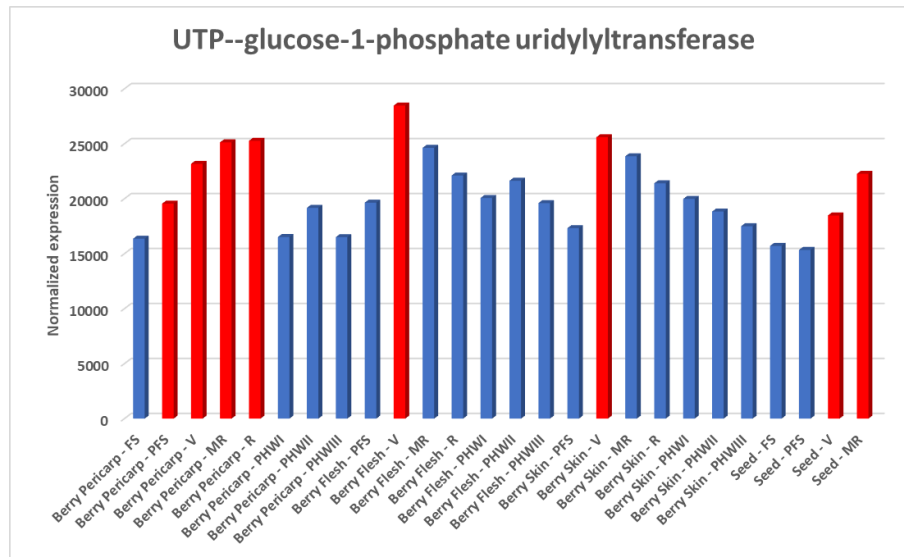


Figure 68: Bar chart reporting the expression profile in the Atlas (Fasoli *et al.*, 2012) of the *UTP-GLUCOSE-1-PHOSPHATE URIDYLYLTRANSFERASE*. Description of ATLAS abbreviations (54 developmental stages): **Berry Pericarp** – FS =fruit set; – PFS = post-fruit set; – V = véraison; – MR = mid-ripening; – R = ripening; – PHWI = post- harvest withering I; – PHWII = post-harvest withering II; – PHWIII = post-harvest withering III; **Berry Skin** – PFS = post-fruit set; – V = véraison; – MR = mid-ripening; – R = ripening; – PHWI = post-harvest withering I; – PHWII = post-harvest withering II; – PHWIII = post-harvest withering III; **Berry Flesh** – PFS = post-fruit set; – V = véraison; – MR = mid-ripening; – R = ripening; – PHWI = post-harvest withering I; – PHWII = post-harvest withering II; – PHWIII = post-harvest withering III; **Seed** – FS = fruit set; – PFS = post-fruit set; – V = véraison; – MR = mid-ripening.

The gene was always abundantly expressed in all the organs at all the developmental stages. However, a significant increase was interestingly noticed in the berry pericarp starting from the post fruit set to the ripening, in the berry flesh and skin at veraison and in the seeds at veraison and mid ripening.

Between the genes regulated by 12 TFs, the *3-METHYL-2-OXOBUTANOATE DEHYDROGENASE* (VIT_18s0001g14980) was found, as expected from the single TF DAP-seq analyses in which it was very often present also in the first positions (q-value based).

Moreover, a *BLH1 EMBRYO SAC DEVELOPMENT ARREST 29*

(VIT_08s0105g00230) and an *EXPANSIN* *VvEXPA18* (VIT_17s0053g00990), important for the plant cell wall growth (Marowa *et al.*, 2016), were also regulated by 12 TFs.

Interestingly, an auxin- and an ethylene-related gene (VIT_00s0184g00110 and VIT_18s0072g00260), the *SENESCENCE-INDUCIBLE CHLOROPLAST STAY-GREEN PROTEIN 1* (VIT_02s0025g04660), a *MYB* gene (VIT_15s0046g02260) and two *LACCASES* (VIT_18s0122g00520 and VIT_18s0122g00690) resulted regulated by 11 *VviNACs*.

Three *WRKY* genes, *VviWRKY14* (VIT_05s0077g00730), *VviWRKY43* (VIT_14s0068g01770) and *VviWRKY52* (VIT_17s0000g01280), two *MYB* genes (VIT_12s0028g00980 and VIT_01s0011g04760) and the *VviNAC01* (VIT_01s0146g00280) resulted direct targets of 10 *VviNACs*.

The presence of *VviNAC01* in this group is very intriguing as it resulted the TF with more *VviNACs* interactions: 28 direct interactions with another *VviNAC* promoter/5'UTR region for a total of 23 *VviNACs* regulated by it and showing also its autoregulation.

VviNAC61 (VIT_08s0007g07640) is the second *VviNAC* most regulated gene with 9 *VviNACs* TF interactions.

Considering the very interesting information that this list could give to define the regulative role of the 14 selected *VviNACs*, in the future a more detailed analysis will be done.

VviNAC60 and ChIP-seq

Considering that the DAP-seq technique gives a global view of all the possible binding sites of a specific transcription factor, without taking into consideration the tissue and developmental stage specificity of regulation, ChIP-seq data were also obtained for *VviNAC60*. The aim was to find direct target of the TF which are related to the berry ripening specific regulation.

The analyses were performed, always using cv Shiraz fruiting cuttings (**Fig. 69**), on berries before veraison ('Green berry'), characterized by a very low expression of *VviNAC60* and used as a sort of negative control, and berries after veraison ('Veraison berry'), characterized by a high expression of the gene. Given the

absence of *VviNAC60* expression in young leaves, these were used as another and more powerful negative controls (‘Young leaf’).



Figure 69: Picture of the fruiting cuttings of cv Shiraz and details of the three tissues used in the ChIP-seq experiment: berries before veraison, characterized by a very low expression of *VviNAC60*, and berries after veraison, characterized by a high expression of the NAC candidate; given the absence of *VviNAC60* expression in young leaves, these were used as negative control.

The ChIP-Seq protocol provided, after the harvesting, the plant tissue fixation using formaldehyde to crosslink TFs–DNA interactions (**Fig. 70**).

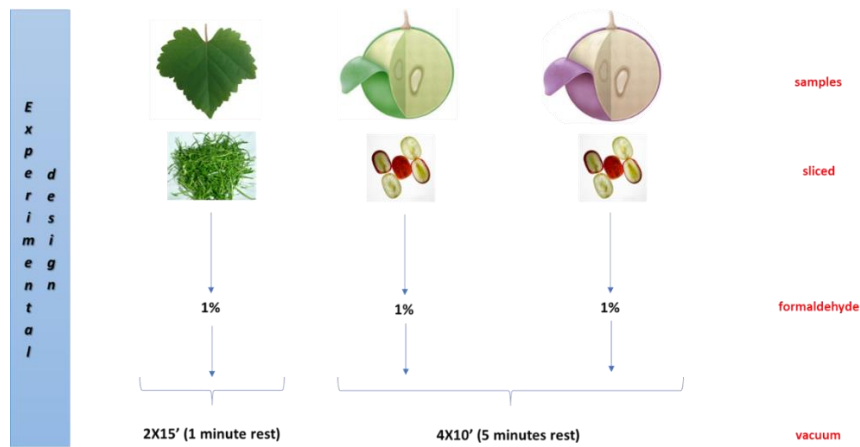


Figure 70: Experimental design of the ChIP-seq assay; the three different tissues harvested, sliced and the TF was crosslinked to the chromatin using 1% formaldehyde under different vacuum condition (depending on the type of tissue).

Then, the isolation of nuclei and the shearing of chromatin were performed. The subsequent sonication permitted to obtain most of the DNA fragments at 200 bp length, the perfect size for the sequencing step. After the precipitation of all the insoluble material, the immunoprecipitation step with the specific antibody against *VviNAC60* was performed and, once the antibody–TF/DNA complexes were isolated, the DNA was released by reverse crosslinking and purified.

Once being able to obtain enough immunoprecipitated material, especially from the ‘Veraison berry’ samples (considering the huge difficulties in extracting genomic DNA from the berry tissues at this particular stage of development), the resulting DNA fragments were sequenced.

Looking at each of the three sample percentages of alignment on the grape genome (**Fig. 71**), the ‘Young leaf’ was in line with the ChIP-seq literature (31,26%); unfortunately, this did not happen for the berry samples for which a 19,73% (‘Green berry’) and a 5,29% (‘Veraison berry’) were obtained.

The ChIP-seq experiment was performed again on the ‘Veraison berry’ sample, increasing of 3 times the chromatin concentration, to obtain a higher correspondence and a more accurate dataset.

Instead, the ‘Green berry’ results was not repeated as the alignment percentage was not too far from the average 25% found in literature and the developmental stage of the berry tissue was not the main protagonist of our investigation.

Unfortunately, with the second sequencing run nothing changed and a very low alignment was obtained again. For this reason, a specific bioinformatic analysis was applied to all the ChIP-seq samples, in order to understand to which organism the alien sequenced DNA belonged to.

All ‘input’ samples (the not immunoprecipitated chromatin of each sample), used as a control, perfectly aligned on the *Vitis vinifera* genome (>89%). On the contrary, most of the sequences of the immunoprecipitated samples belonged to microorganisms that usually live on the leaves and grape surface (**Fig. 71a-c**). For some unknown reasons, during the immuno-precipitation steps this DNA was selected and enriched.

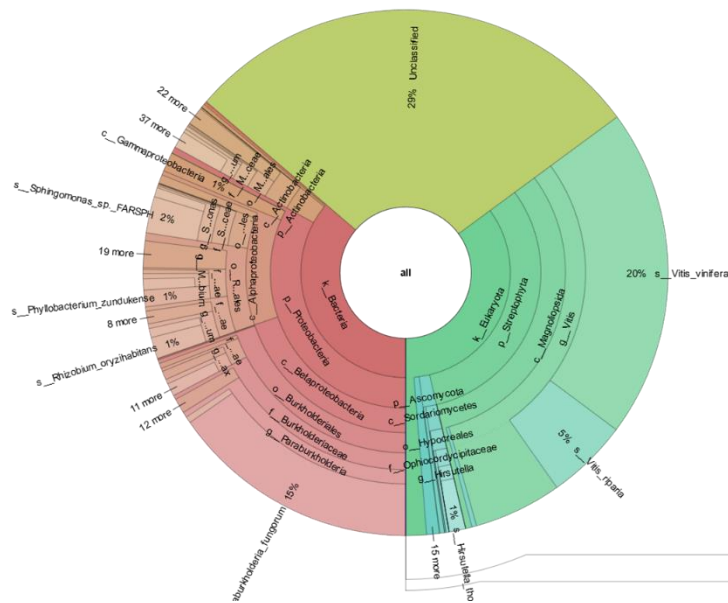
The organisms were the same in all the samples and the changes concerned only the numerical amount of the unwanted contamination, which drastically increase in the berry tissues, in particular in the almost mature one.

If the percentage of the different microorganisms was the same in all the samples, one microorganism, the most enriched one, showed differences.

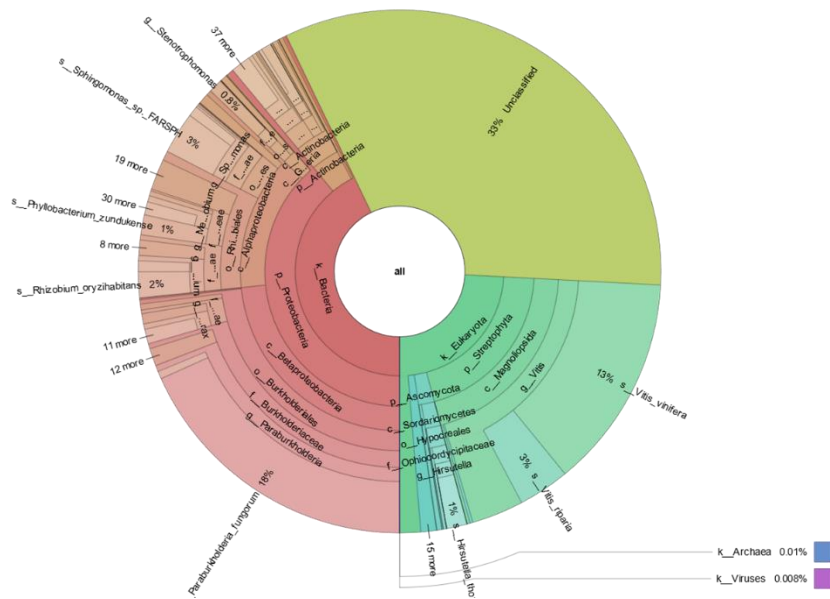
Indeed, the only one that increase between the different tissues and developmental

stages was the *Paraburkholderia fungorum*. This plant probiotic bacterium has never been studied in grapevine; however, a recent study correlates its presence to improvements in growth, yield and content of antioxidants in strawberry fruit (Rahman *et al.*, 2018). Moreover, plant probiotic bacteria are generally known to naturally occur in plant and enhance the growth of the host, sometimes suppressing diseases and providing beneficial effects (Rahman *et al.*, 2018).

a)



b)



c)

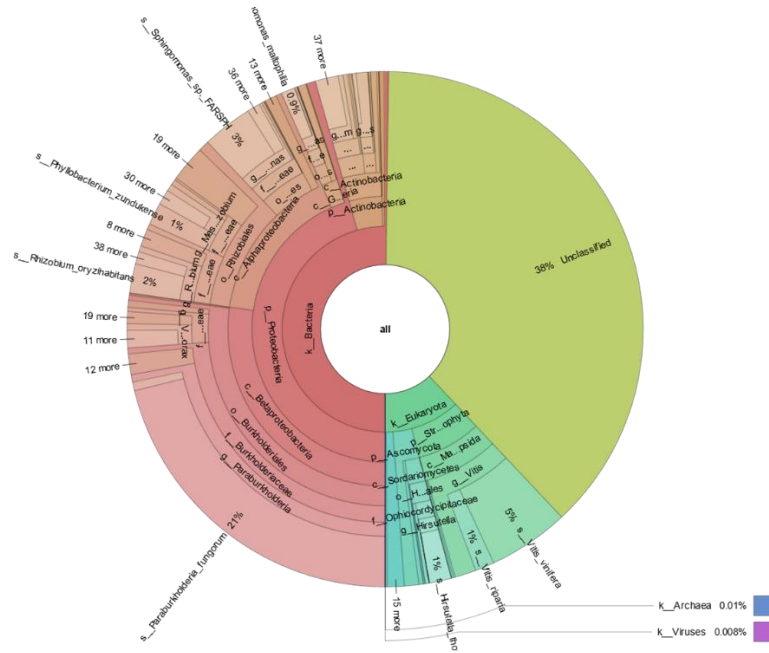


Figure 71: Pie charts of a) the ‘Young leaf’, b) the ‘Green berry’ and c) the ‘Veraison berry’ immunoprecipitated DNA, showing the bacteria DNA enrichment accidentally obtained in the CHIP-seq assay.

However, putting all the sequencing results together and despite the larger amount of alien enriched DNA, the highest number of genes were found in the ‘Veraison berry’ dataset (**Fig. 72**). This was very comforting, especially considering the low amount of analyzable grape DNA of these samples, and this evidence shows the good transcription factor recognition by the antibody and confirms the highest *VviNAC60* expression in the berries after veraison.

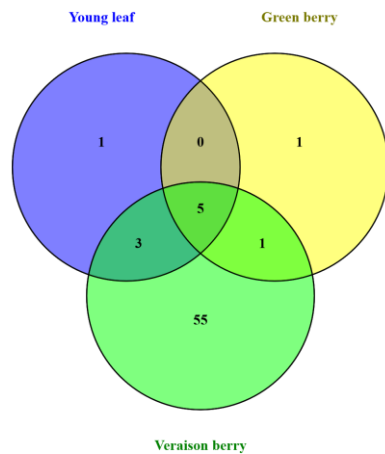


Fig. 72: Venn diagram of the genes found in the CHIP-seq analyzed samples.

Nine genes were found for the ‘Young leaf’ sample (**Table 57**), only one of which resulted leaf specific (VIT_05s0020g02930), and 3 genes were in common with the ‘Veraison sample’ (VIT_12s0178g00200, VIT_08s0007g02780 and VIT_13s0074g00400). Seven genes were found in the ‘Green berry’ sample (**Table 57**): only one was specific of this sample (VIT_15s0107g00120) and another one was in common with ‘Veraison berry’ sample (VIT_00s0366g00010). In addition to the genes in common with the other two samples, which were already reported above, the ‘Veraison berry’ sample had other 55 specific genes (**Table 57**). Five genes (**Table 57**) were found in common between all the samples (VIT_06s0004g03090, VIT_13s0101g00230, VIT_13s0101g00220, VIT_13s0064g00830 and VIT_18s0041g01900).

| Sample | Gene ID | Functional annotation | Young leaf | Green berry | Veraison berry |
|----------------|--------------------|--|------------|-------------|----------------|
| Young leaf | VIT_06s0004g03090 | Syntaxin of plants SYP7 | * | * | * |
| Young leaf | VIT_13s0101g00230 | Unknown | * | * | * |
| Young leaf | VIT_13s0101g00220 | Ribosomal RNA 16S | * | * | * |
| Young leaf | VIT_13s0064g00830 | Disease resistance protein RGA2 (RGA2-1b) | * | * | * |
| Young leaf | VIT_12s0178g00200 | Actin beta/gamma 1 | * | * | * |
| Young leaf | VIT_18s0041g01900 | Elongation factor 1-gamma | * | * | * |
| Young leaf | VIT_08s0007g02780 | Asp/Glu racemase | * | * | * |
| Young leaf | VIT_13s0074g00400 | PTL (PETAL LOSS) | * | * | * |
| Young leaf | VIT_05s0020g02930 | DNA-directed RNA polymerase III subunit C3 | * | * | * |
| Green berry | VIT_06s0004g03090 | Syntaxin of plants SYP7 | * | * | * |
| Green berry | VIT_13s0101g00230 | Unknown | * | * | * |
| Green berry | VIT_00s0366g00010 | No hit | * | * | * |
| Green berry | VIT_13s0101g00220 | Ribosomal RNA 16S | * | * | * |
| Green berry | VIT_15s0107g00120 | putative MADS-box Short Vegetal Phase 3 (vsvSP3) | * | * | * |
| Green berry | VIT_18s0041g01900 | Elongation factor 1-gamma | * | * | * |
| Green berry | VIT_13s0064g00830 | Disease resistance protein RGA2 (RGA2-1b) | * | * | * |
| Veraison berry | VIT_06s0004g03090 | Syntaxin of plants SYP7 | * | * | * |
| Veraison berry | VIT_13s0101g00230 | Unknown | * | * | * |
| Veraison berry | VIT_13s0101g00220 | Ribosomal RNA 16S | * | * | * |
| Veraison berry | VIT_12s0178g00200 | PTL (PETAL LOSS) | * | * | * |
| Veraison berry | VIT_08s0007g02780 | Asp/Glu racemase | * | * | * |
| Veraison berry | VIT_18s0041g01900 | Elongation factor 1-gamma | * | * | * |
| Veraison berry | VIT_13s0064g00830 | Disease resistance protein RGA2 (RGA2-1b) | * | * | * |
| Veraison berry | VIT_13s0106g00500 | RNA recognition motif (RRM)-containing protein | * | * | * |
| Veraison berry | VIT_00s1355g00020 | Expansin-like B1 | * | * | * |
| Veraison berry | VIT_16s0148g00230 | Receptor-like kinase ARK1AS | * | * | * |
| Veraison berry | VIT_09s0054g01070 | Receptor-like protein kinase PRK1 | * | * | * |
| Veraison berry | VIT_11s0037g01330 | No hit | * | * | * |
| Veraison berry | VIT_08s0040g02070 | fasciclin arabinogalactan-protein (FLA11) | * | * | * |
| Veraison berry | VIT_12s0178g00200 | Actin beta/gamma 1 | * | * | * |
| Veraison berry | VIT_15s0107g00090 | Gag-pol polyprotein | * | * | * |
| Veraison berry | VIT_00s0599g00010 | No hit | * | * | * |
| Veraison berry | VIT_00s0125g00020 | Reverse transcriptase | * | * | * |
| Veraison berry | VIT_08s0032g00780 | Calcium Dependent Protein Kinase (vCPK8) | * | * | * |
| Veraison berry | VIT_08s0105g00140 | Bromo-adjacency (BAH) domain-containing protein | * | * | * |
| Veraison berry | VIT_14s0005g00980 | DNA mismatch repair protein Msh1 | * | * | * |
| Veraison berry | VIT_13s0067g03430 | ARR9 typeA | * | * | * |
| Veraison berry | VIT_12s0121g00060 | R protein MLA10 | * | * | * |
| Veraison berry | VIT_18s0041g01130 | RNA binding | * | * | * |
| Veraison berry | VIT_00s0125g00060 | Unknown | * | * | * |
| Veraison berry | VIT_00s0685g00020 | No hit | * | * | * |
| Veraison berry | VIT_01s0013g00430 | Mitotic checkpoint protein BUB3 | * | * | * |
| Veraison berry | VIT_19s0014g01720 | Sodium/calcium exchanger family protein | * | * | * |
| Veraison berry | VIT_04s0044g01360 | Unknown protein | * | * | * |
| Veraison berry | VIT_07s0130g00140 | Thioesterase family | * | * | * |
| Veraison berry | VIT_06s0004g07650 | Taxadien-5-alpha-ol-O-acetyltransferase | * | * | * |
| Veraison berry | VIT_08s0032g01110 | Axial regulator YABBY2 | * | * | * |
| Veraison berry | VIT_08s0007g09040 | DnaJ homolog, subfamily A, member 5 | * | * | * |
| Veraison berry | VIT_09s0002g07250 | No hit | * | * | * |
| Veraison berry | VIT_00s0131g00320 | Annexin ANN3 | * | * | * |
| Veraison berry | VIT_07s0151g00380 | No hit | * | * | * |
| Veraison berry | VIT_00s1328g00020 | Phytosulfokines PSK4 | * | * | * |
| Veraison berry | VIT_15s00045g01140 | Heavy-metal-associated domain-containing protein | * | * | * |
| Veraison berry | VIT_02s0025g02680 | Growth-regulating factor 5 | * | * | * |
| Veraison berry | VIT_00s0236g00020 | RabGAP/TBC domain-containing protein | * | * | * |
| Veraison berry | VIT_06s0004g02170 | Histidinol-phosphate aminotransferase | * | * | * |
| Veraison berry | VIT_12s0059g01110 | Tubulin beta-8 | * | * | * |
| Veraison berry | VIT_00s0366g00010 | No hit | * | * | * |
| Veraison berry | VIT_12s0034g01260 | R protein L6 | * | * | * |
| Veraison berry | VIT_10s0003g04250 | Glutathione S-transferase GSTU22 | * | * | * |
| Veraison berry | VIT_01s0150g00640 | Unknown protein | * | * | * |
| Veraison berry | VIT_16s0013g01320 | Ser/Thr receptor-like kinase1 | * | * | * |
| Veraison berry | VIT_16s0013g00180 | Nectinesterase PPM1E | * | * | * |
| Veraison berry | VIT_12s0038g00340 | Protein binding / zinc ion binding | * | * | * |
| Veraison berry | VIT_14s0036g01060 | Unknown protein | * | * | * |
| Veraison berry | VIT_13s0019g04450 | ATSYTA/NTMC2T1.1/NTMC2TYPE1.1/SYTA | * | * | * |
| Veraison berry | VIT_12s0034g00490 | No hit | * | * | * |
| Veraison berry | VIT_04s0069g00470 | No hit | * | * | * |
| Veraison berry | VIT_00s0169g00110 | No hit | * | * | * |
| Veraison berry | VIT_14s0108g00530 | No hit | * | * | * |
| Veraison berry | VIT_11s0149g00070 | Ribosomal protein S6 | * | * | * |
| Veraison berry | VIT_19s0003g00050 | R protein PRF disease resistance protein | * | * | * |
| Veraison berry | VIT_10s0003g02400 | SRG1 (senescence-related gene 1) oxidoreductase | * | * | * |
| Veraison berry | VIT_09s0009g00830 | R protein disease resistance protein | * | * | * |
| Veraison berry | VIT_04s0043g00490 | No hit | * | * | * |
| Veraison berry | VIT_07s0005g06010 | FAD linked oxidase, N-terminal | * | * | * |
| Veraison berry | VIT_14s0003g01240 | Protein kinase beta-2 subunit 5'-AMP-activated | * | * | * |
| Veraison berry | VIT_16s0003g00820 | EMB1891 (embryo defective 1891) | * | * | * |
| Veraison berry | VIT_13s0106g00470 | RNA-binding protein 45 (RBP45) | * | * | * |
| Veraison berry | VIT_10s0003g05770 | Short-chain dehydrogenase/reductase (SDR) | * | * | * |

Table 57: VviNAC60 ChIP-seq target genes.

Only the small ‘Veraison berry’ dataset was further analyzed and, once removed all the ‘no hit’ and ‘unknown’ genes and all the genes in common with the other two samples, a list of 46 binding sites was obtained (**Table 58**).

Only four genes were found to be regulated in the ‘promoter’ region: *SODIUM/CALCIUM EXCHANGER FAMILY PROTEIN* (VIT_19s0014g01720), *HEAVY-METAL-ASSOCIATED DOMAIN-CONTAINING PROTEIN* (VIT_15s0045g01140), R protein L6 (VIT_12s0034g01260) and *PROTEIN BINDING / ZINC ION BINDING* (VIT_12s0028g03340). Three genes were found regulated in the 3’UTR region, 21 in the distal intergenic region, 7 in the downstream region, 2 in the exons and 9 in the introns. Moreover, this list was crossed with the already described DAP-seq and over expressions dataset to see if some correlation could be found (**Table 58**).

Three genes were also found up regulated by the *VviNAC60* stable over expression: *PROTEIN BINDING / ZINC ION BINDING* (VIT_12s0028g03340), which *VviNAC60* binding site was found in the promoter, *PHYTOSULFOKINES PSK4* (VIT_00s1328g00020) and *RECEPTOR-LIKE KINASE ARK1AS* (VIT_16s0148g00230), which harbors two binding sites in the intron. Only one gene found correlation with the *VviNAC60* transient over expression: *RNA-BINDING PROTEIN 45 RBP45* (VIT_13s0106g00470), which regulation is related to the binding of *VviNAC60* in the distal intergenic region.

Crossing the *VviNAC60* DAP-seq and the ChIP-seq datasets, only one gene was found in common; unfortunately, this gene reveals the TF binding site in two different genic regions, in an exon (745 bp from to the TSS) in the ChIP-seq dataset and in the promoter (-946 bp from to the TSS) in the DAP-seq one. However, this gene, *SRG1- SENESCENCE-RELATED GENE 1 OXIDOREDUCTASE* (VIT_10s0003g02400), seems to be very interesting as it is related to senescence and plant immunity (Cui *et al.*, 2018).

| q-value | Genic region | Gene ID | Distance to TSS | Functional annotation | DAP-seq | Stable OE | Transient OE |
|---------|---|-------------------|-----------------|--|-----------------|-----------|--------------|
| 999.00 | Intron (mRNA383/VIT_06s0004g03090, intron 2 of 8) | VIT_06s0004g03090 | 1735 | Syntaxin of plants SYP7 | | | |
| 256.1 | Intron (mRNA383/VIT_06s0004g03090, intron 2 of 8) | VIT_06s0004g03090 | 1734 | Syntaxin of plants SYP7 | | | |
| 78.09 | 3' UTR | VIT_13s0101g00220 | 735 | Ribosomal RNA 16S | | | |
| 50.62 | Distal Intergenic | VIT_13s0074g00400 | 19535 | PTL (PETAL LOSS) | | | |
| 37.83 | 3' UTR | VIT_13s0101g00220 | 736 | Ribosomal RNA 16S | | | |
| 32.71 | Intron (mRNA3531/VIT_13s0106g00500, intron 5 of 9) | VIT_13s0106g00500 | 3249 | RNA recognition motif (RRM)-containing protein | | | |
| 30.34 | Intron (mRNA23493/VIT_16s0148g00230, intron 1 of 2) | VIT_16s0148g00230 | 5412 | Receptor-like kinase ARK1AS | | 1,50 | |
| 30.18 | 3' UTR | VIT_09s0054g01070 | 2193 | Receptor-like protein kinase PRK1 | | | |
| 16.37 | Downstream (<1kb) | VIT_00s0125g00020 | 1047 | Reverse transcriptase | | | |
| 15.09 | Distal Intergenic | VIT_08s0032g00780 | 13152 | Calcium Dependent Protein Kinase (VvCPK8) | | | |
| 14.97 | Distal Intergenic | VIT_08s0105g00140 | 7371 | Bromo-adjacency (BAH) domain-containing protein | | | |
| 14.96 | Downstream (<1kb) | VIT_14s0006g00980 | 1019 | DNA mismatch repair protein Mlh1 | | | |
| 12.21 | Exon (mRNA25235/VIT_13s0067g03430, exon 5 of 5) | VIT_13s0067g03430 | 939 | ARR9 typeA | | | |
| 12.02 | Distal Intergenic | VIT_12s0121g00060 | 21966 | R protein MLA10 | | | |
| 10.92 | Distal Intergenic | VIT_18s0041g01130 | -33000 | RNA binding | | | |
| 9.79 | Distal Intergenic | VIT_08s0105g00140 | 11152 | Bromo-adjacency (BAH) domain-containing protein | | | |
| 9.51 | Promoter (<-1kb) | VIT_19s0014g01720 | -466 | Sodium/calcium exchanger family protein | | | |
| 8.70 | Downstream (<1kb) | VIT_07s0130g00140 | 3720 | Thioesterase family | | | |
| 8.32 | Downstream (1-2kb) | VIT_06s0004g07650 | 3040 | Taxadien-5-alpha-ol-O-acetyltransferase | | | |
| 7.40 | Intron (mRNA10573/VIT_08s0032g01110, intron 2 of 6) | VIT_08s0032g01110 | 1954 | Axial regulator YABBY2 | | | |
| 7.27 | Distal Intergenic | VIT_08s0007g09040 | -4318 | DnaJ homolog, subfamily A, member 5 | | | |
| 6.51 | Intron (mRNA3531/VIT_13s0106g00500, intron 5 of 9) | VIT_13s0106g00500 | 3252 | RNA recognition motif (RRM)-containing protein | | | |
| 6.19 | Distal Intergenic | VIT_13s0074g00400 | 19533 | PTL (PETAL LOSS) | | | |
| 6.14 | Downstream (1-2kb) | VIT_06s0004g07650 | 3041 | Taxadien-5-alpha-ol-O-acetyltransferase | | | |
| 5.79 | Distal Intergenic | VIT_00s0131g00320 | 25581 | Annexin ANN3 | | | |
| 4.75 | Distal Intergenic | VIT_00s1328g00020 | -9983 | Phytosulfokines PSK4 | | 1,53 | |
| 4.38 | Promoter (<-1kb) | VIT_15s0045g01140 | -252 | Heavy-metal-associated domain-containing protein | | | |
| 4.21 | Downstream (1-2kb) | VIT_02s0025g02680 | 2504 | Growth-regulating factor 5 | | | |
| 3.77 | Distal Intergenic | VIT_06s0004g02170 | -5454 | Histidinol-phosphate aminotransferase | | | |
| 3.39 | Distal Intergenic | VIT_12s0059g01110 | -5619 | Tubulin beta-8 | | | |
| 3.34 | Intron (mRNA23493/VIT_16s0148g00230, intron 1 of 2) | VIT_16s0148g00230 | 5430 | Receptor-like kinase ARK1AS | | 1,50 | |
| 3.12 | Promoter (1-2kb) | VIT_12s0034g01260 | -1022 | R protein L6 | | | |
| 3.11 | Distal Intergenic | VIT_10s0003g04250 | 17969 | Glutathione S-transferase GSTU22 | | | |
| 2.86 | Distal Intergenic | VIT_16s0013g00160 | 46887 | Pectinesterase PPME1 | | | |
| 2.85 | Promoter (1-2kb) | VIT_12s0028g03340 | -1383 | Protein binding / zinc ion binding | | 1,73 | |
| 2.76 | Downstream (1-2kb) | VIT_02s0025g02680 | 2490 | Growth-regulating factor 5 | | | |
| 2.65 | Distal Intergenic | VIT_13s0019g04450 | -12560 | ATSYTA/NTMC2T1.1/NTMC2TYPE1.1/SYTA | | | |
| 2.42 | Distal Intergenic | VIT_19s0093g00050 | -56392 | R protein PRF disease resistance protein | | | |
| 2.42 | Intron (mRNA7571/VIT_11s0149g00070, intron 2 of 4) | VIT_11s0149g00070 | 8771 | Ribosomal protein S6 | | | |
| 2.41 | Exon (mRNA27904/VIT_10s0003g02400, exon 3 of 5) | VIT_10s0003g02400 | 745 | SRG1 (senescence-related gene 1) oxidoreductase | Promoter (-946) | | |
| 2.40 | Distal Intergenic | VIT_09s0096g00830 | -28086 | R protein disease resistance protein | | | |
| 2.27 | Distal Intergenic | VIT_07s0005g06010 | -41522 | FAD linked oxidase, N-terminal | | | |
| 2.18 | Distal Intergenic | VIT_16s0050g00820 | -4733 | EMB1691 (embryo defective 1691) | | | |
| 2.18 | Distal Intergenic | VIT_14s0006g01240 | -23558 | Protein kinase beta-1 subunit 5'-AMP-activated | | | |
| 2.17 | Distal Intergenic | VIT_13s0106g00470 | 16599 | RNA-binding protein 45 (RBP45) | | | 1,76 |
| 2.17 | Intron (mRNA10357/VIT_10s0003g05770, intron 1 of 5) | VIT_10s0003g05770 | 366 | Short-chain dehydrogenase/reductase (SDR) | | | |

Table 58: VvNAC60 ‘Veraison berry’ specific ChIP-seq target genes.

REFERENCES

- Acevedo-Garcia, J., Kusch, S., & Panstruga, R.** (2014). Magical mystery tour: MLO proteins in plant immunity and beyond. *New Phytologist*, *204*(2), 273-281.
- Bönisch, F., Frotscher, J., Stanitzek, S., Rühl, E., Wüst, M., Bitz, O., & Schwab, W.** (2014). A UDP-glucose: monoterpenol glucosyltransferase adds to the chemical diversity of the grapevine metabolome. *Plant Physiology*, *165*(2), 561-581.
- Braidot, E., Zancani, M., Petrusa, E., Peresson, C., Bertolini, A., Patui, S., ... & Vianello, A.** (2008). Transport and accumulation of flavonoids in grapevine (*Vitis vinifera* L.). *Plant signaling & behavior*, *3*(9), 626-632.
- Bu, Q., Jiang, H., Li, C. B., Zhai, Q., Zhang, J., Wu, X., ... & Li, C.** (2008). Role of the *Arabidopsis thaliana* NAC transcription factors ANAC019 and ANAC055 in regulating jasmonic acid-signaled defense responses. *Cell research*, *18*(7), 756-767.
- Cailliatte, R., Schikora, A., Briat, J. F., Mari, S., & Curie, C.** (2010). High-affinity manganese uptake by the metal transporter NRAMP1 is essential for *Arabidopsis* growth in low manganese conditions. *The Plant Cell*, *22*(3), 904-917.
- Cui, B., Pan, Q., Clarke, D., Villarreal, M. O., Umbreen, S., Yuan, B., ... & Loake, G. J.** (2018). S-nitrosylation of the zinc finger protein SRG1 regulates plant immunity. *Nature Communications*, *9*(1), 1-12.
- Daie, J.** (1993). Cytosolic fructose-1, 6-bisphosphatase: a key enzyme in the sucrose biosynthetic pathway. *Photosynthesis research*, *38*(1), 5-14.
- D'Incà E.** 2017. Master regulators of the vegetative-to-mature organ transition in grapevine: the role of NAC transcription factors. PhD thesis. Verona University.
- Fasoli, M., Dal Santo, S., Zenoni, S., Tornielli, G. B., Farina, L., Zamboni, A., ... & Pezzotti, M.** (2012). The grapevine expression atlas reveals a deep transcriptome shift driving the entire plant into a maturation program. *The Plant Cell*, *24*(9), 3489-3505.
- Gachomo, E. W., Jimenez-Lopez, J. C., Baptiste, L. J., & Kotchoni, S. O.** (2014). GIGANTUS1 (GTS1), a member of Transducin/WD40 protein superfamily, controls seed germination, growth and biomass accumulation through ribosome-biogenesis protein interactions in *Arabidopsis thaliana*. *BMC plant biology*, *14*(1), 37.
- Gao, Y., Wang, Y., Xin, H., Li, S., & Liang, Z.** (2017). Involvement of ubiquitin-conjugating enzyme (E2 gene Family) in ripening process and response to cold and heat stress of *Vitis vinifera*. *Scientific reports*, *7*(1), 1-12.
- Goossens, J., Mertens, J., & Goossens, A.** (2017). Role and functioning of bHLH transcription factors in jasmonate signalling. *Journal of Experimental Botany*, *68*(6), 1333-1347.
- Heim, M. A., Jakoby, M., Werber, M., Martin, C., Weisshaar, B., & Bailey, P. C.** (2003). The basic helix-loop-helix transcription factor family in plants: a genome-wide study of protein structure and functional diversity. *Molecular biology and evolution*, *20*(5), 735-747.
- Hu, X., Jia, T., Hörtensteiner, S., Tanaka, A., & Tanaka, R.** (2020). Subcellular localization of chlorophyllase2 reveals it is not involved in chlorophyll degradation during senescence in *Arabidopsis thaliana*. *Plant Science*, *290*, 110314.

- İbrahim, M., Kibar, U., Kazan, K., Özmen, C. Y., Mutaf, F., Aşçı, S. D., ... & Ergül, A.** (2019). Genome-wide identification of the LEA protein gene family in grapevine (*Vitis vinifera* L.). *Tree Genetics & Genomes*, *15*(4), 55.
- Kim, J. H., Kim, B. G., Park, Y., Ko, J. H., Lim, C. E., Lim, J., ... & Ahn, J. H.** (2006). Characterization of flavonoid 7-O-glucosyltransferase from *Arabidopsis thaliana*. *Bioscience, biotechnology, and biochemistry*, *70*(6), 1471-1477.
- Kim JH, Woo HR, Kim J, Lim PO, Lee IC, Choi SH, Hwang D, Nam HG.** (2009). Trifurcate feed-forward regulation of age-dependent cell death involving miR164 in *Arabidopsis*. *Science*. 323(5917):1053-7. doi: 10.1126/science.1166386. PMID: 19229035.
- Kong X, Huang G, Xiong Y, Zhao C, Wang J, Song X, Giri J, Zuo K.** 2019. IBRS regulates leaf serrations development via modulation of the expression of PIN1. *International Journal of Molecular Sciences*. 20(18):4429. doi: 10.3390/ijms20184429. PMID: 31505781; PMCID: PMC6770195.
- Lee, S. J., Lee, B. H., Jung, J. H., Park, S. K., Song, J. T., & Kim, J. H.** (2018). GROWTH-REGULATING FACTOR and GRF-INTERACTING FACTOR specify meristematic cells of gynoecia and anthers. *Plant physiology*, *176*(1), 717-729.
- Liu, Y., Song, Q., Li, D., Yang, X., & Li, D.** (2017). Multifunctional roles of plant dehydrins in response to environmental stresses. *Frontiers in Plant Science*, *8*, 1018.
- Liu, H., Hu, M., Wang, Q., Cheng, L., & Zhang, Z.** (2018). Role of papain-like cysteine proteases in plant development. *Frontiers in plant science*, *9*, 1717.
- Madson, M., Dunand, C., Li, X., Verma, R., Vanzin, G. F., Caplan, J., ... & Reiter, W. D.** (2003). The MUR3 gene of *Arabidopsis* encodes a xyloglucan galactosyltransferase that is evolutionarily related to animal exostosins. *The Plant Cell*, *15*(7), 1662-1670.
- Marowa, P., Ding, A., & Kong, Y.** (2016). Expansins: roles in plant growth and potential applications in crop improvement. *Plant cell reports*, *35*(5), 949-965.
- Massonnet, M., Fasoli, M., Tornielli, G. B., Altieri, M., Sandri, M., Zuccolotto, P., ... & Pezzotti, M.** (2017). Ripening transcriptomic program in red and white grapevine varieties correlates with berry skin anthocyanin accumulation. *Plant Physiology*, *174*(4), 2376-2396.
- Matus, J. T., Cavallini, E., Loyola, R., Höll, J., Finezzo, L., Dal Santo, S., ... & Arce-Johnson, P.** (2017). A group of grapevine MYBA transcription factors located in chromosome 14 control anthocyanin synthesis in vegetative organs with different specificities compared with the berry color locus. *The Plant Journal*, *91*(2), 220-236.
- Nicolas, P., Lecourieux, D., Kappel, C., Cluzet, S., Cramer, G., Delrot, S., & Lecourieux, F.** (2014). The basic leucine zipper transcription factor ABSCISIC ACID RESPONSE ELEMENT-BINDING FACTOR2 is an important transcriptional regulator of abscisic acid-dependent grape berry ripening processes. *Plant Physiology*, *164*(1), 365-383.
- Oda-Yamamizo, C., Mitsuda, N., Sakamoto, S., Ogawa, D., Ohme-Takagi, M., & Ohmiya, A.** (2016). Corrigendum: The NAC transcription factor ANAC046 is a positive regulator of chlorophyll degradation and senescence in *Arabidopsis* leaves. *Scientific reports*, *6*.
- Ohmiya, A., Oda-Yamamizo, C., & Kishimoto, S.** (2019). Overexpression of CONSTANS-like 16 enhances chlorophyll accumulation in petunia corollas. *Plant Science*, *280*, 90-96.
- Oikawa, K., Yamasato, A., Kong, S. G., Kasahara, M., Nakai, M., Takahashi, F., ... & Wada, M.** (2008). Chloroplast outer envelope protein CHUP1 is essential for chloroplast anchorage to the plasma membrane and chloroplast movement. *Plant physiology*, *148*(2), 829-842.

Omidbakhshfard, M. A., Fujikura, U., Olas, J. J., Xue, G. P., Balazadeh, S., & Mueller-Roeber, B. (2018). GROWTH-REGULATING FACTOR 9 negatively regulates Arabidopsis leaf growth by controlling ORG3 and restricting cell proliferation in leaf primordia. *PLoS genetics*, *14*(7), e1007484.

Palumbo, M. C., Zenoni, S., Fasoli, M., Massonnet, M., Farina, L., Castiglione, F., ... & Paci, P. (2014). Integrated network analysis identifies fight-club nodes as a class of hubs encompassing key putative *switch* genes that induce major transcriptome reprogramming during grapevine development. *The Plant Cell*, *26*(12), 4617-4635.

Park, S. Y., Yu, J. W., Park, J. S., Li, J., Yoo, S. C., Lee, N. Y., ... & Paek, N. C. (2007). The senescence-induced staygreen protein regulates chlorophyll degradation. *The Plant Cell*, *19*(5), 1649-1664.

Rahman, M., Sabir, A. A., Mukta, J. A., Khan, M. M. A., Mohi-Ud-Din, M., Miah, M. G., ... & Islam, M. T. (2018). Plant probiotic bacteria *Bacillus* and *Paraburkholderia* improve growth, yield and content of antioxidants in strawberry fruit. *Scientific reports*, *8*(1), 1-11.

Rauf, M., Arif, M., Fisahn, J., Xue, G. P., Balazadeh, S., & Mueller-Roeber, B. (2013). NAC transcription factor speedy hyponastic growth regulates flooding-induced leaf movement in Arabidopsis. *The Plant Cell*, *25*(12), 4941-4955.

Robert, N., Roche, K., Lebeau, Y., Breda, C., Boulay, M., Esnault, R., & Buffard, D. (2002). Expression of grapevine chitinase genes in berries and leaves infected by fungal or bacterial pathogens. *Plant Science*, *162*(3), 389-400.

Sakuraba, Y., Park, S. Y., Kim, Y. S., Wang, S. H., Yoo, S. C., Hörtensteiner, S., & Paek, N. C. (2014). Arabidopsis STAY-GREEN2 is a negative regulator of chlorophyll degradation during leaf senescence. *Molecular plant*, *7*(8), 1288-1302.

Schenk, N., Schelbert, S., Kanwischer, M., Goldschmidt, E. E., Dörmann, P., & Hörtensteiner, S. (2007). The chlorophyllases AtCLH1 and AtCLH2 are not essential for senescence-related chlorophyll breakdown in Arabidopsis thaliana. *Febs Letters*, *581*(28), 5517-5525.

Shen, W., Reyes, M. I., & Hanley-Bowdoin, L. (2009). Arabidopsis protein kinases GRIK1 and GRIK2 specifically activate SnRK1 by phosphorylating its activation loop. *Plant physiology*, *150*(2), 996-1005.

Sun, X., Wang, Y., & Sui, N. (2018). Transcriptional regulation of bHLH during plant response to stress. *Biochemical and biophysical research communications*, *503*(2), 397-401.

Tan, T. T., Endo, H., Sano, R., Kurata, T., Yamaguchi, M., Ohtani, M., & Demura, T. (2018). Transcription factors VND1-VND3 contribute to cotyledon xylem vessel formation. *Plant physiology*, *176*(1), 773-789.

Theodoulou, F. L. (2000). Plant ABC transporters. *Biochimica et Biophysica Acta (BBA)-Biomembranes*, *1465*(1-2), 79-103.

Toth, Z., Winterhagen, P., Kalapos, B., Su, Y., Kovacs, L., & Kiss, E. (2016). Expression of a grapevine NAC transcription factor gene is induced in response to powdery mildew colonization in salicylic acid-independent manner. *Scientific reports*, *6*, 30825.

Vannozzi, A., Wong, D. C. J., Höll, J., Hmnam, I., Matus, J. T., Bogs, J., ... & Lucchin, M. (2018). Combinatorial regulation of stilbene synthase genes by WRKY and MYB transcription factors in grapevine (*Vitis vinifera* L.). *Plant and Cell Physiology*, *59*(5), 1043-1059.

Wang, M., Vannozzi, A., Wang, G., Liang, Y. H., Tornielli, G. B., Zenoni, S., ... & Cheng, Z. M. M. (2014). Genome and transcriptome analysis of the grapevine (*Vitis vinifera* L.) WRKY gene family. *Horticulture research*, *1*(1), 1-16.

Wang, X., Guan, Y., Zhang, D., Dong, X., & Tian, L. (2017). A β -ketoacyl-CoA synthase is involved in rice leaf cuticular wax synthesis and requires a CER2-LIKE protein as a cofactor. *Plant Physiology*, *173*(2), 944-955.

Wang, X., Guo, R., Tu, M., Wang, D., Guo, C., Wan, R., ... & Wang, X. (2017). Ectopic expression of the wild grape WRKY transcription factor VqWRKY52 in *Arabidopsis thaliana* enhances resistance to the biotrophic pathogen powdery mildew but not to the necrotrophic pathogen *Botrytis cinerea*. *Frontiers in plant science*, *8*, 97.

Wang, X., Tu, M., Wang, D., Liu, J., Li, Y., Li, Z., ... & Wang, X. (2018). CRISPR/Cas9-mediated efficient targeted mutagenesis in grape in the first generation. *Plant biotechnology journal*, *16*(4), 844-855.

Wu, B. H., Liu, H. F., Guan, L., Fan, P. G., & Li, S. H. (2011). Carbohydrate metabolism in grape cultivars that differ in sucrose accumulation. *Vitis*, *50*(2), 51-57.

Yoshida, S., Ito, M., Callis, J., Nishida, I., & Watanabe, A. (2002). A delayed leaf senescence mutant is defective in arginyl-tRNA: protein arginyltransferase, a component of the N-end rule pathway in *Arabidopsis*. *The Plant Journal*, *32*(1), 129-137.

Zenoni, S., Dal Santo, S., Tornielli, G. B., D'Incà, E., Filippetti, I., Pastore, C., ... & Poni, S. (2017). Transcriptional responses to pre-flowering leaf defoliation in grapevine berry from different growing sites, years, and genotypes. *Frontiers in plant science*, *8*, 630.

4. THE VviNACs REGULATION NETWORK

4.1 INTRODUCTION

Advance in the *in vivo* and *in vitro* techniques is helping in the determination of TF-binding sites, slowly bringing to the deciphering of the transcriptional regulatory code (Franco-Zorrilla *et al.*, 2014). NAC proteins are among the largest plant specific TF family and are implicated in the regulation of transcriptional reprogramming associated with diverse developmental processes (Kim *et al.*, 2016), which face a wide range of environmental stresses. Indeed, NACs TFs are known to have a regulative role in the temporal expression of maturation-associated genes (in particular during leaf aging/senescence), but many members of the NAC family also have roles in the regulation of multiple stress responses (Balazadeh *et al.*, 2010). Most of the NAC TFs functionally characterized have been shown to be transcriptional activator but a few other NAC proteins are also transcriptional repressors (Yuan *et al.*, 2019). Indeed, many NACs show expression changes during leaf aging in *Arabidopsis* and genetic studies identified many NACs as positive and negative regulators of leaf senescence (Kim *et al.*, 2018). This duality may be achieved by recruiting or interacting with different transcriptional partners (Yuan *et al.*, 2019). Many TFs interact with other proteins, including other types of TFs, to regulate the expression of their target genes or enhance their binding capacity to the *cis* elements in promoters of their target genes (Yuan *et al.*, 2019). Auto- and cross-regulation of members within the same TF family forms one of the control nodes of the growth signalling pathways; it is common that multiple members within the same family share related and redundant roles in mediating their downstream signalling pathways, thereby cross-regulating each other at the transcriptional level (Ng *et al.*, 2018). For example, the three closely related WRKY TFs (WRKY18, WRKY40 and WRKY60) were found to cross-regulate each other in mediating the ABA signalling (Ng *et al.*, 2018). Moreover, the NACs are reported to regulate their own and each other transcription, forming a complex regulatory web and providing a finely tuned control system (Kim *et al.*, 2018); ANAC013 and ANAC017 were found to be involved in the mitochondrial retrograde regulation under oxidative stress and a *cis*-regulatory element can be

found at their promoters, suggesting that a positive feedback regulation enhances their transcripts and targets expression under stresses (Ng *et al.*, 2018).

A recent study demonstrated that nine distantly related NAC TFs were able to bind the same core sequence, though with different affinities; moreover, in line with this result, another paper has shown that several other NAC TFs bind the typical NAC binding core but with considerable sequence differences in the flanking bases (Lindemose *et al.*, 2014). Thus, as seen in bHLH and homeodomain proteins where few amino acids can play a critical role in the definition of DNA specificities for single TFs, the flanking bases next to the core of NAC binding sites in promoters may determine the binding specificities and fine-tune affinity for different NAC TFs *in vivo* (Lindemose *et al.*, 2014). The conformational changes that typically occur in the conserved DNA-binding domain of a TF can influence the dimerization of TFs and DNA binding (Kang *et al.*, 2018). Dimerization of DNA-binding domains is common and can function in modulating the DNA-binding specificity (Müller, 2001). Gel filtration studies on the ANAC NAC domain have shown that it forms mostly dimers in solution (Olsen *et al.*, 2004). The structure determination of the N-terminal domain of ANAC shows that the NAC domain presents a twisted antiparallel β -sheet sandwiched between two helices, suggesting that this domain mediates dimerization of the NAC proteins through conserved interactions and that the DNA binding through the NAC dimer face is rich in positive charges (Ernst *et al.*, 2004). Indeed, NAC proteins were shown to bind DNA as dimers in an EMSA experiment with different-sized NAC proteins and a NAC domain truncation, rendering the domain unable to dimerize, also prevented DNA binding (Olsen *et al.*, 2005). It is plausible that promoters showing palindromic dimer sites could be differentially regulated by combinations of NAC homo- and hetero-dimers thus expanding on the range of signals recognized (Lindemose *et al.*, 2014). Homo- and hetero-dimer interaction among the previously mentioned WRKY18, WRKY40 and WRKY60 were found to alter their DNA binding activities (Ng *et al.*, 2018). Features of transcriptional autoregulation and inter-regulation through homo-dimerization and hetero-dimerization among the NAC TFs have highlighted the huge network complexity in which they operate, even though the relevance of NAC dimers *in vivo* has not yet been established (Kim *et al.*, 2016).

REFERENCES

- Balazadeh, S., Siddiqui, H., Allu, A. D., Matallana-Ramirez, L. P., Caldana, C., Mehrnia, M., ... & Mueller-Roeber, B.** (2010). A gene regulatory network controlled by the NAC transcription factor ANAC092/AtNAC2/ORE1 during salt-promoted senescence. *The Plant Journal*, *62*(2), 250-264.
- Ernst, H. A., Nina Olsen, A., Skriver, K., Larsen, S., & Lo Leggio, L.** (2004). Structure of the conserved domain of ANAC, a member of the NAC family of transcription factors. *EMBO reports*, *5*(3), 297-303.
- Franco-Zorrilla, J. M., López-Vidriero, I., Carrasco, J. L., Godoy, M., Vera, P., & Solano, R.** (2014). DNA-binding specificities of plant transcription factors and their potential to define target genes. *Proceedings of the National Academy of Sciences*, *111*(6), 2367-2372.
- Kang, M., Kim, S., Kim, H. J., Shrestha, P., Yun, J. H., Phee, B. K., ... & Chang, I.** (2018). The C-domain of the NAC transcription factor ANAC019 is necessary for pH-tuned DNA binding through a histidine *switch* in the N-domain. *Cell reports*, *22*(5), 1141-1150.
- Kim, H. J., Nam, H. G., & Lim, P. O.** (2016). Regulatory network of NAC transcription factors in leaf senescence. *Current opinion in plant biology*, *33*, 48-56.
- Kim, H. J., Park, J. H., Kim, J., Kim, J. J., Hong, S., Kim, J., ... & Hwang, D.** (2018). Time-evolving genetic networks reveal a NAC troika that negatively regulates leaf senescence in Arabidopsis. *Proceedings of the National Academy of Sciences*, *115*(21), E4930-E4939.
- Lindemose, S., Jensen, M. K., de Velde, J. V., O'Shea, C., Heyndrickx, K. S., Workman, C. T., ... & Masi, F. D.** (2014). A DNA-binding-site landscape and regulatory network analysis for NAC transcription factors in Arabidopsis thaliana. *Nucleic acids research*, *42*(12), 7681-7693.
- Müller, C. W.** (2001). Transcription factors: global and detailed views. *Current opinion in structural biology*, *11*(1), 26-32.
- Ng, D. W., Abeyasinghe, J. K., & Kamali, M.** (2018). Regulating the regulators: The control of transcription factors in plant defense signaling. *International journal of molecular sciences*, *19*(12), 3737.
- Olsen, A. N., Ernst, H. A., Leggio, L. L., & Skriver, K.** (2005). DNA-binding specificity and molecular functions of NAC transcription factors. *Plant Science*, *169*(4), 785-797.
- Yuan, X., Wang, H., Cai, J., Li, D., & Song, F.** (2019). NAC transcription factors in plant immunity. *Phytopathology Research*, *1*(1), 3.

4.2 MATERIAL AND METHODS

Promoting region isolation and cloning

The promoting sequences were amplified from *Vitis vinifera* cv Shiraz leaf gDNA using KAPA HiFi DNA polymerase (KAPA Biosystems, Wilmington, MA, USA) and the primers listed in **Table 59**.

The PCR products were directionally cloned into the Gateway^R entry vector pENTR/D-TOPO (Invitrogen, Thermo Fisher Scientific, Waltham, MA, USA) and then transferred by site-specific LR Gateway^R recombination into the binary reporter vector pPGWL7.0 (https://gateway.psb.ugent.be/vector/show/pPGWL7/search/index/transcriptional_reporters, Laboratory of Plant System Biology, Ghent University).

The *VviNACs* ORF were previously amplified from a *V. vinifera* cv Shiraz and cv Corvina berry cDNA and cloned into the binary overexpression vector pK7WG2.0.

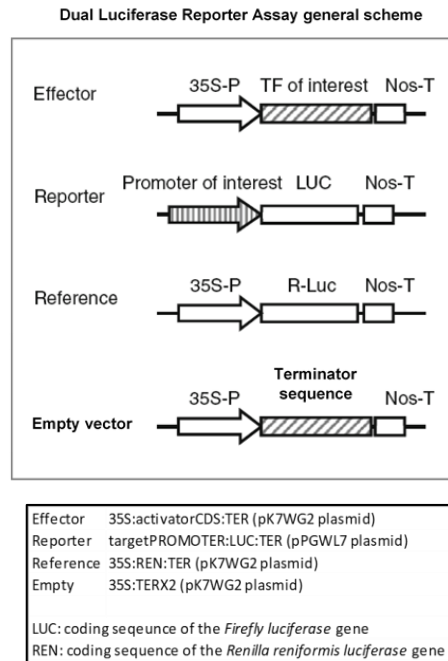
| Gene ID | Functional annotation | Direction | Primer | T _a (°C) | Length (bp) |
|-------------------|-----------------------|-----------|----------------------------------|---------------------|-------------|
| VIT_01s0146g00280 | VviNAC01 | For | 5'-CACCCCTGTTGAGTGGGAACAGCAA-3' | 52 | 922 |
| | | Rev | 5'-CGCTAAAAAATCCTATCAACTCT-3' | | |
| VIT_17s0000g06400 | VviNAC05 | For | 5'-CACCTTGCTTTTGCTATCCGTCCT-3' | 51 | 2142 |
| | | Rev | 5'-CTGATCATCTCCACACTAAGT-3' | | |
| VIT_18s0001g02300 | VviNAC08 | For | 5'-CACCTCCCAACCATAGCTTACCTGTC-3' | 55 | 1024 |
| | | Rev | 5'-ATTAGTTCTCTCTCTTCCCTCTC-3' | | |
| VIT_12s0028g03050 | VviNAC34 | For | 5'-CACCGGGTGCCTAAAATCCCCTGT-3' | 55 | 1014 |
| | | Rev | 5'-TTCTTAGTTTTCTCTAATGCCCA-3' | | |
| VIT_10s0003g00350 | VviNAC37 | For | 5'-CACCTTATCCGCACCTCGGTCA-3' | 55 | 1049 |
| | | Rev | 5'-CCCTGTTGTTGAGCCTCTATG-3' | | |
| VIT_08s0007g07640 | VviNAC61 | For | 5'-CACCAATCTCTGAAAGCGGGGC-3' | 55 | 1051 |
| | | Rev | 5'-AAGGTCATCACCTTGATCGGC-3' | | |

Table 59: Primers list for the isolation of the promoting sequences used in the Dual Luciferase Reporter Assay.

Agrobacterium tumefaciens C5851 transformation

The pPGWL7.0 cloned constructs were inserted into *A. tumefaciens* strain C58C1 by electroporation (Bio-Rad electroporation instrument, 25 μ F, 200 Ω and 2.5 kV) and the transformed colonies were selected by strain antibiotic resistance (tetracycline) and construct antibiotic resistance (streptomycin and spectinomycin).

Dual-Luciferase^R Reporter Assay System (Promega)



- Obtain a 0.2 (OD_{600nm}) resuspension in MMA buffer for each transformed bacteria strain.

The MMA buffer must be fresh and is composed of:

- MES 0.01 M pH 5.6
 - $MgCl_2$ 0.01 M
 - Acetosyringone 0.01 M
- Incubate 2 hours at room temperature with slow shaking.
 - Mix the MMA solution containing the *Agrobacterium* harboring vector of interest basing on your test.

Proportion among effector, reporter and reference vectors has been determined according to the Dual Luciferase Reporter Assay System technical manual (Promega).

For example, to the transactivation of the *geneA* by the *geneB* your mix will be the follow:

Mix_{control}: 8 ml of the Reporter vector (*geneA*promoter:LUC)
 1.7 ml of the Reference
 8 ml of the Empty vector

Mix_{test}: 8 ml of the Reporter vector (*geneA*:promoter:LUC)
1.7 ml of the Reference
8 ml of the Effector vector (35S:*geneB*)

- For each prepared MMA mix, using a 1ml syringe without the needle, infiltrate three 5 weeks old *N. Benthamiana* plants (biological replicates) on the lower side of 3 leaves.
- 72 hours after infection, collect three fresh leaf disks (1cm diameter disks, technical replicates) from the 3rd leaf of each plant in separate eppy tubes.
- Ground the leaf disks with 250 μ l of 1X Passive Lysis Buffer (Promega).
- Centrifuge the lysate for 1 minute at 12.000 g to allow leaf debris to settle.
- Dilute (1:10) the clear supernatant.
- Put 10 μ l of each sample diluted supernatant in a white 96-wells plate.

Detect Firefly and *R. reniformis* luminescence following manufactures instruction (Promega) and using a Tecan Infinite ® M200 PLEX instrument with double injectors.

- Inject in each well 40 μ l of Luciferase Assay Reagent (LARII, Promega).
- Shake the plate and measure firefly luciferase activity for 2 second.
- Inject 40 μ l of 1X Stop & GLO Reagent.
- Shake the plate and measure renilla luciferase activity for 2 second.
- LUC values are analysed relative to the REN value and normalized against the control (empty effector vector).

4.3 RESULTS

The main goal of this chapter is the validation of the interactions between a specific VviNAC and some identified VviNAC target genes. Indeed, many of the selected TFs binding sites were found within the promoter regions of other VviNAC family members; the number of binding sites and regulated genes for each selected transcription factor is reported in **Figure 73**.

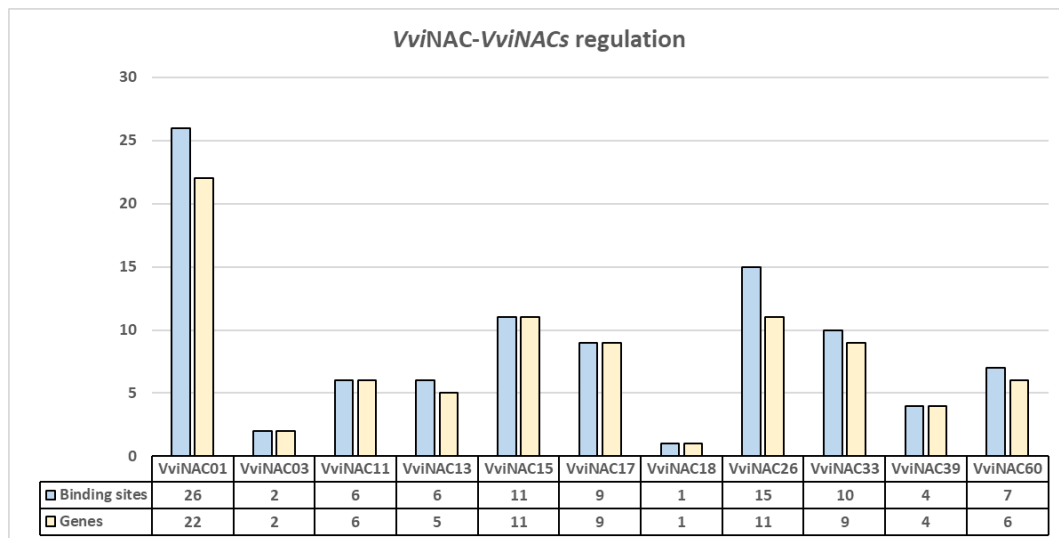


Figure 73: Bar chart reporting the number of interactions between each of the selected VviNAC TFs and the promoting region of VviNAC genes. Moreover, the chart reports also the number of VviNAC genes directly regulated by each transcription factors.

A total of 33 regulated VviNAC target genes were found among all the DAP-seq results (**Table 60**). The final aim is the validation of all these interactions; however, the promoter isolation is a quite long procedure and, for this reason, not all the found interactions were tested in time for this thesis.

The decision was to start isolating and testing the activation/repression of the most represented targets between all the DAP-seq datasets; on the base of this consideration, a ranking (**Table 60**), from the most represented to the least, of the different VviNAC targets founds in all the DAP-seq assays results allowed to select 5 candidates, which promoters were isolated (**Appendix D**) and tested in a dual luciferase assay: VviNAC05 (VIT_17s0000g06400), VviNAC08 (VIT_18s0001g02300), VviNAC34 (VIT_12s0028g03050), VviNAC37 (VIT_10s0003g00350) and VviNAC61 (VIT_08s0007g07640).

Moreover, *VviNAC01* (VIT_01s0146g00280) promoter was also taken into consideration because it seems to be regulated by *VviNAC01* itself; considering the high number of *VviNAC* genes regulated by this TF, it was interesting to see if it could have a positive or negative role on its own regulation.

| Dual Luciferase Reporter Assay | | TFs | | | | | | | | | | Somma | |
|--------------------------------|----------|----------|----------|----------|----------|----------|----------|----------|----------|----------|----------|-------|----------|
| | | VviNAC01 | VviNAC03 | VviNAC11 | VviNAC13 | VviNAC15 | VviNAC17 | VviNAC18 | VviNAC26 | VviNAC33 | VviNAC39 | | VviNAC60 |
| Targets | VviNAC05 | * | * | | | | * | * | * | * | * | * | 7 |
| | VviNAC34 | * | | * | * | * | | | * | * | * | 7 | |
| | VviNAC61 | * | | * | | * | * | | * | * | * | 7 | |
| | VviNAC73 | * | * | | | | * | | * | * | * | 6 | |
| | VviNAC19 | * | | * | * | * | | | * | * | * | 5 | |
| | VviNAC20 | * | | | * | * | * | | | * | * | 5 | |
| | VviNAC37 | * | | * | * | * | | | * | * | * | 5 | |
| | VviNAC08 | * | | | | | * | | * | * | * | 4 | |
| | VviNAC67 | * | | | | * | * | | * | * | * | 4 | |
| | VviNAC39 | * | | | | * | * | | * | * | * | 3 | |
| | VviNAC47 | * | | * | | | * | | | | | 3 | |
| | VviNAC53 | * | | | | * | * | | | | | 3 | |
| | VviNAC21 | * | | | * | | | | | | | 2 | |
| | VviNAC23 | | | | | | | | * | | * | 2 | |
| | VviNAC45 | | | * | | | | | | | * | 2 | |
| | VviNAC58 | | | | | | * | | * | | * | 2 | |
| | VviNAC63 | * | | | | | | | * | * | * | 2 | |
| | VviNAC66 | | | | | | | | * | | * | 2 | |
| | VviNAC01 | * | | | | | | | | | | 1 | |
| | VviNAC07 | | | | | | | | * | | * | 1 | |
| | VviNAC12 | | | | | | | | | * | * | 1 | |
| | VviNAC15 | | | | | | | | | * | * | 1 | |
| | VviNAC17 | * | | | | | | | | | | 1 | |
| | VviNAC25 | * | | | | | | | | | | 1 | |
| | VviNAC29 | * | | | | | | | | | | 1 | |
| | VviNAC40 | | | | | | | | * | | * | 1 | |
| | VviNAC51 | | | | | * | | | | | | 1 | |
| | VviNAC54 | | | | | * | | | | | | 1 | |
| | VviNAC56 | * | | | | | | | | | | 1 | |
| | VviNAC62 | * | | | | | | | | | | 1 | |
| | VviNAC64 | * | | | | | | | | | | 1 | |
| | VviNAC70 | * | | | | | | | | | | 1 | |
| | VviNAC71 | | | | | * | | | | | | 1 | |

Table 60: Ranking list of all the *VviNAC* genes regulated by at least one of the selected TFs. The purple-colored targets on the left are the one chosen to be tested in the DLRA.

The Dual Luciferase Reporter Assay (DLRA) is a powerful technique used for the validation of the interaction between a specific transcription factor and the promoter of a gene; moreover, the assay is quantitative and the analysis permits to identify the investigated TF as an activator or a repressor.

Moreover, considering the binding of more than one selected *VviNAC* TFs on some *VviNACs* promoters, the investigation of a possible correlation between the binding site positions revealed with the DAP-seq and the fluorescence quantitative value of the DLRA, could be useful to understand a little bit more about the different action that the TFs could have on a specific gene.

It is obvious that the understanding of the fine regulatory mechanisms of a gene can hardly be explained on the base of a simply binding site observation, especially in

this specific case in which all the selected TFs present a very similar expression profile in Atlas dataset; however, an attempt has been done.

VviNAC01 was validated as repressor of its own transcription; this was very interesting because a sort of negative feedback regulation on its own transcription could be assumed (**Fig. 74**).

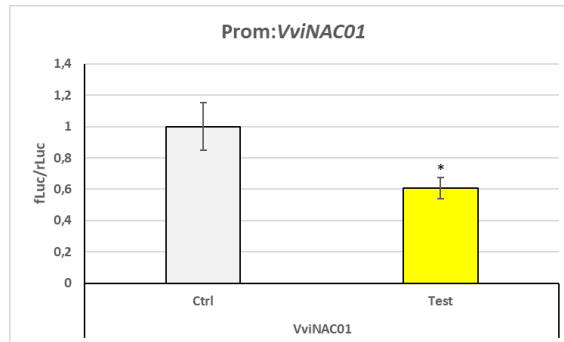


Figure 74: *VviNAC01* promoter activations tested by Dual Luciferase Reporter Assays in infiltrated *Nicotiana benthamiana* leaves. The activity of these promoters was tested in the presence and absence of the 35S:*VviNAC01* effector vector. LUC values are reported relative to the REN value and normalized against the control (empty effector vector). LUC values represent the mean of three biological replicates (three technical replicates each) \pm standard deviation (SD). Asterisks (*) indicate significant differences in promoter activation compared with the control (t-test; $p < 0.05$).

VviNAC05 was repressed by the action of VviNAC01, VviNAC03 and VviNAC17; instead, it resulted activated by VviNAC18, VviNAC26, VviNAC33 and VviNAC60 (**Fig. 75**). VviNAC03 and VviNAC18 are both NOR orthologues and the finding that they both regulate the same gene but in an opposite way is very intriguing.

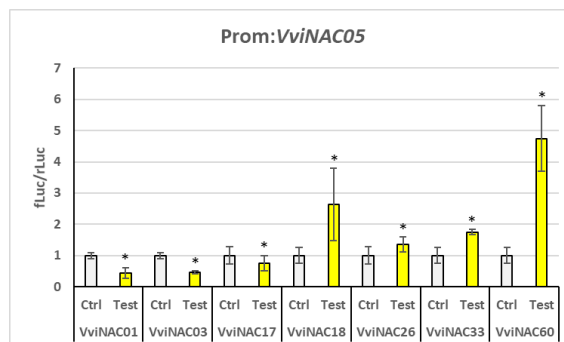


Figure 75: *VviNAC05* promoter activations tested by Dual Luciferase Reporter Assays in infiltrated *Nicotiana benthamiana* leaves. The activity of these promoters was tested in the presence and absence of 7 different 35S:*VviNAC* effector vectors. LUC values are reported relative to the REN value and normalized against the control (empty effector vector). LUC values represent the mean of three biological replicates (three technical replicates each) \pm standard deviation (SD). Asterisks (*) indicate significant differences in promoter activation compared with the control (t-test; $p < 0.05$).

Concerning the *VviNAC05* promoter region, it was clear that the binding of VviNAC17 (-1911) and VviNAC03 (-1859) are specific and always brings to a repression of the gene expression; the other interactions revealed a very close or identical position of the binding sites (**Table 61**). VviNAC01 (repressor), VviNAC18 (activator), VviNAC26 (activator), VviNAC33 (activator) and VviNAC60 (activator) bind the promoter of the gene at 0 bp from the transcription start site (TSS), suggesting a very fine stage- or organ- or tissue- specific, and maybe competitive, role; VviNAC26 (activator) and VviNAC60 (activator) bind very close to each other, at -1867 and -1862 bp from the TSS, respectively, suggesting a possible enhanced activation with the heterodimerization of the two TFs.

| Interaction elements | | Region of interaction | | Over expressions | | DAP-seq | DLRA | |
|----------------------|------------------------|-----------------------|-----------------|------------------|-----------|---------|-----------|--------|
| TFs | Direct regulated genes | Genic region | Distance to TSS | Stable | Transient | q-value | fLuc/rLuc | p<0.05 |
| VviNAC01 | VviNAC05 | Promoter (<=1kb) | 0 | | | 12,84 | -2,30 | * |
| VviNAC03 | VviNAC05 | Promoter (1-2kb) | -1859 | | | 6,66 | -2,20 | * |
| VviNAC17 | VviNAC05 | Promoter (1-2kb) | -1911 | | | 853 | -1,33 | * |
| VviNAC18 | VviNAC05 | Promoter (<=1kb) | 0 | | | 2,89 | 2,62 | * |
| VviNAC26 | VviNAC05 | Promoter (1-2kb) | -1867 | | | 1976 | 1,35 | * |
| VviNAC26 | VviNAC05 | Promoter (<=1kb) | 0 | | | 1295 | 1,35 | * |
| VviNAC33 | VviNAC05 | Promoter (<=1kb) | 0 | | | 2,24 | 1,75 | * |
| VviNAC60 | VviNAC05 | Promoter (1-2kb) | -1862 | | | 33,15 | 4,74 | * |

Table 61: List of all the possible TFs binding sites on the *VviNAC05* promoter, correlated with the over expressions, the DAP-seq q-values and the DLRA fluorescence results. The yellow highlighted interactions indicate the same position on the promoting region of the different TFs and the green one the possible heterodimers elements and sites.

VviNAC08 was activated by VviNAC01 and VviNAC33 but its expression resulted suppressed by the action of VviNAC17 and VviNAC26 (**Fig. 76**).

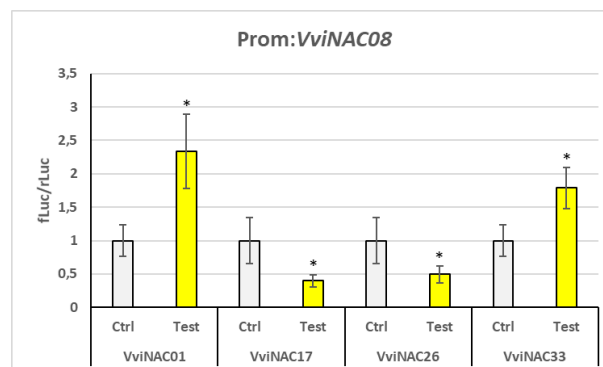


Figure 76: *VviNAC08* promoter activations tested by Dual Luciferase Reporter Assays in infiltrated *Nicotiana benthamiana* leaves. The activity of these promoters was tested in the presence and absence of 4 different 35S:*VviNAC* effector vectors. LUC values are reported relative to the REN value and normalized against the control (empty effector vector). LUC values represent the mean of three biological replicates (three technical replicates each) \pm standard deviation (SD). Asterisks (*) indicate significant differences in promoter activation compared with the control (t-test; $p < 0.05$).

VviNAC08 resulted activated by *VviNAC01* and *VviNAC33*, which present very close binding sites, at -327 and -320 bp from TSS respectively, and suggesting a possible interaction between the two TFs (**Table 62**). The suppression of the expression of the gene was, instead, regulated by two other TFs (*VviNAC17* and *VviNAC26*), which presented the same identical binding position at -29 bp from the TSS and introducing the idea of a very fine differentiation in the regulation mechanism of this gene; moreover, *VviNAC26* also presented a specific repression binding site at -341 bp from the TSS (**Table 62**). Moreover, the two repressors of the *VviNAC08* expression belong to the same clade (III) in the phylogenetic tree (**Fig. 19, Introduction of Chapter 2**) and the activator belongs to another clade (V). *VviNAC01*, which also activated *VviNAC08* expression, belongs to the same clade of the repressors but, in the previous phylogenetic tree (Wang et al, 2013) it was present in another different clade (V).

| Interaction elements | | Region of interaction | | Over expressions | | DAP-seq | DLRA | |
|----------------------|------------------------|-----------------------|-----------------|------------------|-----------|---------|-----------|--------|
| TFs | Direct regulated genes | Genic region | Distance to TSS | Stable | Transient | q-value | fLuc/rLuc | p<0.05 |
| VviNAC01 | VviNAC08 | Promoter (<=1kb) | -327 | | | 2,4 | 2,33 | * |
| VviNAC17 | VviNAC08 | Promoter (<=1kb) | -29 | | | 204 | -2,49 | * |
| VviNAC26 | VviNAC08 | Promoter (<=1kb) | -341 | | | 636 | -2,03 | * |
| VviNAC26 | VviNAC08 | Promoter (<=1kb) | -29 | | | 352 | -2,03 | * |
| VviNAC33 | VviNAC08 | Promoter (<=1kb) | -320 | | | 3,4 | 1,79 | * |

Table 62: List of all the possible TFs binding sites on the *VviNAC08* promoter, correlated with the over expressions, the DAP-seq q-values and the DLRA fluorescence results. The yellow highlighted interactions indicate the same position on the promoting region of the different TFs and the green one the possible heterodimers elements and sites.

VviNAC34 expression resulted positively controlled by *VviNAC11*, which reported the highest induction of the gene with about a 16-fold activation, *VviNAC13*, *VviNAC15*, *VviNAC33* and *VviNAC60*; whereas, it was negatively regulated by *VviNAC26* (**Fig. 77**). Unfortunately, its regulation by *VviNAC01* was not validated and this finding suggests the need of a co-factor (or heterodimerization complex with another *VviNAC* TF) for the activation/repression of this specific gene.

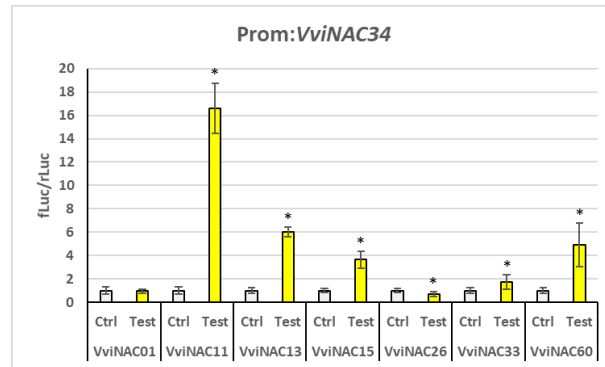


Figure 77: *VviNAC34* promoter activations tested by Dual Luciferase Reporter Assays in infiltrated *Nicotiana benthamiana* leaves. The activity of these promoters was tested in the presence and absence of 7 different 35S:*VviNAC* effector vectors. LUC values are reported relative to the REN value and normalized against the control (empty effector vector). LUC values represent the mean of three biological replicates (three technical replicates each) \pm standard deviation (SD). Asterisks (*) indicate significant differences in promoter activation compared with the control (t-test; $p < 0.05$).

VviNAC34 presented a specific binding site for VviNAC26 (-390 bp from the TSS), which brings to the suppression of the gene expression; all the other TFs activate the expression of *VviNAC34* (**Table 63**). VviNAC60 presents a specific binding sites at -414 bp from the TSS, whereas the other four TFs binding sites suggest possible heterodimerization or, being maybe too close, a fine dynamic regulatory mechanism; indeed, VviNAC11 and VviNAC33 present the binding at -353 and -354 bp from the TSS, and VviNAC13 and VviNAC15 at -200 and -203 bp, respectively (**Table 63**).

Even though the interaction of VviNAC01 with the gene were not validated, it is interesting to notice that *VviNAC34* presented a VviNAC01 specific binding site at -229 bp from the TSS and another site at -353 bp from the TSS, the same position found for VviNAC11 and VviNAC33 (**Table 63**).

| Interaction elements | | Region of interaction | | Over expressions | | DAP-seq | DLRA | |
|----------------------|------------------------|-----------------------|-----------------|------------------|-----------|---------|-----------|--------|
| TFs | Direct regulated genes | Genic region | Distance to TSS | Stable | Transient | q-value | fLuc/rLuc | p<0.05 |
| VviNAC01 | VviNAC34 | Promoter (<=1kb) | -353 | | | 21,71 | -1,05 | |
| VviNAC01 | VviNAC34 | Promoter (<=1kb) | -229 | | | 9,34 | -1,05 | |
| VviNAC11 | VviNAC34 | Promoter (<=1kb) | -353 | | | 3,26 | 16,61 | * |
| VviNAC13 | VviNAC34 | Promoter (<=1kb) | -200 | | | 6,76 | 6,03 | * |
| VviNAC15 | VviNAC34 | Promoter (<=1kb) | -203 | | | 17,55 | 3,67 | * |
| VviNAC26 | VviNAC34 | Promoter (<=1kb) | -390 | | | 348 | -1,39 | * |
| VviNAC33 | VviNAC34 | Promoter (<=1kb) | -354 | | | 5,72 | 1,73 | * |
| VviNAC60 | VviNAC34 | Promoter (<=1kb) | -414 | -2,51 | | 5,76 | 4,93 | * |

Table 63: List of all the possible TFs binding sites on the *VviNAC34* promoter, correlated with the over expressions, the DAP-seq q-values and the DLRA fluorescence results. The green and light-blue highlighted interactions indicate two possible different heterodimers elements and sites; the grey color indicates the not validated interactions.

VviNAC37 regulation resulted to be always in favor of its activation and mediated by *VviNAC11*, *VviNAC13* and *VviNAC33* (**Fig. 78**).

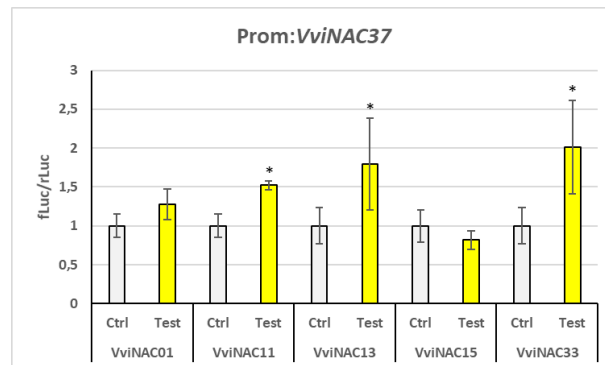


Figure 78: *VviNAC37* promoter activations tested by Dual Luciferase Reporter Assays in infiltrated *Nicotiana benthamiana* leaves. The activity of these promoters was tested in the presence and absence of 5 different 35S:*VviNAC* effector vectors. LUC values are reported relative to the REN value and normalized against the control (empty effector vector). LUC values represent the mean of three biological replicates (three technical replicates each) \pm standard deviation (SD). Asterisks (*) indicate significant differences in promoter activation compared with the control (t-test; $p < 0.05$).

VviNAC37 resulted always activated by three TFs: *VviNAC11*, *VviNAC13* and *VviNAC33*. All present the same binding site position at 0 (or -1) bp from the TSS; however, a *VviNAC33* specific activation binding site was found at -899 bp from the TSS (**Table 64**).

Moreover, the two not validated interactions regarding *VviNAC01* and *VviNAC15* present a very close binding site on the *VviNAC37* promoter (0 bp and -3 bp from the TSS, respectively), suggesting an heterodimerization possibility between the two TFs (**Table 64**).

| Interaction elements | | Region of interaction | | Over expressions | | DAP-seq | DLRA | |
|----------------------|------------------------|-----------------------|-----------------|------------------|-----------|---------|-----------|--------|
| TFs | Direct regulated genes | Genic region | Distance to TSS | Stable | Transient | q-value | fLuc/rLuc | p<0.05 |
| VviNAC01 | VviNAC37 | Promoter (<=1kb) | 0 | | | 15,38 | 1,28 | |
| VviNAC01 | VviNAC37 | Promoter (<=1kb) | -905 | | | 13,63 | 1,28 | |
| VviNAC01 | VviNAC37 | Promoter (<=1kb) | -272 | | | 2,63 | 1,28 | |
| VviNAC11 | VviNAC37 | Promoter (<=1kb) | 0 | | | 2,75 | 1,52 | * |
| VviNAC13 | VviNAC37 | Promoter (<=1kb) | 0 | | | 9,64 | 1,79 | * |
| VviNAC13 | VviNAC37 | Promoter (<=1kb) | -926 | | | 2,3 | 1,79 | * |
| VviNAC15 | VviNAC37 | Promoter (<=1kb) | -3 | | | 7,52 | -1,23 | |
| VviNAC33 | VviNAC37 | Promoter (<=1kb) | -899 | | | 5,72 | 2,01 | * |
| VviNAC33 | VviNAC37 | Promoter (<=1kb) | -1 | | | 3,97 | 2,01 | * |

Table 64: List of all the possible TFs binding sites on the *VviNAC37* promoter, correlated with the over expressions, the DAP-seq q-values and the DLRA fluorescence results. The yellow highlighted interactions indicate the same position on the promoting region of the different TFs and the grey color indicates the not validated interactions.

VviNAC61 resulted activated by VviNAC11, VviNAC33 and VviNAC60, whereas was repressed by the action of VviNAC17 and VviNAC26 (**Fig. 79**).

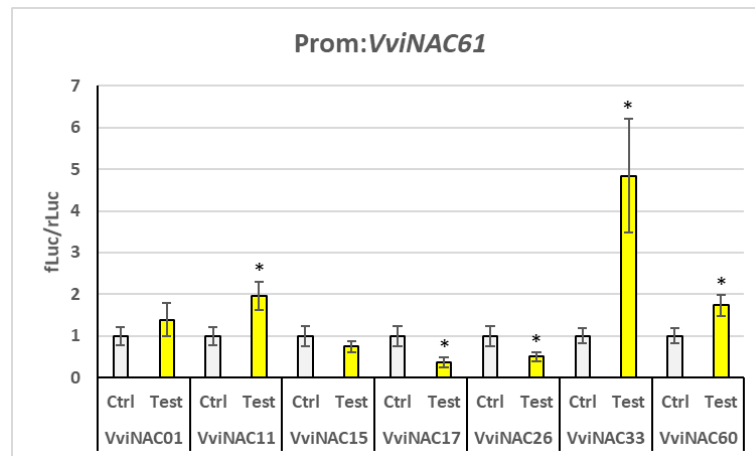


Figure 79: *VviNAC61* promoter activations tested by Dual Luciferase Reporter Assays in infiltrated *Nicotiana benthamiana* leaves. The activity of these promoters was tested in the presence and absence of 7 different 35S:*VviNAC* effector vectors. LUC values are reported relative to the REN value and normalized against the control (empty effector vector). LUC values represent the mean of three biological replicates (three technical replicates each) \pm standard deviation (SD). Asterisks (*) indicate significant differences in promoter activation compared with the control (t-test; $p < 0.05$).

All the transcription factors that regulate this gene present the binding site at 0 bp from the TSS (**Table 65**): VviNAC11, VviNAC33 and VviNAC60 act as activators, whereas VviNAC17 and VviNAC26 as repressors. This evidence could be interpreted in different ways, but the most likely hypothesis is that the activators and repressors probably fine regulate the gene in different developmental stages, whereas the activation or repression mechanisms are orchestrated by the different TFs in different organs or tissues. Moreover, both the not validated interactions present the binding sites at 0 bp from the TSS as all the other TFs.

| Interaction elements | | Region of interaction | | Over expressions | | DAP-seq | DLRA | |
|----------------------|------------------------|-----------------------|-----------------|------------------|-----------|---------|-----------|--------|
| TFs | Direct regulated genes | Genic region | Distance to TSS | Stable | Transient | q-value | fLuc/rLuc | p<0.05 |
| VviNAC01 | VviNAC61 | Promoter (<=1kb) | 0 | | | 27,26 | 1,38 | |
| VviNAC11 | VviNAC61 | Promoter (<=1kb) | 0 | | | 2,55 | 1,96 | * |
| VviNAC15 | VviNAC61 | Promoter (<=1kb) | 0 | | 1,56 | 25,45 | -1,35 | |
| VviNAC17 | VviNAC61 | Promoter (<=1kb) | 0 | | | 1869 | -2,74 | * |
| VviNAC26 | VviNAC61 | Promoter (<=1kb) | 0 | | | 1855 | -2,01 | * |
| VviNAC33 | VviNAC61 | Promoter (<=1kb) | 0 | | | 3,78 | 4,84 | * |
| VviNAC60 | VviNAC61 | Promoter (<=1kb) | 0 | | | 59,84 | 1,73 | * |

Table 65: List of all the possible TFs binding sites on the *VviNAC61* promoter, correlated with the over expressions, the DAP-seq q-values and the DLRA fluorescence results. The yellow highlighted interactions indicate the same position on the promoting region of the different TFs and the grey colour indicates the not validated interactions.

VviNAC11, VviNAC13, VviNAC33 and VviNAC60 appeared to be only

regulators of other *VviNAC* genes, without being present as target themselves (**Appendix E**); they are all *switch* genes, and this evidence highlights once more the importance of these TFs in the regulation of the developmental processes as principal actors.

Moreover, only two interaction presented a match between the over expression and the DLRA results: *VviNAC15-VviNAC61* (**Table 65**) and *VviNAC60-VviNAC34* (**Table 63**). Unfortunately, it was not possible to define a good correlation between the experiments; the repression role of *VviNAC15* on *VviNAC61*, validated by the luciferase assay, did not reflect the up regulation of the gene in the transient over expression, and the role of *VviNAC60* as an activator of *VviNAC34* was also not reconfirmed with the over expression of the TF, where the gene was down regulated.

At the end of all the analyses, a hierarchical network of all the validated regulations was constructed (**Fig. 80**). The transcription factors hierarchy, considering that many other *VviNAC* TFs - *VviNAC* targets interactions need to be validated, was given only considering the number of regulated *VviNAC* genes. In **Appendix E**, the entire possible *VviNAC-VviNACs* network, only DAP-seq results based, shows the enormous complexity of the developmental regulatory mechanisms putatively orchestrated by the *VviNAC* family.

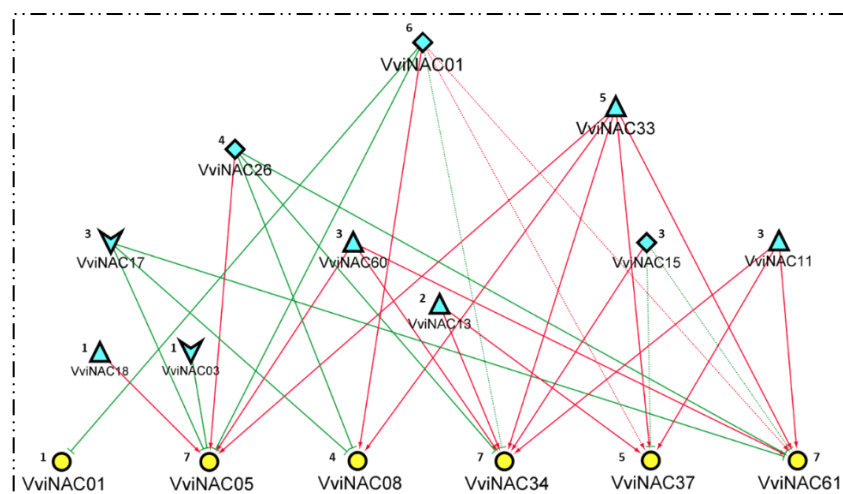


Figure 80: Hierarchical representation of all the validated *VviNAC-VviNACs* interactions. The TFs are highlighted in light-blue and their role as activators, repressors or double-action regulators is represented with a triangle, an arrow and a square, respectively. All the targets are represented as yellow circles. Next to each element of the hierarchy the number of interactions is reported. The red \rightarrow arrows indicate the activation of the related target and the green T arrows show the repression of the targets. The continuous lines indicate the validated interactions ($p < 0.05$) and the dashed lines indicate the not significant interactions.

5. DISCUSSION

The current global warming contest is assuming a notable attention due to its effects on agriculture (Webb *et al.*, 2007). In particular, the grapevine cultivation is highly temperature sensitive and the maintenance of a stable high-quality grape production is a fundamental point for the wide wine industry (Spayd *et al.*, 2002; Marais *et al.*, 2001; Haselgrove 2000; Hannah *et al.*, 2013).

Increase knowledges on the regulation of the developmental process occurring in the plant, in particular concerning the berry ripening, are required to limit the damage caused by the profound climate changes (Pearce and Coombe 2004; Jones and Davis 2000). Studying the transcriptome regulation will help to get a comprehensive picture of the molecular mechanisms of the maturation shift in grapevine which will have an important direct involvement in the management of the vineyard.

The grapevine development is a long and very complex process which is affected by many exogenous and endogenous factors (Duchêne *et al.*, 2010; Jones and Davis, 2000; Coombe and McCarthy, 2000; Martinez-Esteso *et al.*, 2013; Kennedy *et al.*, 2002). The grapevine global gene expression atlas (Fasoli *et al.*, 2012) showed the transcriptional shift during the vegetative-to-mature transition in most of grapevine organs and tissues; afterwards, the main actors of this shift, called *switch* genes, were identified with an integrated network analysis (Palumbo *et al.*, 2014). Some *switch* genes were found in common between the Atlas and a specific berry dataset (Massonnet *et al.*, 2017), suggesting their specific role in the berry ripening. Interestingly, most of these *switch* genes were transcription factors and some of them were identified as markers of the first transition of the onset of berry ripening (Fasoli *et al.*, 2018).

Among the *switches*, particular interest was placed on the *NAC* (*NAM/ATAF/CUC*) genes, which belongs to a large plant-specific transcription factors family, involved in many processes such as plant growth and development, response to abiotic and biotic stress, flower and fruit development, hormone signaling and regulation of secondary metabolic processes (Hendelman *et al.*, 2013; Raman *et al.*, 2008; Fabi *et al.*, 2012; Wang *et al.*, 2013; Sun *et al.*, 2012). Indeed, the identification and characterization of some *VviNAC* genes involved in the grapevine (Wang *et al.*, 2013) maturation, in particular in the berry ripening, was the first step to fully

understand the regulation mechanisms underlying these developmental processes. The investigation started by D'Inca (2017) from a group of five *VviNAC*s, four *switch* genes (*VviNAC11*, *VviNAC13*, *VviNAC33* and *VviNAC60*) and a *NOR* (Giovannoni, 2004; Giovannoni *et al.*, 1995) orthologue (*VviNAC03*). Transient over expression assay combined with microarray analyses were already performed on these genes. Moreover, *VviNAC33* and *VviNAC60* were also stably over expressed and the transgenic grapevines were molecularly (microarray) and phenotypically characterized: *VviNAC33* overexpressing leaves showed a yellowing effect due to a chlorophyll breakdown, *VviNAC60* overexpressing plants showed a slightly plant growth and an earlier stem lignification in comparison to the same-age control plant.

Afterwards, on the base of Atlas (Fasoli *et al.*, 2012) expression profiles similarity to the one of *VviNAC60*, of the distance to *VviNAC60* in the phylogenetic tree construct upon all the *VviNAC* family (Wang *et al.*, 2013) and of some recent RNA-seq transcriptomic analysis performed on grapes (Fasoli *et al.*, 2018), other interesting *VviNAC* genes were identified and isolated: *VviNAC01*, *VviNAC08*, *VviNAC15*, *VviNAC17*, *VviNAC18*, *VviNAC26*, *VviNAC38*, *VviNAC39* and *VviNAC61*. The cv Shiraz isolated coding sequences of the selected *VviNAC*s showed a very high similarity to the one of the cv Pinot noir reference genome, reporting only a few SNPs which brought to aminoacidic changes.

After the isolation and cloning, the transient over expressions of the selected *VviNAC* genes were performed directly in grapevine to gain information about the impact of the over expression of these genes on the leaf transcriptome and to have some hints about the possible targets of these TFs. Microarray analyses of the transcriptomes were carried out to complete what was already started with *VviNAC03*, *VviNAC11*, *VviNAC13*, *VviNAC33* and *VviNAC60* (D'Inca, 2017). For these last two genes, the transient over expression results were also compared with the available stable one. The over expression datasets are very useful to highlight the activation/repression role of a specific TF on a metabolic pathway but, at the same time, are very difficult to interpret in the correct way concerning the direct regulation of a specific gene. Moreover, must be considered that the results of the

different approaches (stable and transient) are very different since the transient over expression focus on the primary transcriptomic changes and the stable on the secondary derived metabolisms or developmental processes alterations.

To avoid possible ‘false positive’ target genes in the direct regulation interpretation of a specific TF, the DAP-seq (Bartlett *et al.*, 2017) on the cv Shiraz genome was performed for all the selected VviNACs.

DAP-seq is a fast, high-throughput, inexpensive, and easily scaled method that permits to obtain a cistrome map of a TF (O’Malley *et al.*, 2016); indeed, the DAP-seq permits to detect all the possible binding sites of transcription factor, losing the chromatin-structure-associated and tissue specificity regulation variables. It couples *in vitro* translated and affinity-purified TFs with next-generation sequencing of a genomic DNA library to discover all the possible protein binding sites (O’Malley *et al.*, 2016; Bartlett *et al.*, 2017); moreover, DNA libraries are constructed using native genomic DNA preserving tissue-specific cytosine methylations that are known to impact TF binding. This represents the first *Vitis vinifera* DAP-seq attempt and some optimization were necessary to assure the good yield of the experiment.

The success of the assay is strongly gDNA libraries quality dependent; for this reason, many protocols were tested to be able to obtain a high amount of very pure genomic DNA (Bartlett *et al.*, 2017). At first three different samples were considered as tests of the DAP-seq experiments, young leaves, green berries and berries at veraison; the starting idea was to try to reveal some possible differences in the binding of the TFs due to cytosine methylation, which could be tissue and developmental stage related (Bartlett *et al.*, 2017). Unfortunately, no protocol tested on the berries at veraison permitted to extract enough genomic DNA to proceed with the library preparation; this was probably due to the high quantity of phenolic compounds present in that type of tissue. Concerning the other two samples (young leaves and green berries), the reported protocol (**Material and methods, Chapter 3**) worked on both, with much higher yields on the leaf tissue, and genomic DNA libraries were efficiently prepared. However, considering the not enough remarkable differences (noticed in the final DAP-seq results) between the two

different tissues and the higher difficulties in obtaining the genomic DNA from the green berries, only the leaf results are reported in this thesis.

The optimization steps highlighted the fact that the use of Nanodrop to quantify the plant genomic DNA for the library preparation is not recommended as minor impurities in the purified genomic DNA sample can make the quantification inaccurate (Bartlett *et al.*, 2017); for this reason, the suggestion is to use the Qubit. Concentrations of the grapevine DNA libraries after the adapter ligation usually range from around 125–180 ng/ μ L (recovering about 50–70% of the original genomic DNA amount), which is a very high yield compared to the literature reported one (Bartlett *et al.*, 2017; Galli *et al.*, 2018). Moreover, the amount of genomic DNA library used in a DAP-seq experiment is highly dependent on genome size (Bartlett *et al.*, 2017); for a relatively small genome, as the *A. thaliana* one, 100 ng are sufficient, but with larger genomes (as the *Vitis vinifera* one) 500–1000 ng produce better results. Indeed, 500 ng and, in some cases, 1000 ng of genomic DNA library were used for all the TFs in this study. However, to establish an optimal genomic DNA input amount, it is useful to perform DNA library titration using positive control proteins; it must be considered that too small quantities of genomic DNA would not allow the detection of all the possible TF binding sites and that, on the contrary, an excessive quantity of genomic DNA could lead to many false positives (Bartlett *et al.*, 2017).

Moreover, a good expression of the tagged protein is crucial for a successful experiment; for this reason, a Western blot analysis could be performed to verify the TF expression before the DAP part (Bartlett *et al.*, 2017). In this type of assay the *in vitro* translation is generally used because, even if it is expensive, it has worked for many TF family. It was noticed that the good translation of the proteins is also family-related; indeed, some TF families showed a higher percentage of success in the DAP-seq assay than others. Concerning the NAC family, generally it works well in this type of assay and the literature findings (Bartlett *et al.*, 2017) reflected the results of this thesis where only three TFs did not work properly, reaching an 80% of successfully translated TFs. However, a standard *E. coli* protein expression and purification can also be performed in this step (Galli *et al.*, 2018).

Finally, the final concentrations of DAP-seq samples can vary, but the typical amounts range from 10–50 ng/ μ L (Bartlett *et al.*, 2017). To assess whether a particular DAP-seq experiment worked well, the DNA must be sequenced and evaluated for the presence of binding peaks. The target number of sequencing reads will depend on the size of the genome; for *Vitis vinifera* samples (~ 500 Mb genome size), 3,5 million reads per DAP-seq sample were sequenced. This value was decided in proportion to the 10 million reads generally considered for the maize genome, which is enormously larger than the grapevine one (Galli *et al.*, 2018).

Even if it represents an easy and fast method, the DAP-seq technique is also subject to some limitations; the causes are generally dependent on the TF-specific DNA binding properties related to the *in vitro* expression and to the absence of co-factors or other protein partners (Bartlett *et al.*, 2017). It is also important to consider that the DAP-seq technique is a powerful but very dispersive way to identify the targets of a transcription factor; performing this assay it was possible to obtain all the possible binding sites of the selected VviNACs on the grapevine genome, without highlighting the tissue or time specific role of these TFs. This means that all the possible actions of each VviNAC family member are written inside the DAP datasets but different keys to read them are required in relation to temporal, organ and tissue dynamics. Appears clear that, to fully understand the role of the selected TFs, a huge work will be required and that the transversality between different biotechnological and bioinformatic approaches is needed.

By comparing transcriptomic analyses, obtained from transient and stable grapevine transformation, with the DAP-seq datasets, the identification of some target genes commonly and consistently modulated was possible.

Indeed, many *switch* genes (many of which were transcription factors) often returned in the different DAP-seq datasets and some of them also have a positive correlation in the over expression one; between the most represented TFs, many Zinc-fingers (Takatsuji, 1998; Ciftci-Yilmaz and Mittler, 2008), NAC (Wang *et al.*, 2013; Sun *et al.*, 2011; Le Henanff *et al.*, 2013;), WRKY (Vannozzi *et al.*, 2018; Amato *et al.*, 2017; Wang *et al.*, 2014; Amato *et al.*, 2019), MYB (Matus *et al.*, 2010; Holl *et al.*, 2013; Vannozzi *et al.*, 2018; Matus *et al.*, 2017; Amato *et al.*, 2019; Koyama *et al.*, 2014; Czemmél *et al.*, 2012) and bHLH (Xu *et al.*, 2014;

Matus *et al.*, 2010) constantly appeared. Moreover, a lot of first and second transition markers were also present in the DAP-seq results (Fasoli *et al.*, 2018); knowing that these genes are responsible of the primary metabolic pathways shutdown, this evidence emphasized the important role of the selected *VviNAC* genes in the regulation of the grapevine development, activating the maturation processes and repressing the vegetative growth, and, considering that they were selected for their high expression in the berry tissues, confirmed their mainly action on the berry ripening regulation. Moreover, some interesting features concerning the regulatory role of each selected *VviNAC* TF were found. For some TFs, a putative role was strongly highlighted, for others this thesis represents a good starting point in the elucidation of more complex regulation mechanisms.

VviNAC01, which in the Atlas resulted co-express with many genes, confirmed its important role in the ethylene pathways showing a lot of *ERF/AP2* (Xie *et al.*, 2019; Feng *et al.*, 2020; Sun *et al.*, 2016) up regulated genes as results of its transient over expression and revealing many ethylene-related genes also between the DAP-seq targets; unfortunately, the ethylene role in grapevine has not been well defined yet. Moreover, also the phylogenetic footprints correlate with *ANAC092*, considered the key positive regulator of leaf senescence, involved in a delicately balanced feed-forward loop that promotes ethylene-mediated chlorophyll degradation (Kim *et al.*, 2009). *VviNAC03*, one of the closest NOR orthologue, did not reveal a well-defined identity; however, its role seems to be plant growth related and probably activates the glycosylation of flavonoids, which is important for the defense responses and for the berries color. *VviNAC08* DAP-seq results highlighted a very low number of direct targets (data validated with multiple DAP-seq assay on this specific TF) and none of them was found in the over expression dataset where, however, a possible role of this TF in the gibberellin-related and circadian mechanisms was noticed. *VviNAC11* seems to be related to the control of the auxin pathways and, even if with some mixed results, in promoting the stop of the lateral organs growth and the chlorophylls degradation. *VviNAC13* revealed almost no correlation between the over expression and the DAP-seq results; for this reason, the interpretation of its putative role is difficult. However, the GO enrichment of the DAP-seq dataset highlighted a probable action in the lignin and

phenylpropanoid metabolic processes. VviNAC15 revealed many TF between its regulated targets and, considering that this evidence perfectly matched with the over expression results where all the TF genes were up regulated, this suggests its fundamental role in the regulation mechanisms orchestration. VviNAC17 appeared to be a regulator of the jasmonic acid-induced gene expression; this hypothesis was also supported by the correlation of this TF with ANAC055 (known to regulate jasmonic acid-induced expression of defense genes) in the binding motif analysed. VviNAC18 analyses reported its role in the chlorophyll degradation. Indeed, the *SGR1* and *SGR2* were found as targets, respectively up and down regulated by the over expression of the TF, strongly suggesting its action in stopping the *SGR2* production (which negatively regulates chlorophylls degradation interfering with *SGR1*) and directly activating the *SGR1* production (Park *et al.*, 2007; Sakuraba *et al.*, 2014). VviNAC26 matching results between the DAP-seq and the over expression presented many genes related to the sugars biosynthesis, which is important in the leaves and berries maturation processes, and in the anthocyanin synthesis. VviNAC33 was the most studied TF; indeed, a paper has been recently accepted (New Phytologist) and its major role in terminating photosynthetic activity and organ growth, as part of a regulatory network governing the vegetative-to-mature phase transition, was already well established. Unfortunately, VviNAC38 DAP-seq resulted not very informative and *VviNAC38* over expression was not performed; the functional analyses on this TF will be done again as soon as possible. VviNAC39 resulted to up regulate the transport of many metabolites (mostly sugars and lipids) and the ubiquitin-conjugating, which was demonstrated to be involved in ripening and post-harvest stage in grapevine (Gao *et al.*, 2017). VviNAC61 revealed a predominant role in the regulation of the metabolic processes, focused on the aromatic compounds biosynthesis. This TF was already known to have a role in the withering processes (Zenoni *et al.*, 2016) and the transient over expression results strongly confirmed this evidence. Unfortunately, the DAP-seq assay did not result very informative and is going to be performed again to complete the information available for this very interesting TF.

VviNAC60 was already identified as the master regulator of the berry ripening; for this reason, a more in-depth analysis was performed on this TF. The DAP-seq

results, combined again with the stable and transient over expression dataset, revealed a lot of hormones related up regulated genes which clearly showed the pro-maturation effects of the VviNAC60 action; whereas the many transcription factors found in its lists resulted regulated by the TF in both positive (when related to secondary metabolic processes activation) and negative (when related to the vegetative growth) ways. This was very interesting because the important and major role of this transcription factor in the grapevine maturation processes was again highlighted. Considering that the DAP-seq technique gives a global view of all the possible binding sites of a specific transcription factor, without taking into consideration the tissue and developmental stage specificity of regulation, ChIP-seq data were also obtained for VviNAC60. The aim was to find direct target of the TF which are related to the berry ripening specific regulation.

ChIP-seq represents a powerful way to study TF-DNA interactions *in vivo* (Kaufmann *et al.*, 2010; Bowler *et al.*, 2004); this methodology has produced numerous applications in studying the composition and dynamics of chromatin landscapes and TF binding, as well as assessing the interplay between different factors in gene regulation under different conditions and developmental phases (Kidder *et al.*, 2011; Kaufmann *et al.*, 2010; Lin *et al.*, 2012; Martel *et al.*, 2011). ChIP-seq approach can be used to study DNA methylation, chromatin structure/histone modifications, and the cooperative binding of TFs.

As for the DAP-seq, this also represent the first *Vitis vinifera* ChIP-seq attempt. Indeed, genome-wide applications of the ChIP-seq methodology in the plant field are still relatively scarce. This delay is partly due to technical difficulties in ChIP sample preparation related to the complexity of plant tissues for the presence of rigid cell walls, high levels of cellulose and lignin and large vacuoles (Kaufmann *et al.*, 2010). The establishment of an efficient ChIP-seq protocols for plant systems (especially for grapevine) is hard and many optimizations were required as different types of tissues were sampled (Bowler *et al.*, 2004); indeed, the chromatin extraction from the berry samples was hard and requires many little precautions to reach a good yield.

The ChIP assay consists in the TF-DNA crosslinking by formaldehyde tissues vacuum infiltration, the isolation of chromatin from the extracted nuclei, the

chromatin fragmentation, the immunoprecipitation of the TF-DNA complexes with a specific antibody, the reverse crosslinking for the recovery of DNA and the final identification of associated DNA sequences through sequencing (Kaufmann *et al.*, 2010).

The formaldehyde percentage is an important parameter that needs to be taken into consideration (Schmiedeberg *et al.*, 2009). It is essential that the samples are treated with a suitable volume of formaldehyde to assure the stable bond between the protein and the DNA: if the formaldehyde concentration is too low or the incubation time is too short, not enough crosslinked material will be produced; on the other hand, a formaldehyde concentration that is too high or an incubation time that is too long also reduces recovery, reflecting the insoluble complexes formation or masking the epitopes recognition by the antibody (Kaufmann *et al.*, 2010; Schmiedeberg *et al.*, 2009; Solomon *et al.*, 1985).

Sonication is the most variable step in the process and will vary greatly depending on the cell type, the quantity of cells, the sonication volume, the crosslinking degree and the specifics of the sonicator used (Kaufmann *et al.*, 2010; Bortz *et al.*, 2011). Sonication is important for the solubilization and shearing of the chromatin; under sonication brings to a loss of resolution of the binding sites and over sonication can lead to protein denaturation. The optimal chromatin fragments length ranges between 150 and 300 bp (Kaufmann *et al.*, 2010).

The quality of antibodies used for ChIP-seq is one of the most important factors that contribute to the quality of the generated data (Park, 2009; Kidder *et al.*, 2011). Antibodies that offer high sensitivity and specificity are necessary for ChIP-seq because they allow the detection of enrichment peaks without substantial background noise (Kaufmann *et al.*, 2010; Busby *et al.*, 2016); indeed, the specificity of an antibody should be directly addressed by immunoblot analysis of the protein of interest. It is also important to consider the potential cross-reactivity of antibodies with closely related family members. The heterogeneity of the antibody should also be considered in the selection of an antibody; monoclonal antibodies, which recognize a single epitope on an antigen, may be a good choice for diminishing background noise in ChIP studies but, however, the use of monoclonal antibodies may result in a lower signal if the epitope is masked by

surrounding chromatin components or if the protein is part of a larger protein complex (Busby *et al.*, 2016; Kaufmann *et al.*, 2010). The polyclonal antibodies represent the best solution as they offer the flexibility of multiple epitopes recognition (Kaufmann *et al.*, 2010; Busby *et al.*, 2016).

In this thesis the specificity analyses of the used polyclonal antibody are not reported; however, many Western blot analyses were carried out before using the specific anti-VviNAC60 polyclonal antibody. The obtained results were useful to assure the antibody specific recognition of the TF of interest and be confident of the right fragment selection in the immunoprecipitation step.

The ChIP-seq results were very hard to obtain because of the above-described technical issues that appeared during the setting up of the experiment; however, the efforts brought to a few but interesting observations. Even if the percentages of alignment on the grape genome of the immunoprecipitated chromatin fragments were, for the berry samples, very low (the lowest is the 5,29% of the berries at veraison), the highest number of VviNAC60 regulated genes was found in the veraison berries sample, the main subject of the investigation, where indeed the TF is more expressed.

This result matched with the Atlas (Fasoli *et al.*, 2012) transcriptomic findings despite the higher number of contaminants present in that sample; indeed, the most of the immunoprecipitated sequences belonged to microorganisms that usually live on the fruit and leaves surface (Menendez and Garcia-Fraile, 2017). The organisms were the same in all the samples and the percentage of the different microorganisms was almost the same; what increased the contamination in different sequenced samples was the DNA of only one microorganism, the *Paraburkholderia fungorum*. Searching in the literature, this plant probiotic bacterium was found correlated with fruit growth improvements (Rahman *et al.*, 2018; Menendez and Garcia-Fraile, 2017); this finding made of this enriched, unexpected and unwanted bacterial DNA a real interesting observation, useful for further studies.

The small 'Veraison berry' dataset was analyzed and 46 binding sites were obtained. Only four genes found correlations with the VviNAC60 stable and transient over expression DEGs and only one of these, the *PROTEIN BINDING/ ZINC ION BINDING* (VIT_12s0028g03340), resulted up regulated by the action of

the TF in promoter region; unfortunately, almost nothing is present in literature concerning this gene. Moreover, this list of the ChIP-seq found gene was crossed with the DAP-seq one but, again, only one gene matched. Unfortunately, this gene, *SRG1- SENESCENCE-RELATED GENE 1 OXIDOREDUCTASE* (VIT_10s0003g02400), revealed the TF binding site in two different genic regions, in an exon in the ChIP-seq dataset and in the promoter in the DAP-seq one. However, this gene, seems to be very interesting as it is related to senescence, a maturation process. Senescence brings to a huge macromolecular catabolism which dismantles the chloroplasts and decreases the photosynthetic capacity of the leaves; moreover, a recent study provided evidence that a delayed leaves senescence enhances carbon assimilation that, ultimately, increased the number of fleshy fruits and their total soluble solid content (Lira *et al.*, 2017). Indeed, it was found that one way to delay senescence initiation is the relation of key TFs involved in triggering this process, such as the NAC (Lira *et al.*, 2017). For this reason, the fact that VviNAC60 directly regulates *SRG1* only in the veraison berry tissue once again gives strength to the role of this master regulator in the berry ripening and encourages new optimizations on this promising first ChIP-seq attempt.

After many technical and biological considerations, we do not think that the ChIP-seq results were due to the non-specificity antibody issue; probably, the probiotic microorganisms are simply more abundant on berries at veraison (Menendez and Garcia-Fraile, 2017) and this tissue- and developmental stage-specific characteristic is reflected in the sequencing results. However, a solution is needed to avoid the unwanted material selection and to obtain more accurate ChIP-seq results; in the future, a further setting-up of the ChIP-seq protocol will be carried out to better clean the starting harvest tissues, to find a way to increase the chromatin extraction yield from the berries and to avoid the selection and enrichment of the contaminants (for example trying to use a different preclearing method).

After all the individual analyses on all the 14 above described VviNACs, with the aim to try understanding the general regulative role of the selected VviNAC family members on the grapevine transcriptome, a global analysis of all the possible interactions obtained with the DAP-seq assays was performed. The *UTP GLUCOSE-1-PHOSPHATE URIDYLYLTRANSFERASE* (VIT_04s0044g00710),

resulted regulated by 13 of the 14 *VviNACs*. Not much information is available in literature concerning this gene, excluding the fact that it encodes for an enzyme obviously related to the carbohydrate metabolism; however, looking at the Atlas (Fasoli *et al.*, 2012), the gene showed a significant increase in its expression in the berry pericarp starting from the post fruit set to the ripening, in the berry flesh and skin at veraison and in the seeds at veraison and mid ripening. Considering the role of the *UTP GLUCOSE-1-PHOSPHATE URIDYLYLTRANSFERASE* in the sugar metabolism and the interesting results obtained with its expression profile investigation, this gene could really represent an important target in the *VviNAC*-mediated berry development.

As said previously in this chapter, many *VviNAC* genes were found as targets of the selected TFs; to assess if these genes were for sure direct targets of the *VviNACs* regulation, another experimental approach, the Dual Luciferase Reporter Assay (DLRA), was used. The DLRA is a powerful technique used for the validation of the interaction between a specific transcription factor and the promoter of a gene using a fluorescent reporter; moreover, the assay is quantitative and the analysis permits to identify the investigated TFs as activators or repressors (Sherf *et al.*, 1996). Considering the binding of more than one selected *VviNAC* TFs on some *VviNAC* promoters, the fluorescence quantitative value of the DLRA, correlated with the q-value of the DAP-seq and the FC of the over expression, could also be useful to understand which TF has the predominant regulative role on a gene.

The decision of starting from the identification of a possible mechanism of regulation between *VviNACs* comes from the idea that the understanding of the connection between the members of this family could facilitate the further interpretation of a wider regulation network, especially being conscious of the high expression similarity between the selected TFs. Indeed, many genes were found as common targets of more than one TF and the specific single *VviNAC*-related genes most of the times belonged to biological and metabolic processes regulation functional categories, which have a fundamental but very generic role in the development scenario.

The final aim is, of course, to validate all of them; however, the promoters isolation and cloning are long and difficult steps considering the possible differences

between the reference genome (Pinot Noir) and the selected cultivar for this thesis (Shiraz), the A and T enrichment generally present in the promoting regions which makes specific primers design hard and the possible similarity between the promoters of genes belonging to the same family. For all these reasons, the decision was to start testing the activation/repression effects of some selected TFs on five of the most represented *VviNAC* genes between all the DAP-seq datasets: *VviNAC05*, *VviNAC34* and *VviNAC61* were found to be regulated by seven of the 14 TFs; *VviNAC37* by five of them and *VviNAC08* by four. Moreover, *VviNAC01* was also taken into consideration because it resulted directly regulated by *VviNAC01* itself. It was very interesting to find *VviNAC61* between the most DAP-seq represented regulated genes; this TF was already known to have a role in the withering processes (Zenoni *et al.*, 2016) and the transient over expression results confirm this evidence. The fact that it seems to be regulated by such a high number of *VviNAC* TFs could be related to its role in secondary metabolic processes, which are relevant in the last stages of the development and in the post harvesting phase and could place it downstream of the regulatory network of the *NAC* TFs. Moreover, *VviNAC61* presented a very low number of binding sites in its DAP-seq dataset, with no interactions found with the promoters of other *VviNACs*. Looking at the DEGs, *VviNAC61* over expression regulated 1135 gene, supporting the hypothesis of its role in the downstream processes of development.

The DLRA was performed on *N. benthamiana* leaves; this choice has the limit that, working on a different plant species, no hypothetical grapevine co-factor is available and, knowing that *VviNACs* often form homodimers in their regulatory action, some activation/repression could be lost. This consideration must be done when correlating the over expression results with the fluorescence quantification: all the over expressions were performed in the plant of interest (*V. vinifera*) and all the other *VviNACs* are also present and could interact, bringing to the regulation of a gene. However, the DLRA gives the possibility to test the action on a gene of more TFs together, permitting to identify possible heterodimerizations; this part has not been performed yet but will be a crucial point of the *VviNACs* investigation.

The results obtained in this thesis showed that *VviNAC01* can act both as an activator and a repressor; indeed, it directly repressed *VviNAC05* expression,

whereas activated the *VviNAC08* one. Moreover, *VviNAC01* was validated as repressor of its own transcription; this was very interesting because, also considering the high number of genes regulated by this TF, a sort of negative feedback regulation on its own transcription could be assumed. No significant fluorescence values were obtained, in comparison to the control, concerning the other three DAP-seq identified regulated genes (*VviNAC34*, *VviNAC37* and *VviNAC61*); probably a partner is needed in these specific cases. *VviNAC03* was confirmed in its action on the *VviNAC05* expression and results a repressor of this gene. *VviNAC11* acted always as an activator in all the validated interactions and directly regulates *VviNAC34*, *VviNAC37* and *VviNAC61*. Moreover, the *VviNAC34* expression activation was the highest revealed, with a 16-fold induction compared to the control. *VviNAC13*, which also acted always as an activator, results to regulate *VviNAC34* and *VviNAC37* expression. *VviNAC15* presented a binding site on three of the six selected *VviNAC* genes (*VviNAC34*, *VviNAC37* and *VviNAC61*) but only one interaction was significantly validated; indeed, it results an activator of *VviNAC34*. Unfortunately, this demonstrated *VviNAC61* repression by *VviNAC15* did not reflect the transient over expression findings, where the gene was found between the up regulated DEGs. *VviNAC17* acted always as a repressor and significantly down regulates *VviNAC05*, *VviNAC08* and *VviNAC61* expression. *VviNAC18* resulted a direct activator of *VviNAC05*. Worth notices that *VviNAC18* and *VviNAC03* are both NOR orthologues (Giovannoni *et al.*, 1995; Giovannoni *et al.*, 2004) and present very similar expression profiles; these knowledges, together with the fact that in the DAP-seq results they presented two totally different binding position on *VviNAC05*, indicate that they do not compete and suggests that they could probably be partners of other TFs which activate or repress the gene in relation to different dynamics. *VviNAC26* acts both as an activator and a repressor; indeed, it positively regulates the expression of *VviNAC05* and directly down regulates the *VviNAC08*, *VviNAC34* and *VviNAC61* expression. *VviNAC33* was found as a direct activator of *VviNAC05*, *VviNAC08*, *VviNAC34*, *VviNAC37* and *VviNAC61* expression. The other master regulator *VviNAC60* was also found to only direct up regulate the expression of the DAP-seq identified target; indeed, high fluorescence values were induced when it regulated *VviNAC05*, *VviNAC34* and

VviNAC61. Unfortunately, the activation acted by *VviNAC60* on *VviNAC34* found no confirmation in the *VviNAC60* stable over expression results, where the gene was down regulated.

Not looking only at the single validated activations/repressions and at the specific found binding sites, it was very interesting to see that more TFs could bind to the same *VviNAC* promoter region, sometimes exactly at the same site, other times very close to each other. The presence of more than one transcription factor binding site in the promoter region of a gene could highlight the ability of the TFs to form homo- or hetero- dimers (Wehner *et al.*, 2011; Mitsuda and Ohme-Takagi, 2009). Generally, these complexes contribute to increase the regulatory effect of a gene in comparison to the result of a single TF binding on the DNA; indeed, it is plausible that the presence of more binding sites brings to a synergic regulation of the gene expression (Malhotra and Sowdhamini, 2014; Lai *et al.*, 2019). Considering the highly similar expression profiles of the selected TFs and the fact that sometimes more than two TFs binds very close to each other on the same promoter, it is hard to confidently hypothesize an organ or tissue dependent fine regulation mechanism or to identify only one specific heterodimerization complex; moreover, even in the case of great diversity among the regulators, it would still be difficult to identify the biological causes of possible interactions between TFs. Whether more than one transcription factor binding sites on the promoter of a target gene increase the gene regulation is dependent on several factors (such as proximity), most of them still unclarified; the transcription factor binding attribution to a specific associated gene regulation is an ongoing issue which is mainly bioinformatically studied and does not present many biological validations (Spadafore *et al.*, 2017; Tian *et al.*, 2020). Thanks to the genome editing technology, it would be possible to individually mutate each binding site maintaining its real biological context, identifying in this way the specific binding position-related role of a TF; unfortunately, this is not trivial, especially considering the well know difficulty of working with a not model crop species such as grapevine.

Concerning the DLRA not matching results with the DEGs values, must be considered that the over expressions have helped in the definition of a more specific role of these TFs but the limits of this type of technique are many and the

interpretation of the results is sometimes hard. Only a few cases (for example VviNAC61 and VviNAC01, the most evident) exhibited a clear regulative role from the DAP-seq results and the DEGs analysis correlation; looking at the stable VviNACs over expression, probably what was in most of the cases seen is the long-term action of the TF regulation, on the other way, the transient over expression can give a more instant picture of the transcriptome regulation but the results are highly infiltration-dependent. Moreover, in both the over expressions must be considered the fact that, performing the experiments in grapevine, all the possible co-factors of the TF were available and the identified DEGs could have been positively or negatively regulated by a combination of different TF; as said before, the ability of the NAC TFs to form homodimers is, indeed, well known. It was also very interesting to see that the *switch* master regulators VviNAC33 and VviNAC60, together with the *NOR* orthologues VviNAC03 and VviNAC18, and with other two Atlas switch TFs VviNAC11 and VviNAC13, did not present regulation by any VviNACs. Probably they are placed at the very beginning of the development regulatory network induced by the VviNAC family and orchestrate all the possible mechanisms of control.

Considering all the ongoing climate changes (Hannah *et al.*, 2013; Webb *et al.*, 2007; Spayd *et al.*, 2002), in particular the continuous temperature increasing that is altering the maturation process, that could modify the physiological characteristics of grape, its final quality and consequently the wine one, the development of different strategies to prevent these negative effects is fundamental. Indeed, the study and the interpretation of the molecular mechanisms controlling the onset of berry ripening could provide a solution to the all the current agronomical problems. This thesis represents another little step in the definition of a clear regulatory network of the grapevine maturation processes, particularly focused on the VviNAC TFs and their direct regulated target genes.

In the future, many other putative target genes (and not also between the VviNAC family) will be investigated to obtain more information about the roles of all the VviNACs, but these preliminary results clearly highlight the crucial roles of the VviNAC transcription factors in the regulation of grapevine development through an inter-family network.

REFERENCES

- Amato, A., Cavallini, E., Walker, A. R., Pezzotti, M., Bliet, M., Quattrocchio, F., ... & Tornielli, G. B.** (2019). The MYB 5-driven MBW complex recruits a WRKY factor to enhance the expression of targets involved in vacuolar hyper-acidification and trafficking in grapevine. *The Plant Journal*, 99(6), 1220-1241.
- Amato, A., Cavallini, E., Zenoni, S., Finezzo, L., Begheldo, M., Ruperti, B., & Tornielli, G. B.** (2017). A grapevine TTG2-like WRKY transcription factor is involved in regulating vacuolar transport and flavonoid biosynthesis. *Frontiers in plant science*, 7, 1979.
- Bartlett, A., O'Malley, R. C., Huang, S. S. C., Galli, M., Nery, J. R., Gallavotti, A., & Ecker, J. R.** (2017). Mapping genome-wide transcription-factor binding sites using DAP-seq. *Nature protocols*, 12(8), 1659.
- Bortz, P. D. S., & Wamhoff, B. R.** (2011). Chromatin immunoprecipitation (ChIP): revisiting the efficacy of sample preparation, sonication, quantification of sheared DNA, and analysis via PCR. *PLoS one*, 6(10), e26015.
- Bowler, C., Benvenuto, G., Laflamme, P., Molino, D., Probst, A. V., Tariq, M., & Paszkowski, J.** (2004). Chromatin techniques for plant cells. *The Plant Journal*, 39(5), 776-789.
- Busby, M., Xue, C., Li, C., Farjoun, Y., Gienger, E., Yofe, I., ... & Goren, A.** (2016). Systematic comparison of monoclonal versus polyclonal antibodies for mapping histone modifications by ChIP-seq. *Epigenetics & chromatin*, 9(1), 1-16.
- Ciftci-Yilmaz, S., & Mittler, R.** (2008). The zinc finger network of plants. *Cellular and Molecular Life Sciences*, 65(7), 1150-1160.
- Coombe BG, Mccarthy MG** (2000). Dynamics of grape berry growth and physiology of ripening. *Aust J Grape Wine R.* 6, 131-135.
- Coombe BG, Mccarthy MG.** (2000). Dynamics of grape berry growth and physiology of ripening. *Aust J Grape Wine R.* 6, 131-135.
- Czemmel, S., Heppel, S. C., & Bogs, J.** (2012). R2R3 MYB transcription factors: key regulators of the flavonoid biosynthetic pathway in grapevine. *Protoplasma*, 249(2), 109-118.
- D'Incà E.** (2017). Master regulators of the vegetative-to-mature organ transition in grapevine: the role of NAC transcription factors. PhD thesis. Verona University.
- Duchêne E, Huard F, Dumas V, Schneider C, Merdinoglu D** (2010). The challenge of adapting grapevine varieties to climate change. *Clim Res.* 41, 193- 204.
- Fabi JP, Seymour GB, Graham NS, Broadley MR, May ST, Lajolo FM, Cordenunsi BR, Oliveira do Nascimento JR.** (2012). Analysis of ripening-related gene expression in papaya using an Arabidopsis-based microarray. *BMC Plant Biol.* 12, 242.
- Fasoli M, Dal Santo S, Zenoni S, Tornielli GB, Farina L, Zamboni A, Porceddu A, Venturini L, Bicego M, Murino V, Ferrarini A, Delledonne M, Pezzotti M.** (2012). The grapevine expression atlas reveals a deep transcriptome shift driving the entire plant into a maturation program. *Plant Cell.* 24(9):3489- 505.
- Fasoli M., Richter C. L., Zenoni S., Bertini E., Vitulo N., Dal Santo S., Dokoozlian N., Pezzotti M., Tornielli G.B.** (2018). The timing and order of the molecular events that mark the onset of berry ripening in grapevine. *Plant Physiology*. Vol. 178: 1187-1206.

- Feng, K., Hou, X. L., Xing, G. M., Liu, J. X., Duan, A. Q., Xu, Z. S., ... & Xiong, A. S.** (2020). Advances in AP2/ERF super-family transcription factors in plant. *Critical Reviews in Biotechnology*, 40(6), 750-776.
- Galli, M., Khakhar, A., Lu, Z., Chen, Z., Sen, S., Joshi, T., ... & Gallavotti, A.** (2018). The DNA binding landscape of the maize AUXIN RESPONSE FACTOR family. *Nature communications*, 9(1), 1-14.
- Giovannoni J** (2004). Genetic regulation of fruit development and ripening. *Plant Cell*. 16, S170-S180.
- Giovannoni J, Noensie EN, Ruezinsky DM, Lu X, Tracy SL, Ganal MW, Martin GB, Pillen K, Alpert K, Tanksley SD** (1995) Molecular genetic analysis of the ripening-inhibitor and non-ripening loci of tomato: a first step in genetic map-based cloning of fruit ripening genes. *Mol Gen Genet*. 248, 195-206.
- Hannah L, Roehrdanz PR, Ikegami M, Shepard AV, Shaw MR, Tabor G, et al.** (2013). Climate change, wine, and conservation. *Proc Natl Acad Sci USA*. 110, 6907-12.
- Haselgrove L, Botting D, Van Heeswijck R, HØJ PB, Dry PR, Ford C, Iland PG** (2000). Canopy microclimate and berry composition: The effect of bunch exposure on the phenolic composition of *Vitis vinifera* cv. Shiraz grape berries. *Aust J Grape Wine R*. 6, 141-149.
- Hendelman A, Stav R, Zemach H, Arazi T** (2013). The tomato NAC transcription factor SINAM2 is involved in flower-boundary morphogenesis. *J Exp Bot*. 64, 5497-5507.
- Höll, J., Vannozzi, A., Czemplak, S., D'Onofrio, C., Walker, A. R., Rausch, T., ... & Bogs, J.** (2013). The R2R3-MYB transcription factors MYB14 and MYB15 regulate stilbene biosynthesis in *Vitis vinifera*. *The Plant Cell*, 25(10), 4135-4149.
- Jones GV, Davis RE** (2000). Climate Influences on Grapevine Phenology, Grape Composition, and Wine Production and Quality for Bordeaux, France. *Am J Enol Vitic*. 51, 249-261.
- Kaufmann, K., Muino, J. M., Østerås, M., Farinelli, L., Krajewski, P., & Angenent, G. C.** (2010). Chromatin immunoprecipitation (ChIP) of plant transcription factors followed by sequencing (ChIP-SEQ) or hybridization to whole genome arrays (ChIP-CHIP). *Nature protocols*, 5(3), 457-472.
- Kennedy JA, Matthews MA, Waterhouse AL** (2002). Effect of maturity and vine water status on grape skin and wine flavonoids. *Amer J Enol Vitic*. 53, 268- 274.
- Kidder, B.L., Hu, G., and Zhao, K.** (2011). ChIP-Seq: technical considerations for obtaining high-quality data. *Nat. Immunol*. 12, 918–922.
- Kim JH, Woo HR, Kim J, Lim PO, Lee IC, Choi SH, Hwang D, Nam HG.** (2009). Trifurcate feed-forward regulation of age-dependent cell death involving miR164 in *Arabidopsis*. *Science*. 323(5917):1053-7. doi: 10.1126/science.1166386. PMID: 19229035.
- Koyama, K., Numata, M., Nakajima, I., Goto-Yamamoto, N., Matsumura, H., & Tanaka, N.** (2014). Functional characterization of a new grapevine MYB transcription factor and regulation of proanthocyanidin biosynthesis in grapes. *Journal of Experimental Botany*, 65(15), 4433-4449.
- Lai, X., Stigliani, A., Vachon, G., Carles, C., Smaczniak, C., Zubieta, C., ... & Parcy, F.** (2019). Building transcription factor binding site models to understand gene regulation in plants. *Molecular plant*, 12(6), 743-763.
- Le Hénanff, G., Profizi, C., Courteaux, B., Rabenoelina, F., Gérard, C., Clément, C., ... & Dhondt-Cordelier, S.** (2013). Grapevine NAC1 transcription factor as a convergent node in

developmental processes, abiotic stresses, and necrotrophic/biotrophic pathogen tolerance. *Journal of experimental botany*, 64(16), 4877-4893.

Lin, X., Tirichine, L., & Bowler, C. (2012). Protocol: Chromatin immunoprecipitation (ChIP) methodology to investigate histone modifications in two model diatom species. *Plant methods*, 8(1), 1-9.

Lira, B. S., Gramegna, G., Trench, B. A., Alves, F. R., Silva, E. M., Silva, G. F., ... & Rossi, M. (2017). Manipulation of a senescence-associated gene improves fleshy fruit yield. *Plant physiology*, 175(1), 77-91.

Malhotra, S., & Sowdhamini, R. (2014). Interactions among plant transcription factors regulating expression of stress-responsive genes. *Bioinformatics and Biology insights*, 8, BBI-S16313.

Marais G, Mouchiroud D, Duret L (2001). Does recombination improve selection on codon usage? Lessons from nematode and fly complete genomes. *Proc Natl Acad Sci USA*. 98, 5688-5692.

Martel, C., Vrebalov, J., Tafelmeyer, P., & Giovannoni, J. J. (2011). The tomato MADS-box transcription factor RIPENING INHIBITOR interacts with promoters involved in numerous ripening processes in a COLORLESS NONRIPENING-dependent manner. *Plant physiology*, 157(3), 1568-1579.

Martínez-Esteso MJ, Vilella-Antón MT, Pedreño MA, Valero ML, Bru- Martínez R (2013). iTRAQ-based protein profiling provides insights into the central metabolism changes driving grape berry development and ripening. *BMC Plant Biol*. 13, 167.

Massonnet M, Fasoli M, Tornielli G.B., Altieri M, Sandri M, Zuccolotto P, Paci P, Gardiman M, Zenoni S. and Pezzotti M. (2017) Ripening Transcriptomic Program in Red and White Grapevine Varieties Correlates with Berry Skin Anthocyanin Accumulation. *Plant Physiology*. Vol. 174: 2376–2396.

Matus, J. T., Cavallini, E., Loyola, R., Höll, J., Finezzo, L., Dal Santo, S., ... & Arce-Johnson, P. (2017). A group of grapevine MYBA transcription factors located in chromosome 14 control anthocyanin synthesis in vegetative organs with different specificities compared with the berry color locus. *The Plant Journal*, 91(2), 220-236.

Matus, J. T., Poupin, M. J., Cañón, P., Bordeu, E., Alcalde, J. A., & Arce-Johnson, P. (2010). Isolation of WDR and bHLH genes related to flavonoid synthesis in grapevine (*Vitis vinifera* L.). *Plant molecular biology*, 72(6), 607-620.

Menendez, E., & Garcia-Fraile, P. (2017). Plant probiotic bacteria: solutions to feed the world. *AIMS microbiology*, 3(3), 502.

Mitsuda, N., & Ohme-Takagi, M. (2009). Functional analysis of transcription factors in Arabidopsis. *Plant and Cell Physiology*, 50(7), 1232-1248.

O'Malley, R. C., Huang, S. S. C., Song, L., Lewsey, M. G., Bartlett, A., Nery, J. R., ... & Ecker, J. R. (2016). Cistrome and epicistrome features shape the regulatory DNA landscape. *Cell*, 165(5), 1280-1292.

Palumbo MC, Zenoni S, Fasoli M, Massonnet M, Farina L, Castiglione F, Pezzotti M, Paci P (2014). Integrated network analysis identifies fight-club nodes as a class of hubs encompassing key putative switch genes that induce major transcriptome reprogramming during grapevine development. *Plant Cell*. 26(12), 4617-35.

Park, P. J. (2009). ChIP-seq: advantages and challenges of a maturing technology. *Nature reviews genetics*, 10(10), 669-680.

Park, S. Y., Yu, J. W., Park, J. S., Li, J., Yoo, S. C., Lee, N. Y., ... & Paek, N. C. (2007). The senescence-induced staygreen protein regulates chlorophyll degradation. *The Plant Cell*, 19(5), 1649-1664.

Pearce I, Coombe B (2004). Grapevine phenology. Viticulture: Volume 1 – Resources, Eds. P.R. Dry and B.G. Coombe (Winetitles: Adelaide, South Australia) pp. 150-166.

Rahman, M., Sabir, A. A., Mukta, J. A., Khan, M. M. A., Mohi-Ud-Din, M., Miah, M. G., ... & Islam, M. T. (2018). Plant probiotic bacteria *Bacillus* and *Paraburkholderia* improve growth, yield and content of antioxidants in strawberry fruit. *Scientific reports*, 8(1), 1-11.

Raman S, Greb T, Peaucelle A, Blein T, Laufs P, Theres K (2008). Interplay of miR164, CUP-SHAPED COTYLEDON genes and LATERAL SUPPRESSOR controls axillary meristem formation in *Arabidopsis thaliana*. *Plant J*. 55, 65-76.

Sakuraba, Y., Park, S. Y., Kim, Y. S., Wang, S. H., Yoo, S. C., Hörtensteiner, S., & Paek, N. C. (2014). *Arabidopsis* STAY-GREEN2 is a negative regulator of chlorophyll degradation during leaf senescence. *Molecular plant*, 7(8), 1288-1302.

Schmiedeberg, L., Skene, P., Deaton, A., & Bird, A. (2009). A temporal threshold for formaldehyde crosslinking and fixation. *PLoS One*, 4(2), e4636.

Sherf, B. A., Navarro, S. L., Hannah, R. R., & Wood, K. V. (1996). Dual-luciferase reporter assay: an advanced co-reporter technology integrating firefly and *Renilla* luciferase assays. *Promega Notes*, 57(2), 2-8.

Solomon, M. J., & Varshavsky, A. (1985). Formaldehyde-mediated DNA-protein crosslinking: a probe for in vivo chromatin structures. *Proceedings of the National Academy of Sciences*, 82(19), 6470-6474.

Spadafore, M., Najarian, K., & Boyle, A. P. (2017). A proximity-based graph clustering method for the identification and application of transcription factor clusters. *BMC bioinformatics*, 18(1), 1-14.

Spayd SE, Tarara JM, Mee DL, Ferguson JC (2002). Separation of sunlight and temperature effects on the composition of *Vitis vinifera* cv. 'Merlot' berries. *Amer J Enol and Vitic.* 53, 171-182.

Sun X, Korir NK, Han J, Shangguan LF, Kayesh E, Leng XP, Fang JG (2012). Characterization of grapevine microR164 and its target genes. *Mol. Biol. Rep.* 39, 9463-9472.

Sun, X., Shangguan, L., Fang, J., Song, C., Wang, C., & Mu, Q. (2011). Bioinformatics analysis of the NAC transcription factor family in grapevine. *Genomics and Applied Biology*, 30(2), 229-242.

Sun, X., Zhao, T., Gan, S., Ren, X., Fang, L., Karungo, S. K., ... & Xin, H. (2016). Ethylene positively regulates cold tolerance in grapevine by modulating the expression of ETHYLENE RESPONSE FACTOR 057. *Scientific reports*, 6(1), 1-14.

Takatsuji, H. (1998). Zinc-finger transcription factors in plants. *Cellular and Molecular Life Sciences CMLS*, 54(6), 582-596.

Tian, F., Yang, D. C., Meng, Y. Q., Jin, J., & Gao, G. (2020). PlantRegMap: charting functional regulatory maps in plants. *Nucleic acids research*, 48(D1), D1104-D1113.

Vannozzi, A., Wong, D. C. J., Höll, J., Hmam, I., Matus, J. T., Bogs, J., ... & Lucchin, M. (2018). Combinatorial regulation of stilbene synthase genes by WRKY and MYB transcription factors in grapevine (*Vitis vinifera* L.). *Plant and Cell Physiology*, 59(5), 1043-1059.

Wang N, Zheng, Y, Xin H, Fang L, Li S (2013). Comprehensive analysis of NAC domain transcription factor gene family in *Vitis vinifera*. *Plant Cell Rep.* 32, 61-75.

Wang, M., Vannozzi, A., Wang, G., Liang, Y. H., Tornielli, G. B., Zenoni, S., ... & Cheng, Z. M. M. (2014). Genome and transcriptome analysis of the grapevine (*Vitis vinifera* L.) WRKY gene family. *Horticulture research*, 1(1), 1-16.

Webb L, Whetton P, Barlow EWR (2007). Modelled impact of future climate change on phenology of wine grapes in Australia. *Aust J Grape Wine R.* 13, 165- 175.

Wehner, N., Weiste, C., & Dröge-Laser, W. (2011). Molecular screening tools to study *Arabidopsis* transcription factors. *Frontiers in plant science*, 2, 68.

Xie, Z., Nolan, T. M., Jiang, H., & Yin, Y. (2019). AP2/ERF transcription factor regulatory networks in hormone and abiotic stress responses in *Arabidopsis*. *Frontiers in plant science*, 10, 228.

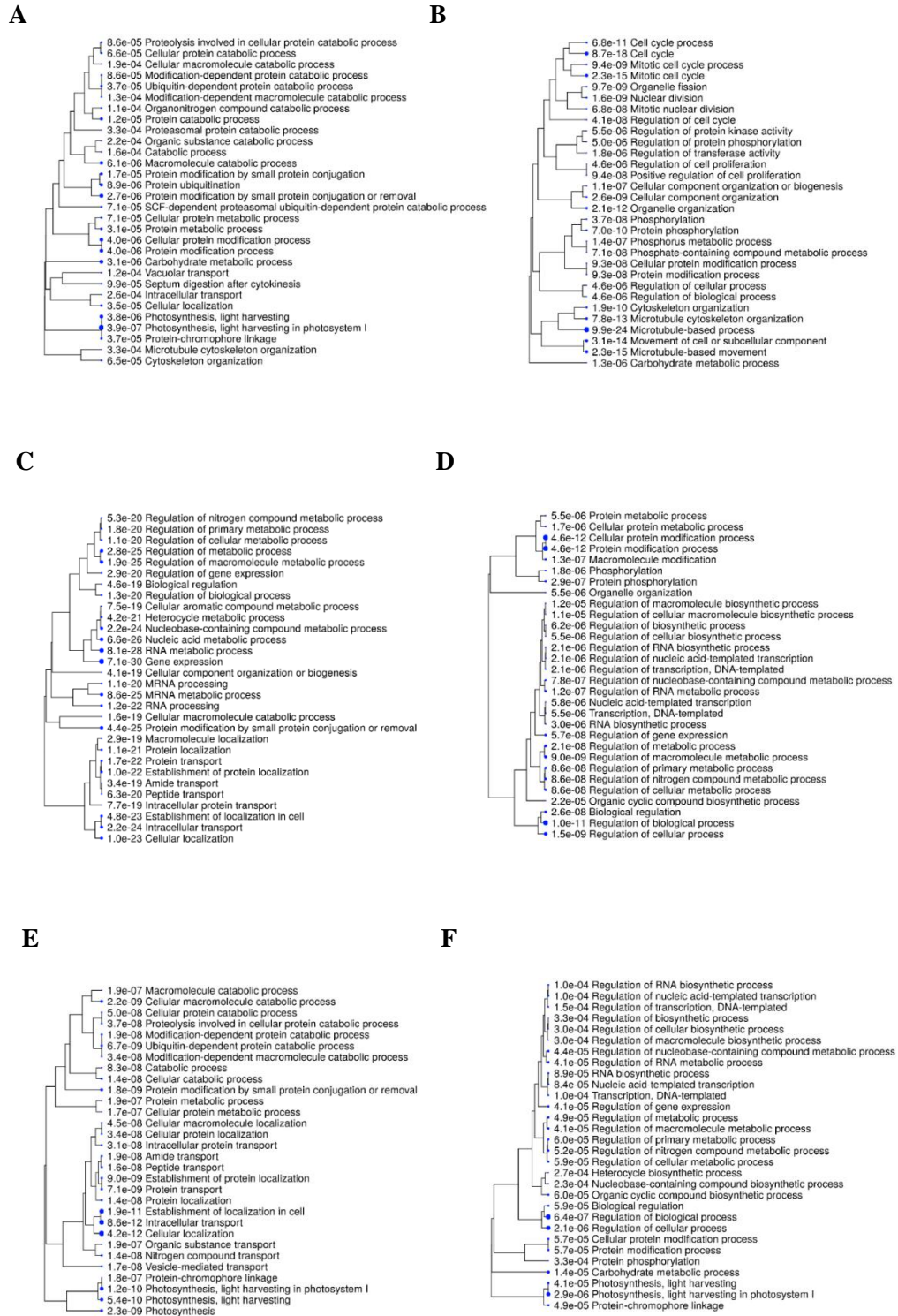
Xu, W., Zhang, N., Jiao, Y., Li, R., Xiao, D., & Wang, Z. (2014). The grapevine basic helix-loop-helix (bHLH) transcription factor positively modulates CBF-pathway and confers tolerance to cold-stress in *Arabidopsis*. *Molecular Biology Reports*, 41(8), 5329-5342.

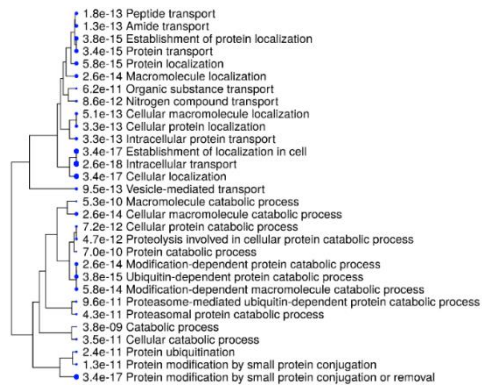
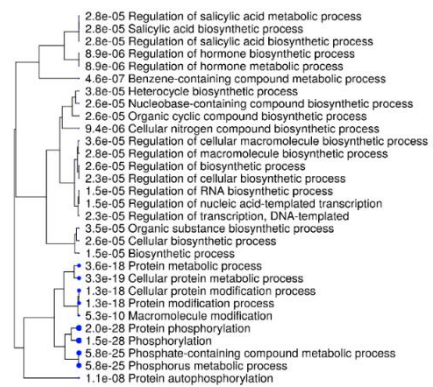
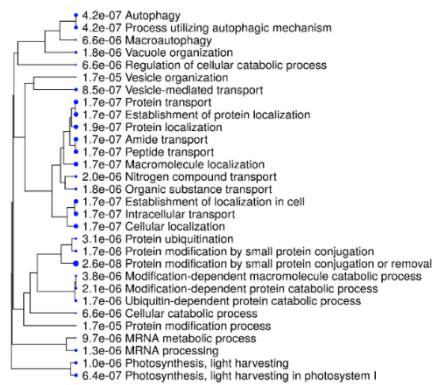
Zenoni, S., Fasoli, M., Guzzo, F., Dal Santo, S., Amato, A., Anesi, A., ... & Tornielli, G. B. (2016). Disclosing the molecular basis of the postharvest life of berry in different grapevine genotypes. *Plant Physiology*, 172(3), 1821-1843.

Zhang, Y., Liu, T., Meyer, C.A., Eeckhoute, J., Johnson, D.S., Bernstein, B.E., Nussbaum, C., Myers, R.M., Brown, M., Li, W., et al. (2008). Model-based analysis of ChIP-seq MACS. *Genome Biol.* 9, R137.1–R137.9.

APPENDIX

Appendix A: A) *VviNAC01*, B) *VviNAC08*, C) *VviNAC15*, D) *VviNAC17*, E) *VviNAC18*, F) *VviNAC26*, G) *VviNAC38*, H) *VviNAC39* and I) *VviNAC61* co-expressing genes GO enrichment analyses using ShinyGO.



G**H****I**

Appendix B: Alignments of A) *VviNAC01*, B) *VviNAC08*, C) *VviNAC15*, D) *VviNAC17*, E) *VviNAC18*, F) *VviNAC26*, G) *VviNAC38*, H) *VviNAC39* and I) *VviNAC61* nucleotide sequences from Shiraz and Pinot Noir cultivars.

A

| | |
|--------------------|---|
| VviNAC01_Shiraz | ATGGAGAAGCTCAATTTTGTGAAGAATGGCGTCCTCAGATTGCCTCCTGGCTTCCGCTTC |
| VviNAC01_Reference | ATGGAGAAGCTCAATTTTGTGAAGAATGGCGTCCTCAGATTGCCTCCTGGCTTCCGCTTC ***** |
| VviNAC01_Shiraz | CATCCTACTGATGAAGAGCTGGTGGTGCAGTACTTGAAGCGCAAGGCTATTCTTGCCCC |
| VviNAC01_Reference | CATCCTACTGATGAAGAGCTGGTGGTGCAGTACTTGAAGCGCAAGGCTATTCTTGCCCC ***** |
| VviNAC01_Shiraz | CTGCCCGCTCCATCATCCCTGAGGTCGATGTCTGCAAGGCTGATCCTTGGGATTTGCCA |
| VviNAC01_Reference | CTGCCCGCTCCATCATCCCTGAGGTCGATGTCTGCAAGGCTGATCCTTGGGATTTGCCA ***** |
| VviNAC01_Shiraz | GGTGATTTGGAGCAGGAGAGGTACTTCTTCAGCACCAGGAGGCCAAGTACCCGAATGGA |
| VviNAC01_Reference | GGTGATTTGGAGCAGGAGAGGTACTTCTTCAGCACCAGGAGGCCAAGTACCCGAATGGA ***** |
| VviNAC01_Shiraz | AACCGGTCGAATAGAGCCACGGTTTCGGGTTACTGGAAGGCAACTGGAATTGACAAGCAA |
| VviNAC01_Reference | AACCGGTCGAATAGAGCCACGGTTTCGGGTTACTGGAAGGCAACTGGAATTGACAAGCAA ***** |
| VviNAC01_Shiraz | ATTGTAGCTTCCAAGGGGAACCGGTTGTGGGGATGAAGAAAACCTTGGTTTTTTATAGA |
| VviNAC01_Reference | ATTGTAGCTTCCAAGGGGAACCGGTTGTGGGGATGAAGAAAACCTTGGTTTTTTATAGA ***** |
| VviNAC01_Shiraz | GGAAAGCCTCCACATGGGTCGAGAACCGATTGGATCATGCACGAATACCGGCTTGTGTGT |
| VviNAC01_Reference | GGAAAGCCTCCACATGGGTCGAGAACCGATTGGATCATGCACGAATACCGGCTTGTGTGT ***** |
| VviNAC01_Shiraz | GCTGAAACCAACCCACAGAAAAGAGCTCGACAACCTCAGAGCTCAATGGCGCAAGCGGAG |
| VviNAC01_Reference | GCTGAAACCAACCCACAGAAAAGAGCTCGACAACCTCAGAGCTCAATGGCGCAAGCGGAG ***** |
| VviNAC01_Shiraz | AACTGGGTGTTGTGCCGCATATTCCTGAAGAAACGGGGCACGAAAAATGATGAGGAGATG |
| VviNAC01_Reference | AACTGGGTGTTGTGCCGCATATTCCTGAAGAAACGGGGCACGAAAAATGATGAGGAGATG ***** |
| VviNAC01_Shiraz | ATGCAAACCAACAATGAGAACCGGGTGGTTCAGAAGTTGAGGAGCAGCAGGCTGTTTTTC |
| VviNAC01_Reference | ATGCAAACCAACAATGAGAACCGGGTGGTTCAGAAGTTGAGGAGCAGCAGGCTGTTTTTC ***** |
| VviNAC01_Shiraz | TATGATTTCTTGACAAGGGACAGGGATGATACTAATCTTGCTTCTTCCAATTCTTCGGGT |
| VviNAC01_Reference | TATGATTTCTTGACAAGGGACAGGGATGATACTAATCTTGCTTCTTCCAATTCTTCGGGT ***** |
| VviNAC01_Shiraz | TCAAGTGGGATCACAGAGGTGTGCAATACCGAATCAGAAGAACACGAAGAAGCAGTAGT |
| VviNAC01_Reference | TCAAGTGGGATCACAGAGGTGTGCAATACCGAATCAGAAGAACACGAAGAAGCAGTAGT ***** |
| VviNAC01_Shiraz | TGCAATAGTTTCTCGCCTTTCAGAAGAAAACCATAA |
| VviNAC01_Reference | TGCAATAGTTTCTCGCCTTTCAGAAGAAAACCATAA ***** |

B

```

VviNAC08_Shiraz      ATGACAGCGGAGTTGCAGTTACCTCCAGGCTTCAGGTTCCATCCGACGGATGAGGAGCTT
VviNAC08_Reference    ATGACAGCGGAGTTGCAGTTACCTCCAGGCTTCAGGTTCCATCCGACGGATGAGGAGCTT
*****

VviNAC08_Shiraz      GTGATGCACTATCTGTGCCGTAATGTGCATCGCAATCGATCGCCGTGCCGATCATTGCC
VviNAC08_Reference    GTGATGCACTATCTGTGCCGTAATGTGCATCGCAATCGATCGCCGTGCCGATCATTGCC
*****

VviNAC08_Shiraz      GAAATTGATCTCTACAAATTCGATCCCTGGCAGCTTCCCTGAGATGGCCTTGTACGGAGAG
VviNAC08_Reference    GAAATTGATCTCTACAAATTCGATCCCTGGCAGCTTCCCTGAGATGGCCTTGTACGGAGAG
*****

VviNAC08_Shiraz      AAAGAGTGGTACTTCTTTTCGCCGAGAGATCGGAAATATCCGAACGGTTCAAGGCCGAAC
VviNAC08_Reference    AAAGAGTGGTACTTCTTTTCGCCGAGAGATCGGAAATATCCGAACGGTTCAAGGCCGAAC
*****

VviNAC08_Shiraz      CGGGCAGCGGGAACAGGGTACTGGAAGGCCACCGGAGCGGATAAGCCTATTGGGCATCCG
VviNAC08_Reference    CGGGCAGCGGGAACAGGGTACTGGAAGGCCACCGGAGCGGATAAGCCTATTGGGCATCCG
*****

VviNAC08_Shiraz      AAACCGGTTGGGATTAAGAAGGCTTTGGTTTTTATGCCGAAAAGCCCCAGGGGAGAG
VviNAC08_Reference    AAACCGGTTGGGATTAAGAAGGCTTTGGTTTTTATGCCGAAAAGCCCCAGGGGAGAG
** *****

VviNAC08_Shiraz      AAGACAAATTGGATTATGCATGAATACCGGCTGGCAGACGTGGACCGGTCCGGCTCGCAAG
VviNAC08_Reference    AAGACAAATTGGATTATGCATGAATACCGGCTGGCAGACGTGGACCGGTCCGGCTCGCAAG
*****

VviNAC08_Shiraz      AAGAATAATAGCTTAAGGTTGGACGATTGGGTTCTGTGCCGCATATACAACAAGAAGGGC
VviNAC08_Reference    AAGAATAATAGCTTAAGGTTGGACGATTGGGTTCTGTGCCGCATATACAACAAGAAGGGC
*****

VviNAC08_Shiraz      ATTGTCGAGAAACAACACCCGCTGCCCGAAATCAGATTGCTCCGATGTTGAGGATCAA
VviNAC08_Reference    ATTGTCGAGAAACAACACCCGCTGCCCGAAATCAGATTGCTCCGATGTTGAGGATCAA
*****

VviNAC08_Shiraz      AAGCCTGGACCTCTTGCTCTAAGCAGGAAGGTAGGTGCGATGCCCTCCACCTCCGCCGCCG
VviNAC08_Reference    AAGCCTGGACCTCTTGCTCTAAGCAGGAAGGTAGGTGCGATGCCCTCCACCTCCGCCGCCG
*****

VviNAC08_Shiraz      TCGTCCTCTACGGCACCAACTGCGACAGCGGCACTGGACGATTTGGTGTACTTCGACTCA
VviNAC08_Reference    TCGTCCTCTACGGCACCAACTGCGACAGCGGCACTGGACGATTTGGTGTACTTCGACTCA
*****

VviNAC08_Shiraz      TCGGATTCCGGTCCCGCCCTCCACACCCGACTCGAGCTGTTCCGAGCACGTGGTGTGCCCG
VviNAC08_Reference    TCGGATTCCGGTCCCGCCCTCCACACCCGACTCGAGCTGTTCCGAGCACGTGGTGTGCCCG
*****

VviNAC08_Shiraz      GAGTTCACGTGCGAGAGGGAGGTGCAGAGCGAGCCCAAGTGAAGGAGTGGGAAAATCCC
VviNAC08_Reference    GAGTTCACGTGCGAGAGGGAGGTGCAGAGCGAGCCCAAGTGAAGGAGTGGGAAAATCCC
*****

VviNAC08_Shiraz      ATGGACTTTTCGTACAATTACATGGATGCCACAGTTGACAACGCATTTTGTCTCAGTTC
VviNAC08_Reference    ATGGACTTTTCGTACAATTACATGGATGCCACAGTTGACAACGCATTTTGTCTCAGTTC
*****

VviNAC08_Shiraz      CCGAATAATCAGATGTCGCCATTGCAGGACATGTTTCATGTACCTGCAGAAGCCCTTCTGA
VviNAC08_Reference    CCGAATAATCAGATGTCGCCATTGCAGGACATGTTTCATGTACCTGCAGAAGCCCTTCTGA
*****

```

C

VviNAC15_Shiraz ATGAAGGTGACAGTGGGTGATTTCGTCGCGTGTCTTGACGGAGACGAAAAGTCTGCGTGG
VviNAC15_Reference ATGAAGGTGACAGTGGGTGATTTCGTCGCGTGTCTTGACGGAGACGAAAAGTCTGCGTGG

VviNAC15_Shiraz CCACCCGGTTCCGATTCCATCCCACCGATGAAGAGCTGGTTCTGTATTATCTGAAGAAG
VviNAC15_Reference CCACCCGGTTCCGATTCCATCCCACCGATGAAGAGCTGGTTCTGTATTATCTGAAGAAG

VviNAC15_Shiraz AAGATCTGCCGGCAGCGCTGAAGCTCGATATCATCGCCGAGGTCGATGTCTACAAGTGG
VviNAC15_Reference AAGATCTGCCGGCAGCGCTGAAGCTCGATATCATCGCCGAGGTCGATGTCTACAAGTGG

VviNAC15_Shiraz GACCCCGAGGATTTGCCTGGCTATCTAAATTGAAGACAGGAGATAGGCAATGGTTCTTT
VviNAC15_Reference GACCCCGAGGATTTGCCTGGCTATCTAAATTGAAGACAGGAGATAGGCAATGGTTCTTT

VviNAC15_Shiraz TTTAGCCCCAGAGACAGGAAGTACCCTAATGGAGCTAGGTCTAATAGGGCAACCAGGCAT
VviNAC15_Reference TTTAGCCCCAGAGACAGGAAGTACCCTAATGGAGCTAGGTCTAATAGGGCAACCAGGCAT

VviNAC15_Shiraz GGATACTGAAAGCAACAGGAAAGGATCGAACTATTAGCTGTAATATTCGGTCAGTTGGT
VviNAC15_Reference GGATACTGAAAGCAACAGGAAAGGATCGAACTATTAGCTGTAATATTCGGTCAGTTGGT

VviNAC15_Shiraz GTGAAGAAGACCTTGGTTTTCTATAAAGGCCGTGCTCCAAGTAAAGAGCCACAGACTGG
VviNAC15_Reference GTGAAGAAGACCTTGGTTTTCTATAAAGGCCGTGCTCCAAGTAAAGAGCCACAGACTGG

VviNAC15_Shiraz GTGATGCATGAGTATACAATGGATGAAGAGGAGCTCAAGAGATGCCCGAATGTGCAGGAT
VviNAC15_Reference GTGATGCATGAGTATACAATGGATGAAGAGGAGCTCAAGAGATGCCCGAATGTGCAGGAT

VviNAC15_Shiraz TATTATGCACTTTATAAGGTCTTCAAGAAGAGTGGACCTGGTCCCAAAAATGGTGAGCAA
VviNAC15_Reference TATTATGCACTTTATAAGGTCTTCAAGAAGAGTGGACCTGGTCCCAAAAATGGTGAGCAA

VviNAC15_Shiraz TACGGGGCTCCATTTAAAGAAGAGGAATGGGCTGACGAAGATGACCTAGATGTTAGTAAC
VviNAC15_Reference TACGGGGCTCCATTTAAAGAAGAGGAATGGGCTGACGAAGATGACCTAGATGTTAGTAAC

VviNAC15_Shiraz TACTCTGTTGAAGAGACTCCTCCAGAGCAGTTGAATGGCGTTATTTCTGTCAATAATTC
VviNAC15_Reference TACTCTGTTGAAGAGACTCCTCCAGAGCAGTTGAATGGCGTTATTTCTGTCAATAATTC

VviNAC15_Shiraz AAACCTAATGGGCAAGACTGTCAAGCAGATGCTTGGGATGACATCTGAAAGGACTTGCA
VviNAC15_Reference AAACCTAATGGGCAAGACTGTCAAGCAGATGCTTGGGATGACATCTGAAAGGACTTGCA

VviNAC15_Shiraz GAAGCACCTCCAGTTGTTCTCTGCGTGTGATGATTATGTTAATCTACTAGCTCAGGTT
VviNAC15_Reference GAAGCACCTCCAGTTGTTCTCTGCGTGTGATGATTATGTTAATCTACTAGCTCAGGTT

VviNAC15_Shiraz ATTGGTGAAGAAGAAGCTCAAACCTCTTGGTGGATTCACTCAATGGAGCTTTCGTT
VviNAC15_Reference ATTGGTGAAGAAGAAGCTCAAACCTCTTGGTGGATTCACTCAATGGAGCTTTCGTT

VviNAC15_Shiraz GCTGATCCAATAAGCACAGTATTAACCCCTACCTCTCAGCAGTATGCTGTGCCAGAGAAC
VviNAC15_Reference GCTGATCCAATAAGCACAGTATTAACCCCTACCTCTCAGCAGTATGCTGTGCCAGAGAAC

VviNAC15_Shiraz GTTGAGTTTACACAATCAGCCTCCTCTCAGTTGCAATTGCACGAGGCACCTGAGGTCACA
VviNAC15_Reference GTTGAGTTTACACAATCAGCCTCCTCTCAGTTGCAATTGCACGAGGCACCTGAGGTCACA

VviNAC15_Shiraz TCTGCTCCTAACATTAGTGAGCAGGAACGTGGATTAAGTGAGGAGGACTTCTAGAAATG
VviNAC15_Reference TCTGCTCCTAACATTAGTGAGCAGGAACGTGGATTAAGTGAGGAGGACTTCTAGAAATG

VviNAC15_Shiraz GATGATCTCCTTGGTCCAGAACCATTCTCAAACCTATGAAAAAAGTGGAGGAACTTG
VviNAC15_Reference GATGATCTCCTTGGTCCAGAACCATTCTCAAACCTATGAAAAAAGTGGAGGAACTTG

VviNAC15_Shiraz CAGTTTGAAGCCGATGGATTGAGCATGCTTGACCTGTACCATGATGCAGCCATGTTCTTT
VviNAC15_Reference CAGTTTGAAGCCGATGGATTGAGCATGCTTGACCTGTACCATGATGCAGCCATGTTCTTT

VviNAC15_Shiraz CGTGACATTTGGCCCTATTGATCAAGGAACGGTCCGCATCCATATTGAATACCATTGAG
VviNAC15_Reference CGTGACATTTGGCCCTATTGATCAAGGAACGGTCCGCATCCATATTGAATACCATTGAG

VviNAC15_Shiraz AATGAGATGGTGAACAGTTGAATTACCAGCTGCAGCCCCATTCTGTTGGTGCAGATCAG
VviNAC15_Reference AATGAGATGGTGAACAGTTGAATTACCAGCTGCAGCCCCATTCTGTTGGTGCAGATCAG

VviNAC15_Shiraz ATTAGTGGTCAGCTGTGGACACTCGATCAAAGTGTCTGTACCTCAGCAGAATCTATTTCAG
VviNAC15_Reference ATTAGTGGTCAGCTGTGGACACTCGATCAAAGTGTCTGTACCTCAGCAGAATCTATTTCAG

```

VviNAC15_Shiraz      GGGATCATTTGGGCAGCCAACCTCAGGTGTGGTATATGCCAGCAGTTCTACAAATGTTCCC
VviNAC15_Reference    GGGATCATTTGGGCAGCCAACCTCAGGTGTGGTATATGCCAGCAGTTCTACAAATGTTCCC
*****

VviNAC15_Shiraz      ACCGAAGGAAATCAAACATGAATGGCGAAGGGGTAACGGTGCAGGGAACCGATTCACT
VviNAC15_Reference    ACCGAAGGAAATCAAACATGAATGGCGAAGGGGTAACGGTGCAGGGAACCGATTCACT
*****

VviNAC15_Shiraz      TCTGCTCTATGGTCCTTTGTGGAGTCAATACCTACCACACCTGCATCAGCTTCAGAAAAAT
VviNAC15_Reference    TCTGCTCTATGGTCCTTTGTGGAGTCAATACCTACCACACCTGCATCAGCTTCAGAAAAAT
*****

VviNAC15_Shiraz      GCGTTGGTAAATCGGGCATTTGGTGAGAATGTCTAGCTTTAGTAGGATGAGAATGAATGCA
VviNAC15_Reference    GCGTTGGTAAATCGGGCATTTGGTGAGAATGTCTAGCTTTAGTAGGATGAGAATGAATGCA
*****

VviNAC15_Shiraz      TTGAACACAAATGCAGGTAATGGAGGTGCAGCCACATGGAAGGGAGGTATAAATAAGGGG
VviNAC15_Reference    TTGAACACAAATGCAGGTAATGGAGGTGCAGCCACATGGAAGGGAGGTATAAATAAGGGG
*****

VviNAC15_Shiraz      GGATTCATCATTCCTTTCAGTTATTGGAGCACTGATAGCTATATTCTGGGTCCTAATGCTA
VviNAC15_Reference    GGATTCATCATTCCTTTCAGTTATTGGAGCACTGATAGCTATATTCTGGGTCCTAATGCTA
*****

VviNAC15_Shiraz      GGACCTGTGAAGATGTTAGGAAGATGCCTCCCTCATGA
VviNAC15_Reference    GGACCTGTGAAGATGTTAGGAAGATGCCTCCCTCATGA
*****

```

D

| | |
|--------------------|--|
| VviNAC17_Shiraz | ATGGGTGTACCGGAGACTGACCCGCTTTCACAGCTTAGTTTCCCGCTGGGTCCGATTT |
| VviNAC17_Reference | ATGGGTGTACCGGAGACTGACCCGCTTTCACAGCTTAGTTTCCCGCTGGGTCCGATTT ***** |
| VviNAC17_Shiraz | TATCCCACCGATGAGGAGCTTCTGGTGCAGTATCTCTGCCGAAAGTGCCCGACAGGGG |
| VviNAC17_Reference | TATCCCACCGATGAGGAGCTTCTGGTGCAGTATCTCTGCCGAAAGTGCCCGACAGGGG ***** |
| VviNAC17_Shiraz | TTTTCAATTGGAGATAATTGGCGAAATCGATCTGTACAAGTTTGACCCATGGGTTCTTCCC |
| VviNAC17_Reference | TTTTCAATTGGAGATAATTGGCGAAATCGATCTGTACAAGTTTGACCCATGGGTTCTTCCC ***** |
| VviNAC17_Shiraz | AGTAAAGCTATATTTGGAGAGAAAGAGTGGTACTTTTTTCAGTCCCAGAGATCGGAAGTAC |
| VviNAC17_Reference | AGTAAAGCTATATTTGGAGAGAAAGAGTGGTACTTTTTTCAGTCCCAGAGATCGGAAGTAC ***** |
| VviNAC17_Shiraz | CCAAATGGGTCCAGACCCAATAGGGTTGCTGGGTCTGGGTATTGGAAGGCCACCGGAAC |
| VviNAC17_Reference | CCAAATGGGTCCAGACCCAATAGGGTTGCTGGGTCTGGGTATTGGAAGGCCACCGGAAC ***** |
| VviNAC17_Shiraz | GATAAGGTGATTACCACCGAGGCCGAAAGTTGGCATCAAGAAAGCTCTGGTGTTTTAC |
| VviNAC17_Reference | GATAAGGTGATTACCACCGAGGCCGAAAGTTGGCATCAAGAAAGCTCTGGTGTTTTAC ***** |
| VviNAC17_Shiraz | GTCGGCAAAGCTCCAAAAGGAACAAAATAATGGATCATGCATGAGTACAGACTCCTA |
| VviNAC17_Reference | GTCGGCAAAGCTCCAAAAGGAACAAAATAATGGATCATGCATGAGTACAGACTCCTA ***** |
| VviNAC17_Shiraz | GAAAATTCGAGGAAAAATGGAAGCTCCAAGTTGGATGATTGGGTTCTGTGCCGAATTTAC |
| VviNAC17_Reference | GAAAATTCGAGGAAAAATGGAAGCTCCAAGTTGGATGATTGGGTTCTGTGCCGAATTTAC ***** |
| VviNAC17_Shiraz | AAGAAGAAATCCAACCTCTCGAAACCCATAGCAGCTGTACTTCCCAGCAAAGCGCACAGC |
| VviNAC17_Reference | AAGAAGAAATCCAACCTCTCGAAACCCATAGCAGCTGTACTTCCCAGCAAAGCGCACAGC ***** |
| VviNAC17_Shiraz | AACGGCTCGTCATCGTCATCGTCGTCACCTCGACGACGTCCTGGAGTCGCTGCCGGAG |
| VviNAC17_Reference | AACGGCTCGTCATCGTCATCGTCGTCACCTCGACGACGTCCTGGAGTCGCTGCCGGAG ***** |
| VviNAC17_Shiraz | ATCGATGACAGGTTCTTTCTCCCAATCGGATGAATTCCTGAGAGTTTCACAGCCGGAC |
| VviNAC17_Reference | ATCGATGACAGGTTCTTTCTCCCAATCGGATGAATTCCTGAGAGTTTCACAGCCGGAC ***** |
| VviNAC17_Shiraz | GAGAAAGTCAACTTCCATAACCTGGGCTCGGGCAACTTCGACTGGGCCACTCTAGCAGGC |
| VviNAC17_Reference | GAGAAAGTCAACTTCCATAACCTGGGCTCGGGCAACTTCGACTGGGCCACTCTAGCAGGC ***** |
| VviNAC17_Shiraz | GTCTCCTCCTGACAGGAGTTGGTCTCCGGCGTCCAATCCACGCCAGCCTCCCGCAGCT |
| VviNAC17_Reference | GTCTCCTCCTGACAGGAGTTGGTCTCCGGCGTCCAATCCACGCCAGCCTCCCGCAGCT ***** |
| VviNAC17_Shiraz | GTCAACAACAGCAACGAAATGTACGTTCCGTCACGTGCCGCCGTAATCCAAGCCGAAGAA |
| VviNAC17_Reference | GTCAACAACAGCAACGAAATGTACGTTCCGTCACGTGCCGCCGTAATCCAAGCCGAAGAA ***** |
| VviNAC17_Shiraz | GAAGTCCAGAGCGGACTCAGAACCAGAGATCGACCCAGTAATGAACCAAGGGTTCTTC |
| VviNAC17_Reference | GAAGTCCAGAGCGGACTCAGAACCAGAGATCGACCCAGTAATGAACCAAGGGTTCTTC ***** |
| VviNAC17_Shiraz | CCGCAGAACTCGAACGCGTTCAGTCAGAGTTTCTCTAACTCACTCGACCCGTTCCGGGTTT |
| VviNAC17_Reference | CCGCAGAACTCGAACGCGTTCAGTCAGAGTTTCTCTAACTCACTCGACCCGTTCCGGGTTT ***** |
| VviNAC17_Shiraz | CGGTACCCGACCAACCTAGCGGATTGGATATAGCAGTAA |
| VviNAC17_Reference | CGGTACCCGACCAACCTAGCGGATTGGATATAGCAGTAA ***** |

E

| | |
|--------------------|---|
| VviNAC18_Shiraz | ATGGAGAGCACCGATTTCATCTTCGGGCTCGCCGACGCCGACGCTTCCACCGGGTTCCGC |
| VviNAC18_Reference | ATGGAGAGCACCGATTTCATCTTCGGGCTCGCCGACGCCGACGCTTCCACCGGGTTCCGC ***** |
| VviNAC18_Shiraz | TTCACCCACCGATGAAGAGTTAGTAGTTCACTATCTGAAGAAGAAGGCCTCATCTGCT |
| VviNAC18_Reference | TTCACCCACCGATGAAGAGTTAGTAGTTCACTATCTGAAGAAGAAGGCCTCATCTGCT ***** |
| VviNAC18_Shiraz | CCTCTTCGGTTCGCCATAATCGCAGAGGTTGATCTCTATAAGTTGATCCCTGGGAACTC |
| VviNAC18_Reference | CCTCTTCGGTTCGCCATAATCGCAGAGGTTGATCTCTATAAGTTGATCCCTGGGAACTC ***** |
| VviNAC18_Shiraz | CCTGCTAAGGCCAGTTTGGAGAACAGGAATGGTACTTCTTCAGCCCTAGAGACCGGAAG |
| VviNAC18_Reference | CCTGCTAAGGCCAGTTTGGAGAACAGGAATGGTACTTCTTCAGCCCTAGAGACCGGAAG ** ***** |
| VviNAC18_Shiraz | TACCCAAACGGGGCTCGGCCTAATCGAGCGGCGACTTCTGGTTATTGGAAGGCGACGGGG |
| VviNAC18_Reference | TACCCAAACGGGGCTCGGCCTAATCGAGCGGCGACTTCTGGTTATTGGAAGGCGACGGGG ***** |
| VviNAC18_Shiraz | ACGGACAAGCCGGTGTGACCTCTGGGGTACTCAGAAGTGGGTGTGAAGAAGGCGCTG |
| VviNAC18_Reference | ACGGACAAGCCGGTGTGACCTCTGGGGTACTCAGAAGTGGGTGTGAAGAAGGCGCTG ***** |
| VviNAC18_Shiraz | GTTTCTATGAGGGAAGCCCCAAAGGGGATCAAAACCAATTGGATCATGCATGAGTAC |
| VviNAC18_Reference | GTTTCTATGAGGGAAGCCCCAAAGGGGATCAAAACCAATTGGATCATGCATGAGTAC ***** |
| VviNAC18_Shiraz | AGGCTTGCTGACAACAAGGTTAACACAAAGCCTCCCGGATGCGATATGGGCAACAAGAAG |
| VviNAC18_Reference | AGGCTTGCTGACAACAAGGTTAACACAAAGCCTCCCGGATGCGATATGGGCAACAAGAAG ***** |
| VviNAC18_Shiraz | AACTCTTTCGGCTTGATGATTGGGTGCTATGTCGAATCTACAAGAAGAACAACACGCAT |
| VviNAC18_Reference | AACTCTTTCGGCTTGATGATTGGGTGCTATGTCGAATCTACAAGAAGAACAACACGCAT ***** |
| VviNAC18_Shiraz | AGAACGCTGGATCCTGACAAGGATGACTCCATGGACGACATGCTTGGGCCGGTGCCGAGC |
| VviNAC18_Reference | AGAACGCTGGATCCTGACAAGGATGACTCCATGGACGACATGCTTGGGCCGGTGCCGAGC ***** |
| VviNAC18_Shiraz | TCGATCTCGATGGGGCAACAAGCCTGAAACTGCAGTTCCCAAAGTCCCAAACACAGT |
| VviNAC18_Reference | TCGATCTCGATGGGGCAACAAGCCTGAAACTGCAGTTCCCAAAGTCCCAAACACAGT ***** |
| VviNAC18_Shiraz | GCATTGCTAGAAAATGAGCAGAGCCTGTTTGAAGGGATGATAAACAGCGATGGTATCAAC |
| VviNAC18_Reference | GCATTGCTAGAAAATGAGCAGAGCCTGTTTGAAGGGATGATAAACAGCGATGGTATCAAC ***** |
| VviNAC18_Shiraz | AGTTCGGCACTATTTCTCAGCTGGCCTGCTCAAGCTCAAAGCCGGATCACCTCTCTTG |
| VviNAC18_Reference | AGTTCGGCACTATTTCTCAGCTGGCCTGCTCAAGCTCAAAGCCGGATCACCTCTCTTG ***** |
| VviNAC18_Shiraz | GTTGCAGCCACAACATCAAGCATCCTCCCTCTGAAGCGAAGCCTCCCTTCTCTATACTGG |
| VviNAC18_Reference | GTTGCAGCCACAACATCAAGCATCCTCCCTCTGAAGCGAAGCCTCCCTTCTCTATACTGG ***** |
| VviNAC18_Shiraz | AACGACGATGATACTGCCGTCCTTCCACGACAAAGAGGTTCCAAGCCGAAAACACAGAT |
| VviNAC18_Reference | AACGACGATGATACTGCCGTCCTTCCACGACAAAGAGGTTCCAAGCCGAAAACACAGAT ***** |
| VviNAC18_Shiraz | GGAAACATTGGTAGAACAACCTGATGGGAACAATCCATCGCCACTCTGCTCAGCCAGCTT |
| VviNAC18_Reference | GGAAACATTGGTAGAACAACCTGATGGGAACAATCCATCGCCACTCTGCTCAGCCAGCTT ***** |
| VviNAC18_Shiraz | CCGCAAGCTCCTTTCATGACCAACAGTCAATGCTGGGGTCTCTTGGCGAAGGCGTTTTT |
| VviNAC18_Reference | CCGCAAGCTCCTTTCATGACCAACAGTCAATGCTGGGGTCTCTTGGCGAAGGCGTTTTT ***** |
| VviNAC18_Shiraz | CGGCAACCCTTTCAACTCCCTGGCATGAATTGGTATGCTTAG |
| VviNAC18_Reference | CGGCAACCCTTTCAACTCCCTGGCATGAATTGGTATGCTTAG ***** |

F

| | |
|--------------------|---|
| VviNAC26_Shiraz | ATGGATGGAAAAGGCAGCTCTCAACTTCCTCCCGGTTTTAGATTCCACCCACCCGACGAG |
| VviNAC26_Reference | ATGGATGGAAAAGGCAGCTCTCAACTTCCTCCCGGTTTTAGATTCCACCCACCCGACGAG ***** |
| VviNAC26_Shiraz | GAACTCATCATGTATTACCTCAAAAACCAAGCCACTTCCAAGCCATGCCCCGTATCCATT |
| VviNAC26_Reference | GAACTCATCATGTATTACCTCAAAAACCAAGCCACTTCCAAGCCATGCCCCGTATCCATT ***** |
| VviNAC26_Shiraz | ATCCCCGAAGTGGATATCTACAAATTCGAGCCTTGGGAATTGCCTGAGAAGCGGAATTT |
| VviNAC26_Reference | ATCCCCGAAGTGGATATCTACAAATTCGAGCCTTGGGAATTGCCTGAGAAGCGGAATTT ***** |
| VviNAC26_Shiraz | GGAGAAAATGAGTGGTATTCTTTAGCCC GCGTGACCGTAAGTATCCCAATGGGGCTAGA |
| VviNAC26_Reference | GGAGAAAATGAGTGGTATTCTTTAGCCC GCGTGACCGTAAGTATCCCAATGGGGCTAGA ***** |
| VviNAC26_Shiraz | CCCAACCGAGCTACAGTGTCCGGCTACTGGAAAGCCACAGGACAGACAAGGCAATCTAC |
| VviNAC26_Reference | CCCAACCGAGCTACAGTGTCCGGCTACTGGAAAGCCACAGGACAGACAAGGCAATCTAC ***** |
| VviNAC26_Shiraz | AGTGGGGCTAAGTATGTGGGGGTGAAAAGGCTCTTGTGTCTACAAGGGTAGGCCTCCT |
| VviNAC26_Reference | AGTGGGGCTAAGTATGTGGGGGTGAAAAGGCTCTTGTGTCTACAAGGGTAGGCCTCCT ***** |
| VviNAC26_Shiraz | AAGGGCATTAAAGCCGATTGGATTATGCATGAATATCGCCTTAGTGATTCAAGGCCACGC |
| VviNAC26_Reference | AAGGGCATTAAAGCCGATTGGATTATGCATGAATATCGCCTTAGTGATTCAAGGCCACGC ***** |
| VviNAC26_Shiraz | CCCAAGAAGCACAATGGTTCCATGAGATTGGATGATTGGGTGCTATGTAGGATCTATAAG |
| VviNAC26_Reference | CCCAAGAAGCACAATGGTTCCATGAGATTGGATGATTGGGTGCTATGTAGGATCTATAAG ***** |
| VviNAC26_Shiraz | AAGAAGCATGTGGGGAGAATTTTGGAAAGAGAAGAAGAAAATTTAGGTCCCAAAATACCC |
| VviNAC26_Reference | AAGAAGCATGTGGGGAGAATTTTGGAAAGAGAAGAAGAAAATTTAGGTCCCAAAATACCC ***** |
| VviNAC26_Shiraz | GTTACAAATTCAGATGATGGCGGTGAGCAGCACCAGTGAATTTCCAAGGACTTTTTC |
| VviNAC26_Reference | GTTACAAATTCAGATGATGGCGGTGAGCAGCACCAGTGAATTTCCAAGGACTTTTTC ***** |
| VviNAC26_Shiraz | CTTGCTCATTTATTGGACATGGAATACTTGGGTCCAATTTCACAACTTCTAGGTGACAA |
| VviNAC26_Reference | CTTGCTCATTTATTGGACATGGAATACTTGGGTCCAATTTCACAACTTCTAGGTGACAA ***** |
| VviNAC26_Shiraz | TCATACCATTAGCCTTTGATTTCCAAGGCACCATAAGCAATATTGCCGGAACCGACCCC |
| VviNAC26_Reference | TCATACCATTAGCCTTTGATTTCCAAGGCACCATAAGCAATATTGCCGGAACCGACCCC ***** |
| VviNAC26_Shiraz | CCTGGCGTGGACAAATTCGAGTTATTCCAAGTCCCATGCCAATACAACGATTCAACCAAG |
| VviNAC26_Reference | CCTGGCGTGGACAAATTCGAGTTATTCCAAGTCCCATGCCAATACAACGATTCAACCAAG ***** |
| VviNAC26_Shiraz | TTCCAAGTGAATCAGAATCACATTCGGAACCGCCTCTATTGTGAACCCAGTGTATGAA |
| VviNAC26_Reference | TTCCAAGTGAATCAGAATCACATTCGGAACCGCCTCTATTGTGAACCCAGTGTATGAA ***** |
| VviNAC26_Shiraz | TTTCAGTGA |
| VviNAC26_Reference | TTTCAGTGA ***** |

G

| | |
|--------------------|---|
| VviNAC38_Shiraz | ATGATGGGGAAGGGTTCCAAGAGCAATTGCAAGTCGGCGTCCCACAAGATGTTCAAGGAC |
| VviNAC38_Reference | ATGATGGGGAAGGGTTCCAAGAGCAATTGCAAGTCGGCGTCCCACAAGATGTTCAAGGAC ***** |
| VviNAC38_Shiraz | AAGCCAAGAACCCTGTTGATGATCTACAGGGGATGTTACCGGATCTGCAGTCTCGGAGG |
| VviNAC38_Reference | AAGCCAAGAACCCTGTTGATGATCTACAGGGGATGTTACCGGATCTGCAGTCTCGGAGG ***** |
| VviNAC38_Shiraz | AAGGAGAGCCGATCGGTGGATGTCGGGTCCTTGAGGAGCAGCTTCATCAGATGCTTCGT |
| VviNAC38_Reference | AAGGAGAGCCGATCGGTGGATGTCGGGTCCTTGAGGAGCAGCTTCATCAGATGCTTCGT ***** |
| VviNAC38_Shiraz | GAGTGGAAAGCCGAACCTCAACGAACCCCTCCCGCATCTTCTCTACAAGGCGGTAGTCTG |
| VviNAC38_Reference | GAGTGGAAAGCCGAACCTCAACGAACCCCTCCCGCATCTTCTCTACAAGGCGGTAGTCTG ***** |
| VviNAC38_Shiraz | GGGTCGTTTTCTCGGACATTTGCCGGCTGTGCAGCTTTGTGAAGAGGAGGACGATGCC |
| VviNAC38_Reference | GGGTCGTTTTCTCGGACATTTGCCGGCTGTGCAGCTTTGTGAAGAGGAGGACGATGCC ***** |
| VviNAC38_Shiraz | ACTAGTGCCTTAGCTGATGGGGCAGTGCCCAAACCTGAGCCTGATGCTCAAGGCCATCAA |
| VviNAC38_Reference | ACTAGTGCCTTAGCTGATGGGGCAGTGCCCAAACCTGAGCCTGATGCTCAAGGCCATCAA ***** |
| VviNAC38_Shiraz | ATTGGAGCTAGTGTGCTTTTCCAAGAGCGCTATAATAAGGGCCACAGGAGCATGGCTTT |
| VviNAC38_Reference | ATTGGAGCTAGTGTGCTTTTCCAAGAGCGCTATAATAAGGGCCACAGGAGCATGGCTTT ***** |
| VviNAC38_Shiraz | CAATTGGTGGATCAATGCAAAATTTCTCCTTCAGGTGCTCACAATATGGGAGTTCACAAT |
| VviNAC38_Reference | CAATTGGTGGATCAATGCAAAATTTCTCCTTCAGGTGCTCACAATATGGGAGTTCACAAT ***** |
| VviNAC38_Shiraz | TTGGAAGGAGCTACTCAGTTGGACTATCGTCAGTTTGATTTGCAACAAGACTTTGAGCAA |
| VviNAC38_Reference | TTGGAAGGAGCTACTCAGTTGGACTATCGTCAGTTTGATTTGCAACAAGACTTTGAGCAA ***** |
| VviNAC38_Shiraz | AACTTCTTTGCTGGTTATGATGGGACTGGTCTGTGTGGAGAGGATGCTATGCCTCATATT |
| VviNAC38_Reference | AACTTCTTTGCTGGTTATGATGGGACTGGTCTGTGTGGAGAGGATGCTATGCCTCATATT ***** |
| VviNAC38_Shiraz | TCTAGCTTTTGGCAAGTATTTGCCTTCCACCTTCTGCATTCTTGGGCCAAAATGTGCA |
| VviNAC38_Reference | TCTAGCTTTTGGCAAGTATTTGCCTTCCACCTTCTGCATTCTTGGGCCAAAATGTGCA ***** |
| VviNAC38_Shiraz | CTCTGGGATTGCCCCAGGCCAGCTCAAGGGATGGATTGGTGTCAAACCTATTGCGCAGC |
| VviNAC38_Reference | CTCTGGGATTGCCCCAGGCCAGCTCAAGGGATGGATTGGTGTCAAACCTATTGCGCAGC ***** |
| VviNAC38_Shiraz | TTTCATGCTACTCTGGCATTGAGTGAAGCCCTCCTGGTATGACCCAGTTCACGACCT |
| VviNAC38_Reference | TTTCATGCTACTCTGGCATTGAGTGAAGCCCTCCTGGTATGACCCAGTTCACGACCT ***** |
| VviNAC38_Shiraz | GGGGGCATTGGCCTGAAGGATGGTCTGCTTTTGTGCTCTTAGTGCAAAGGTGCAAGGA |
| VviNAC38_Reference | GGGGGCATTGGCCTGAAGGATGGTCTGCTTTTGTGCTCTTAGTGCAAAGGTGCAAGGA ***** |
| VviNAC38_Shiraz | AAAGATGTTGGTATCCCAGAATGTGAAGGGCTGCAACTGCAAAATCCCCATGGAATGCT |
| VviNAC38_Reference | AAAGATGTTGGTATCCCAGAATGTGAAGGGCTGCAACTGCAAAATCCCCATGGAATGCT ***** |
| VviNAC38_Shiraz | CCTGAGCTATTTGATCTGTCAGTTCTTGAGGGTGAACAATAGGGAATGGCTTTTTTTTT |
| VviNAC38_Reference | CCTGAGCTATTTGATCTGTCAGTTCTTGAGGGTGAACAATAGGGAATGGCTTTTTTTTT ***** |
| VviNAC38_Shiraz | GACAAGCCTCGAAGAGCATTGAGAGTGGAAATAGAAAGCAGAGGTCATTGCCAGATTAT |
| VviNAC38_Reference | GACAAGCCTCGAAGAGCATTGAGAGTGGAAATAGAAAGCAGAGGTCATTGCCAGATTAT ***** |
| VviNAC38_Shiraz | AGTGGGCGTGGTTGGCATGAGTCAAGGAAGCAAGTGATGAATGAATATGGGGACTGAAA |
| VviNAC38_Reference | AGTGGGCGTGGTTGGCATGAGTCAAGGAAGCAAGTGATGAATGAATATGGGGACTGAAA ***** |
| VviNAC38_Shiraz | AGATCTTACTACATGGATCCGCAACCTCTGAACCATTTTGTGAGTGGCACCTTTATGAATAT |
| VviNAC38_Reference | AGATCTTACTACATGGATCCGCAACCTCTGAACCATTTTGTGAGTGGCACCTTTATGAATAT ***** |
| VviNAC38_Shiraz | GAAATCAGTAAAGTGTGATGCTTGTGCCCTGTATAGTTGGAAGTGAAGCTTGTGTATGGG |
| VviNAC38_Reference | GAAATCAGTAAAGTGTGATGCTTGTGCCCTGTATAGTTGGAAGTGAAGCTTGTGTATGGG ***** |

```

VviNAC38_Shiraz      AAGAAGA GTTCCAAGCAAAGCAACTGATTCAGTGGCTGATCTGCAGAAGCAGATG
VviNAC38_Reference   AAGAAGA-----
*****

VviNAC38_Shiraz      GGAAGGCTTACTGCTGAGTTCCCTTCACCATGATGGGGAAGG GTTCCAAGCAAAGCA
VviNAC38_Reference   -----GTTCCAAGCAAAGCA
*****

VviNAC38_Shiraz      ACAACTGATTCAGTGGCTGATCTGCAGAAGCAGATGGGAAGGCTTACTGCTGAGTTCCC
VviNAC38_Reference   ACAACTGATTCAGTGGCTGATCTGCAGAAGCAGATGGGAAGGCTTACTGCTGAGTTCCC
*****

VviNAC38_Shiraz      TTAGATAACAAGCGCTCTGTTAAAGGAAGGACAAAAATTAATATGAAGGATGGTGTGGA
VviNAC38_Reference   TTAGATAACAAGCGCTCTGTTAAAGGAAGGACAAAAATTAATATGAAGGATGGTGTGGA
*****

VviNAC38_Shiraz      GATGTTTATTCTACTCCAATCGGGTAGGACCTCCAATCAACAAGGTGATTATGGGGTA
VviNAC38_Reference   GATGTTTATTCTACTCCAATCGGGTAGGACCTCCAATCAACAAGGTGATTATGGGGTA
*****

VviNAC38_Shiraz      GGAGGACCTTACGATTATCTTGTGGAGAATTTAGGTGACTATTATTGACATGA
VviNAC38_Reference   GGAGGACCTTACGATTATCTTGTGGAGAATTTAGGTGACTATTATTGACATGA
*****

```

H

VviNAC39_Shiraz ATGATGAGCGGAGATCAGTTGCAGTTGCCGGCTGGTTTCAGATTTTCATCCGACGGACGAG
VviNAC39_Reference ATGATGAGCGGAGATCAGTTGCAGTTGCCGGCTGGTTTCAGATTTTCATCCGACGGACGAG

VviNAC39_Shiraz GAGCTCGTGGTGCATTATCTGGTTCGTAATGCGCATCACAGAGCATCTCCGTTCCGATT
VviNAC39_Reference GAGCTCGTGGTGCATTATCTGGTTCGTAATGCGCATCACAGAGCATCTCCGTTCCGATT

VviNAC39_Shiraz ATTGCCGAGGTTGATCTCTACAAGTACGATCCATGGCAGCTTCCAGGAATGGCTCTGTAC
VviNAC39_Reference ATTGCCGAGGTTGATCTCTACAAGTACGATCCATGGCAGCTTCCAGGAATGGCTCTGTAC

VviNAC39_Shiraz GGTGAAAAGGAGTGGTACTTCTTCTCTCCAAGGACCGCGAATATCTCAACGGTTCAAGG
VviNAC39_Reference GGTGAAAAGGAGTGGTACTTCTTCTCTCCAAGGACCGCGAATATCTCAACGGTTCAAGG

VviNAC39_Shiraz CCTAACCGGGCGGCCGGATCCGGCTACTGGAAGGCCACCGCGCCGATAAGCCCATCGGC
VviNAC39_Reference CCTAACCGGGCGGCCGGATCCGGCTACTGGAAGGCCACCGCGCCGATAAGCCCATCGGC

VviNAC39_Shiraz CGACCCAAGACGGTCGGAATTAATAAAGGCACTCGTATTTTATGCCGGCAAAGCTCCGAGA
VviNAC39_Reference CGACCCAAGACGGTCGGAATTAATAAAGGCACTCGTATTTTATGCCGGCAAAGCTCCGAGA

VviNAC39_Shiraz GGTGTCAAAACCAATTGGATCATGCACGAGTATCGCCTCGCCAATGTTGATCGATCCGCC
VviNAC39_Reference GGTGTCAAAACCAATTGGATCATGCACGAGTATCGCCTCGCCAATGTTGATCGATCCGCC

VviNAC39_Shiraz GGCAAGAAAAACAACCTTAAGGCTTGACGATTGGGTCTTATGTGCAATATACAACAAGAAA
VviNAC39_Reference GGCAAGAAAAACAACCTTAAGGCTTGACGATTGGGTCTTATGTGCAATATACAACAAGAAA

VviNAC39_Shiraz GGCAGCGCCGAGAAACAGCACACCTTTGATCAATAGTCAATGAAATATCCAGAACTTGAA
VviNAC39_Reference GGCAGCGCCGAGAAACAGCACACCTTTGATCAATAGTCAATGAAATATCCAGAACTTGAA

VviNAC39_Shiraz GACCAGAAGCCAAAAATAATCAACGGTTCAAAGATAAAGTAGTACCCTCTTATTGCGG
VviNAC39_Reference GACCAGAAGCCAAAAATAATCAACGGTTCAAAGATAAAGTAGTACCCTCTTATTGCGG

VviNAC39_Shiraz TCCCTACCTCCGATGCCTGCGCCGCAACAACCAATGACTACCTATACTTCGAGACATCT
VviNAC39_Reference TCCCTACCTCCGATGCCTGCGCCGCAACAACCAATGACTACCTATACTTCGAGACATCT

VviNAC39_Shiraz GATTTCAGTGCCGAGGTTACACACTCACACAGATTCTAGTGGTTCCGAACAAGTAATGTCA
VviNAC39_Reference GATTTCAGTGCCGAGGTTACACACTCACACAGATTCTAGTGGTTCCGAACAAGTAATGTCA

VviNAC39_Shiraz CCGGAGAAGGAGGTTCAAAGCGAGCCTAAGTGAATGACTTTGATTTAGCCTCTATATG
VviNAC39_Reference CCGGAGAAGGAGGTTCAAAGCGAGCCTAAGTGAATGACTTTGATTTAGCCTCTATATG

VviNAC39_Shiraz GATGGTTTTGCCAACGACCCTTTTGCCTCTCAAGCACAGTTTTCGGGAGACTTTTAACA
VviNAC39_Reference GATGGTTTTGCCAACGACCCTTTTGCCTCTCAAGCACAGTTTTCGGGAGACTTTTAACA

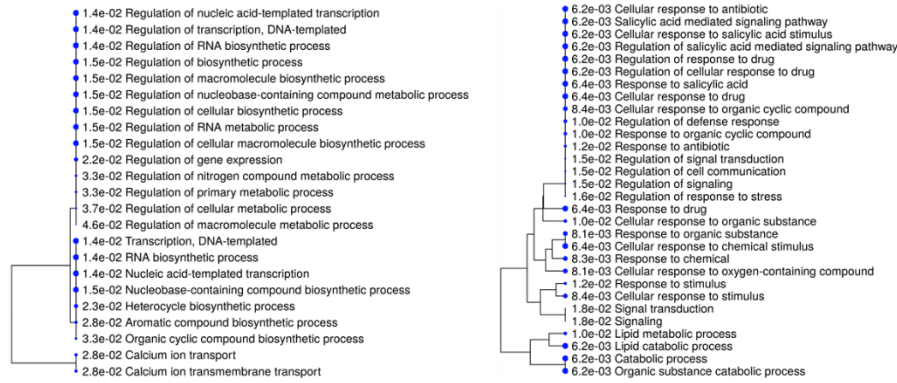
VviNAC39_Shiraz TCGTCGTGGCAGGACATGTTGATGTTCTCGAACAAGTCATTTGA
VviNAC39_Reference TCGTCGTGGCAGGACATGTTGATGTTCTCGAACAAGTCATTTGA

I

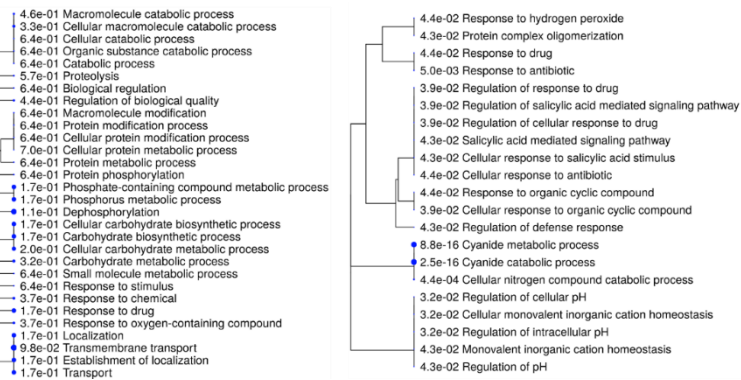
| | |
|--------------------|---|
| VviNAC61_Shiraz | ATGGAAGAGGCTTCACTTGCCGATCAAGGTGATGACCTTATGGATTGCCCCAGGTTTT |
| VviNAC61_Reference | ATGGAAGAGGCTTCACTTGCCGATCAAGGTGATGACCTTATGGATTGCCCCAGGTTTT ***** |
| VviNAC61_Shiraz | AGATTCCACCCACAGATGAAGAGATCATATCTTATTATCTCACGGAGAGGGTGATGAAT |
| VviNAC61_Reference | AGATTCCACCCACAGATGAAGAGATCATATCTTATTATCTCACGGAGAGGGTGATGAAT ***** |
| VviNAC61_Shiraz | AGTAGCTTCAGTGCAAGAGCTATTGGAGAAGTTGACCTTAACAAGTGTGACCCCTGGGAT |
| VviNAC61_Reference | AGTAGCTTCAGTGCAAGAGCTATTGGAGAAGTTGACCTTAACAAGTGTGACCCCTGGGAT ***** |
| VviNAC61_Shiraz | TTACCTAAGAAAAGCAAAGATGGGAGAGAAGGAATGGTATTTCTTTGCGAGAGATAGG |
| VviNAC61_Reference | TTACCTAAGAAAAGCAAAGATGGGAGAGAAGGAATGGTATTTCTTTGCGAGAGATAGG ***** |
| VviNAC61_Shiraz | AAGTATCCTACAGGCATGAGAACGAATCGAGCTACCGAATCTGGTACTGGAAGGCCACT |
| VviNAC61_Reference | AAGTATCCTACAGGCATGAGAACGAATCGAGCTACCGAATCTGGTACTGGAAGGCCACT ***** |
| VviNAC61_Shiraz | GGAAAGGATAAAGAGATTTACAAGGGGAGGGTTGTCTTGTGGGATGAAGAAGACCCCTT |
| VviNAC61_Reference | GGAAAGGATAAAGAGATTTACAAGGGGAGGGTTGTCTTGTGGGATGAAGAAGACCCCTT ***** |
| VviNAC61_Shiraz | GTTTTCTACCGAGGAGAGCCCCAAAGGAGAGAAAAGCAATTGGTTCATGCACGAATAC |
| VviNAC61_Reference | GTTTTCTACCGAGGAGAGCCCCAAAGGAGAGAAAAGCAATTGGTTCATGCACGAATAC ***** |
| VviNAC61_Shiraz | AGACTGGAAGGCAAATTCATATTACAACCTCCCCAAAGCCGAAAGGATGAATGGGTC |
| VviNAC61_Reference | AGACTGGAAGGCAAATTCATATTACAACCTCCCCAAAGCCGAAAGGATGAATGGGTC ***** |
| VviNAC61_Shiraz | GTCTGTAGGGTATCCACAAGAGCGCGGGGATCAAACGAAGTCTTATTCCTGCGCCGATA |
| VviNAC61_Reference | GTCTGTAGGGTATCCACAAGAGCGCGGGGATCAAACGAAGTCTTATTCCTGCGCCGATA ***** |
| VviNAC61_Shiraz | AGGATGAACCTCTTTGGGGATGATCTCTTGACTGTTCTTCTTACCCTCTTATGAC |
| VviNAC61_Reference | AGGATGAACCTCTTTGGGGATGATCTCTTGACTGTTCTTCTTACCCTCTTATGAC ***** |
| VviNAC61_Shiraz | CCTCCTATTCCAACCCCAACAAAATGATTCCTGCTTTACAAATGGTGAAGATGAATTC |
| VviNAC61_Reference | CCTCCTATTCCAACCCCAACAAAATGATTCCTGCTTTACAAATGGTGAAGATGAATTC ***** |
| VviNAC61_Shiraz | AAGGGATCATCAACCAGATTTTCAGATGGAACCACCCTACCCTTACTTCTCCCCACC |
| VviNAC61_Reference | AAGGGATCATCAACCAGATTTTCAGATGGAACCACCCTACCCTTACTTCTCCCCACC ***** |
| VviNAC61_Shiraz | ATAAACGGTCATCAACTGCAAAAGCAACAAGATCAGAAGAGCTTTCTTCTATCCCCAAT |
| VviNAC61_Reference | ATAAACGGTCATCAACTGCAAAAGCAACAAGATCAGAAGAGCTTTCTTCTATCCCCAAT ***** |
| VviNAC61_Shiraz | AACGTGCACACCCTCCAACCTACCAAGCCACCCTAAGCAACCTTACCAAACTCCATT |
| VviNAC61_Reference | AACGTGCACACCCTCCAACCTACCAAGCCACCCTAAGCAACCTTACCAAACTCCATT ***** |
| VviNAC61_Shiraz | TTCTACCCCAAGTTTCTCCCTCGAATCCTCTTTTCCCCTTCCAAGCATCCCCAATCCT |
| VviNAC61_Reference | TTCTACCCCAAGTTTCTCCCTCGAATCCTCTTTTCCCCTTCCAAGCATCCCCAATCCT ***** |
| VviNAC61_Shiraz | AGTTATTCACACTGGCAGATGGGTAGTTTCCAAGCTTCCGGCTCTGGCTTCAA |
| VviNAC61_Reference | AGTTATTCACACTGGCAGATGGGTAGTTTCCAAGCTTCCGGCTCTGGCTTCAA ***** |
| VviNAC61_Shiraz | GGTAGTGATCCGACCAGTACCGTAAGAGCCAGACATCTGGCGTACAGAGCAATGCAAG |
| VviNAC61_Reference | GGTAGTGATCCGACCAGTACCGTAAGAGCCAGACATCTGGCGTACAGAGCAATGCAAG ***** |
| VviNAC61_Shiraz | GTGGAGCAGTTCTCATCCAACAGTCTATGGTCAGCCTCTCGCAGGACACCGGACTCAGC |
| VviNAC61_Reference | GTGGAGCAGTTCTCATCCAACAGTCTATGGTCAGCCTCTCGCAGGACACCGGACTCAGC ***** |
| VviNAC61_Shiraz | ACTGACATGAACCGGAGATATCCTCTGTGCTTTCAAAGCATCAAGACACAGGAAACAAC |
| VviNAC61_Reference | ACTGACATGAACCGGAGATATCCTCTGTGCTTTCAAAGCATCAAGACACAGGAAACAAC ***** |
| VviNAC61_Shiraz | AGGTCTTACGAAGATCTTCAAGTCCATCGGTCGGCCAAATCGGAGATTGGATTATTTA |
| VviNAC61_Reference | AGGTCTTACGAAGATCTTCAAGTCCATCGGTCGGCCAAATCGGAGATTGGATTATTTA ***** |
| VviNAC61_Shiraz | CTCGACTACTGA |
| VviNAC61_Reference | CTCGACTACTGA ***** |

Appendix C: GO enrichment analysis tree of the A) *VviNAC01*, B) *VviNAC08*, C) *VviNAC15*, D) *VviNAC17*, E) *VviNAC18*, F) *VviNAC26*, G) *VviNAC39* and H) *VviNAC61* over expression DEGs, divided into up-regulated (on the left) and down-regulated (on the right).

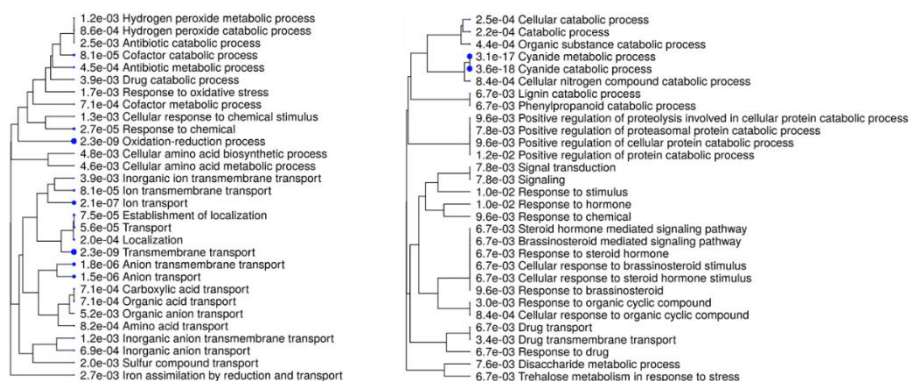
A



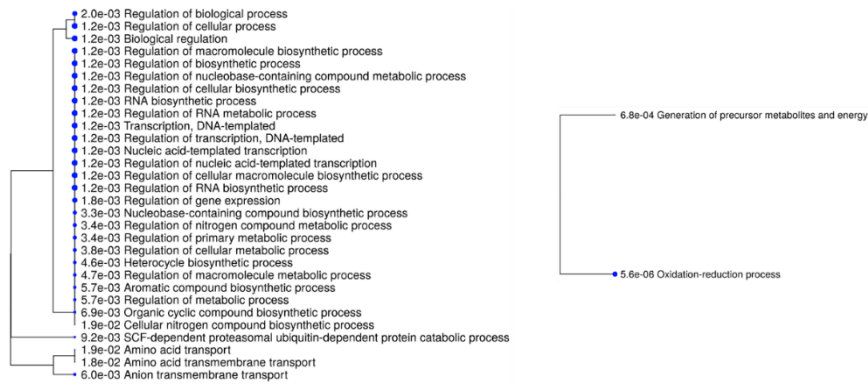
B



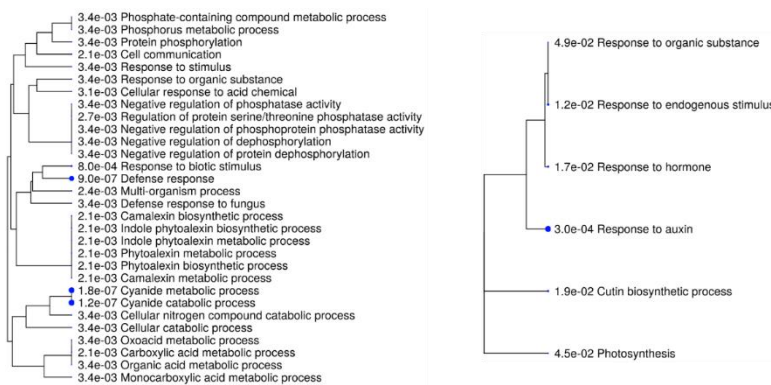
C



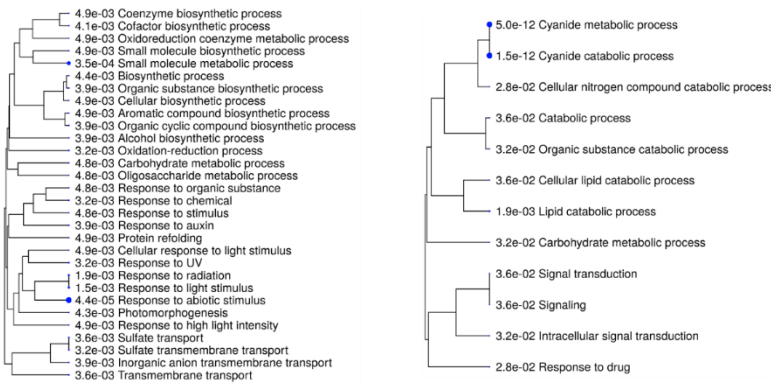
D



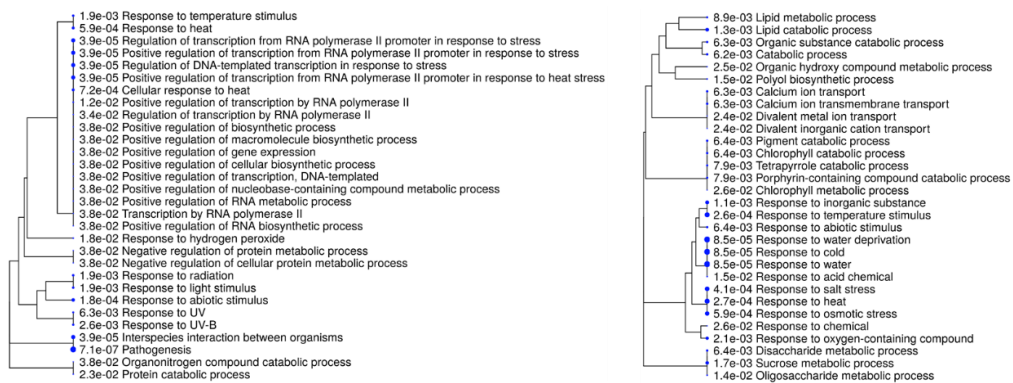
E



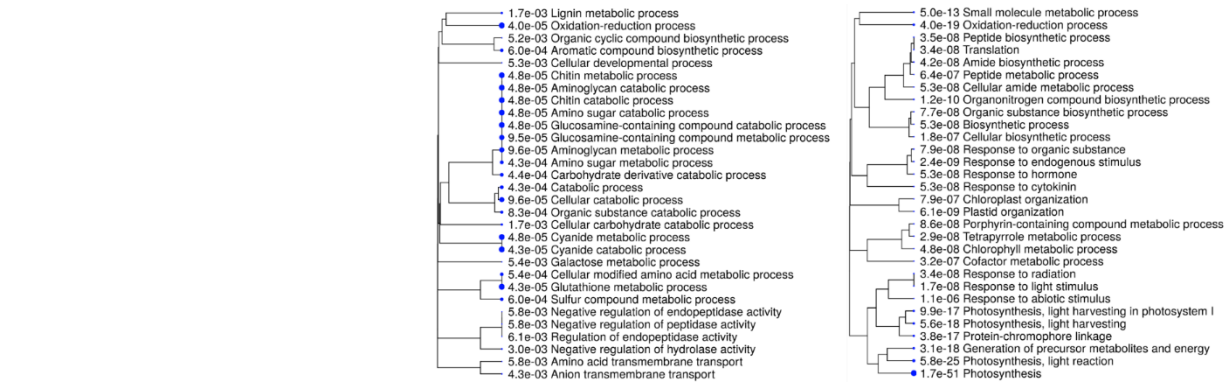
F



G



H



Appendix D: Alignments of A) *VviNAC01*, B) *VviNAC05*, C) *VviNAC08*, D) *VviNAC34*, E) *VviNAC37* and F) *VviNAC61* promoters nucleotide sequences from Shiraz and Pinot Noir cultivars.

A

```

PromoterVviNAC01_Pinot      CTGTTGAGTGGGAACAGCAAGTAATCTGAAGGACCCTCGTGACCGTTTTCTGGCAGCGCA
PromoterVviNAC01_Shiraz    CTGTTGAGTGGGAACAGCAAGTAATCTGAAGGACCCTCGTGACCGTTTTCTGGCAGCGCA
*****

PromoterVviNAC01_Pinot      GCATAGAGGCAAAAATATTTCTGTCCCTCATGCTCAGCATCCACAAAAAGGAAAAAAG
PromoterVviNAC01_Shiraz    GCATAGAGGCAAAAATATTTCTGTCCCTCATGCTCAGCATCCACAAAAAGGAAAAAAG
*****

PromoterVviNAC01_Pinot      GAAACCAAAAAAAAAAAAAAAAAA-AAAAACCCTAGGGGTAATCATGTACTTTCACATCT
PromoterVviNAC01_Shiraz    GAAACCAAAAAAAAAAAAAAAAAA-AAAAACCCTAGGGGTAATCATGTACTTTCACATCT
*****

PromoterVviNAC01_Pinot      CAATTAAGGCACCTTTGTGCCCTCCAGCTGTGAGCATGACATAAGGTGACTTACCCCTTAC
PromoterVviNAC01_Shiraz    CAATTAAGGCACCTTTGTGCCCTCCAGCTGTGAGCATGACATAAGGTGACTTACCCCTTAC
*****

PromoterVviNAC01_Pinot      GAGACTGCGAGGGTGGCAATTTTCTTCGAAATGACTAAAACACCCTTCATTAGGATCCTT
PromoterVviNAC01_Shiraz    GAGACTGCGAGGGTGGCAATTTTCTTCGAAATGACTAAAACACCCTTCATTAGGATCCTT
*****

PromoterVviNAC01_Pinot      GATGACAGAATCGCCCATCCCACCGTCCACAAATTAGACCACATCGCGATTTTATTGGGT
PromoterVviNAC01_Shiraz    GATGACAGAATCGCCCATCCCACCGTCCACAAATTAGACCACATCGCGATTTTATTGGGT
*****

PromoterVviNAC01_Pinot      ACGCACGGTGAGGGAAGAAAGGGTGTGTTGGTCAATTTTACAACCACAGGGGATTCGA
PromoterVviNAC01_Shiraz    ACGCACGGTGAGGGAAGAAAGGGTGTGTTGGTCAATTTTACAACCACAGGGGATTCGA
*****

PromoterVviNAC01_Pinot      AGGTCCCTTTAGCAGCTTCGGTTATTCACACACAAGGTGCAACACAACCTAAGAAACG
PromoterVviNAC01_Shiraz    AGGTCCCTTTAGCAGCTTCGGTTATTCACACACAAGGTGCAACACAACCTAAGAAACG
*****

PromoterVviNAC01_Pinot      TTAACCTATTGGAAAGCGGCCGTAATTAATTAATCTCTCTAAACCTTTTGTAAAATCAT
PromoterVviNAC01_Shiraz    TTAACCTATTGGAAAGCGGCCGTAATTAATTAATCTCTCTAAACCTTTTGTAAAATCAT
*****

PromoterVviNAC01_Pinot      GATCCGAGGAGAAAATTTGGAAAAGAAGGAAAAGAAAAAAGAAAGAGTTTGTAGTCTTG
PromoterVviNAC01_Shiraz    GATCCGAGGAGAAAATTTGGAAAAGAAGGAAAAGAAAAAAGAAAGAGTTTGTAGTCTTG
*****

PromoterVviNAC01_Pinot      TTTACGCCAAAGGGTTCGTGATTTCTATTTCTCTCTCTGCGAGACCTTGCTCGCCGC
PromoterVviNAC01_Shiraz    TTTACGCCAAAGGGTTCGTGATTTCTATTTCTCTCTCTGCGAGACCTTGCTCGCCGC
*****

PromoterVviNAC01_Pinot      ACCATTTATATAAAGAACCAGCACTTTATCTCTCAACCCACACCCACCTTTTCGCCTTTT
PromoterVviNAC01_Shiraz    ACCATTTATATAAAGAACCAGCACTTTATCTCTCAACCCACACCCACCTTTTCGCCTTTT
*****

PromoterVviNAC01_Pinot      CTTTCTTTCTTTCTTTTACACCAGTCCCCTCCCTTCTTTTCTCCTCTCTTTT
PromoterVviNAC01_Shiraz    CTTTCTTTCTTTCTTTTACACCAGTCCCCTCCCTTCTTTTCTCCTCTCTTTT
*****

PromoterVviNAC01_Pinot      TCTTATCTCTTACTTTGCTGGATTATAAGTACTACCACATATGTCTTCTTCGAATTGG
PromoterVviNAC01_Shiraz    TCTTATCTCTTACTTTGCTGGATTATAAGTACTACCACATATGTCTTCTTCGAATTGG
*****

PromoterVviNAC01_Pinot      ACCTCAATCAGTTATCATTCTCAACTAGTCTCTTCTTCTCTCCTTCAGCTTCAGCTCT
PromoterVviNAC01_Shiraz    ACCTCAATCAGTTATCATTCTCAACTAGTCTCTTCTTCTCTCCTTCAGCTTCAGCTCT
*****

PromoterVviNAC01_Pinot      AGAGTTGATAGGATTTTTTAGCG
PromoterVviNAC01_Shiraz    AGAGTTGATAGGATTTTTTAGCG
*****

```

B

| | |
|-------------------------|--|
| PromoterVviNAC05_Pinot | TTGCTTTTGCTATCCGTCTACAATTTTATTTTATTTTAAATTTTTTAAATTTTAAATGC |
| PromoterVviNAC05_Shiraz | TTGCTTTTGCTATCCGTCTACAATTTTATTTTATTTTAAATTTTTTAAATTTTAAATGC ***** |
| PromoterVviNAC05_Pinot | ATATCAAATGACTCAATTACCCTCATCTTAGTTGTATTTACCTCCACCCAATCATTCTA |
| PromoterVviNAC05_Shiraz | ATATCAAATGACTCAATTACCCTCATCTTAGTTGTATTTACCTCCACCCAATCATTCTA ***** |
| PromoterVviNAC05_Pinot | ATTATTTTAAAAATAAAAATAAAAATAAAGAATACGAAGAATTAATAATATATATATATG |
| PromoterVviNAC05_Shiraz | ATTATTTTAAAAATAAAAATAAAAATAAAGAATACGAAGAATTAATAATATATATATATG ***** |
| PromoterVviNAC05_Pinot | GTATTAATGGTAATATGATTAATCTTTCACACCATATTTTAAAACTTGTTGACTTAT |
| PromoterVviNAC05_Shiraz | GTATTAATGGTAATATGATTAATCTTTCACACCATATTTTAAAACTTGTTGACTTAT ***** |
| PromoterVviNAC05_Pinot | TTTATTCAAAATTAAGTCTAACAGTCAAATATGATTAATTAGTATAAATATAATAAA |
| PromoterVviNAC05_Shiraz | TTTATTCAAAATTAAGTCTAACAGTCAAATATGATTAATTAGTATAAATATAATAAA ***** |
| PromoterVviNAC05_Pinot | GTTAATCAACATAAATTATAAATGATTAATATGAATTAAGTTGTATTGATAAGTTGAT |
| PromoterVviNAC05_Shiraz | GTTAATCAACATAAATTATAAATGATTAATATGAATTAAGTTGTATTGATAAGTTGAT ***** |
| PromoterVviNAC05_Pinot | TAAAAATAATCTATTCCCTTAAACAATTATGTAATTTGACATAAATTTGATATAAACAG |
| PromoterVviNAC05_Shiraz | TAAAAATAATCTATTCCCTTAAACAATTATGTAATTTGACATAAATTTGATATAAACAG ***** |
| PromoterVviNAC05_Pinot | GATAAAAAACACATTAGATTCGAGTAAAAATATCATATTTTCTCACCATTATGTGATGT |
| PromoterVviNAC05_Shiraz | GATAAAAAACACATTAGATTCGAGTAAAAATATCATATTTTCTCACCATTATGTGATGT ***** |
| PromoterVviNAC05_Pinot | TAAAAATGGCATGTCAAGCACAATGAAAAATTTGGGAATAAAGTTGCAAAATACGCAATT |
| PromoterVviNAC05_Shiraz | TAAAAATGGCATGTCAAGCACAATGAAAAATTTGGGAATAAAGTTGCAAAATACGCAATT ***** |
| PromoterVviNAC05_Pinot | GGGTCAAATTACTTGGTTACCCCTCAACAGAGGGGCACCTTGACTTAAATCCAACGTTTGG |
| PromoterVviNAC05_Shiraz | GGGTCAAATTACTTGGTTACCCCTCAACAGAGGGGCACCTTGACTTAAATCCAACGTTTGG ***** |
| PromoterVviNAC05_Pinot | AAATTGAGTTTTTTCATGGGTAGTTGGATTTAGGTCGGGAATTAGAAAAAACGGGAGA |
| PromoterVviNAC05_Shiraz | AAATTGAGTTTTTTCATGGGTAGTTGGATTTAGGTCGGGAATTAGAAAAAACGGGAGA ***** |
| PromoterVviNAC05_Pinot | TTTATTGAACCTTGTAATTCGGGCTTAAATGACTCAACTTATGGGGTTGATGCCATA |
| PromoterVviNAC05_Shiraz | TTTATTGAACCTTGTAATTCGGGCTTAAATGACTCAACTTATGGGGTTGATGCCATA ***** |
| PromoterVviNAC05_Pinot | GTTTGGAGGAGGATAGAGATGTCCCAAGCAAAGTGTGACAAGCATTTCGTATGTGGAT |
| PromoterVviNAC05_Shiraz | GTTTGGAGGAGGATAGAGATGTCCCAAGCAAAGTGTGACAAGCATTTCGTATGTGGAT ***** |
| PromoterVviNAC05_Pinot | GGTTTATTTATTTAAGTCCCATGAAAGTCGTCTGAAAACCTTAGGATAAGTTTCATAAAAA |
| PromoterVviNAC05_Shiraz | GGTTTATTTATTTAAGTCCCATGAAAGTCGTCTGAAAACCTTAGGATAAGTTTCATAAAAA ***** |
| PromoterVviNAC05_Pinot | GGAGAGTCATATTGTATTTAGCTTAAAGTGATCGGAAAAAAGATAGTGACCTTTTCTGA |
| PromoterVviNAC05_Shiraz | GGAGAGTCATATTGTATTTAGCTTAAAGTGATCGGAAAAAAGATAGTGACCTTTTCTGA ***** |
| PromoterVviNAC05_Pinot | TTTGTTTTTACCTGGAATAGCTGAAAGATCAAAGTGCATGTTTAGCTTGTGTTTGC |
| PromoterVviNAC05_Shiraz | TTTGTTTTTACCTGGAATAGCTGAAAGATCAAAGTGCATGTTTAGCTTGTGTTTGC ***** |
| PromoterVviNAC05_Pinot | AAGGTGCTCAACTTCCTCCACACCCAAGGAGATAAATGCCTCTCAACTACAAGTCACTT |
| PromoterVviNAC05_Shiraz | AAGGTGCTCAACTTCCTCCACACCCAAGGAGATAAATGCCTCTCAACTACAAGTCACTT ***** |
| PromoterVviNAC05_Pinot | TATTCATGTACACCTCCTTTGCAAGAAGGTCAAACCACATTTAATTTGTGAGGACCCCA |
| PromoterVviNAC05_Shiraz | TATTCATGTACACCTCCTTTGCAAGAAGGTCAAACCACATTTAATTTGTGAGGACCCCA ***** |

PromoterVviNAC05_Pinot
PromoterVviNAC05_Shiraz
AAAGATTAACCTGGTGAAAAAATGAGATGATTTGATTGGTCTTGACCTATTAACATATT
AAAGATTAACCTGGTGAAAAAATGAGATGATTTGATTGGTCTTGACCTATTAACATATT

PromoterVviNAC05_Pinot
PromoterVviNAC05_Shiraz
CAAGATTTATGAGGTTTTGGGCCCTCCAGGGGAGGCCCTACTTTATCCTAACTCCATGA
CAAGATTTATGAGGTTTTGGGCCCTCCAGGGGAGGCCCTACTTTATCCTAACTCCATGA

PromoterVviNAC05_Pinot
PromoterVviNAC05_Shiraz
CACCAATGATGGTCAGCTTTCATTTATAACACACCTAAAGCATCTTGCCTTAGATATTTA
CACCAATGATGGTCAGCTTTCATTTATAACACACCTAAAGCATCTTGCCTTAGATATTTA

PromoterVviNAC05_Pinot
PromoterVviNAC05_Shiraz
TTTAGAAAGGGAAGGCCAATAGGGTGATTTTGGATATCTTAGAGTCGAATAAATGGAAT
TTTAGAAAGGGAAGGCCAATAGGGTGATTTTGGATATCTTAGAGTCGAATAAATGGAAT

PromoterVviNAC05_Pinot
PromoterVviNAC05_Shiraz
CTTTTAAAGAAGCTAAGATGGGAGCATCTGTAATTCCTATGCATCCAACAGATGTTAC
CTTTTAAAGAAGCTAAGATGGGAGCATCTGTAATTCCTATGCATCCAACAGATGTTAC

PromoterVviNAC05_Pinot
PromoterVviNAC05_Shiraz
CAGCTGCTGAGATAAACCAGCTTTATTTGGGAATGCCCATTCCATTCTTGGCCAACCT
CAGCTGCTGAGATAAACCAGCTTTATTTGGGAATGCCCATTCCATTCTTGGCCAACCT

PromoterVviNAC05_Pinot
PromoterVviNAC05_Shiraz
ATTATTACAATGCATGATGGACAATTTGGGTACTGATGAAACAAGCTGTGAAGTTGAC
ATTATTACAATGCATGATGGACAATTTGGGTACTGATGAAACAAGCTGTGAAGTTGAC

PromoterVviNAC05_Pinot
PromoterVviNAC05_Shiraz
ACCAAAGGCTTCATGGGTGTTCTTGCTGCAGATGATAATTCCTCTTTAATTCAGATTTT
ACCAAAGGCTTCATGGGTGTTCTTGCTGCAGATGATAATTCCTCTTTAATTCAGATTTT

PromoterVviNAC05_Pinot
PromoterVviNAC05_Shiraz
TGTGAAAAATAAATGGGAATACTTGAATTAGTAAATGGTAAGTATCAAAATACATGC
TGTGAAAAATAAATGGGAATACTTGAATTAGTAAATGGTAAGTATCAAAATACATGC

PromoterVviNAC05_Pinot
PromoterVviNAC05_Shiraz
AGAGGGTTGGAGATGAGTTGTCTTTGGTCAAATTTTGAAGGATAGATTTATGGCAGAAA
AGAGGGTTGGAGATGAGTTGTCTTTGGTCAAATTTTGAAGGATAGATTTATGGCAGAAA

PromoterVviNAC05_Pinot
PromoterVviNAC05_Shiraz
AGTTAAAGGAGGAGATGAAACAACAACAAGTGCCTTACATTCACGGTTTCTCTCT
AGTTAAAGGAGGAGATGAAACAACAACAAGTGCCTTACATTCACGGTTTCTCTCT

PromoterVviNAC05_Pinot
PromoterVviNAC05_Shiraz
CTCCAAACACCAGTATTTAGGGGCTTCTGTTCCATGTATTGCTTTTTTCTTAAACACTCT
CTCCAAACACCAGTATTTAGGGGCTTCTGTTCCATGTATTGCTTTTTTCTTAAACACTCT

PromoterVviNAC05_Pinot
PromoterVviNAC05_Shiraz
CCATCTTTCAGGTTTACAGCTTTTAGTTCATGGCTTCCCTGCCTTTTCTCTCTGCCTTT
CCATCTTTCAGGTTTACAGCTTTTAGTTCATGGCTTCCCTGCCTTTTCTCTCTGCCTTT

PromoterVviNAC05_Pinot
PromoterVviNAC05_Shiraz
TGTTGCCAAATTTATGGCTTTTCTTCATGCTTTTCTTCTAGTTCCTAGAAATCTACTTT
TGTTGCCAAATTTATGGCTTTTCTTCATGCTTTTCTTCTAGTTCCTAGAAATCTACTTT

PromoterVviNAC05_Pinot
PromoterVviNAC05_Shiraz
CTATTTGAATTTCCAGGCTTCTCGGTGGATGCTCCTGAATTTAGAAATTTGGACAGT
CTATTTGAATTTCCAGGCTTCTCGGTGGATGCTCCTGAATTTAGAAATTTGGACAGT

PromoterVviNAC05_Pinot
PromoterVviNAC05_Shiraz
TTGTTGGTACCCATTTGAAATATAGGGGCTCCTAGGGGCTGGGTGTAGGAATTGAGGTA
TTGTTGGTACCCATTTGAAATATAGGGGCTCCTAGGGGCTGGGTGTAGGAATTGAGGTA

PromoterVviNAC05_Pinot
PromoterVviNAC05_Shiraz
GAGTAGTGGAGGTTTACAGCTTTTAAATCAGAACCCTACTGAGATTTAGCGGACTTTCAA
GAGTAGTGGAGGTTTACAGCTTTTAAATCAGAACCCTACTGAGATTTAGCGGACTTTCAA

PromoterVviNAC05_Pinot
PromoterVviNAC05_Shiraz
AGAATGGAACATTTGCTGGACTTAGTGTGGAAGATGATCAG
AGAATGGAACATTTGCTGGACTTAGTGTGGAAGATGATCAG

C

```

PromoterVviNAC08_Pinot      TCCCAACCATAGCTTACCTGTCATTTATTGAGGCCAAACCGTTTTGACGTGTCTAGACGT
PromoterVviNAC08_Shiraz     TCCCAACCATAGCTTACCTGTCATTTATTGAGGCCAAACCGTTTTGACGTGTCTAGACGT
*****

PromoterVviNAC08_Pinot      TTCTTCGCATGATTTTGGCATTAAATGCTTCCACCATTCTGTAACCACGACGGACACG
PromoterVviNAC08_Shiraz     TTCTTCGCATGATTTTGGCATTAAATGCTTCCACCATTCTGTAACCACGACGGACACG
*****

PromoterVviNAC08_Pinot      TGGTATCTACGTGGCCCTTTTTTTTTTCTGGTAGTGTCTTATTCTGACAATATTTTAT
PromoterVviNAC08_Shiraz     TGGTATCTACGTGGCCCTTTTTTTTTTCTGGTAGTGTCTTATTCTGACAATATTTTAT
*****

PromoterVviNAC08_Pinot      CTGCCTGGTTCTAACCTTTTTTTTTTTAAAATACATTAATTAATTAAGACGACC
PromoterVviNAC08_Shiraz     CTGCCTGGTTCTAACCTTTTTTTTTTTAAAATACATTAATTAATTAAGACGACC
*****

PromoterVviNAC08_Pinot      TAAACAGGATGTTGGACCATAAGATAAATGAAACAATCGTTATCAACCCAACAGTACC
PromoterVviNAC08_Shiraz     TAAACAGGATGTTGGACCATAAGATAAATGAAACAATCGTTATCAACCCAACAGTACC
*****

PromoterVviNAC08_Pinot      TCAAATAATTC AATTC A ACGTGCACATGAAAAATTGATAAAATCGATTTAAACGCCGTC
PromoterVviNAC08_Shiraz     TCAAATAATTC AATTC A ACGTGCACATGAAAAATTGATAAAATCGATTTAAACGCCGTC
*****

PromoterVviNAC08_Pinot      TAACCGACAATTGCATTTTTTTTCAAACCACAAGGTTGAAAAAAAAAAAAAAAAAGGTT
PromoterVviNAC08_Shiraz     TAACCGACAATTGCATTTTTTTTCAAACCACAAGGTTGAAAAAAAAAAAAAAAAAGGTT
***

PromoterVviNAC08_Pinot      TTATGAAAAATAAGTACCAGCGCATATATTTATTTC AATATGGGGCCACAGGAAAACCC
PromoterVviNAC08_Shiraz     TTATGAAAAATAAGTACCAGCGCATATATTTATTTC AATATGGGGCCACAGGAAAACCC
*****

PromoterVviNAC08_Pinot      AGGTCTAACGTTTCACGACACACGTTGAAGGCTCCCACTA AACTGCACCGGCTGACATCAG
PromoterVviNAC08_Shiraz     AGGTCTAACGTTTCACGACACACGTTGAAGGCTCCCACTA AACTGCACCGGCTGACATCAG
*****

PromoterVviNAC08_Pinot      CGTCGCACGTGGATGATCCACGATGACGTGGACATGAATCCACCGTTAAACTGTCGGCT
PromoterVviNAC08_Shiraz     CGTCGCACGTGGATGATCCACGATGACGTGGACATGAATCCACCGTTAAACTGTCGGCT
*****

PromoterVviNAC08_Pinot      CAGCGACCAAGAGAAAAGAGGAGGAAAACCAAGCGGAGCCGTCGACTGCACACGGTTCCC
PromoterVviNAC08_Shiraz     CAGCGACCAAGAGAAAAGAGGAGGAAAACCAAGCGGAGCCGTCGACTGCACACGGTTCCC
*****

PromoterVviNAC08_Pinot      CATGACAGTTGGTCCCATATGACTCGCAGCTGCGTCCAAAACAGGTGACGCAAGCAGTG
PromoterVviNAC08_Shiraz     CATGACAGTTGGTCCCATATGACTCGCAGCTGCGTCCAAAACAGGTGACGCAAGCAGTG
*****

PromoterVviNAC08_Pinot      ACTAAATCACAGAGTGTGGGCTCTCGACACGCATACACTCACACTTCATAATCCGCCACG
PromoterVviNAC08_Shiraz     ACTAAATCACAGAGTGTGGGCTCTCGACACGCATACACTCACACTTCATAATCCGCCACG
*****

PromoterVviNAC08_Pinot      TGTCCGGCTGCGGTCAGAATGGTGGCTATTC C C C T A G A A C A A C C G A A A A T A T T A T C G C
PromoterVviNAC08_Shiraz     TGTCCGGCTGCGGTCAGAATGGTGGCTATTC C C C T A G A A C A A C C G A A A A T A T T A T C G C
*****

PromoterVviNAC08_Pinot      CCACGTGATTTCTAATAACCACCGTTCCCACTGCCACGTGTCCTCTTTTCTCTATAAA
PromoterVviNAC08_Shiraz     CCACGTGATTTCTAATAACCACCGTTCCCACTGCCACGTGTCCTCTTTTCTCTATAAA
*****

PromoterVviNAC08_Pinot      TTCTTCGCTCTCCCTTCCGGTCTAAGTTTCAAGCGCGCTCTGGCTCAGAGCAAAGCCGT
PromoterVviNAC08_Shiraz     TTCTTCGCTCTCCCTTCCGGTCTAAGTTTCAAGCGCGCTCTGGCTCAGAGCAAAGCCGT
*****

PromoterVviNAC08_Pinot      GAGAGAAGAGAAAAAAGGTCAGGAGAAACATTCATTCAAGAGAGGAGGAGAGAGAA
PromoterVviNAC08_Shiraz     GAGAGAAGAGAAAAAAGGTCAGGAGAAACATTCATTCAAGAGAGGAGGAGAGAGAA
*****

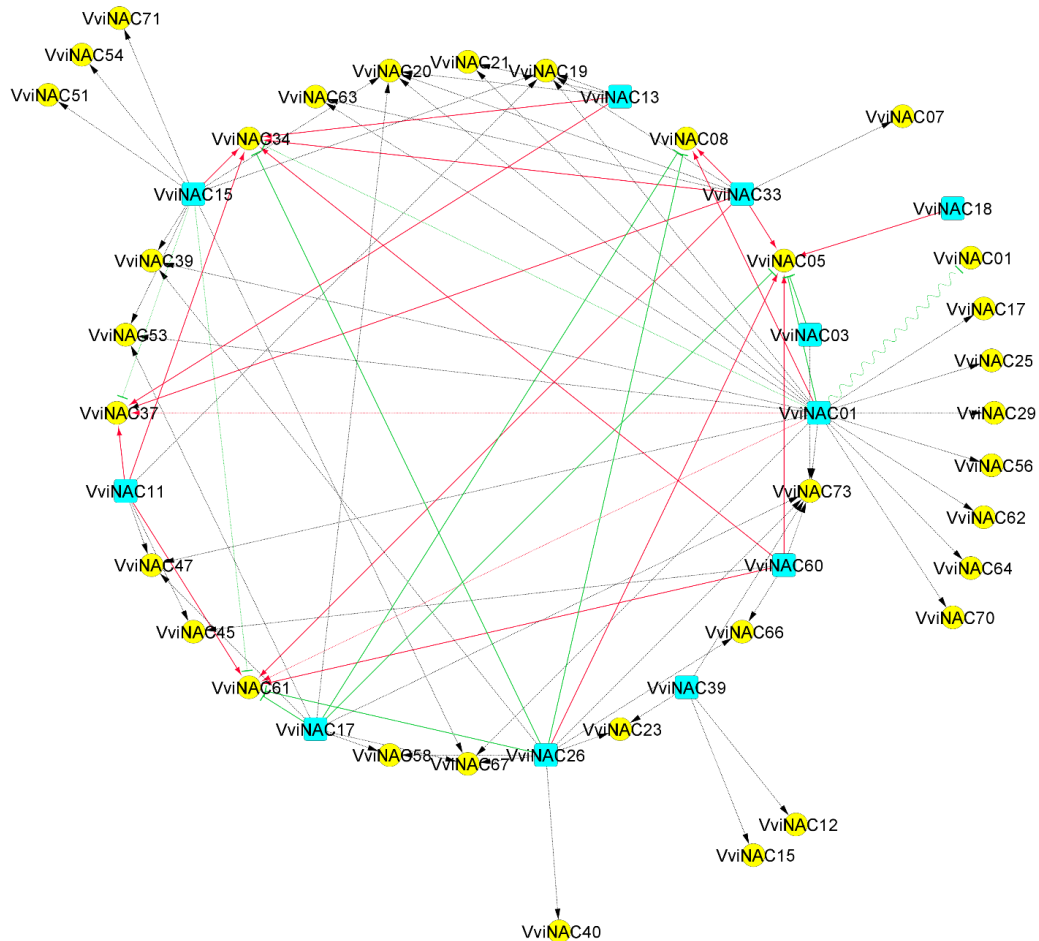
PromoterVviNAC08_Pinot      GCTAAT
PromoterVviNAC08_Shiraz     GCTAAT
*****

```


F

| | |
|-------------------------|---|
| PromoterVviNAC61_Pinot | AATCTCTCTGAAAGCGGGGCTGGGCTTGGAGTTGAAGTTTGGAGTTGCCAGCGCGCACCT |
| PromoterVviNAC61_Shiraz | AATTTCTCTGAAAGCGGGGCTGGGCTTGGAGTTGAAGTTTGGAGTTGCCAGCGCGCACCT *** ***** |
| PromoterVviNAC61_Pinot | TTTCTCAGTCGGCGCTTCATGTTTACTTTTTATTTTTTTTAAAAAATTTCCCATATG |
| PromoterVviNAC61_Shiraz | TTTTCAGTCGGCGCTTCATGTTTACTTTTTATTTTTTTTAAAAAATTTCCCATATG *** ***** |
| PromoterVviNAC61_Pinot | CACGTGGGGATTCCCTTTCTCCACACCCCACTGGATTTCTGCAAAATAAAAGATGGG |
| PromoterVviNAC61_Shiraz | CACGTGGGGATTCCCTTTCTCCACACCCCACTGGATTTCTGCAAAATAAAAGATGGG ***** |
| PromoterVviNAC61_Pinot | TAAGCTTGATTTGTGAAATATGAAAAAAAAATACAATATACTGGACAAAAATTCAA |
| PromoterVviNAC61_Shiraz | TAAGCTTGATTTGTGAAATATGAAAAAAAAATACAATATACTGGACAAAAATTCAA ***** |
| PromoterVviNAC61_Pinot | AAAGTTGTAAGAGATTAATATAAATATGAATGTATGTTGGGAGTATGCTAATTTGACA |
| PromoterVviNAC61_Shiraz | AAAGTTGTAAGAGATTAATATAAATATGAATGTATGTTGGGAGTATGCTAATTTGACA ***** |
| PromoterVviNAC61_Pinot | GAACCTCCAAGTGGCTTCTCCAGTCATGGATCCATGTTCTGGAAGGGACAAGATAT |
| PromoterVviNAC61_Shiraz | GAACCTCCAAGTGGCTTCTCCAGTCATGGATCCATGTTCTGGAAGGGACAAGATAT ***** |
| PromoterVviNAC61_Pinot | TACAAGGAGAAAGCTTAGGAAAATATGGAGGATAATGGGAGTGAAGCTGGGAGGAGGAT |
| PromoterVviNAC61_Shiraz | TACAAGGAGAAAGCTTAGGAAAATATGGAGGATAATGGGAGTGAAGCTGGGAGGAGGAT ***** |
| PromoterVviNAC61_Pinot | GAGGATGGGGCTGGGGCTTAAGCCAGGAGTGCGCCACTTCGAAATGGATGGATTTGACAT |
| PromoterVviNAC61_Shiraz | GAGGATGGGGCTGGGGCTTAAGCCAGGAGTGCGCCACTTCGAAATGGATGGATTTGACAT ***** |
| PromoterVviNAC61_Pinot | TTTCCCAAAGCATTAAAGGGGGAGTGTGTGGTTAGGGATGAGGGATGAGGGATGAAG |
| PromoterVviNAC61_Shiraz | TTTCCCAAAGCATTAAAGGGGGAGTGTGTGGTTAGGGATGAGGGATGAGGGATGAAG ***** |
| PromoterVviNAC61_Pinot | GGGGATTAAGACGAAATCCAAATCCAAAGTCGTATTTTAAATGTGAAGGGAGCTGGA |
| PromoterVviNAC61_Shiraz | GGGGATTAAGACGAAATCCAAATCCAAAGTCGTATTTTAAATGTGAAGGGAGCTGGA ***** |
| PromoterVviNAC61_Pinot | AACATGGGTCCCAGACGCCCAACATAGAAACACCTTGACCATTTCCCTTTTCAA |
| PromoterVviNAC61_Shiraz | AACATGGGTCCCAGACGCCCAACATAGAAACACCTTGACCATTTCCCTTTTCAA ***** |
| PromoterVviNAC61_Pinot | GAGGTAGATAAAGCTAATTAAGAAAATACACAAAAGGACAAGAGGAAAACCAAAAA |
| PromoterVviNAC61_Shiraz | GAGGTAGATAAAGCTAATTAAGAAAATACACAAAAGGACAAGAGGAAAACCAAAAA ***** |
| PromoterVviNAC61_Pinot | AAATGATATTGTAAGGCTTCTCGGAGAAGTGCCGTGCAGCGCAAGGATCTTATGACTTGT |
| PromoterVviNAC61_Shiraz | AAATGATATTGTAAGGCTTCTCGGAGAAGTGCCGTGCAGCGCAAGGATCTTATGACTTGT ***** |
| PromoterVviNAC61_Pinot | GAGCTGCGGGCGAAGCTCCTCTATTTAAGCTCCTTTTCTTCTTCTACTTTCTTA |
| PromoterVviNAC61_Shiraz | GAGCTGCGGGCGAAGCTCCTCTATTTAAGCTCCTTTTCTTCTTCTACTTTCTTA ***** |
| PromoterVviNAC61_Pinot | ACTGCTCTCTTTGAAAACCTTCAATACAGGCTCTTCTCTCCCTTGCTTTCTGCTATTG |
| PromoterVviNAC61_Shiraz | ACTGCTCTCTTTGAAAACCTTCAATACAGGCTCTTCTCTCCCTTGCTTTCTGCTATTG ***** |
| PromoterVviNAC61_Pinot | TTGTTTGTGCGTATTGGTTTGGAAATTAATCTTCTTTCTGATTCTACATTCGCTTAGA |
| PromoterVviNAC61_Shiraz | TTGTTTGTGCGTATTGGTTTGGAAATTAATCTTCTTTCTGATTCTACATTCGCTTAGA ***** |
| PromoterVviNAC61_Pinot | GCTTTATTTTTTTTTTAAAGGTAATAATGATATACAGTAGTGGTGAACCATGGAAGA |
| PromoterVviNAC61_Shiraz | GCTTTATTTTTTTTTTAAAGGTAATAATGATATACAGTAGTGGTGAACCATGGAAGA ***** |
| PromoterVviNAC61_Pinot | GGCTTCACTTGCCGATCAAGGTGATGACCTT |
| PromoterVviNAC61_Shiraz | GGCTTCACTTGCCGATCAAGGTGATGACCTT ***** |

Appendix E: Circular representation of all the *VviNAC-VviNACs* interactions revealed in the DAP-seq datasets. The TFs are highlighted in light-blue squares and the targets are represented as yellow circles. The red \rightarrow arrows indicate the activations and the green **T** arrows show the repressions; the curved arrow indicates the autoregulation of *VviNAC01*. The continuous lines indicate the validated interactions ($p < 0.05$) and the dashed lines indicate the not significant interactions. The image was done with Cytoscape.



Non sono mai stata brava con le parole e proprio per questo non ho mai scritto dei ringraziamenti. La pandemia mi ha tuttavia spinta a tentare; il non poter vedere le persone a me care mi ha fatto capire che la vicinanza e l'affetto vadano talvolta dimostrate anche in maniera diversa...o per lo meno bisogna provarci.

Mi ritrovo quindi a scrivere la parte più difficile della mia tesi, quella non basata su dati scientifici, quella dove solo le mie sensazioni possono essere prese in considerazione. Tre anni sono volati ma non sono stati di certo sempre facili. Le ansie, le preoccupazioni e le difficoltà che derivano dal trovarsi a sviluppare un progetto di ricerca sono molte; ciò che mi ha spinto ad andare avanti è sicuramente la passione verso il mio lavoro ma ha anche dei nomi e delle facce.

Ringrazio Sara, per avermi affidato questo progetto ambizioso ma allo stesso tempo intrigante e per aver creduto in me anche quando l'unica cosa che riuscivo ad immunoprecipitare era il nulla cosmico. Grazie anche per l'esperienza americana dalla quale ho imparato molto, sia dal punto di vista scientifico che umano, e che mi ha permesso di capire che, nonostante le scarse liquidità investite in Italia nella ricerca, l'arte di arrangiarsi sarà sempre un buon fondo da cui attingere.

Ringrazio i miei compagni di laboratorio Erica, Alessandra, Edoardo, Chiara e Anne-Marie per il supporto scientifico e psicologico che mi hanno sempre dato. In particolare, un super grazie alla mia compagna di banco Ericuz per avermi aiutata ad integrarmi fin da subito nel progetto NAC, per aver visto bande anche dove un elfo della Terra di Mezzo sarebbe stato cieco e per aver curato costantemente la mia idratazione.

Ringrazio Peter per le tante serate passate insieme, per avermi sempre fatto vedere i miei problemi con uno spirito più allegro, per le risate con la piccola Lia e per avermi spronata ad essere più calma e riflessiva, permettendomi così di mantenere la giusta distanza dalle mie inutili preoccupazioni.

Ringrazio la ormai tedeschissima Alice per il sostegno, le risate, le strigliate, la schiettezza e l'essere sempre presente come amica nonostante i troppi chilometri di distanza. Con te ho capito quanto non mollare mai e farsi sempre valere per quello in cui si crede sia fondamentale, soprattutto nell'ambito della ricerca.

Grazie a te, Di, perché, per fortuna, sei stranamente tu! La nostra amicizia inaspettata mi ha sempre accompagnata durante il nostro dottorato ed è diventata sempre più preziosa...direi insostituibile. Sei la spinta positiva di molti miei momenti bui, la peculiarità nelle mie valutazioni banali e sappi che una bistecca sarà sempre data a Casa Foresti a chi (come te) se la merita.

Ringrazio il rosso più monello che ci sia, Stefano, per le chiacchierate e le confidenze, per gli innumerevoli 'Ciao come va?', per gli scherzi ricevuti, per le tante esperienze fatte insieme, per tutte le volte che le litigate hanno rafforzato il nostro rapporto e per essere un mio grande sostenitore. Ci sei sempre stato e sai quanto tu sia un amico prezioso per me.

Grazie alla mia bolzanina preferita, Cuccuruccucù Paloma, che mi sostiene sempre ed è sempre pronta a mangiare con me una briochinaaaaa. Tutte le volte rimango stupita da come tu riesca a rasserenarmi anche solo con un semplice messaggio o qualche (forse non solo qualche) meme assurdo che solo tu puoi trovare.

Un ringraziamento con tampone negativo (che così arriva anche in Portogallo) va al mio stravagante amico Scia che, nonostante i pronostici, sta sopravvivendo a ben tre traslochi, due dottorati e molte (anche se non riconosciute) spasimanti. Le tue vicissitudini assurde riescono sempre a farmi tornare il sorriso...ma mai quanto vederti saltellare con il tuo latte per i corridoi dell'università.

Grazie a Richi per avermi copiato tutte le pizze mangiate e tutte le birre bevute in compagnia e per aver mantenuto in vita un gruppo su Telegram con ben tre partecipanti! La tua presenza costante, gentile e discreta mi ha sempre rallegrata e rassicurata.

Grazie al mio talent scout di fiducia Charles per le magnifiche serate, per i tanti consigli dispensati, per il giro in monopattino, per gli aggiornamenti costanti sui Brooke e Ridge di Verona, per essere il mio vice rafforza carattere e per avermi concesso di entrare nel #Clann (questa solo perché te l'avevo promessa eh...).

Grazie alla mia Pinko Panka Linda per aver sopportato e supportato sempre le mie fisse mentali facendomi sentire vagamente normale, per la tua risata contagiosa, per le nostre mille avventure insieme e per volermi bene sempre e comunque.

Ringrazio le mie amichette bisbetiche e per nulla domate di una vita, Paolenzi e Meggionzi, per tutte le stalkerate, le acidate e i pettegolezzi che hanno reso le mie giornate più allegre e per avermi fatto realizzare che non c'è mai limite al disagio.

Ringrazio la piccola ma vulcanica Lizia per tutte le chiamate (a cui puntualmente non ho risposto perché ero troppo indaffarata al lavoro) che mi hanno sempre fatto sentire la sua vicinanza, per il sostegno, per i pettegolezzi montoriesi e per la pazienza nell'aspettare che io abbia due settimane di ferie per andare in vacanza...Please, don't stop believing!

Un grazie immenso alla mia amica Carlo, fin dal liceo anima gemella di sfortune, gioie, dolori e risate...sei sempre stata e sempre sarai la mia dolce metà! Abbiamo visto cose che voi umani non potreste immaginarvi: casi umani da combattimento a flote al largo dei bastioni di Verona, e abbiamo visto spasimanti impensabili balenare nel buio vicino alle porte di casa. E tutti questi momenti non andranno perduti nel tempo, proprio come la nostra angoscia condivisa in piena pandemia. È tempo di andare a Lourdes!

Infine, il ringraziamento più sentito va alla mia mamma e al mio papà. Mi avete sempre dato tutto, anche più di quello di cui avessi realmente bisogno. Grazie di tutto...per come siete, per come mi avete permesso di essere e per tutti i sogni che solo grazie a voi ho realizzato. Siete e sarete sempre le persone più importanti della mia vita.